PDE constrained kernel regression methods

Iain Henderson

THÈSE

En vue de l'obtention du

DOCTORAT DE L'UNIVERSITÉ DE TOULOUSE

Délivré par : *l'Université Toulouse 3 Paul Sabatier (UT3 Paul Sabatier)*

Présentée et soutenue le *28 Septembre 2023* **par :**

Iain HENDERSON

Méthodes de régression à noyau sous contraintes d'équations aux dérivées partielles

---

JURY

Eric SAVIN	ONERA, Palaiseau	Président du jury
Josselin GARNIER	Ecole Polytechnique, Palaiseau	Rapporteur
Clémentine PRIEUR	Université Grenoble Alpes	Rapporteure
Anne ESTRADE	Université Paris Descartes	Examinatrice
Pascal NOBLE	Université Paul Sabatier	Directeur de thèse
Olivier ROUSTANT	Université Paul Sabatier	Directeur de thèse
Rémy BARAILLE	SHOM, Toulouse	Invité

École doctorale et spécialité :
MITT : Domaine Mathématiques : Mathématiques appliquées
Unité de Recherche :
INSA Toulouse, Institut de Mathématiques de Toulouse (UMR 5219)
Directeur(s) de Thèse :
Pascal NOBLE et *Olivier ROUSTANT*
Rapporteurs :
Josselin GARNIER et *Clémentine PRIEUR*

It's still magic even if you know how it's done.

Terry Pratchett
in *A hat full of sky*

Avant-propos

Ce manuscrit traite de l'étude des méthodes de régression dites "à noyau", situées à l'interface entre apprentissage machine et équations aux dérivées partielles, spécifiquement calibrées pour traiter certains problèmes issus de la physique. Plusieurs points de vue, déterministes ou probabilistes, permettent d'introduire ces méthodes de régression.

Le fil rouge de ce mémoire de thèse est la mise en relation de ces méthodes à noyau (dans leurs différentes formulations) avec certains aspects théoriques et numériques concernant les équations aux dérivées partielles, et leur formulation reposant sur l'analyse fonctionnelle en particulier. Un des objectifs de fond est d'identifier dans quelle mesure les principes de chaque discipline peuvent s'articuler les uns aux autres. Cette question est motivée par l'ébullition d'un domaine nouveau et prometteur (le "physics-informed machine learning"), objet de nombreux fantasmes mais dont le véritable champs des possibles demeure encore mal compris.

Dans cette optique, la démarche que j'ai suivie est très exploratoire. Les choix qui ont été faits tout au long de la thèse ne sont certainement pas les seuls possibles, en particulier concernant le parti pris initial de se tourner vers les méthodes à noyau. Les résultats présentés dans ce manuscrit sauront peut-être justifier la pertinence des choix que nous avons faits.

Remerciements

Je voudrais tout d'abord remercier Pascal et Olivier, qui m'ont encadré pendant ces trois années de thèse, ainsi que pendant mon stage de Master. Ils m'ont fait confiance tout au long de ce long voyage. En effet, ils m'ont laissé beaucoup de liberté sur les différentes directions de recherche qui se sont présentées durant ces trois années. En ce sens, je voudrais souligner leur ouverture d'esprit et leur sens de la pédagogie. Ils ont aussi su me pousser et m'accompagner dans des projets ambitieux, que ce soit pendant la thèse ou lors de la préparation de l'après-thèse. Enfin, ils ont toujours été très réactifs pour prendre tout le temps nécessaire lorsque j'en avais besoin, malgré leurs emplois du temps (sur)chargés, ce pourquoi je les remercie grandement.

Un grand merci à Clémentine Prieur et Josselin Garnier, qui ont accepté de rapporter ma thèse, pendant l'été qui plus est. Il en va de même pour Anne Estrade et Eric Savin, qui ont accepté d'être examinateurs.

Il me faut bien sûr aussi remercier le SHOM qui financé cette thèse, et qui a aussi fait preuve d'une grande flexibilité quant aux directions de recherche possibles. Au sein du SHOM, je souhaite remercier tout particulièrement Rémy Baraille, pour ses encouragements ainsi que l'intérêt et la curiosité qu'il a porté pour mes travaux. Au même titre qu'Olivier et Pascal, j'ai pu compter sur son soutien pendant la thèse, mais aussi concernant l'après-thèse. Je voudrais également souligner que le SHOM m'a donné la chance de partir en conférence, de surcroît dans des endroits extrêment désagréables tels que la Grande Motte, le Croisic, Berne ou encore Braga au Portugal (en plus il faisait beau).

Je souhaite ensuite remercier tous les membres du GMM, pour l'ambiance de travail très agréable qu'ils amènent avec eux, malgré le contexte étrange d'un début de thèse en plein covid. Je pense particulièrement à Sandrine, et à son infinie patience envers mes retards de déclaration d'OM. Je souhaite aussi remercier les équipes MAC et Stat-Optim de l'IMT, ainsi que les organisateurs de leurs séminaires respectifs. J'ai eu un grand plaisir à assister à ces derniers. Du côté des doctorants, je remercie d'abord Julie pour ces trois ans et demi passés à partager le même bureau. J'éprouve une certaine fierté à la pensée de ces quelques journées estivales durant lesquelles notre bureau concentrait, à nous deux, entre 50% et 67% de l'effectif total des personnes présentes au GMM ce jour-là. Un grand merci aux autres doctorants de l'INSA, anciens et nouveaux, avec qui nous avons partagé moult cafés, mots croisés, devinettes géographiques mais aussi de belles galères de thèse comme on les aime : Clément, Alban, Hippolyte, Mahmoud, Evgeniia, Amandine, Nathanël, Hugo.

Je veux particulièrement remercier Romain, qui a bien voulu écouter mes vagabondages mathématiques et qui m'a aussi raconté les siens (désolé Aude d'avoir autant colonisé votre bureau...). En dehors de l'INSA aussi, on se

souviendra des sorties au parc de la Grande plaine et des soirées haletantes passées à chasser des trésors (inutiles d'ailleurs) sur Sea of Thieves.

Je voudrais te remercier Antoine car, malgré la distance et notre déficit flagrant en compétences communicationnelles, nous sommes parvenus à rester proches. Cela m'amuse toujours de constater à quel point, lorsqu'on se voit, il est difficile de nous empêcher de parler de maths, d'informatique et de répliques d'anime japonais (Ultimato Doragon Tayger ...). J'espère pouvoir partager encore avec toi nos fameux sandwichs garniture chips et jambon (fumé), souvenir innocent de deux années de prépa beaucoup moins candides.

Je veux aussi remercier mes amis du lycée, Paul, Florian, Sébastien, Thomas, Anthony, Adrien, François-Xavier. Comme il est étrange de voir comment nous avons grandi.

Après le travail et les amis, c'est vers ma famille que je me tourne. Merci à Claude et Xavier, qui se sont attelés avec courage au problème NP-difficile consistant à être parents. Encore merci pour vos encouragements et pour votre confiance indéflectible. Aussi, merci d'avoir éveillé ma curiosité très tôt dans mon enfance, d'avoir accepté mon caractère indépendant voire solitaire, d'avoir su me pousser vers le meilleur et, fait non moins important, d'avoir réussi à faire de moi un individu (à peu près) fonctionnel. Il y a certainement un peu de vous dans ce manuscrit. Merci à ma Bonne Maman, mon Bon Papa et à mes oncles et tantes (Anne et Jean-Paul en particulier), chez qui je me suis souvent échappé pendant et après les années prépas. Enfin, je veux remercier mes grandes soeurs, Isabelle et Hélène, avec qui j'ai grandi et continue de grandir malgré la distance (il paraît que nous sommes des adultes maintenant !). Merci de m'avoir souvent accueilli dans vos différents appartements à taille très variable, et de m'avoir bien souvent montré la voie, que ce soit à l'école, dans les études, ou autre part encore (dans les bars par exemple ?).

Et enfin, bien sûr, merci Nathalie. Merci pour ta présence quotidienne, ta tendresse, ta patience, ton aide aussi, et pour l'intérêt que tu portes à ce que je fais, malgré mes tentatives d'explications souvent plus embrouillantes qu'autre chose. Je crois que tout est plus facile (thèse inclue) lorsqu'on a un joli foyer où rentrer. D'ailleurs, même si traverser une thèse est une belle étape, je crois bien que nous avons beaucoup d'autres aventures à vivre ensemble. Je veux aussi remercier la famille de Nathalie, pour leur accueil toujours aussi chaleureux. Enfin, je termine par remercier nos chats (et oui, j'ose), Minette et Ninou, qui savent si bien nous rappeler aux choses vraiment importantes dans la vie (le thon).

Table des matières

1 Chapitre introductif **1**

1.1 Contexte général de l'apprentissage machine 4

1.1.1 Quelques principes de l'apprentissage machine 4

1.1.2 La systématisation de l'utilisation de l'apprentissage machine 5

1.2 Outils d'apprentissage machine 8

1.2.1 Formulation générale de l'apprentissage supervisé . . . 9

1.2.2 Approche bayésienne pour les problèmes inverses . . . 11

1.2.3 Mesures gaussiennes et régression par processus gaussiens 14

1.2.4 Espaces de Hilbert à noyau reproduisant 21

1.2.5 Méthodes à noyau et réseaux de neurones 24

1.3 Equations aux dérivées partielles 26

1.3.1 Quelques propriétés des EDPs 26

1.3.2 Espaces de Sobolev et formulations faibles 29

1.3.3 Formulation distributionnelle et fonction de Green . . . 32

1.3.4 Méthodes numériques pour la résolution des EDP . . . 36

1.3.5 Le problème de l'apprentissage machine sous contraintes d'EDP 37

1.4 Description des chapitres 40

1.4.1 Chapitre 2 : processus aléatoires sous contraintes distributionnelles d'EDPs linéaires 42

1.4.2 Chapitre 3 : régularité Sobolev des trajectoires d'un processus gaussien 46

1.4.3 Chapitre 4 : régression par processus gaussiens pour l'équation des ondes en trois dimensions 58

1.4.4 Chapitre 5 : régression par processus gaussiens et méthode des différences finies 62

2 Characterization of the second order random fields subject to linear distributional PDE constraints **69**

2.1 Introduction 71

2.2 Background 77

2.2.1 Random fields 77

2.2.2 Tools from functional analysis 79

2.3 Random fields under linear differential constraints 83

2.3.1 The case of classical derivatives 84

2.3.2 The case of distributional derivatives 85

2.3.3 A heredity property for Gaussian process regression . . 93
2.4 Gaussian processes and the 3 dimensional wave equation . . . 94
2.4.1 General solution to the 3 dimensional wave equation . 95
2.4.2 Gaussian process modelling of the solution 96
2.5 Conclusion and perspectives 102

3 Sobolev regularity of Gaussian random fields 105
3.1 Introduction 107
3.2 Preliminary notions and results 111
3.2.1 Definition of weak derivatives and Sobolev spaces . . . 111
3.2.2 Characterization of $W^{m,p}$-regularity for locally integrable functions 112
3.2.3 Sobolev regularity and generalized functions 113
3.2.4 Tools from operator theory 115
3.2.5 Gaussian processes, Gaussian measures over Banach spaces 117
3.3 Sobolev regularity of Gaussian processes : the general case, $1 < p < +\infty$ 121
3.4 Sobolev regularity of Gaussian processes : the Hilbert space case, $p = 2$ 137
3.4.1 Reproducing Kernel Hilbert Spaces (RKHS, [24]) . . . 138
3.4.2 Ellipsoids of Hilbert spaces and canonical Gaussian processes 138
3.5 Application to the selection of covariance kernels 150
3.6 Concluding remarks and perspectives 156
3.7 Proofs of intermediary results and lemmas 157

4 GPR for the three dimensional wave equation 167
4.1 Introduction 169
4.2 Background on Gaussian process regression 172
4.2.1 Random fields, Gaussian processes, positive definite functions 172
4.2.2 Gaussian process regression [166] 173
4.3 Gaussian process priors for the 3D wave equation 175
4.3.1 General solution to the wave equation 175
4.3.2 Gaussian process priors for the wave equation 175
4.3.3 The point source limit 186
4.3.4 Computational speedups 196
4.3.5 Initial condition reconstruction and error bounds . . . 200
4.4 Numerical experiments 203
4.4.1 Test case for $k_{\mathrm{u}}^{\mathrm{wave}}$ 207
4.4.2 Test case for $k_{\mathrm{v}}^{\mathrm{wave}} + k_{\mathrm{u}}^{\mathrm{wave}}$ 208

4.5 Conclusion and perspectives 213

5 GPR methods and finite difference schemes 215
5.1 Introduction 217
5.2 Finite difference schemes for the advection equation 221
5.2.1 First order hyperbolic PDEs 221
5.2.2 Finite difference schemes 222
5.2.3 Gaussian process regression and finite difference schemes in the flat limit regime 227
5.2.4 Finite difference schemes via GPR in the non flat regime 240
5.3 Transparent boundary conditions 247
5.3.1 Context 247
5.3.2 The two dimensional wave equation 249
5.3.3 A matched Dirichlet boundary condition strategy . . . 250
5.4 Conclusion and perspectives 251
5.5 Appendix : proofs 254

6 General Conclusion and perspectives 261

Table des figures

1.1 Vraie u_0 (colonne de gauche) vs u_0 estimée (colonne de droite). 15 capteurs ont été utilisés. Les images correspondent à une évaluation des fonctions en $z = 0.5$. 62
1.2 Exemple numérique de conditions aux bords transparentes obtenue selon la stratégie décrite plus haut (extrait de la figure 5.7). 67

4.1 Negative log marginal likelihood as a function of $x_0 \in \mathbb{R}^3$. Are only represented values of the negative log marginal likelihood that are below 2.035×10^9. There only remains thin spherical shells. Red crosses: sensor locations. Black cross: source position. The source is located at the intersection of spheres centered at the sensor locations. 188
4.2 Visualization of signal and WIGPR results for the test case #1 206
4.3 Box plots for the sensibility analysis, test case #1 208
4.4 Test case #2, excerpt of captured signals. Dashed line: noiseless data. Solid line: noisy data. 210
4.5 Test case #2: top and lateral view of the reconstructions of u_0 (Figure 4.5a) and v_0 (Figure 4.5b) provided by WIGPR, in comparison with u_0 and v_0. Left columns: true IC. Right columns: WIGPR IC reconstructions. 20 sensors were used. . 211
4.6 Box plots for the sensibility analysis, test case#2 212

5.1 Coefficients a_{-1} (blue), a_0 (orange) and a_1 (green) of the ν-scheme for $\nu = 1/2,\ 1,\ 3/2,\ 2$, as functions of $\lambda \in [-1, 1]$. . . 234
5.2 Plot of the map $\lambda \mapsto D(\nu, \lambda)$, $\lambda \in [-1, 1]$, for several values of $\nu \in [1/2, 2]$. These plots confirm Conjecture 5.2.8. 235
5.3 Convergence plots for several ν-schemes, with $\lambda = 0.75$ 237
5.4 Visualization of the numerical solutions associated to ν-schemes, with smooth (Gaussian) and non smooth (door type) initial conditions. 239
5.5 Absolute value of the negative overshoot (equation (5.2.50)) of the solution associated to the ln-scheme with a door type initial condition, as a function of time, in log scale. The overshoots are less and less dampened as ν approaches 2, while those of the Lax-Wendroff scheme actually seem to grow. 239
5.6 Numerical example showing that the outgoing waves produced by WIGPR do not suffer from numerical reflection issues. . . . 248

5.7 Numerical example of matched Dirichlet transparent boundary conditions using WIGPR. 252

Liste des tableaux

4.1 Hyperparameter estimation and relative errors, test case #1 . 208
4.2 Hyperparameter estimation and relative errors, test case #2 . 210

Chapitre 1

Chapitre Introductif

Avant-propos du premier chapitre. Ce chapitre est d'abord l'occasion de contextualiser et de motiver les choix qui ont été faits lors de mes travaux de recherche. Pour cela nous décrivons, de façon simplifiée, quelques principes importants de l'apprentissage machine, ainsi que les raisons qui ont fait émerger le thème de l'apprentissage machine appliqué à des problèmes issus de la physique. En particulier, même si la thèse ne traitera jamais de régression basée sur des réseaux de neurones, ces derniers ont joué un rôle crucial dans la généalogie des thématiques abordées dans ce manuscrit ; ils constituent aussi la méthode de régression reine sur les problèmes généraux d'apprentissage machine. C'est pourquoi j'ai fait le choix de leur accorder une place relativement importante dans ce chapitre. Cela servira aussi à justifier l'intérêt qu'ont les méthodes à noyau, lorsque nous décrirons certains liens étroits existant entre ces méthodes et les réseaux de neurones. Cela nous permettra en outre d'expliciter certains avantages (fiabilité et interprétabilité) qu'ont les méthodes à noyau sur les réseaux de neurones, dans le cas précis d'applications sur des modèles physiques.

Si la diversité des concepts que nous aborderons tout au long de ce texte est une source de richesse mathématique, c'est aussi une source de difficulté. En effet, le coût d'entrée est double, puisqu'il nous faudra manipuler autant de notions de probabilités et de statistiques que d'équations aux dérivées partielles. Partant du principe que ce manuscrit s'adresse autant au probabiliste qu'au statisticien ou à l'analyste ("l'edpiste"), ce chapitre introductif est donc aussi l'occasion de resituer certains concepts que j'ai jugés importants, et qui sont issus des différentes disciplines entrant en jeu. Certains détails seront certainement des évidences pour le probabiliste mais pas pour l'analyste, et réciproquement. Etant donné que cette dernière communauté est parfois hésitante ou frileuse à la vue d'outils de statistiques, et que la situation miroir se produit tout autant, j'ai pris le parti d'aller assez loin dans le détail d'exemples simples mais illustratifs, plutôt que de laisser le lecteur intéressé mais non initié se perdre dans des ouvrages spécialisés. L'introduction des différents concepts est accompagnée de commentaires à visée pédagogique. Le choix d'une telle présentation s'est aussi fait dans l'espoir qu'elle rende relativement "naturelles" les questions auxquelles nous avons donné une réponse dans les chapitres suivants.

Résumé

La première partie de ce chapitre décrit rapidement les grands principes de l'apprentissage machine, puis dresse un paysage simplifié de l'apprentissage machine, à l'heure actuelle. Cette partie décrit notamment certaines raisons qui ont amené l'apparition de l'apprentissage machine dans les problèmes de la physique en particulier. La deuxième partie motive et décrit le formalisme et les outils mathématiques que nous utilisons dans le manuscrit. Cela comprend les méthodes à noyau dans leur formalisme probabiliste et déterministe d'une part, et les formulations faibles et distributionnelles des équations aux dérivées partielles d'autre part. Chaque discipline est rapidement décrite ; nous discutons aussi des liens entre méthodes à noyau et réseaux de neurones, et des différentes stratégies existantes en apprentissage machine informé par la physique. La troisième partie décrit les chapitres de la thèse. En particulier, les questions traitées dans chaque chapitre sont motivées, et la stratégie générale de résolution est décrite.

Contents

1.1 Contexte général de l'apprentissage machine 4
1.1.1 Quelques principes de l'apprentissage machine 4
1.1.2 La systématisation de l'utilisation de l'apprentissage machine 5
1.2 Outils d'apprentissage machine 8
1.2.1 Formulation générale de l'apprentissage supervisé . . . 9
1.2.2 Approche bayésienne pour les problèmes inverses . . . 11
1.2.3 Mesures gaussiennes et régression par processus gaussiens 14
1.2.4 Espaces de Hilbert à noyau reproduisant 21
1.2.5 Méthodes à noyau et réseaux de neurones 24
1.3 Equations aux dérivées partielles 26
1.3.1 Quelques propriétés des EDPs 26
1.3.2 Espaces de Sobolev et formulations faibles 29
1.3.3 Formulation distributionnelle et fonction de Green . . 32
1.3.4 Méthodes numériques pour la résolution des EDP . . . 36
1.3.5 Le problème de l'apprentissage machine sous contraintes d'EDP 37
1.4 Description des chapitres 40
1.4.1 Chapitre 2 : processus aléatoires sous contraintes distributionnelles d'EDPs linéaires 42
1.4.2 Chapitre 3 : régularité Sobolev des trajectoires d'un processus gaussien 46
1.4.3 Chapitre 4 : régression par processus gaussiens pour l'équation des ondes en trois dimensions 58
1.4.4 Chapitre 5 : régression par processus gaussiens et méthode des différences finies 62

1.1 Contexte général de l'apprentissage machine

1.1.1 Quelques principes de l'apprentissage machine

Parmi les bouleversements scientifiques et techniques des cinquante dernières années, nous pouvons certainement citer l'essor de l'apprentissage machine ("machine learning"). Considérons un ensemble de données labelisées, par exemple des images chacune munies d'un ensemble de mots la décrivant (chat, maison...). Un des champs d'application de l'apprentissage machine concerne la conception d'algorithmes qui, à partir de la connaissance de cet ensemble de données, doivent décider si une image qu'ils n'ont jamais vue peut être décrite par un autre ensemble de mots. Pour cela, une première étape dite *d'apprentissage* est d'abord mise en place, pendant laquelle l'algorithme est calibré pour coller aux données. Puis vient l'étape de *prédiction*, où l'on se sert de l'algorithme sur de nouveaux exemples. Des étapes intermédiaires de *validation* de l'algorithme sont souvent mises en place, afin de s'assurer que les résultats de la phase de calibration ne donnent pas de résultats aberrants. En général, un compromis doit être trouvé entre bonne approximation de la base de données et bonnes propriétés de prédiction (ou "généralisation"). Dans notre exemple, l'apprentissage est dit *supervisé* car les données ont été labelisées.

Dans la version classique de l'apprentissage machine, la partie calibration se fait essentiellement en interagissant avec le modèle en question, sans connaître a priori les propriétés fines ou "internes" du modèle. L'espoir sous-jacent est que l'algorithme retrouve, de façon relativement autonome, ces dites propriétés. C'est pourquoi nous parlons aussi d'apprentissage *automatique*, mais aussi d'approche "guidée par les données" (*data driven*). Le modèle est donc souvent vu comme une sorte de boîte noire, soit impénétrable, soit qu'on ne souhaite pas pénétrer, dont nous ne connaissons que certaines entrées et sorties. Cette abstraction des structures spécifiques du modèle en question est une des grandes forces des méthodes d'apprentissage machine, puisque par construction ces méthodes peuvent s'appliquer à tout type de données [1]. Il se trouve aussi qu'une des seules théories mathématiques (la seule ?) qui subsiste à un tel niveau de généralité, et qui arrive à concilier des données de nature aussi hétérogènes, est la théorie des statistiques. Il n'est donc pas surprenant que ce soit cette théorie qui soit la plus rencontrée en apprentissage machine.

1. Le simple fait qu'une telle approche puisse fournir des résultats non triviaux peut sembler surprenant, et diverses théories (mathématiques ou non) ont tenté d'expliquer de tels succès, par exemple en arguant que la majorité des phénomènes que nous rencontrons (et donc les données qu'ils génèrent) possèdent une structure de système hiérarchique [188].

Dans l'exemple de classification d'images décrit plus haut (et en apprentissage machine en général) il est clair que la quantité de données disponibles, le choix du type d'algorithme et le choix de la méthode de calibration, auront des impacts importants sur la qualité de la prédiction. En ce sens, l'apprentissage machine s'est aussi développé en parallèle avec les avancées en puissance de calcul, en traitement de données massives, en optimisation en grande dimension et en informatique en général. Citons, entre autres, la systématisation de l'utilisation d'algorithmes de différentiation automatique, de descente de gradient stochastique ou la démocratisation d'outils logiciels comme Keras, Pytorch ou Tensorflow.

Depuis les années 2010, les réseaux de neurones (profonds) se sont imposés comme méthode hégémonique d'apprentissage machine, aussi est-il difficile de parler d'apprentissage machine sans dire un mot sur ces algorithmes. Un réseau de neurones artificiels a la structure générale suivante

$$R_\theta(x) \coloneqq (W_L \circ \sigma \circ W_{L-1} \circ \sigma \circ \cdots \circ \sigma \circ W_1)(x). \tag{1.1.1}$$

où σ est une fonction non linéaire ponctuelle, représentant typiquement une opération de seuillage, et $W_k : \mathbb{R}^{d_k} \to \mathbb{R}^{d_{k+1}}$ est une transformation affine [2] (une non linéarité peut être appliquée ou non sur la dernière couche). Chaque couche W_k possède des paramètres $\theta_k \in \mathbb{R}^{n_k}$, et la calibration du réseau se fait typiquement en cherchant les paramètres $\theta^* = (\theta_1^*, ..., \theta_{\mathcal{L}}^*)$ le plus en accord avec les données $\mathcal{B}$:

$$\theta^* = \arg\min_\theta S_{\mathcal{B}}(\theta). \tag{1.1.2}$$

Ici, S est une fonction de coût choisie au préalable, pénalisant par exemple le non-respect des données. Le nombre de paramètres du réseau $n = n_1 + ... + n_L$ peut aller de quelques dizaines à quelques milliards.

Terminons cette section en soulignant que certains algorithmes utilisés en apprentissage machine n'ont pas attendu l'arrivée de l'informatique pour voir le jour, puisque la méthode des moindres carrés a été introduite dès la fin du XIX^e siècle par de grand noms comme Pierre Simon Laplace ou encore Carl Friedrich Gauss ([62], p. 451).

1.1.2 La systématisation de l'utilisation de l'apprentissage machine

L'efficacité déraisonnable de l'apprentissage machine En 1960, Eugene P. Wigner publie un article intitulé "The Unreasonable Effectiveness of

2. Cette structure (interconnexion et fontion d'activation) est bien sûr inspirée de celle des réseaux de neurones biologiques.

Mathematics in the Natural Sciences" [215]. Dans cet article, Wigner montre à quel point il est troublant que des modèles mathématiques arrivent à expliquer si fidèlement de nombreux phénomènes observés empiriquement.

Il semble qu'aujourd'hui, la question soulevée par Wigner se pose aussi pour l'apprentissage machine et l'apprentissage profond en particulier. Quelque soit le domaine où des techniques d'apprentissage machine ont été appliquées, des avancées (d'incrémentales à révolutionnaires) ont été faites.

Il semblerait donc que la structure des réseaux de neurones soit capable de capturer les propriétés fines de nombreux jeux de données issus de contextes très différents. D'un point de vue mathématique cependant, cette structure présente le défaut d'être très difficile à étudier. Autre fait remarquable, les réseaux de neurones dit *hyperparamétrés* semblent échapper à certains grands principes de la théorie des statistiques classiques comme le compromis biais-variance [20]. Ainsi, à la différence des questions soulevées par Wigner, nous ne disposons pas de théorie mathématique capable d'expliquer les performances de certains réseaux de neurones. Plusieurs articles dont [185] ont d'ailleurs repris (de façon plus ou moins sérieuse) le titre de l'article de Wigner, dans des contextes d'apprentissage machine. En conséquence, les méthodes de certification d'algorithmes basés sur des réseaux de neurones se limitent à des algorithmes de validation croisée ou à des tests statistiques ; malheureusement ces méthodes de validation sont vulnérables aux biais inhérents contenus dans les données d'apprentissage et de test.

En pratique, il existe en fait des exemples montrant que certains réseaux de neurones, très performants par ailleurs, peuvent commettre de grossières erreurs de classification d'image lorsqu'un bruit invisible à l'oeil nu (mais bien choisi) est ajouté à une image [197]. Cela signifie que de tels réseaux de neurones sont par nature instables, un fait qui se formalise et se prouve en utilisant le langage de la théorie de l'approximation de fonctions (voir par exemple la présentation [41]).

S'il est vrai qu'une théorisation systématique de l'apprentissage machine n'est pas une fin désirable en soi [31], il existe des domaines d'application pour lesquels la compréhension fine des capacités explicatives de l'algorithme choisi, la connaissance de ses limitations, et l'existence de garanties théoriques fiables associées, sont des questions critiques (pensons à la conception d'une centrale nucléaire). Dans ce cadre, l'absence de théorie adéquate devient problématique.

Apprentissage hybride et modèles physiques Dans un engouement généralisé pour l'application des réseaux de neurones, l'apprentissage machine a graduellement infiltré de nombreux autres domaines scientifiques. Pour les spécialistes des domaines concernés, il fut sans doute assez frustrant de consta-

ter que les réseaux de neurones ont surpassé bien des méthodes basées sur des modèles physiques et mathématiques pourtant étudiés depuis longtemps. Un exemple frappant est celui de la classification d'images, pour lequel l'article [117] [3] datant de 2012 a irrémédiablement fait basculer l'état de l'art du côté des méthodes basées sur les réseaux de neurones.

Si nous sommes obligés d'accepter cet état de fait, cela ne signifie pas pour autant que les théories précédant l'arrivée des réseaux de neurones doivent être abandonnées. Après le premier bouleversement initié par la popularisation de l'utilisation des réseaux de neurones, plusieurs approches *hybrides* visant à combiner apprentissage machine et modèles mathématiques ont été mises en place. Dans certains domaines, y compris l'imagerie, ce sont actuellement ces méthodes qui sont les plus performantes. Pour plus de détails sur ce cas spécifique, nous renvoyons vers le manuscrit [89], qui présente des exemples de méthodes hybrides (méthodes *Plug&Play* et réseaux *unrolled*) dans des contextes d'imagerie. Les approches hybrides s'écartent de l'approche "guidée par les données", puisque dans ce cas les informations utilisées par le modèle ne sont plus uniquement contenues dans les données. La boîte noire devient alors une boîte grise.

En ce qui concerne l'apprentissage machine appliqué à la physique, l'introduction de méthodes basées sur les réseaux de neurones date essentiellement de l'article [162], mis en ligne pour la première fois en 2017. La méthode qui y est introduite est une méthode hybride ; de telles méthodes semblent en effet constituer une bonne direction de recherche (voir aussi [112]). En ce sens, nous relevons dès à présent quelques caractéristiques qui démarquent les problèmes d'apprentissage contraints par la physique des problèmes classiques d'apprentissage machine.

(*i*) Ces problèmes sont relativement simples, au sens où ils sont régis par moins d'équations (on n'ose imaginer toutes les équations nécessaires pour décrire une salle meublée, ce que certains réseaux de neurones semblent pourtant capables d'émuler [161]). Cependant, les contraintes imposées par les équations de la physique sont souvent *rigides*. Cela signifie que certaines des structures qu'elles imposent sur leurs solutions sont très spécifiques, et donc très difficiles à inférer sans en avoir la connaissance a priori. Par exemple, l'écoulement d'un fluide doit impérativement respecter la conservation de la masse.

(*ii*) La quantité de données ainsi que leur diversité est parfois moindre, comparée aux problèmes classiques d'apprentissage. Un exemple de facteur limitant peut être le nombre de capteurs utilisés lors de la capture des données (pensons à des balises en mer). Compléter les données avec un modèle physique devient donc une nécessité.

3. cité plus de 130 000 fois selon Google Scholar...

(*iii*) Un savoir-faire préexistant très conséquent existe, ici la théorie des équations aux dérivées partielles ainsi que les méthodes numériques associées.

(*iv*) De nombreuses applications en lien avec la physique sont critiques, telles que la météorologie, l'aérodynamique ou la construction, et nécessitent donc des garanties de fiabilité en plus d'une solution informatique.

Nous détaillerons certains aspects du point (*iii*) dans la section 1.3. De façon pragmatique, le contenu de ce manuscrit sera essentiellement consacré à l'étude de méthodes d'approximation de solutions d'équations aux dérivées partielles, à l'aide de méthodes initialement développées pour l'apprentissage machine [166]. Bien que nous avons mis l'accent sur le paradigme de l'apprentissage machine, les approches hybrides que nous étudierons sont aussi pertinentes dans d'autres disciplines reposant sur des modèles "boîte noire" et des modèles "de substitution" (*surrogate models*), comme la quantification et la propagation d'incertitudes ([91], chapitre 8), l'optimisation bayésienne (([91], chapitre 7) ou l'analyse de sensibilité ([174], chapitre 7), en ce qui concerne l'étude de codes complexes pour la physique en particulier. Ces domaines ont aussi été transformés par l'émergence des réseaux de neurones, et sont tous étroitement liés.

Le but des deux prochaines sections est de balayer les différents outils et points de vue conceptuels qui nous guideront tout au long de la thèse, dans l'objectif de les motiver. Ces sections sont aussi à visée pédagogique, aussi sont-elles accompagnées d'exemples simples et illustratifs.

1.2 Outils d'apprentissage machine

Cette section est consacrée à la présentation des outils d'apprentissage machine que nous utiliserons tout au long de la thèse. Après une courte formalisation du problème de l'apprentissage machine (section 1.2.1), nous introduisons les méthodes dites à noyau, que nous utiliserons à peu près sous toutes leurs formes. Il en existe essentiellement trois, entre lesquelles les délimitations sont poreuses. La première est celle de l'inférence bayésienne, qui s'inspire de la théorie de la mesure et des statistiques (sections 1.2.2 et 1.2.3). La deuxième (que l'on pourrait ranger avec la première), probabiliste de nature, puise sa source dans la théorie des processus gaussiens (section 1.2.3). La troisième, déterministe et s'appuyant sur l'analyse fonctionnelle, est celle des espaces de Hilbert à noyau reproduisant (section 1.2.4) [4]. Une dernière partie (section 1.2.5) discute des différents liens profonds qui lient les méthodes à noyau et les réseaux de neurones.

4. Il existe aussi une approche plus algébrique des (méthodes à) noyaux, voir par exemple [87] et [23]. Nous n'utiliserons pas vraiment ce point de vue dans ce manuscrit.

1.2.1 Formulation générale de l'apprentissage supervisé

Un problème d'approximation de fonction Considérons un ensemble de données $\mathcal{B} \coloneqq \{(x_i, y_i)\}_{1 \leq i \leq n}$ où $x_i \in E$ désigne une valeur d'entrée, par exemple une image pixelisée, et $y_i \in F$ désigne la variable d'intérêt, par exemple la classe de l'image (auquel cas $E = \mathbb{R}^d, d \gg 1$, et F sera un ensemble de mots). Dans la thèse, x_i désignera plutôt une position dans l'espace et y_i une mesure d'un champ physique. Formellement, il existe donc une correspondance entre les variables d'entrée et les observations sous la forme d'une fonction

$$f : \begin{cases} E & \longrightarrow F \\ x & \longmapsto f(x) \end{cases} \tag{1.2.1}$$

et nous avons $y_i = f(x_i) + \varepsilon_i$, où ε_i est une variable aléatoire représentant un bruit de mesure ou une erreur de discrétisation (nous avons donc supposé ici que le bruit était additif). Il se trouve qu'un très grand nombre de problèmes d'apprentissage machine peuvent se formaliser de cette façon. Tout le problème de l'apprentissage machine supervisé consiste alors à approcher la fonction f étant donné la connaissance des données $\mathcal{B}$. C'est donc fondamentalement un problème d'approximation de fonctions [50, 51], dont la résolution se situe à l'intersection de nombreux domaines : statistiques, analyse fonctionnelle, problèmes inverses, optimisation, algorithmie ou encore informatique. Si nous adoptons ici une approche mathématique, il ne faut pas ignorer qu'il existe d'autres approches très différentes en ce qui concerne l'apprentissage machine, chacune apportant son éclairage. Si f peut prendre un continuum de valeurs, alors c'est un problème dit de régression. Si F est un ensemble fini ou discret, on parle de problème de classification. Cette thèse s'intéressera uniquement à des problèmes de régression. Dans l'exemple 1.2.1, nous décrivons la méthode de régression la plus simple, la régression linéaire.

Théorie de l'approximation et modélisation statistique Il est possible de diviser la théorie de l'approximation de fonctions en deux catégories, qui peuvent bien sûr interagir l'une avec l'autre. Une première consiste à voir les données comme déterministes. Par exemple, on peut supposer que la fonction cible f appartient à un certain espace de fonctions connu a priori, ce qui permet l'utilisation de méthodes d'analyse fonctionnelle (voir par exemple [42]). Dans l'exemple de l'analyse hilbertienne, les approximants de f sont typiquement obtenus comme des projections orthogonales de f sur certains sous-espaces de dimension finie déterminés par les données.

En apprentissage machine cependant, il est plus commun de voir les données $\{(x_i, y_i)\}_{1 \leq i \leq n}$ comme des réalisations de variables aléatoires $\{(X_i, Y_i)\}_{1 \leq i \leq n}$

définies sur un même espace de probabilité $(\Omega, \mathcal{F}, \mathbb{P})$, indépendantes et de même loi [5] ([166], p. xiv). Dans certains cas, c'est une hypothèse naturelle, par exemple lorsque la capture des données n'est pas une expérience reproductible. Dans ce cas, il s'agira plutôt d'estimer la loi des couples (X_i, Y_i), ou certaines de ses caractéristiques comme ses moments ou ses quantiles. Le langage privilégié sera celui des probabilités et des statistiques, et l'espace de prédilection sera $L^2(\mathbb{P})$, l'espace des variables aléatoires à variance finie.

L'exemple ci-dessous décrit en détail un exemple très simple de modèle de régression, dans ses approches déterministes et aléatoires. Nous pouvons voir les méthodes à noyau comme des généralisations de cette méthode. En particulier, certaines idées profondes, qui seront importantes dans la suite, sont déjà présentes dans ce modèle.

Exemple 1.2.1 (Méthode des moindres carrés et régression linéaire). Le modèle de régression le plus simple est probablement le suivant. Considérons p variables d'entrées $X = (x_1, ..., x_p)^T \in \mathbb{R}^p$, (variables explicatives) et une variable scalaire de sortie y (variable expliquée). Considérons n observations du modèle, $\{(X_i, y_i), 1 \leq i \leq n\}$, avec $X_i = (x_{1i}, ..., x_{pi})^T$. On note M la matrice de taille $n \times p$ dont la ligne i est donnée par X_i^T. La méthode des moindres carrés consiste d'abord à supposer une dépendence linéaire de la sortie en les données selon un vecteur $\beta \in \mathbb{R}^p$,

$$\hat{y}_i = \sum_{k=1}^{p} x_{ik}\beta_k = X_i^T\beta, \quad \text{soit} \quad M\beta = \hat{y}. \tag{1.2.2}$$

Une dépendance affine peut être considérée en modifiant X_i par $(1, X_i) \in \mathbb{R}^{p+1}$. On cherche ensuite les coefficients $(\beta_1, ..., \beta_p)$ qui minimisent la distance euclidienne entre le modèle et les données (moindres carrés), c'est à dire $\beta^* = \arg\min_\beta S(\beta)$ où $S(\beta) = \sum_{i=1}^n (y_i - \hat{y}_i)^2 = \sum_{i=1}^n (y_i - X_i^T\beta)^2$. Cette fonction admet toujours un minimiseur, qui est unique si X^TX est inversible. La solution correspondante est

$$\hat{\beta} = M^+ y, \tag{1.2.3}$$

où M^+ est le pseudo-inverse de Moore-Penrose de M. Si M^TM est inversible, nous avons $M^+ = (M^TM)^{-1}M^T$. M^+ est cependant tout le temps défini même si M^TM n'est pas inversible, auquel cas M^+y est la solution de norme minimale parmi toutes les solutions. De plus, MM^+ est la projection orthogonale sur $\mathrm{Im}(M)$ et M^+M est la projection orthogonale sur $\mathrm{Im}(M^T)$ (voir par exemple [88], pp. 257-258). Pour une nouvelle observation $X_0 = (x_{10}, ..., x_{p0})$, la phase de prédiction consiste à estimer la vraie sortie correspondante y_0 par

5. Une réalisation du couple (X_i, Y_i) est un couple $(X_i(\omega), Y_i(\omega))$, étant donné un $\omega \in \Omega$.

$\hat{y}_0 = X_0^T\hat{\beta}$. Nous obtenons aussi que $\hat{y} = MM^+y$, donc $\hat{y}$ est la projection orthogonale, dans $\mathbb{R}^n$, de y sur $\mathrm{Im}(M)$. Enfin, dans l'hypothèse (ici peu raisonnable) où le modèle était vraiment linéaire, i.e. $y_i = X_i^T\alpha$ pour un certain α, alors $y = M\alpha$ et $\beta = M^+M\alpha$. Dans ce cas, β correspond à la projection orthogonale de α sur $\mathrm{Im}(M^T) = \mathrm{Vect}(X_1^T, ..., X_n^T)$.

Supposons maintenant que les observations sont plutôt données par

$$y_i = X_i\beta + \varepsilon_i,$$

où β et X_i sont déterministes, mais où les ε_i sont des variables aléatoires centrées de même variance finie et indépendantes. Les valeurs observées sont donc des réalisations de variables aléatoires. Nous pouvons tenter d'estimer β sous la forme d'une combinaison linéaire des données (régression linéaire) : $\hat{\beta}_i = C_i^TY$, avec C_i un vecteur déterministe. Parmi tous les estimateurs non biaisés de β (i.e. vérifiant $\mathbb{E}[\hat{\beta}] = \beta$) de la forme ci-dessus, celui minimisant cette fois l'erreur *en moyenne quadratique*

$$S(\hat{\beta}) \coloneqq \mathbb{E}\big[\|\beta - \hat{\beta}\|^2\big] = \mathbb{E}\Big[\sum_{i=1}^{p}(\beta_i - \hat{\beta}_i)^2\Big] \tag{1.2.4}$$

vaut "encore" $\hat{\beta} = M^+Y$. $\hat{\beta}$ est donc le meilleur estimateur linéaire non biaisé (Best Unbiaised Linear Predictor, ou BLUP). Cette fois, $\hat{Y} = M\hat{\beta} = MM^+Y$, c'est donc la projection orthogonale, dans $L^2(\mathbb{P}, \mathbb{R}^n)$, du vecteur aléatoire Y sur l'espace déterministe $\mathrm{Im}(M)$. Nous avons ainsi un premier exemple de correspondance entre projection orthogonale déterministe et projection aléatoire.

Un défaut de la régression linéaire présentée ainsi est sa faible *expressivité* : ses approximants se limitent à des combinaisons linéaires des données. Il se trouve cependant que certains modèles de régression en apprentissage machine sont des versions plus ou moins sophistiquées de la régression linéaire, formulées dans des espaces bien choisis qui sont définis à partir de nouvelles variables (ou "features"), elles-mêmes obtenues par transformation des variables initiales (ici, X). Les méthodes de régression à noyau en font partie.

1.2.2 Approche bayésienne pour les problèmes inverses

Le théorème de Bayes Le point de vue aléatoire présente un avantage théorique sur le point de vue déterministe, car il permet d'utiliser la notion de probabilité conditionnelle ainsi que le théorème de Bayes. Ces deux outils semblent particulièrement adaptées pour la prise en compte de données "partielles", dans un cadre très large. Rappelons le théorème de Bayes dans sa forme la plus élémentaire. D'abord, la probabilité conditionnelle de A sachant B (où

$\mathbb{P}(B) \neq 0$), notée $\mathbb{P}(A|B)$, est définie comme $\mathbb{P}(A|B) \coloneqq \mathbb{P}(A \cap B)/\mathbb{P}(B)$[6]. Le théorème de Bayes stipule alors que la probabilité de A sachant B peut s'obtenir à partir de la probabilité de B sachant A selon l'égalité

$$\mathbb{P}(A|B) = \mathbb{P}(B|A)\mathbb{P}(A)/\mathbb{P}(B). \tag{1.2.5}$$

Sous cette forme, ce théorème est une conséquence immédiate de la définition de $\mathbb{P}(A|B)$ et de $\mathbb{P}(B|A)$. Pour un couple (X, Y) de variables aléatoires à densité $p_{(X,Y)}$ (par rapport à une mesure de référence), ce théorème s'écrit aussi en termes de densité. En définissant la densité conditionnelle par $p_{X|Y=y}(x) \coloneqq p_{(X,Y)}(x, y)/p_Y(y)$ quand $p_Y(y) \neq 0$, le théorème de Bayes s'écrit alors, pour tout couple (x, y),

$$p_{X|Y=y}(x) = p_{Y|X=x}(y)p_X(x)/p_Y(y). \tag{1.2.6}$$

L'équation (1.2.6) est une version infinitésimale de l'équation (1.2.5). Notons que $p_Y(y)$ ne dépend pas de x et lorsqu'on ne considérera que la dépendance en x, on pourra noter $p_{X|Y=y}(x) \propto p_{Y|X=x}(y)p_X(x)$. L'équation (1.2.6) permet notamment de conditionner selon certains évenements de probabilité nulle mais dont la densité associée est non nulle, typiquement des évenements de la forme $\{x\}$.

Inférence bayésienne Celle-ci se déroule en trois étapes. Etant donnée une quantité inconnue u, on la voit comme réalisation d'une variable aléatoire U de loi μ_U. Etant donné des observations y (vues comme réalisation d'une variable aléatoire Y) contenant des informations sur u, on conditionne la loi μ_U aux observations selon le théorème de Bayes, ce qui fournit une loi μ_U^y. Dans ce formalisme, μ_U s'appelle la loi *a priori* de U, et μ_U^y s'appelle la loi *a posteriori* de U (ou encore, le *prior* et le *posterior* respectivement). Comme son nom l'indique, le prior est un bon outil pour incorporer tout type d'information connue a priori. Dans le cadre des problèmes inverses, la relation de dépendance entre U et Y est typiquement traduite par une relation de la forme

$$Y = G(U) + \varepsilon, \tag{1.2.7}$$

où ε est un bruit aléatoire de loi μ_ε indépendant de U, et G est une opération de mesure [55]. Dans ce cas, le couple (U, Y) n'est autre que $(U, G(U) + \varepsilon)$ et si μ_U et μ_ε admettent des densités p_U et p_ε, la loi du couple (U, Y) admet

6. Le conditionnement peut faire penser à une sorte d'opération de projection de mesure, mais dans un cadre indépendant de structure hilbertienne (en fait, de toute structure topologique).

pour densité la fonction $p_{(U,Y)} : (u, y) \mapsto p_\varepsilon(y - G(u))p_U(u)$. Nous voyons aussi que $p_{Y|U=u}(y) = p_\varepsilon(y - G(u))$. Dans le cadre de l'inférence bayésienne, cette quantité s'appelle la vraisemblance, car elle reflète la probabilité d'obtenir la mesure y sous l'hypothèse que U prenne la valeur u. Une estimation numérique de U à partir de la loi a posteriori est obtenu en moyennant tous les candidats u possibles selon la loi a posteriori :

$$\hat{U} = \mathbb{E}[U|Y = y] = \int u\mu_U^y(du) = \int up_{U|Y=y}(u)du. \tag{1.2.8}$$

La fonction $y \mapsto \mathbb{E}[U|Y = y]$ s'appelle la fonction de régression. L'équation (1.2.8) se généralise en n'imposant pas de valeur y de Y, auquel cas nous obtenons $\hat{U} = \mathbb{E}[U|Y]$, l'espérance conditionnelle de U sachant Y. $\mathbb{E}[U|Y]$ est exactement la projection orthogonale dans $L^2(\Omega, \mathcal{F}, \mathbb{P})$ de U sur le sous-espace vectoriel fermé $L^2(\Omega, \sigma(Y), \mathbb{P})$, où $\sigma(Y)$ est la tribu engendrée par Y. Une autre estimation possible de U est obtenue en cherchant le candidat u^* qui maximise la densité a posteriori $p_{U|Y=y}$. C'est l'estimateur MAP (Maximum A Posteriori) qui correspond à la valeur "la plus probable d'être tirée" au vu des données. Dans tous les cas que nous rencontrerons dans cette thèse (vraisemblance et prior gaussiens), espérance conditionnelle et MAP coïncident.

Nous voyons un autre intérêt de l'approche bayésienne, en ce que la loi a posteriori fournit une mesure d'incertitude a posteriori, par exemple au travers de sa covariance si elle est définie (voir l'équation (1.2.15)).

Exemple 1.2.2 (Régression linéaire, approche bayésienne, [166], section 2.1.1). On considère toujours un modèle de régression linéaire

$$y_i = X_i^T\beta + \varepsilon_i. \tag{1.2.9}$$

Les valeurs des variables explicatives X_i sont connues, alors que β et le bruit $\varepsilon = (\varepsilon_1, ..., \varepsilon_n)$ sont incertains. Nous allons donc considérer un prior gaussien sur β ainsi que sur ε, ici $\beta \sim \mathcal{N}(0, v_\beta I_p)$ et $\varepsilon \sim \mathcal{N}(0, v_\varepsilon I_n)$ avec β et ε indépendants. Ici, $v_\beta > 0$ et $v_\varepsilon > 0$ désignent les variances de β et ε, respectivement. L'opérateur de mesure correspond ici à $G : \mathbb{R}^p \to \mathbb{R}^n$, $\eta \mapsto M\eta$ où M est définie dans l'exemple 1.2.1. Appliquons le théorème de Bayes (1.2.6). Tout d'abord, la vraisemblance s'écrit

$$p_{Y|\beta=\eta}(y) = p_\varepsilon(y - G(\eta)) = \frac{1}{(\sqrt{2\pi}v_\varepsilon)^n} \exp\Big(-\frac{1}{2v_\varepsilon}\big|y - M\eta\big|^2\Big). \tag{1.2.10}$$

Ainsi, étant donné le prior $p_\beta(\eta) \propto \exp(-|\eta|^2/2v_\beta)$ et en mettant le polynôme en η sous forme canonique ([166], p. 9), nous obtenons

$$p_{\beta|Y=y}(\eta) \propto \exp\Big(-\frac{1}{2v_\varepsilon}\big|y - M\eta\big|^2\Big) \exp\Big(-\frac{1}{2v_\beta}|\eta|^2\Big)$$

$$\propto \exp\Big(-\frac{1}{2}(\eta-\bar{\eta})^T\big(v_\varepsilon^{-1}M^TM + v_\beta^{-1}I_p\big)(\eta-\bar{\eta})\Big), \qquad (1.2.11)$$

avec $\bar{\eta} = (M^TM + v_\varepsilon v_\beta^{-1}I_p)^{-1}M^Ty$. On reconnaît la forme d'une densité de probabilité gaussienne de moyenne $\bar{\eta}$ et de matrice de covariance $(v_\varepsilon^{-1}M^TM + v_\beta^{-1}I_p)^{-1}$ (voir les équations (1.2.11) et (1.2.12)). L'estimateur bayésien, qui ici est aussi le MAP, est donné par $\bar{\eta}$. De plus, $\bar{\eta}_i = \mathbb{E}[\beta_i|Y_1,...,Y_n]$ est la projection orthogonale, dans $L^2(\Omega,\mathcal{F},\mathbb{P})$, de β_i sur $L^2(\Omega,\sigma(Y_1,...,Y_n),\mathbb{P})$ mais aussi sur $\mathrm{Vect}(Y_1,...,Y_n)$ (particularité du cas gaussien). Enfin, on retrouve la méthode des moindres carrés lorsque $v_\beta \to +\infty$, c'est à dire dans la limite d'un prior uniformément plat (en quelque sorte non informatif, ou impropre, [211], section 11.6). Nous verrons d'autres types de limites "plates" apparaître de façon assez surprenante dans le chapitre 5.

Notons tout de même que l'approche bayésienne et probabiliste est une vue de l'esprit : il est possible que la modélisation par des variables aléatoires soit déconnectée de la réalité. Dans de tels cas, l'unique but de cette modélisation est qu'elle donne accès au calcul des probabilitéset au théorème de Bayes en particulier.

Dans le cadre de nos problèmes de régression, l'approche décrite ci-dessus devient pertinente lorsque U est une fonction. L'opérateur de mesure G peut par exemple correspondre à l'observation de valeurs ponctuelles de U (problème d'interpolation). Notons que dans ce cas, la topologie de l'espace auquel appartiendra U, ou plutôt, son approximant, devra être compatible avec l'évaluation ponctuelle de ses éléments. Cela nous mènera "naturellement" à la notion d'espace de Hilbert à noyau reproduisant. Enfin, quoiqu'attractif sur le plan théorique, l'inférence bayésienne nécessite souvent des calculs numériques lourds car les intégrales en grande dimension de la forme (1.2.8) ont rarement une forme explicite. Comme souligné dans [166], le cas gaussien est une exception car d'une part la majorité des calculs sont explicites, et d'autre part, les modèles d'inférences résultants demeurent relativement généraux et flexibles.

1.2.3 Mesures gaussiennes et régression par processus gaussiens

Mesures gaussiennes Dans l'approche bayésienne d'un problème de régression, nous avons besoin d'une mesure de probabilité sur un espace adéquat de fonctions E, par exemple $E = L^2(\mathcal{D})$ où $\mathcal{D}$ est un ouvert de $\mathbb{R}^d$, ou $E = C(K)$ où K est un compact de $\mathbb{R}^d$. Ces espaces sont de dimension infinie. Une première question est celle de la tribu à considérer sur de tels espaces. Nous considérerons toujours la tribu borélienne $\mathcal{B}(E)$, c'est à dire celle engendrée par les ouverts de E (notons qu'il nous suffirait pour cela que E soit

un espace vectoriel topologique). L'intérêt principal de cette tribu est qu'elle rend mesurable les applications continues, et les formes linéaires continues en particulier. Il se trouve ensuite que la construction de mesures intéressantes sur de tels espaces mesurables n'est pas du tout triviale. Le premier obstacle est le résultat suivant :

Proposition 1.2.3 ([103], p. 2)**.** *Soit E un espace de Banach séparable (i.e. admettant une partie dénombrable dense) de dimension infinie. Soit μ une mesure sur la tribu borélienne de E, et supposons que μ soit invariante par translation. Alors $\mu \equiv 0$ ou $\mu \equiv +\infty$.*

Ce théorème implique entre autres qu'il n'y a pas d'analogue de la mesure de Lebesgue en dimension infinie. Une explication intuitive de ce résultat vient du fait que l'invariance par translation d'une mesure μ sur $\mathbb{R}^d$ lui impose une propriété de *dilatation* en r^d : $\mu(B(0,r)) = r^d \mu(B(0,1))$. Dans le cas formel où $d = +\infty$, cette relation implique bien que μ est soit nulle partout soit infinie partout (comme E est supposé séparable, les boules ouvertes engendrent sa tribu borélienne...).

Après la mesure de Lebesgue, la deuxième classe de mesures la plus naturelle en dimension finie est celle des mesures gaussiennes. Heureusement pour nous, ces mesures perdurent en dimension infinie. Dans $\mathbb{R}^d$, une mesure gaussienne est une mesure à densité (par rapport à la mesure de Lebesgue) dont cette dernière s'écrit

$$p(x) = \frac{1}{(2\pi)^{d/2} \det K^{1/2}} \exp\Big(-\frac{1}{2}(x-m)^T K^{-1}(x-m)\Big). \tag{1.2.12}$$

où m est un vecteur de $\mathbb{R}^d$ et K est une matrice symétrique définie positive (de spectre inclus dans $\mathbb{R}_+^*$). On note $\mathcal{N}(m,K)$ une telle loi. L'équation (1.2.12) se généralise au cas où K est semi-définie positive, ou *dégénérée* (spectre inclus dans $\mathbb{R}_+$) en changeant K^{-1} par le pseudo-inverse K^+, et en n'utilisant que les valeurs propres strictement positives de K dans le terme $\det K$. En particulier, une masse de Dirac en x_0 est une mesure gaussienne $\mathcal{N}(x_0, 0)$.

On appelle vecteur gaussien à valeur dans $\mathbb{R}^d$ tout vecteur aléatoire dont la loi est de la forme (1.2.12), en autorisant les matrices K dégénérées. Dans ce cadre, le vecteur m correspond au vecteur moyenne du vecteur gaussien tandis que la matrice K correspond à sa matrice de covariance. A tout vecteur gaussien à valeur dans $\mathbb{R}^d$ correspond une mesure gaussienne sur $\mathbb{R}^d$ et vice versa.

Les vecteurs gaussiens ont la propriété remarquable suivante : pour tout vecteur gaussien $U = (U_1, ..., U_d)$ et vecteur $a = (a_1, ..., a_d) \in \mathbb{R}^d$, $a^T U$ est une variable aléatoire gaussienne (scalaire). Cette propriété, qui sert aussi de définition des vecteurs gaussiens, est une conséquence des propriétés de

stabilité par convolution des densités gaussiennes [7]. Notons que cette propriété revient à dire que pour tout $a \in \mathbb{R}^d \cong (\mathbb{R}^d)^*$ (dual de $\mathbb{R}^d$), la mesure image (ou *pushforward*) d'une mesure gaussienne par l'application $x \mapsto a^T x$ est une mesure gaussienne sur la droite réelle. Cette propriété sert de définition en dimension infinie :

Définition 1.2.4. Soit E un espace de Banach E muni de sa tribu borélienne, et soit E^* son dual topologique (ensemble des formes linéaires continues). On appelle mesure gaussienne sur E toute mesure μ telle que pour tout $\ell \in E^*$, la mesure $\mu_{\#\ell}$, définie pour tout borélien A de $\mathbb{R}$ par $\mu_{\#\ell}(A) \coloneqq \mu(\{x \in E : l(x) \in A\})$, est une loi normale sur $\mathbb{R}$.

Il est un peu miraculeux que des mesures définies par des densités en dimension finie continuent d'exister en dimension infinie. De nombreux détails sur les mesures gaussiennes, dans des contextes très généraux, sont décrits dans [29]. L'article de référence [195] décrit certaines utilisations de priors de mesures gaussiennes sur des problèmes d'estimation de fonction.

Processus aléatoires et mesures sur des espaces de fonctions. Un processus aléatoire (scalaire réel) sur un ensemble $\mathcal{D}$, ou processus stochastique, n'est rien d'autre qu'un ensemble de variables aléatoires réelles $(U(x))_{x\in\mathcal{D}}$ indexé par $\mathcal{D}$, toutes définies sur le même espace probabilisé $(\Omega, \mathcal{F}, \mathbb{P})$. La notion la plus importante associée aux processus aléatoires est celle de trajectoire ou de réalisation : étant donné $\omega \in \Omega$, la trajectoire associée est la fonction déterministe $U_\omega : x \mapsto U(x)(\omega)$. De cette façon, un processus aléatoire définit une application à valeur dans $\mathcal{F}(\mathcal{D}, \mathbb{R})$, l'espace des fonctions définies de $\mathcal{D}$ à valeur dans $\mathbb{R}$:

$$\tilde{U} : \begin{cases} (\Omega, \mathcal{F}, \mathbb{P}) & \longrightarrow (\mathcal{F}(\mathcal{D}, \mathbb{R}), \mathcal{E}) \\ \omega & \longmapsto U_\omega \end{cases} \tag{1.2.13}$$

Ici, $\mathcal{E}$ est la tribu produit de $\mathcal{F}(\mathcal{D}, \mathbb{R})$; c'est la plus petite tribu rendant mesurable les applications "projection sur la x^{ie} coordonnée", $\ell_x : f \mapsto f(x)$. Un tel choix de tribu rend l'application $\tilde{U}$ mesurable ([110], section 9.2). La mesure image de $\tilde{U}$ définit donc une mesure de probabilité sur l'espace de fonctions

7. Les lois ayant ce type de propriété sont les lois dites *stables* ([150], chapitre 1). En particulier, contrairement aux lois gaussiennes, la loi de Lévy $\mathcal{L}(0, c)$ a l'intéressante propriété d'être supportée sur l'intervalle $(0, +\infty)$, ce qui peut être intéressant pour les EDPs hyperboliques (voir aussi la remarque 4.3.2). Malheureusement, les seules lois stables qui admettent une variance finie sont les lois gaussiennes. Pour nos applications, l'utilisation des autres lois stables comme prior nécessiterait donc probablement un formalisme bien différent de celui exposé dans cette thèse (mais le théorème de Bayes tient toujours !). Le récent article [196] considère cependant de tels priors dans le cadre de problèmes inverses.

$(\mathcal{F}(\mathcal{D},\mathbb{R}),\mathcal{E})$. Malheureusement, cet espace a une structure très pauvre [8], et nous serons plutôt intéressés au cas où l'application $\tilde{U}$ est à valeurs dans un espace de Sobolev $W^{m,p}$ (centraux en équations aux dérivées partielles). Les tribus boréliennes de ces espaces ne contiennent pas $\mathcal{E}$ (sauf si $m > d/p$), ce qui les rend, en un sens, "orthogonales" à $\mathcal{E}$. La construction d'applications $\tilde{U}$ mesurables à valeur dans de tels espaces devient alors non évidente.

Processus gaussiens De même qu'en dimension finie, il existe (formellement) un pendant probabiliste des mesures gaussiennes. Ce sont les processus gaussiens, qui sont des processus aléatoires tels que pour tout $(x_1,...,x_n) \in \mathcal{D}^n$, $(U(x_1),...,U(x_n))$ est un vecteur aléatoire gaussien. L'existence d'un tel processus déterminé par ses lois fini-dimensionelles est assurée par le théorème d'extension de Kolmogorov, [110], section 9.4. En conséquence de la propriété de stabilité par combinaison linéaire des vecteurs gaussiens, les processus gaussiens peuvent être vus comme les processus aléatoires à variance finie les plus "linéaires", similairement aux espaces vectoriels parmi les variétés [9]. Cela justifie le rôle central des processus gaussiens dans de nombreux domaines des mathématiques. Citons entre autres l'intégration stochastique, les équations aux dérivées partielles stochastiques, l'analyse de sensibilité ou la quantification d'incertitudes. La loi d'un processus gaussien, au sens de la mesure image de l'application (1.2.13), est caractérisée par les fonctions moyenne et covariance du processus, définies respectivement par

$$m(x) \coloneqq \mathbb{E}[U(x)], \tag{1.2.14}$$

$$k(x,x') \coloneqq \mathrm{Cov}(U(x),U(x')) = \mathbb{E}[U(x)U(x')] - \mathbb{E}[U(x)]\mathbb{E}[U(x')]. \tag{1.2.15}$$

Nous notons $GP(m,k)$ cette loi (pour *Gaussian process*). Dans la majorité de la thèse nous supposerons que $m \equiv 0$. La fonction de covariance, que nous appelerons aussi *noyau* (de covariance), jouit de très bonnes propriétés

8. Sa topologie usuelle est celle de la convergence ponctuelle, ou encore, celle engendrée par la famille non dénombrable de semi-normes $\mathcal{P} \coloneqq \{f \mapsto |f(x)|,\ x \in \mathcal{D}\}$. Muni de cette topologie, cet espace est quasi-complet ([184], p. 124) ; il n'est cependant ni normable ni même métrisable (comme il est quasi-complet, sa métrisabilité impliquerait que $\mathcal{P}$ pourrait être restreinte à une famille dénombrable, [202], proposition 8.1), ni séparable (car il admet un sous espace non séparable, section 3.4.1 du chapitre 3), ni nucléaire (car il admet un sous espace non nucléaire (n'importe quel RKHS de dimension infinie), [202], proposition 50.1), et donc ne tombe dans aucune catégorie agréable d'espaces fonctionnels, à part celle des espaces localement convexes.

9. Nous pourrions même aller plus loin en concentrant la comparaison avec sur variétés de classe C^1, dont les espaces tangents sont bien définis. En effet, le théorème centrale limite (et ses équivalents fonctionnels) montre qu'en un certain sens, les variables aléatoires gaussiennes appraissent comme une approximation "à l'ordre un" de certaines variables aléatoires à variance finie.

géométriques puisqu'elle est définie positive : pour tout $(x_1, ..., x_n) \in \mathcal{D}^n$, la matrice $(k(x_i, x_j))_{1 \leq i,j \leq n}$ est *semi*-définie positive[10]. Nous dirons qu'elle est strictement définie positive si les matrices de covariance associées sont toutes définies positives, si les x_i sont distincts deux à deux. Pour toute fonction m et fonction définie positive k, il existe un processus gaussien de loi $GP(m, k)$. Une famille importante de fonctions définies positives sur $\mathbb{R}^d$ est celle des noyau de Matérn. En notant $|\cdot|$ la norme euclidienne sur $\mathbb{R}^d$, elles sont données par

$$k_\nu(x, x') = \sigma^2 \frac{2^{1-\nu}}{\Gamma(\nu)} \left(\frac{\sqrt{2\nu}|x - x'|}{\ell} \right)^\nu K_\nu \left(\frac{\sqrt{2\nu}|x - x'|}{\ell} \right), \tag{1.2.16}$$

où $\sigma > 0$, $\nu > 0$, $\ell > 0$ et où K_ν est la fonction de Bessel modifiée du second type d'ordre ν ([166], p. 84). L'expression (1.2.16) se simplifie lorsque $\nu = p + 1/2$ avec $p \in \mathbb{N}$([166], p. 85). Pour $\nu = +\infty$, nous obtenons le noyau gaussien $k_\infty(x, x') = \exp(-|x - x'|^2/2\ell^2)$. Nous donnons ci-dessous un premier exemple de correspondance entre mesure gaussiennes et processus gaussiens. Pour cela nous avons besoin de la notion de processus mesurable.

Définition 1.2.5. Soit $\mathcal{D}$ une partie d'un espace topologique. Nous disons qu'un processus aléatoire $(U(x))_{x \in \mathcal{D}}$ est mesurable si l'application produit $(\omega, x) \mapsto U(x)(\omega)$ est mesurable, lorsqu'on munit l'espace $\Omega \times \mathcal{D}$ de la tribu produit $\mathcal{F} \otimes \mathcal{B}(\mathcal{D})$.

Les processus aléatoires à trajectoires continues en probabilité ainsi que ceux définis par des décompositions de type Karhunen-Loève (somme de produits tensoriels) sont des exemples de processus aléatoires mesurables (voir la section 2.2.1.2). Nous pouvons maintenant énoncer la correspondance suivante :

Proposition 1.2.6 (Proposition 3.2.9 simplifiée)**.** *Soit $\mathcal{D}$ un ouvert de $\mathbb{R}^d$, $p \in [1, +\infty)$. Alors nous avons les deux faits suivants.*
(i) Si $(U(x))_{x \in \mathcal{D}}$ est un processus gaussien mesurable à trajectoires dans $L^p(\mathcal{D})$ presque sûrement, alors il induit une mesure gaussienne sur $L^p(\mathcal{D})$, qui est la mesure image de $\mathbb{P}$ via l'application $(\Omega, \mathcal{F}, \mathbb{P}) \to (L^p(\mathcal{D}), \mathcal{B}(L^p(\mathcal{D}))),\ \omega \mapsto U_\omega$.
(ii) Toute mesure gaussienne sur $L^p(\mathcal{D})$ s'obtient comme mesure image d'un certain processus gaussien mesurable, au sens de l'application ci-dessus.

Dans le point (*i*), il est intéressant de noter que le fait que les trajectoires d'un processus gaussien centré mesurable soit contenues dans $L^p(\mathcal{D})$ presque sûrement est équivalent au critère intégral suivant,

$$\int_{\mathcal{D}} k(x, x)^{p/2} dx < +\infty, \tag{1.2.17}$$

10. Le hiatus de vocabulaire, entre défini positif pour les fonctions de covariance et semi-défini positif pour les matrices, est un héritage d'usages historiques.

où k est la fonction de covariance du processus (proposition 3.2.9). Par ailleurs, notons que dans le point *(ii)*, il n'y a pas du tout unicité du processus gaussien mesurable : étant donné un tel processus gaussien $(U(x))_{x\in\mathcal{D}}$ et $x_0 \in \mathcal{D}$, le processus épointé $V(x) \coloneqq \mathbb{1}_{\mathcal{D}\setminus\{x_0\}}(x)U(x)$ induit la même mesure gaussienne. Cela s'explique par le fait que dans l'espace $L^p(\mathcal{D})$, des fonctions sont égales lorsqu'elles sont égales presque partout. En particulier, la tribu borélienne de $L^p(\mathcal{D})$ ne contient pas $\mathcal{E}$.

Dans une grande partie de la thèse, nous nous focaliserons sur l'étude des processus gaussiens. Une telle attention pourra peut-être donner l'impression que ces derniers sont l'outil "optimal" pour régler un certain nombre de problèmes. Nous terminons donc ce paragraphe en soulignant que les processus gaussiens (et les mesures gaussiennes) peuvent aussi avoir des propriétés assez extrêmes. En ce sens, un exemple de résultat surprenant est le théorème de Fernique, dont nous citons une version simplifiée dans le cas L^p. Nous notons $\|u\|_p = (\int_{\mathcal{D}} |u(x)|^p dx)^{1/p}$.

Proposition 1.2.7. *Soit $(U(x))_{x\in\mathcal{D}}$ un processus gaussien mesurable. Notons $\|U\|_p$ la variable aléatoire réelle $\omega \mapsto \|U(\cdot)(\omega)\|_p$ (bien mesurable par le théorème de Fubini). Supposons que $\mathbb{P}(\|U\|_p < +\infty) = 1$. Alors il existe $\varepsilon > 0$ tel que*

$$\mathbb{E}\Big[\exp\left(\varepsilon\|U\|_p^2\right)\Big] < +\infty. \tag{1.2.18}$$

En particulier, la norme aléatoire $\|U\|_p$ a tous ses moments finis.

Ce théorème demeure vrai dans un cadre beaucoup plus large (plus large que celui des espaces de Banach, [29], Théorème 2.8.5), et est un des piliers de la théorie des mesures gaussiennes. Pour les normes de processus gaussiens, il n'existe donc pas d'intermédiaire entre être finie presque sûrement et admettre des moments "exponentiels carrés", ce qui est une propriété d'intégrabilité extrêmement forte.

Régression par processus gaussiens ([166], section 2.2) Nous pouvons dès à présent utiliser un prior de processus gaussien à des fins de régression. Donnons-nous donc une fonction $u : \mathcal{D} \to \mathbb{R}$ à approcher à partir d'un ensemble de valeurs ponctuelles $y_i = u(x_i)+\varepsilon_i$. Choisissons un prior de processus gaussien centré sur u avec $U \sim GP(0, k)$, ce qui revient encore à supposer que u est une réalisation d'un processus gaussien de loi $GP(0, k)$, via l'équation (1.2.13). Nous choisissons aussi un prior gaussien sur le bruit, $\varepsilon \sim \mathcal{N}(0, \lambda I_n)$ (indépendant de U). Les observations s'écrivent encore de façon vectorielle $Y = U(X) + \varepsilon$.

Soit $x \in \mathcal{D}$. Nous notons $k(X,X)$ la matrice donnée par $k(X,X)_{ij} = k(x_i,x_j)$ et $k(x,X)$ le vecteur colonne donné par $k(x,X)_i = k(x,x_i)$. Pour estimer $u(x)$, considérons le vecteur gaussien $(U(x_1),...,U(x_n),U(x))$. Sa loi a posteriori se calcule exactement comme dans l'équation (1.2.11). C'est celle d'un vecteur gaussien dont la dernière coordonnée du vecteur moyenne est

$$\begin{aligned}\tilde{m}(x) :&= \mathbb{E}[U(x)|U(x_i)+\varepsilon_i = y_i, \forall \in \{1,...,n\}] \\ &= k(x,X)^T(k(X,X)+\lambda I_n)^{-1}y. \end{aligned} \tag{1.2.19}$$

Une formule similaire pour $m \neq 0$ est obtenue en considérant le processus centré $V(x) = U(x) - m(x)$. Pour le calcul de la covariance a posteriori, il faut considérer cette fois le vecteur gaussien $(U(x_1),...,U(x_n),U(x),U(x'))$. Un calcul similaire donne

$$\begin{aligned}\tilde{k}(x,x') :&= \mathrm{Cov}(U(x),U(x')|U(x_i)+\varepsilon_i = y_i, \forall \in \{1,...,n\}) \\ &= k(x,x') - k(x,X)^T(k(X,X)+\lambda I_n)^{-1}k(x',X). \end{aligned} \tag{1.2.20}$$

La fonction $\tilde{k}$ est encore définie positive. Nous voyons donc que les équations (1.2.19) et (1.2.20) définissent à leur tour la loi d'un processus gaussien, de fonction moyenne et covariance données par les équations (1.2.19) et (1.2.20). L'estimateur bayésien est obtenu en remplaçant y_i par $U(x_i)+\varepsilon_i$, ce qui donne

$$\begin{aligned}&\mathbb{E}[U(x)|U(x_1)+\varepsilon_1,...,U(x_n)+\varepsilon_n] \\ &\qquad = k(x,X)^T(k(X,X)+\lambda I_n)^{-1}(U(X)+\varepsilon). \end{aligned} \tag{1.2.21}$$

et c'est encore la projection orthogonale de $U(x)$ sur $\mathrm{Vect}(U(x_1)+\varepsilon_1,...,U(x_n)+\varepsilon_n)$, dans $L^2(\mathbb{P})$. Comme dans la régression linéaire, c'est le meilleur prédicteur linéaire non biaisé.

Dans ce formalisme, la question du choix du prior $GP(0,k)$ se pose. Par exemple, dans le cas du noyau (1.2.16), il est nécessaire de sélectionner au préalable les paramètres $\theta = (\sigma,\ell,\nu)$. Une façon de le faire consiste à maximiser la fonction $\theta \mapsto p_{Y,\theta}(y)$, où $p_{Y,\theta}(y)$ est la densité de probabilité du vecteur aléatoire Y d'obtenir les données y étant donné les paramètres θ. Dans le formalisme bayésien on note encore $p_{Y,\theta}(y) = p_Y(y|\theta)$. Cette optimisation revient à sélectionner les paramètres θ qui expliquent le mieux les données, ce qui correspond en fait à une phase d'entraînement dans un cadre d'apprentissage machine. Cette quantité s'appelle la vraisemblance marginale, car elle s'écrit comme l'intégrale de la vraisemblance contre le prior : $p_Y(y|\theta) = \int p_{(U(X),Y)}(u',y|\theta)du' = \int p_Y(y|U(X)=u'|\theta)p_{U(X)}(u'|\theta)du'$. Une expression détaillée de $p_Y(y|\theta)$ est donnée dans l'équation (4.2.3).

Nous appelerons "processus conditionné" n'importe quel processus gaussien de loi la loi conditionnée $GP(\tilde{m},\tilde{k})$, mais soulignons tout de même que spécifier

une loi ne suffit pas à définir une variable aléatoire. Rigoureusement, nous ne pouvons conditionner que des lois et des espérances. En particulier, la notation $(U(x)|U(x_i) = y_i)$ n'a pas de sens canonique au niveau de la variable aléatoire, et si jamais nous utilisons cette notation, nous n'utiliserons en fait que sa loi (elle, définie sans ambiguité).

La régression par processus gaussiens s'appelle encore le krigeage (Kriging), en référence à l'ingénieur Danie G. Krige qui utilisa cette technique dans un contexte de géostatistiques (voir par exemple [49] pour une description détaillée de l'histoire du krigeage).

1.2.4 Espaces de Hilbert à noyau reproduisant

Nous avons vu que la fonction de covariance d'un processus gaussien (en fait, de tout processus stochastique) était définie positive. Cette propriété permet en fait de définir une structure d'espace de Hilbert de fonctions en considérant d'abord $H_k^0 := \mathrm{Vect}(k(x,\cdot), x \in \mathcal{D})$, l'espace vectoriel constitué des combinaisons linéaires finies de fonctions de la forme $k(x,\cdot)$, et en le munissant de la forme bilinéaire suivante, étant donné $f = \sum_{i=1}^n a_i k(x_i,\cdot)$ et $g = \sum_{j=1}^p b_j k(y_j,\cdot)$:

$$\langle f, g\rangle_k = \left\langle \sum_{i=1}^n a_i k(x_i,\cdot), \sum_{j=1}^p b_j k(y_j,\cdot) \right\rangle_k := \sum_{i=1}^n \sum_{j=1}^p a_i b_j k(x_i, y_j). \quad (1.2.22)$$

Cette forme bilinéaire est bien symétrique et positive. En conséquence elle vérifie l'inégalité de Cauchy-Schwarz. Elle vérifie aussi les propriétés dites de "reproduction" suivantes

$$\langle k(x,\cdot), k(x',\cdot)\rangle_k = k(x,x') \quad \text{et} \quad \langle f, k(x,\cdot)\rangle_k = f(x) \ \ \forall f \in H_k^0. \quad (1.2.23)$$

Nous notons $|f|_k := \langle f, f\rangle^{1/2}$, qui n'est a priori qu'une semi-norme. C'est en fait une norme, même si k n'est pas strictement défini positif[11]. Pour le voir, considérons $f \in H_k^0$ telle que $|f|_k = 0$. Alors pour tout $x \in \mathcal{D}$, l'inégalité de Cauchy-Schwarz donne

$$|f(x)| = |\langle f, k(x,\cdot)\rangle_k| \leq |f|_k k(x,x)^{1/2} = 0, \quad (1.2.24)$$

et donc $f \equiv 0$. H_k^0 est donc un espace préhilbertien, et son complété H_k est un espace de Hilbert de fonctions dont on note $\|\cdot\|_k$ la norme (les détails techniques montrant que les limites de suites de Cauchy s'interprètent

11. Ce cas général est évoqué dans l'article fondateur [14] ainsi que dans l'ouvrage [24] mais étonnament, certains textes modernes de références comme [212] ou [77] ne traitent que les cas des fonctions (conditionnellement) *strictement* définies positives.

encore comme des fonctions se trouvent dans [212]). En référence aux équations (1.2.23), l'espace H_k s'appelle un espace de Hilbert à noyau reproduisant (*reproducing kernel Hilbert space*, ou RKHS, [14]). Nous noterons souvent $k_x \coloneqq k(x, \cdot)$.

Les RKHS sont des espaces de Hilbert dont la topologie est compatible avec l'évaluation ponctuelle, étant donné que les formes linéaires d'évaluation sont continues : $|f(x)| \leq k(x,x)^{1/2}\|f\|_k$ (équation (1.2.24)). En fait, la continuité des formes linéaires d'évaluation est une définition alternative des RKHS, et il existe une bijection entre de tels espaces et les fonctions définies positives. Via les injections de Sobolev dans les espaces de fonctions continues de type Hölder, cela montre par exemple que les espaces de Sobolev $H^s(\mathcal{D})$ avec $\mathcal{D} \subset \mathbb{R}^d$ un ouvert régulier et $s > d/2$, sont des RKHS (un noyau engendrant une norme équivalente à $\|\cdot\|_{H^s}$ est d'ailleurs k_ν introduit dans l'équation (1.2.16), pour $\nu = s - d/2$). Plus spécifiquement, les RKHS sont exactement les sous-espaces hilbertiens de $\mathcal{F}(\mathcal{D}, \mathbb{R})$ dont l'injection dans $\mathcal{F}(\mathcal{D}, \mathbb{R})$ est continue lorsqu'on munit $\mathcal{F}(\mathcal{D}, \mathbb{R})$ de la topologie de la convergence ponctuelle ([184], section 9). En ce sens, les RKHS fournissent un cadre particulièrement adapté à l'utilisation de l'analyse hilbertienne sur des problèmes de régression et d'interpolation.

Reconstruction optimale dans les RKHS (régression à noyau, [212]) [12]
Considérons donc le problème de régression régularisé suivant, étant donné $\lambda > 0$:

$$\min_{v \in H_k} \sum_{i=1}^{n} (y_i - v(x_i))^2 + \lambda \|v\|_k^2. \tag{1.2.25}$$

Le premier terme est un terme d'attache aux données quantifiant l'erreur d'approximation de $v \in H_k$, tandis que le deuxième terme pénalise les candidats v de trop grande norme (trop "irréguliers"). C'est donc un terme de régularisation. Ce problème se résout explicitement ([166], section 6.2.2), sa solution est

$$v^*(x) = k(x, X)^T (k(X, X) + \lambda I_n)^{-1} y. \tag{1.2.26}$$

Lorsque λ tend vers 0, nous obtenons un problème d'interpolation régularisé

$$\min_{v \in H_k} \|v\|_k \quad \text{sous la contrainte} \quad v(x_i) = y_i, \quad \forall i \in \{1, ..., n\}, \tag{1.2.27}$$

12. En statistiques, le terme de "régression à noyau" fait souvent réference à une autre méthode de régression utilisée notamment pour l'estimation de densité de probabilité, voir par exemple [211], section 20.3.

dont la solution s'écrit cette fois, si $k(X,X)$ est inversible,

$$v^*(x) = k(x,X)^T k(X,X)^{-1} y. \tag{1.2.28}$$

Ce n'est autre que l'estimateur de la régression par processus gaussiens. Notons qu'il est possible de considérer des formes linéaires continues générales $\ell_i(v) = \langle e_i, v\rangle_k$ dans les problèmes (1.2.25) et (1.2.27), et non simplement $\langle k(x_i,\cdot), v\rangle_k = v(x_i)$.

Parallèle avec la régression linéaire Notons $M : H_k \to \mathbb{R}^n$ l'opérateur d'observation défini par $Mv = (v(x_1), ..., v(x_n))$. Nous montrons alors que l'opérateur de $\mathbb{R}^n$ à valeur dans H_k qui à y associe v^* dans l'équation (1.2.28) n'est rien d'autre que M^+, le pseudo inverse de Moore-Penrose de M (voir [71], p. 45 pour les pseudo-inverses dans un cadre très général). En effet, un calcul d'adjoint montre que si $z \in \mathbb{R}^n$, alors $M^* z = \sum_{i=1}^n z_i k(x_i,\cdot)$, et que $MM^* = k(X,X)$, d'où, pour v^* dans l'équation (1.2.28),

$$v^* = M^*(MM^*)^{-1} y = M^+ y. \tag{1.2.29}$$

En effet, $M^+ = M^*(MM^*)^{-1}$ si MM^* est inversible. Supposons maintenant que $u \in H_k$, alors on a pour tout x que

$$u(x) = \langle k(x,\cdot), u\rangle_k \quad \text{et} \quad y = Mu. \tag{1.2.30}$$

Nous avons alors que $v^* = M^+ Mu$, et donc v^* est la projection orthogonale de u sur $F = \mathrm{Im}(M^*) = \mathrm{Vect}(k(x_1,\cdot), ..., k(x_n,\cdot))$. Il est aussi possible de voir que la covariance a posteriori (dans le cas $\lambda = 0$) s'écrit comme $\tilde{k}(x,x') = p_{F^\perp}(k(x,\cdot))(x')$, et qu'elle contrôle l'erreur d'approximation selon

$$|u(x) - v^*(x)| \leq \tilde{k}(x,x)^{1/2} \|u\|_k. \tag{1.2.31}$$

(voir par exemple [212], section 11 et son théorème 11.4.) Dans le cadre des RKHS, la fonction $x \mapsto \tilde{k}(x,x)^{1/2}$ s'appelle la *power function* [212].

En terme de l'opérateur M, la comparaison entre la méthode des moindres carrés et la régression à noyau est transparente, ce qui montre que les principes d'optimalité décrits plus hauts étaient déjà présents dans la méthode des moindres carrés. La différence cruciale entre les deux méthodes est la suivante : au lieu de chercher un approximant linéaire de u, nous avons au préalable envoyé x, de façon non linéaire, dans un espace bien plus riche (ici, H_k) via une application ϕ appelée "feature map". L'espoir sous-jacent est (i) d'échapper à l'expressivité limitée de la régression linéaire, et (ii) que le problème devienne approximativement linéaire dans le nouvel espace H_k. Dans ce contexte, l'espace cible H_k s'appelle aussi l'espace des caractéristiques, ou

features, et ϕ est simplement donnée par $\phi(x) = k(x, \cdot) \in H_k$. Cela donne aussi que $k(x, x') = \langle \phi(x), \phi(x') \rangle_k$, donc k donne une mesure de similarité entre $\phi(x)$ et $\phi(x')$. [13] La recherche du coefficient α d'approximation linéaire $\hat{u}(x) = x^T \alpha$ a ensuite été substituée par celle du meilleur vecteur $\alpha \in H_k$, selon la forme calquée "$\hat{u}(x) = \phi(x)^T \alpha$", ou rigoureusement, $\hat{u}(x) = \langle \phi(x), \alpha \rangle_k$.

Nous avons vu les liens étroits qui lient deux très belles théories, celles des processus gaussiens et celle des espaces de Hilbert à noyau reproduisant. Nous appelerons méthodes à noyau les méthodes de régression utilisant l'un ou l'autre de ces paradigmes.

1.2.5 Méthodes à noyau et réseaux de neurones

Au début de ce chapitre, nous avons motivé l'application de l'apprentissage machine sur des problèmes de physique au travers de l'exemple des réseaux de neurones. Dans cette section, nous exposons quelques correspondances fortes entre ces derniers et les méthodes à noyau. Cela terminera de motiver l'étude des méthodes à noyau, sur lesquelles se concentre la majeure partie de la thèse.

Du point de vue historique, les méthodes à noyau ont longtemps représenté l'état de l'art sur de nombreux problèmes d'apprentissage machine. Ce n'est que depuis le début des années 2010 que l'utilisation des réseaux de neurones profonds, déverouillée par de nombreuses avancées algorithmiques et informatiques, ont commencé à surclasser les méthodes à noyau (voir par exemple [85] ou [167]), en particulier lorsque de nombreuses données sont disponibles. En effet, les méthodes à noyau (dans leur formulation standard) sont difficiles à mettre en oeuvre lorsque les données sont très nombreuses, à cause de la matrice de covariance à inverser. Nous revenons sur ce point en fin de section. En contrepartie, les méthodes à noyau sont généralement plus adaptées aux cas où peu de données sont disponibles, comme lors de l'émulation de codes de calculs onéreux [174, 91]. [14]. De même, la régression par processus gaussiens est particulièrement populaire dans des contextes de quantification d'incertitude ([91], p. xiv), grâce à la mesure a posteriori qu'elle fournit.

Il existe pourtant des liens profonds entre les méthodes à noyau et les réseaux de neurones. Un premier exemple datant de 1996 est décrit dans [147], section 2.1. Il y est observé qu'en mettant un prior sur les poids θ d'un réseau

13. Ce dernier point est un autre avantage de l'approche à noyau : pour calculer le produit scalaire entre $\phi(x)$ et $\phi(x')$ (tâche a priori compliquée ou coûteuse), il suffit en fait d'évaluer le scalaire $k(x, x')$. Il suffit donc de se donner k, et pas ϕ : c'est "l'astuce du noyau" (*kernel trick*).

14. Il semblerait pourtant que certains réseaux de neurones puissent aussi fournir de bonnes performances avec peu de données, voir notamment [15]. De façon intéressante, cette étude passe par une formulation équivalente du réseau de neurones...à l'aide d'une méthode à noyau !

de neurones $x \mapsto R_\theta(x)$ à une couche cachée (en supposant les priors sur chaque neurone indépendants et identiquement distribués), on obtient un prior de fonction sur $x \mapsto R_\theta(x)$ qui converge vers un prior de processus gaussien dans la limite du nombre de neurones tendant vers l'infini. Cela se déduit en fait d'une application directe du théorème central limite ([166], section 4.2.3). De telles approches appartiennent aux modèles de type "random features", en référence aux feature maps introduites plus haut.

De nombreux liens similaires ont depuis été établis, notamment pour les réseaux de neurones profonds [128]. Nous renvoyons aux études bibliographiques de [128] ou du plus récent article [26] pour plus d'exemples de liens de ce type. Par ailleurs, [106] a récemment montré que la régression avec un réseau de neurones pour lequel les poids ont peu varié lors de la phase d'apprentissage (régime "paresseux", ou *lazy regime*) était en fait équivalente à une méthode à noyau dont le noyau est dicté par le réseau. Ce noyau s'appelle le *neural tangent kernel*.

Plus largement, il est possible de voir certaines méthodes de régression basées sur les réseaux de neurones comme des méthodes à noyau pour lesquelles le noyau a été appris à partir des données. Pour le cas des *ResNets*, cette correspondance a été rendue explicite dans [152], dans la limite continue du nombre de couches. Ce même article montre que la régression à l'aide de ResNets est une forme (quasi) infini-dimensionnelle d'algorithmes variationnels bien connus en recalage d'image (*image registration*).

Dans les applications aussi, il est observé dans [21] que les réseaux de neurones et les méthodes à noyau ont des comportements très voisins sur de nombreux exemples. Ces deux méthodes offrent notamment des propriétés de généralisation (i.e. de prédiction sur de nouveaux exemples) très similaires. Cela renforce l'idée que la compréhension des propriétés de généralisation des méthodes à noyau peut apporter des éclairages sur celles des réseaux de neurones. nous renvoyons à [85] pour plus de détails bibliographiques sur des études similaires.

Enfin, le récent article [17] établit une correspondance entre la régression basées sur des réseaux de neurones dont la fonction d'activation est une spline de la forme $\sigma(u) = \max(u, 0)^\alpha$, $\alpha \in \mathbb{N}$, et l'interpolation avec les mêmes splines. Pour certaines valeurs de α, σ correspond à une spline dite "polyharmonique" (voir [204] ou [129]). La régression avec de telles splines, dans sa formulation usuelle, n'est pas une méthode de régression dans un RKHS car les splines polyharmoniques ne sont que conditionnellement définies positives (il existe cependant une formulation équivalente de la régression à l'aide de splines conditionnellement définies positives, dans un RKHS auxiliaire, [212], théorème 10.20). il se trouve aussi que la correspondance entre l'interpolation avec des splines polyharmoniques et l'interpolation dans des RKHS de régu-

larité finie, dans le régime de la limite plate, est connue depuis le début des années 2010 [191] (et, sous forme cachée, depuis au moins 1974, même pour les splines d'ordre fractionnaire, dans l'article [143] passé inaperçu).

Toutes ces correspondances, en plus du cadre mathématique agréable des processus gaussiens et des RKHS, justifient pourquoi aujourd'hui encore, une partie importante de la recherche en apprentissage machine est consacrée aux méthodes à noyau. De plus, les sections précédentes ont montré que ces méthodes reposaient sur un cadre mathématique agréable ayant de bonnes propriétés d'interprétabilité, par exemple en termes de projections orthogonales et d'espérances conditionnelles. Les hypothèses nécessaires pour manipuler les méthodes à noyau semblent facilement identifiables, et l'obtention de garanties théoriques d'approximation semble être un objectif atteignable dans ce formalisme. Terminons en notant qu'il existe des méthodes permettant de rendre les méthodes à noyau viables pour un plus grand nombre de données (*inducing points* [159] et autres méthodes de bas rang [190], ou priors pour lesquels $k(X, X)^{-1}$ est creuse [135]). C'est pour ces raisons que nous concentrerons sur ces outils dans la suite de la thèse.

Nous nous tournons maintenant vers le deuxième grand thème de ce mémoire de thèse, celui des équations aux dérivées partielles.

1.3 Equations aux dérivées partielles

Cette section est consacrée à l'introduction et à l'illustration ce certaines notions centrales en équations aux dérivées partielles, qui seront les équations que nous utiliserons pour modéliser la physique. Ces notions nous guiderons tout au long de la thèse. Après une courte description des propriétés typiques que l'on peut attendre des solutions d'EDPs (section 1.3.1), nous introduisons les espaces de Sobolev et les formulations faibles associées (section 1.3.2). Puis, nous introduisons la formulation distributionnelle (section 1.3.3), et dans une moindre mesure les méthodes numériques de résolution des EDPs (section 1.3.4). Une dernière partie (section 1.3.5) discute des différentes stratégies existantes concernant l'apprentissage machine informé par la physique. Nous nous basons essentiellement sur [73, 33] pour les sections 1.3.1 et 1.3.2, et [202, 173] pour la section 1.3.3.

1.3.1 Quelques propriétés des EDPs

Une grande partie des équations de la physique sont des traductions plus ou moins directes de grands principes de conservation, d'équilibre ou de dissipation (frottements). Les plus grands de ces principes sont certainement les

principes de conservation de la masse, de l'énergie ou de la quantité de mouvement. Un moyen efficace de traduire mathématiquement ces principes consiste à les voir comme des équilibres ou des échanges de flux. A l'échelle infinitésimale, ces derniers se traduisent finalement comme des équations liant les différents *taux de variations*, temporels et/ou spatiaux, des différentes quantités intervenant dans le phénomène physique en question. Ces équations sont des *équations aux dérivées partielles* (EDP). De façon générale, elles prennent la forme suivante, étant donné un ouvert $\mathcal{D} \subset \mathbb{R}^d$:

$$\mathcal{L}(x, \{\partial^\alpha u(x)\}_{|\alpha|\leq m}) = f(x), \quad \forall x \in \mathcal{D}, \tag{1.3.1}$$
$$\mathcal{B}(x, \{\partial^\alpha u(x)\}_{|\alpha|\leq m}) = g(x), \quad \forall x \in \partial\mathcal{D}. \tag{1.3.2}$$

Ici, m est l'ordre de l'équation. Etant donné $\alpha \in \mathbb{N}^d$, nous avons noté $|\alpha| := \alpha_1 + ... + \alpha_d$, et la notation $\partial^\alpha u(x)$ signifie

$$\partial^\alpha u(x) = \left[\left(\frac{\partial}{\partial x_1}\right)^{\alpha_1} \cdots \left(\frac{\partial}{\partial x_d}\right)^{\alpha_d} u \right](x). \tag{1.3.3}$$

Les applications $\mathcal{L}$ et $\mathcal{B}$ (par exemple continues) sont à valeur scalaires, f et g sont des termes sources mesurables et u est l'inconnue (les généralisations vectorielles sont directes). Dans les équations, nous supposons pour l'instant que u est de classe C^m. L'équation (1.3.1) traduit une contrainte à l'intérieur du domaine, et l'équation (1.3.2) traduit une contrainte au bord du domaine. Une EDP est dite linéaire si les applications $\mathcal{L}$ et $\mathcal{B}$ le sont. Bien que de nombreuses EDPs réalistes soient non linéaires (en mécanique des fluides en particulier), les EDPs linéaires demeurent centrales dans de nombreuses applications physiques ainsi que dans les fondements théoriques des EDPs. De plus, elles admettent des formules de représentations intéressantes que nous utiliserons par la suite (voir notamment la section 1.3.3). C'est pourquoi une grande partie de la thèse sera dédiée à l'étude des EDPs linéaires.

Les applications des EDPs sont innombrables, tant dans des domaines appliqués que théoriques. Si nous nous focaliserons sur des problèmes en lien avec des applications pratiques, la portée des EDPs ne s'y restreint pas. En ce sens, l'étude des EDPs figure encore parmi les thèmes de recherches actuels les plus actifs.

Classification des EDPs Parmi les EDPs, trois classes principales (mais non exhaustives) apparaissent. Ces classes s'introduisent d'abord lorsque $\mathcal{L}$ est linéaire ; leur généralisation aux EDPs non linéaires se fait au cas par cas. La première classe est celle des EDPs *elliptiques*[15], qui décrivent des

15. La distinction entre équations elliptiques, paraboliques et hyperboliques est issue de la similarité formelle entre les EDPs linéaires à deux variables et d'ordre deux et la classification des coniques.

problèmes stationnaires, de la forme $Lu = f$. L doit être un opérateur elliptique (possédant de fortes propriétés de positivité), dont le prototype est $-\Delta = -\sum_{i=1}^{d} \partial^2_{x_i x_i}$, l'opposé du Laplacien (avec conditions aux bords adéquates). Les EDPs correspondantes sont les équations de Laplace, $\Delta u = 0$, et de Poisson, $-\Delta u = f$. La deuxième classe est celle des équations *paraboliques*. Elles sont typiquement de la forme $\partial_t u + Lu = 0$, où L est un opérateur elliptique. Elles décrivent des phénomènes de diffusion et leur prototype est l'équation de la (diffusion de la) chaleur, $\partial_t u - \Delta u = 0$. Etant donné la condition initiale $u(t = 0) = u_0$, et en notant $|\cdot|$ la norme euclidienne sur $\mathbb{R}^d$, sa solution est donnée par

$$u(x,t) = \int_{\mathbb{R}^d} \frac{1}{(4\pi t)^{d/2}} e^{\frac{-|x-y|^2}{4t}} u_0(y) dy, \quad x \in \mathbb{R}^d,\ t \geq 0. \tag{1.3.4}$$

Enfin, la troisième classe est celle des équations *hyperboliques*. Ces dernières sont particulièrement adaptées aux lois de conservation et décrivent des phénomènes de propagation à vitesse finie. Elles sont typiquement de la forme $\partial^2_{tt} u + Lu = 0$ où L est elliptique (ordre deux), ou $\partial_t u + \mathrm{div}(au) = 0$ avec $\mathrm{div}(f) := \sum_{i=1}^{d} \partial_{x_i} f_i$ si f est définie de $\mathbb{R}^d$ à valeur dans $\mathbb{R}^d$ avec $f(x) = (f_1(x), ..., f_d(x))^T$ (ordre un). Leurs prototypes sont l'équation des ondes, $c^{-2}\partial_{tt} u - \Delta u = 0$, ainsi que l'équation de transport (ou d'advection), $\partial_t u + a^T \nabla u = 0$ où $a \in \mathbb{R}^d$, $\nabla u := (\partial_{x_1} u, ..., \partial_{x_d} u)^T$ et u est à valeur scalaire. Etant donné la condition initiale $u(t = 0) = u_0$, la solution de cette dernière s'écrit

$$u(x,t) = u_0(x - ta), \quad x \in \mathbb{R}^d,\ t \geq 0. \tag{1.3.5}$$

Régularité des solutions d'une EDP Les solutions d'équations elliptiques, paraboliques et hyperboliques possèdent des propriétés très différentes. D'un côté, les équations elliptiques et paraboliques linéaires régularisent leur terme source : les solutions de l'équation de Laplace avec condition de Dirichlet sont de classe C^∞ à l'intérieur du domaine ([73], p. 28) et dans le cas de l'équation de la chaleur, la solution en espace est de classe C^∞ pour tout $t > 0$ (équation (1.3.4)). De l'autre côté, les équations hyperboliques n'ont pas de propriété régularisante au sens ci-dessus. Pour l'équation d'advection, la régularité de la solution à l'instant t est la même que celle de la condition intiale (équation (1.3.5)). Pire, pour une EDP hyperbolique non linéaire, des discontinuités peuvent apparaître en temps fini. La solution continue cependant d'exister (disons empiriquement pour l'instant) mais la présence d'une discontinuité interroge sur le sens à donner aux équations (1.3.1) et (1.3.2) : comment dériver une fonction discontinue ? Ce type de discontinuité n'est pas qu'un artefact mathématique : ce sont par exemple elles qui apparaissent lorsqu'un avion dépasse le mur du son, les équations d'Euler formant un système hyperbolique ([186], p. 4 ou [132], chapitre 14).

Ces propriétés, étonnantes au premier abord, ne signifient pas que les équations hyperboliques ont moins de sens physique que leurs équivalents elliptiques et paraboliques. Au contraire, l'absence de régularisation suggère par exemple que les EDPs hyperboliques ont des bonnes propriétés de propagation d'information ainsi que de réversibilité (en l'absence de chocs non linéaires... voir par exemple l'équation (1.3.11)). A contrario, l'équation de la chaleur propage l'information à vitesse infinie (dans l'équation (1.3.4), $u(x,t) \neq 0$ si $t > 0$ même si le support de u_0 est compact), et sa version rétrograde (changer t par $-t$) est sévèrement mal posée ([105], exemple 2.1.1).

1.3.2 Espaces de Sobolev et formulations faibles

Normes de Sobolev Nous avons vu que bons nombres d'EDPs sont le fruit de principes d'équilibre. En ce sens, une notion centrale est celle de fonctionnelle d'énergie qui, pour une fonction donnée, correspond à sa norme euclidienne $\|u\|_{L^2}^2 = \int u(x)^2 dx$. Rappelons que l'espace L^2 a de très bonnes propriétés topologiques : c'et un espace de Hilbert séparable, qui admet donc une base hilbertienne. Il est aussi connu que ses éléments n'ont pas de raisons d'être continus. Selon ce point de vue, il peut donc sembler que la régularité L^2 soit au moins aussi pertinente que la régularité C^0 pour étudier certaines EDPs. De même, une fonction doit pouvoir admettre des dérivées d'énergie finie sans pour autant qu'elles soient continues. Dans le cas des équations types que nous avons évoquées, cette idée est renforcée par le fait que l'opérateur laplacien possède de très bonnes propriétés en lien avec le produit scalaire dans L^2. En effet, étant donné deux fonctions u, v qu'on suppose d'abord à support compact et de classe C^1, une intégration par parties (termes de bord nuls) donne

$$\begin{aligned}\langle u, -\Delta v\rangle_{L^2(\mathbb{R}^d,\mathbb{R})} &= -\int_{\mathbb{R}^d} u(x)\Delta v(x)dx = \int_{\mathbb{R}^d} \nabla u(x)\cdot\nabla v(x)dx \\ &= \langle \nabla u, \nabla v\rangle_{L^2(\mathbb{R}^d,\mathbb{R}^d)}. \end{aligned} \tag{1.3.6}$$

Cette expression est à comparer avec la forme bilinéaire positive associée à une matrice semi-définie positive, $(u,v) \mapsto \langle u, Av\rangle = u^T Av$. Tous ces éléments suggèrent l'existence d'une structure hilbertienne dans laquelle certaines EDPs peuvent être agréablement reformulées. Ces structures correspondent à des espaces dit de Sobolev. De façon similaire à l'espace $C^m(\mathbb{R}^d)$, l'espace de Sobolev $H^m(\mathbb{R}^d)$ correspond aux fonctions d'énergie finie dont toutes les dérivées d'ordre au plus m sont aussi d'énergie finie. Il peut être construit en considérant l'espace $C_c^m(\mathbb{R}^d)$ des fonctions de classe C^m à support compact muni du

produit scalaire

$$\langle u, v\rangle_{H^m} = \sum_{|\alpha|\leq m} \langle \partial^\alpha u, \partial^\alpha v\rangle_{L^2}, \tag{1.3.7}$$

et en le complétant par la norme induite par ce produit scalaire. De façon générale, les éléments de $H^m(\mathbb{R}^d)$ ainsi définis ne sont pas de classe C^m, ni même continus sauf si $m > d/2$ (par les injections de Sobolev). Alternativement, les dérivées *faibles* $\partial^\alpha f$ d'une fonction f localement intégrable (i.e. intégrable sur tout compact) sont définies comme les uniques fonctions localement intégrables, si elles existent, vérifiant la propriété d'intégration par parties suivante :

$$\forall \varphi \in C_c^m(\mathbb{R}^d),\ \forall |\alpha| \leq m,\ \int_{\mathbb{R}^d} \partial^\alpha \varphi(x) f(x) dx = (-1)^{|\alpha|} \int_{\mathbb{R}^d} \varphi(x) \partial^\alpha f(x) dx.$$

L'espace $H^m(\mathbb{R}^d)$ est ensuite défini comme l'ensemble des fonctions f dont les dérivées faibles d'ordre au plus m existent et sont dans L^2. Cette approche permet notamment de définir les espaces de Sobolev sur des ouverts $\mathcal{D} \subset \mathbb{R}^d$ arbitraires.

Formulations faibles A titre d'illustration, étant donné $f \in L^2(\mathbb{R}^d)$, l'équation $-\Delta u + u = f$ dans $\mathbb{R}^d$ est reformulée de la façon suivante. Supposons d'abord que u soit de classe C^2. Considérons ensuite $\varphi \in C_c^1(\mathbb{R}^d)$, multiplions l'équation par φ et intégrons sur tout $\mathbb{R}^d$:

$$\forall \varphi \in C_c^1(\mathbb{R}^d),\ -\int_{\mathbb{R}^d} \varphi \Delta u + \int_{\mathbb{R}^d} \varphi u = \int_{\mathbb{R}^d} \varphi f. \tag{1.3.8}$$

Cette approche revient à *tester* l'équation par des moyennes locales (car φ est à support compact). C'est notamment ce point de vue qui est à l'origine de la méthode des éléments finis et plus largement des méthodes de Galerkine continues et discontinues (nous renvoyons à [217] pour d'autres interprétations physiques de cette approche). Après une intégration par parties selon l'équation (1.3.6), nous obtenons que

$$\forall \varphi \in C_c^1(\mathbb{R}^d),\quad \langle \varphi, u\rangle_{H_1} = \langle \varphi, f\rangle_{L^2}. \tag{1.3.9}$$

La continuité sur $H^1(\mathbb{R}^d)$ des formes linéaires $\varphi \mapsto \langle \varphi, f\rangle_{L^2}$ et $\varphi \mapsto \langle \nabla\varphi, \nabla u\rangle_{L^2}$ ainsi que la densité de $C_c^1(\mathbb{R}^d)$ dans $H^1(\mathbb{R}^d)$ permettent d'étendre cette égalité à $H^1(\mathbb{R}^d)$, donnant finalement que

$$\forall \varphi \in H^1(\mathbb{R}^d),\quad \langle \varphi, u\rangle_{H_1} = \langle \varphi, f\rangle_{L^2}. \tag{1.3.10}$$

Ainsi, nous avons transformé notre équation en un problème de représentation de formes linéaires et bilinéaires continues dans un espace de Hilbert. L'équation (1.3.10) s'appelle la formulation faible de l'EDP $-\Delta u + u = f$. Comme cette équation est aussi obtenue en minimisant la fonctionnelle $u \mapsto \frac{1}{2}\|u\|_{H^1}^2 - \langle u, f\rangle_{L^2}$, nous parlons aussi de formulation variationnelle. Dans le cas de cette équation elliptique, la théorie de Lax-Milgram permet d'établir des théorèmes d'existence et d'unicité de la solution, ainsi que la continuité de l'opérateur inverse $(-\Delta + I)^{-1}$. [16]

De nombreux principes de conservation ou de décroissance d'énergie, qui traduisent une forme de stabilité, s'expriment facilement grâce aux normes H^m. Par exemple, pour l'équation des ondes $\partial_{tt}u - \Delta u = 0$ dans $\mathbb{R}^d$ munie des conditions initiales $u(t=0) = u_0$ et $\partial_t u(t=0) = v_0$, nous avons (par exemple en utilisant l'équation (1.3.6))

$$\partial_t \Big(\|\partial_t u(\cdot,t)\|_{L^2}^2 + \|\nabla u(\cdot,t)\|_{L^2}^2 \Big) = 0, \tag{1.3.11}$$

et donc $\|\partial_t u(\cdot,t)\|_{L^2}^2 + \|\nabla u(\cdot,t)\|_{L^2}^2 = \|v_0\|_{L^2}^2 + \|\nabla u_0\|_{L^2}^2$. Pour l'équation de la chaleur $\partial_t u = \Delta u$ munie de la condition initiale $u(t=0) = u_0$, nous avons cette fois

$$\frac{1}{2}\partial_t \|u(\cdot,t)\|_{L^2}^2 = -\|\nabla u(\cdot,t)\|_{L^2}^2 \leq 0, \tag{1.3.12}$$

donc $\|u(\cdot,t)\|_{L^2} \leq \|u_0\|_{L^2}$ et l'énergie du terme source a été dissipée.

Certaines équations possèdent des structures qui sont mieux révélées par des espaces non hilbertiens. Citons par exemple l'équation de Schrödinger non linéaire donnée par $i\partial_t u + \Delta u = \kappa |u|^2 u$, pour laquelle le terme $|u|^2 u$ ne semble pas vraiment adapté à L^2, mais plutôt à un espace de type L^p (voir par exemple [200], section 2.3). Cela motive l'introduction d'espaces de Sobolev $W^{m,p}$ non hilbertiens, étant donné $p \in [1, +\infty)$, obtenus en considérant cette fois la norme

$$\|u\|_{W^{m,p}} := \Big(\sum_{|\alpha| \leq m} \|\partial^\alpha u\|_{L^p}^p \Big)^{1/p}. \tag{1.3.13}$$

Le cas $p = \infty$ est défini comme $\|u\|_{W^{m,\infty}} := \max_{|\alpha|\leq m} \|\partial^\alpha u\|_{L^\infty}$. Les espaces résultants sont des espaces de Banach. On peut alors espérer obtenir des équations de la forme (1.3.11) ou (1.3.12) en fonction des normes $\|u\|_{W^{m,p}}$, selon l'EDP étudiée (voir [200], section 2.3 pour des exemples).

Tout espace de Banach E est muni d'une sorte de produit scalaire non symétrique en la forme du crochet de dualité, défini par $\langle T, u\rangle := T(u)$, étant

16. La validité de ces trois points sert de définition de la notion d'EDP *bien posée* au sens de Hadamard.

donné $u \in E$ et $T \in E^*$. Si l'on munit E^* de la norme d'opérateur, il vérifie "l'inégalité de Cauchy-Schwarz" : $|\langle T, u\rangle| \leq \|T\|_{E^*}\|u\|_E$. Parmi les espaces de Banach remarquables se trouvent les espaces réflexifs, pour lesquels l'application qui à $u \in E$ associe la forme linéaire sur E^* donnée par $T \mapsto \langle T, u\rangle_{E^*,E}$, et une bijection de E sur E^{**} (autrement dit, le lemme de Riesz est vérifié). Ainsi, parmi les espaces de Banach non hilbertiens, les espaces réflexifs sont les plus proches des espaces de Hilbert. Les espaces $L^p, 1 < p < +\infty$, sont réflexifs (en plus d'être séparables), et à ce titre l'application $u \mapsto \|u\|^p_{W^{m,p}}$ est souvent interprétée comme une fonctionnelle d'énergie généralisée. Elle est notamment convexe (voire un peu mieux par les inégalités de Clarkson, [169], théorème 2.38). A contrario, l'espace $C(K)$ des fonctions continues sur un compact K de $\mathbb{R}^d$ est séparable mais pas réflexif.

Terminons en soulignant qu'il n'existe pas de définition consacrée pour le terme "formulation faible". En effet les formulations faibles, et leurs espaces fonctionnels en particulier, dépendent de l'EDP qu'elles visent à résoudre (voir la section 2.1 pour des exemples et références). Par ailleurs, en considérant le cas $\mathcal{D} = \mathbb{R}^d$, nous n'avons pas discuté du rôle des conditions aux bords (l'équation (1.3.2)). Dans le cas général, elles jouent un rôle important dans la formulation faible (1.3.10) en intervenant soit dans les formes linéaires de la formulation, soit dans le choix de l'espace de fonctions tests, soit dans les deux.

1.3.3 Formulation distributionnelle et fonction de Green

Formulation distributionnelle Bien que très agréable, le cadre des espaces de Sobolev n'est pourtant pas suffisant pour formuler toutes les EDPs physiquement pertinentes, ainsi que pour rendre compte de toutes leurs solutions. Par exemple, quel sens donner à l'équation de transport unidimensionnelle

$$\partial_t u + a\partial_x u = 0 \tag{1.3.14}$$

si la condition initiale u_0 est discontinue ? En effet, la représentation (1.3.5) suggère dans ce cas que à t fixé, la solution u doit aussi être discontinue. Il se trouve aussi (particularité de la dimension 1) que $H^1(\mathbb{R}) \subset C^0(\mathbb{R})$, et donc le cadre pourtant naturel fourni par l'espace $H^1(\mathbb{R})$ est trop rigide pour rendre compte de telles solutions. Nous sommes donc contraints à changer d'espace fonctionnel.

Dans la construction de la formulation faible (1.3.10), nous avons transformé la dérivée Δu en une forme linéaire continue sur l'espace $H^1(\mathbb{R}^d)$. Cela nous a entre autres permis d'assouplir les contraintes de différentiabilité sur

la solution u. Nous allons donc suivre cette même démarche mais en limitant l'espace des fonctions tests à un espace beaucoup plus restreint, l'espace des fonctions de classe C^∞ et à support compact, que l'on note $C_c^\infty(\mathcal{D})$ si le domaine ambiant est un ouvert $\mathcal{D} \subset \mathbb{R}^d$. Pour l'équation de transport unidimensionnelle avec condition initiale en $t = 0$, nous obtenons alors que

$$\forall \varphi \in C_c^\infty(\mathbb{R} \times \mathbb{R}_+^*), \quad \int_{\mathbb{R}\times\mathbb{R}_+^*} \varphi(x,t)\big(\partial_t u(x,t) + a\partial_x u(x,t)\big)dxdt = 0.$$

Cette approche consiste donc à considérer toutes les moyennes lisses et locales en espace-temps, à la place de la formulation ponctuelle de l'EDP. Comme précédemment, des intégrations par parties donnent que pour tout $\varphi \in C_c^\infty(\mathbb{R} \times \mathbb{R}_+^*)$,

$$\int_{\mathbb{R}\times\mathbb{R}_+^*} \big(\partial_t \varphi(x,t) + a\partial_x \varphi(x,t)\big)u(x,t)dxdt = 0. \tag{1.3.15}$$

Notons que cette formulation permet de rendre compte des solutions discontinues s'il y en a, la seule hypothèse de régularité nécessaire pour donner un sens à l'équation (1.3.15) étant que u soit localement intégrable. Il est même possible de considérer des solutions mesures en remplaçant $u(x,t)dxdt$ par $\mu(dx,dt)$.

Il est possible de se demander s'il existe une interprétation de l'équation (1.3.15) en termes de formes linéaires continues, similairement à la formulation faible (1.3.10) [17]. Seulement, l'espace des fonctions tests est ici restreint à $C_c^\infty(\mathbb{R} \times \mathbb{R}_+^*)$, et donc une question centrale est celle de la bonne topologie à considérer sur cet espace. La réponse fut donnée par Laurent Schwartz en 1946 [183], donnant ainsi naissance à la théorie des *distributions* [18], terme désignant les éléments du dual de C_c^∞. C'est pourquoi nous appelons l'équation (1.3.15) la formulation distributionnelle de l'équation de transport. Dans les chapitres suivants, nous noterons $\mathscr{D}(\mathcal{D}) := C_c^\infty(\mathcal{D})$, en référence aux notations de Schwartz ($\mathscr{D}$ signifie "différentiable"). Dans ce chapitre introductif cependant, nous gardons la notation C_c^∞, un peu plus explicite.

Cette topologie sur C_c^∞, dite "topologie LF" et dont nous retardons la description à la section 2.2.2.2, est fondamentalement différente de celles des

17. De façon générale, en dimension infinie, l'ensemble des toutes les formes linéaires est bien trop gros pour avoir des propriétés agréables. A contrario, par une analogie lointaine avec les espaces de Hilbert et de Banach, se restreindre aux formes linéaires continues permet d'espérer accéder à des propriétés "géométriques" du crochet de dualité, et aux opérateurs adjoints en particulier. Par exemple, une transformée de Fourier très générale est obtenue en considérant l'opérateur adjoint de la transformée de Fourier usuelle définie de l'espace des fonctions à décroissance rapide $\mathcal{S}(\mathbb{R}^d)$ à valeur dans lui-même.

18. Ce terme est inspiré des distributions de charge en électrostatique. Cette théorie lui vaudra l'attribution de la médaille Fields en 1950.

espaces de Sobolev car elle n'est pas normable ni même métrisable. Elle permet en contrepartie de donner une définition des dérivées, de tout ordre, de toute fonction localement intégrable sur un ouvert $\mathcal{D} \subset \mathbb{R}^d$. En notant $\langle \cdot, \cdot \rangle$ le crochet de dualité entre $C_c^\infty(\mathcal{D})$ et son dual, la dérivée distributionnelle $\partial^\alpha u$ est *définie* comme la forme linéaire sur $C_c^\infty(\mathbb{R}^d)$ suivante, étant donné $\varphi \in C_c^\infty(\mathcal{D})$

$$\langle \partial^\alpha u, \varphi \rangle \coloneqq \langle u, (-1)^{|\alpha|} \partial^\alpha \varphi \rangle = (-1)^{|\alpha|} \int_{\mathcal{D}} u(x) \partial^\alpha \varphi(x) dx, \tag{1.3.16}$$

qui se trouve bien être continue sur $C_c^\infty(\mathcal{D})$ si u est localement intégrable. Notons que cette définition "copie" l'étape d'intégration par parties dans la définition des dérivées faibles, comme si $\langle \cdot, \cdot \rangle$ était le produit scalaire L^2. Ce calcul revient en fait à calculer l'adjoint de l'opérateur différentiel $\partial^\alpha : C_c^\infty(\mathcal{D}) \to C_c^\infty(\mathcal{D})$. Outre la formulation distributionnelle des EDPs, la théorie des distributions possède de nombreuses applications importantes, comme en analyse de Fourier ou en théorie des équations intégrales [139].

Fonction de Green L'approche distributionnelle peut sembler un peu artificielle ou inutilement compliquée. Pourtant l'étude de certaines solutions d'EDPs, centrales d'un point de vue physique, nécessitent l'adoption de ce point de vue. L'exemple le plus important est celui de la fonction de Green d'une EDP [19]. Etant donné un opérateur différentiel linéaire à coefficients constants $\mathcal{L}$, sa fonction de Green est la solution de l'équation suivante, posée sur $\mathbb{R}^d$:

$$\mathcal{L}G = \delta_0, \tag{1.3.17}$$

où δ_0 est la masse de Dirac en 0 [20]. Il est aussi possible de placer la masse de Dirac dans l'équation de bord (1.3.2), comme dans le cas de conditions initiales. Rappelons que la masse de Dirac peut être vue comme une mesure définie par $\int f(x)\delta_0(dx) = f(0)$ pour toute fonction continue f. En traitement du signal, G correspondrait à la réponse impulsionnelle de l'opérateur $\mathcal{L}$. Cette dernière a un rôle important car on peut ensuite écrire, au moins formellement, qu'une/la solution de l'EDP $\mathcal{L}u = f$ s'écrit comme $u = G * f$ où $(f * g)(x) = \int f(y)g(x-y)dy$. En effet, formellement,

$$\mathcal{L}(G * f)(x) = \mathcal{L} \int f(y)G(x-y)dy = \int f(y)(\mathcal{L}G)(x-y)dy$$

19. Cette fonction est mal nommée puisque nous verrons que ce n'est pas toujours une fonction à proprement parler.

20. La fonction de Green est parfois non unique ; son existence pour un opérateur linéaire à coefficients constants est assurée par le théorème de Malgrange-Ehrenpeis [33], p. 117.

$$= \int f(y)\delta_0(x-y)dy = (\delta_0 * f)(x) = f(x). \tag{1.3.18}$$

Informellement, la formule $u = G * f$ dit que "toute la physique" de $\mathcal{L}$ est contenue dans G.

Pour résoudre l'équation (1.3.17), nous ne pouvons pas suivre à la lettre la construction de la formulation faible (1.3.10) car le second membre δ_0 n'est pas un élément de L^2, ni même un élément du dual de $H^m(\mathbb{R}^d)$ (sauf si $m > d/2$). C'est cependant un élément du dual de $C_c^\infty(\mathbb{R}^d)$ et donc on peut considérer la formulation distributionnelle de l'équation (1.3.17). Pour l'équation de transport (1.3.14), sa fonction de Green est la mesure sur $\mathbb{R}\times\mathbb{R}$ donnée par $G = \mathbb{1}_{\mathbb{R}_+}(t)\delta_{at}(dx)dt$. Vérifions-le : soit $\varphi \in C_c^\infty(\mathbb{R}\times\mathbb{R})$ et notons $\psi(t) \coloneqq \varphi(at,t)$, de dérivée $\psi'(t) = a\partial_x\phi(at,t) + \partial_t\phi(at,t)$. La définition de la forme linéaire $\mathcal{L}G = \partial_t G + a\partial_x G$ sur $C_c^\infty(\mathbb{R}\times\mathbb{R})$ donne :

$$\begin{aligned}
\langle \mathcal{L}G, \varphi\rangle &= \langle \partial_t G + a\partial_x G, \varphi\rangle = -\langle G, \partial_t\varphi + a\partial_x\varphi\rangle \\
&= -\int_{-\infty}^{+\infty}\int_{-\infty}^{+\infty} (\partial_t\varphi + a\partial_x\varphi)(x,t)\mathbb{1}_{\mathbb{R}_+}(t)\delta_{at}(dx)dt \\
&= -\int_{-\infty}^{+\infty} (\partial_t\varphi + a\partial_x\varphi)(at,t)\mathbb{1}_{\mathbb{R}_+}(t)dt \\
&= -\int_0^{+\infty} (\partial_t\varphi + a\partial_x\varphi)(at,t)dt = -\int_0^{+\infty}\psi'(t)dt \\
&= \psi(0) = \varphi(0,0) = \langle \delta_{(0,0)}, \varphi\rangle.
\end{aligned}$$

Ainsi, $\mathcal{L}G = \delta_{(0,0)}$ dans l'espace des distributions. G est une mesure singulière par rapport à la mesure de Lebesgue de $\mathbb{R}\times\mathbb{R}$ et il est clair qu'une formulation faible n'aurait pas pu permettre de faire surgir G, puisque ce n'est pas une fonction ! Voici un autre exemple avec un sens physique plus important, avec l'équation des ondes en trois dimensions, $\frac{1}{c^2}\partial_{tt}G - \Delta G = \delta_0$. Dans ce cas, G s'interprête comme la détonation acoustique produite par un claquement de mains [21]. Sa fonction de Green est cette fois formellement donnée par $G(x,t) = \delta(t-|x|/c)/4\pi|x|$ où $|\cdot|$ dénote encore une fois la norme euclidienne, soit rigoureusement,

$$\forall\varphi \in C_c^\infty(\mathbb{R}^3\times\mathbb{R}), \quad \langle G,\varphi\rangle = \int_0^{+\infty}\int_{S(0,c|t|)} \frac{1}{4\pi c|t|}\varphi(x,t)\Omega(dx)dt. \tag{1.3.19}$$

Ici, Ω est la mesure de Lebesgue sur $S(0,c|t|)$, la sphère centrée en 0 de rayon $c|t|$. Nous renvoyons à la section 4.3.1 pour plus de détails sur cette intégrale. Dans ces deux exemples, la singularité de la fonction de Green est

21. Ceci explique l'envie irrépressible qu'ont de nombreux férus d'acoustique de claquer des mains dans les salles vides : ils calculent des fonctions de Green !

liée à l'hyperbolicité de l'EDP associée. A contrario, la fonction de Green de l'équation de la chaleur dans $\mathbb{R}^d$ est $G(x,t) = \mathbb{1}_{\mathbb{R}_+}(t)\exp(-|x|^2/4t)/(4\pi t)^{d/2}$, qui est analytique en espace.

Nous terminons cette section en soulignant que la formulation distributionnelle décorrèle les notions d' "être solution d'une EDP" et d' "être suffisamment régulier". En conséquence, la formulation distributionnelle fournit un cadre unifié pour traiter la grande majorité des EDPs linéaires (une exception notable concerne les EDPs de la forme $\mathrm{div}(a\nabla u) = f$ où a est peu régulière, par exemple $a \in L^\infty$; ce cas ne permet pas transférer toutes les dérivées sur la fonction test. Cette équation est l'équation de la chaleur stationnaire avec conductivité thermique a variable). La même chose ne peut être dite des formulations faibles.

En conclusion, nous avons donc introduit les notions d'espace de Sobolev, de dérivée faible et de dérivée distributionnelle, conjointement aux formulations associées. Nous avons aussi motivé le rôle central de ces différents points de vue dans la théorie des EDPs. La courte section suivante décrit la dernière étape de la résolution d'une EDP : sa résolution numérique.

1.3.4 Méthodes numériques pour la résolution des EDP

Puisque la plupart des EDPs n'ont pas de forme fermée pour leur solution, il est nécessaire de les résoudre à l'aide de méthodes numériques. Même dans les cas où l'EDP est linéaire et où sa fonction de Green est connue, le coût de calcul de la convolution peut être très grand, voire prohibitif [35] (comme quoi la fonction de Green ne fait pas tout). Ainsi, au même titre que l'étude théorique des EDPs, la conception et l'analyse de méthodes de résolution numérique des EDPs concerne encore aujourd'hui une grande part de la recherche mathématique.

Toute méthode numérique s'appuie sur une forme de discrétisation de l'EDP qu'elle vise à résoudre. Nous décrivons ci-dessous les principales méthodes numériques et leurs contextes d'utilisation. Selon le cas, ces méthodes sont plus ou moins adaptées aux EDPs linéaires et non linéaires.

• La méthode des éléments finis s'appuie sur la discrétisation de formulations faibles, en ne testant l'équation qu'avec un nombre fini de fonctions φ polynomiales par morceaux et en supposant en même temps que la solution appartient à l'espace engendré par ces fonctions. Elle nécessite un maillage non nécessairement cartésien ou régulier du domaine de résolution. Cette méthode est particulièrement adaptée aux équations elliptiques et paraboliques, car les systèmes linéaires résultants sont symétriques définis positifs. Cette méthode revient à calculer une projection orthogonale de la vraie solution sur l'espace engendré par les fonctions de test.

• La méthode des différences finies consiste à discrétiser les opérateurs différentiels de façon similaire à la méthode d'Euler. L'équation différentielle est ainsi remplacée par une équation de récurrence. Elle est très adaptée aux maillages cartésiens du domaine de résolution, puisque son étude repose sur des développements de Taylor. Nous l'étudierons plus en détail dans le chapitre 5.

• La méthode des volumes finis consiste à approcher la solution par ses moyennes locales (intégrales) sur des cellules numériques, non nécessairement structurées. Elle est particulièrement adaptée aux équations hyperboliques non linéaires (dont les solutions peuvent devenir discontinues) car elle ne suppose pas que la solution calculée est différentiable. Elle possède certains liens profonds avec la méthode des différences finies ([132], chapitre 4).

D'autres méthodes plus sophistiquées existent comme la méthode de Galerkine discontinue. Enfin, certaines méthodes sont directement basées sur la fonction de Green de l'équation, comme la méthode des éléments frontières.

Ayant ces principes théoriques et numériques en tête, nous terminons la section en décrivant plusieurs approches possibles pour aborder quelques problèmes d'apprentissage machine sous contraintes physiques.

1.3.5 Le problème de l'apprentissage machine sous contraintes d'EDP

Cette dernière section est dédiée à la description des différentes approches existantes concernant l'apprentissage machine sur des problèmes issus de la physique. La description de la combinaison des concepts des sections 1.2 (apprentissage machine) et 1.3 (EDPs) est quant à elle retardée à la section 1.4, dans laquelle nous détaillons les autres chapitres de la thèse.

Afin de fixer les idées, nous décrivons le type de problème qui nous motivera tout au long du manuscrit. Etant donné un ouvert $\mathcal{D} \subset \mathbb{R}^d$ dont on note $\partial\mathcal{D}$ le bord, et deux opérateurs différentiels non nécessairement linéaires, nous considérons l'EDP

$$\mathcal{L}_{\theta_{\mathcal{L}}}(u) = f \quad \text{dans} \quad \mathcal{D}, \quad \mathcal{B}_{\theta_{\mathcal{B}}}(u) = g \quad \text{dans} \quad \partial\mathcal{D}. \tag{1.3.20}$$

Ici, $\theta_{\mathcal{L}}$ et $\theta_{\mathcal{B}}$ désignent les paramètres des opérateurs $\mathcal{L}$ et $\mathcal{B}$, respectivement. Ils peuvent être fini-dimensionnel,s comme dans le cas de l'équation des ondes à célérité $c \in \mathbb{R}$ constante (milieu homogène), ou infini-dimensionnels, comme dans le cas de l'équation des ondes à célérité $c(x)$ variable en espace (milieu hétérogène). Nous nous donnons aussi un ensemble d'observations de la solution, par exemple de la forme $\mathcal{B} = \{(x_i, u(x_i) + \varepsilon_i)\}_{i\in\{1,\dots,n\}}$. Cela constitue

notre base de données. Etant donné $\mathcal{B}$ et le modèle (1.3.20), plusieurs questions possibles se posent, par exemple :

(i) comment estimer la fonction u ?

(ii) comment estimer les paramètres $\theta_{\mathcal{L}}$ et $\theta_{\mathcal{B}}$?

(iii) comment estimer les fonctions f et g ?

(iv) est-il possible de résoudre plusieurs de ces questions en même temps ?

Dans la section 1.2.1, nous avons décrit quelques particularités des problèmes issus de la physique, suggérant une approche hybride dans l'application de méthodes d'apprentissage machine sur de tels problèmes. Une première catégorie concerne des méthodes à noyau, et une deuxième concerne des méthodes basées sur des réseaux de neurones.

Noyaux informés par la physique Les propriétés des méthodes de regression à noyau sont entièrement contrôlées par celles du noyau utilisé. Pour certaines équations (linéaires en particulier), il est possible de fabriquer des fonctions définies positives telles que le RKHS associé soit un sous espace de l'ensemble des solutions de l'EDP étudiée. Cela revient aussi (formellement pour l'instant) à choisir un prior de processus gaussien dans lequel les contraintes physiques sont déjà respectées, au niveau des trajectoires du processus. En guise d'exemple, étant donné un noyau $k_0 : \mathbb{R}^d \times \mathbb{R}^d \to \mathbb{R}$ et $a \in \mathbb{R}^d$, le noyau espace-temps défini par

$$k((x,t),(x',t')) \coloneqq k_0(x - ta, x' - t'a) \tag{1.3.21}$$

vérifie, pour tout (x_0, t_0) (et au sens des distributions !),

$$\partial_t k(\cdot,(x_0,t_0)) + a^T \nabla k(\cdot,(x_0,t_0)) = 0, \tag{1.3.22}$$

Comme le RKHS associé est engendré par les fonctions de la forme $k(\cdot,(x_0,t_0))$ (section 1.2.4), il est uniquement constitué de solutions de cette équation. Nous pouvons donc penser qu'un modèle de régression utilisant ce noyau aura de très bonnes performances pour approcher les solutions de l'équation de transport (une telle méthode ne pourra cependant résoudre que cette équation). C'est ce type de noyau que nous étudierons dans les chapitres 2 et 4. Nous renvoyons à ces deux chapitres pour une présentation de la littérature associée. Par ailleurs, les propriétés de stabilité par linéarité des processus gaussiens suggèrent que le modèle probabiliste associé peut lui aussi bien se comporter par rapport aux contraintes strictes d'EDPs linéaires.

Régression à noyau sous contrainte locale d'EDP Dans l'ouvrage de référence [212] (section 16.3) datant de 2004, une méthode d'interpolation à noyau permettant de résoudre des EDPs linéaires est décrite. Cette méthode consiste à résoudre le problème (1.2.27) en imposant la contrainte d'EDP $\mathcal{L}(u)(x_i) = f(x_i)$ en des points $(x_1, ..., x_n)$ appelés points de collocation. En effet, l'opération $u \mapsto \mathcal{L}(u)(x_i)$ pouvant être vue comme une forme linéaire continue sur un RKHS si le noyau associé est suffisamment régulier. Cette méthode ancienne a depuis été généralisée aux EDPs non linéaires dans l'article récent [36], ouvrant ainsi la voie à de nombreuses applications. Fait non négligeable, l'article [36] fournit un théorème de convergence de l'interpolant vers la solution lorsque les points de collocation remplissent le domaine d'interpolation, si la solution est forte (i.e. vérifie l'EDP ponctuellement). Ce manuscrit ne traite pas directement de cette méthode ; cependant, les résultats quantitatifs présentés dans le chapitre 3 ouvrent des perspectives d'applications pour cette méthode et son étude théorique de en particulier.

Il est par ailleurs possible de combiner cette approche avec les noyaux informés par la physique, notamment dans le cas d'un système d'équations combinant EDPs linéaires et non linéaires. C'est par exemple le cas pour les équations de Navier-Stokes, pour lesquelles une telle démarche a été décrite dans [153].

Réseaux de neurones informés par la physique Les *physics-informed neural networks* (PINNs) sont une méthode de régression pouvant être appliquée dans les modèles directs et inverses, dans laquelle la contrainte physique apparaît dans la fonction de coût [162, 112]. Etant donné une équation aux dérivées partielles potentiellement non linéaire $\mathcal{L}(u) = 0$, un ensemble de données d'observation $\{(x_i, u(x_i))\}_{1\leq i\leq n}$ et $\{y_j\}_{1\leq j\leq p}$ des points de collocation cible, la méthode consiste à entraîner un réseau de neurones R_θ en trouvant les poids qui minimisent la fonction de coût

$$S(\theta) \coloneqq \frac{1}{n}\sum_{i=1}^{n}(R_\theta(x_i) - u(x_i))^2 + \frac{1}{p}\sum_{j=1}^{p}[\mathcal{L}(R_\theta)(y_j)]^2. \tag{1.3.23}$$

La première somme mesure l'erreur d'approximation sur les observations, et la deuxième somme pénalise le non-respect de l'équation aux points de collocation. Contrairement aux deux approches précédentes, il n'y a aucune garantie que la contrainte d'EDP soit effectivement imposée sur le réseau de neurones, même approximativement, et même aux points de collocation. Dans les faits, les PINNs peuvent résoudre certains problèmes complexes avec une efficacité remarquable [165], mais peuvent aussi échouer sur des exemples simples ([206], section 6).

Réseaux de neurones à valeurs fonctionnelles Les réseaux de neurones peuvent être utilisés pour approcher une application entre deux espaces de fonctions. Une première approche est celle des "DeepONet" [138] (Le "O" désigne le mot "opérateur"). Cette approche est justifiée par un théorème d'approximation universelle pour certaines applications continues entre espaces de Banach. Une deuxième approche concerne les *Fourier neural operators* [116], qui ont aussi été utilisés dans des contextes de réduction de modèle [133, 25].

1.4 Description des chapitres

La question du choix d'un prior gaussien Afin de traiter les questions soulevées dans la section 1.3.5 concernant l'équation (1.3.20), nous allons considérer un prior de processus gaussien sur la solution u à des fins de régression. Se pose alors immédiatement la question du choix d'un tel prior : quels sont les "bons" processus gaussiens au vu de la contrainte de modèle (1.3.20) ? Pour traiter cette question, un point important est d'abord le sens que l'on donne à l'équation (1.3.20) : ponctuel, faible ou distributionnel (ou autre chose). Une question intimement liée est celle de la régularité Sobolev d'un processus gaussien. Nous étudierons ces propriétés au niveau des réalisations (trajectoires) du processus, en vertu de la modélisation décrite en section 1.2.3 et de l'application (1.2.13) en particulier. De même que dans la proposition 1.2.6, les processus gaussiens dont les trajectoires sont contenues dans $W^{m,p}(\mathcal{D})$ presque sûrement fournissent naturellement une mesure gaussienne sur le même espace de Sobolev.

Il se trouve aussi qu'un bon nombre d'EDPs importantes sont linéaires et homogènes, ce dernier terme signifiant que dans (1.3.20), le terme source f est nul dans l'équation intérieure. Ce type d'équation correspond à des lois de conservation. Dans ce cas, l'information que $f \equiv 0$ peut être prise comme une information a priori, et l'on pourra directement chercher les processus gaussiens dont toutes les trajectoires vérifient la contrainte $\mathcal{L}u = 0$. De telles propriétés sont parfois connues comme des propriétés de "dégénerescence" [86].

Enfin, l'évaluation numérique de la moyenne a posteriori d'un prior de processus gaussien gaussien adapté à une EDP peut se comprendre comme une forme de méthode numérique. Il convient donc d'étudier s'il existe des correspondances entre une telle méthode d'approximation de fonction et les méthodes numériques classiques de résolution des EDPs.

Toutes ces observations mènent au cahier des charges suivant, auquel nous essaieront d'apporter des éléments de réponse.

(i) Caractériser les priors de processus gaussiens compatibles avec des contraintes d'EDPs linéaires, avec éventuellement une méthode constructive accom-

pagnée d'exemples explicites. Comme la formulation distributionnelle permet de traiter la grande majorité des EDPs linéaires, ce cadre semble adapté pour une première étude.

(*ii*) Comprendre comment caractériser et contrôler la régularité Sobolev des processus gaussiens, si possible dans un cadre assez général.

(*iii*) Comprendre comment les méthodes à noyau se positionnent par rapport aux méthodes numériques déjà connues. En particulier, le point de vue bayésien peut peut-être venir enrichir ou éclairer les méthodes numériques classiques.

Les différents chapitres du manuscrit offrent chacun des éléments de réponse aux questions soulevées plus haut. Les chapitres 2 et 3 traitent de questions théoriques, et les chapitres 4 et 5 traitent de questions plus appliquées. Plus spécifiquement :

• Le chapitre 2, qui correspond à l'article [97], donne une caractérisation des processus aléatoires à variance finie (non nécessairement gaussiens) dont presque toutes les trajecteoires vérifient la même EDP linéaire et homogène, au sens des distributions. Le résultat est ensuite appliqué sur deux EDPs hyperboliques : l'équation d'advection et l'équation des ondes en trois dimensions, centrale en acoustique et en électromagnétisme notamment.

• Le chapitre 3, qui correspond à l'article [96], donne plusieurs conditions nécessaires et suffisantes pour que les trajectoires d'un processus gaussien soient presque surement contenues dans l'espace de Sobolev $W^{m,p}(\mathcal{D})$, où $m \in \mathbb{N}, 1 < p < +\infty$ et où $\mathcal{D}$ est un ouvert quelconque de $\mathbb{R}^d$. Ces résultats sont accompagnés de bornes utilisables en pratique. Une courte section discute ensuite d'applications en régression par processus gaussiens, en ce qui concerne la sélection de noyaux compatibles avec la régularité Sobolev.

• Le chapitre 4, qui correspond à l'article [98], décrit certains priors de processus gaussiens explicites dont les trajectroires vérifient l'équation des ondes. Il est une continuation du chapitre 2. Plusieurs applications de tels priors sont ensuite décrites, notamment pour l'estimation des paramètres de l'EDP et la reconstruction de ses conditions initiales. Un lien inattendu est établi entre cette méthode et la localisation GPS.

• Le chapitre 5 décrit certains liens explicites entre quelques schémas numériques classiques et certains régimes de régression par processus gaussiens. Ceux-ci concernent le régime dit de la "limite plate" (*flat limits*), ainsi qu'un régime non asymptotique contraint aux équations dites de "consistance" des schémas aux différences finies. Une partie est consacrée aux conditions aux bords transparentes.

Les sections qui suivent présentent chacune un résumé de chaque chapitre. Les résultats principaux y sont décrits, parfois accompagnés d'éléments de preuves.

1.4.1 Chapitre 2 : processus aléatoires sous contraintes distributionnelles d'EDPs linéaires

Contraindre les trajectoires en contraignant le noyau De façon très générale, étant donné un processus aléatoire U centré d'ordre deux (i.e. vérifiant $\mathbb{E}[U(x)^2] < +\infty$ pour tout x) et un opérateur linéaire $\mathcal{L} : E \to F$ où E contient presque sûrement les trajectoires de U, il est commun d'avoir l'équivalence suivante :

$$\mathbb{P}(\{\omega \in \Omega : \mathcal{L}(U_\omega) = 0\}) = 1 \iff \forall x \in E, \mathcal{L}(k_x) = 0. \tag{1.4.1}$$

L'article [86] décrit de telles correspondances dans un certain nombre de cadres différents. Le but de ce chapitre est d'obtenir un critère de ce type lorsque $\mathcal{L}$ est un opérateur différentiel. Pour cela, nous considérons un ouvert $\mathcal{D} \subset \mathbb{R}^d$ et un opérateur différentiel linéaire $\mathcal{L}$ d'ordre m sur $\mathcal{D}$, donné par

$$\mathcal{L}u = \sum_{|\alpha| \leq m} a_\alpha \partial^\alpha u. \tag{1.4.2}$$

Ici, les coefficients a_α non nécessairement constants sont supposés de classe $C^{|\alpha|}(\mathcal{D})$. L'adjoint formel de $\mathcal{L}$ (obtenu par intégrations par parties successives contre des éléments de $C_c^\infty(\mathcal{D})$) est défini comme

$$\mathcal{L}^*\varphi := \sum_{|\alpha| \leq m} (-1)^{|\alpha|} \partial^\alpha (a_\alpha \varphi). \tag{1.4.3}$$

Ainsi, la formulation distributionnelle de l'EDP $\mathcal{L}u = 0$ s'écrit

$$\forall \varphi \in C_c^\infty(\mathcal{D}), \quad \int_{\mathcal{D}} u(x) \mathcal{L}^*\varphi(x) dx = 0. \tag{1.4.4}$$

La question que nous nous posons est la suivante : peut-on caractériser les processus aléatoires $(U(x))_{x \in \mathcal{D}}$ centrés d'ordre d'ordre deux dont les trajectoires vérifient l'équation (1.4.4) avec probabilité 1 ? La réponse est oui et constitue le résultat principal du chapitre. Nous donnons ce résultat dans la proposition 1.4.1 ci-dessous. Notons qu'ici, la formulation distributionnelle permet de s'affranchir d'hypothèses de gaussianité sur le processus $(U(x))_{x \in \mathcal{D}}$. Nous notons aussi $L^1_{loc}(\mathcal{D})$ l'ensemble des fonctions f telles que $\int_K |f| < +\infty$ pour tout compact $K \subset \mathcal{D}$.

Proposition 1.4.1. *Supposons que $(U(x))_{x\in\mathcal{D}}$ soit mesurable et centré, et que $\sigma \in L^1_{loc}(\mathcal{D})$, où $\sigma : x \mapsto k(x,x)^{1/2}$ et k est sa fonction de covariance.*
1) Alors $\mathbb{P}(U \in L^1_{loc}(\mathcal{D})) = 1$ et pour tout $x \in \mathcal{D}, k_x \in L^1_{loc}(\mathcal{D})$.
2) Les deux points suivants sont équivalents :

(i) $\mathbb{P}(\mathcal{L}(U) = 0$ *au sens des distributions*$) = 1$.

(ii) $\forall x \in \mathcal{D},\ \mathcal{L}(k_x) = 0$ *au sens des distributions.*

Explicitement, le point (i) signifie qu'il existe un évenement $A \in \mathcal{F}$ avec $\mathbb{P}(A) = 1$ tel que

$$\forall \omega \in A, \quad \forall \varphi \in C_c^\infty(\mathcal{D}), \quad \int_{\mathcal{D}} U_\omega(x)\mathcal{L}^*\varphi(x)dx = 0. \tag{1.4.5}$$

Une généralisation directe au cas non centré est donné dans la proposition 2.3.5. La stratégie de preuve est assez simple, et repose sur des applications répétées du théorème de Fubini ; ceci explique pourquoi l'hypothèse de mesurabilité du processus est quasi inévitable. Une partie conséquente de la preuve complète consiste à vérifier que les hypothèses d'intégrabilité du théorème de Fubini sont vérifiées. L'autre hypothèse de régularité, $\sigma \in L^1_{loc}(\mathcal{D})$, sert en fait à assurer la continuité d'un certain nombre de formes linéaires sur $C_c^\infty(\mathcal{D})$, ainsi que les hypothèses d'intégrabilité du théorème de Fubini.

Avant de commencer l'esquisse de preuve, citons une des définitions équivalentes de la topologie de $C_c^\infty(\mathcal{D})$, où $\mathcal{D}$ est un ouvert de $\mathbb{R}^d$. Rappelons que $\mathrm{Supp}(f)$, le support d'une fonction f, est la fermeture dans $\mathcal{D}$ de l'ensemble $\{x \in \mathcal{D} : f(x) \neq 0\}$. La topologie de $C_c^\infty(\mathcal{D})$ est celle correspondant à la notion de convergence suivante : φ_n converge vers φ dans $C_c^\infty(\mathcal{D})$ s'il existe un compact $K \subset \mathcal{D}$ tel que pour tout entier n, $\mathrm{Supp}(\varphi_n) \subset K$ et pour tout $\alpha \in \mathbb{N}^d, \|\partial^\alpha\varphi_n - \partial^\alpha\varphi\|_\infty \to 0$ (convergence uniforme des dérivées de tout ordre).

Esquisse de preuve. Nous admettons le point (1), qui se vérifie facilement grâce au théorème de Fubini, et aux estimations $\mathbb{E}[|U(x)|] \leq \sigma(x)$ et $|k_x(y)| \leq \sigma(x)\sigma(y)$ (deux inégalités de Cauchy-Schwarz). Le point (1) assure que les points $(2)(i)$ et $(2)(ii)$ ont bien un sens, du point de vue des distributions.
$\underline{(i) \implies (ii)}$: on se donne une fonction test $\varphi \in C_c^\infty(\mathcal{D})$. Nous pouvons ensuite écrire

$$\begin{aligned} 0 &= \mathbb{E}\left[U(x')\int_{\mathcal{D}} U(x)\mathcal{L}^*\varphi(x)dx\right] = \int_{\mathcal{D}} \mathcal{L}^*\varphi(x)\mathbb{E}[U(x)U(x')]dx \\ &= \int_{\mathcal{D}} \mathcal{L}^*\varphi(x)k(x,x')dx. \end{aligned}$$

Comme cette propriété est vraie pour tout $\varphi \in C_c^\infty(\mathcal{D})$, cela donne bien le point (ii).
$(ii) \implies (i)$: on se donne encore une fonction test $\varphi \in C_c^\infty(\mathcal{D})$, et on montre dans un premier temps que la variable aléatoire $U_\varphi := \int_{\mathcal{D}} U(x)\mathcal{L}^*\varphi(x)dx$ est nulle presque sûrement. Il suffit pour cela de montrer que $\mathbb{E}[U_\varphi^2] = 0$, et par le point (ii) on a en effet que

$$\begin{aligned} 0 &= \int_{\mathcal{D}} \mathcal{L}^*\varphi(x') \left(\int_{\mathcal{D}} \mathcal{L}^*\varphi(x) k(x,x') dx \right) dx' \\ &= \int_{\mathcal{D}} \int_{\mathcal{D}} \mathcal{L}^*\varphi(x)\mathcal{L}^*\varphi(x')\mathbb{E}[U(x)U(x')] dx dx' \\ &= \mathbb{E}\left[\left(\int_{\mathcal{D}} \mathcal{L}^*\varphi(x) U(x) dx \right)^2 \right] = \mathbb{E}\big[U_\varphi^2\big]. \end{aligned}$$

Cela fournit donc un ensemble $A_\varphi \subset \Omega$ de probabilité 1 sur lequel la variable U_φ est nulle. Le candidat naturel pour la partie A dans l'équation (1.4.5) est donc

$$A \coloneqq \bigcap_{\varphi \in C_c^\infty(\mathcal{D})} A_\varphi. \tag{1.4.6}$$

Malheureusement, cette intersection est indénombrable, et donc A n'a aucune raison d'être de probabilité 1 ni même d'être mesurable. Pour résoudre ce problème, nous allons utiliser deux faits. Premièrement, l'espace $C_c^\infty(\mathcal{D})$ est *séquentiellement séparable* muni de sa topologie usuelle, ce qui signifie qu'il existe une partie $F \subset C_c^\infty(\mathcal{D})$ dénombrable telle que pour tout $\varphi \in C_c^\infty(\mathcal{D})$, il existe une suite $(\varphi_n) \subset F$ telle que $\varphi_n \to \varphi$ au sens de la topologie de $C_c^\infty(\mathcal{D})$ (c'est le contenu du lemme 2.3.6). Deuxièmement, toutes les intégrales de la forme $\int_{\mathcal{D}} v(x)\mathcal{L}^*\varphi(x)dx$ avec $v \in L^1_{loc}(\mathcal{D})$ sont, en tant que fonction de φ, des formes linéaires séquentiellement continues sur $C_c^\infty(\mathcal{D})$ muni de la même topologie (c'est ici que l'hypothèse $a_\alpha \in C^{|\alpha|}$ intervient). Rappelons que par le point (1), les trajectoires de U sont dans $L^1_{loc}(\mathcal{D})$ presque sûrement ; notons B l'évènement associé, de probabilité 1. Ainsi, en considérant l'ensemble

$$A \coloneqq B \cap \left(\bigcap_{\varphi \in F} A_\varphi \right), \tag{1.4.7}$$

nous pouvons en fait montrer que le contrainte de nullité sur F implique la nullité pour toutes les fonctions tests, c'est à dire que

$$\forall \omega \in A, \quad \forall \varphi \in C_c^\infty(\mathcal{D}), \quad \int_{\mathcal{D}} U_\omega(x)\mathcal{L}^*\varphi(x)dx = 0. \tag{1.4.8}$$

De plus, on a bien cette fois que $\mathbb{P}(A) = 1$, puisque F est dénombrable et que $\mathbb{P}(A_\varphi) = 1$ pour tout $\varphi \in F$. Ceci termine la preuve de $(ii) \implies (i)$. □

Cette preuve montre que l'hypothèse que $\sigma \in L^1_{loc}(\mathcal{D})$, en apparence inoffensive, est en fait cruciale : c'est la bonne hypothèse à utiliser conjointement à la séparabilité séquentielle de de $C^\infty_c(\mathcal{D})$, afin de permuter les quantificateurs "presque sûrement" et "pour tout $\varphi \in C^\infty_c(\mathcal{D})$". Enfin, dans le cas des processus gaussiens mesurables, notons que le fait que $\mathbb{P}(U \in L^1_{loc}(\mathcal{D})) = 1$ implique en fait que $\sigma \in L^1_{loc}(\mathcal{D})$ (appliquer par exemple l'équation (3.2.30) de la proposition 3.2.9).

Une première application à l'équation des ondes La caractérisation de la proposition 1.4.1 est agréable, notamment concernant l'étude de modèles de covariance pour les EDPs hyperboliques dont les solutions sont parfois peu régulières. C'est pourquoi la deuxième partie du chapitre est dédiée à la description des fonctions de covariance pour l'équation des ondes en trois dimensions, centrale en acoustique et en électromagnétisme :

$$\big(\frac{1}{c^2}\partial^2_{tt} - \Delta\big)w = 0 \qquad \forall (x,t) \in \mathbb{R}^3 \times \mathbb{R}^*_+, \tag{1.4.9}$$

munie des conditions initiales $u(x,0) = u_0(x)$ et $(\partial_t u)(x,0) = v_0(x)$. Pour cela, nous nous reposons sur une formule de représentation de la solution, la formule de Kirschhoff :

$$w(x,t) = \int_{S(0,1)} t v_0(x - c|t|\gamma) + u_0(x - c|t|\gamma) - c|t|\gamma \cdot \nabla u_0(x - c|t|\gamma)\frac{d\Omega}{4\pi}.$$

Cette formule s'écrit en fait de façon compacte à l'aide de convolutions des conditions initiales contre des distributions :

$$w(x,t) = (F_t * v_0)(x) + (\dot{F}_t * u_0)(x) \qquad \forall (x,t) \in \mathbb{R}^3 \times \mathbb{R}^*_+. \tag{1.4.10}$$

Ici, F_t est un multiple de la mesure de Lebesgue sur la sphère de centre 0 et de rayon $c|t|$, et $\dot{F}_t$ désigne sa dérivée temporelle, au sens des distributions. Cette représentation permet en fait de décrire les fonctions de covariance des processus dont les trajectoires sont solutions de l'équation (1.4.9). En effet, choisissons des priors de processus gaussiens indépendants sur les conditions initiales, $U^0 \sim GP(0, k_{\mathrm{u}})$ and $V^0 \sim GP(0, k_{\mathrm{v}})$ (avec hypothèses minimales sur k_{u} et k_{v} données dans le chapitre 2). En notant $z = (x,t)$ la variable spatio-temporelle, nous obtenons deux processus stochastiques définis par des intégrales de trajectoires,

$$V(z) : \omega \longmapsto (F_t * V^0_\omega)(x) \;\text{ et }\; U(z) : \omega \longmapsto (\dot{F}_t * U^0_\omega)(x). \tag{1.4.11}$$

et nous définissons leur somme par $W(z) = U(z) + V(z)$. La proposition suivante décrit les lois des processus U, V et W.

Proposition 1.4.2. *Définissons les deux fonctions*

$$k_{\mathrm{v}}^{\mathrm{wave}}(z,z') := [(F_t \otimes F_{t'}) * k_{\mathrm{v}}](x,x'), \tag{1.4.12}$$
$$k_{\mathrm{u}}^{\mathrm{wave}}(z,z') := [(\dot{F}_t \otimes \dot{F}_{t'}) * k_{\mathrm{u}}](x,x'). \tag{1.4.13}$$

(i) Alors $U = (U(z))_{z\in\mathbb{R}^3\times\mathbb{R}}$ *et* $V = (V(z))_{z\in\mathbb{R}^3\times\mathbb{R}}$ *définis dans l'équation* (1.4.11) *sont deux processus gaussiens centrés et indépendants, de fonctions de covariance* $k_{\mathrm{u}}^{\mathrm{wave}}$ *et* $k_{\mathrm{v}}^{\mathrm{wave}}$ *respectivement. En conséquence,* $(W(z))_{z\in\mathbb{R}^3\times\mathbb{R}}$ *est un processus gaussien centré de fonction de covariance*

$$k_W(z,z') = k_{\mathrm{v}}^{\mathrm{wave}}(z,z') + k_{\mathrm{u}}^{\mathrm{wave}}(z,z'). \tag{1.4.14}$$

(ii) Réciproquement, tout processus aléatoire mesurable d'ordre deux dont la fonction de covariance est k_W *a ses trajectoires solutions de l'équation des ondes* (2.4.1)*, au sens des distributions, presque sûrement.*

Ce résultat est encore une fois le fruit d'applications répétées du théorème de Fubini. La difficulté se situe essentiellement dans la vérification des hypothèses d'intégrabilité, et dans la définition de $(\dot{F}_t \otimes \dot{F}_{t'}) * k_{\mathrm{u}}$. Notons que nous pouvons donner un sens à ces formules pour $t < 0$, grâce à la réversibilité de l'équation des ondes (section 2.4.1).

Perspectives La représentation agréable du noyau de covariance du processus solution W suggère la possibilité d'applications pratiques pour l'équation des ondes. Cette question est l'objet du chapitre 4. De plus, un théorème général décrivant les noyaux vérifiant la contrainte du point (ii) de la proposition 1.4.1 (par exemple à l'aide de fonctions de Green) serait un bon complément à cette même proposition. Des applications pratiques à des équations dont les coefficients sont non constants constituent aussi une direction de recherche intéressante.

1.4.2 Chapitre 3 : régularité Sobolev des trajectoires d'un processus gaussien

Ce chapitre est le plus long et le plus technique de ce manuscrit. En comparaison avec les autres chapitres, j'ai donc fait le choix d'aller un peu plus loin dans la présentation des résultats, outils techniques et idées de preuve du chapitre. Quelques discussions et comparaisons préliminaires (non présentes dans le chapitre 3) concernant l'étude de la régularité classique des processus gaussiens sont aussi fournies.

Continuité des processus gaussiens et mesures gaussiennes sur les espaces L^p Dans l'introduction, nous avons motivé l'importance de la régularité de type Sobolev dans l'étude des équations aux dérivées partielles. De façon étonnante, la régularité Sobolev des trajectoires des processus gaussiens généraux est pourtant assez peu étudiée, notamment dans sa définition générale (ouvert $\mathcal{D} \subset \mathbb{R}^d$ quelconque). Ceci entre en contrast avec les travaux consacrés à l'étude de leur régularité classique (C^k), à mon avis pourtant plus difficile à maîtriser, en témoigne le chapitre 1 de [2]. Il se trouve aussi les méthodes les plus fines de contrôle de la régularité classique des trajectoires des processus gaussiens nécessitent des outils relativement difficiles à mettre en oeuvre en pratique : entropie métrique ([2], section 1.3), mesures majorantes ([2], section 1.5) ou encore chaînage ([199], Appendix B). Une des conditions suffisantes les plus manipulables dans les applications est la suivante, conséquence de la borne d'entropie métrique de Dudley ([199], équation (A.23)) :

Proposition 1.4.3 ([2], théorème 1.4.1)**.** *Soit $(U(x))_{x\in\mathcal{D}}$ un processus gaussien, où $\mathcal{D} \subset \mathbb{R}^d$. Posons $d(s,t)^2 := \mathbb{E}[(U(s)-U(t))^2]$ et $p(u) := \sup_{|s-t|\leq u} d(s,t)$ (mesurable car croissante). Supposons qu'il existe $\delta > 0$ tel que*

$$\int_\delta^{+\infty} p\big(e^{-u^2}\big)du < +\infty. \tag{1.4.15}$$

Alors il existe une modification du processus $(U(x))_{x\in\mathcal{D}}$ à trajectoires continues presque sûrement.

Cette caractérisation est aussi nécessaire dans le cas stationnaire, sous une condition supplémentaire de décroissance de la fonction de covariance ([2], Corollaire 1.5.5). Elle ne l'est pas dans le cas générale ([2], contre-exemple p. 20) [22]. Les conditions nécessaires et suffisantes de continuité sont difficiles à établir ; une réponse est donnée par la théorie des mesures majorantes ([2], théorème 1.5.1 ; voir aussi [199]).

Dans le cas de la continuité trajectorielle des processus gaussiens, un des principes centraux est le fait que cette propriété est quasiment équivalente au fait d'être fini presque sûrement ([2], théorème 1.5.4 ou plusieurs endroits dans [67]). En effet, la continuité peut se contrôler à l'aide du module de continuité, qui est lui-même un supremum ([2], p. 14). En un certain sens, nous utiliserons le même type de correspondance en écrivant la norme L^p comme un supremum indexé par la boule unité de L^q, $q = p/(p-1)$, en vertu de la dualité (réciproque, par réflexité) entre L^p et L^q lorsque $p \in (1, +\infty)$.

Les caractérisations de la régularité $W^{m,p}$ que nous obtenons sont de plusieurs natures. Elles offrent différentes interprétations d'une même propriété,

22. Il y a d'ailleurs une coquille dans ce contre-exemple de [2] : il faut prendre $f(t) = w(\sqrt{h(t)})$, $t \in [0,1]$, où $w(t)$ est le mouvement brownien standard et $h(t) = \ln 4/\ln(4/t)$.

ainsi que différents moyens de construction et de vérification qu'un processus gaussien à ses trajectoires dans $W^{m,p}$.

- L'une est intégrale, à la manière du critère de l'équation (1.2.17).
- L'une est "spectrale", à la manière de la décomposition de Mercer.
- L'une s'exprime à travers les propriétés du RKHS du noyau du processus, à la manière du théorème de Driscoll ([111], théorème 4.9).

Il se trouve qu'une partie de l'étude, pour la décomposition de Mercer "généralisée" en particulier, a déjà été faite si l'on se ramène à l'étude de mesures gaussiennes sur L^p. En effet, le noyau de covariance k d'un processus gaussien mesurable à trajectoires dans $L^p(\mathcal{D})$ engendre un opérateur intégral $\mathcal{E}_k : L^q(\mathcal{D}) \to L^p(\mathcal{D})$ qui se trouve être l'opérateur de covariance de la mesure gaussienne engendrée par le processus gaussien. $\mathcal{E}_k$ est défini par

$$\mathcal{E}_k f(x) := \int_{\mathcal{D}} k(x,y) f(y) dy. \tag{1.4.16}$$

Notons que l'injectivité de l'application $k \mapsto \mathcal{E}_k$ (avec espaces de départ et d'arrivée appropriés...) est assurée par le théorème du noyau de Schwartz ([202], theorème 51.7 ; voir l'équation (3.4.36) pour une application). Si $p \in [2, +\infty)$, les opérateurs de covariance des mesures gaussiennes sur $L^p(\mathcal{D})$ sont exactement les opérateurs symmétriques, positifs et nucléaires, ce qui signifie qu'il existe une décomposition du noyau k, dans $L^p(\mathcal{D} \times \mathcal{D})$, de la forme suivante :

$$k = \sum_{n=0}^{+\infty} \lambda_n e_n \otimes e_n, \tag{1.4.17}$$

où $(\lambda_n) \subset \mathbb{R}_+, (e_n) \subset L^p(\mathcal{D})$ et où $\sum_n \lambda_n \|e_n\|_p^2 < +\infty$ (convergence absolue de la série de fonctions (1.4.17)). la norme nucléaire de $\mathcal{E}_k$ est définie comme

$$\nu(\mathcal{E}_k) := \inf \left\{ \sum_{n=0}^{+\infty} \|x_n\|_p \|y_n\|_p \text{ tel que } \mathcal{E}_k = \sum_{n=0}^{+\infty} x_n \otimes y_n \right\}. \tag{1.4.18}$$

Dans le cas $p = 2$, cela correspond exactement aux opérateurs autoadjoints positifs à trace finie (spectre sommable). Dans le cas où $p \in [1, 2)$, tous les opérateurs de la forme (1.4.17) ne sont pas des opérateurs de covariance de mesure gaussienne (voir l'exemple 3.2.10). Pour obtenir des opérateurs de covariance de mesure gaussienne, il est nécessaire et suffisant de rajouter la condition supplémentaire que les vecteurs e_n puissent être obtenus comme l'image d'une base orthonormée (g_n) de $L^2(\mathcal{D})$ par un opérateur linéaire continu $A : L^2(\mathcal{D}) \to L^p(\mathcal{D})$ $(e_n = Ag_n)$.

Le cadre général que nous considérons est le suivant. Nous nous donnons un ouvert $\mathcal{D} \subset \mathbb{R}^d$ quelconque, un processus gaussien $(U(x))_{x\in\mathcal{D}}$ mesurable, et nous souhaitons étudier la régularité $W^{m,p}(\mathcal{D})$ des trajectoires du processus $(U(x))_{x\in\mathcal{D}}$ étant donné un entier $m \in \mathbb{N}$ et un exposant $p \in (1, +\infty)$. Nous justifions plus tard l'exclusion des cas $p = 1$ et $p = \infty$. Notons que nous ne faisons pas d'hypothèses de continuité sur le noyau k ainsi que sur les trajectoires du processus. Ceci sort du cadre standard de l'étude des processus aléatoires, qui sont quasi systématiquement supposés à trajectoires continues au moins en probabilité ([63], théorème 2.6 ou [127], section 6.5.1). Comme évoqué dans la section 1.3.2, il est néanmoins important (au moins dans un premier temps) de s'écarter de telles hypothèses de régularité classique dans l'étude des EDPs.

Une caractérisation dénombrable de la régularité Sobolev pour les fonctions localement intégrables Le cas où $\mathcal{D}$ est un ouvert quelconque interdit des caractérisations à l'aide de la transformée de Fourier. En effet, cette approche n'est valide que dans le cas $\mathcal{D} = \mathbb{R}^d$, et l'existence d'un opérateur d'extension $E : W^{m,p}(\mathcal{D}) \to W^{m,p}(\mathbb{R}^d)$ permettant de se ramener au cas $\mathcal{D} = \mathbb{R}^d$ n'est assurée que lorsque $\mathcal{D}$ est suffisamment régulier ([169], théorèmes 5.24 et 5.28).

En l'absence d'approche de type Fourier, la régularité Sobolev se caractérise par des propriétés variationnelles sur l'espace $C_c^\infty(\mathcal{D})$ ainsi qu'en terme d'opérateur de différences finies. Les caractérisations que nous utiliserons sont décrites ci-dessous, dans le cas simplifié où $\mathcal{D} = \mathbb{R}$ et où $m = 1$. Le cas général (identique en essence) est présenté dans la proposition 3.2.1. L'hypothèse minimale pour manipuler ces caractérisations est encore une fois la régularité L^1_{loc}. Soit $p \in (1, +\infty)$. Nous notons $\|\cdot\|_p := \|\cdot\|_{L^p}, q := p/(p-1)$, et τ_h l'opérateur de translation par h, soit $(\tau_h u)(x) := u(x + h)$.

Proposition 1.4.4. *Soit $u \in L^1_{loc}(\mathbb{R})$. Alors il y a équivalence entre les faits suivants.*

(i) $u \in W^{1,p}(\mathbb{R})$.

(ii) Les deux suprema suivants sont finis :

$$\sup_{\varphi\in C_c^\infty(\mathbb{R})\setminus\{0\}} \left| \int_{\mathbb{R}} u(x) \frac{\varphi(x)}{\|\varphi\|_q} dx \right| < +\infty, \tag{1.4.19}$$

$$\sup_{\varphi\in C_c^\infty(\mathbb{R})\setminus\{0\}} \left| \int_{\mathbb{R}} u(x) \frac{\varphi'(x)}{\|\varphi\|_q} dx \right| < +\infty. \tag{1.4.20}$$

auquel cas, ces suprema valent $\|u\|_p$ et $\|u'\|_p$ respectivement.

(iii) Il existe une constante $C > 0$ telle que pour tout $h > 0$,

$$\|\tau_h u - u\|_p \leq Ch. \tag{1.4.21}$$

auquel cas nous pouvons prendre $C = ||u||_{W^{1,p}}$.

Les équations (1.4.19) et (1.4.20) impliquent que $u \in L^p(\mathbb{R})$ et $u' \in L^p(\mathbb{R})$, respectivement. Ce sont des applications du lemme de Riesz dans $L^p(\mathbb{R})$ pour $p \in (1, +\infty)$, conjointement à la densité de $C_c^\infty(\mathcal{D})$ dans $L^p(\mathcal{D})$. Le point *(iii)* sera utile lorsque nous étudierons la caractérisation de la régularité H^m des trajectoires selon les propriétés du RKHS du processus. Quant au point *(ii)*, il nous incite à considérer les variables aléatoires $U_\varphi(\omega) := \int_{\mathbb{R}} U_\omega(x)\varphi'(x)dx/\|\varphi\|_q$, puis à montrer que l'application

$$|U| : \omega \mapsto \sup_{\varphi \in C_c^\infty(\mathbb{R})\setminus\{0\}} |U_\varphi(\omega)|, \tag{1.4.22}$$

est finie presque sûrement. Une condition suffisante (qui se trouvera être aussi nécessaire) pour le montrer est de prouver que $\mathbb{E}\big[|U|\big] < +\infty$. Malheureusement, comme dans l'équation (1.4.6), il y a encore un problème de mesurabilité apparent pour $|U|$, étant donné que le supremum est indénombrable. L'approche classique permettant d'éviter ce problème ([2], p. 15 ou [199], p. 13) consiste à redéfinir l'espérance du supremum comme

$$\mathbb{E}\big[|U|\big] := \sup_{\substack{I \subset C_c^\infty(\mathbb{R})\setminus\{0\} \\ I \text{ fini}}} \mathbb{E}\Big[\sup_{\varphi \in I} |U_\varphi|\Big]. \tag{1.4.23}$$

Cette méthode, bien qu'élégante dans le cas général, est un peu décevante, car nous ne retombons pas sur le critère *(ii)* au niveau des trajectoires du processus. Nous adopterons donc une autre approche qui, comme pour l'équation (1.4.6), consistera à montrer que le supremum (1.4.20) peut être obtenu comme un supremum dénombrable et indépendant de $u \in L^1_{loc}(\mathcal{D})$ (et donc des trajectoires du processus gaussien étudié). Pour cela nous avons besoin de la séparabilité de $L^q(\mathcal{D})$ (dual de $L^p(\mathcal{D})$), ce qui explique pourquoi nous excluons $p = 1$ et $p = \infty$. En effet, $L^\infty(\mathcal{D})$ n'est pas séparable ([33], Remarque 8 p. 103), et de même pour son dual. De plus, des difficultés techniques supplémentaires apparaissent lorsqu'on considère des mesures gaussiennes sur des espaces (de Banach) non séparables ([29], chapitre 3).

Une première partie technique du chapitre est donc consacrée à la construction d'une partie $F_q \subset C_c^\infty(\mathcal{D})$ dénombrable telle que les suprema (1.4.19) et (1.4.20) soit égaux aux suprema obtenus en se restreignant à l'ensemble F_q. C'est le contenu du lemme 3.2.2. Cette construction repose sur la séparabilité de $L^q(\mathcal{D})$, $q \in (1, +\infty)$, sur la densité de $C_c^\infty(\mathcal{D})$ dans $L^q(\mathcal{D})$ et sur la séparabilité séquentielle de $C_c^\infty(\mathbb{R})$, c'est à dire le lemme 2.3.6. La construction de

l'ensemble F_q à l'aide d'un $\mathbb{Q}$-espace vectoriel dénombrable s'inspire en fait de la preuve de la séparabilité de L^q (voir par exemple [33], théorème 4.1.3). L'existence de cet ensemble montre aussi que l'application (1.4.22) est en fait bien mesurable. Cet ensemble F_q est construit comme un sous ensemble de la sphère unité de L^q, ce qui nous permettra par la suite d'ignorer la renormalisation par $\|\varphi\|_q$.

1.4.2.1 Caractérisation de la régularité $W^{m,p}$ des trajectoires d'un processus gaussien mesurable

Une fois l'existence de l'ensemble F_q établie, nous pouvons commencer l'étude de la régularité $W^{m,p}$ des trajectoires des processus gaussiens mesurables. Etant donné $f \in L^p(\mathcal{D})$, nous disons qu'une fonction mesurable g définie ponctuellement est un représentant de f dans $L^p(\mathcal{D})$ si $\|f-g\|_p = 0$. Enfin nous reprenons la notation $\|U\|_p : \omega \mapsto \|U_\omega\|_p$ de la proposition 1.2.7. La proposition ci-dessous est un énoncé simplifié du théorème général (proposition 3.3.1), dans le cas où $\mathcal{D} = \mathbb{R}$ et $m = 1$. Nous notons $\partial_x\partial_y k$ la dérivée croisée du noyau $(x,y) \mapsto k(x,y)$, si elle existe.

Proposition 1.4.5. *Soit $(U(x))_{x\in\mathbb{R}} \sim GP(0,k)$ un processus gaussien mesurable tel que la fonction $x \mapsto k(x,x)^{1/2}$ soit localement intégrable. Alors les points suivants sont équivalents.*

(i) Les trajectoires de $(U(x))_{x\in\mathbb{R}}$ sont dans $W^{1,p}(\mathbb{R})$ presque sûrement.

(ii) (Critère intégral) On a $k \in L^p(\mathbb{R}\times\mathbb{R})$, la dérivée faible $\partial_x\partial_y k$ existe et $\partial_x\partial_y k \in L^p(\mathbb{R}\times\mathbb{R})$. De plus il existe un représentant $\tilde{k}$ de $\partial_x\partial_y k$ dans $L^p(\mathbb{R}\times\mathbb{R})$ qui est la fonction de covariance d'un processus gaussien. Enfin,

$$\int_{\mathbb{R}} k(x,x)^{p/2}dx < +\infty \quad et \quad \int_{\mathbb{R}} \tilde{k}(x,x)^{p/2}dx < +\infty. \tag{1.4.24}$$

(iii) (Décomposition de Mercer généralisée) On a $k \in L^p(\mathbb{R}\times\mathbb{R})$, la dérivée faible $\partial_x\partial_y k$ existe et $\partial_x\partial_y k \in L^p(\mathbb{R}\times\mathbb{R})$. De plus, il existe deux suites positives $(\lambda_n) \subset \mathbb{R}_+$ et $(\mu_n) \subset \mathbb{R}_+$, et deux suites de fonctions $(e_n) \subset L^p(\mathbb{R})$ et $(f_n) \subset L^p(\mathbb{R})$ vérifiant

$$\sum_{n=0}^{+\infty} \lambda_n \|e_n\|_p^2 < +\infty \quad et \quad \sum_{n=0}^{+\infty} \mu_n \|f_n\|_p^2 < +\infty, \tag{1.4.25}$$

telles que les deux égalités suivantes soient vraies dans $L^p(\mathbb{R}\times\mathbb{R})$:

$$k = \sum_{n=0}^{+\infty} \lambda_n e_n \otimes e_n \quad et \quad \partial_x\partial_y k = \sum_{n=0}^{+\infty} \mu_n f_n \otimes f_n. \tag{1.4.26}$$

Si de plus $p \in (1,2)$, alors il existe une base orthonormée (g_n) de $L^2(\mathbb{R})$ et deux opérateurs continus A_0 et A_1 de $L^2(\mathbb{R})$ dans $L^p(\mathbb{R})$ tels que $e_n = A_0 g_n$ et $f_n = A_1 g_n$ pour tout entier n.

Notons que le critère *(ii)* nécessite que les fonctions intégrées soient bien mesurables sur leur diagonale. Pour k, cette propriété est assurée par la mesurabilité du processus gaussien sous-jacent, par le théorème de Fubini. Pour $\partial_x\partial_y k$ cependant, cette propriété est bien moins évidente puisque $\partial_x\partial_y k$ n'est a priori défini que comme un élément de $L^p(\mathbb{R}\times\mathbb{R})$ (donc à un ensemble de mesure nulle près), et l'ensemble $\{(x,x),\ x\in\mathbb{R}\}$ est de mesure nulle dans $\mathbb{R}\times\mathbb{R}$. De fait, le critère *(ii)* se trouve être faux si l'on considère l'évaluation ponctuelle de n'importe quel représentant de $\partial_x\partial_y k$ dans $L^p(\mathbb{R}\times\mathbb{R})$ (voir la discussion après la proposition 3.3.1). Il est cependant vrai si ce représentant est la fonction de covariance d'un autre processus gaussien mesurable (ou, si $p \geq 2$, ce représentant correspond à l'évaluation ponctuelle d'une décomposition nucléaire du noyau, par le lemme 3.3.7). Il est aussi naturel de se demander si dans la décomposition nucléaire de $\partial_x\partial_y k$, on ne pourrait pas tout simplement distribuer les dérivées, c'est à dire prendre $\mu_n = \lambda_n$ et $f_n = e_n'$ (on peut en effet montrer que la dérivée faible e_n' existe et que $e_n' \in L^p(\mathbb{R})$). Ce fait est inconditionnellement vrai si $p = 2$, probablement vrai si $p \in (1,2)$ mais il devient faux si $p \in (2,+\infty)$ (Remarque 3.3.4).

Eléments de preuve Nous montrons la chaîne d'implications suivante : $(i) \implies (ii)$ & (iii), $(ii) \implies (i)$ et $(iii) \implies (ii)$.
$(i) \implies (ii)$ & (iii) : les propriétés des points *(ii)* et *(iii)* concernant le noyau non dérivé k sont en fait déjà assurées par la proposition 3.2.9. Il nous faut maintenant prouver celles concernant le noyau dérivé. Pour cela, nous montrons que l'application suivante (bien définie par hypothèse)

$$\begin{cases} (\Omega,\mathcal{F},\mathbb{P}) & \to \big(L^p(\mathbb{R}), \mathcal{B}(L^p(\mathbb{R}))\big) \\ \omega & \mapsto U'_\omega \end{cases} \tag{1.4.27}$$

où U'_ω désigne la dérivée faible de la trajectoire U_ω, est mesurable, et qu'elle induit une mesure gaussienne μ sur $(L^p(\mathbb{R}), \mathcal{B}(L^p(\mathbb{R})))$. Nous identifions ensuite l'opérateur de covariance associé. Nous montrons que c'est l'opérateur intégral associé à la dérivée faible $\partial_x\partial_y k$, et nous montrons donc au passage que la dérivée faible $\partial_x\partial_y k$ existe et est dans $L^p(\mathbb{R}\times\mathbb{R})$. Le point *(iii)* est assuré par la description des opérateurs de covariance de mesure gaussienne sur les espaces L^p (propositions 3.2.7 et 3.2.8). Enfin, puisque la mesure gaussienne μ est engendrée par un processus gaussien mesurable à trajectoires dans $L^p(\mathbb{R})$ (proposition 1.2.6), la fonction de covariance d'un tel processus fournit un représentant $\tilde{k}$ de $\partial_x\partial_y k$ dans $L^p(\mathbb{R}\times\mathbb{R})$ qui, par l'équation (1.2.17), vérifie

bien le critère intégral du point *(ii)*.
(ii) $\implies$ *(i)* : Soit $(V(x))_{x\in\mathbb{R}}$ un processus gaussien centré de fonction de covariance $\tilde{k}$, où $\tilde{k} = \partial_x\partial_y k$ dans $L^p(\mathbb{R}\times\mathbb{R})$. Etant donné $\varphi \in C_c^\infty(\mathbb{R})$, on définit les variables aléatoires

$$V_\varphi : \omega \mapsto \int_{\mathbb{R}} V_\omega(x)\varphi(x)dx, \quad U_\varphi : \omega \mapsto -\int_{\mathbb{R}} U_\omega(x)\varphi'(x)dx. \tag{1.4.28}$$

On constate que les processus $(U_\varphi)_{\varphi\in F_q}$ et $(V_\varphi)_{\varphi\in F_q}$ ont les mêmes lois finidimensionnelles. En effet, ils sont bien définis, ce sont des suites gaussiennes (processus gaussiens indexés par un ensemble dénombrable, lemme 3.2.5), elles sont centrées et ont même fonction de covariance : par le théorème de Fubini,

$$\begin{aligned}\mathbb{E}[V_\varphi V_\psi] &= \int_{\mathbb{R}\times\mathbb{R}} \varphi(y)\psi(x)\tilde{k}(x,y)dxdy = \int_{\mathbb{R}\times\mathbb{R}} \varphi(y)\psi(x)\partial_x\partial_y k(x,y)dxdy \\ &= \int_{\mathbb{R}\times\mathbb{R}} \varphi'(y)\psi'(x)k(x,y)dxdy. \qquad (1.4.29)\\ \mathbb{E}[U_\varphi U_\psi] &= \int_{\mathbb{R}\times\mathbb{R}} \varphi'(y)\psi'(x)k(x,y)dxdy. \qquad (1.4.30)\end{aligned}$$

Ainsi, les variables aléatoires $\sup_{\varphi\in F_q}|U_\varphi|$ et $\sup_{\varphi\in F_q}|V_\varphi|$ ont même loi, les suprema étant dénombrables. D'où,

$$1 = \mathbb{P}(\|V\|_p < +\infty) = \mathbb{P}(\sup_{\varphi\in F_q}|V_\varphi| < +\infty) = \mathbb{P}(\sup_{\varphi\in F_q}|U_\varphi| < +\infty), \tag{1.4.31}$$

ce qui montre que $U'_\omega \in L^p(\mathbb{R})$ presque sûrement.
(iii) $\implies$ *(ii)* : cette implication est assurée par la théorie des mesures gaussiennes sur les espaces L^p (propositions 3.2.7 ou 3.2.8). □

Notons que les points *(ii)* et *(iii)* de la proposition 1.4.5 reposent sur la finitude de deux quantités : les normes L^p des fonctions écart type d'un côté, et les normes nucléaires des opérateurs de covariance de l'autre (avec une condition supplémentaire lorsque $p \in (1,2)$). Il convient donc de trouver des encadrements de chacune de ces quantités en fonction l'une de l'autre. C'est le contenu de la proposition suivante (qui, elle, autorise le cas $p = 1$).

Proposition 1.4.6. *Soit μ une mesure gaussienne centrée sur $L^p(\mathcal{D})$, où $1 \le p < +\infty$. Soit $k \in L^p(\mathcal{D}\times\mathcal{D})$ le noyau intégral de son opérateur de covariance, choisi de façon à ce qu'il soit aussi la fonction de covariance d'une processus gaussien mesurable $(U(x))_{x\in\mathbb{R}}$, par la proposition 3.2.9. Posons $\sigma(x) \coloneqq k(x,x)^{1/2}$ et $C_p \coloneqq 2^{p/2}\Gamma((p+1)/2)/\sqrt{\pi}$ ($C_p = \mathbb{E}[|X|^p]$ si $X \sim \mathcal{N}(0,1)$). Alors les bornes suivantes sont vraies.*

• *si* $1 \leq p < 2$*, il existe un opérateur symétrique, positif et à trace finie* S *sur* $L^2(\mathcal{D})$ *et un opérateur borné* $A : L^2(\mathcal{D}) \to L^p(\mathcal{D})$ *tel que* $\mathcal{E}_k = ASA^*$*. De plus,*

$$\nu(\mathcal{E}_k) \leq \inf_{\substack{A,S \text{ s.t.} \\ \mathcal{E}_k = ASA^*}} \|A\|^2 \nu(S) \leq \|\sigma\|_p^2 \leq C_p^{-2/p} \inf_{\substack{A,S \text{ s.t.} \\ \mathcal{E}_k = ASA^*}} \|A\|^2 \nu(S). \tag{1.4.32}$$

• *si* $2 \leq p < +\infty$*, alors* $\mathcal{E}_k$ *est symétrique, positif et nucléaire, et*

$$C_p^{-2/p} \nu(\mathcal{E}_k) \leq \|\sigma\|_p^2 \leq \nu(\mathcal{E}_k). \tag{1.4.33}$$

Eléments de preuve Cette proposition est le résultat d'un certain nombre de calculs "directs", qui reposent en grande partie sur l'égalité suivante

$$\mathbb{E}\left[\int_{\mathcal{D}} |U(x)|^p dx\right] = \int_{\mathcal{D}} C_p \sigma(x)^p dx = C_p \|\sigma\|_p^p, \tag{1.4.34}$$

ainsi que sur l'application répétée de l'inégalité de Jensen pour les fonctions concaves ou convexes, selon que $p/2 \geq 1$ ou $p/2 < 1$. Nous utilisons aussi des estimations classiques concernant les mesures gaussiennes et les opérateurs nucléaires. Ces faits concernent l'inégalité de gauche dans (1.4.32), l'inégalité de droite dans (1.4.32) et l'inégalité de gauche dans (1.4.33). La preuve de l'inégalité du milieu dans (1.4.32) est remarquable car elle se fait à l'aide d'opérateurs S et A explicites, donnés par

$$Af(x) = f(x)\sigma(x)^{1-p/2} \quad \text{(opérateur de multiplication)}, \tag{1.4.35}$$

et $S = \mathcal{E}_{k_0}$ avec $k_0(x,y) \coloneqq k(x,y)\sigma(x)^{p/2-1}\sigma(y)^{p/2-1}$. Ces opérateurs vérifient $\mathcal{E}_k = A\mathcal{E}_{k_0}A^*$, avec $\|A\| = \|A^*\| \leq \|\sigma\|_p^{1-p/2}$ et $\nu(S) = \mathrm{Tr}(S) = \|\sigma\|_p^p$. Cela donne bien $\|A\|^2\nu(\mathcal{E}_{k_0}) \leq \|\sigma\|_p^{2-p}\|\sigma\|_p^p = \|\sigma\|_p^2$. Enfin, l'inégalité de droite dans (1.4.33) est une conséquence de l'inégalité de Minkowski dans $L^{p/2}$ et du fait que pour toute décomposition nucléaire $k = \sum_n \mu_n \psi_n \otimes \phi_n$, nous avons

$$\int_{\mathcal{D}} k(x,x)^{p/2} dx = \int_{\mathcal{D}} \left| \sum_{n=0}^{+\infty} \mu_n \psi_n(x)\phi_n(x) \right|^{p/2} dx. \tag{1.4.36}$$

Cette égalité n'est pas triviale, pour les raisons de mesurabilité évoquées plus haut. Elle se trouve être vraie mais sa preuve est tout à fait non triviale. C'est pourquoi un lemme à part entière lui est dédié (le lemme 3.3.7). Cette preuve, qui utilise de façon cruciale les hypothèses de mesurabilité du processus gaussien de fonction de covariance k ainsi que de nucléarité de la décomposition de k, repose sur l'inégalité de Hardy-Littlewood (équation (3.3.61)). □

1.4.2.2 Caractérisation de la régularité H^m des trajectoires d'un processus gaussien mesurable

Dans le cas spécifique des espaces de Sobolev hibertiens ($p = 2$), une condition nécessaire et suffisante supplémentaire peut être obtenue en considérant l'injection du RKHS H_k dans $H^m(\mathcal{D})$. Pour cela, nous avons besoin de la notion d'opérateur de type Hilbert-Schmidt et à trace finie. Nous disons qu'un opérateur linéaire continu A entre deux espaces de Hilbert séparables H_1 et H_2 est de type Hilbert-Schmidt si pour une (toute) base orthonormée (e_n) de H_1, nous avons

$$\|A\|_{HS}^2 \coloneqq \sum_{n=0}^{+\infty} \|Ae_n\|_{H_2}^2 < +\infty. \tag{1.4.37}$$

Cette quantité est indépendante du choix de la base (e_n) et vaut le carré de $\|A\|_{HS}$, la norme Hilbert-Schmidt de A. Si $H_1 = H_2 = H$, nous définissons la trace d'un opérateur borné A autoadjoint et positif ($\langle Af, f\rangle_H \geq 0$) par la série à termes positifs suivante, convergente ou non :

$$\mathrm{Tr}(A) \coloneqq \sum_n \langle Ae_n, e_n\rangle_H, \tag{1.4.38}$$

étant donnée une base orthonormée (e_n) de H. Si cette somme converge pour une base, alors elle converge quelque soit la base vers la même valeur. De plus, $\mathrm{Tr}(A) = \nu(A)$ pour les opérateurs autoadjoints positifs. Le résultat principal de cette partie est le suivant, qui est une version simplifiée de la proposition 3.4.4.

Proposition 1.4.7. *Soit $(U(x))_{x\in\mathbb{R}} \sim GP(0, k)$ un processus gaussien mesurable tel que la fonction $x \mapsto k(x, x)^{1/2}$ soit localement intégrable. Alors les points suivants sont équivalents.*

(i) Les trajectoires de $(U(x))_{x\in\mathbb{R}}$ sont dans $H^1(\mathbb{R})$ presque sûrement.

(ii) (Critère intégral) On a $k \in L^2(\mathbb{R}\times\mathbb{R})$, la dérivée faible $\partial_x\partial_y k$ existe et $\partial_x\partial_y k \in L^2(\mathbb{R}\times\mathbb{R})$. De plus il existe un représentant $\tilde{k}$ de $\partial_x\partial_y k$ dans $L^2(\mathbb{R}\times\mathbb{R})$ qui est la fonction de covariance d'un processus gaussien. Enfin,

$$Tr(\mathcal{E}_k) = \int_{\mathbb{R}} k(x, x)dx < +\infty \quad et \quad Tr(\mathcal{E}_{\tilde{k}}) = \int_{\mathbb{R}} \tilde{k}(x, x)dx < +\infty. \tag{1.4.39}$$

(iii) (Décomposition de Mercer) On a $k \in L^2(\mathbb{R}\times\mathbb{R})$, la dérivée faible $\partial_x\partial_y k$ existe et $\partial_x\partial_y k \in L^2(\mathbb{R}\times\mathbb{R})$. De plus, il existe suite positive $(\lambda_n) \subset \mathbb{R}_+$ et une suite de fonctions $(\phi_n) \subset L^2(\mathbb{R})$ vérifiant $k = \sum_n \lambda_n\phi_n \otimes \phi_n$ dans $L^2(\mathbb{R}\times\mathbb{R})$.

Pour toute décomposition de cette forme, nous avons que $\phi'_n \in L^2(\mathbb{R})$ *si* $\lambda_n \neq 0$*, ainsi que les égalités*

$$Tr(\mathcal{E}_k) = \sum_{n=0}^{+\infty} \lambda_n \|\phi_n\|_2^2 < +\infty \quad et \quad Tr(\mathcal{E}_k) = \sum_{n=0}^{+\infty} \lambda_n \|\phi'_n\|_2^2 < +\infty. \quad (1.4.40)$$

(iv) (plongement du RKHS) $H_k \subset H^1(\mathbb{R})$*, l'opérateur de plongement correspondant* $i : H_k \to H^1(\mathbb{R})$ *est continu et* $ii^* : H^1(\mathbb{R}) \to H^1(\mathbb{R})$ *est à trace finie. De façon équivalente,* $\ker(i)^\perp$ *muni de la topologie de* H_k *est un espace de Hilbert séparable et* $j := i_{|\ker(i)^\perp} : \ker(i)^\perp \to H^1(\mathbb{R})$ *est de type Hilbert-Schmidt. De plus, la norme Hilbert-Schmidt de* j *est donnée par*

$$\|j\|_{HS}^2 = Tr(ii^*) = Tr(\mathcal{E}_k) + Tr(\mathcal{E}_{\tilde{k}}). \quad (1.4.41)$$

En comparaison avec les résultats de la proposition 1.4.5, cette proposition montre en plus que toutes les quantités numériques intervenant dans les points *(ii)*, *(iii)* et *(iv)* correspondent essentiellement à la même chose, ici une trace. C'est en fait le contenu de la proposition 1.4.6 (le cas $p = 2$ sature les inégalités de la proposition 1.4.6), à ceci près que nous prouvons en plus que ces traces se calculent à l'aide de n'importe quelle représentation de Mercer du noyau, lorsque $p = 2$. Cette propriété devient fausse si $p > 2$ (Remarque 3.3.4).

Notons qu'une difficulté apparaît pour définir la notion d'opérateur de type Hilbert-Schmidt lorsque l'espace de Hilbert H_k n'est pas séparable (cela peut arriver en pratique, voir la remarque 3.4.1). C'est pourquoi il est nécessaire d'introduire l'application j.

Stratégie de preuve de l'équivalence *(iii)* $\iff$ *(iv)* **:** L'implication *(iii)* $\implies$ *(iv)* s'obtient en étudiant le comportement en norme L^2 des différences finies $\tau_h f - f$ des éléments f de H_k, afin d'utiliser le point *(iii)* du lemme 1.4.4. L'implication réciproque repose sur la diagonalisation de l'opérateur ii^* dans une base orthonormée de $H^1(\mathbb{R})$. Les calculs de trace sont "élémentaires" (ils n'utilisent pas d'outils fins d'analyse) mais ils sont aussi assez piégeux, car ils nécessitent d'alterner entre fonctions définies ponctuellement, définies presque partout dans $L^2(\mathbb{R})$ et presque partout dans $L^2(\mathbb{R} \times \mathbb{R})$.

Lien avec le processus gaussien canonique d'un espace de Hilbert Le cas hilbertien permet une autre preuve de l'équivalence *(i)* $\iff$ *(ii)*. Celle-ci repose sur l'étude des *ellipsoïdes* (i.e. les images de la boule unité par un opérateur linéaire) d'un espace de Hilbert séparable H en relation avec son processus gaussien (centré) "canonique" $(V_f)_{f \in H}$, de fonction de covariance $\mathbb{E}[V_f V_g] = \langle f, g \rangle_H$. En effet, étant donné un opérateur continu, autoadjoint

et positif $A : H \to H$ et en notant B la boule unité de H, il est connu que la variable $\sup_{f\in A(B)} |V_f| = \sup_{g\in B} |V_{Ag}|$ est finie presque sûrement si et seulement si A est de type Hilbert-Schmidt (proposition 3.4.3). Etant donné un processus gaussien mesurable $(U(x))_{x\in\mathcal{D}}$, cette propriété peut être exploitée en exprimant la loi de la suite gaussienne $(U_\varphi)_{\varphi\in F_2}$ (où $U_\varphi(\omega) \coloneqq \int_{\mathcal{D}} U_\omega(x)\varphi(x)dx$ si $\varphi \in C_c^\infty(\mathcal{D})$) en fonction de la loi du processus gaussien canonique de l'espace de Hilbert $H = L^2(\mathcal{D})$, à la manière de la preuve de l'implication $(ii) \implies (i)$ dans la proposition 1.4.5 (explicitement, il faut poser $A \coloneqq \mathcal{E}_k^{1/2}$, $A \coloneqq \mathcal{E}_{\partial_x\partial_y k}^{1/2}$ et ainsi de suite). Nous laissons les détails techniques dans le corps du chapitre.

Application à la sélection de noyau de covariance La dernière section du chapitre 3 propose une application des critères quantitatifs de la régularité Sobolev de la proposition (i), pour la sélection de noyau. La stratégie de sélection vise à choisir le noyau dont la moyenne de krigeage m_k associée (l'interpolant) est de norme Sobolev minimale :

$$\min_{\text{tous les noyaux } k} \|m_k\|_{H^m}. \tag{1.4.42}$$

Une version fini-dimensionnelle de ce problème d'optimisation est obtenue en considérant une famille de noyaux de rang fini : $k_\Lambda(x,y) \coloneqq \sum_{i=1}^d \lambda_i\phi_i(x)\phi_i(y)$, où les modes $\phi_i \in H^m$ sont fixés ainsi que le rang $d \in \mathbb{N}$, $\Lambda \coloneqq (\lambda_1,\dots,\lambda_d) \in \mathbb{R}_+^d$ est la variable d'optimisation. Enfin, une version relaxée de ce problème est obtenue en notant que pour tout $f \in H_k$,

$$\begin{aligned}\|f\|_{H^m} = \|i(f)\|_{H^m} &\le \|i\|_{\mathcal{L}(H_k,H^m)}\|f\|_{H_k} \le \|i\|_{HS}\|f\|_{H_k} \\ &\le \frac{1}{2}\Big(\varepsilon\|i\|_{HS}^2 + \varepsilon^{-1}\|f\|_{H_k}^2\Big).\end{aligned} \tag{1.4.43}$$

Le terme $\|i\|_{HS}^2$ est donné dans la proposition (i), et la norme $\|m_k\|_{H_k}$ est elle aussi explicite. Nous obtenons finalement le problème de minimisation suivant

$$\min_{\Lambda\in\mathbb{R}_+^d} \varepsilon\sum_{i=1}^d \lambda_i\|\phi_i\|_{H^m}^2 + \frac{1}{\varepsilon}u(X)^T K_\Lambda^+ u(X), \tag{1.4.44}$$

que nous résolvons "explicitement" dans la limite de $\lambda_0 \to 0$ (proposition 3.5.3).

Perspectives L'étude de critères similaires pour les espaces de Sobolev d'ordre fractionnaire ainsi que pour les espaces de Besov est une direction de recherche intéressante. En effet, ces espaces apparaissent naturellement dans l'étude d'EDPs avec conditions de bord. Par ailleurs, autre la sélection

de noyau, les critères quantitatifs obtenus dans les propositions 1.4.5, 1.4.6 et 1.4.7 peuvent certainement être utilisés dans l'étude des méthodes à noyaux sous contrainte locale d'EDP décrite dans la section 1.3.5.

1.4.3 Chapitre 4 : régression par processus gaussiens pour l'équation des ondes en trois dimensions

Ce chapitre est une continuation du chapitre 4, et repose sur les formules de convolutions données dans la proposition 1.4.2. Plusieurs applications de tels priors sont ensuite décrites, notamment pour l'estimation des paramètres de l'EDP et la reconstruction de ses conditions initiales. Un lien inattendu est établi entre cette méthode et la localisation GPS.

1.4.3.1 Quelques priors pour l'équation des ondes

Il se trouve que les formules données dans la proposition 1.4.2 sont extrêmement coûteuses à évaluer sous leur forme de convolution, en temps mais aussi en mémoire, puisqu'elles nécessitent au mieux une FFT en 4 (voire 6) dimensions. La première partie du chapitre est donc consacrée à la simplification de ces formules sous des hypothèses supplémentaires, qui correspondent ici à celles de la stationarité et de la symétrie radiale des conditions initiales. Dans le cas de la stationarité, nous avons la proposition suivante.

Proposition 1.4.8. *Supposons que k_{v} soit continue et stationnaire : $k_{\mathrm{v}}(x,x') = k_S(x-x')$ pour une fonction continue k_S.*
(i) Alors $k_{\mathrm{v}}^{\mathrm{wave}}$ est stationnaire en espace et

$$[(F_t \otimes F_{t'}) * k_{\mathrm{v}}](x,x') = (F_t * F_{t'} * k_S)(x-x'). \tag{1.4.45}$$

(ii) De plus, la mesure $F_t * F_{t'}$ est absolument continue sur $\mathbb{R}^3$. En notant $|h|$ la norme euclidienne de $h \in \mathbb{R}^3$ et en identifiant $F_t * F_{t'}$ avec sa densité, nous avons

$$(F_t * F_{t'})(h) = \frac{sgn(t)sgn(t')}{8\pi c^2 |h|} \mathbb{1}_{\left[c\left||t|-|t'|\right|, c(|t|+|t'|)\right]}(|h|). \tag{1.4.46}$$

Des formules similaires peuvent ensuite être obtenues pour $k_{\mathrm{u}}^{\mathrm{wave}}$, en utilisant la relation $\dot{F}_t = \partial_t F_t$. La preuve du point *(ii)* se fait dans le domaine de Fourier en espace, et utilise plusieurs propriétés spécifiques à la dimension 3. Si k_S est le noyau gaussien, il est possible d'obtenir une formule explicite pour l'équation (1.4.45) à l'aide de la fonction d'erreur *erf*, ou encore, de la fonction de répartition de la densité gaussienne (équation (4.3.23)).

Dans le cas de la symétrie radiale autour d'un point $x_0 \in \mathbb{R}^3$, nous avons cette fois la description suivante.

Proposition 1.4.9. *Supposons que les trajectoires des processus U^0 et V^0 soient à symétrie radiale autour d'un même point $x_0 \in \mathbb{R}^3$, presque sûrement. Alors il existe deux fonctions de covariance (explicites) sur $\mathbb{R}_+$, K_{v} et K_{u} telles que pour tout $z = (x,t) \in \mathbb{R}^3 \times \mathbb{R}$ et $z' = (x',t') \in \mathbb{R}^3 \times \mathbb{R}$, en notant $r = |x - x_0|$ et $r' = |x' - x_0|$,*

$$k_{\mathrm{v}}^{\mathrm{wave}}(z,z') = \frac{sgn(tt')}{16c^2rr'} \sum_{\varepsilon,\varepsilon' \in \{-1,1\}} \varepsilon\varepsilon' K_{\mathrm{v}}\big((r+\varepsilon c|t|)^2, (r'+\varepsilon' c|t'|)^2\big), \quad (1.4.47)$$

$$k_{\mathrm{u}}^{\mathrm{wave}}(z,z') = \frac{1}{4rr'} \sum_{\varepsilon,\varepsilon' \in \{-1,1\}} (r+\varepsilon c|t|)(r'+\varepsilon' c|t'|) \times K_{\mathrm{u}}\big((r+\varepsilon c|t|)^2, (r'+\varepsilon' c|t'|)^2\big). \quad (1.4.48)$$

La proposition 4.3.6 est une version de la proposition 1.4.9 sous l'hypothèse supplémentaire que les conditions initiales soient à support compact. Ce cas est intéressant en pratique car la propagation du support de la solution de l'équation des ondes en trois dimensions possède des propriétés remarquables : c'est le principe de Huygens (section 4.3.2.4). Ces formules montrent aussi qu'il est possible de voir les paramètres physiques de l'EDP (ici, la célérité c, la position de la source x_0 et la taille de la source si son support est compact) comme des hyperparamètres du noyau. En conséquence, ces paramètres peuvent être estimés en maximisant la vraisemblance marginale, ou plutôt, en minimisant l'opposé de son logarithme.

Ces formules ouvrent les portes à de premières applications pratiques. Avant leur application cependant, nous étudions plus en profondeur le cas du support compact, dans la limite du rayon du support tendant vers 0.

1.4.3.2 Le cas de la source ponctuelle

Comme évoqué dans la section 1.3.3, il peut être intéressant d'étudier le cas où le terme source (ici, les conditions initiales) est réduit à une masse de Dirac. Considérons, pour v_0, le noyau tronqué défini par

$$k_{\mathrm{v}}^R(x,x') \coloneqq (4\pi R^3/3)^{-2} \mathbb{1}_{[0,R]}(r) \mathbb{1}_{[0,R]}(r') k(x,x') \quad (1.4.49)$$

où $k(x,x')$ est un noyau donné. Lorsque R tend vers 0, le noyau k_{v}^R dégénère en la *mesure singulière produit* donnée par $k(x_0,x_0)\delta_{x_0}(dx)\delta_{x_0}(dx')$, ce qui correspond encore à la fonction de covariance du "processus gaussien" donné par $V_0(x) = \xi\delta_{x_0}(x)$ où $\xi \sim \mathcal{N}(0, k(x_0,x_0))$. Ce modèle n'est pas très intéressant du point de vue des formules de krigeage car il n'est capable de rendre compte que des multiples d'une masse de Dirac. Pour autant, il est intéressant d'étudier la vraisemblance marginale associée car le centre $x_0 \in \mathbb{R}^3$ est un

hyperparamètre du noyau ; l'optimisation de la vraisemblance marginale peut donc (en principe) traiter le problème de la localisation de source ponctuelle pour l'équation des ondes.

Pour étudier cette question, nous fixons tous les hyperparamètres du noyau, autres que la position x_0 et le niveau de bruit λ (aux bonnes valeurs si nous les connaissons, la célérité c en particulier). Ainsi, la log vraisemblance marginale négative devient une application $(x_0, \lambda) \mapsto \mathcal{L}(x_0, \lambda)$, à minimiser.

Les données sont récoltées par N capteurs supposés fixes aux positions x_i qui mesurent des séries temporelles de taille q (il y a donc $n = Nq$ mesures). L'ensemble des coordonnées espace-temps (x_i, t_j) sont stockées dans un grand vecteur $Z \in (\mathbb{R}^4)^n$. La figure 4.1 du chapitre 4 montre, sur un exemple, toutes les valeurs de cette vraisemblance marginale en dessous d'un certain seuil, à λ fixé, en fonction de x_0. De façon surprenante au premier abord, nous obtenons des sphères centrées autour de chaque capteur qui s'intersectent en un unique point, qui correspond à la véritable position de la source. Ce n'est pas sans rappeler la méthode de localisation utilisée dans les systèmes GPS [23]. Cette section est dédiée à l'étude de ce phénomène ; nous renvoyons à la section 4.3.3 pour plus de détails de modélisation du problème et d'interprétation de la figure 4.1.

Pour cette étude donc, nous étudions d'abord le comportement du noyau $k_{\mathrm{v}}^{\mathrm{wave}}$ (équation (1.4.12)) avec $k_{\mathrm{v}} = k_{\mathrm{v}}^R$ (équation (1.4.49)), dans la limite de R tendant vers 0. De même que pour k_{v}^R, le noyau $k_{\mathrm{v}}^{\mathrm{wave}}$ se comporte alors comme un produit tensoriel de mesures (proposition 4.3.8). En particulier, il s'apparente à un noyau de rang 1. Ce résultat nous incite à introduire une vraisemblance "régularisée" $\mathcal{L}_{\mathrm{reg}}$, qui prend en compte ce comportement de rang 1 de la mesure limite tout en évitant sa singularité par rapport à la mesure de Lebesgue. Plus précisément, la fonction $\mathcal{L}_{\mathrm{reg}}$ est obtenue en remplaçant k_{v}^R par un noyau $k_{\mathrm{reg}}((x,t),(x',t'))$, lui-même obtenu en convoluant la mesure limite avec une approximation de l'unité (*mollification*) ; c'est l'équation (4.3.42). En particulier, le noyau $k_{\mathrm{reg}}((x,t),(x',t'))$ est de rang 1 et d'hyperparamètre x_0.

Nous stockons les observations de tous les capteurs dans un grand vecteur concaténé W (avec ordre de concaténation approprié), et nous notons F_{x_0} le vecteur tel que la matrice de covariance associée aux mesures s'écrive comme $k_{\mathrm{reg}}(Z,Z) = F_{x_0} F_{x_0}^T$. Le bilan de l'étude de la vraisemblance marginale régularisée $\mathcal{L}_{reg}$ est concentré dans le résultat suivant.

Proposition 1.4.10. *Définissons le coefficient de corrélation entre F_{x_0} et W par $r(x_0) := \langle F_{x_0}, W\rangle_{\mathbb{R}^n} / (||W||_{\mathbb{R}^n} ||F_{x_0}||_{\mathbb{R}^n})$. Si $F_{x_0} = 0$, nous posons $r(x_0) = 0$.*

23. Voir par exemple [76] ou la page suivante pour une introduction "pédagogique" : `https://en.wikipedia.org/wiki/True-range_multilateration`

Alors nous avons la convergence ponctuelle suivante :

$$\forall x_0 \in \mathbb{R}^3, \quad \left|\lambda \mathcal{L}_{\text{reg}}(x_0, \lambda) - ||W||^2_{\mathbb{R}^n}\left(1 - r(x_0)^2\right)\right| = O_{\lambda \to 0}(\lambda \log \lambda),$$

Ce résultat découle d'une étude explicite de $\mathcal{L}_{\text{reg}}(x_0, \lambda)$, rendue possible par la formule de Sherman-Morrison, qui exprime l'inverse de $A + uv^T$ en fonction de A^{-1}, u et v. La convergence ponctuelle peut être raffinée (proposition 4.3.9) et d'autres régimes asymptotiques peuvent être considérés (proposition 4.3.11). Ces résultats permettent tous de retrouver les phénomènes observés sur la figure 4.1 (voir la section 4.3.3.4).

1.4.3.3 Quelques applications aux problèmes inverses

Les priors que nous avons décrits peuvent être utilisés sur des cas pratiques. Par ailleurs, le problème de l'estimation de la solution toute entière w se réduit à l'estimation de ses conditions initiales, si jamais les paramètres physiques sont connus ou ont été correctement estimés (proposition 4.3.14). La reconstruction de condition initiale est l'objectif de la tomographie photoacoustique (PAT).

Les cas tests que nous examinons se limitent à la symétrie radiale à support compact (proposition 4.3.6), le cas d'une condition initiale stationnaire ayant a priori moins de sens physique. Nous générons des données à partir d'une simulation numérique, et effectuons une régression par processus gaussien en utilisant les noyaux de la proposition 4.3.6. La figure 1.1 donne un exemple de reconstruction d'une condition initiale. Les tables 4.1 et 4.2 résument les erreurs d'estimation des paramètres et de reconstrution des conditions initiales (en norme relative L^1, L^2 et L^∞), en fonction du nombre de capteurs utilisés, pour une configuration de 30 capteurs donnée. Par ailleurs, les figures 4.3 et 4.6 présentent une étude de la sensibilité de la phase de reconstruction en fonction de la disposition des capteurs, sur un échantillon de 40 dispositions des capteurs en hypercube latin.

Perspectives L'extension des applications des formules de covariance au delà de la symétrie radiale est une direction de recherche claire, qui permettrait peut-être des applications en tomographie photoacoustique. Par ailleurs, l'application au cas d'une vitesse c non constante aurait des applications intéressantes en problèmes inverses notamment. Une application potentielle intéressante concerne la conception de conditions aux bords transparentes pour l'équation des ondes. Ce sujet est abordé dans le chapitre 5. Enfin, l'équation des ondes à deux dimensions possède des propriétés différentes de celle en trois dimensions (au niveau du principe de Hugyens par exemple), et intervient en

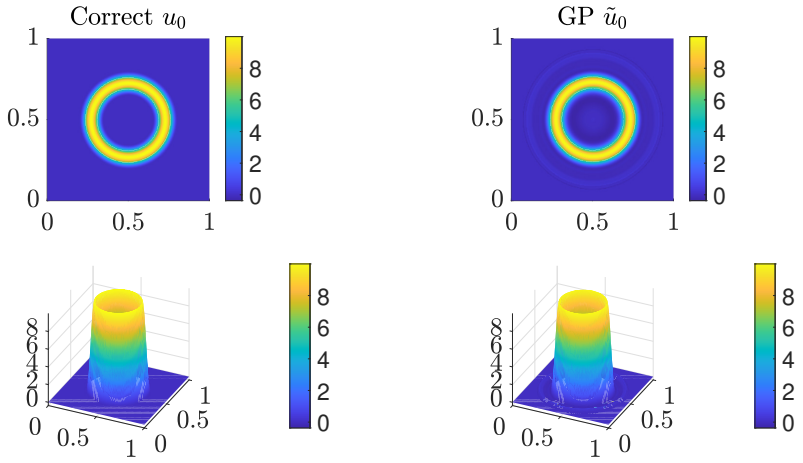

FIGURE 1.1 – Vraie u_0 (colonne de gauche) vs u_0 estimée (colonne de droite). 15 capteurs ont été utilisés. Les images correspondent à une évaluation des fonctions en $z = 0.5$.

océanographie notamment ; une étude spécifique de modèles de régression à noyau pour cette équation paraît donc pertinente.

1.4.4 Chapitre 5 : régression par processus gaussiens et méthode des différences finies

Ce chapitre est dédié à l'étude de certains liens explicites entre les méthodes de régression à noyau et la méthode des différences finies, qui figure parmi les méthodes de base de résolution numérique des équations aux dérivées partielles. Le contenu de ce chapitre est le fruit de recherches récentes ; c'est pourquoi certaines directions de recherche n'ont pas encore été explorées. Plusieurs conjectures sont fournies.

A titre d'illustration de la méthode des différences finies, considérons l'équation d'advection

$$\partial_t u + c\partial_x u = 0, \quad (x,t) \in \mathbb{R} \times \mathbb{R}_+. \tag{1.4.50}$$

Cette équation sert de modèle pour les EDPs hyperboliques d'ordre un, dont la solution n'est en général pas connue explicitement. Il se trouve que l'étude des méthodes servant à résoudre numériquement de telles équations (dont la méthode des différences finies) passe très souvent par par leur étude sur l'équation d'advection, pour des raisons expliquées dans le chapitre 5. La méthode des différences finies consiste à remplacer les dérivées apparaissant dans l'EDP par des opérateurs de "différences finies", comme des taux d'accroissements. Considérons un pas de temps $\Delta t > 0$ et un pas d'espace $\Delta x > 0$. Par exemple,

si nous utilisons la méthode d'Euler explicite pour ∂_t et ∂_x, l'équation (1.4.50) est transformée en l'équation suivante, d'inconnue la suite $(u_j^n)_{j\in\mathbb{Z},n\in\mathbb{N}}$,

$$\frac{u_j^{n+1}-u_j^n}{\Delta t}+c\frac{u_{j+1}^n-u_j^n}{\Delta x}=0. \tag{1.4.51}$$

Ici, la quantité u_j^n joue le rôle d'une approximation de $u(j\Delta x, n\Delta t)$. Il se trouve aussi que l'équation (1.4.51) peut ensuite être écrite comme une relation de récurrence exprimant $u_\cdot^{n+1}$ en fonction de $u_\cdot^n$, elle-même facilement implémentable sur une machine. Les schémas upwind, de Lax-Wendroff ou encore de Lax-Friedrichs sont des exemples classiques de schémas aux différences finies.

L'approximation de la suite $(u(j\Delta x,(n+1)\Delta t))_{j\in\mathbb{Z}}$ à l'aide de la suite $(u(j\Delta x,n\Delta t))_{j\in\mathbb{Z}}$ peut être vue comme un problème de régression, qui peut donc être traité par régression par processus gaussiens. En particulier, si l'on tente d'approcher la valeur $u(j\Delta x,\Delta t)$ à l'aide des valeurs $u_{j-1}^0 \coloneqq u((j-1)\Delta x,0)$, $u_j^0 \coloneqq u(j\Delta x,0)$ et $u_{j+1}^0 \coloneqq u((j+1)\Delta x,0)$ selon une méthode de krigeage, il se trouve que nous écrivons une équation de la forme

$$\tilde{m}(j\Delta x,\Delta t)=a_{-1,j}u_{j-1}^0+a_{0,j}u_j^0+a_{1,j}^0u_{j+1}^0, \tag{1.4.52}$$

où $\tilde{m}$ est la moyenne de krigeage et où le vecteur $(a_{-1,j},a_{0,j},a_{1,j})$ est donné par les formules de krigeage. La relation (1.4.52) ressemble à un schéma aux différences finies. Ce chapitre est dédié à l'étude de la proximité de formules de la forme (1.4.52) avec la méthode des différences finies, lorsque le noyau est choisi de façon à respecter l'équation d'advection. Pour cette équation, de tels noyaux sont de la forme $k((x,t),(x',t'))=k_0(x-ct,x'-ct')$ pour un noyau k_0 quelconque, correspondant à un prior de processus gaussien sur la condition initiale de l'équation d'advection. Si de plus k_0 est stationnaire ($k_0(x,x')=k_S(x-x')$ pour un certain k_S), nous pouvons écrire

$$k((x,t),(x',t'))=k_S(x-x'-c(t-t')). \tag{1.4.53}$$

Pour un tel noyau, les coefficients $(a_{-1,j},a_{0,j},a_{1,j})$ ne dépendent plus de j et nous avons donc

$$\tilde{m}(j\Delta x,\Delta t)=a_{-1}u_{j-1}^0+a_0u_j^0+a_1^0u_{j+1}^0. \tag{1.4.54}$$

Dans ce chapitre, nous étudions deux façons d'obtenir des schémas aux différences finies intéressants à l'aide du noyau (1.4.53). Une première méthode consiste à étudier le régime dit de la limite plate, que nous décrivons ci-dessous. De façon remarquable, nous obtenons une famille continue de schémas contenants en particulier les schémas upwind et de Lax-Wendroff. Ce résultat, liant méthodes à noyau et méthodes numériques classiques, est dans la lignée de

ceux de la section 4.3.3 du chapitre 4. Une deuxième méthode consiste à observer que les coefficients (a_{-1}, a_0, a_1) donnés par les équations de krigeage minimisent une certaine forme quadratique. Ainsi, nous obtenons un schéma consistant (notion décrite ci-dessous) en contraignant le problème de minimisation de cette forme quadratique aux équations de consistance. La consistance est une propriété minimale pour qu'un schéma aux différences finies soit utilisable en pratique.

Quelques propriétés des schémas aux différences finies Parmi les nombreuses propriétés intéressantes des schémas numériques de type différences finies, trois notions sont particulièrement importantes. Tout d'abord, un schéma est "consistant" s'il est bien un approximation de l'EDP qu'il est supposé approcher. Il est possible de voir qu'un schéma est consistant pour l'équation d'advection s'il vérifie l'équation (5.2.9). Un schéma consistant est d'ordre $s > 0$ en espace si la solution numérique converge vers la vraie solution à la vitesse $O(\Delta x^s)$ lorsque Δx tend vers 0 (la même définition vaut pour l'ordre en temps). un schéma est "stable" pour une certaine norme discrète $\|\cdot\|$ sur l'espace des suites indexées par $\mathbb{Z}$ si (informellement) la norme $\|u_\cdot^n\|$ de sa solution à l'itération n reste bornée lorsque n tend vers l'infini. Il se trouve que de nombreux schémas sont stables sous une condition dite de Courant-Friedrichs-Lewy (CFL) de la forme $|\lambda| \leq \lambda_0$, où $\lambda \coloneqq c\Delta t/\Delta x$ s'appelle le nombre de Courant.

1.4.4.1 Le régime de la limite plate

Considérons un noyau de covariance k et introduisons sa dilatation par $\ell > 0$, donnée par $k_\ell(x, x') \coloneqq k(x/\ell, x'/\ell)$. le paramètre ℓ correspond donc à la longueur caractéristique du noyau de covariance. Dans un contexte général de régression, l'étude de la limite plate consiste à étudier le comportement de la moyenne de krigeage issue d'une régression avec le noyau k_ℓ, dans la limite de ℓ qui tend vers l'infini. Dans ce cas, le noyau k_ℓ devient uniformément plat. Il est connu que lorsque k est de classe C^∞, la moyenne de krigeage converge vers l'interpolant polynomial de Lagrange [178] (ou son équivalent multidimensionel si $x, x' \in \mathbb{R}^d$), si la limite existe. Lorsque le noyau a une régularité finie, l'interpolant converge cette fois vers la solution d'un problème d'interpolation avec splines polyharmoniques généralisées [130] (toujours si la limite existe).

Dans la section 5.2.3.3 du chapitre 5, nous étudions le cas des schémas à trois points centrés lorsque nous utilisons un noyau de Matérn de paramètre de régularité $\nu > 0$ (équation (1.2.16)) pour k_0. Le résultat le plus intéressant est la proposition 5.2.5, dont une version raccourcie est donnée ci-dessous.

Proposition 1.4.11. *Supposons que $1 < \nu < 2$. Alors dans le régime de la limite plate, nous obtenons les coefficients*

$$a_{-1} = \frac{\lambda + D(\nu,\lambda)}{2}, \quad a_0 = 1 - D(\nu,\lambda), \quad a_1 = \frac{-\lambda + D(\nu,\lambda)}{2}, \tag{1.4.55}$$

où le coefficient $D(\nu,\lambda)$ est donné par

$$D(\nu,\lambda) \coloneqq \frac{|\lambda+1|^{2\nu} + |\lambda-1|^{2\nu} - 2|\lambda|^{2\nu} - 2}{4^\nu - 4}. \tag{1.4.56}$$

En particulier, le schéma est consistant.

Dans le cas $\nu \in (0,1)$, nous obtenons des schémas qui ne sont pas consistants à part si $\nu = 1/2$, auquel cas nous retrouvons le schéma upwind (proposition 5.2.4). Le cas $\nu = 1$ nécessite un calcul de limite lorsque ν tend vers 1 ; le schéma résultant est lui aussi consistant (proposition 5.2.7). Dans le cas où $\nu \geq 2$, nous retrouvons le schéma de Lax-Wendroff, indépendamment de ν (propositions 5.2.7 et 5.2.6).

Nous présentons une étude théorique et numérique des schémas donnés dans la proposition 1.4.11 ainsi que du schéma correspondant à $\nu = 1$ dans la section 5.2.3.4. La figure 5.3 contient notamment une étude numérique de l'ordre de convergence de ces schémas.

1.4.4.2 Régime non asymptotique

Le régime de la limite plate possède le désavantage d'avoir une variance a posteriori $\tilde{k}_\ell(x,x)$ convergeant vers 0, pour tout x, lorsque ℓ tend vers $+\infty$ (proposition 5.2.9). En particulier, cela semble empêcher toute utilisation intéressante de la mesure a posteriori pour l'estimation probabiliste de l'erreur d'approximation. Plus largement, cela empêche l'interprétation bayésienne habituellement associée aux méthodes à noyau, en ce qui concerne les schémas obtenus dans la section précédente. la question d'un régime non asymptotique se pose alors ; malheureusement, les coefficients obtenus de cette façon ne fournissent pas un schéma consistant (en fait, ils sont consistants dans un sens relâché de l'équation (5.2.10)). Une façon de contourner ce problème consiste à observer que les poids de krigeage (i.e. le vecteur (a_{-1}, a_0, a_1) apparaissant dans l'équation (1.4.54)) minimisent la forme quadratique

$$Q(b) \coloneqq \mathbb{E}\Big[\big(U(c\Delta t) - b^T U(X)\big)^2\Big], \tag{1.4.57}$$

où $(U(x))_{x\in\mathbb{R}} \sim GP(0,k)$ et où $U(X) = (U(-\Delta x), U(0), U(\Delta x))^T$ (dans le cas d'un schéma à trois points centré). Il est donc possible de considérer la

minimisation de cette forme quadratique, mais sous la contrainte des équations de consistance.

La section 5.2.4 du chapitre 5 est dédiée à l'étude de cette méthode, toujours dans le cas des schémas à trois points centrés. En particulier, une formule explicite est donnée dans la proposition 5.2.10. Nous la donnons aussi ci-dessous.

Proposition 1.4.12. *Soit $k : \mathbb{R} \times \mathbb{R} \to \mathbb{R}$ un noyau stationnaire. Alors le schéma obtenu en minimisant la forme quadratique (1.4.57) sous la constrainte des équations de consistance est celui dont les coefficients sont donnés par*

$$a_{-1} = \frac{\lambda + D_k}{2}, \quad a_0 = 1 - D_k, \quad a_1 = \frac{-\lambda + D_k}{2}, \tag{1.4.58}$$

où le coefficient D_k est donné par

$$D_k := \frac{[(S \otimes \Delta_d)k](0,0)}{[(\Delta_d \otimes \Delta_d)k](0,0)}. \tag{1.4.59}$$

Dans la proposition 1.4.12 ci-dessus, l'opérateur Δ_d est un Laplacien discret (voir l'équation (5.2.65)) et l'opérateur S est l'opérateur appliquant le schéma centré (voir l'équation (5.2.64)). Une étude partielle de la stabilité du schéma associé est donnée dans les propositions 5.2.11, 5.2.12 et 5.2.13, ainsi que dans la conjecture 5.2.14. Les résultats de ces propositions s'expriment en fonction des propriétés de la mesure spectrale du noyau k.

1.4.4.3 Conditions aux bords transparentes

La thématique de cette section est un problème classique d'analyse numérique. Elle est liée à la question de la résolution numérique d'équations aux dérivées partielles posées en domaine non borné. En effet, tout domaine de résolution numérique est nécessairement fini donc par nature borné. En particulier, il est nécessaire de prescrire un comportement au bord du domaine numérique. Les conditions au bord classiques comprennent les conditions de Dirichlet ou de Neumann ; lorsqu'il s'agit de simuler un problème non borné (dans l'espace tout entier par exemple), il semble naturel d'essayer d'encoder des conditions aux bords correspondant à un domaine dont les bords sont "transparents", permettant aux ondes simulées de sortir du domaine numérique.

Il se trouve que la conception de telles conditions aux bords est un problème difficile, en particulier lorsque le domaine numérique comporte des angles (comme un carré ou un cube). Comme la régression à noyau est une méthode sans maillage d'approximation de fonctions, elle semble adaptée à des géométries arbitraires. Cette section est dédiée à la description d'une stratégie

simple de TBC pour l'équation des ondes en deux dimensions. Cette méthode consiste à imposer une condition de Dirichlet non homogène au bord du domaine numérique, correspondant à l'évaluation ponctuelle d'une moyenne de krigeage. Cette moyenne de krigeage, "informée par la physique", correspond à celle obtenue avec un noyau de la forme (1.4.14), conditionnée à des évaluations ponctuelles des conditions initiales. La figure 1.2 montre un exemple de résultat numérique correspondant à la stratégie décrite plus haut. Cette figure est un extrait de la plus grande figure 5.7.

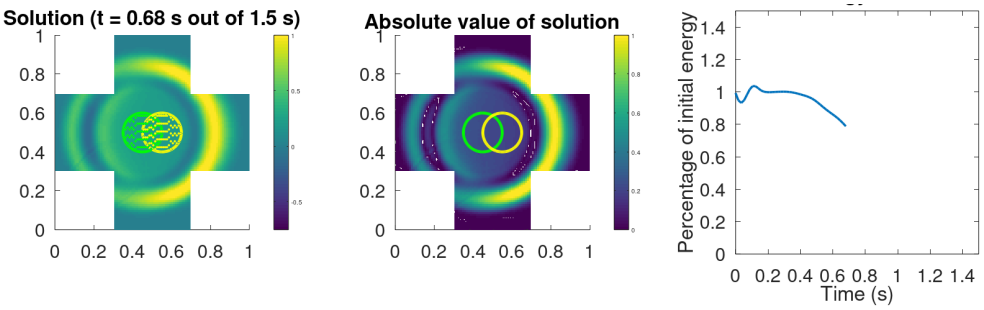

FIGURE 1.2 – Exemple numérique de conditions aux bords transparentes obtenue selon la stratégie décrite plus haut (extrait de la figure 5.7).

Perspectives L'étude théorique et numérique des schémas numériques obtenus par limites plates, dans le cas d'un nombre arbitraire de points, est une direction intéressante de recherche. Pour les schémas obtenus dans le régime non asymptotique contraints sur les équations de consistance, l'analyse de la stabilité et de l'ordre des schémas doit être poursuivie. L'étude de ces derniers schémas dans le cas d'un noyau non stationnaire peut aussi avoir des applications intéressantes. L'application de toutes ces méthodes à d'autres EDPs est aussi une perspective prometteuse. En ce qui concerne les TBC, l'étude de la méthode proposée (ainsi que de méthodes alternatives aussi basées sur des noyaux "informés par la physique") doit être poursuivie.

Chapter 2

Characterization of the second order random fields subject to linear distributional PDE constraints

---

This chapter corresponds to the article [97], which has been published in Bernoulli in 2023.

Abstract

Let L be a linear differential operator acting on functions defined over an open set $\mathcal{D} \subset \mathbb{R}^d$. In this article, we characterize the measurable second order random fields $U = (U(x))_{x\in\mathcal{D}}$ whose sample paths all verify the partial differential equation (PDE) $L(u) = 0$, solely in terms of their first two moments. When compared to previous similar results, the novelty lies in that the equality $L(u) = 0$ is understood in the *sense of distributions*, which is a powerful functional analysis framework mostly designed to study linear PDEs. This framework enables to reduce to the minimum the required differentiability assumptions over the first two moments of $(U(x))_{x\in\mathcal{D}}$ as well as over its sample paths in order to make sense of the PDE $L(U_\omega) = 0$. In view of Gaussian process regression (GPR) applications, we show that when $(U(x))_{x\in\mathcal{D}}$ is a Gaussian process (GP), the sample paths of $(U(x))_{x\in\mathcal{D}}$ conditioned on pointwise observations still verify the constraint $L(u) = 0$ in the distributional sense. We finish by deriving a simple but instructive example, a GP model for the 3D linear wave equation, for which our theorem is applicable and where the previous results from the literature do not apply in general.

Contents

2.1 Introduction 71
2.2 Background 77
2.2.1 Random fields 77
2.2.2 Tools from functional analysis 79
2.3 Random fields under linear differential constraints . 83
2.3.1 The case of classical derivatives 84
2.3.2 The case of distributional derivatives 85
2.3.3 A heredity property for Gaussian process regression . . 93
2.4 Gaussian processes and the 3 dimensional wave equation 94
2.4.1 General solution to the 3 dimensional wave equation . 95
2.4.2 Gaussian process modelling of the solution 96
2.5 Conclusion and perspectives 102

2.1 Introduction

When dealing with an unknown function of interest $u : \mathcal{D} \to \mathbb{R}$ where say $\mathcal{D} \subset \mathbb{R}^d$, it is common (as e.g. in Bayesian inverse problems) to assume that it is a sample path of a random field $U = (U(x))_{x\in\mathcal{D}}$. Incorporating prior knowledge over u, such as smoothness, is then achieved by constraining the law of U accordingly. Sometimes, this prior knowledge comes from physical considerations. If u describes a positive quantity such as mass or energy, then the random variables $U(x)$ should all be positive almost surely (a.s.). In many cases, this physical constraint can be more precisely translated as a partial differential equation (PDE). Such equations are a pivotal tool for modelling, understanding and predicting real-life phenomena such as those arising from fluid mechanics, electromagnetics or biology to name a few. The most simple (yet central) PDEs are those that are linear. In this article, we will only consider homogeneous linear PDEs, which take the form

$$L(u) \coloneqq \sum_{|\alpha|\leq n} a_\alpha(x)\partial^\alpha u = 0. \tag{2.1.1}$$

Above, u is the unknown function of interest, defined over an open set $\mathcal{D} \subset \mathbb{R}^d$, and L is a linear partial differential operator. In (2.1.1), for a multi-index $\alpha = (\alpha_1, ..., \alpha_d)^T \in \mathbb{N}^d$, we used the notations $|\alpha| = \alpha_1 + ... + \alpha_d$ and $\partial^\alpha = (\partial_{x_1})^{\alpha_1}...(\partial_{x_d})^{\alpha_d}$. Homogeneous PDEs, i.e. PDEs with a null term on the right-hand side of (2.1.1), are often encountered to describe conservation laws, such as conservation of mass, energy or momentum in closed systems [186].

In order to incorporate the knowledge that $L(u) = 0$ in the prior U, a natural question is whether one can characterize, in terms of their law, the random fields U whose sample paths are all solutions to the PDE (2.1.1). Let U be a centered second order random field with covariance function k: under the assumption that U is a Gaussian process (GP) whose sample paths are n times differentiable, [86] proved for some classes of differential operators L of order n that ([86], Sections 3.3 and 4.1)

$$\mathbb{P}(L(U) = 0) = 1 \iff \forall x \in \mathcal{D}, L(k(x, \cdot)) = 0. \tag{2.1.2}$$

This property provides a simple characterization of the GPs that incorporate the PDE constraint (2.1.1) sample path-wise. Such GPs would fall in the category of "physics-informed" GPs in the machine learning community. In the proof of this property, the fact that the sample paths are n times differentiable, i.e. that the PDE (2.1.1) can be understood *pointwise*, is central. These functions are then *strong* solutions of the PDE (2.1.1) (see Definition 2.3.1).

In the standard PDE approach though, equation (2.1.1) is reinterpreted by weakening the definition of the derivatives of u, thereby weakening the required regularity assumptions over u. It can indeed happen in practice that the sought solutions of the PDE $L(u) = 0$ are not n times differentiable or even continuous (see e.g. [73], Section 2.1), and they are only solutions of some weakened formulation of equation (2.1.1). This is typically the case for hyperbolic PDEs such as the wave equation presented in Section 2.4. We introduce here the distributional formulation of the PDE (2.1.1), where the regularity assumptions over u are relaxed to the maximum. As such, this formulation enables working with potentially singular solutions of equation (2.1.1), solutions which are not allowed to appear in more restrictive functional frameworks (see also the upcoming Remark 2.3.4). Another advantage of the distributional formulation is that it provides a unifying framework for dealing with linear PDEs, independently of their nature. In contrast, traditional weak or variational formulations vary greatly depending on the nature of the PDE. As an illustration, in [73], one can compare the different function spaces for weak solutions associated to elliptic PDEs (Section 6.1.2), parabolic PDEs (Section 7.1.1(b)) and hyperbolic PDEs (Section 7.2.1(b)). The distributional formulation will be our main object of interest in this article, and can be seen as a weakened form of weak formulations of PDEs. Consider equation (2.1.1), and "test it locally": that is, multiply it by a compactly supported, infinitely differentiable test function φ (i.e. $\varphi \in C_c^\infty(\mathcal{D})$) and integrate over $\mathcal{D}$:

$$\forall \varphi \in C_c^\infty(\mathcal{D}),\ \sum_{|\alpha| \leq n} \int_{\mathcal{D}} \varphi(x) a_\alpha(x) \partial^\alpha u(x) dx = 0. \tag{2.1.3}$$

For each integral term above, perform $|\alpha|$ successive integrations by parts to transfer the derivatives from u to φ. Since φ is identically null on a neighbourhood of the boundary of $\mathcal{D}$, the boundary terms of each integration by parts vanish and we obtain that

$$\forall \varphi \in C_c^\infty(\mathcal{D}),\ \int_{\mathcal{D}} u(x) \sum_{|\alpha| \leq n} (-1)^{|\alpha|} \partial^\alpha (a_\alpha \varphi)(x) dx = 0. \tag{2.1.4}$$

To make sense of (2.1.4), one only requires u to be locally integrable, i.e. $\int_K |u(x)| dx < +\infty$ for all compact set $K \subset \mathcal{D}$. We then say that a locally integrable function u is a solution to $L(u) = 0$ in the sense of distributions, or distributional sense, if u verifies (2.1.4). In this case, u is a solution to equation (2.1.1) in the sense of "all smooth local averages" (i.e. for all $\varphi \in C_c^\infty(\mathcal{D})$), though not pointwise in general: taking $\varphi(x) = \delta_0(x - x_0)$ is not allowed without additional assumptions over u.

The distributional formulation of the PDE $L(u) = 0$ is "compliant with physics" too, as pointed out by W. Rudin ([173], p. 150): most of the sensors

we use in practice are only capable of computing local averages of the physical quantity they are measuring. Suppose one wishes to check experimentally that a temperature field obeys the heat equation, by using a set of thermometers: then one will actually only deal with the distributional formulation of the heat equation.

The natural question that follows from this new definition is whether one can characterize, in terms of their law, the random fields whose sample paths are solutions to the PDE $L(u) = 0$ *in the distributional sense*. The answer is yes, and is the main content of this article. Under the assumptions that U is a measurable centered second order random field and that its standard deviation function $\sigma : x \longmapsto \sqrt{k(x,x)}$ is locally integrable, we show in Proposition 2.3.5 that

$$\begin{aligned}\mathbb{P}(L(U) = 0 \text{ in the distributional sense}) = 1 \\ \iff \forall x \in \mathcal{D}, L(k(x,\cdot)) = 0 \text{ in the distributional sense.}\end{aligned} \quad (2.1.5)$$

Related literature

It is known, at least since the fifties, that some covariance functions are naturally linked to certain stochastic partial derivative equations (SPDEs), i.e. PDEs where the source term is random. For example, it was already observed in 1954 by [214] that the covariance function of a stationary GP U verifying the two dimensional SPDE $(\alpha^2 - \partial^2_{xx} - \partial^2_{yy})^{3/4} U = W_S$, where W_S is a spatial white noise process, is exponential, i.e. of the form $\mathrm{Cov}(U(x+h), U(x)) = C \exp(-\alpha|h|)$. Already for this SPDE, the differentiation has to be understood in a weakened sense as white noise processes are not random fields in the usual sense. In [170], SPDEs describing the random motion of micro-particles are introduced to link certain covariance functions, Matérn in particular, with an underlying physical model. We also refer to [135] for a large overview of the possible applications and recent developments pertaining to random fields defined by SPDEs. A general framework for the study of SPDEs was recently reintroduced in [207], which was then used to classify the stationary *generalized* random fields that are solutions of a wide class of linear SPDEs. In particular, [207] provides a description of all the second order stationary generalized random fields that are solutions to certain homogeneous PDEs, and the 3D wave equation in particular (which we also study in Section 2.4), in terms of their covariance operator. Loosely speaking, generalized random fields are function-indexed random fields where the covariance function is replaced by a covariance operator. From a functional analysis point of view, this is actually very close to the tools we use here, although in this article we constrain ourselves to work with (standard) random fields with well-defined

sample paths, as these are the objects that arise the most in the random function models met in practice. The two other key differences between this work and [207] are that (i) we do not focus on *stationary* random field models for u and (ii) we focus on the *homogeneous* case for PDE $L(u) = 0$.

The literature concerning random fields that are PDE-constrained at the level of the sample paths is rather sparse. In [86], general theorems are exposed for many different classes of linear operators acting on suitable spaces of functions. These theorems take the form of equation (2.1.2), and can in turn be applied to certain differential operators (see [86], Sections 3.3 and 4.1). [182] builds covariance functions that ensure that the sample path of a given two or three dimensional random vector field are either divergence or curl free. This result is notable because "any" three dimensional vector field can be decomposed as a sum of divergence and curl free vector fields through the Helmholtz-Hodge decomposition theorem. Moreover, divergence or curl free vector fields are commonly encountered in fluid mechanics. [78] extends the results of [182] to random fields on the sphere of $\mathbb{R}^3$, which has been rediscovered later in [75]. In [72], stationary GPs are represented in terms of a random wavevector. [72] then characterizes the stationary GPs whose sample paths verify a homogeneous linear PDE, in terms of the spectral measure of the GP and in terms of its random wavevector. [72] additionally requires that the sample paths be infinitely differentiable, that the PDE's coefficients be constant and that only even orders of differentiation appear in the PDE. This is then applied to a few wave models. A simple algorithm for building linearly constrained GPs is proposed in [109], based on formal GPR derivations upon (2.1.1); however, partly because the assumed regularity of u is not fully addressed, the claim that the sample paths of the underlying GP are indeed linearly constrained is left unproved. This is clarified in [123], where the requirement that $u \in C^\infty(\mathbb{R}^d)$ is made explicit and the enforcement of the PDE on the sample paths is proved for GPs whose sample paths are smooth. The algorithm from [109] is then supplemented in [123], where parametrizations of the solution spaces of (2.1.1) thanks to Gröbner bases are proposed. In [124], the same author completes the approach from [123] by incorporating boundary conditions on hypersurfaces in the Gröbner basis parametrization. With the idea to apply GPR to rigid body dynamics, [83] enforces Gauss' principle of least constraint on the sample paths of a GP.

One can understand our main result (Proposition 2.3.5) as a characterization of the "physics-informed" random fields that incorporate the distributional PDE constraint $L(u) = 0$ at the level of the sample paths. It turns out that the design of similar "physics-informed priors" has received a lot a attention from the machine learning community since the early 2000' ([90]), in the context of Gaussian process regression (GPR); see Section 2.3.3.1 for a

description of this technique. GPR is a Bayesian framework for function regression and interpolation which is well suited for handling linear constraints, partly because GPs are "stable under linear combinations", see Section 2.2.1.3. The recurring idea is to assume that the function u in equation (2.1.1) is a sample path of a (centered) GP U and to draw the consequences of equation (2.1.1) on the covariance function of U. The covariance function of U is then expected to incorporate the constraint $L(u) = 0$ in some sense. The majority of these works (except those mentioned above) do not aim at analysing whether the obtained covariance function indeed yields sample path PDE constraints over U: this is justified by the fact that they are only concerned with imposing the constraints on the function provided by GPR to approximate u. This approximation of u, which we denote by $\tilde{m}$, is called the Kriging mean in the GPR context; see equation (2.3.16) for a definition.

While they do not primarily focus on investigating sample path PDE constraints (contrarily to this article), the works coming from the GPR community are still very connected to this article. Indeed, they are concerned with designing explicit covariance functions that verify constraints of the form $L(k(\cdot, x)) = 0$ for all $x \in \mathcal{D}$ (the PDE is understood in the strong sense in these works). Indeed, this constraint ensures that all the possible regression functions $\tilde{m}$ provided by the corresponding GPR model verify the constraint $L(\tilde{m}) = 0$ (as seen in equation (2.3.16)). Note that "$L(k(\cdot, x)) = 0 \; \forall x \in \mathcal{D}$" is the right-hand side of equation (2.1.2): actually knowing covariance functions that verify this constraint is a necessary complement to the condition we prove in this article (Proposition 2.3.5 is otherwise useless in practice). Explicit PDE constrained covariance functions were designed for a number of classical PDEs, namely: divergence-free vector fields [146, 182], curl-free vector fields [81, 182], the Laplace equation [179, 142, 5], Maxwell's equations [209, 109, 123] (although [209, 109] only exploit curl/divergence free constraints), the 1D heat equation [5], Helmholtz' 2D equations [5], and linear solid mechanics [108]. [124] and [94] enforce homogeneous boundary conditions on the covariance function.

We finish with a brief overview of the alternative "physics-informed" GPR models. Contrarily to the equation (2.1.1) considered here, one may put a random source term f in the PDE and study instead the SPDE $L(u) = f$: see [163], [8] and [151] for entry points on the related literature. A recent article [36] extended the use of GPR to nonlinear PDEs by imposing the nonlinear interpolation constraints on the collocation points, setting the way forward for many possible applications of GPR to nonlinear realistic PDE models, as found e.g. in fluid mechanics. In [148], the variational formulation (see [73], Section 6.1.2 for a definition) of certain linear PDEs has been incorporated into a GPR framework. This approach requires the use of Gaussian

generalized random fields (see [24], Section 2.2.1.1), or "functional Gaussian processes" following [148]. The variational formulation of a PDE differs from its distributional formulation in the choice of the space of test functions.

Contribution and organisation of the paper

Consider the PDE in equation (2.1.1), where the coefficients of the differential operator L have possibly limited smoothness. Consider also a centered second order measurable stochastic process $U = (U(x))_{x\in\mathcal{D}}$ with covariance function $k(x, x')$ (see Sections 2.2.1.2 and 2.2.1.3). Under the assumption that its standard deviation function $\sigma : x \longmapsto k(x, x)^{1/2}$ is locally integrable, we show in Proposition 2.3.5 that the announced equation (2.1.5) holds. The result is then compared to a previous result from [86], which ensures pointwise linear differential degeneracy of the sample paths of U under stronger assumptions. We then provide a simple corollary which states that linear distributional differential constraints are preserved when a GP U is conditioned on pointwise observations, in view of GPR applications.

As an application example, we derive a general Gaussian process model for the homogeneous 3D free space wave equation, for which the solutions are not smooth in general. This equation is central for describing finite speed propagation phenomena as found e.g. in acoustics. Plugging this model in a GPR framework yields potential applications in different inverse problems related to this PDE, such as thermoacoustic tomography (i.e. initial condition reconstruction, [118], Section 19.3.1.1), source localization or propagation speed estimation, following e.g. the GPR methodology from [163] or [86], Section 4.2.

This model is derived by putting GP priors over the initial conditions of the wave equation and in Proposition 2.4.1, we obtain "explicit" formulas for the covariance function of the solution process, in the form of convolutions. From Propositions 2.3.5 and 2.4.1, we obtain that the sample paths of the corresponding (nonstationary) GP all verify the wave equation in the distributional sense. When the covariance functions of the initial conditions are not smooth enough, the result from [86] cannot be applied. Explicitly, for this PDE, choosing the commonly used 3/2-Matérn covariance functions for the initial position is enough to land outside the scope of the result from [86] (Section 2.4.2.1).

We emphasize that the covariance expressions exposed in Proposition 2.4.1 are original and interesting in themselves, as they can be used for efficient GPR for the wave equation. Specifically, the key difference with the wave equation covariance functions presented in [207] is that here, no stationarity assumptions are made on the solution stochastic process U. In particular the

spectral measure provided by Bochner's theorem [166], which is the key tool used in [207], is not available anymore. We thus resort to more standard integration techniques to prove Proposition 2.4.1.

The paper is organized as follow. For self-containment, Section 2.2 is dedicated to reminders on random fields and generalized functions. This Section and all the proofs are detailed enough so that this article is accessible to the analyst, the probability theorist and the statistician. In Section 2.3, we state and prove our new necessary and sufficient condition on random fields that are subject to linear distributional differential constraints. Section 2.4 is dedicated to the study of a GP model for the wave equation. We conclude in Section 2.5.

2.2 Background

2.2.1 Random fields

Let $(\Omega, \mathcal{A}, \mathbb{P})$ be a probability space. For convenience, we will assume that it is complete, i.e. that $\mathcal{A}$ contains the subsets of sets $A \in \mathcal{A}$ such that $\mathbb{P}(A) = 0$.

2.2.1.1 Basic definitions

Let $\mathcal{D} \subset \mathbb{R}^d$ be an open set. In this article, a random field $U = (U(x))_{x \in \mathcal{D}}$ is a collection of real random variables defined on Ω. We define its sample path at point $\omega \in \Omega$ to be the deterministic function $x \longmapsto U(x)(\omega)$, and we denote it by U_ω. Given an operator acting on the sample paths of U, an event of the form $\{L(U) \in A\}$ will always be understood sample path wise: that is, by definition, $\{L(U) \in A\} \coloneqq \{\omega \in \Omega : L(U_\omega) \in A\}$. Such sets are not automatically measurable; still, they are measurable as soon as they contain an event of probability 1 (as the ones in Propositions 2.3.2 and 2.3.5), since $(\Omega, \mathcal{A}, \mathbb{P})$ is a complete probability space.

2.2.1.2 Measurable random fields

In view of our main theorem, a necessary notion is that of the measurability of the random field U. U is said to be measurable ([63], p. 60 or [127], p. 34) if it is measurable seen as a bivariate map $U : (\Omega \times \mathcal{D}, \mathcal{A} \otimes \mathcal{B}(\mathcal{D})) \longrightarrow (\mathbb{R}, \mathcal{B}(\mathbb{R}))$, $(\omega, x) \mapsto U(x)(\omega)$. Here, $\mathcal{B}(S)$ denotes the Borel σ-algebra of S and $\mathcal{A} \otimes \mathcal{B}(\mathcal{D})$ denotes the product σ-algebra of $\mathcal{A}$ and $\mathcal{B}(\mathcal{D})$.

To work with measurable random fields, one will often consider random fields U which are continuous *in probability*, i.e. for all $x \in \mathcal{D}$ and $\varepsilon >$

$0, \mathbb{P}(|U(x)-U(x+h)| > \varepsilon) \to 0$ when $h \to 0$. Indeed, continuity in probability implies the existence of a measurable modification of U, i.e. a measurable random field $\tilde{U}$ such that $\mathbb{P}(\tilde{U}(x) = U(x)) = 1$ for all $x \in \mathcal{D}$ ([63], Theorem 2.6, p. 61). One then implicitly works with $\tilde{U}$. In this article, we will directly assume that we deal with measurable random fields instead of assuming any continuity regularity on the sample paths of the said stochastic process. This is because pointwise continuity is not really relevant when working with PDEs in a weak sense; actually, one of the main points of working with weakened formulations is to avoid strong (i.e. pointwise) formulations. Note however that ensuring measurability outside of the above mentioned theorem, though possible, rapidly becomes tedious (see e.g. [64], Theorem 2.3). A famous theorem from Kolmogorov ([52], Theorem 3.3 p. 73 and Theorem 3.4 p. 74) provides sufficient conditions for almost sure continuity of the sample paths, which in turn implies continuity in probability of the random field. This condition is phrased in terms of a sufficient Hölder control of the expectation of the increments of the process. Refinements in the case of Gaussian processes exist: see e.g. [2], Theorem 1.4.1, p. 20. On a final note, the measurability assumption is discussed in [193] (Theorem 3.3), where it is shown to be a necessary condition for the existence of Karhunen-Loève expansions of second order random fields.

2.2.1.3 Second order random fields, Gaussian processes.

Note $L^2(\mathbb{P})$ the Hilbert space of real valued random variables X such that $\mathbb{E}[X^2] < +\infty$. A stochastic process $(U(x))_{x\in\mathcal{D}}$ is said to be second order if for all $x \in \mathcal{D}$, $U(x) \in L^2(\mathbb{P})$. One can then define its mean and covariance functions by $m(x) = \mathbb{E}[U(x)]$ and $k(x, x') = \mathbb{E}[(U(x) - m(x))(U(x') - m(x'))]$ respectively. One can then also define its standard deviation function

$$\sigma : x \mapsto \sqrt{k(x, x)}. \tag{2.2.1}$$

A Gaussian process $(U(x))_{x\in\mathcal{D}}$ over $\mathcal{D}$ is a random field over $\mathcal{D}$ such that for any $(x_1, ..., x_n) \in \mathcal{D}^n$ and any $(a_1, ..., a_n) \in \mathbb{R}^n, \sum_i a_i U(x_i)$ is a Gaussian random variable; that is, the law of $(U(x_1), ..., U(x_n))^T$ is a multivariate normal distribution. The law of a GP is characterized by its mean and covariance functions ([107], Section 8). We write $(U(x))_{x\in\mathcal{D}} \sim GP(m, k)$. Given a GP $(U(x))_{x\in\mathcal{D}}$, we will sometimes use the space $\mathcal{L}(U) = \overline{\text{Span}(U(x), x \in \mathcal{D})}$, i.e. the Hilbert subspace of $L^2(\mathbb{P})$ induced by U. Since $L^2(\mathbb{P})$-limits of Gaussian random variables drawn from the same GP remain Gaussian ([107], Section 1.3), $\mathcal{L}(U)$ only encompasses Gaussian random variables.

Whereas m can be any function, the covariance function k has to be symmetric and positive definite: for all $(x_1, ..., x_n)$ in $\mathcal{D}^n$, the matrix $(k(x_i, x_j))_{1 \leq i,j \leq n}$ is symmetric and nonnegative definite.

Symmetric positive definite functions verify the Cauchy-Schwarz inequality [166]:

$$\forall x, x' \in \mathcal{D}, \quad |k(x, x')| \leq \sqrt{k(x, x)}\sqrt{k(x', x')}. \tag{2.2.2}$$

Note that there is a one-to-one correspondence between positive definite functions and the laws of centered GPs ([63], Theorem 3.1). We provide below two examples of radial Matérn covariance functions ([166], pp. 84-85), which will be useful in Section 2.4. Set $r = \|x - x'\|$, the Euclidean distance between x and x', then the following two functions are valid covariance functions, given any $l > 0$:

$$k_{1/2}(x, x') = \exp(-r/l), \qquad k_{3/2}(x, x') = (1 + r/l)\exp(-r/l). \tag{2.2.3}$$

These covariance functions are widely used in machine learning, especially $k_{3/2}$. Almost surely, the sample paths of a GP with a Matérn covariance function k_ν with $\nu = m + 1/2$, $m \in \mathbb{N}$, are of differentiability class C^m and not C^{m+1}. They are thus commonly used to model functions with finite smoothness.

2.2.2 Tools from functional analysis

We refer to [173] and [202] for further details on generalized functions and Radon measures. In this whole subsection, $\mathcal{D}$ is an open set of $\mathbb{R}^d$.

2.2.2.1 Class C^m functions, test functions, locally integrable functions

Given $m \in \mathbb{N}$, $C^m(\mathcal{D})$ denotes the space of real-valued functions defined over $\mathcal{D}$ of class C^m, and $C_c^m(\mathcal{D})$ denotes the subspace of $C^m(\mathcal{D})$ of functions φ whose support $\mathrm{Supp}(\varphi)$ is compact. Recall that $\mathrm{Supp}(\varphi)$ is the closure of the set $\{x : \varphi(x) \neq 0\}$. The space $C_c^\infty(\mathcal{D})$, which we will rather denote $\mathscr{D}(\mathcal{D})$, is the space of compactly supported infinitely differentiable functions supported on $\mathcal{D}$, also known as test functions. $L^1_{loc}(\mathcal{D})$ denotes the space of measurable scalar functions f defined on $\mathcal{D}$ that are locally integrable, i.e. such that $\int_K |f| < +\infty$ for all compact sets $K \subset \mathcal{D}$. Two locally integrable functions are equal in $L^1_{loc}(\mathcal{D})$ when they are equal almost everywhere (a.e.) in the sense of the Lebesgue measure over $\mathbb{R}^d$. $L^1_{loc}(\mathcal{D})$ is a very large space which contains the space of piecewise continuous functions, but also all the local Lebesgue

spaces $L^p_{loc}(\mathcal{D}), p \geq 1$ and thus all the Sobolev spaces of nonnegative exponent. It is in fact the largest space of functions that can be alternatively viewed as continuous linear forms over $\mathscr{D}(\mathcal{D})$ (see Section 2.2.2.4 below).

2.2.2.2 Generalized functions

We endow $\mathscr{D}(\mathcal{D})$ with its usual LF-space topology, defined for example in [202], Chapter 13. LF stands for "strict inductive limit of Fréchet spaces". As it will appear in several places later on, we briefly describe the LF topology following [202], although this is not necessary for understanding the article. Assume that a vector space E can be written as $E = \bigcup_n E_n$ where (E_n) is an increasing sequence of Fréchet spaces (i.e. metrizable complete locally convex topological vector spaces), such that the natural injection $E_n \to E_{n+1}$ is a linear homeomorphism over its range. The LF topology over E is defined as follow: a convex set $V \subset E$ is a neighborhood of 0 if and only if $V \cap E_n$ is a neighborhood of 0 for all n. It is remarkable that LF topologies are *not* metrizable except if for some n_0, $E_n = E_{n_0}$ for all $n \geq n_0$ ([202], Remark 13.1). In return, this allows for some other very nice topological properties to hold, e.g., LF spaces are complete ([202], Theorem 13.1).

For $\mathscr{D}(\mathcal{D})$, the LF topology is the one corresponding to the decomposition $\mathscr{D}(\mathcal{D}) = \bigcup_i \mathscr{D}_{K_i}(\mathcal{D})$, where $\mathscr{D}_{K_i}(\mathcal{D}) \coloneqq \{\varphi \in C^\infty(\mathcal{D}) : \mathrm{Supp}(\varphi) \subset K_i\}$, and $(K_i)_{i\in\mathbb{N}}$ is an increasing sequence of compact subsets of $\mathcal{D}$ such that $\bigcup_i K_i = \mathcal{D}$ ([202], pp. 131-133). This LF topology does not depend on the choice of $(K_i)_{i\in\mathbb{N}}$. An example of metric inducing the Fréchet topology of $\mathscr{D}_{K_i}(\mathcal{D})$ is the following:

$$d_i(\varphi,\psi) \coloneqq \sup_{N\in\mathbb{N}} 2^{-N} \frac{p_{N,i}(\varphi-\psi)}{1+p_{N,i}(\varphi-\psi)}, \quad p_{N,i}(\varphi) \coloneqq \max_{|\alpha|\leq N} \sup_{x\in K_i} |\partial^\alpha \varphi(x)|. \quad (2.2.4)$$

It is given in [173], Section 1.46 p. 34 and Remark 1.38(c) p. 29. Explicitly, a sequence $(\varphi_n) \subset \mathscr{D}(\mathcal{D})$ converges to $\varphi \in \mathscr{D}(\mathcal{D})$ if there exists a compact set $K \subset \mathcal{D}$ such that $\mathrm{Supp}(\varphi_n) \subset K$ for all $n \in \mathbb{N}$ and for all $\alpha \in \mathbb{N}^d$, $\|\partial^\alpha \varphi_n - \partial^\alpha \varphi\|_\infty \to 0$ ([173], Theorem 6.5(f) and the remark following p. 154).

We call generalized function any continuous linear form on $\mathscr{D}(\mathcal{D})$, i.e. any element of $\mathscr{D}(\mathcal{D})'$, the topological dual of $\mathscr{D}(\mathcal{D})$. We will rather denote it by $\mathscr{D}'(\mathcal{D})$ as in [202], Notation 21.1. The topology of $\mathscr{D}(\mathcal{D})$ is such that $T \in \mathscr{D}'(\mathcal{D})$ if and only if for all compact set $K \subset \mathcal{D}$, there exists $C_K > 0$ and a nonnegative integer n_K such that

$$\forall \varphi \in \mathscr{D}(\mathcal{D}) \text{ such that } \mathrm{Supp}(\varphi) \subset K, \quad |T(\varphi)| \leq C_K \sum_{|\alpha|\leq n_K} \|\partial^\alpha \varphi\|_\infty. \quad (2.2.5)$$

We recall that we use the following notations: given a multi-index $\alpha = (\alpha_1, ..., \alpha_d) \in \mathbb{N}^d$, we denote $|\alpha| = \alpha_1 + ... + \alpha_d$ and $\partial^\alpha := (\partial_{x_1})^{\alpha_1} ... (\partial_{x_d})^{\alpha_d}$ where $\partial_{x_i}^{\alpha_i}$ is the α_i^{th} derivative with reference to the i^{th} coordinate x_i. Generalized functions are also called "distributions", a terminology we will only use when there is no risk of confusion with probability distributions. The duality bracket will be denoted $\langle , \rangle$: for all $\varphi \in \mathscr{D}(\mathcal{D})$ and $T \in \mathscr{D}'(\mathcal{D})$, we have $\langle T, \varphi \rangle := T(\varphi)$.

2.2.2.3 Generalized functions and differentiation

Any generalized function T can be infinitely differentiated ([173], Section 6.12, p. 158 or [202], pp. 248-250) according to the following definition

$$\partial^\alpha T : \varphi \longmapsto \langle T, (-1)^{|\alpha|} \partial^\alpha \varphi \rangle. \tag{2.2.6}$$

The derivative $\partial^\alpha T$ is then also a continuous linear form over $\mathscr{D}(\mathcal{D})$, i.e. $\partial^\alpha T \in \mathscr{D}'(\mathcal{D})$.

2.2.2.4 Regular generalized functions

Any function $f \in L^1_{loc}(\mathcal{D})$ can be injectively identified to a generalized function T_f ([202], p. 224 or [173], Section 6.11, p. 157) defined as follow

$$\forall \varphi \in \mathscr{D}(\mathcal{D}), \quad \langle T_f, \varphi \rangle := \int_{\mathcal{D}} f(x)\varphi(x)dx. \tag{2.2.7}$$

The map $L^1_{loc}(\mathcal{D}) \ni f \longmapsto T_f$ is linear and injective; any generalized function T that is of the form T_f for some $f \in^1_{loc} (\mathcal{D})$ is said to be regular. Throughout this article, we will use the abusive notation $\langle T_f, \varphi \rangle = \langle f, \varphi \rangle$, as if $\langle , \rangle$ were the L^2 inner product. Observe that equations (2.2.6) and (2.2.7) combined provide a flexible definition of the derivatives of any function $f \in L^1_{loc}(\mathcal{D})$ up to any order. One also sees that *weak* derivatives, as encountered in Sobolev spaces ([33], Section 9.1) and weak formulations of PDEs, are particular cases of distributional derivatives: given $\alpha \in \mathbb{N}^d$ and two locally integrable functions f and f_α, f admits f_α for its α^{th} weak derivative if and only if $\partial^\alpha T_f = T_{f_\alpha}$. One then conveniently writes $\partial^\alpha f = f_\alpha$ ($\partial^\alpha f$ is unique in $L^1_{loc}(\mathcal{D})$ from the injectivity of the mapping (2.2.7)).

2.2.2.5 Radon measures

This subsection and the ones that follow are only necessary for dealing with the wave equation in Section 2.4. In this article, we call positive Radon measure any positive measure over $\mathcal{D}$ that is Borel regular ([74], Definition 1.9)

and that has finite mass over any compact subset of $\mathcal{D}$. A Radon measure is a linear combination of positive Radon measures. In [122], Chapter 9, it is proved that the space of Radon measures over $\mathcal{D}$ is isomorphic to the space of continuous linear forms over $C_c(\mathcal{D})$, the space of compactly supported continuous functions on $\mathcal{D}$ endowed with its usual LF-space topology described e.g. in [202], pp. 131-133. The corresponding isomorphism is given by

$$\mu \longmapsto T_\mu : \begin{cases} C_c(\mathcal{D}) & \longrightarrow \mathbb{R} \\ f & \longmapsto \int_{\mathcal{D}} f(x)\mu(dx). \end{cases} \tag{2.2.8}$$

We have the following facts. (i) Any signed measure that admits a density f with reference to the Lebesgue measure such that $f \in L^1_{loc}(\mathcal{D})$ is a Radon measure ([202], p. 217). (ii) Any Radon measure can be injectively identified to a generalized function T_μ by replacing $C_c(\mathcal{D})$ by $\mathscr{D}(\mathcal{D})$ in equation (2.2.8). In particular, Radon measures can be differentiated up to any order through equation (2.2.6). (iii) Any Radon measure μ, can be uniquely written as $\mu = \mu^+ - \mu^-$ where μ^+ and μ^- are positive Radon measures ([122], Chapter 9). We then define its total variation by $|\mu| \coloneqq \mu^+ + \mu^-$.

2.2.2.6 Finite order generalized functions

A generalized function T is said to be of finite order if there exists a nonnegative integer m such that one can take $n_K = m$, independently of K, in the definition of the continuity of T, i.e. equation (2.2.5). The order of T is then the smallest of those integers m. The space of generalized functions of order m is isomorphic to $C_c^m(\mathcal{D})'$, the space of continuous linear forms over $C_c^m(\mathcal{D})$, when $C_c^m(\mathcal{D})$ is endowed with its usual LF-space topology ([202], pp. 131-133). The key property for us is that such generalized functions can be represented thanks to Radon measures. If L is of order m, there exists a family of Radon measures $\{\mu_p\}_{|p|\leq m}$ over $\mathcal{D}$ such that

$$T = \sum_{|p|\leq m} \partial^p \mu_p, \tag{2.2.9}$$

where the equality in equation (2.2.9) holds in $\mathscr{D}'(\mathcal{D})$ and $C_c^m(\mathcal{D})'$ ([202], p 259). Among the finite order generalized functions are those that are *compactly supported*, i.e. those for which the measures μ_p such that $T = \sum_{|p|\leq m} \partial^p \mu_p$ all have compact support.

2.2.2.7 Convolution with generalized functions

As above, we consider $C_c^m(\mathbb{R}^d)$ endowed with its LF-space topology. Let $f \in C_c^m(\mathbb{R}^d)$ and $T \in C_c^m(\mathbb{R}^d)'$. Note $\tau_x f$ the function $y \longmapsto f(y-x)$ and $\check{f}$

the function $y \longmapsto f(-y)$. Then ([202], p. 287, Section 27) one may define the convolution between T and f by

$$T * f : x \longmapsto \langle T, \tau_{-x}\check{f} \rangle, \tag{2.2.10}$$

and $T * f$ is a function in the classical sense, i.e. defined pointwise. When T is a regular generalized function, equation (2.2.10) reduces to the usual convolution of functions through the identification defined in equation (2.2.7). Similarly if T is in fact a Radon measure μ:

$$(T * f)(x) = \int_{\mathbb{R}^d} f(x - y)\mu(dy). \tag{2.2.11}$$

More general definitions of generalized function convolution are available ([202], Chapter 27) but this one is sufficient for our use.

2.2.2.8 Tensor product of generalized functions

For two generalized functions $T_1 \in \mathscr{D}'(\mathcal{D}_1)$ and $T_2 \in \mathscr{D}'(\mathcal{D}_2)$, $T_1 \otimes T_2 \in \mathscr{D}'(\mathcal{D}_1 \times \mathcal{D}_2)$ denotes their tensor product([202], pp. 416-417), which is uniquely determined by the following tensor property:

$$\forall \varphi_1 \in \mathscr{D}(\mathcal{D}_1), \forall \varphi_2 \in \mathscr{D}(\mathcal{D}_2),\ \langle T_1 \otimes T_2, \varphi_1 \otimes \varphi_2 \rangle = \langle T_1, \varphi_1 \rangle \times \langle T_2, \varphi_2 \rangle. \tag{2.2.12}$$

$T_1 \otimes T_2$ reduces to the tensor product of functions (respectively, measures) when T_1 and T_2 are functions (respectively, measures) through the identification of equation (2.2.7) (respectively, equation (2.2.8)).

2.3 Random fields under linear differential constraints

The results in this section state that under suitable assumptions over the first two moments of a given second order random field $U = (U(x))_{x \in \mathcal{D}}$, sample path degeneracy properties with reference to differential constraints can be read on the first two moments of U, namely the mean function and the functions $k_x : y \longmapsto k(x, y)$, where k is the covariance function of U. This is remarkable because the space induced by the sample paths of U is a priori much larger than the space spanned by the functions $k_x, x \in \mathcal{D}$. Moreover, the functions k_x are "accessible", i.e. checking that these functions indeed verify the linear constraint can usually be done with direct computations.

We begin by recalling a result from [86] in the case of pointwise defined derivatives. We next state and prove a result similar to that of [86], where we interpret the derivatives in the distributional sense.

2.3.1 The case of classical derivatives

We start by properly defining the notion of strong solutions of a PDE.

Definition 2.3.1 (Strong/classical solutions)**.** Let L be a differential operator defined as in equation (2.1.1), with continuous coefficients. We say that a function u is a classical or strong solution to the PDE $L(u) = 0$ if u is n times differentiable and u verifies the PDE pointwise:

$$\forall x \in \mathcal{D}, \quad L(u)(x) = \sum_{|\alpha| \leq n} a_\alpha(x) \partial^\alpha u(x) = 0. \tag{2.3.1}$$

Note that the space of n times differentiable functions does not have the nice topological properties of $C^n(\mathcal{D})$ and in most cases met in practice, one rather requires that strong solutions lie in $C^n(\mathcal{D})$. It is however in the sense of the definition 2.3.1 that the theorem from [86] is best understood. This theorem, which we remind in Proposition 2.3.2, is the one proved and used in [86] to build a Gaussian process whose sample paths are all strong solutions to the Laplace equation on a 2D circular domain.

We first introduce some notations. Let $(U(x))_{x \in \mathcal{D}}$ be a centered Gaussian process with covariance function k. Denote $\mathcal{F}(\mathcal{D}, \mathbb{R})$ the space of real-valued pointwise-defined functions on $\mathcal{D}$ (often alternatively denoted $\mathbb{R}^{\mathcal{D}}$). We will only use $\mathcal{F}(\mathcal{D}, \mathbb{R})$ as a set, therefore we do not consider any topology over it. We refer to [184], Section 9, for details on $\mathcal{F}(\mathcal{D}, \mathbb{R})$ seen as a topological vector space. Denote $\mathcal{H}_k$ the reproducing kernel Hilbert space (RKHS) associated to k (see [24], Definition 1 p. 7 and Theorem 3, p. 19). $\mathcal{H}_k$ is a Hilbert space of pointwise-defined functions (i.e. $\mathcal{H}_k \subset \mathcal{F}(\mathcal{D}, \mathbb{R})$ as sets), such that the pointwise evaluation maps $l_x : f \mapsto f(x)$ are continuous functionals. Although belonging to $\mathcal{F}(\mathcal{D}, \mathbb{R})$ does not seem very restrictive at first glance, this clashes with the usual L^p and Sobolev spaces encountered in PDE theory, which are sets of functions defined up to a set of null Lebesgue measure.

Proposition 2.3.2 (sample paths of GPs under linear constraints [86])**.** *Let $\big(U(x)\big)_{x \in \mathcal{D}} \sim GP(0, k)$. Note for all $x \in \mathcal{D}$ the function $k_x : y \longmapsto k(x, y)$. Let E be a real vector space of functions defined on $\mathcal{D}$ that contains the sample paths of U almost surely and $L : E \longrightarrow \mathcal{F}(\mathcal{D}, \mathbb{R})$ be a linear operator. Assume that for all $x \in \mathcal{D}$, $L(U)(x) \in \mathcal{L}(U)$, where $\mathcal{L}(U)$ is the closure of $Span\{U(x), x \in \mathcal{D}\}$ in $L^2(\mathbb{P})$. Then there exists a unique linear operator $\mathscr{L} : \mathcal{H}_k \longrightarrow \mathcal{F}(\mathcal{D}, \mathbb{R})$ such that*

$$\forall x, y \in \mathcal{D}, \quad \mathbb{E}[L(U)(x)U(y)] = \mathscr{L}(k_y)(x),$$

and such that for all $x \in \mathcal{D}, h \in \mathcal{H}_k$ and sequence $(h_n) \subset \mathcal{H}_k$ such that $h_n \to h$ for the topology of $\mathcal{H}_k$, we have $\mathscr{L}(h_n)(x) \longrightarrow \mathscr{L}(h)(x)$. Finally, the following statements are equivalent:

(*i*) $\mathbb{P}(L(U) = 0) = 1$.
(*ii*) $\forall x \in \mathcal{D}, \mathscr{L}(k_x) = 0$.

A sufficient condition ensuring that the sample paths of a GP lie in $C^n(\mathcal{D})$ is found in [2], Theorem 1.4.2. More broadly, both necessary and sufficient conditions over the first two moments of a GP for its sample path to be (Hölder) continuous are well-known: see e.g. [3], Theorems 3.3.3 and 8.3.2.

The proof of Proposition 2.3.2 heavily relies on the Loève isometry ([24], Theorem 35, p. 65) between the two Hilbert spaces $\mathcal{H}_k$ and $\mathcal{L}(U)$ (see Section 2.2.1.3 for details on $\mathcal{L}(U)$). This theorem can be applied when L is a differential operator as discussed in [86]. However, in Proposition 2.3.2, the differential operator L of order n has to be valued in $\mathcal{F}(\mathcal{D}, \mathbb{R})$; in particular for $u \in E$, the function $L(u)$ has to be defined pointwise in order to use the Loève isometry. To summarize, in all generality the derivatives in L have to be understood in a classical sense and E has to be contained in $\mathscr{D}^n(\mathcal{D})$, the space of n times differentiable functions on $\mathcal{D}$. Requiring that $E \subset \mathscr{D}^n(\mathcal{D})$ is a very strong assumption with reference to the sample paths of U; furthermore, this is not compliant with the usual way of studying PDEs where derivatives are understood in a weaker sense. We present in Proposition 2.3.5 an adaptation of Proposition 2.3.2 where the derivatives are understood in the distributional sense. By transferring all the derivatives on the test function, we will be liberated from any differentiability assumptions over the sample paths of U, effectively replacing $\mathscr{D}^n(\mathcal{D})$ with $L^1_{loc}(\mathcal{D})$. Finally, the random field U will not be assumed Gaussian and will only be required to be measurable second order.

2.3.2 The case of distributional derivatives

2.3.2.1 Distributional solutions of PDEs

In this section, we elaborate a bit more on the notion of distributional solutions to a given PDE. Let $L = \sum_{|\alpha| \leq n} a_\alpha(x)\partial^\alpha$ be a linear differential operator, and assume for the moment that its coefficients are infinitely differentiable. We briefly recall the steps described in the introduction that lead to the definition of distributional solutions presented in equation (2.1.4). Start from a strong solution u of class C^n of $L(u) = 0$, multiply this PDE by a test function $\varphi \in \mathscr{D}(\mathcal{D})$, integrate over $\mathcal{D}$ and perform $|\alpha|$ integration by parts to transfer all derivatives from u to φ. Since the support of φ is a compact subset of the open set $\mathcal{D}$, the boundary terms of each integration by parts vanish, leading to

$$\forall \varphi \in \mathscr{D}(\mathcal{D}), \quad \int_{\mathcal{D}} u(x) \sum_{|\alpha| \leq n} (-1)^{|\alpha|} \partial^\alpha (a_\alpha \varphi)(x) dx = 0. \tag{2.3.2}$$

Following equation (2.3.2) we introduce L^*, the formal adjoint of L, acting on $\mathscr{D}(\mathcal{D})$, defined by the following formula ([202], pp. 247-249)

$$L^* : \varphi \longmapsto \sum_{|\alpha| \leq n} (-1)^{|\alpha|} \partial^\alpha (a_\alpha \varphi). \tag{2.3.3}$$

Note that for equation (2.3.2) to be well defined, the assumptions that $u \in L^1_{loc}(\mathcal{D})$ and $a_\alpha \in C^{|\alpha|}(\mathcal{D})$ are sufficient. More precisely, these assumptions are enough to show that the map $L(u)$ defined by duality

$$L(u) : \begin{cases} \mathscr{D}(\mathcal{D}) & \longrightarrow \mathbb{R} \\ \varphi & \longmapsto \int_{\mathcal{D}} L^*(\varphi)(x) u(x) dx \end{cases} \tag{2.3.4}$$

defines a continuous linear form over $\mathscr{D}(\mathcal{D})$, i.e. $L(u) \in \mathscr{D}'(\mathcal{D})$ (see equations (2.2.5) and (2.3.9) for a rigorous proof of this statement). This definition extends the definition of distributional derivatives from Section 2.2.2.3 to differential operators. By construction, L and L^* verify a duality identity: given $\varphi \in \mathscr{D}(\mathcal{D})$ and $u \in L^1_{loc}(\mathcal{D})$, $\langle L(u), \varphi \rangle = \langle u, L^*(\varphi) \rangle$.

As in Section 2.2.2.4, the assumption that $u \in L^1_{loc}(\mathcal{D})$ is in fact a *continuity* assumption over the associated linear form $L(u)$ (a more general and theoretical analysis of such observations can be found in [202], pp. 247-251). This finally leads to the following definition, following e.g. [69], p. 10:

Definition 2.3.3 (Distributional solutions)**.** A function $u \in L^1_{loc}(\mathcal{D})$ is said to be a solution to the PDE $L(u) = 0$ in the sense of distributions if $L(u) = 0$ in $\mathscr{D}'(\mathcal{D})$, i.e. when $L(u)$ is seen as en element of $\mathscr{D}'(\mathcal{D})$ through equation (2.3.4) and 0 is the null linear form over $\mathscr{D}(\mathcal{D})$.

As weak derivatives are a particular case of distributional derivatives (Section 2.2.2.4), one expects that the distributional solutions of a PDE that admit some weak derivatives are in fact weak solutions, i.e. solutions of some weak formulation of that PDE. Rigorous statements of this general fact have to be checked on a case-by-case basis, depending on the weak formulation at hand (a more in-depth discussion falls outside of the scope of this article). As an example, this is the case for the weak formulation of elliptic PDEs in $H^1_0(\mathcal{D})$ (see e.g. [73], Section 6.2), where $H^1_0(\mathcal{D})$ is the closure of $\mathscr{D}(\mathcal{D})$ in the Sobolev space $H^1(\mathcal{D}) := \{u \in L^2(\mathcal{D}) : \nabla u \text{ exists as a weak derivative and } \nabla u \in L^2(\mathcal{D})^d\}$.

Remark 2.3.4 (Measure-valued solutions of PDEs). Although it is not the main focus of the paper, we can even allow u in Definition 2.3.3 to be a Radon measure by replacing $u(x)dx$ with $\mu(dx)$ in equation (2.3.4). This will be useful in Section 2.4.1, where we will encounter a measure-valued PDE solution which is central from a physical viewpoint, with the wave equation's Green's function

(it is *not* actually a function!). Notice that weak formulations in Sobolev spaces, say $H^1(\mathcal{D})$, are not well-equipped to work with such solutions, and our distributional framework becomes needed.

2.3.2.2 Random fields under distributional differential constraints

We can now state the following proposition, based on Definition 2.3.3.

Proposition 2.3.5 (sample paths of random fields under linear differential constraints, distributional derivatives)**.** *Let $\mathcal{D} \subset \mathbb{R}^d$ be an open set and let $L = \sum a_\alpha(x)\partial^\alpha$, $|\alpha| \leq n$, be a linear differential operator of order n with coefficients $a_\alpha(x) \in C^{|\alpha|}(\mathcal{D})$. Let $U = \big(U(x)\big)_{x\in\mathcal{D}}$ be a measurable second order random field with mean function $m(x)$ and covariance function $k(x, x')$. For all $x \in \mathcal{D}$, note $k_x : y \longmapsto k(x, y)$. Suppose that $m \in L^1_{loc}(\mathcal{D})$ and $\sigma \in L^1_{loc}(\mathcal{D})$, where $\sigma : x \mapsto k(x, x)^{1/2}$.*
1) Then $\mathbb{P}(U \in L^1_{loc}(\mathcal{D})) = 1$ and for all $x \in \mathcal{D}, k_x \in L^1_{loc}(\mathcal{D})$.
2) Suppose that $L(m) = 0$ in the sense of distributions. Then the following statements are equivalent:

(i) $\mathbb{P}(L(U) = 0$ *in the sense of distributions*$) = 1$.

(ii) $\forall x \in \mathcal{D},\ L(k_x) = 0$ *in the sense of distributions.*

Explicitly, by (i) we mean that there exists a set $A \in \mathcal{A}$ with $\mathbb{P}(A) = 1$ such that for all $\omega \in A$,

$$\forall \varphi \in \mathscr{D}(\mathcal{D}),\quad \langle U_\omega, L^*\varphi\rangle = \int_{\mathcal{D}} U_\omega(x) L^*\varphi(x)dx = 0. \tag{2.3.5}$$

The fact that the functions $x \longmapsto U_\omega(x)$ and $y \longmapsto k_x(y)$ lie in $L^1_{loc}(\mathcal{D})$ ensure the existence of the integrals in equations (2.3.5) (see Point 2 of the proof of Proposition 2.3.5) as well as the continuity of the associated linear forms over $\mathscr{D}(\mathcal{D})$, following the definition of equation (2.3.4). The assumption that $a_\alpha \in C^{|\alpha|}(\mathcal{D})$ is not very strong, in the sense that it is the minimal assumption to ensure that the adjoint L^* is well-defined (equation (2.3.3)), and thus that Definition 2.3.3 even makes sense. Likewise, requiring that $\sigma \in L^1_{loc}(\mathcal{D})$ is not very restrictive (see Section 2.2.2.1). However, ensuring the measurability of the random process U is more demanding in practice, because it is difficult to ensure this property outside of having continuity in probability (see Section 2.2.1.2).

The following lemma will be crucial for the proof of Proposition 2.3.5:

Lemma 2.3.6. *$\mathscr{D}(\mathcal{D})$ is sequentially separable, i.e. there exists a countable subset $F \subset \mathscr{D}(\mathcal{D})$ such that for all $\varphi \in \mathscr{D}(\mathcal{D})$, there exists a sequence $(\varphi_n) \subset F$ such that $\varphi_n \to \varphi$ in $\mathscr{D}(\mathcal{D})$ for its LF topology.*

Recall that a topological space E is separable if there exists a countable subset $F \subset E$ such that its closure in E is equal to E. If the topology of E is metrizable (as e.g. for Fréchet spaces), sequential separability and separability are equivalent. If this topology is *not* metrizable (as e.g. for LF spaces), then sequential separability implies separability but the converse need not hold. Below, we provide a short proof of Lemma 2.3.6, as we could not find it in the literature. The weaker property that $\mathscr{D}(\mathcal{D})$ is separable is already difficult to track down, see e.g. [82], Corollaire (1).2, p. 78 or [84], p. 73, (3).

Proof. We first show that the spaces $\mathscr{D}_{K_i}(\mathcal{D})$ introduced in Section 2.2.2.2 are separable Fréchet spaces. The Fréchet topology of $\mathscr{D}_{K_i}(\mathcal{D})$ is the one induced by the usual Fréchet topology of $C^\infty(\mathcal{D})$ when $\mathscr{D}_{K_i}(\mathcal{D})$ is seen as a subspace of $C^\infty(\mathcal{D})$ ([202], pp. 131-132). As a Fréchet space, $C^\infty(\mathcal{D})$ is metrizable ([202], p. 85). But $C^\infty(\mathcal{D})$ is also a Montel space ([202], Proposition 34.4, p. 357): as a metrizable Montel space, it is automatically separable ([180], p. 195 or [61]). Thus $\mathscr{D}_{K_i}(\mathcal{D})$ is also separable as a subset of the separable metrizable space $C^\infty(\mathcal{D})$ ([33], Proposition 3.25, p. 73).

Denote now F_i a countable dense subset of $\mathscr{D}_{K_i}(\mathcal{D})$ and consider $F \coloneqq \bigcup_{i\in\mathbb{N}} F_i$. Let $\varphi \in \mathscr{D}(\mathcal{D})$ and $i \in \mathbb{N}$ such that $\mathrm{Supp}(\varphi) \subset K_i$, where $(K_i)_{i\in\mathbb{N}}$ is the sequence of compact sets from Section 2.2.2.2. Then $\varphi \in \mathscr{D}_{K_i}(\mathcal{D})$ and there exists a sequence $(\varphi_n) \subset F_i \subset F$ such that $\varphi_n \to \varphi$ in the sense of the Fréchet topology of $\mathscr{D}_{K_i}(\mathcal{D})$, i.e. the metric d_i in equation (2.2.4). From equation (2.2.4), $\|\partial^\alpha \varphi_n - \partial^\alpha \varphi\|_\infty \to 0$ for all $\alpha \in \mathbb{N}^d$. Since $\mathrm{Supp}(\varphi_n) \subset K_i$ for all $n \in \mathbb{N}$, we have that $\varphi_n \to \varphi$ in $\mathscr{D}(\mathcal{D})$ (see Section 2.2.2.2). □

We are now able to prove Proposition 2.3.5.

Proof. Suppose first that U is centered, i.e. $m \equiv 0$.
1) We begin by showing that the sample paths of U almost surely lie in $L^1_{loc}(\mathcal{D})$. Note first that thanks to the Cauchy-Schwarz inequality, $\mathbb{E}[|U(x)|] \leq \sigma(x)$. Now, let $(K_i)_{i\in\mathbb{N}}$ be an increasing sequence of compact subsets of $\mathcal{D}$ such that $\bigcup_{i\in\mathbb{N}} K_i = \mathcal{D}$. Using Tonelli's theorem, we have that for any $n \in \mathbb{N}$,

$$\mathbb{E}\left[\int_{K_i} |U(x)|dx\right] = \int_{K_i} \mathbb{E}[|U(x)|]dx \leq \int_{K_i} \sigma(x)dx < +\infty, \tag{2.3.6}$$

since $\sigma \in L^1_{loc}(\mathcal{D})$. Note that in order for the integrals above to be well defined, imposing that U is a measurable random field cannot be circumvented. Equation (2.3.6) yields a set $B_n \subset \Omega$ of probability 1 over which the random variable $\omega \longmapsto \int_{K_i} |U_\omega(x)|dx$ is finite (from Fubini's theorem again, the map $\omega \longmapsto \int_{K_i} |U_\omega(x)|dx$ is measurable). Consider now the set $B = \bigcap_{n\in\mathbb{N}} B_n$

which remains of probability 1. For all compact subset $K \subset \mathcal{D}$, there exists an integer n_K such that $K \subset K_{n_K}$ and thus for all $\omega \in B$,

$$\int_K |U_\omega(x)|dx \leq \int_{K_{n_K}} |U_\omega(x)|dx < +\infty, \tag{2.3.7}$$

which shows that the sample paths of U lie in $L^1_{loc}(\mathcal{D})$ almost surely. Similarly, we check that for all $x \in \mathcal{D}, k_x$ lies in $L^1_{loc}(\mathcal{D})$: for any compact set K, since $\sigma \in L^1_{loc}(\mathcal{D})$ and because of equation (2.2.2),

$$\int_K |k_x(y)|dy = \int_K |k(x,y)|dy \leq \sigma(x) \int_K \sigma(y)dy < \infty.$$

2) Let us check in advance that whatever $f \in L^1_{loc}(\mathcal{D})$, the map $T(f) : \varphi \longmapsto \langle f, L^*\varphi \rangle$ is a continuous linear form over $\mathscr{D}(\mathcal{D})$. Since $a_\alpha \in C^{|\alpha|}(\mathcal{D})$, we can apply Leibniz' rule on $L^*\varphi = \sum_{|\alpha| \leq n} (-1)^{|\alpha|} \partial^\alpha (a_\alpha \varphi)$. This yields a family $\{f_\alpha\}_{|\alpha| \leq n}$ of continuous functions over $\mathcal{D}$ such that

$$\forall \varphi \in \mathscr{D}(\mathcal{D}), \quad \forall x \in \mathcal{D}, \quad L^*\varphi(x) = \sum_{|\alpha| \leq n} f_\alpha(x) \partial^\alpha \varphi(x). \tag{2.3.8}$$

For all $f \in L^1_{loc}(\mathcal{D})$, for all compact set $K \subset \mathcal{D}$ and for all $\varphi \in \mathscr{D}(\mathcal{D})$ such that $\mathrm{Supp}(\varphi) \subset K$, we have $\mathrm{Supp}(L^*\varphi) \subset K$ and equation (2.3.8) yields

$$\begin{aligned} |\langle f, L^*\varphi \rangle| &\leq \int_{\mathcal{D}} |f(x)||L^*\varphi(x)|dx \\ &\leq \left(\int_K |f(x)|dx \times \max_{|\alpha| \leq n} \sup_{x \in K} |f_\alpha(x)| \right) \times \sum_{|\alpha| \leq n} \|\partial^\alpha \varphi\|_\infty < +\infty. \end{aligned} \tag{2.3.9}$$

This proves that $T(f) : \varphi \longmapsto \langle f, L^*\varphi \rangle$ is a continuous linear form over $\mathscr{D}(\mathcal{D})$ (see equation (2.2.5)).

$\underline{(i) \implies (ii)}$: Suppose (i). Let $\varphi \in \mathscr{D}(\mathcal{D})$. There exists a set $A \subset \Omega$ such that $\mathbb{P}(A) = 1$ and such that

$$\forall \omega \in A, \quad \langle U_\omega, L^*\varphi \rangle = \int_{\mathcal{D}} U_\omega(x) L^*\phi(x)dx = 0.$$

Multiplying equation above with the random variable $U(x')$, taking the expectation and formally permuting (for now) the integral and the expectation, we obtain

$$0 = \mathbb{E}\left[U(x') \int_{\mathcal{D}} U(x) L^*\varphi(x)dx \right] = \int_{\mathcal{D}} L^*\varphi(x) \mathbb{E}[U(x)U(x')]dx$$

$$= \int_{\mathcal{D}} L^*\varphi(x)k(x,x')dx = \langle k_{x'}, L^*\varphi\rangle.$$

The integral-expectation permutation is justified by writing down the expectation as an integral and using Fubini's theorem, checking that the below quantity is finite. We use Tonelli's theorem and the Cauchy-Schwarz inequality:

$$\begin{aligned}\mathbb{E}\left[\int_{\mathcal{D}} |U(x')U(x)L^*\varphi(x)|dx\right] &= \int_{\mathcal{D}} |L^*\varphi(x)|\mathbb{E}[|U(x)U(x')|]dx \\ &\leq \int_{\mathcal{D}} |L^*\varphi(x)|\mathbb{E}[U(x)^2]^{1/2}\mathbb{E}[U(x')^2]^{1/2}dx \\ &\leq \sigma(x')\int_{\mathcal{D}} |L^*\varphi(x)|\sigma(x)dx < +\infty.\end{aligned}$$

Indeed, since $\sigma \in L^1_{loc}(\mathcal{D})$, setting $f = \sigma$ in equation (2.3.9) shows that the last integral is indeed finite. Thus, $\forall x \in \mathcal{D}, \forall \varphi \in \mathscr{D}(\mathcal{D}), \langle k_x, L^*\varphi\rangle = 0$ which proves that $(i) \implies (ii)$.
$(ii) \implies (i)$: Suppose (ii). Let $\varphi \in \mathscr{D}(\mathcal{D})$, we have $\langle k_{x'}, L^*\varphi\rangle = 0$. Multiplying this with $L^*\varphi(x')$ and integrating with reference to x' yields

$$\begin{aligned}0 &= \int_{\mathcal{D}} L^*\varphi(x')\int_{\mathcal{D}} L^*\varphi(x)k(x,x')dxdx' \\ &= \int_{\mathcal{D}}\int_{\mathcal{D}} L^*\varphi(x)L^*\varphi(x')\mathbb{E}[U(x)U(x')]dxdx'.\end{aligned}$$

Permuting formally the expectation and the integrals (justified in equation (2.3.10)) yields

$$\begin{aligned}0 &= \int_{\mathcal{D}}\int_{\mathcal{D}} L^*\varphi(x)L^*\varphi(x')\mathbb{E}[U(x)U(x')]dxdx' \\ &= \mathbb{E}\left[\left(\int_{\mathcal{D}} L^*\varphi(x)U(x)dx\right)^2\right] = \mathbb{E}\left[\langle U, L^*\varphi\rangle^2\right],\end{aligned}$$

and thus $\langle U, L^*\varphi\rangle = 0$ a.s. : there exists $A_\varphi \in \mathcal{A}$ with $\mathbb{P}(A_\varphi) = 1$ such that $\forall \omega \in A_\varphi, \langle U_\omega, L^*\varphi\rangle = 0$. We justify the expectation-integral permutation with the computation below

$$\begin{aligned}&\int_{\mathcal{D}}\int_{\mathcal{D}} |L^*\varphi(x)L^*\varphi(x')|\mathbb{E}[|U(x)U(x')|]dxdx' \\ &\qquad\leq \int_{\mathcal{D}}\int_{\mathcal{D}} |L^*\varphi(x)L^*\varphi(x')|\sigma(x)\sigma(x')dxdx' \\ &\qquad\leq \left(\int_{\mathcal{D}} |L^*\varphi(x)|\sigma(x)dx\right)^2 < +\infty. \qquad (2.3.10)\end{aligned}$$

As previously, setting $f = \sigma$ in equation (2.3.9) shows that the integral above is indeed finite.

This does not finish the proof as we need to find a set A with $\mathbb{P}(A) = 1$, independently from φ, such that $\forall \omega \in A, \langle U_\omega, L^*\varphi \rangle = 0$. For this we shall use Lemma 2.3.6. Let

$$A \coloneqq B \cap \big(\bigcap_{\varphi \in F} A_\varphi \big), \tag{2.3.11}$$

where the set F is introduced in Lemma 2.3.6. Then $\mathbb{P}(A) = 1$ since $\mathbb{P}(B) = 1, \mathbb{P}(A_\varphi) = 1$ and F is countable. Let $\omega \in A$. Since $U_\omega \in L^1_{loc}(\mathcal{D})$, equation (2.3.9) shows that the map $T_\omega : \varphi \longmapsto \langle U_\omega, L^*\varphi \rangle$ is a continuous linear form on $\mathscr{D}(\mathcal{D})$. In particular, Theorem 6.6(c) p. 155 from [173] states that T_ω is in fact *sequentially* continuous. Let $\varphi \in \mathscr{D}(\mathcal{D})$ and $(\varphi_n) \subset F$ be such that $\varphi_n \to \varphi$ in $\mathscr{D}(\mathcal{D})$, from Lemma 2.3.6. From the sequential continuity of T_ω, $T_\omega(\varphi) = \lim_{n\to\infty} T_\omega(\varphi_n) = 0$ since $\forall n \in \mathbb{N}, T_\omega(\varphi_n) = 0$. That is, we have proved that

$$\forall \omega \in A, \quad \forall \varphi \in \mathscr{D}(\mathcal{D}), \quad \langle U_\omega, \ L^*\varphi \rangle = T_\omega(\varphi) = 0.$$

Since $\mathbb{P}(A) = 1$, this shows that $(ii) \implies (i)$.

When U is not centered, consider the centered random field V defined by $V(x) = U(x) - m(x)$ for which the above proof can be applied. Since L is linear and m is assumed to verify $L(m) = 0$ in the sense of distributions, the probabilistic sets $A_U = \{L(U) = 0 \text{ in the sense of distributions}\}$ and $A_V = \{L(V) = 0 \text{ in the sense of distributions}\}$ coincide and thus, $A \subset A_U$. Finally, U and V have the same covariance function $k(x, x')$. Thus,

$$\begin{aligned} &\mathbb{P}(L(U) = 0 \text{ in the sense of distributions}) = 1 \\ &\qquad \iff \mathbb{P}(L(V) = 0 \text{ in the sense of distributions}) = 1 \\ &\qquad \iff \forall x \in \mathcal{D}, L(k_x) = 0 \text{ in the sense of distributions}, \end{aligned}$$

which finishes the proof in the general case. □

Remark 2.3.7. Distributional solutions are the weakest types of solutions for PDEs. In general, additional regularity conditions have to be imposed to obtain physically realistic solutions, such as Sobolev regularity or entropy conditions as for nonlinear hyperbolic PDEs [186]. However, every step in the above proof remains valid when replacing $\varphi \in \mathscr{D}(\mathcal{D})$ with $\varphi \in C^n_c(\mathcal{D})$. Although we have not explicited the usual topology of $C^n_c(\mathcal{D})$ in this article, we state that this is enough to show that the equalities stated in Proposition 2.3.5 also hold in $C^n_c(\mathcal{D})'$, the space of finite order generalized functions of order n, rather than just in $\mathscr{D}'(\mathcal{D})$. $C^n_c(\mathcal{D})'$ is a smaller space than $\mathscr{D}'(\mathcal{D})$, though less used in functional analysis than $\mathscr{D}'(\mathcal{D})$.

We partially recover Proposition 2.3.2 when the sample paths of U are n times differentiable with locally integrable n^{th} derivative and $k \in C^{n,n}(\mathcal{D}\times\mathcal{D})$. Indeed, in that case one can show that if $L = \sum_{|\alpha|\leq n} a_\alpha(x)\partial^\alpha$, then we simply have $\mathscr{L} = L$ in Proposition 2.3.2. Additionally, $L(U_\omega)$ and $L(k_x)$ both lie in $\mathcal{F}(\mathcal{D},\mathbb{R}) \cap L^1_{loc}(\mathcal{D})$. In that framework, Proposition 2.3.2 states that

$$\forall x \in \mathcal{D},\ L(k_x) = 0 \iff \mathbb{P}(L(U) = 0) = 1, \tag{2.3.12}$$

where the function equalities of the form $L(f) = 0$ in equation (2.3.12) are valid everywhere on $\mathcal{D}$. In contrast, for any function g that lies in $L^1_{loc}(\mathcal{D})$, we have

$$g = 0 \text{ in the sense of distributions} \iff g = 0 \ a.e. \tag{2.3.13}$$

Equation (2.3.13) is just another way of saying that the linear map $f \longmapsto T_f$ given in (2.2.7) is injective. Following equation (2.3.13), Proposition 2.3.5 states a slightly weaker result than (2.3.12), namely that

$$\forall x \in \mathcal{D},\quad L(k_x) = 0 \ a.e. \iff \mathbb{P}(L(U) = 0 \ a.e.) = 1. \tag{2.3.14}$$

If we actually have that the sample paths of U lie in $C^n(\mathcal{D})$, nullity almost everywhere implies nullity everywhere and we recover equation (2.3.12) from equation (2.3.14).

Instead of having the sample paths of U lie in $C^n(\mathcal{D})$ though, one may rather encounter the case where U is *mean-square* differentiable up to a certain order m. Under some continuity assumptions over the covariance function of U and up to suitable modifications, [181] showed that the sample paths of the mean-square differentiated process are actually weak derivatives of the sample paths of U. As observed after Definition 2.3.3, we thus expect that the sample paths of the mean-square differentiable random fields verifying Point 2, (ii) of Proposition 2.3.5 are solutions of some weak formulation of the PDE, rather than just distributional solutions.

Example 2.3.8 (A first order PDE). Consider a continuous, nondifferentiable one dimensional covariance function $k_0 : \mathbb{R}\times\mathbb{R} \to \mathbb{R}$, for example $k_0(x,x') = \exp(-|x-x'|)$. It is then readily checked that the function $k : \mathbb{R}^2\times\mathbb{R}^2 \to \mathbb{R}$ defined by $k((x,y),(x',y')) = k_0(x-y,x'-y')$ is positive definite and verifies Point 2, (ii) of Proposition 2.3.5 for the PDE

$$\partial_x u + \partial_y u = 0 \quad \text{in } \mathbb{R}^2. \tag{2.3.15}$$

Consider now a centered second order random field $(U(x,y))_{(x,y)\in\mathbb{R}^2}$ with covariance function k, passing to a measurable version of U if necessary (it exists from Section 2.2.1.2, as the continuity of k yields the continuity in probability

of U). Then almost surely, its sample paths verify the PDE (2.3.15) in the sense of distributions, even though they are not expected to be differentiable. An example of random field whose covariance function is k as defined above, is the GP $(U_0(x-y))_{(x,y)\in\mathbb{R}^2}$ where $(U_0(x))_{x\in\mathbb{R}} \sim GP(0, k_0)$. These formulas can be obtained by viewing the PDE (2.3.15) as a transport equation under the condition that $U(x,0) = U_0(x)$, following the same approach as in the upcoming Section 2.4.2.

2.3.3 A heredity property for Gaussian process regression

2.3.3.1 Gaussian process regression in a nutshell

GPs can be used for function interpolation. Let u be a function defined on $\mathcal{D}$ for which we know a dataset of values $B = \{u(x_1), ..., u(x_n)\}$. Conditioning the law of a GP $(U(x))_{x\in\mathcal{D}} \sim GP(m, k)$ on the database B yields a second GP $\tilde{U}$ given by $\tilde{U}(x) \coloneqq (U(x)|U(x_i) = u(x_i), i = 1, ..., n)$. The law of $\tilde{U}$ is known: $(\tilde{U}(x))_{x\in\mathcal{D}} \sim GP(\tilde{m}, \tilde{k})$. $\tilde{m}$ and $\tilde{k}$ are given by the so-called *Kriging* equations (2.3.16) and (2.3.17). Let $X = (x_1, ..., x_n)^T$, denote $m(X)$ the column vector such that $m(X)_i = m(x_i)$, $k(X,X)$ the square matrix such that $k(X,X)_{ij} = k(x_i, x_j)$ and given $x \in \mathcal{D}$, $k(X,x)$ the column vector such that $k(X,x)_i = k(x_i, x)$. Suppose that $K(X,X)$ is invertible, then [166]

$$\begin{cases} \tilde{m}(x) &= m(x) + k(X,x)^T k(X,X)^{-1}(u(X) - m(X)), & (2.3.16) \\ \tilde{k}(x,x') &= k(x,x') - k(X,x)^T k(X,X)^{-1} k(X,x'). & (2.3.17) \end{cases}$$

The Kriging standard deviation function is then given by

$$\tilde{\sigma}(x) = \tilde{k}(x,x)^{1/2}. \tag{2.3.18}$$

The so-called Kriging mean $\tilde{m}$ plays the role of an approximation of u; in particular, it interpolates u at the observation points: $\tilde{m}(x_i) = u(x_i)$ for all $i = 1, ..., n$. Moreover, the Kriging covariance $\tilde{k}$ can be used to further control the distance between u and $\tilde{m}$.

2.3.3.2 Conditioned Gaussian processes under linear differential constraints

We can now state the following corollary, which draws the consequences of Proposition 2.3.5 when applied to GPR.

Proposition 2.3.9 (Heredity of Proposition 2.3.5 to conditioned GPs)**.** *Let $\mathcal{D}$ and L be as defined in Proposition 2.3.5. Let $(U(x))_{x\in\mathcal{D}} \sim GP(m, k)$ be a*

Gaussian process that verifies the assumptions of Proposition 2.3.5. Suppose also that

$$L(m) = 0 \quad \textit{and} \quad \forall x \in \mathcal{D},\ L(k_x) = 0 \quad \textit{both in the sense of distributions.} \tag{2.3.19}$$

(i) Then whatever the integer p, the vector $u = (u_1, ..., u_p)^T \in \mathbb{R}^p$ and the vector $X = (x_1, ..., x_p)^T \in \mathcal{D}^p$ such that $k(X, X)$ is invertible, the Kriging mean $\tilde{m}(x)$ and the Kriging standard deviation function $\tilde{\sigma}$ both lie in $L^1_{loc}(\mathcal{D})$, and we have

$$L(\tilde{m}) = 0 \quad \textit{and} \quad \forall x \in \mathcal{D},\ L(\tilde{k}_x) = 0 \quad \textit{both in the sense of distributions.}$$

where $\tilde{m}$ and $\tilde{k}$ are defined in equations (2.3.16) and (2.3.17).
(ii) As such, the sample paths of the conditioned Gaussian process $\left(\tilde{U}(x)\right)_{x\in\mathcal{D}}$ defined by $\tilde{U}(x) = (U(x)|U(x_i) = u_i\ \forall i = 1, ..., p)$ are almost surely solutions of the equation $L(f) = 0$ in the sense of distributions:

$$\mathbb{P}(L(\tilde{U}) = 0 \textit{ in the sense of distributions}) = 1.$$

Proof. Note first that for all $x \in \mathcal{D}, \tilde{k}(x, x) \leq k(x, x)$ ([77], p. 117). Thus the function $\tilde{\sigma} : x \longmapsto \tilde{k}(x, x)^{1/2}$ also lies in $L^1_{loc}(\mathcal{D})$. Point (i) is then a direct consequence of the definition of $\tilde{m}$ and $\tilde{k}$ in equations (2.3.16) and (2.3.17), and the linearity of L. Proposition 2.3.5 can then be applied conjointly with (i), which yields point (ii) since the mean and covariance functions of the GP $\tilde{U}$ are $\tilde{m}$ and $\tilde{k}$ (see equations (2.3.16) and (2.3.17)). □

Proposition 2.3.9 shows that when U is a GP, the results of Proposition 2.3.5 are inherited on the conditioned posterior process $\tilde{U}$. One weak consequence of Proposition 2.3.9 is that if GPR is performed with a covariance function k that verifies point (ii) of Proposition 2.3.5, then all the possible Kriging means provided by GPR remain solutions of the PDE $L(\tilde{m}) = 0$.

2.4 Gaussian processes and the 3 dimensional wave equation

The formalism we used in the previous section is necessary to tackle hyperbolic PDEs as in some cases, their solutions only verify the PDE in a weaker sense, e.g. the distributional sense ([73], Sections 2.1.1 and 7.2). Hyperbolic PDEs are typically encountered when describing finite speed propagation phenomena and their prototype is the wave equation (see equation (2.4.1)); this equation is central in a number of fields such as acoustics, electromagnetics

and quantum mechanics. In this section, we derive a GP model for the solutions of the homogeneous 3D wave equation, with explicit covariance formulas in the form of convolutions.

We show on one example that the model we obtain below is capable of dealing with an initial speed v_0 that is piecewise continuous and an initial position u_0 that has piecewise continuous derivatives, when the initial discontinuity surfaces are "nice enough". This is an advantage with reference to the previous models, where the sample paths actually had to be sufficiently differentiable to obtain sample path degeneracy with reference to the PDE.

2.4.1 General solution to the 3 dimensional wave equation

Denote the 3D Laplace operator $\Delta = \partial^2_{xx} + \partial^2_{yy} + \partial^2_{zz}$ and the d'Alembert operator $\Box = 1/c^2\partial^2_{tt} - \Delta$ with constant wave speed $c > 0$. We focus on the general initial value problem in the free space $\mathbb{R}^3$

$$\begin{cases} \Box w & = 0 & \forall (x,t) \in \mathbb{R}^3 \times \mathbb{R}^*_+, \\ w(x,0) & = u_0(x) & \forall x \in \mathbb{R}^3, \\ (\partial_t w)(x,0) & = v_0(x) & \forall x \in \mathbb{R}^3. \end{cases} \tag{2.4.1}$$

Throughout this article, we will refer to u_0 as the initial position and v_0 as the initial speed. The solution of this problem is unique in the distributional sense ([69], p. 164). It can be extended to all $t \in \mathbb{R}$ ([69], p. 295) and is represented as follow ([69], p. 295 again)

$$w(x,t) = (F_t * v_0)(x) + (\dot{F}_t * u_0)(x) \qquad \forall (x,t) \in \mathbb{R}^3 \times \mathbb{R}, \tag{2.4.2}$$

where F_t and $\dot{F}_t$ are known generalized functions. That is, the function $w(x,t)$ above is a solution of the system (2.4.1), in which t is now allowed to lie in $\mathbb{R}$ rather than $\mathbb{R}^*_+$. The existence of such an extension is possible because of the time reversibility of the wave equation (in the language of semigroup theory, its semigroup can be embedded in a group, [155], Theorem 4.5 p. 222). In dimension 3, F_t and $\dot{F}_t$ are compactly supported generalized functions of order 0 and 1 respectively. They are given by

$$F_t = \frac{\sigma_{c|t|}}{4\pi c^2 t} \quad \text{and} \quad \dot{F}_t = \partial_t F_t \quad \forall t \in \mathbb{R}, \tag{2.4.3}$$

where σ_R is the surface measure of the sphere of center 0 and radius R; $\dot{F}_t = \partial_t F_t$ means that for all $f \in C^1_c(\mathbb{R}^3)$, $\langle \dot{F}_t, f\rangle = \partial_t \langle F_t, f\rangle$. We make these expressions more explicit in equation (2.4.4), using spherical coordinates. It is worth noting that $(F_t)_{t\in\mathbb{R}}$ corresponds to the *Green's function* of the wave

equation, in the sense that it verifies the system (2.4.1) with $u_0 = 0$ and $v_0 = \delta_0$ where δ_0 is the Dirac mass ([69], pp. 294-295). As discussed in Remark 2.3.4, $(F_t)_{t\in\mathbb{R}}$ is a family of singular measures and this PDE system has to be understood in the distributional sense. Note also that equations (2.4.3) show that F_t and $\dot{F}_t$ are supported on the sphere of radius $c|t|$: "the support of F_t propagates at finite speed c". This property is known as the Huygens principle for the three dimensional wave equation, see [73], p. 80.

Suppose that $u_0 \in C^1(\mathbb{R}^3)$ and $v_0 \in C^0(\mathbb{R}^3)$, then w as defined in equation (2.4.2) is a pointwise defined function (Section 2.2.2.7) and in that case an explicit formula for such convolutions is reminded in equation (2.2.10) (yet one may actually make sense out of (2.4.2) when u_0 and v_0 are only required to be any generalized functions, see [202], Chapter 27).

Equation (2.4.2) can be written using means over spheres. Denote (r, θ, ϕ), $r \geq 0, \theta \in [0, \pi], \phi \in [0, 2\pi]$ the spherical coordinates, $S(0, 1)$ the unit sphere of $\mathbb{R}^3$ and $\gamma = (\sin\theta\cos\phi, \sin\theta\sin\phi, \cos\theta)^T \in S(0, 1)$ the corresponding parametrization of $S(0, 1)$ ($\|\gamma\|_2 = 1$). We write $d\Omega = \sin\theta d\theta d\phi$ the surface differential element of $S(0, 1)$. The formulas (2.4.2) and (2.4.3) then lead to the Kirschoff formula ([73], p. 72):

$$w(x,t) = \int_{S(0,1)} tv_0(x - c|t|\gamma) + u_0(x - c|t|\gamma) - c|t|\gamma \cdot \nabla u_0(x - c|t|\gamma)\frac{d\Omega}{4\pi} \tag{2.4.4}$$

2.4.2 Gaussian process modelling of the solution

Suppose now that u_0 and v_0 are unknown, and only pointwise values of w are observed. We thus model u_0 and v_0 as random functions and put Gaussian process priors over u_0 and v_0. More precisely, we make the following assumptions.

(A_1) Suppose that the initial conditions u_0 and v_0 of Problem (2.4.1) are sample paths drawn from two independent Gaussian processes $U^0 \sim GP(0, k_{\mathrm{u}})$ and $V^0 \sim GP(0, k_{\mathrm{v}})$: $\exists\omega \in \Omega, \forall x \in \mathbb{R}^3, u_0(x) = U^0_\omega(x)$ and $v_0(x) = V^0_\omega(x)$.

(A_2) Suppose that all sample paths of U^0 lie in $C^1(\mathbb{R}^3)$ and that those of V^0 lie in $C^0(\mathbb{R}^3)$, almost surely. A sufficient condition for this is given in [2], Theorem 1.4.2. This theorem states that under mild technical assumptions, the paths of $(U(x))_{x\in\mathcal{D}} \sim GP(0, k)$ lie in C^l a.s. as soon as $k \in C^{2l}(\mathcal{D} \times \mathcal{D})$, *which we assume from now on.* This is e.g. fulfilled by the Matérn covariance functions from equation (2.2.3), with $l = 0$ for $k_{1/2}$ and $l = 1$ for $k_{3/2}$.

We now analyse the consequence of these two assumptions. First, they imply that by solving (2.4.1), one obtains a time-space stochastic process $W(x, t)$

defined by

$$W(x,t) : \Omega \ni \omega \longmapsto (F_t * V^0_\omega)(x) + (\dot{F}_t * U^0_\omega)(x). \tag{2.4.5}$$

Here again, V^0_ω denotes the sample path of V^0 at $\omega \in \Omega$ and likewise for U^0_ω. In particular, thanks to assumption (A_2), equation (2.4.5) defines a random variable for all (x,t). Note the space-time variable $z = (x,t)$ and note the random variables

$$V(z) : \omega \longmapsto (F_t * V^0_\omega)(x) \quad \text{and} \quad U(z) : \omega \longmapsto (\dot{F}_t * U^0_\omega)(x), \tag{2.4.6}$$

that is, $W(z) = U(z) + V(z)$. We show in the next proposition that the random fields U, V and W are GPs as well. In particular we describe their covariance functions.

Proposition 2.4.1. *Define the two functions*

$$k^{\text{wave}}_{\text{v}}(z,z') = [(F_t \otimes F_{t'}) * k_{\text{v}}](x,x'), \tag{2.4.7}$$
$$k^{\text{wave}}_{\text{u}}(z,z') = [(\dot{F}_t \otimes \dot{F}_{t'}) * k_{\text{u}}](x,x'). \tag{2.4.8}$$

(i) Then $U = (U(z))_{z\in\mathbb{R}^3\times\mathbb{R}}$ and $V = (V(z))_{z\in\mathbb{R}^3\times\mathbb{R}}$ as defined in (2.4.6) are two independent centered GPs with covariance functions $k^{\text{wave}}_{\text{u}}$ and $k^{\text{wave}}_{\text{v}}$ respectively. Consequently, $(W(z))_{z\in\mathbb{R}^3\times\mathbb{R}}$ is a centered GP whose covariance function is given by

$$k_W(z,z') = k^{\text{wave}}_{\text{v}}(z,z') + k^{\text{wave}}_{\text{u}}(z,z'). \tag{2.4.9}$$

(ii) Conversely, any measurable centered second order random field with covariance function k_W has its sample paths solution of the wave equation (2.4.1), in the sense of distributions, almost surely.

The formulas (2.4.7) and (2.4.8) can easily be derived formally, by running computations as if F_t and $\dot{F}_t$ were regular generalized functions (Section 2.2.2.4). This is somewhat justified because any generalized function can be approximated with a sequence of smooth compactly supported functions, by a "cutting and regularizing" argument ([202], Theorem 28.2, Chapter 28). However, checking that this procedure passes to the limit everywhere is tedious. Here, we rather make use of representations of F_t and $\dot{F}_t$ thanks to Radon measures (Sections 2.2.2.5 and 2.2.2.6) and use Fubini's theorem. We refer to Sections 2.2.2.6 and 2.2.2.8 for the definition of $\dot{F}_t \otimes \dot{F}_{t'}$, and Section 2.2.2.7 for the definition of $(\dot{F}_t \otimes \dot{F}_{t'}) * k_{\text{u}}$.

Proof. (i) : first we prove that U and V are GPs. Since U^0 and V^0 are GPs, $\mathcal{L}(U^0)$ and $\mathcal{L}(V^0)$ are only comprised of Gaussian random variables (see

Section 2.2.1.3). We then rely on the Kirschoff formula (2.4.4), writing the integrals as limits of Riemann sums. We start with V, that is, we focus on the first term in Kirschoff's formula (2.4.4). To show that V is a Gaussian process, we only need to show that for any z, $V(z) \in \mathcal{L}(V^0)$ as this will ensure the Gaussian process property. Since the sample paths of V^0 are continuous almost surely, there exists a sequence of numbers $(a_k^n) \subset \mathbb{R}$ and points $(y_k^n) \subset S(0,1)$ such that for almost any $\omega \in \Omega$,

$$\begin{aligned} V(z)(\omega) = (F_t * V_\omega^0)(x) &= t \int_{S(0,1)} V^0(x - c|t|\gamma)(\omega) \frac{d\Omega}{4\pi} \\ &= \frac{t}{4\pi} \int_0^{2\pi} \int_0^{\pi} V^0(x - c|t|\gamma(\theta,\phi))(\omega) \sin(\theta) d\theta d\phi \\ &= \lim_{n\to\infty} \sum_{k=1}^{n} a_k^n V^0(x - c|t|y_k^n)(\omega). \end{aligned}$$

This shows that $V(z)$ is the a.s. limit of the sequence of centered Gaussian random variables $(Y_n) \subset \mathcal{L}(V^0)$, where $Y_n = \sum_{k=1}^n a_k^n V^0(x - c|t|y_k^n)$; Y_n is Gaussian because V^0 is a GP. Almost sure convergence implies convergence in law. From [127], Proposition 1.1, $V(z)$ is normally distributed and the convergence also takes place in $L^2(\mathbb{P})$. Therefore, $V(z) \in \mathcal{L}(V^0)$ and V is a Gaussian process. From the same proposition, $V(z)$ is centered because the variables Y_n are centered. Note that since F_t is supported on the compact set $S(0, c|t|)$, we only required the sample paths of V^0 to be continuous rather than continuous and compactly supported.

We apply the same reasoning to U, by applying the above steps to the second part of Kirschoff's formula (2.4.4). One's ability to write out the integrals as a limit of Riemann sums is ensured when the sample paths of U^0 lie in $C^1(\mathbb{R}^3)$.

Finally, since U^0 and V^0 are independent, $\mathcal{L}(U^0)$ and $\mathcal{L}(V^0)$ are orthogonal in $L^2(\mathbb{P})$. Since $\mathcal{L}(U) \subset \mathcal{L}(U^0)$ and likewise for V, U and V are independent Gaussian processes as for Gaussian random variables, independence is equivalent to null covariance. Finally, the sum of independent Gaussian random variables is a Gaussian random variable. Therefore $\mathcal{L}(W) \subset \mathcal{L}(U) + \mathcal{L}(V)$ is only comprised of Gaussian random variables and W is a Gaussian process. Now, we prove that

$$\mathbb{E}[U(z)U(z')] = [(\dot{F}_t \otimes \dot{F}_{t'}) * k_{\mathrm{u}}](x, x'). \tag{2.4.10}$$

The main argument is Fubini's theorem for Radon measures. For this we use the fact that $\dot{F}_t$ is a distribution of order 1 and can be identified to a sum of derivatives of measures (see equation (2.2.9)): for all $t \in \mathbb{R}$, there exists

$\{\mu_\alpha^t\}_{\alpha\in\mathbb{N}^3,|\alpha|\leq 1}$ a family of Radon measures such that

$$\dot{F}_t = \sum_{|\alpha|\leq 1} \partial^\alpha \mu_\alpha^t \quad \text{in the sense of distributions.} \tag{2.4.11}$$

Moreover, $\dot{F}_t$ is compactly supported, therefore all the measures μ_α^t are also compactly supported. First, we write $U_\omega(z)$ in integral form:

$$U_\omega(z) = \big(\dot{F}_t * U_\omega^0\big)(x) = \langle \dot{F}_t, \tau_{-x}\check{U}_\omega^0\rangle = \Big\langle \sum_{|\alpha|\leq 1} \partial^\alpha \mu_\alpha^t, \tau_{-x}\check{U}_\omega^0\Big\rangle \tag{2.4.12}$$

$$= \sum_{|\alpha|\leq 1} \langle \mu_\alpha^t, (-1)^{|\alpha|}\partial^\alpha \tau_{-x}\check{U}_\omega^0\rangle = \sum_{|\alpha|\leq 1} \int_{\mathbb{R}^3} (-1)^{|\alpha|}\partial^\alpha U_\omega^0(x-y)\mu_\alpha^t(dy). \tag{2.4.13}$$

Before applying Fubini's theorem, we need to check an integrability condition. Let $\alpha \in \mathbb{N}^3$ be such that $|\alpha| \leq 1$. Recall that $|\mu_t^\alpha|$ is defined in Section 2.2.2.5; denote also $\sigma_{\partial^\alpha U^0}(x) = \sqrt{\mathrm{Var}(\partial^\alpha U_0(x))}$. Since the sample paths of U^0 lie in $C^1(\mathcal{D})$ a.s, those of $\partial^\alpha U^0$ lie in $C^0(\mathcal{D})$ and thus the function $x \longmapsto \mathrm{Var}(\partial^\alpha U_0(x))$ also lies in $C^0(\mathcal{D})$ ([16], chapter 1, Section 4.3). Therefore the function $x \longmapsto \sigma_{\partial^\alpha U^0}(x)$ also lies in $C^0(\mathcal{D})$. We now check that the integral I below is finite. We use Tonelli's theorem and the Cauchy-Schwarz inequality:

$$\begin{aligned}
I &:= \int_\Omega \sum_{|\alpha|\leq 1} \int_{\mathbb{R}^3} \Big|\partial^\alpha U_\omega^0(x-y)\Big| |\mu_\alpha^t|(dy) \sum_{|\alpha'|\leq 1} \int_{\mathbb{R}^3} \Big|\partial^{\alpha'} U_\omega^0(x'-y')\Big| |\mu_{\alpha'}^{t'}|(dy')\mathbb{P}(d\omega) \\
&= \sum_{|\alpha|,|\alpha'|\leq 1} \int_{\mathbb{R}^3}\int_{\mathbb{R}^3}\int_\Omega \Big|\partial^\alpha U_\omega^0(x-y)\partial^{\alpha'} U_\omega^0(x'-y')\Big| \mathbb{P}(d\omega)|\mu_\alpha^t|(dy)|\mu_{\alpha'}^{t'}|(dy') \\
&= \sum_{|\alpha|,|\alpha'|\leq 1} \int_{\mathbb{R}^3}\int_{\mathbb{R}^3} \mathbb{E}\big[|\partial^\alpha U^0(x-y)\partial^{\alpha'} U^0(x'-y')|\big] |\mu_\alpha^t|(dy)|\mu_{\alpha'}^{t'}|(dy') \\
&\leq \sum_{|\alpha|,|\alpha'|\leq 1} \int_{\mathbb{R}^3}\int_{\mathbb{R}^3} \Big(\mathbb{E}\big[\partial^\alpha U^0(x-y)^2\big]\mathbb{E}\big[\partial^{\alpha'} U^0(x'-y')^2\big]\Big)^{1/2} |\mu_\alpha^t|(dy)|\mu_{\alpha'}^{t'}|(dy') \\
&\leq \Bigg(\sum_{|\alpha|\leq 1} \int_{\mathbb{R}^3} \Big(\mathbb{E}\big[\partial^\alpha U^0(x-y)^2\big]\Big)^{1/2} |\mu_\alpha^t|(dy)\Bigg) \\
&\qquad\qquad \times \Bigg(\sum_{|\alpha|\leq 1} \int_{\mathbb{R}^3} \Big(\mathbb{E}\big[\partial^\alpha U^0(x-y)^2\big]\Big)^{1/2} |\mu_\alpha^{t'}|(dy)\Bigg) \\
&\leq \Big(\sum_{|\alpha|\leq 1} (|\mu_\alpha^t| * \sigma_{\partial^\alpha U^0})(x)\Big) \times \Big(\sum_{|\alpha|\leq 1} (|\mu_\alpha^{t'}| * \sigma_{\partial^\alpha U^0})(x')\Big) < +\infty.
\end{aligned}$$

For all multi-index α, the scalar $(|\mu_\alpha^t| * \sigma_{\partial^\alpha U^0})(x)$ is finite because $x \longmapsto \sigma_{\partial^\alpha U^0}(x)$ is continuous and $|\mu_\alpha^t|$ is compactly supported. Note also that from

Assumption (A_2), the GP U^0 is *mean square differentiable* up to order 1, which implies ([168], Section III.1.4) that we have, for all multi-indexes α, α' such that $|\alpha|, |\alpha'| \leq 1$, x and x':

$$\mathbb{E}\big[\partial^\alpha U^0(x)\partial^{\alpha'} U^0(x')\big] = \partial_1^\alpha \partial_2^{\alpha'} k_{\mathrm{u}}(x, x'). \tag{2.4.14}$$

where ∂_1 (respectively ∂_2) denotes derivatives with reference to the first (respectively second) argument of k_{u}. We may thus permute integrals and differential operators in $\mathbb{E}\big[U(z)U(z')\big]$:

$$\begin{aligned}
&\mathbb{E}\big[U(z)U(z')\big] \\
&= \mathbb{E}\left[\sum_{|\alpha|\leq 1}\int_{\mathbb{R}^3}(-1)^{|\alpha|}\partial^\alpha U^0(x-y)\mu_\alpha^t(dy))\sum_{|\alpha'|\leq 1}\int_{\mathbb{R}^3}(-1)^{|\alpha'|}\partial^{\alpha'}U^0(x-y)\mu_{\alpha'}^{t'}(dy')\right] \\
&= \sum_{|\alpha|,|\alpha'|\leq 1}\int_{\mathbb{R}^3}\int_{\mathbb{R}^3}(-1)^{|\alpha|}(-1)^{|\alpha'|}\partial_1^\alpha\partial_2^{\alpha'}\mathbb{E}\big[U^0(x-y)U^0(x'-y')\big]\mu_\alpha^t(dy)\mu_{\alpha'}^{t'}(dy') \\
&= \sum_{|\alpha|,|\alpha'|\leq 1}\int_{\mathbb{R}^3}\int_{\mathbb{R}^3}(-1)^{|\alpha|}(-1)^{|\alpha'|}\partial_1^\alpha\partial_2^{\alpha'}k_{\mathrm{u}}(x-y,x'-y')\mu_\alpha^t(dy)\mu_{\alpha'}^{t'}(dy') \\
&= \left[\Big(\sum_{|\alpha|\leq 1}\partial^\alpha\mu_\alpha^t\otimes\sum_{|\alpha'|\leq 1}\partial^{\alpha'}\mu_{\alpha'}^{t'}\Big)*k_{\mathrm{u}}\right](x,x') = [(\dot{F}_t\otimes\dot{F}_{t'})*k_{\mathrm{u}}](x,x'),
\end{aligned}$$

which proves (2.4.10). One proves that $\mathbb{E}\big[V(z)V(z')\big] = [(F_t\otimes F_{t'})*k_{\mathrm{v}}](x,x')$ the exact same way, which is actually simpler as F_t is directly a measure. To conclude,

$$\begin{aligned}
k_W(z,z') &= \mathrm{Cov}(W(z),W(z')) \\
&= \mathbb{E}[(W(z)W(z')] = \mathbb{E}\big[\big(U(z)+V(z)\big)\big(U(z')+V(z')\big)\big] \\
&= \mathbb{E}\big[U(z)U(z')\big] + \mathbb{E}\big[U(z)V(z')\big] + \mathbb{E}\big[V(z)U(z')\big] + \mathbb{E}\big[V(z)V(z')\big] \\
&= [(\dot{F}_t\otimes\dot{F}_{t'})*k_{\mathrm{u}}](x,x') + [(F_t\otimes F_{t'})*k_{\mathrm{v}}](x,x').
\end{aligned} \tag{2.4.15}$$

The cross terms are null because $U(z)$ and $V(z')$ are independent as well as $U(z')$ and $V(z)$.
(ii) : with expression (2.4.9), one checks that for any fixed z', the function $z \longmapsto k_W(z,z')$ is of the form (2.4.2) and thus verifies $\Box k_{x'} = 0$ in the sense of distributions. (ii) is then a direct consequence of Proposition 2.3.5. □

Remark 2.4.2. If U and V are not independent, then the two terms $[(\dot{F}_t\otimes F_{t'})*k_{uv}](x,x')$ and $[(F_t\otimes\dot{F}_{t'})*k_{vu}](x,x')$ must be added to equation (2.4.9), where $k_{uv}(x,x')$ denotes the cross covariance between U and V : $k_{uv}(x,x') = \mathrm{Cov}(U(x),V(x'))$ and $k_{vu}(x,x') = \mathrm{Cov}(V(x),U(x')) = k_{uv}(x',x)$.

More explicitly, we have the following Kirschoff-like integral formulas for $k_{\mathrm{v}}^{\mathrm{wave}}$ and $k_{\mathrm{u}}^{\mathrm{wave}}$:

$$[(F_t \otimes F_{t'}) * k_{\mathrm{v}}](x,x') = tt' \int_{S(0,1)\times S(0,1)} k_v(x - c|t|\gamma, x' - c|t'|\gamma') \frac{d\Omega d\Omega'}{(4\pi)^2}, \tag{2.4.16}$$

$$\begin{aligned}[(\dot{F}_t \otimes \dot{F}_{t'}) * k_{\mathrm{u}}](x,x') = \int_{S(0,1)\times S(0,1)} \Big(& k_u(x - c|t|\gamma, x' - c|t'|\gamma') \\ & - c|t|\nabla_1 k_u(x - c|t|\gamma, x' - c|t'|\gamma') \cdot \gamma \\ & - c|t'|\nabla_2 k_u(x - c|t|\gamma, x' - c|t'|\gamma') \cdot \gamma' \\ & + c^2 tt' \gamma^T \nabla_1 \nabla_2 k_u(x - c|t|\gamma, x' - c|t'|\gamma')\gamma' \Big) \frac{d\Omega d\Omega'}{(4\pi)^2}.\end{aligned} \tag{2.4.17}$$

Above, $\nabla_1 k_u(x,x')$ is the gradient vector of k_u with reference to x, $\nabla_2 k_u(x,x')$ is the gradient vector of k_u with reference to x' and $\nabla_1\nabla_2 k_u(x,x')$ is the matrix whose entry (i,j) is given by

$$\nabla_1\nabla_2 k_u(x,x')_{ij} = \partial_{x_i^1}\partial_{x_j^2} k_u(x,x'). \tag{2.4.18}$$

($\partial_{x_i^1}$ is the derivative with reference to the i^{th} coordinate of x, $\partial_{x_j^2}$ is the derivative with reference to the j^{th} coordinate of x').

2.4.2.1 Extending the covariance functions $k_{\mathrm{u}}^{\mathrm{wave}}$ and $k_{\mathrm{v}}^{\mathrm{wave}}$ to initial conditions u_0 and v_0 with piecewise regularity

The formulas (2.4.16) and (2.4.17) are valid in a more general context than that of assumptions (A_1) and (A_2). We provide below examples where these formulas yield valid covariance functions (in particular, functions defined for *all* values of (x,t) and (x',t')) corresponding to initial conditions with some forms of piecewise discontinuities. Assume, for example, that the initial speed v_0 is compactly supported on a ball $B(x_0,R)$ centered on some point x_0 with radius R. This is a natural model when v_0 is assumed to be a localized source. For the process V^0, this translates as $V^0(x) = 0$ *a.s.* if x is outside the ball $B(x_0,R)$. One can thus truncate the covariance function of V^0 accordingly, e.g. choosing the following function for k_{v} (see Section 2.2.1.3 for $k_{1/2}$)

$$k_{\mathrm{v}}(x,x') = k_{1/2}(x,x')\mathbb{1}_{[0,R]}(\|x - x_0\|)\mathbb{1}_{[0,R]}(\|x' - x_0\|). \tag{2.4.19}$$

Above, $\|x\|$ denotes the Euclidean norm of x. Such a covariance function indeed verifies $k_{\mathrm{v}}(x,x) = \mathrm{Var}(V^0)(x)) = 0$ if $\|x - x_0\| > R$ and the GP

corresponding to k_{v} is $V^0(x) = V_{1/2}(x)\mathbb{1}_{[0,R]}(\|x - x_0\|)$, where $V_{1/2}$ is a continuous modification of a GP with covariance function $k_{1/2}$. Note that the sample paths of V^0 are piecewise continuous and that V as defined in (2.4.6) is well-defined and measurable. The integrals in (2.4.16) still make sense and point (ii) from Proposition is still valid: the sample paths of the process V whose covariance function is $k_{\mathrm{v}}^{\mathrm{wave}}$ (or any other measurable centered second order random field with this covariance function) remains a solution of the wave equation in the distributional sense. One can perform the same kind of discussions on $k_{\mathrm{u}}^{\mathrm{wave}}$: for example, equation (2.4.17) shows that when $k_{\mathrm{u}} \in C^{1,1}(\mathbb{R}^3 \times \mathbb{R}^3) \setminus C^{2,2}(\mathbb{R}^3 \times \mathbb{R}^3)$, $k_{\mathrm{u}}^{\mathrm{wave}}$ is only expected to lie in $C^{1,1}(\mathbb{R}^3 \times \mathbb{R}^3)$; the sample paths of the GP with covariance function $k_{\mathrm{u}}^{\mathrm{wave}}$ will be at most of class C^1 and thus cannot be strong solutions of equation (2.4.1). This is the case when k_{u} is the $k_{3/2}$ Matérn covariance function from equation (2.2.3).

More generally, one can incorporate a finite number of discontinuities on k_{v} and on the derivatives of k_{u} so that they remain piecewise continuous: the integrals above will remain well defined and the sample paths of the corresponding GPs will remain distributional solutions to the wave equation, even though they will not be sufficiently differentiable to be strong solutions.

2.5 Conclusion and perspectives

In Section 2.3, we have presented a new result that provides a simple characterization of the measurable second order random fields $(U(x))_{x\in\mathcal{D}}$ whose sample paths verify homogeneous linear differential constraints within the framework of generalized functions. This characterization is valid for any linear differential operator L, provided that its coefficients fulfil minimal smoothness requirements, and no stationarity assumptions over $(U(x))_{x\in\mathcal{D}}$ are required. Motivated by physical applications, we described in Section 2.4 a Gaussian process model of the wave equation which is central to describe propagation phenomena. This PDE served as an application case for Proposition 2.3.5, and the GP model was derived by putting a GP prior on the wave equation's initial conditions. In Proposition 2.4.1, we presented covariance formulas that are tailored to the wave equation and take the form of convolutions; these expressions are interesting in themselves and call for physics-informed GPR applications for this equation. In particular, we showed that these formulas can model piecewise continuously differentiable solutions for the wave equation. Moreover, this setting provides a natural way to incorporate any type of information, both numerical or experimental. In a forthcoming paper, we will show how to use GPR conjointly with the covariance functions from

Proposition 2.4.1 in a numerical setting, in order to construct approximate solutions of the wave equation based on scattered observations. This in turn provides a natural method for solving different inverse problems, by using the likelihood of GPR as well as the reconstructed solution. An other application concerns the design of transparent boundary conditions (TBC): this provides artificial boundary conditions on a computational domain so that the computed solution is exactly an approximation of a solution on the whole space. Those conditions are usually nonlocal and restricted to simple geometries. A GPR strategy is meshless therefore suitable to design TBC on any type of computational domains.

Proposition 2.3.5 constitutes a first step towards understanding PDE constrained random fields in an weakened sense; different functional analysis frameworks can now be considered, obvious extensions being the weak or variational formulations of equation (2.1.1). These formulations are obtained by transferring only a part of the derivatives of the PDE to the test function and are for instance the canonical way of studying elliptic PDEs ([73], Section 6.1.2). The natural spaces arising from these formulations are Sobolev spaces rather than $\mathscr{D}'(\mathcal{D})$. An attached question, as studied in [181], is that of the Sobolev regularity of a given second order random field; a current research topic is whether or not one may relax the continuity assumptions required in [181]. Finally, the matter of using random fields for modelling and approximating solutions of nonlinear PDEs is a natural direction for future research.

Acknowledgements

Research of all the authors was supported by SHOM (Service Hydrographique et Océanographique de la Marine) project "Machine Learning Methods in Oceanography" no-20CP07. We thank Rémy Baraille in particular for his personal involvement in the project. We are thankful to the reviewers and the editor for their interesting and constructive remarks, leading to an improved and enriched version of the manuscript.

Chapter 3

Sobolev regularity of Gaussian random fields

This chapter corresponds to the article [96], where Example 3.2.10, Remark 3.3.4 and Section 3.5 were subsequently added. An improved version of the article [96] is currently in minor revision for the Journal of Functional Analysis.

Abstract

In this article, we fully characterize the measurable Gaussian processes $(U(x))_{x\in\mathcal{D}}$ whose sample paths lie in the Sobolev space of integer order $W^{m,p}(\mathcal{D})$, $m \in \mathbb{N}$, $1 < p < +\infty$, where $\mathcal{D}$ is an arbitrary open set of $\mathbb{R}^d$. The result is phrased in terms of a form of Sobolev regularity of the covariance function on the diagonal. This is then linked to the existence of suitable Mercer or otherwise nuclear decompositions of the integral operators associated to the covariance function and its cross-derivatives. In the Hilbert case $p = 2$, additional links are made w.r.t. the Mercer decompositions of the said integral operators, their trace and the imbedding of the RKHS in $W^{m,2}(\mathcal{D})$. We provide simple examples and partially recover recent results pertaining to the Sobolev regularity of Gaussian processes.

Contents

3.1 Introduction 107
3.2 Preliminary notions and results 111
3.2.1 Definition of weak derivatives and Sobolev spaces . . . 111
3.2.2 Characterization of $W^{m,p}$-regularity for locally integrable functions 112
3.2.3 Sobolev regularity and generalized functions 113
3.2.4 Tools from operator theory 115
3.2.5 Gaussian processes, Gaussian measures over Banach spaces 117
3.3 Sobolev regularity of Gaussian processes : the general case, $1 < p < +\infty$ 121
3.4 Sobolev regularity of Gaussian processes : the Hilbert space case, $p = 2$ 137
3.4.1 Reproducing Kernel Hilbert Spaces (RKHS, [24]) . . . 138
3.4.2 Ellipsoids of Hilbert spaces and canonical Gaussian processes 138
3.5 Application to the selection of covariance kernels . . 150
3.6 Concluding remarks and perspectives 156
3.7 Proofs of intermediary results and lemmas 157

3.1 Introduction

Sobolev spaces $W^{m,p}(\mathcal{D})$ are central tools in modern mathematics, most notably in the study of partial differential equations (PDEs). These spaces are built upon the notion of weak derivative: v is the weak derivative of u in the direction x_i if for all smooth compactly supported function $\varphi \in C_c^\infty(\mathcal{D})$,

$$\int_{\mathcal{D}} u(x)\frac{\partial \varphi}{\partial x_i}(x)dx = -\int_{\mathcal{D}} v(x)\varphi(x)dx. \tag{3.1.1}$$

Weak derivatives generalize classical, pointwise defined derivatives. In particular, there are cases where weak derivatives are well defined and pointwise differentiation otherwise fails (see e.g. [73], Examples 3 and 4 p. 260). The popularity of Sobolev spaces is justified by a number of reasons: first, they are separable reflexive Banach spaces when $1 < p < +\infty$, and separable Hilbert spaces when $p = 2$ ([169], Theorem 3.6 p. 61). Through duality, this allows for geometrical interpretations of PDEs which in turn lead to numerous quantitative theoretical results in the study of PDEs [73]. Second, as the Sobolev norm is defined through integrals of powers of the function and its weak derivatives, it is easily interpreted as an energy functional of the said function, which complies with physical interpretations of PDEs. This is a desirable feature as PDEs are generally used for describing physical phenomena. Finally, Sobolev spaces are useful for practical purposes as they are the natural mathematical framework for the celebrated finite element method when seeking numerical solutions to PDEs ([32], Chapter 1).

When a function of interest $u : \mathcal{D} \to \mathbb{R}$ is unknown, it may be relevant to model it as a sample path of a random field $(U(x))_{x\in\mathcal{D}}$, say a Gaussian process, whose realizations lie in a suitable function space. This is e.g. frequent in Bayesian inference of functions [205]. Such suitable spaces can indeed happen to be Sobolev spaces, for example when u describes a physical quantity. The question at hand in this article is thus the following: when do the sample paths of a given Gaussian process lie in some Sobolev space? This question is closely linked to the recent attention that Gaussian processes have drawn for tackling machine learning problems arising from PDE models; see e.g. [163, 209, 151, 123]. Notably (see [36]), Gaussian processes seem to provide a numerically competitive and mathematically tractable alternative to the now widespread "physics informed neural networks" (PINNs, [162]). For the moment though, the machine learning techniques involving Gaussian processes have only been studied within the framework of spaces of functions with classical smoothness : C^0, C^1, etc. As argued before, these spaces are often not as well-suited for studying PDEs as Sobolev spaces.

Though weak differentiability is more general, it is less direct to check than classical differentiability. Weak derivatives are defined implicitly and in the

most general case, ensuring Sobolev regularity is not usually done by directly verifying that an integral or a series is finite, as would be the case in L^p spaces; variational or boundedness criteria are used instead (see Proposition 3.2.1).

In many important cases however, handy characterizations of such regularity do exist, which have effectively been used to bypass the implicit definition of Sobolev regularity and generate results on the sample path regularity of Gaussian processes. When $\mathcal{D} = \mathbb{R}^d$, the space $W^{m,p}(\mathbb{R}^d)$ can be characterized in terms of a sufficient decay of of the Fourier transform ([192], Theorem 3 p. 135; [73], Section 5.8.5; [169], Section 7.63). Still in the case $\mathcal{D} = \mathbb{R}^d$, Sobolev regularity is equivalent to the convergence of its de la Vallée Poussin expansion in a suitable space ([149], Section 8.9). This fact has been the first to be employed for characterizing the Sobolev regularity of stationary Gaussian processes indexed by the unit cube of $\mathbb{R}^d$ in [40, 104], in terms of the spectral measure of its covariance. For some Banach spaces, explicit Schauder bases are known and lying in such spaces can be translated as the convergence of some coordinate series. This has been exploited in [39] for studying the Besov and Besov-Orlicz regularity of one dimensional Gaussian processes (they are natural generalizations of Sobolev regularity, [169]). Wavelet analysis is also available for describing Sobolev regularity ([169], Section 7.70) and has been used for studying the smoothness of the Brownian motion [38, 172]. More complex notions such as the existence of an underlying Dirichlet structure have been put to use in [115]. The latter work deals with Besov $B^s_{\infty,\infty}$ regularity, $s > 0$, on compact metric spaces, and relies on a convergence analysis of suitable spectral coefficients, based on the so called Littlewood-Paley decomposition. In [193], Karhunen-Loève expansions are used to study whether or not the sample paths of a general second order random process lie in interpolation spaces between the reproducing kernel Hilbert space (RKHS, Section 3.4.1 below) of the process and $L^2(\nu)$, where ν is a σ-finite measure. This is then applied to study H^s-regularity properties of the corresponding sample paths when $s > d/2$ (Corollary 4.5 and 5.7 in [193]), with applications to Gaussian processes in particular. Note that RKHS are also popular function spaces in the machine learning community [24]. Using the notion of mean square derivatives, [181] shows that the sample paths of a general second order random field lie in $W^{m,2}(\mathcal{D})$ under an integrability condition of the symmetric cross derivatives of the kernel over the diagonal ([181], Theorem 1). This result strongly suggests that a purely spectral criteria for Sobolev regularity of a random process should exist as the integrals appearing in Theorem 1 of [181] exactly correspond to the trace of specific integral operators which are naturally linked to the covariance of the process; in fact, we provide such a criteria in Proposition 3.4.4. For the suitable definition and use of the mean square derivatives of the process, [181] additionally requires that the covari-

ance function be continuous over the diagonal as well as its symmetric cross derivatives.

The purpose of this article is to uncover necessary and sufficient characterizations of the Sobolev regularity of nonnegative integer order of a given Gaussian process, in terms of its covariance function. In an attempt to make them both as general and concise as possible, we set the following targets and assumptions.

• The covariance function of the Gaussian process will only be assumed measurable, as in [193]. This contrasts with some of the previously mentioned works [39, 181, 115], where the covariance function is assumed continuous. It seems though that assuming the continuity of the covariance (and thus more or less that of the sample paths, [16] p. 31) to examine some Sobolev regularity of potentially low order is an unnatural hypothesis. This is especially true as the dimension of $\mathcal{D}$ increases, since $W^{m,p}(\mathcal{D})$ is embedded in $C_B^0(\mathcal{D})$, the Banach space of continuous and bounded functions over $\mathcal{D}$, only when $m > d/p$ ([169], Theorems 4.12 and 7.34).

• We will not make any regularity or shape assumptions on the open set $\mathcal{D}$. Indeed, Sobolev spaces of integer order are easily defined over arbitrary open sets $\mathcal{D} \subset \mathbb{R}^d$, and thus some results should exist within this general setting. As a result though, we will not deal with fractional Sobolev spaces nor Besov spaces. Indeed, those spaces may have some pathological properties without additional hypotheses on $\mathcal{D}$, namely enjoying a Lipschitz boundary or the cone condition (see e.g. [59], Example 9.1). We will see that elementary characterizations of Sobolev regularity (Lemmas 3.2.1 and 3.2.4) will prove to be enough for our purpose.

• Our results should lie outside of the assumption that $m > d/p$, where m, p and d correspond to the notation $W^{m,p}(\mathcal{D})$, $\mathcal{D} \subset \mathbb{R}^d$. Indeed, many previous results concerning the Sobolev regularity of a given Gaussian process concern the spaces $H^m(\mathcal{D}) = W^{m,2}(\mathcal{D})$, $\mathcal{D} \subset \mathbb{R}^d$, only in the case $m > d/2$. This is convenient because it ensures that $H^m(\mathcal{D})$ is continuously embedded in $C_B^0(\mathcal{D})$ when $\mathcal{D}$ is smooth enough, which suppresses the ambiguity of choosing a representative of a function in $H^m(\mathcal{D})$. However, $m > d/2$ excludes the spaces $H^1(\mathbb{R}^2)$ and $H^1(\mathbb{R}^3)$, which are central in the study of many important second order PDEs such as the wave equation, the heat equation, Laplace's equation or Schrödinger's equation.

Our characterizations of measurable Gaussian processes with sample paths in $W^{m,p}(\mathcal{D})$ is phrased in terms of a form of Sobolev regularity of the covariance function on the diagonal. It is then linked to the existence of suitable Mercer or otherwise nuclear decompositions of the integral operators associated to the covariance function and its symmetric weak cross-derivatives. In the Hilbert

case $p = 2$, additional links are made w.r.t. the Mercer decompositions of the said integral operators, their trace and the Hilbert-Schmidt nature of the imbedding of the RKHS in $W^{m,2}(\mathcal{D})$. Our results are strongly reminiscient of those found in [181], where we removed the continuity asusmptions over the covariance. In particular, this shows that contrarily to what is suggested in [193], p. 370, the Sobolev regularity of the sample paths of a given Gaussian process is not about $d/2$ less than that of the functions of its RKHS. This regularity is rather characterized by purely spectral properties of the covariance operator of the associated Gaussian measure. It just happens that in many standard cases such as with the Matérn kernels of order ν on "nice" bounded domain $\mathcal{D} \subset \mathbb{R}^d$, their RKHS turns out to be $H^{\nu+d/2}(\mathcal{D})$ ([193], Example 4.8) and the imbedding of $H^{\nu+d/2}(\mathcal{D})$ in $H^s(\mathcal{D})$ is Hilbert-Schmidt when $s < \nu$. See Example 3.4.5 for further details.

The article is organized as follow. In Section 3.2, we introduce the necessary notions for properly stating our results as well as some useful lemmas directly related to these notions. In Sections 3.3 and 3.4, we state and prove the main results of this article, which treat the general case $p \in (1, +\infty)$ and the special case $p = 2$ respectively. In Section 3.6, we conclude and provide some further outlooks. We prove the intermediary lemmas used in the main proofs in Section 3.7.

Notations Given a Banach space X, X^* denotes its topological dual. Given $x \in X$ and $l \in X^*$, we denote the duality bracket as follow: $l(x) = \langle l, x \rangle_{X^*,X}$. $\mathcal{B}(X)$ denotes the Borel σ-algebra of X for its norm topology. Given two linear operators $A : X_1 \to Y_1$ and $B : X_2 \to Y_2$, $A \otimes B : X_1 \otimes X_2 \to Y_1 \otimes Y_2$ denotes their tensor product which verifies $(A \otimes B)(a \otimes b) = (Aa) \otimes (Bb)$. Given two real valued functions f and g, $f \otimes g$ denotes their tensor product defined by $(f \otimes g)(x, y) = f(x)g(y)$. Given $h \in \mathbb{R}^d$, $|h|$ denotes its Euclidean norm. Given $p \in (1, +\infty)$, q will always denote its conjugate: $1/p + 1/q = 1$ i.e. $q = p/(p-1)$. As usual, when $\mathcal{D}$ is an open set of $\mathbb{R}^d$, we identify the dual of $L^p(\mathcal{D})$ with $L^q(\mathcal{D})$. Explicitly, if $f \in L^p(\mathcal{D})$ and $g \in L^q(\mathcal{D})$, we have

$$\langle f, g \rangle_{L^p,L^q} = \int_{\mathcal{D}} f(x)g(x)dx = \langle g, f \rangle_{L^q,L^p}. \tag{3.1.2}$$

When there is no risk of confusion, we will write $\|f\|_p \coloneqq \|f\|_{L^p(\mathcal{D})}$. If H is a Hilbert space, $\langle \cdot, \cdot \rangle_H$ denotes its inner product. Given an open set $\mathcal{D} \subset \mathbb{R}^d$, we write $\mathcal{D}_0 \Subset \mathcal{D}$ if $\mathcal{D}_0 \subset \mathcal{D}$ and $\overline{\mathcal{D}_0}$ is compact. $L^1_{loc}(\mathcal{D})$ denotes the space of equivalence classes of locally integrable functions over $\mathcal{D}$, i.e. such that $\int_K |f(x)|dx < +\infty$ for all $K \Subset \mathcal{D}$. Elements of $L^1_{loc}(\mathcal{D})$ are identified when they are equal almost everywhere w.r.t. the Lebesgue measure. Given an equivalence class $f \in L^1_{loc}(\mathcal{D})$, a *representative* of f is a function $\widehat{f} : \mathcal{D} \to \mathbb{R}$

such that the equivalence class of $\widehat{f}$ in $L^1_{loc}(\mathcal{D})$ is f. We will sometimes denote f and $\widehat{f}$ with the same symbol, e.g. f. Given a function k defined over $\mathcal{D}\times\mathcal{D}$, $\mathcal{E}_k$ denotes the associated integral operator (if well defined):

$$(\mathcal{E}_k f)(x) = \int_{\mathcal{D}} k(x,y)f(y)dy. \tag{3.1.3}$$

The input and output spaces of $\mathcal{E}_k$ will be specified on a case-by-case basis.

3.2 Preliminary notions and results

In Sections 3.2.1, 3.2.2 and 3.2.3, we introduce Sobolev regularity through the prisms of weak derivatives and generalized functions, and provide handy characterizations of this regularity. We present useful notions from operator theory in Section 3.2.4. In Section 3.2.5, we recall some useful results related to Gaussian processes and Gaussian measures.

3.2.1 Definition of weak derivatives and Sobolev spaces

Let $\alpha = (\alpha_1, ..., \alpha_d) \in \mathbb{N}^d$. Denote $\partial^\alpha = \partial^{\alpha_1}_{x_1}...\partial^{\alpha_d}_{x_d}$ the α^{th} derivative, and $|\alpha| \coloneqq \sum_{i=1}^d |\alpha_i|$. In this article, the statement "let $|\alpha| \leq m$" will mean "let $\alpha = (\alpha_1, ..., \alpha_d) \in \mathbb{N}^d$ be such that $|\alpha| \leq m$". Given a function k defined on $\mathcal{D}\times\mathcal{D}$, $\partial^{\alpha,\alpha}k$ denotes its symmetric cross derivative: $\partial^{\alpha,\alpha}k(x,y) \coloneqq \partial^{\alpha_1}_{x_1}...\partial^{\alpha_d}_{x_d}\partial^{\alpha_1}_{y_1}...\partial^{\alpha_d}_{y_d}k(x,y)$ (formally, $\partial^{\alpha,\alpha} = \partial^\alpha \otimes \partial^\alpha$). A function $u \in L^1_{loc}(\mathcal{D})$ has $v \in L^1_{loc}(\mathcal{D})$ for its α^{th} weak derivative if ([169], section 1.62)

$$\forall \varphi \in C^\infty_c(\mathcal{D}), \quad \int_{\mathcal{D}} u(x)\partial^\alpha\varphi(x)dx = (-1)^{|\alpha|}\int_{\mathcal{D}} v(x)\varphi(x)dx. \tag{3.2.1}$$

v is then unique in $L^1_{loc}(\mathcal{D})$ and is denoted $v = \partial^\alpha u$. Let $p \in [1, +\infty]$. The Sobolev space $W^{m,p}(\mathcal{D})$ is defined as ([169], section 3.2)

$$W^{m,p}(\mathcal{D}) = \{u \in L^p(\mathcal{D}) : \forall\ |\alpha| \leq m, \partial^\alpha u \in L^p(\mathcal{D})\}. \tag{3.2.2}$$

Sobolev spaces are Banach spaces for the norm $\|u\|_{W^{m,p}} \coloneqq (\sum_{|\alpha|\leq m} \|\partial^\alpha u\|_p^p)^{1/p}$; they are separable when $p \neq +\infty$ ([169], Theorem 3.6 p. 61). When $p = 2$, $W^{m,p}(\mathcal{D})$ is usually denoted $H^m(\mathcal{D})$ and is a Hilbert space for the following inner product

$$\langle u, v\rangle_{H^m(\mathcal{D})} \coloneqq \sum_{|\alpha|\leq m} \langle \partial^\alpha u, \partial^\alpha v\rangle_{L^2(\mathcal{D})}. \tag{3.2.3}$$

Note that we made no assumptions on the regularity of the open set $\mathcal{D}$.

3.2.2 Characterization of $W^{m,p}$-regularity for locally integrable functions

As for pointwise derivatives, finite difference operators can be used for characterizing Sobolev regularity. Given $h \in \mathbb{R}^d$, introduce the translation operator $(\tau_h u)(x) = u(x+h)$, which is bounded over $L^p(\mathbb{R}^d)$. Introduce the associated finite difference operator:

$$\Delta_h = \tau_h - Id. \tag{3.2.4}$$

The linear subspace of bounded operators over $L^p(\mathbb{R}^d)$ induced by the translation operators is commutative, as $\tau_{h_1} \circ \tau_{h_2} = \tau_{h_1+h_2} = \tau_{h_2} \circ \tau_{h_1}$. Let $h = (h_1, ..., h_m) \in (\mathbb{R}^d)^m$, we define the m^{th} order finite difference operator associated to h to be $\Delta_h \coloneqq \prod_{i=1}^m \Delta_{h_i}$ where the product symbol denotes the composition of operators. When $h \in \mathbb{R}^d$, the adjoint of Δ_h is also a finite difference operator, which is computable using the change of variable formula. If $h \in \mathbb{R}^d$, then

$$\Delta_h^* = \tau_{-h} - Id. \tag{3.2.5}$$

Finally, when $\alpha = (\alpha_1, ..., \alpha_d) \in \mathbb{N}^d$ and $h = (h_1, ..., h_d) \in (\mathbb{R}_+^*)^d$, we denote by δ_h^α the finite difference approximation of ∂^α defined by

$$\delta_h^\alpha = \prod_{i=1}^d \left(\frac{\Delta_{h_i e_i}}{h_i} \right)^{\alpha_i} = \left(\frac{\Delta_{h_1 e_1}}{h_1} \right)^{\alpha_1} \cdots \left(\frac{\Delta_{h_d e_d}}{h_d} \right)^{\alpha_d}. \tag{3.2.6}$$

Above, $(e_1, ..., e_d)$ is the canonical basis of $\mathbb{R}^d$. Depending on which one is the most convenient, we will either use Δ_h or δ_h^α. We will use the following characterizations of $W^{m,p}$-regularity, which are straightforward generalizations of Proposition 9.3 from [33] to multiple derivatives. We prove them in Section 3.7, as we could not find them stated as such in the literature.

Lemma 3.2.1. *Suppose that $u \in L^1_{loc}(\mathcal{D})$. Let $m \in \mathbb{N}$, $p \in (1, +\infty]$ and introduce $q \geq 1$ the conjugate of p : $1/p + 1/q = 1$. Then the following statements are equivalent*

(i) $u \in W^{m,p}(\mathcal{D})$

(ii) (Variational control) for all α such that $|\alpha| \leq m$, there exists a constant C_α such that

$$\forall \varphi \in C_c^\infty(\mathcal{D}), \quad \left| \int_{\mathcal{D}} u(x) \partial^\alpha \varphi(x) dx \right| \leq C_\alpha \|\varphi\|_{L^q(\mathcal{D})}. \tag{3.2.7}$$

In this case, the L^p norm of $\partial^\alpha u$ is given by

$$\|\partial^\alpha u\|_{L^p(\mathcal{D})} = \sup_{\varphi \in C_c^\infty(\mathcal{D}) \setminus \{0\}} \left| \int_{\mathcal{D}} u(x) \frac{\partial^\alpha \varphi(x)}{\|\varphi\|_{L^q}} dx \right|. \tag{3.2.8}$$

(iii) (Finite difference control) there exists a constant C such that for all open set $\mathcal{D}_0 \Subset \mathcal{D}$, for all $l \leq m$ and all $h = (h_1, ..., h_l) \in (\mathbb{R}^d)^l$ such that $\sum_i |h_i| < dist(\mathcal{D}_0, \partial\mathcal{D})$,

$$\|\Delta_h u\|_{L^p(\mathcal{D}_0)} \leq C|h_1| \times ... \times |h_l|. \tag{3.2.9}$$

Moreover, $\|\partial^\alpha u\|_{L^p(\mathcal{D})} \leq C$ for any C verifying equation (3.2.9) and one can actually take $C = \|u\|_{W^{m,p}(\mathcal{D})}$ in equation (3.2.9).

In Point *(iii)* above, the assumption that $\sum_i |h_i| < \text{dist}(\mathcal{D}_0, \partial\mathcal{D})$ is only there to ensure that the quantity $\Delta_h u(x)$ makes sense when $x \in \mathcal{D}_0$.

3.2.3 Sobolev regularity and generalized functions

The theory of generalized functions (or distributions) provides a flexible way of characterizing Sobolev regularity, by building a larger space in which partial derivatives are always defined. Given an open set $\mathcal{D}$, denote $C_c^\infty(\mathcal{D})$ the space of smooth functions with compact support in $\mathcal{D}$. Endow it with its usual LF topology, defined e.g. in [202], Chapter 13. This topology is such that the sequence (φ_n) converges to φ in $C_c^\infty(\mathcal{D})$ if and only if there exists a compact set $K \subset \mathcal{D}$ such that $\text{Supp}(\varphi_n) \subset K$ for all n and

$$\forall \alpha = (\alpha_1, ..., \alpha_d) \in \mathbb{N}^d, \quad \sup_{x \in K} |\partial^\alpha \varphi_n(x) - \partial^\alpha \varphi(x)| \longrightarrow 0. \tag{3.2.10}$$

With $C_c^\infty(\mathcal{D})$ endowed with this topology, the space of generalized functions, or distributions, is then defined as the topological dual of $C_c^\infty(\mathcal{D})$ i.e. the set of all continuous linear forms over $C_c^\infty(\mathcal{D})$. It is traditionally denoted as follow: $\mathscr{D}'(\mathcal{D}) := C_c^\infty(\mathcal{D})'$ ([202], Notation 21.1). A generalized function $T \in \mathscr{D}'(\mathcal{D})$ is said to be regular ([202], p. 224) if it is of the form

$$\forall \varphi \in C_c^\infty(\mathcal{D}), \quad T(\varphi) = \int_{\mathcal{D}} u(x)\varphi(x)dx. \tag{3.2.11}$$

for some $u \in L^1_{loc}(\mathcal{D})$, in which case one writes $T = T_u$. Given any function $u \in L^1_{loc}(\mathcal{D})$ and $\alpha \in \mathbb{N}^d$, its distributional derivative $D^\alpha u$ is *defined* by the following formula ([202], pp. 248-250):

$$D^\alpha u : \varphi \longmapsto (-1)^{|\alpha|} \int_{\mathcal{D}} \partial^\alpha \varphi(x) u(x) dx. \tag{3.2.12}$$

$D^\alpha u$ then also lies in $\mathscr{D}'(\mathcal{D})$. Sobolev regularity can now be rephrased as follow : u lies in $W^{m,p}(\mathcal{D})$ iff for all $|\alpha| \leq m$, the distributional derivative $D^\alpha u$ is in fact a regular generalized function represented by some $v_\alpha \in L^p(\mathcal{D})$ i.e.

$D^\alpha u = T_{v_\alpha}$. Then v_α is unique in $L^p(\mathcal{D})$ and $\partial^\alpha u = v_\alpha$ in $L^p(\mathcal{D})$, where $\partial^\alpha u$ is the α^{th} weak derivative of u.

Moreover, the control equation (3.2.7) shows that $\partial^\alpha u$ exists and lies in $L^p(\mathcal{D})$ if and only if $D^\alpha u : C_c^\infty(\mathcal{D}) \to \mathbb{R}$ can be extended as a continuous linear form over $L^q(\mathcal{D})$. Ensuring the existence of such extensions will thus be of prime interest for us, and is the topic of the next lemma. Specifically, the next result states that given continuous linear or bilinear forms over $C_c^\infty(\mathcal{D})$, the existence of extensions of these maps to $L^q(\mathcal{D})$ can be ensured by obtaining suitable estimates on a well chosen *countable* set $E_q \subset C_c^\infty(\mathcal{D})$. Restricting ourselves to E_q will allow us to eliminate any measurability issues when introducing the supremum of certain random variables indexed by E_q, as a countable supremum of random variables remains a random variable (i.e. a measurable map). Below, we write $\|\cdot\|_q \coloneqq \|\cdot\|_{L^q(\mathcal{D})}$ for short.

Lemma 3.2.2 (Extending continuous linear and bilinear forms over $C_c^\infty(\mathcal{D})$ to $L^p(\mathcal{D})$)**.** *Let $p \in (1, +\infty)$. There exists a countable $\mathbb{Q}-$vector space $E_q = \{\Phi_n^q, n \in \mathbb{N}\} \subset C_c^\infty(\mathcal{D})$ with the following property.*

(i) A distribution $T \in \mathscr{D}'(\mathcal{D})$ is a regular distribution, $T = T_v$, for some $v \in L^p(\mathcal{D})$ iff it verifies the countable estimate for some constant $C > 0$

$$\forall \varphi \in E_q, \quad |T(\varphi)| \leq C\|\varphi\|_q. \tag{3.2.13}$$

or equivalently, $\sup_{n\in\mathbb{N}^*} |T(\Phi_n^q)|/\|\Phi_n^q\|_q < +\infty$ (here, setting $\Phi_0^p = 0$ without loss of generality). This is equivalent to T admitting an extension over $L^q(\mathcal{D})$ which is then uniquely given by $T(f) = \int_{\mathcal{D}} f(x)v(x)dx$. Moreover,

$$\sup_{n\in\mathbb{N}^*} \frac{|T(\Phi_n^q)|}{\|\Phi_n^q\|_q} = \sup_{\varphi\in C_c^\infty(\mathcal{D})} \frac{|T(\varphi)|}{\|\varphi\|_q}, \tag{3.2.14}$$

whether these quantities are finite or not.

(ii) Let b be a continuous bilinear form over $C_c^\infty(\mathcal{D})$. Then b can be extended to a continuous bilinear form over $L^q(\mathcal{D})$ iff it verifies the countable estimate

$$\forall \varphi, \psi \in E_q, \quad |b(\varphi, \psi)| \leq C\|\varphi\|_q\|\psi\|_q. \tag{3.2.15}$$

In this case, such an extension is unique and there will exist a unique bounded operator $B : L^q(\mathcal{D}) \to L^p(\mathcal{D})$ verifying the following identity

$$\forall \varphi, \psi \in C_c^\infty(\mathcal{D}), \quad b(\varphi, \psi) = \langle B\varphi, \psi\rangle_{L^p, L^q}. \tag{3.2.16}$$

The proof of this result can be found in Section 3.7. It is based on Lemma 3.2.3 below, which is interesting in itself. Recall that a topological space X is *sequentially separable* if there exists a countable subset $Y \subset X$ such that for every $x \in X$, there exists a sequence $(x_n) \subset Y$ such that $x_n \to x$. Then the following holds.

Lemma 3.2.3. *$C_c^\infty(\mathcal{D})$ endowed with its LF-topology is sequentially separable.*

This result is Lemma 2.3.6 from Chapter 2. Given the set E_q provided by Lemma 3.2.2, we next define the countable set F_q to be

$$F_q \coloneqq \{\varphi/\|\varphi\|_q, \varphi \in E_q, \varphi \neq 0\} = \{f_n^q, n \in \mathbb{N}^*\} \subset S_q(0,1). \tag{3.2.17}$$

Above, $(f_n^q)_{n\in\mathbb{N}^*}$ is an enumeration of F_q and $S_q(0,1)$ is the unit sphere of $L^q(\mathcal{D})$. The next lemma is then a direct consequence of Lemmas 3.2.1 and 3.2.2.

Lemma 3.2.4 (Countable characterization of Sobolev regularity)**.** *Let $p \in (1,+\infty)$. For any $u \in L^1_{loc}(\mathcal{D})$, u lies in $W^{m,p}(\mathcal{D})$ iff for all multi index α such that $|\alpha| \leq m$, there exists a constant C_α such that*

$$\forall \varphi \in E_q, \quad \left| \int_{\mathcal{D}} u(x)\partial^\alpha \varphi(x)dx \right| \leq C_\alpha \|\varphi\|_q, \tag{3.2.18}$$

or equivalently, in terms of the set F_q defined in equation (3.2.17),

$$\sup_{\varphi\in F_q} \left| \int_{\mathcal{D}} u(x)\partial^\alpha \varphi(x)dx \right| = \sup_{n\in\mathbb{N}^*} \left| \int_{\mathcal{D}} u(x)\partial^\alpha f_n^q(x)dx \right| < +\infty. \tag{3.2.19}$$

Moreover,

$$\sup_{\varphi\in F_q} \left| \int_{\mathcal{D}} u(x)\partial^\alpha \varphi(x)dx \right| = \sup_{\varphi\in C_c^\infty(\mathcal{D})\setminus\{0\}} \left| \int_{\mathcal{D}} u(x)\frac{\partial^\alpha \varphi(x)}{\|\varphi\|_q}dx \right|, \tag{3.2.20}$$

whether these quantities are finite or not. If one of them is finite, then it is equal to $\|\partial^\alpha u\|_{L^p(\mathcal{D})}$.

This lemma provides us with a somewhat explicit *countable* criteria for Sobolev regularity, which is valid whatever the open set $\mathcal{D}$.

3.2.4 Tools from operator theory

The following reminders may be found in [29], Section A.2. Let H_1 and H_2 be two Hilbert spaces, and X and Y two Banach spaces.

(i) A linear operator $T : X \to Y$ is bounded if $\|T\| \coloneqq \sup_{\|x\|_X=1} \|Tx\|_Y < +\infty$. A bounded operator $T : X \to Y$ is compact if $\overline{T(B)}$ is a compact set of Y, where B is the closed unit ball of X. When $X = Y$, the spectrum of a compact operator is purely discrete, and can be reordered as a sequence $(\lambda_n)_{n\in\mathbb{N}}$ which converges to 0.

(ii) If $T : H_1 \to H_2$ is compact, then $T^*T : H_1 \to H_1$ is compact, self-adjoint and nonnegative ($\forall x \in H_1, \langle x, T^*Tx\rangle_{H_1} \geq 0$). If H_1 is separable, T^*T can be diagonalized in an orthonormal basis (e_n) of H_1. The nonnegative eigenvalues of T^*T, (s_n^2), are called the singular values of T. If H_1 is separable, T is said to be Hilbert-Schmidt if $\sum_{n\in\mathbb{N}} \|Te_n\|_{H_2}^2 < +\infty$ for one (equivalently, all) orthonormal basis (e_n) of H_1. Its Hilbert-Schmidt norm, defined as the sum above, is then also the sum of its singular values:

$$\|T\|_{HS}^2 = \sum_{n\in\mathbb{N}} \|Te_n\|_{H_2}^2 = \sum_{n\in\mathbb{N}} s_n^2 \tag{3.2.21}$$

Every Hilbert-Schmidt operator is compact, and every Hilbert-Schmidt operator T acting on $L^2(\mathcal{D})$ can be written in integral form ([29], Lemma A.2.13): there exists a "kernel" $k \in L^2(\mathcal{D}\times\mathcal{D})$ such that for all $f \in L^2(\mathcal{D})$,

$$(Tf)(x) = \int_{\mathcal{D}} k(x,y)f(y)dy = (\mathcal{E}_k f)(x). \tag{3.2.22}$$

If T is symmetric, nonnegative and Hilbert-Schmidt, there exists an orthonormal basis (ϕ_n) of $L^2(\mathcal{D})$ of eigenvectors of T with nonnegative eigenvalues (λ_n), such that in $L^2(\mathcal{D}\times\mathcal{D})$, we have

$$k(x,y) = \sum_{n\in\mathbb{N}} \lambda_n \phi_n(x)\phi_n(y). \tag{3.2.23}$$

We will refer to decompositions of f of the form of equation (3.2.23) as *Mercer decompositions*, in reference to the celebrated Mercer's theorem ([34], Theorem 1.2).

(iii) If H_1 is separable, T is said to be trace-class (or nuclear) if $\sum_{n\in\mathbb{N}} s_n < +\infty$. One can then define its trace as the following linear functional, which is independent of the choice of basis (e_n), and equal to the series of the eigenvalues of T (Lidskii's theorem)

$$\mathrm{Tr}(T) \coloneqq \sum_{n\in\mathbb{N}} \langle Te_n, e_n\rangle = \sum_{n\in\mathbb{N}} \lambda_n. \tag{3.2.24}$$

Any trace-class operator is Hilbert-Schmidt, and T is Hilbert-Schmidt if and only if T^*T is trace-class, in which case $\mathrm{Tr}(T^*T) = \|T\|_{HS}^2 = \|T^*\|_{HS}^2$. If $H_1 = H_2 = L^2(\mathcal{D})$, if T is trace class with kernel k and if k is sufficiently smooth (say continuous), then the trace of $T = \mathcal{E}_k$ is given by $\mathrm{Tr}(T) = \int_{\mathcal{D}} k(x,x)dx$. Extensions of this formula to general Hilbert-Schmidt kernels $k \in L^2(\mathcal{D}\times\mathcal{D})$ of trace class operators is studied in [34]; see also Proposition 3.2.9 and Lemma 3.3.7 below. If $T : H_1 \to H_1$ is bounded, self-adjoint and nonnegative, then we define its trace as the possibly infinite series of nonnegative scalars $\mathrm{Tr}(T) \coloneqq \sum_{n\in\mathbb{N}} \langle Te_n, e_n\rangle$.

(*iv*) ([134], p. 160) A bounded operator $T : X \to Y$ is nuclear if there exists sequences $(x_n) \subset X^*$ and $(y_n) \subset Y$ with $\sum_{n=1}^{+\infty} \|x_n\|_{X^*}\|y_n\|_Y < +\infty$ such that $Tx = \sum_{n=1}^{+\infty} \langle x_n, x\rangle_{X^*,X} y_n$ for all $x \in X$. In this case, we write abusively $T = \sum_{n=1}^{+\infty} x_n \otimes y_n$. The nuclear norm of T is then defined as

$$\nu(T) \coloneqq \inf\left\{ \sum_{n=1}^{+\infty} \|x_n\|_{X^*}\|y_n\|_Y \text{ such that } T = \sum_{n=1}^{+\infty} x_n \otimes y_n \right\}. \tag{3.2.25}$$

A bounded operator $K : X^* \to X$ is symmetric if for all $x, y \in X^*$, $\langle x, Ry\rangle = \langle y, Rx\rangle$, and nonnegative if $\langle x, Rx\rangle \geq 0$. When $X = Y = H$ where H is a separable Hilbert space, the sets of trace class and nuclear operators coincide; moreover, the same can be said for the trace functional (3.2.24) and the nuclear norm (3.2.25) if T has a nonnegative spectrum : $\nu(T) = \mathrm{Tr}(T)$.

3.2.5 Gaussian processes, Gaussian measures over Banach spaces

Throughout this article, $(\Omega, \mathcal{F}, \mathbb{P})$ denotes the same probability space. Given $p \in (1, +\infty)$, $L^p(\mathbb{P})$ denotes the space of real valued random variables X such that $\mathbb{E}[|X|^p] < +\infty$.

(*i*) If $(E, \mathcal{B})$ is a measurable space, the *law* $\mathbb{P}_X$ of a random variable $X : \Omega \to E$ is the pushforward measure of $\mathbb{P}$ through X, which is defined by $\mathbb{P}_X(B) \coloneqq \mathbb{P}(X^{-1}(B))$ for all measurable set $B \in \mathcal{B}$ ([30], Section 3.7).

(*ii*) A *Gaussian process* ([2], Section 1.2) $(U(x))_{x\in\mathcal{D}}$ is a family of Gaussian random variables defined over $(\Omega, \mathcal{F}, \mathbb{P})$ such that for all $n \in \mathbb{N}^*$, $(a_1, ..., a_n) \in \mathbb{R}^n$ and $(x_1, ..., x_n) \in \mathcal{D}^n$, $\sum_{i=1}^n a_i U(x_i)$ is a Gaussian random variable. The law it induces over the function space $\mathbb{R}^{\mathcal{D}}$ endowed with its product σ-algebra is uniquely determined by its mean and covariance functions, $m(x) = \mathbb{E}[U(x)]$ and $k(x, x') = \mathrm{Cov}(U(x), U(x'))$ ([110], Section 9.8). We write $(U(x))_{x\in\mathcal{D}} \sim GP(m, k)$. The covariance function k is positive definite over $\mathcal{D}$, which means that for all positive integer n and $(x_1, ..., x_n) \in \mathcal{D}^n$, the matrix $(k(x_i, x_j))_{1\leq i,j\leq n}$ is nonnegative definite. Conversely, given a positive definite function over an arbitrary set $\mathcal{D}$, there exists a centered Gaussian process indexed by $\mathcal{D}$ with the this function as its covariance function ([2], p. 11). We will often denote $\sigma(x) \coloneqq k(x, x)^{1/2}$. Given $\omega \in \Omega$, the corresponding sample path (or realization) of $(U(x))_{x\in\mathcal{D}}$ is the following deterministic function $U_\omega : \mathcal{D} \to \mathbb{R}$ defined by $U_\omega(x) \coloneqq U(x)(\omega)$. A Gaussian process is said to be measurable if the map $(\Omega \times \mathcal{D}, \mathcal{F} \otimes \mathcal{B}(\mathcal{D})) \to (\mathbb{R}, \mathcal{B}(\mathbb{R})), (\omega, x) \mapsto U(x)(\omega)$ is measurable. If $(U(x))_{x\in\mathcal{D}}$ is measurable, then from Fubini's theorem the maps of the form $x \mapsto k(x, x'), x \mapsto k(x, x)$, etc, are measurable. We further discuss this property in Remark 3.2.11.

We will need the following lemma pertaining to the sample path-wise integration of Gaussian processes.

Lemma 3.2.5. *Let $\mathcal{D} \subset \mathbb{R}^d$ be an open set. Let $(U(x))_{x\in\mathcal{D}} \sim GP(0,k)$ be a measurable centered Gaussian process such that its standard deviation function σ lies in $L^1_{loc}(\mathcal{D})$. Then the sample paths of U lie in $L^1_{loc}(\mathcal{D})$ almost surely and given $\varphi \in C^\infty_c(\mathcal{D})$, the map defined by*

$$U^\alpha_\varphi : \Omega \ni \omega \longmapsto (-1)^{|\alpha|} \int_{\mathcal{D}} U(x)(\omega)\partial^\alpha\varphi(x)dx \tag{3.2.26}$$

is a Gaussian random variable. Moreover, for all $p \in (1,+\infty)$, $(U^\alpha_\varphi)_{\varphi\in F_q}$ is a centered Gaussian sequence (i.e. a Gaussian process indexed by a countable set), where F_q is defined in equation (3.2.17).

We will also use the following fact about bounded Gaussian sequences, which can be seen as a weak form of Fernique's theorem ([29], Theorem 2.8.5, p. 75).

Lemma 3.2.6 ([2], Theorem 2.1.2)**.** *Let $(U_n)_{n\in\mathbb{N}}$ be a Gaussian sequence and set $|U| \coloneqq \sup_n |U_n|$. Suppose that $\mathbb{P}(|U| < +\infty) = 1$. Then there exists $\varepsilon > 0$ such that*

$$\mathbb{E}[\exp(\varepsilon|U|^2)] < +\infty. \tag{3.2.27}$$

In particular, $\mathbb{E}[|U|^p] < +\infty$ for all $p \in \mathbb{N}$.

(iii) A *Gaussian measure* μ ([29], Definition 2.2.1) over a Banach space X is a measure over its Borel σ-algebra such that given any $x^* \in X^*$, the pushforward measure of μ through the functional x^* is a Gaussian measure over $\mathbb{R}$ (see Section 3.2.5(*i*) for a definition of the pushforward). Gaussian measures are equipped with a mean vector $a_\mu \in X^{**}$ and a covariance operator $K_\mu : X^* \to X^{**}$, defined in [29], Definition 2.2.7. When X is separable, μ is Radon ([29], p. 125). This implies that a_μ lies in X and that the covariance operator K_μ maps X^* to X ([29], Theorem 3.2.3). The vector a_μ and the covariance operator K_μ are defined by the following formulas

$$\forall x \in X^*,\ \langle a_\mu, x\rangle = \int_X \langle x, z\rangle \mu(dz), \tag{3.2.28}$$

$$\forall x, y \in X^*, \langle y, K_\mu x\rangle = \int_X \langle x - a_\mu, z\rangle\ \langle y - a_\mu, z\rangle \mu(dz). \tag{3.2.29}$$

Any operator $K : X^* \to X^{**}$ which is the covariance operator of a Gaussian measure is called a Gaussian covariance operator. In Propositions 3.2.7 and

3.2.8, we present useful characterizations of Gaussian measures μ over two important classes of Banach spaces: spaces of type 2 and cotype 2 respectively. For a definition of spaces of type 2 and cotype 2, see e.g. [37]. In this article, we will only use the fact that $L^p(\mathcal{D})$ is of type 2 when $p \geq 2$, and cotype 2 when $1 \leq p \leq 2$ (see [29], p. 152). Moreover we will restrict ourselves to the case where X is separable. This implies that μ is Radon, which removes problems pertaining to extensions of measures otherwise considered in [134] and [37].

Proposition 3.2.7 ([134], Theorem 4)**.** *Let X be a separable Banach space of type 2, and let μ be a Gaussian measure over X. Then its covariance operator is symmetric, nonnegative and nuclear. Conversely, given any $a \in X$ and any symmetric, nonnegative and nuclear operator $K : X^* \to X$, there exists a Gaussian measure over X with mean vector a and covariance operator K.*

Denote l^2 the Hilbert space of square summable sequences.

Proposition 3.2.8 ([37], Theorem 4.1 and Corollary 4.1)**.** *Let X be a separable Banach space of cotype 2, and let μ be a Gaussian measure over X. Then there exists a continuous linear map $A : l^2 \to X$ and a symmetric, nonnegative and trace-class operator $S : l^2 \to l^2$ such that covariance operator of μ is given by ASA^* (in particular, the covariance operator of μ is nuclear). In other words, μ is the pushforward measure of a Gaussian measure μ_0 over l^2 through some bounded linear map A. Conversely, given any $a \in X$ and any operator of the form $K = ASA^*$ where $A : l^2 \to X$ is a bounded linear map and S a symmetric, nonnegative and trace class operator over l^2, there exists a Gaussian measure over X with mean vector a and covariance operator K.*

In practice, we will replace l^2 with $L^2(\mathcal{D})$, which are isomorphic Hilbert spaces. The propositions 3.2.7 and 3.2.8 generalize the case where X is a separable Hilbert space, which can be found in [29], Theorem 2.3.1. We finish with the following handy result describing centered Gaussian measures over L^p-spaces.

Proposition 3.2.9 ([29], Proposition 3.11.15 and Example 2.3.16)**.**

• *Let μ be a centered Gaussian measure over $L^p(\mathcal{D})$ where $1 \leq p < +\infty$ and $\mathcal{D} \subset \mathbb{R}^d$ is an open set. Then there exists a function $k \in L^p(\mathcal{D} \times \mathcal{D})$ such that the covariance operator of μ is $\mathcal{E}_k : L^q(\mathcal{D}) \to L^p(\mathcal{D})$, the integral operator associated to k. Moreover, there exists a centered measurable Gaussian process $(U(x))_{x\in\mathcal{D}}$ whose covariance function $\tilde{k}$ verifies $\tilde{k} = k$ in $L^p(\mathcal{D}\times\mathcal{D})$, and whose sample paths lie in $L^p(\mathcal{D})$ a.s.. Setting $\sigma(x) = \tilde{k}(x,x)^{1/2}$, $\tilde{k}$ verifies*

$$\int_{\mathcal{D}} \tilde{k}(x,x)^{p/2} dx = \int_{\mathcal{D}} \sigma(x)^p dx < +\infty. \tag{3.2.30}$$

Additionally, $\mathbb{P}_U = \mu$*, where* $\mathbb{P}_U$ *is the pushforward of* $\mathbb{P}$ *through the Borel-measurable map* $\omega \mapsto U_\omega \in L^p(\mathcal{D})$*. Conversely, given any measurable nonnegative definite function* k *verifying* (3.2.30)*, the corresponding integral operator* $\mathcal{E}_k : L^q(\mathcal{D}) \to L^p(\mathcal{D})$ *is the covariance operator of a centered Gaussian measure* μ *over* $L^p(\mathcal{D})$*.*

• *Given a centered measurable Gaussian process* $(U(x))_{x\in\mathcal{D}}$ *whose covariance function we denote* $\tilde{k}$*, the condition* (3.2.30) *is equivalent to* $(U(x))_{x\in\mathcal{D}}$ *having its sample paths lie in* $L^p(\mathcal{D})$ *a.s..*

This result is quite strong, as it ensures the existence of a representative in $L^p(\mathcal{D}\times\mathcal{D})$ of the kernel of any Gaussian covariance operator, which is the covariance function of a measurable Gaussian process. This will enable us to remove awkward measurability issues w.r.t. k over its diagonal and equation (3.2.30). Without the use of an underlying measurable Gaussian process, these issues are not trivial to deal with, see e.g. [34] for an analysis of the Hilbert case $p = 2$. We deal with the $p \in [2, +\infty)$ case in Proposition 3.3.5 and in Lemma 3.3.7 in particular.

Example 3.2.10 (A nuclear operator over $L^p, 1 \le p < 2$, which is not a Gaussian covariance operator). Consider the cotype 2 space $L^p(\mathbb{R}_+^*), 1 \le p < 2$, and the covariance function defined on $\mathbb{R}_+^* \times \mathbb{R}_+^*$ given by

$$k(x,y) = \sum_{n=0}^{+\infty} e^{-nx}e^{-ny} = \frac{1}{1-e^{-x-y}}. \tag{3.2.31}$$

Let $\phi_n(x) \coloneqq \exp(-nx)$, then

$$\|\phi_n\|_p^p = \int_{\mathbb{R}^+} e^{-npx}dx = \frac{1}{np+1}. \tag{3.2.32}$$

Thus, $\|\phi_n\|_p^2 \sim p^{-2/p}n^{-2/p}$ and the series $\sum_n \|\phi_n\|_p^2$ converges if and only if $p < 2$. In this case, the series of functions $\sum \phi_n \otimes \phi_n$ converges in norm in $L^p(\mathbb{R}_+^* \times \mathbb{R}_+^*)$, thus converges in $L^p(\mathbb{R}_+^* \times \mathbb{R}_+^*)$ (as L^p spaces are complete). Thus, $\mathcal{E}_k : L^q(\mathbb{R}_+^*) \to L^p(\mathbb{R}_+^*)$ is well-defined and nuclear if $1 \le p < 2$. However, $k(x,x) = 1/(1-\exp(-2x)) \sim_{+\infty} 1$ and thus, for all $p \in [1, +\infty)$,

$$\int_{\mathbb{R}^+} k(x,x)^{p/2}dx = +\infty, \tag{3.2.33}$$

and $\mathcal{E}_k$ is not a Gaussian covariance operator over $L^p(\mathbb{R}_+^*)$, for any $p \in [1, +\infty)$.

Remark 3.2.11. Proposition 3.2.9 shows that the assumption that a given Gaussian process is measurable is slightly less demanding that it might seem. Ensuring the existence of a measurable modification of a general random process is difficult outside of it being continuous in probability ([63], Theorem

2.6 p. 61). Tedious extensions of this result exist ([64], Theorem 2.3). For a Gaussian process $(U(x))_{x\in\mathcal{D}} \sim GP(0, k_u)$ however, Propositions 3.2.7, 3.2.8 and 3.2.9 shows that the measurability of its covariance function over $\mathcal{D}\times\mathcal{D}$ and the integrability of its standard deviation in $L^p(\mathcal{D})$ (or equivalently, suitable nuclear decompositions of its associated integral operator $\mathcal{E}_k$) ensure the existence of a measurable Gaussian process $(V(x))_{x\in\mathcal{D}} \sim GP(0, k_v)$ with the same covariance function in $L^1_{loc}(\mathcal{D}\times\mathcal{D})$. Consequently, $k_u = k_v$ a.e. on $\mathcal{D}\times\mathcal{D}$. Note though that the process V need not be a modification of U. Since $k_u = k_v$ a.e., we only have that U and V have the same finite dimensional marginals "almost everywhere" in the sense of the Lebesgue measure: for all $n \in \mathbb{N}^*$ and almost every $(x_1, ..., x_n) \in \mathcal{D}^n$, $(U(x_1), ..., U(x_n))$ and $(V(x_1), ..., V(x_n))$ have the same law.

Throughout this article, we will only consider centered Gaussian processes ($\mathbb{E}[U(x)] \equiv 0$) and Gaussian measures ($a_\mu = 0$). Generalizations of the results of this article to non centered Gaussian processes are straightforward.

3.3 Sobolev regularity of Gaussian processes : the general case, $1 < p < +\infty$

We can now state our first result, which deals with $W^{m,p}(\mathcal{D})$-regularity of Gaussian processes, given any $p \in (1, +\infty)$ and any open set $\mathcal{D} \subset \mathbb{R}^d$.

Proposition 3.3.1 (Sample path Banach-Sobolev regularity for Gaussian processes)**.** *Let $\mathcal{D} \subset \mathbb{R}^d$ be an open set. Let $(U(x))_{x\in\mathcal{D}} \sim GP(0, k)$ be a measurable centered Gaussian process, defined on a probability set $(\Omega, \mathcal{F}, \mathbb{P})$, such that its standard deviation function σ lies in $L^1_{loc}(\mathcal{D})$. Let $p \in (1, +\infty)$. Then the following statements are equivalent :*

(i) (Sample path regularity) The sample paths of $(U(x))_{x\in\mathcal{D}}$ lie in $W^{m,p}(\mathcal{D})$ almost surely.

(ii) (Integral criteria) For all $|\alpha| \leq m$, the distributional derivative $\partial^{\alpha,\alpha}k$ lies in $L^p(\mathcal{D}\times\mathcal{D})$ and admits a representative k_α in $L^p(\mathcal{D}\times\mathcal{D})$ which is the covariance function of a measurable Gaussian process. Note $\sigma_\alpha(x) := k_\alpha(x, x)^{1/2}$, then additionally

$$\int_{\mathcal{D}} \sigma_\alpha(x)^p dx < +\infty. \tag{3.3.1}$$

(iii) (Covariance structure) For all $|\alpha| \leq m$, the distributional derivative $\partial^{\alpha,\alpha}k$ lies in $L^p(\mathcal{D}\times\mathcal{D})$ and the associated integral operator $\mathcal{E}^\alpha_k : L^q(\mathcal{D}) \to$

$L^p(\mathcal{D})$ defined by

$$\mathcal{E}_k^\alpha f(x) = \int_{\mathcal{D}} \partial^{\alpha,\alpha} k(x,y) f(y) dy \tag{3.3.2}$$

is symmetric, nonnegative and nuclear: there exists $(\lambda_n^\alpha)_{n\in\mathbb{N}} \geq 0$ and $(\psi_n^\alpha)_{n\in\mathbb{N}} \subset L^p(\mathcal{D})$ such that

$$\begin{cases} \displaystyle\sum_{n=0}^{+\infty} \lambda_n^\alpha \|\psi_n^\alpha\|_{L^p(\mathcal{D})}^2 < +\infty, & (3.3.3) \\ \partial^{\alpha,\alpha} k(x,y) = \displaystyle\sum_{n=0}^{+\infty} \lambda_n^\alpha \psi_n^\alpha(x)\psi_n^\alpha(y) \quad \textit{in} \quad L^p(\mathcal{D}\times\mathcal{D}). & (3.3.4) \end{cases}$$

If $1 \leq p \leq 2$, then one can choose (λ_n^α) such that $\sum_n \lambda_n^\alpha < +\infty$, and there exists a bounded operator $A_\alpha : L^2(\mathcal{D}) \to L^p(\mathcal{D})$ and an orthonormal basis (ϕ_n^α) of $L^2(\mathcal{D})$ such that $\psi_n^\alpha = A_\alpha \phi_n^\alpha$ for all $n \geq 0$ (in particular, we have the uniform bound $\|\psi_n^\alpha\|_p \leq \|A_\alpha\|$).

The proposition above shows that a suitable L^p control of the function $\partial^{\alpha,\alpha}k$ over the diagonal is necessary and sufficient for ensuring the Sobolev regularity of the sample paths of the Gaussian process with covariance function k. Formally speaking, the function $(x,y) \mapsto \partial^{\alpha,\alpha}k(x,y)$ is the covariance function of the differentiated process, $(\omega, x) \mapsto \partial^\alpha U_\omega(x)$. This is formal only, as the weak derivative of the sample paths are only defined up to a set of Lebesgue measure zero, and thus there is no obvious way of defining the joint map $(\omega, x) \mapsto \partial^\alpha U_\omega(x)$. Note also that the idea of ensuring a suitable control of this covariance function near its diagonal is not with reminding more standard results pertaining to the differentiability in the *mean square* sense of a random process (see e.g. [2], Section 1.4.2). See [181] for similar remarks on the Sobolev regularity of random fields.

Observe also that there is an asymmetry between Point *(ii)* and Point *(iii)* of Proposition 3.3.1, as one depends on whether p is lower or greater than 2 while the other does not. Moreover, both points rely on the finiteness of some quantity, so explicit bounds should be sought so that Point *(ii)* controls Point *(iii)* and conversely. This is the content of Proposition 3.3.5.

Finally, observe that the integrability criteria (ii) cannot be expected to hold for any positive definite representative $\tilde{k}_\alpha$ of $\partial^{\alpha,\alpha}k$, even if $\tilde{k}_\alpha$ is measurable on its diagonal. For example, set $\tilde{k}_\alpha(x,y) := k_\alpha(x,y) + \delta_{x,y}$ where $\delta_{x,y}$ is the Kronecker delta, which verifies $\tilde{k}_\alpha = \partial^{\alpha,\alpha}k$ in $L^p(\mathcal{D}\times\mathcal{D})$. But if $\mathcal{D}$ has infinite Lebesgue measure, it is also clear that $\int_{\mathcal{D}} \tilde{k}_\alpha(x,x)^{p/2} dx \geq \int_{\mathcal{D}} \delta_{x,x} dx = +\infty$. Lemma 3.3.7 describes a natural set of "admissible" representatives for which Point (ii) holds, in the case $p \geq 2$.

Remark 3.3.2. Under the assumption that $(U(x))_{x\in\mathcal{D}}$ is measurable, the statement that its sample paths lie in some Sobolev space is *not* up to a modification of the process. This is a consequence of Lemmas 3.2.4, 3.2.5 and 3.2.6, which show that the Sobolev regularity of its paths is fully determined by the finite dimensional marginals of the process (see equation (3.3.7)). This contrasts with more classical results, e.g. pertaining to the continuity of the process ([16], Section 1.4.1). Still, ensuring the measurability of the process is not really straightforward (see Remark 3.2.11).

Example 3.3.3 (Finite rank covariance functions). Let $p \in (1, +\infty)$, $m \in \mathbb{N}^*$ and $N \in \mathbb{N}^*$. Consider $f_1, ..., f_N \in W^{m,p}(\mathcal{D})$ and choose once and for all representatives of those functions in $L^p(\mathcal{D})$, also denoted by $f_1, ..., f_N$, so that they may be understood as functions in the classical sense. Consider the covariance function $k(x, x') \coloneqq \sum_{i=1}^N f_i(x)f_i(x')$. Then obviously, for all $|\alpha| \leq m$, the weak derivative $\partial^{\alpha,\alpha}k$ is given by

$$\partial^{\alpha,\alpha}k(x, x') = \sum_{i=1}^N \partial^\alpha f_i(x)\partial^\alpha f_i(x') \quad \text{in } L^p(\mathcal{D} \times \mathcal{D}), \tag{3.3.5}$$

and the associated integral operators fulfill the criteria *(iii)* of Proposition 3.3.1. Thus the corresponding measurable Gaussian process has its sample paths in $W^{m,p}(\mathcal{D})$ almost surely. Note that this was obvious in the first place, since this Gaussian process can be written as $U(x) = \sum_{i=1}^N \xi_i f_i(x)$ where $\xi_1, ..., \xi_N$ are independent standard Gaussian random variables (checking that the covariance function is the right one is trivial). Still, this example fell out of the scope of the previous results pertaining to the Sobolev regularity of Gaussian processes.

Proof. (Proposition 3.3.1) We show $(i) \implies (ii)$ & (iii), $(ii) \implies (i)$ and $(iii) \implies (ii)$.
$(i) \implies (ii)$ & (iii) : Suppose (i) and let $|\alpha| \leq m$. We first prove that the map $N_\alpha : (\Omega, \mathcal{F}, \mathbb{P}) \to (\mathbb{R}, \mathcal{B}(\mathbb{R}))$, $\omega \mapsto \|\partial^\alpha U_\omega\|_{L^p(\mathcal{D})}$ is measurable. Indeed, given $\varphi \in F_q$ (see equation (3.2.17) for the definition of F_q), the map

$$U_\varphi^\alpha : \omega \longmapsto \int_\mathcal{D} \partial^\alpha U_\omega(x)\varphi(x)dx = (-1)^{|\alpha|} \int_\mathcal{D} U_\omega(x)\partial^\alpha\varphi(x)dx \tag{3.3.6}$$

is a real valued random variable (this follows from Lemma 3.2.5). From Lemma 3.2.4, one also has

$$\left(\omega \mapsto \|\partial^\alpha U_\omega\|_{L^p(\mathcal{D})}\right) = \sup_{\varphi\in F_q} |U_\varphi^\alpha|. \tag{3.3.7}$$

The supremum being taken over a countable set, N_α is indeed a measurable map. Given any $f \in L^p(\mathcal{D})$, a slight modification of this proof shows that

$\omega \mapsto \|\partial^\alpha U_\omega - f\|_{L^p(\mathcal{D})}$ is also measurable. We can now show the map $T_\alpha : (\Omega, \mathcal{F}, \mathbb{P}) \to (L^p(\mathcal{D}), \mathcal{B}(L^p(\mathcal{D})))$, $\omega \mapsto \partial^\alpha U_\omega$ is measurable. Let $f \in L^p(\mathcal{D}), r > 0$ and $B = B(f, r)$ be an open ball in $L^p(\mathcal{D})$. Then from the measurability of $\omega \mapsto \|\partial^\alpha U_\omega - f\|_{L^p(\mathcal{D})}$,

$$T_\alpha^{-1}(B) = \{\omega \in \Omega : \|\partial^\alpha u - f\|_{L^p(\mathcal{D})} < r\} \in \mathcal{F}. \tag{3.3.8}$$

Since $L^p(\mathcal{D})$ is a separable metric space, its Borel σ-algebra is generated by the open balls of $L^p(\mathcal{D})$ (see e.g. [30], Exercise 6.10.28). Thus T_α is Borel-measurable and the pushforward of $\mathbb{P}$ through T_α induces a (centered) probability measure μ_α over the Banach space $L^p(\mathcal{D})$. We show that it is Gaussian. Let $f \in L^q(\mathcal{D})$ and denote T_f the associated linear form over $L^p(\mathcal{D})$. Let $(\phi_n) \subset C_c^\infty(\mathcal{D})$ be such that $\phi_n \to f$ in $L^q(\mathcal{D})$ and $\omega \in \Omega$ be such that U_ω lies in $L^1_{loc}(\mathcal{D})$:

$$T_f(\partial^\alpha U_\omega) = \int_{\mathcal{D}} \partial^\alpha U_\omega(x) f(x) dx = \lim_{n\to\infty} \int_{\mathcal{D}} \partial^\alpha U_\omega(x) \phi_n(x) dx \tag{3.3.9}$$

$$= \lim_{n\to\infty} (-1)^{|\alpha|} \int_{\mathcal{D}} U_\omega(x) \partial^\alpha \phi_n(x) dx. \tag{3.3.10}$$

For each value of n, Lemma 3.2.5 shows that the map given by

$$\omega \mapsto (-1)^{|\alpha|} \int_{\mathcal{D}} U_\omega(x) \partial^\alpha \phi_n(x) dx,$$

is a Gaussian random variable. Thus $\omega \mapsto T_f(\partial^\alpha U_\omega)$ is a Gaussian random variable as an a.s. limit of Gaussian random variables. This shows that the pushforward of μ_α through T_f is Gaussian (see Section 3.2.5(i) for the pushforward), since for all Borel set $B \in \mathcal{B}(\mathbb{R})$,

$$\mu_\alpha(T_f^{-1}(B)) = \mu_\alpha(\{g \in L^p(\mathcal{D}) : T_f(g) \in B\}) = \mathbb{P}(\{\omega \in \Omega : T_f(\partial^\alpha U_\omega) \in B\}).$$

Hence, μ_α is a Gaussian measure. We next show that $\partial^{\alpha,\alpha} k \in L^p(\mathcal{D} \times \mathcal{D})$ and that the covariance operator of μ_α is the integral operator $\mathcal{E}_k^\alpha : L^q(\mathcal{D}) \to L^p(\mathcal{D})$ with kernel $\partial^{\alpha,\alpha} k$. Let $\mathcal{D}_0 \Subset \mathcal{D} \times \mathcal{D}$ and $K_0 \Subset \mathcal{D}$ be such that $\mathcal{D}_0 \subset K_0 \times K_0$ (for example, set $K_1 := \overline{\{x \in \mathcal{D} : \exists y \in \mathcal{D}, (x, y) \in K\}}$, $K_2 := \overline{\{y \in \mathcal{D} : \exists x \in \mathcal{D}, (x, y) \in K\}}$ which are both compact subsets of $\mathcal{D}$ and $K_0 := K_1 \cup K_2$). Let $h = (h_1, ..., h_d) \in (\mathbb{R}_+^*)^d$ be such that $\sum_i \alpha_i h_i < \operatorname{dist}(K_0, \mathcal{D}_0)$. Use then the bilinearity of the covariance operator:

$$\int_{\mathcal{D}_0} |(\delta_h^\alpha \otimes \delta_h^\alpha) k(x, y)|^p dx dy = \int_{\mathcal{D}_0} |\mathbb{E}[\delta_h^\alpha U(x) \delta_h^\alpha U(y)]|^p dx dy \tag{3.3.11}$$

$$\leq \int_{K_0 \times K_0} |\mathbb{E}[\delta_h^\alpha U(x) \delta_h^\alpha U(y)]|^p dx dy \tag{3.3.12}$$

$$\leq \int_{K_0 \times K_0} \mathbb{E}[|\delta_h^\alpha U(x) \delta_h^\alpha U(y)|^p] dxdy \tag{3.3.13}$$

$$\leq \mathbb{E}\left[\left(\int_{K_0} |\delta_h^\alpha U(x)|^p dx \right)^2 \right] = \mathbb{E}[\|\delta_h^\alpha U\|_p^{2p}]$$

$$\leq \mathbb{E}[\|U\|_{W^{m,p}(\mathcal{D})}^{2p}] =: C^p < +\infty. \tag{3.3.14}$$

The expectation in equation (3.3.14) is indeed finite because of the following. Given $|\alpha| \leq m$, equation (3.3.7) shows that the map $\omega \mapsto \|\partial^\alpha U_\omega\|_p$ is the supremum of a Gaussian sequence which is finite a.s. by assumption; Lemma 3.2.6 then implies that all the moments of this supremum are finite. Writing then $\|U\|_{W^{m,p}}$ in terms of these L^p norms yields equation (3.3.14). To see that the control (3.3.14) implies that $\partial^{\alpha,\alpha} k \in L^p(\mathcal{D} \times \mathcal{D})$, we copy the steps of equations (3.7.2)-(3.7.3)-(3.7.4) in the proof of Lemma 3.2.1. Let $\varphi \in C_c^\infty(\mathcal{D} \times \mathcal{D})$. Since it is compactly supported in $\mathcal{D} \times \mathcal{D}$, find an open set $\mathcal{D}_0 \Subset \mathcal{D}$ such that $\mathrm{Supp}(\varphi) \subset \mathcal{D}_0$. Use Hölder's inequality and equation (3.3.14):

$$\left| \int_{\mathcal{D} \times \mathcal{D}} (\delta_h^\alpha \otimes \delta_h^\alpha) k(x,y) \varphi(x,y) dxdy \right| \leq \|(\delta_h^\alpha \otimes \delta_h^\alpha) k\|_p \|\varphi\|_q \leq C \|\varphi\|_q. \tag{3.3.15}$$

Next, use the discrete integration by parts formula:

$$\int_{\mathcal{D} \times \mathcal{D}} (\delta_h^\alpha \otimes \delta_h^\alpha) k(x,y) \varphi(x,y) dxdy = \int_{\mathcal{D}} k(x,y) (\delta_h^\alpha \otimes \delta_h^\alpha)^* \varphi(x,y) dxdy. \tag{3.3.16}$$

When $h \to 0$, observe that $(\delta_h^\alpha \otimes \delta_h^\alpha)^* \varphi(x,y) \to \partial^{\alpha,\alpha} \varphi(x,y)$ pointwise. Use Lebesgue's dominated convergence theorem and equation (3.3.15) to obtain

$$\left| \int_{\mathcal{D} \times \mathcal{D}} k(x,y) \partial^{\alpha,\alpha} \varphi(x,y) dxdy \right| \leq C \|\varphi\|_q, \tag{3.3.17}$$

which indeed shows that $\partial^{\alpha,\alpha} k \in L^p(\mathcal{D} \times \mathcal{D})$, from Riesz' lemma. We now identify K_α, the covariance operator of μ_α, in terms of $\partial^{\alpha,\alpha} k$. Let $f, g \in L^q(\mathcal{D})$ and using the density of $C_c^\infty(\mathcal{D})$ in $L^q(\mathcal{D})$ ([169], Corollary 2.30), let $(f_n), (g_n) \subset C_c^\infty(\mathcal{D})$ be two sequences such that $f_n \to f$ in $L^q(\mathcal{D})$ and likewise for g_n and g. Then (explanation below),

$$\langle f, K_\alpha g \rangle_{L^q, L^p} = \lim_{n \to \infty} \langle f_n, K_\alpha g_n \rangle_{L^q, L^p} \tag{3.3.18}$$

$$= \lim_{n \to \infty} \int_{L^p(\mathcal{D})} \langle f_n, h \rangle_{L^q, L^p} \langle g_n, h \rangle_{L^q, L^p} d\mu_\alpha(h)$$

$$= \lim_{n \to \infty} \int_\Omega \langle f_n, \partial^\alpha U_\omega \rangle_{L^q, L^p} \langle g_n, \partial^\alpha U_\omega \rangle_{L^q, L^p} d\mathbb{P}(\omega) \tag{3.3.19}$$

$$= \lim_{n\to\infty} \int_\Omega \langle \partial^\alpha f_n, U_\omega \rangle_{L^q,L^p} \langle \partial^\alpha g_n, U_\omega \rangle_{L^q,L^p} d\mathbb{P}(\omega)$$

$$= \lim_{n\to\infty} \int_{\mathcal{D}\times\mathcal{D}} \partial^\alpha f_n(x) \partial^\alpha g_n(y) k(x,y) dxdy \tag{3.3.20}$$

$$= \lim_{n\to\infty} \int_{\mathcal{D}\times\mathcal{D}} f_n(x) g_n(y) \partial^{\alpha,\alpha} k(x,y) dxdy$$

$$= \int_{\mathcal{D}\times\mathcal{D}} f(x) g(y) \partial^{\alpha,\alpha} k(x,y) dxdy = \langle f, \mathcal{E}_k^\alpha g \rangle_{L^q,L^p} \tag{3.3.21}$$

We used the sequential continuity of K_α in equation (3.3.18), the transfer theorem for pushforward measure integration ([30], Theorem 3.6.1) in equation (3.3.19) and Fubini's theorem in equation (3.3.20). THus $K_\alpha = \mathcal{E}_k^\alpha$. According to Proposition 3.2.9, since μ_α is a Gaussian measure over $L^p(\mathcal{D})$, there exists a representative k_α of $\partial^{\alpha,\alpha} k$ in $L^p(\mathcal{D}\times\mathcal{D})$ which is the covariance function of a measurable Gaussian process. Note $\sigma_\alpha(x) = k_\alpha(x,x)^{1/2}$, then the same proposition shows that

$$\int_{\mathcal{D}} \sigma_\alpha(x)^p dx < +\infty, \tag{3.3.22}$$

which shows (ii). By Corollary 3.5.11 from [29], $\mathcal{E}_k^\alpha$ is nuclear and admits a symmetric nonnegative representation as the one in equation (3.3.4). if $1 \leq p \leq 2$, then $L^p(\mathcal{D})$ is of cotype 2 and since $\mathcal{E}_k^\alpha$ is a Gaussian covariance operator, from Proposition 3.2.8 there exists a bounded operator $A_\alpha : L^2(\mathcal{D}) \to L^p(\mathcal{D})$ and a trace class operator $S_\alpha : L^2(\mathcal{D}) \to L^2(\mathcal{D})$ such that $\mathcal{E}_k^\alpha = A_\alpha S_\alpha A_\alpha^*$. Introduce a Mercer decomposition of S_α (equation (3.2.23)): $S_\alpha = \sum_n \lambda_n^\alpha \phi_n^\alpha \otimes \phi_n^\alpha$. Use the continuity of A_α and A_α^* to obtain that $\partial^{\alpha,\alpha} k(x,y) = \sum_n \lambda_n^\alpha (A_\alpha \phi_n^\alpha)(x)(A_\alpha \phi_n^\alpha)(y)$ in $L^p(\mathcal{D}\times\mathcal{D})$, which finishes to prove (iii).

$(ii) \implies (i)$: from Proposition 3.2.9, let (V^α) be a centered measurable Gaussian process with covariance function k_α. Then its sample paths lie in $L^p(\mathcal{D})$ a.s. and the Gaussian measure it induces over $L^p(\mathcal{D})$ through the map $\omega \mapsto V_\omega^\alpha \in L^p(\mathcal{D})$ is the centered Gaussian measure with covariance operator $\mathcal{E}_k^\alpha$. Given $\varphi \in C_c^\infty(\mathcal{D})$, denote V_φ^α the following random variable

$$\omega \mapsto \int_{\mathcal{D}} V_\omega^\alpha(x) \varphi(x) dx. \tag{3.3.23}$$

From Lemma 3.2.5, $(V_\varphi^\alpha)_{\varphi\in F_q}$ is a Gaussian sequence. It is also centered and using Fubini's theorem to permute $\mathbb{E}$ and $\int$, we have that

$$\mathbb{E}[V_\varphi^\alpha V_\psi^\alpha] = \int_{\mathcal{D}\times\mathcal{D}} \varphi(y)\psi(x) k_\alpha(x,y) dxdy = \int_{\mathcal{D}\times\mathcal{D}} \varphi(y)\psi(x) \partial^{\alpha,\alpha} k(x,y) dxdy$$

$$= \int_{\mathcal{D}\times\mathcal{D}} \partial^\alpha\varphi(y)\partial^\alpha\psi(x)k(x,y)dxdy. \tag{3.3.24}$$

$$\mathbb{E}[U^\alpha_\varphi U^\alpha_\psi] = \int_{\mathcal{D}\times\mathcal{D}} \partial^\alpha\varphi(y)\partial^\alpha\psi(x)k(x,y)dxdy. \tag{3.3.25}$$

Having the same mean and covariance, the two Gaussian sequences $(V^\alpha_\varphi)_{\varphi\in F_q}$ and $(U^\alpha_\varphi)_{\varphi\in F_q}$ have the same finite dimensional marginals. One checks in an elementary fashion that their countable suprema over F_q then have the same probability law (e.g. by showing that they have the same cumulative distribution function). Recalling from Lemma 3.2.4 that $\|V^\alpha_\omega\|_p = \sup_{\varphi\in F_q}|V^\alpha_\varphi(\omega)|$, we obtain that

$$1 = \mathbb{P}(\|V^\alpha_\omega\|_p < +\infty) = \mathbb{P}(\sup_{\varphi\in F_q}|V^\alpha_\varphi| < +\infty) = \mathbb{P}(\sup_{\varphi\in F_q}|U^\alpha_\varphi| < +\infty), \tag{3.3.26}$$

which shows that $\partial^\alpha U \in L^p(\mathcal{D})$ almost surely. This is true for all $|\alpha| \leq m$, which shows (i).

$(iii) \implies (ii)$: if (iii), then from either Proposition 3.2.7 or 3.2.8 depending on whether $p \leq 2$ or $p \geq 2$, there exists a Gaussian measure over $L^p(\mathcal{D})$ whose covariance operator is $\mathcal{E}^\alpha_k$ as defined in equation (3.3.2). Proposition 3.2.9 yields (ii). □

Remark 3.3.4 (Distributing derivatives over nuclear decompositions). In Point (iii) of Proposition 3.3.1, it is very tempting to distribute the cross derivative $\partial^{\alpha,\alpha}$ over the nuclear decomposition of k (i.e. when $\alpha = 0$, setting $\lambda_n := \lambda^0_n$ and $\psi_n := \psi^0_n$), thus setting $\lambda^\alpha_n = \lambda_n$ and $\psi^\alpha_n = \partial^\alpha\psi_n$. While we can show that $\partial^\alpha\psi_n \in L^p(\mathcal{D})$ (copy the proof of Lemma 3.4.9, Point (i)), it is not clear whether the obtained decomposition converges in $L^p(\mathcal{D}\times\mathcal{D})$, or that it corresponds to a nuclear one, i.e. $\sum_n \lambda_n\|\partial^\alpha\psi_n\|^2_p < +\infty$ (it is not even clear in what sense this derivative can be distributed, apart from the distributional sense). When $p = 2$, it turns out that this is true (see the upcoming Proposition 3.4.4).

When $p > 2$ though, the following example shows that disbtributing derivatives over a nuclear decomposition do not, in general, yield nuclear decompositions, even if nuclear decompositions of the differentiated kernel exist. Explicitly, we build a covariance function g defined over $(0,1)\times(0,1)$, decomposed as $g = \sum_n \psi_n \otimes \psi_n$ with the following properties.

- (i) $\sum_n \|\psi_n\|^2_p < +\infty$, we have $\int_0^1 g(x,x)^{p/2}dx < +\infty$ and thus the sample paths of the associated GP lie in $L^p((0,1))$.
- (ii) $\partial_x\partial_y g(x,y)$ is well defined for all $x, y \in (0,1)$ except on a countable set, and $\partial_x\partial_y g \in L^p((0,1)\times(0,1))$.
- (iii) $\int_0^1 \partial_x\partial_y g(x,x)^{p/2}dx < +\infty$, hence the sample paths of the GP with covariance function g lie in $W^{1,p}((0,1))$.

• (iv) $\sum_n \|\psi_n'\|_p^2 = +\infty$, hence the decomposition $\partial_x\partial_y g = \sum \psi_n' \otimes \psi_n'$ is not nuclear (even though such decompositions do exist, since $\int_0^1 \partial_x\partial_y g(x,x)^{p/2}dx < +\infty$).

Let $\alpha > 0$, set $s_n := n^{-\alpha}$, $m_n := (s_n + s_{n+1})/2$ and consider the functions defined on $(0,1)$ by

$$\phi_n(x) := \mathbb{1}_{[s_{n+1},m_n]}(x) - \mathbb{1}_{[m_n,s_n]}(x), \quad \psi_n(x) = \int_0^x \phi_n(s)ds. \tag{3.3.27}$$

The functions ψ_n are nonnegative hat functions supported on $[s_{n+1}, s_n]$, with slope ± 1. Consider now the following covariance functions defined for *all* $(x,y) \in (0,1)^2$ by

$$g(x,y) = \sum_{n=0}^{+\infty} \psi_n(x)\psi_n(y), \quad k(x,y) = \sum_{n=0}^{+\infty} \phi_n(x)\phi_n(y). \tag{3.3.28}$$

The infinite sums above has in fact only one non zero term, given any fixed $(x,y) \in (0,1)^2$, hence the functions g and k are well-defined. We now prove the announced properties.

(i) : We have that

$$\|\psi_n\|_p^p = 2\int_0^{s_n - m_n} x^p dx = 2\frac{(s_n - m_n)^{p+1}}{p+1}, \tag{3.3.29}$$

$$\|\psi_n\|_p^2 = \left(\frac{2}{p+1}\right)^{2/p} (s_n - m_n)^{2+2/p}. \tag{3.3.30}$$

hence, since $s_n - m_n \sim \alpha/2n^{\alpha+1}$, $(s_n - m_n)^{2+2/p} \sim C_p/n^{(2+2/p)(\alpha+1)}$ for some $C_p > 0$ and $\sum_n \|\psi_n\|_p^2$ converges.

(ii) : observe that for all $x, y \in (0,1)$, from Tonelli's theorem,

$$\sum_{n=0}^{+\infty} \int_0^x \int_0^y |\phi_n(s)\|\phi_n(t)|dsdt = \int_0^x \int_0^y \sum_{n=0}^{+\infty} |\phi_n(s)\|\phi_n(t)|dsdt \tag{3.3.31}$$

$$= \int_0^x \int_0^y 1 dsdt = xy < +\infty. \tag{3.3.32}$$

Hence, from Fubini's theorem,

$$\int_0^x \int_0^y k(s,t)dsdt = \sum_{n=0}^{+\infty} \int_0^x \phi_n(s)ds \int_0^y \phi_n(s)ds = g(x,y). \tag{3.3.33}$$

From this equation it is also readily seen that for all $x, y \neq s_n$ or m_n,

$$\partial_x\partial_y g(x,y) = k(x,y). \tag{3.3.34}$$

(*iii*) Now, observe that $k(x,x) = 1$ for all $x \in (0,1)$ (except for $x = s_n$ or m_n for some $n \in \mathbb{N}^*$), thus

$$\int_0^1 k(x,x)^{p/2} dx = \int_0^1 dx = 1 < +\infty. \tag{3.3.35}$$

This also shows that nuclear decompositions of $k = \partial_x \partial_y g$ exist, Gaussian covariance operators being nuclear (see e.g. Proposition 3.2.7).
(*iv*) However,

$$\|\phi_n\|_p^p = \int_{s_{n+1}}^{s_n} dx = s_n - s_{n+1} \sim \alpha/2n^{\alpha+1}. \tag{3.3.36}$$

Thus, $\|\phi_n\|_p^2 \sim C_p \times 1/n^{2(\alpha+1)/p}$ and $\sum_n \|\phi_n\|_p^2$ converges only if $\alpha > p/2 - 1$. Therefore, our conterexample is found by taking any $\alpha \in (0, p/2-1]$. Observe that when $p = 2$, this interval becomes empty!

When $1 < p < 2$, the following formal computation shows that we should expect that derivatives may be distributed over nuclear decompositions to yield nuclear distributions. Assume formally that the derivative can be distributed pointwise, and introduce the functions $v_\alpha(x) \coloneqq \sum_n \lambda_n \partial^\alpha \psi_n(x)^2$ and $\sigma_\alpha(x) \coloneqq v_\alpha(x)^{1/2}$. From Proposition 3.3.1, we expect that $\|\sigma_\alpha\|_p < +\infty$. When $1 \leq p < 2$, the *reverse* Minkowski inequality in $L^{p/2}(\mathcal{D})$ (see [169], Theorem 2.13 p. 28) then yields

$$\begin{aligned}\sum_{n=0}^{+\infty} \lambda_n \|\partial^\alpha \psi_n\|_p^2 &= \sum_{n=0}^{+\infty} \lambda_n \|\partial^\alpha \psi_n^2\|_{p/2} \\ &\leq \left\| \sum_{n=0}^{+\infty} \lambda_n \partial^\alpha \psi_n^2 \right\|_{p/2} = \|v_\alpha\|_{p/2} = \|\sigma_\alpha\|_p^2 < +\infty,\end{aligned} \tag{3.3.37}$$

so that the series $\sum_n \lambda_n \|\partial^\alpha \psi_n\|_p^2$ converges. From this, it is then readily checked that the equality $\partial^{\alpha,\alpha} k = \sum_n \lambda_n \partial^\alpha \psi_n \otimes \partial^\alpha \psi_n$ holds in $L^p(\mathcal{D} \times \mathcal{D})$, which is then a nuclear decomposition of $\partial^{\alpha,\alpha} k$. Still, recall that in spaces of cotype 2, Gaussian covariance operators are not just nuclear (Proposition 3.2.8).

The following proposition deals with the apparent asymmetry in p between Points (*ii*) and (*iii*) of Proposition 3.3.1. We recall that the nuclear norm $\nu(T)$ is defined in equation (3.2.25). Contrarily to Proposition 3.3.1, we do not exclude $p = 1$.

Proposition 3.3.5. *Let μ be a centered Gaussian measure over $L^p(\mathcal{D})$, where $1 \leq p < +\infty$. Let $k \in L^p(\mathcal{D} \times \mathcal{D})$ be the kernel of its covariance operator ($K_\mu = \mathcal{E}_k$), chosen such that k is also the covariance function of a measurable*

Gaussian process $(U(x))_{x\in\mathcal{D}}$*, from Proposition 3.2.9. Define* $\sigma(x) = k(x,x)^{1/2}$ *and set* $C_p = 2^{p/2}\Gamma((p+1)/2)/\sqrt{\pi}$ ($C_p = \mathbb{E}[|X|^p]$ *where* $X \sim \mathcal{N}(0,1)$)*. Then the following bounds hold.*

- *if* $1 \leq p < 2$*, there exists a symmetric, nonnegative and trace class operator* S *over* $L^2(\mathcal{D})$ *and a bounded operator* $A : L^2(\mathcal{D}) \to L^p(\mathcal{D})$ *such that* $\mathcal{E}_k = ASA^*$*. Moreover,*

$$\nu(\mathcal{E}_k) \leq \inf_{\substack{A,S \text{ s.t.} \\ \mathcal{E}_k = ASA^*}} \|A\|^2 \nu(S) \leq \|\sigma\|_p^2 \leq C_p^{-2/p} \inf_{\substack{A,S \text{ s.t.} \\ \mathcal{E}_k = ASA^*}} \|A\|^2 \nu(S). \tag{3.3.38}$$

- *if* $2 \leq p < +\infty$*, then* $\mathcal{E}_k$ *is symmetric, nonnegative and nuclear, and*

$$C_p^{-2/p} \nu(\mathcal{E}_k) \leq \|\sigma\|_p^2 \leq \nu(\mathcal{E}_k). \tag{3.3.39}$$

Observe that if $p = 2$ then $C_2 = 1$ and equation (3.3.39) yields $\|\sigma\|_2^2 = \nu(\mathcal{E}_k) = \mathrm{Tr}(\mathcal{E}_k)$. It is expected that the nuclear norm of $\mathcal{E}_k$ cannot directly appear on the right hand side of equation (3.3.38), as not all nuclear operators are Gaussian covariance operators when $1 \leq p < 2$ (Proposition 3.2.8). Proposition 3.3.5 in fact suggests that for general Banach spaces X of cotype 2, the following map defined over the set of Gaussian covariance operators $B : X^* \to X$,

$$B \mapsto \inf_{\substack{A,S \text{ s.t.} \\ B = ASA^*}} \|A\|^2 \nu(S) \tag{3.3.40}$$

is the natural measurement of the "size" of such operators. When X is of type 2, this would be the case for the nuclear norm $B \mapsto \nu(B)$.

Remark 3.3.6. Proposition 3.3.5 is interesting from an application point of view because it states that the operator norms appearing in this proposition, as well as the L^p norm of the standard deviation function σ, are suitable quantities for quantitatively controlling the L^p norm of the sample paths of the underlying Gaussian process. For instance, we have the following L^p control in expectation: $\mathbb{E}[\|U\|_p^p] = C_p \|\sigma\|_p^p$ (see equation (3.3.42)). Applying this fact recursively, we obtain that the $W^{m,p}$-Sobolev norm of the sample paths of the Gaussian process in question is controlled as follow, denoting $\sigma_\alpha(x) = \partial^{\alpha,\alpha} k(x,x)^{1/2}$ (choosing the representative of $\partial^{\alpha,\alpha} k$ which is the covariance of a measurable Gaussian process)

$$\mathbb{E}\big[\|U\|_{W^{m,p}}^p\big] = C_p \sum_{|\alpha| \leq m} \|\sigma_\alpha\|_p^p. \tag{3.3.41}$$

If such a control cannot be obtained, then it means that the sample paths of U do not lie in $W^{m,p}(\mathcal{D})$ in the first place. Finally, we have the following asymptotic behaviour of the constant when $p \to +\infty : C_p^{-2/p} \sim \exp(1)/(p-1)$.

Proof. (Proposition 3.3.5) We begin with the following general fact concerning the measurable Gaussian process $(U(x))_{x\in\mathcal{D}}$, observing from Fubini's theorem that

$$\mathbb{E}[\|U\|_p^p] = \mathbb{E}\left[\int_{\mathcal{D}} |U(x)|^p dx\right] = \int_{\mathcal{D}} \mathbb{E}[|U(x)|^p]dx \tag{3.3.42}$$

$$= \int_{\mathcal{D}} C_p \sigma(x)^p dx = C_p \|\sigma\|_p^p, \tag{3.3.43}$$

where $C_p = 2^{p/2}\Gamma((p+1)/2)/\sqrt{\pi}$. Indeed, given $X \sim \mathcal{N}(0,\sigma^2)$, then $\mathbb{E}[|X|^p] = C_p\sigma^p$.

Suppose now that $1 \le p < 2$. Let μ_0 be a Gaussian measure on $L^2(\mathcal{D})$ and $A : L^2(\mathcal{D}) \to L^p(\mathcal{D})$ a bounded operator such that $\mu = \mu_{0A}$ (pushforward of μ_0 through A, see Section 3.2.5(i)) and S the trace class covariance operator associated to μ_0 (see Proposition 3.2.8). Recall also that from Proposition 3.2.9, $\mu = \mathbb{P}_U$. Then (explanation below),

$$C_p\|\sigma\|_p^p = \mathbb{E}[\|U\|_p^p] = \int_\Omega \|U_\omega\|_p^p \mathbb{P}(d\omega) = \int_{L^p(\mathcal{D})} \|f\|_p^p \mu(df) \tag{3.3.44}$$

$$= \int_{L^2(\mathcal{D})} \|Ag\|_p^p \mu_0(dg) \le \|A\|^p \int_{L^2(\mathcal{D})} \|g\|_2^p \mu_0(dg) \tag{3.3.45}$$

$$\le \|A\|^p \int_{L^2(\mathcal{D})} \langle g,g\rangle_{L^2}^{p/2} \mu_0(dg)$$

$$\le \|A\|^p \left(\int_{L^2(\mathcal{D})} \langle g,g\rangle_{L^2} \mu_0(dg)\right)^{p/2} \tag{3.3.46}$$

$$\le \|A\|^p \ \mathrm{Tr}(S)^{p/2} = \|A\|^p \nu(S)^{p/2}. \tag{3.3.47}$$

In equation (3.3.44), we used equation (3.3.42) and pushforward integration to write the integral w.r.t. $\mathbb{P}$ as an integral w.r.t. $\mu = \mathbb{P}_U$. Likewise in equation (3.3.45) where we write the integral w.r.t. μ as an integral w.r.t. μ_0 using the pushforward identity $\mu = \mu_{0A}$. In equation (3.3.46), we used Jensen's inequality for concave functions ($0 < p/2 < 1$). In equation (3.3.47), we used the trace identity for Gaussian measures over Hilbert spaces from [29], equation 2.3.2 and the one following p. 49. Moreover, from the nuclear norm estimate of [202], Proposition 47.1 pp. 479-480,

$$\nu(\mathcal{E}_k) = \nu(ASA^*) \le \|A\|\nu(S)\|A^*\| \le \|A\|^2\nu(S). \tag{3.3.48}$$

In equations (3.3.47) and (3.3.48), taking the infimum over all representations $\mathcal{E}_k = ASA^*$ yields

$$\nu(\mathcal{E}_k) \le \inf_{\substack{A,S \text{ s.t.} \\ \mathcal{E}_k = ASA^*}} \|A\|^2\nu(S), \quad \|\sigma\|_p^2 \le C_p^{-\frac{2}{p}} \inf_{\substack{A,S \text{ s.t.} \\ \mathcal{E}_k = ASA^*}} \|A\|^2\nu(S). \tag{3.3.49}$$

To prove the remaining inequality ($\inf_{\mathcal{E}_k=ASA^*} \|A\|^2\nu(S) \leq \|\sigma\|_p^2$), we use an explicit decomposition $\mathcal{E}_k = ASA^*$ by first setting

$$Af(x) = f(x)\sigma(x)^{1-p/2}. \tag{3.3.50}$$

Using Hölder's inequality with $a = 2/p, 1/a + 1/b = 1$ (notice that $a > 1$), we obtain

$$\|Af\|_p^p = \int_{\mathcal{D}} |f(x)|^p \sigma(x)^{p(1-p/2)} dx \tag{3.3.51}$$

$$\leq \left(\int_{\mathcal{D}} |f(x)|^2 dx \right)^{p/2} \left(\int_{\mathcal{D}} \sigma(x)^{bp(1-p/2)} dx \right)^{1/b}. \tag{3.3.52}$$

But $b = \frac{a}{a-1} = \frac{2/p}{2/p-1} = \frac{1}{1-p/2}$ and $b(1-p/2) = 1$, which together with equation (3.3.51) yields

$$\|Af\|_p^p \leq \|f\|_2^p \|\sigma\|_p^{p(1-p/2)}. \tag{3.3.53}$$

Thus $A : L^2(\mathcal{D}) \to L^p(\mathcal{D})$ is bounded and $\|A\| \leq \|\sigma\|_p^{1-p/2}$. One also verifies that $A^* : L^q(\mathcal{D}) \to L^2(\mathcal{D})$ is given by $A^* f(x) = f(x)\sigma(x)^{1-p/2}$, with $\|A\| = \|A^*\|$. Introduce the functions $k_0(x, y) := k(x, y)\sigma(x)^{p/2-1}\sigma(y)^{p/2-1}$, and $\sigma_0(x) = k_0(x, x)^{1/2}$; k_0 is the covariance function of the measurable Gaussian process $V(x) := \sigma(x)^{p/2-1}U(x)$, and verifies

$$\|\sigma_0\|_2^2 = \int_{\mathcal{D}} \sigma_0(x)^2 dx = \int_{\mathcal{D}} k_0(x, x) dx = \int_{\mathcal{D}} \sigma(x)^p dx = \|\sigma\|_p^p < +\infty. \tag{3.3.54}$$

Therefore $\mathcal{E}_{k_0}$, the integral operator over $L^2(\mathcal{D})$ associated to k_0, is trace class (Proposition 3.3.1(*ii*)). Observe also that $k = (A \otimes A)k_0$ also yields that $\mathcal{E}_k = A\mathcal{E}_{k_0}A^*$. Thus,

$$\inf_{\substack{A,S \text{ s.t.} \\ \mathcal{E}_k=ASA^*}} \|A\|^2\nu(S) \leq \|A\|^2\nu(\mathcal{E}_{k_0}) \leq \|\sigma\|_p^{2-p}\|\sigma\|_p^p = \|\sigma\|_p^2. \tag{3.3.55}$$

Combining equations (3.3.49) and (3.3.55) yields the desired result of equation (3.3.38).

Suppose now that $p \geq 2$. Recall that $\mu = \mathbb{P}_U$. We successively use the transfer theorem for pushforward measure integration, Jensen's inequality for probability measures ($p/2 \geq 1$) and the nuclear norm estimate from [134], Theorem 3:

$$\mathbb{E}[\|U\|_p^p] = \int_\Omega \|U_\omega\|_p^p \mathbb{P}(d\omega) = \int_{L^p(\mathcal{D})} \|f\|_p^p \mu(df) = \int_{L^p(\mathcal{D})} \|f\|_p^{2\times p/2} \mu(df) \tag{3.3.56}$$

$$\geq \left(\int_{L^p(\mathcal{D})} \|f\|_p^2 \mu(df) \right)^{p/2} \geq \nu(\mathcal{E}_k)^{p/2}, \tag{3.3.57}$$

which together with equation (3.3.42) yields $\|\sigma\|_p^2 \geq C_p^{-2/p} \nu(\mathcal{E}_k)$. We now prove the last remaining inequality, i.e. $\|\sigma\|_p^2 \leq \nu(\mathcal{E}_k)$. For this, consider $k(x,y) = \sum_n \mu_n \psi_n(x) \phi_n(y)$, a nuclear representation of k in $L^p(\mathcal{D} \times \mathcal{D})$, with $\|\psi_n\|_p = \|\phi_n\|_p = 1$ and $S := \sum_n |\mu_n| < +\infty$. Denote by v the function $v : x \mapsto \sum_{n=0}^{+\infty} \mu_n \psi_n(x) \phi_n(x)$. Minkowski's inequality in $L^{p/2}(\mathcal{D})$ shows that $x \mapsto \sum_{n=0}^{+\infty} |\mu_n \psi_n(x) \phi_n(x)|$ is finite a.e. and in fact that $v \in L^{p/2}(\mathcal{D})$:

$$\begin{aligned} \|v\|_{p/2} = \left|\left| \sum_{n=0}^{+\infty} \mu_n \psi_n \phi_n \right|\right|_{p/2} &\leq \sum_{n=0}^{+\infty} |\mu_n| \times \left|\left| \psi_n \phi_n \right|\right|_{p/2} \\ &\leq \sum_{n=0}^{+\infty} |\mu_n| \times \|\psi_n\|_p \|\phi_n\|_p = S. \end{aligned} \tag{3.3.58}$$

In equation (3.3.58) above, we used used the Cauchy-Schwarz inequality on $\|\phi_n \psi_n\|_{p/2}$. From the nuclear decomposition of k, it is very tempting to write $\|\sigma\|_p^2 = \|v\|_{p/2}$, but unfortunately the diagonal of $\mathcal{D} \times \mathcal{D}$ has a null Lebesgue measure. This equality turns out to be true but this fact is non trivial and deferred to Lemma 3.3.7 below. From this lemma and equation (3.3.58) which holds whatever the nuclear decomposition of $\mathcal{E}_k$, taking the infimum over all nuclear representations of $\mathcal{E}_k$ in equation (3.3.58) yields $\|\sigma\|_p^2 \leq \nu(\mathcal{E}_k)$. This finishes the proof. □

The next lemma, which was key in the proof of equation (3.3.39), states that evaluating the $L^{p/2}$-norm of the diagonal of a nuclear representation of a Gaussian covariance operator K in $L^p(\mathcal{D}), p \geq 2$, yields the same result as evaluating $L^{p/2}$-norm of the diagonal of the covariance function k of any measurable Gaussian process $(U(x))_{x \in \mathcal{D}}$ such that $\mathcal{E}_k = K$. This fact is not obvious at all, as the diagonal of $\mathcal{D} \times \mathcal{D}$ has null Lebesgue measure and different representatives of k in $L^p(\mathcal{D} \times \mathcal{D})$ have no reason a priori to agree on sets of null measure. However, the assumptions that the representation is nuclear and that U is measurable turn out to be strong enough to yield the desired conclusion. The proof ideas for this result should largely be credited to [34]; we generalized them in a straightforward fashion from $L^2(\mathcal{D})$ to $L^p(\mathcal{D})$ and applied them to the Gaussian process $(U(x))_{x \in \mathcal{D}}$ of Proposition 3.3.5. They are based on the Hardy-Littlewood maximal inequality.

Lemma 3.3.7. *Let $2 \leq p < +\infty$, $\mathcal{D} \subset \mathbb{R}^d$ be an open set and $(U(x))_{x \in \mathcal{D}} \sim GP(0,k)$ be a measurable Gaussian process whose sample paths lie in $L^p(\mathcal{D})$ a.s.. Then $\mathcal{E}_k : L^q(\mathcal{D}) \to L^p(\mathcal{D})$ is nuclear and there exists sequences $(\mu_n) \subset$*

$\mathbb{R}, (\psi_n), (\phi_n) \subset L^p(\mathcal{D})$ *such that* $k = \sum_n \mu_n \psi_n \otimes \phi_n$ *in* $L^p(\mathcal{D} \times \mathcal{D})$, *with* $\|\psi_n\|_p = \|\phi_n\|_p = 1$ *and* $\sum_n |\mu_n| < +\infty$ *(Propositions 3.2.9 and 3.2.7). Then* $x \mapsto \sum_{n=0}^{\infty} |\mu_n \psi_n(x) \phi_n(x)|$ *is finite a.e. and* $v : x \mapsto \sum_{n=0}^{\infty} \mu_n \psi_n(x) \phi_n(x)$ *is nonnegative a.e.. Moreover,*

$$\|\sigma\|_p^p = \int_{\mathcal{D}} k(x,x)^{p/2} dx = \int_{\mathcal{D}} \left(\sum_{n=0}^{+\infty} \mu_n \psi_n(x) \phi_n(x) \right)^{p/2} dx = \|v\|_{p/2}^{p/2} \quad (3.3.59)$$

A remarkable consequence of this result is that the $L^{p/2}$-norm of the diagonal of a nuclear representation of $\mathcal{E}_k = \sum_n \mu_n \psi_n \otimes \phi_n$ is *invariant* w.r.t. said nuclear decomposition (much like the trace if $p = 2$), while its finiteness fully characterizes the nuclearity of $\mathcal{E}_k$ (Proposition 3.3.5(ii)); the same invariance property does not hold for $\sum_n |\mu_n|$, hence the need to define the nuclear norm of $\mathcal{E}_k$ as the infimum over such quantities.

Proof of Lemma 3.3.7. We first prove the statement when $\mathcal{D} = \mathbb{R}^d$. We begin with some definitions and observations. For $r > 0$, denote $C_r \coloneqq [-r, r]^d$ and $C_r(x) \coloneqq x + C_r$. For $f \in L^p(\mathbb{R}^d)$ (resp. $g \in L^p(\mathbb{R}^d \times \mathbb{R}^d)$), denote its average over $C_r(x)$ (resp. $C_r(x) \times C_r(x)$) as

$$A_r^{(d)} f(x) \coloneqq \frac{1}{|C_r|} \int_{C_r(x)} f(t) dt, \quad A_r^{(2d)} g(x) \coloneqq \frac{1}{|C_r|^2} \int_{C_r(x)} \int_{C_r(x)} g(s,t) ds dt$$

The functions $A_r^{(d)} f$ and $A_r^{(2d)} g$ are defined pointwise and continuous. The point of averaging over cubes rather than balls is that we have $A_r^{(2d)} = A_r^{(d)} \otimes A_r^{(d)}$. One then introduces the Hardy-Littlewood maximal functions of f and g, as

$$M^{(d)} f(x) \coloneqq \sup_{r>0} \frac{1}{|C_r|} \int_{C_r(x)} |f(t)| dt,$$
$$M^{(2d)} g(x,y) \coloneqq \sup_{r>0} \frac{1}{|C_r|^2} \int_{C_r(x)} \int_{C_r(x)} |g(s,t)| ds dt.$$

$M^{(d)} f$ (resp. $M^{(2d)} g$) is measurable, nonnegative and defined pointwise over $\mathbb{R}^d$ (resp. $\mathbb{R}^d \times \mathbb{R}^d$). For all $x \in \mathbb{R}^d$, we obviously have the pointwise majoration

$$|A_r^{(d)} f(x)| \leq M^{(d)} f(x), \quad (3.3.60)$$

and likewise for $M^{(2d)} g$. A key point for us will be the Hardy-Littlewood maximal theorem ([192], Theorem 1 p. 5), which states that there exists a constant $S_p > 0$ such that for all $f \in L^p(\mathbb{R}^d)$,

$$\|M^{(d)} f\|_p \leq S_p \|f\|_p. \quad (3.3.61)$$

This theorem allows a first general observation, given $f \in L^p(\mathbb{R}^d)$. Indeed, the Lebesgue differentiation theorem ([192], Corollary 1 p. 5) states that $A_r^{(d)} f(x) \to f(x)$ a.e.; but we also have the pointwise domination

$$|A_r^{(d)} f(x) - f(x)| \leq |A_r^{(d)} f(x)| + |f(x)| \leq M^{(d)} f(x) + |f(x)| \quad \text{a.e..} \tag{3.3.62}$$

From equation (3.3.61), the function on the right-hand side of equation (3.3.62) lies in $L^p(\mathbb{R}^d)$ and Lebesgue's dominated convergence theorem in $L^p(\mathcal{D})$ yields that we also have convergence:

$$\|A_r^{(d)} f - f\|_{L^p(\mathbb{R}^d)} \xrightarrow[r \to 0]{} 0. \tag{3.3.63}$$

We will also use that the nonlinear operator M is submutliplicative and sub-additive:

$$M^{(2d)}(\psi \otimes \varphi)(x, y) \leq M^{(d)}\psi(x) M^{(d)}\varphi(y), \tag{3.3.64}$$

$$M^{(d)}(\psi + \varphi)(x) \leq M^{(d)}\psi(x) + M^{(d)}\varphi(x). \tag{3.3.65}$$

With equations (3.3.63), (3.3.64) and (3.3.65), we now prove the desired result. We first focus on the decomposition $k = \sum_n \mu_n \psi_n \otimes \phi_n$, for which the following pointwise equality holds ([34], Corollary 2.2 and Lemma 2.3, or equation 3.6 from [34])

$$A_r^{(2d)} k(x, y) = \sum_{n=0}^{+\infty} \mu_n A_r^{(d)} \psi_n(x) A_r^{(d)} \phi_n(y) \quad \forall (x, y) \in \mathbb{R}^d \times \mathbb{R}^d. \tag{3.3.66}$$

We now prove that from this decomposition, we can deduce a first important fact, which is

$$\lim_{r \to 0} A_r^{(2d)} k(x, x) = \sum_{n=0}^{+\infty} \mu_n \psi_n(x) \phi_n(x) \quad \text{a.e..} \tag{3.3.67}$$

For this, first observe that for all $x \in \mathbb{R}^d$ and $n \in \mathbb{N}$, the following domination holds:

$$|\mu_n| \times |A_r^{(d)} \psi_n(x) A_r^{(d)} \phi_n(x)| \leq |\mu_n| \times M^{(d)} \psi_n(x) M^{(d)} \phi_n(x). \tag{3.3.68}$$

But the series obtained by summing the right-hand side term of equation (3.3.68) is an a.e. finite function of x, as Minkowski's inequality in $L^{p/2}(\mathbb{R}^d)$ and equation (3.3.61) yield:

$$\left|\left| \sum_{n=0}^{+\infty} |\mu_n| M^{(d)} \psi_n M^{(d)} \phi_n \right|\right|_{p/2} \leq \sum_{n=0}^{+\infty} |\mu_n| \times \left|\left| M^{(d)} \psi_n M^{(d)} \phi_n \right|\right|_{p/2}$$

$$\leq \sum_{n=0}^{+\infty} |\mu_n| \times \left|\left|M^{(d)}\psi_n\right|\right|_p \left|\left|M^{(d)}\phi_n\right|\right|_p \tag{3.3.69}$$

$$\leq \sum_{n=0}^{+\infty} |\mu_n| \times S_p^2 \|\psi_n\|_p \|\phi_n\|_p \tag{3.3.70}$$

$$= S_p^2 \sum_{n=0}^{+\infty} |\mu_n| < +\infty. \tag{3.3.71}$$

We used the Cauchy-Schwarz inequality in equation (3.3.69). Choose now a conull set $T \subset \mathbb{R}^d$, on which the Lebesgue differentiation theorem applies for all ψ_n and ϕ_n, and on which $x \mapsto \sum_n |\mu_n| M^{(d)}\psi_n(x) M^{(d)}\phi_n(x)$ is finite (such a set exists from the finiteness of its $L^{p/2}$-norm). For all $x \in T$, the Lebesgue dominated convergence theorem for the discrete measure $\sum_{n\in\mathbb{N}} \delta_n$ (using the domination (3.3.68)) yields the equality (3.3.67).

We now focus on the Gaussian process $(U(x))_{x\in\mathbb{R}^d}$. Since its sample paths U_ω lie in $L^p(\mathbb{R}^d)$ almost surely, equation (3.3.63) yields that for almost every $\omega \in \Omega$,

$$\|A_r^{(d)} U_\omega - U_\omega\|_p^p \xrightarrow[r\to 0]{} 0. \tag{3.3.72}$$

We also have that for every such $\omega \in \Omega$ and $r > 0$,

$$\|A_r^{(d)} U_\omega - U_\omega\|_p \leq \|A_r^{(d)} U_\omega\|_p + \|U_\omega\|_p \tag{3.3.73}$$

$$\leq \|M^{(d)} U_\omega\|_p + \|U_\omega\|_p \leq (S_p + 1)\|U_\omega\|_p, \tag{3.3.74}$$

and from Fubini's theorem, the right-hand side of equation (3.3.74) lies in $L^p(\mathbb{P})$:

$$\mathbb{E}[\omega \mapsto \|U_\omega\|_p^p] = \mathbb{E}[\|U\|_p^p] = \int_{\mathbb{R}^d} \mathbb{E}[|U(x)|^p] dx = C_p \|\sigma\|_p^p < +\infty \tag{3.3.75}$$

Thus, from equations (3.3.72), (3.3.74), (3.3.75) and Lebesgue's dominated convergence in $L^p(\mathbb{P})$,

$$\mathbb{E}[\|A_r^{(d)} U - U\|_p^p] \xrightarrow[r\to 0]{} 0. \tag{3.3.76}$$

In particular, using the reverse triangle inequality on the norm $V \mapsto \mathbb{E}[\|V\|_p^p]^{1/p}$, we have

$$\mathbb{E}\big[\|A_r^{(d)} U\|_p^p\big] \xrightarrow[r\to 0]{} \mathbb{E}\big[\|U\|_p^p\big] = C_p \|\sigma\|_p^p. \tag{3.3.77}$$

We then wish to use equations (3.3.77) and (3.3.67) to prove the desired result. For this, observe that from the linearity of the operator $A_r^{(d)}$, $(A_r^{(d)} U(x))_{x\in\mathcal{D}}$

is a centered measurable Gaussian process whose covariance function is given by the following formula, given any $(x, y) \in \mathbb{R}^d \times \mathbb{R}^d$,

$$\mathrm{Cov}(A_r^{(d)}U(x), A_r^{(d)}U(y)) = \big(A_r^{(d)} \otimes A_r^{(d)}\big)k(x, y) = A_r^{(2d)}k(x, y).$$

(Note then that $A_r^{(2d)}k(x, x) = \mathrm{Var}(A_r^{(d)}U(x)) \geq 0$, which also shows that the limit in equation (3.3.67) is nonnegative a.e.) The proof of the Gaussianity of $(A_r^{(d)}U(x))_{x\in\mathcal{D}}$ is carried out similarly as for Lemma 3.2.5, and the expression of its covariance function follows from the measurability of U and Fubini's theorem. Fubini's theorem and the fact that $\mathbb{E}[|X|^p] = C_p s^p$ if $X \sim \mathcal{N}(0, s^2)$ then lead to

$$\mathbb{E}[\|A_r^{(d)}U\|_p^p] = \int_{\mathbb{R}^d} \mathbb{E}[|A_r^{(d)}U(x)|^p]dx = C_p \int_{\mathbb{R}^d} \Big(A_r^{(2d)}k(x, x)\Big)^{p/2} dx \quad (3.3.78)$$

We will finally apply Lebesgue's dominated convergence theorem on equation (3.3.78) when r goes to zero, using the limit given in equation (3.3.67). For this, observe that equation (3.3.60) together with the sublinear properties of $M^{(d)}$ (equations (3.3.64) and (3.3.65)) lead to the domination

$$|A_r^{(2d)}k(x, x)| \leq M^{(2d)}k(x, x) \leq \sum_{n=0}^{+\infty} |\mu_n| M^{(d)}\psi_n(x)M^{(d)}\phi_n(x) \quad \forall x \in \mathbb{R}^d, \quad (3.3.79)$$

and the right-hand side of equation (3.3.79) indeed lies in $L^{p/2}(\mathcal{D})$, from equation (3.3.71). We finally conclude from Lebesgue's dominated convergence theorem that

$$\begin{aligned}\lim_{r\to 0} \mathbb{E}[\|A_r^{(d)}U\|_p^p] &= C_p \int_{\mathbb{R}^d} \lim_{r\to 0} \Big(A_r^{(2d)}k(x, x)\Big)^{p/2} dx \\ &= C_p \int_{\mathbb{R}^d} \Big(\sum_{n=0}^{+\infty} \mu_n\psi_n(x)\phi_n(x)\Big)^{p/2} dx,\end{aligned}$$

which, together with equation (3.3.77), finishes the proof.

To deal with the general case where $\mathcal{D}$ is only an open subset of $\mathbb{R}^d$, extend any function $f \in L^p(\mathcal{D})$ to a function $\tilde{f} \in L^p(\mathbb{R}^d)$ by setting $\tilde{f}(x) = f(x)$ if $x \in \mathcal{D}$, $\tilde{f}(x) = 0$ elsewhere. $\tilde{f}$ remains measurable, and all the arguments and results stated above are preserved. □

3.4 Sobolev regularity of Gaussian processes : the Hilbert space case, $p = 2$

In the case $p = 2$, we provide an alternative proof of the integral and spectral criteria of Proposition 3.3.1, based on the study of the "ellipsoids"

of Hilbert spaces (see Section 3.4.2). These geometrical objects are well understood in relation with Gaussian processes (see [67] or [199], Section 2.5). Compared with the general case $p \in (1, +\infty)$, we draw additional links between the different Mercer decompositions of the kernels $\partial^{\alpha,\alpha}k$, the trace of $\mathcal{E}_k^\alpha$ and the Hilbert-Schmidt nature of the imbedding of the reproducing kernel Hilbert space (see Section 3.4.1 below) associated to k in $H^m(\mathcal{D})$.

3.4.1 Reproducing Kernel Hilbert Spaces (RKHS, [24])

Consider a general set $\mathcal{D}$ and a positive definite function $k : \mathcal{D}\times\mathcal{D} \to \mathbb{R}$, i.e. such that given any $n \in \mathbb{N}^*$ and $(x_1, ..., x_n) \in \mathcal{D}^n$, the matrix $(k(x_i, x_j))_{1\leq i,j\leq n}$ is nonnegative definite. One can then build a Hilbert space H_k of functions defined over $\mathcal{D}$ which contains the functions $k(x, \cdot), x \in \mathcal{D}$ and verifies the *reproducing* identities

$$\langle k(x,\cdot), k(x',\cdot)\rangle_{H_k} = k(x,x') \qquad \forall x, x' \in \mathcal{D}, \tag{3.4.1}$$

$$\langle k(x,\cdot), f\rangle_{H_k} = f(x) \qquad \forall x \in \mathcal{D},\ \forall f \in H_k. \tag{3.4.2}$$

H_k is the RKHS of k. This space is exactly the set of functions of the form $f(x) = \sum_{i=1}^{+\infty} a_i k(x_i, x)$ such that $\|f\|^2_{H_k} = \sum_{i,j=1}^{+\infty} a_i a_j k(x_i, x_j) < +\infty$. If for all $x \in \mathcal{D}$, $k(x, \cdot)$ is measurable, then H_k only contains measurable functions. One may then consider imbedding H_k in some Sobolev space $H^m(\mathcal{D})$. Recall that in $H^m(\mathcal{D})$, functions are equal up to a set of Lebesgue measure zero. If such an imbedding $i : H_k \to H^m(\mathcal{D})$ is well-defined (i.e. if $f \in H_k$ then its weak derivatives $\partial^\alpha f$ exist and lie in $L^2(\mathcal{D})$ for all $|\alpha| \leq m$), we will sometimes use the same notation for $f \in H_k$ and its equivalence class $f \in H^m(\mathcal{D})$; strictly speaking, the latter should be denoted $i(f)$. It may then happen that i is not injective, as with the RKHS associated to the Kronecker delta $k(x, x') = \delta_{x,x'}$ (in this case, we even have $i(H_k) = \{0\}$).

Remark 3.4.1. In Proposition 3.4.4, we will be interested in the Hilbert-Schmidt nature of the imbedding i. However, it may happen that H_k is not separable, such as with the RKHS associated to the Kronecker delta $\delta_{x,x'}$. This results in additional care required for defining the notion of Hilbert Schmidt operators, as the definition from Section 3.2.4(ii) cannot hold. Still, this case is dealt with in Proposition 3.4.4(iv). See [154] and [29], Remark 3.2.9 p. 103 for discussions on non separable RKHS.

3.4.2 Ellipsoids of Hilbert spaces and canonical Gaussian processes

Let $(H; \langle, \rangle_H)$ be a separable Hilbert space. We introduce $(V_x)_{x\in H}$ the canonical Gaussian process of H ([67]), defined as the centered Gaussian

process whose covariance function is the inner product of H:

$$\mathbb{E}[V_x V_y] = \langle x, y \rangle_H. \tag{3.4.3}$$

A subset K of H is said to be Gaussian bounded (GB) if

$$\mathbb{P}(\sup_{x \in K} |V_x| < +\infty) = 1. \tag{3.4.4}$$

The GB property was first introduced for studying the compact sets of Hilbert spaces, see [67] on that topic. In equation (3.4.4), the random variable is defined as $\sup_{x \in K} |V_x| := \sup_{x \in A} |V_x|$ where A is any countable subset of K, dense in K. Different choices of A only modify $\sup_{x \in K} |V_x|$ on a set of probability 0 ([67], p. 291), which leaves equation (3.4.3) unchanged. We will use the two following results below, taken from [67].

Proposition 3.4.2 ([67], p. 293 and [67], Proposition 3.4)**.** *We have the two following facts.*

(i) If K is a GB-set, then its closed, convex, symmetric hull is a GB-set.

(ii) The closure of a GB-set is compact.

Given a self-adjoint compact operator $T : H \to H$, introduce a basis of eigenvectors x_n and its real eigenvalues λ_n, $\lambda_n \to 0$. The image of the closed unit ball of H, $B = B_H(0, 1)$ is the following "ellipsoid" ([67], p. 312)

$$T(B) = \left\{ \sum_{\lambda_n > 0} a_n x_n \ s.t. \ \sum_{\lambda_n > 0} a_n^2 / \lambda_n^2 \leq 1 \right\}. \tag{3.4.5}$$

The main result we will use is the following.

Proposition 3.4.3 ([67], Proposition 6.3)**.** *Suppose that T is compact and self-adjoint. Then $T(B)$ is a GB-set if and only if $\sum_{n \in \mathbb{N}} \lambda_n^2 < \infty$, i.e. $T(B)$ is a "Schmidt ellipsoid".*

We can now state our result pertaining to the $H^m(\mathcal{D})$-regularity of Gaussian processes, given an arbitrary open set $\mathcal{D} \subset \mathbb{R}^d$.

Proposition 3.4.4 (Sample path Hilbert-Sobolev regularity for Gaussian processes)**.** *Let $\mathcal{D} \subset \mathbb{R}^d$ be an open set. Let $(U(x))_{x \in \mathcal{D}} \sim GP(0, k)$ be a measurable centered Gaussian process, defined on a probability set $(\Omega, \mathcal{F}, \mathbb{P})$, such that its standard deviation function σ lies in $L^1_{loc}(\mathcal{D})$. The following statements are equivalent:*

(i) (Sample path regularity) The sample paths of U lie in $H^m(\mathcal{D})$ almost surely.

(ii) (Spectral structure) For all $|\alpha| \leq m$, the distributional derivative $\partial^{\alpha,\alpha}k$ lies in $L^2(\mathcal{D}\times\mathcal{D})$ and the associated integral operator

$$\mathcal{E}_k^\alpha f(x) = \int_{\mathcal{D}} \partial^{\alpha,\alpha}k(x,y)f(y)dy \tag{3.4.6}$$

is trace class. Equivalently, there exists a representative k_α of $\partial^{\alpha,\alpha}k$ in $L^2(\mathcal{D}\times\mathcal{D})$ which is the covariance function of a measurable Gaussian process. Note $\sigma_\alpha(x) \coloneqq k_\alpha(x,x)^{1/2}$, then additionally

$$Tr(\mathcal{E}_k^\alpha) = \int_{\mathcal{D}} k_\alpha(x,x)dx < +\infty. \tag{3.4.7}$$

(iii) (Mercer decomposition) The kernel k has the following Mercer decomposition

$$k(x,y) = \sum_{n=0}^{+\infty} \lambda_n \phi_n(x)\phi_n(y) \qquad \text{in } L^2(\mathcal{D}\times\mathcal{D}), \tag{3.4.8}$$

where (λ_n) is a nonnegative sequence and (ϕ_n) is an orthonormal basis of $L^2(\mathcal{D})$. Moreover, for all $n \in \mathbb{N}$ such that $\lambda_n \neq 0$, $\partial^\alpha\phi_n \in L^2(\mathcal{D})$, $\partial^{\alpha,\alpha}k \in L^2(\mathcal{D}\times\mathcal{D})$, the following equalities hold

$$\begin{cases} Tr(\mathcal{E}_k^\alpha) = \displaystyle\sum_{n=0}^{+\infty} \lambda_n \|\partial^\alpha\phi_n\|_2^2 < +\infty, & (3.4.9) \\ \partial^{\alpha,\alpha}k(x,y) = \displaystyle\sum_{n=0}^{+\infty} \lambda_n \partial^\alpha\phi_n(x)\partial^\alpha\phi_n(y) \qquad \text{in } L^2(\mathcal{D}\times\mathcal{D}). & (3.4.10) \end{cases}$$

(iv) (imbedding of the RKHS) $H_k \subset H^m(\mathcal{D})$, the corresponding natural imbedding $i : H_k \to H^m(\mathcal{D})$ is continuous and $ii^* : H^m(\mathcal{D}) \to H^m(\mathcal{D})$ is trace class. Equivalently, $\ker(i)^\perp$ endowed with the topology of H_k is a separable Hilbert space and $j \coloneqq i_{|\ker(i)^\perp} : \ker(i)^\perp \to H^m(\mathcal{D})$ is Hilbert-Schmidt. Moreover, the Hilbert-Schmidt norm of j (see Section 3.2.4(ii) and (iii)) is given by

$$\|j\|_{HS}^2 = Tr(ii^*) = \sum_{|\alpha|\leq m} Tr(\mathcal{E}_k^\alpha). \tag{3.4.11}$$

Before proving this result, we discuss Proposition 3.4.4 in relation with previous results from the literature. First, point *(iv)* is not without reminding Driscoll's theorem ([111], Theorem 4.9) which is well-known in the machine learning/RKHS community; this theorem states the following. Let k and r be two positive definite functions defined over $\mathcal{D}$, and let $U \sim GP(0,k)$. Suppose

that $H_k \subset H_r$ with a Hilbert-Schmidt imbedding, then the sample paths of U lie in H_r almost surely.

Second, Proposition 3.4.4 and equation (3.4.7) in particular, is a generalization of Theorem 1 from [181] in the case of Gaussian processes. By removing the assumption in [181] that the covariance function be continuous on its diagonal as well as its symmetric cross derivatives, the sufficient condition derived in [181] becomes also necessary. Finally, Proposition 3.4.4 shows that if $p = 2$, then in the nuclear decomposition of $\mathcal{E}_k^\alpha$ (see Proposition 3.3.1(iii)) one can choose $\lambda_n^\alpha = \lambda_n$ and $\psi_n^\alpha = \partial^\alpha \psi_n$. It is not obvious that this should hold when $p \neq 2$ (see Remark 3.3.4).

Example 3.4.5 (Hilbert-Schmidt imbeddings of Sobolev spaces). Proposition 3.4.4 can be compared with the results found in [193] and its Corollary 4.5 in particular. This corollary states that if $\mathcal{D} \subset \mathbb{R}^d$ is sufficiently smooth, if $H_k \subset H^t(\mathcal{D})$ with a continuous imbedding and if $t > d/2$, then the sample paths of the centered Gaussian process with covariance function k lie in $H^m(\mathcal{D})$ for all real number $m \in [0, t-d/2)$. For example, this holds when k is a Matérn covariance function of order $t - d/2$; its RKHs is then exactly $H^t(\mathcal{D})$ ([193], Example 4.8).

In the particular case where in addition m is an integer, we recover this result from Proposition 3.4.4. Indeed, it is known that when $m \in (0, t - d/2)$, the imbedding of $H^t(\mathcal{D})$ in $H^m(\mathcal{D})$ is Hilbert-Schmidt. When the involved indexes are nonnegative integers, this is known as Maurin's theorem ([169], Theorem 6.61, p. 202). Maurin's theorem is generalized to fractional exponents in [203], Folgerung 1 p. 310 (in German) or [121], Proposition 7.1 (in French). if $H_k \subset H^t(\mathcal{D})$ with a continuous imbedding, then the inclusion map of H_k in $H^m(\mathcal{D})$ is Hilbert-Schmidt for all $m \in [0, t - d/2) \cap \mathbb{N}$. From Proposition 3.4.4, we obtain that the sample paths of the corresponding Gaussian process indeed lie in $H^m(\mathcal{D})$.

However, not all RKHS that are subspaces of $H^m(\mathcal{D})$ with a Hilbert-Schmidt imbedding are contained in some $H^t(\mathcal{D})$ with $t > m + d/2$, as the following trivial example shows. Fix any $\varepsilon > 0$ and consider the rank one kernel $k(x, x') = f(x)f(x')$ where f is chosen such that $f \in H^m(\mathcal{D})$ and $f \notin H^{m+\varepsilon}(\mathcal{D})$ (choose a representative of f in $L^2(\mathcal{D})$ so that f is a function in the classical sense). Then $H_k = \mathrm{Span}(f)$ and the imbedding of H_k in $H^m(\mathcal{D})$ is Hilbert-Schmidt since it is rank one; but $H_k \not\subset H^{m+\varepsilon}(\mathcal{D})$. Proposition 3.4.4 yields that the associated trivial Gaussian process $U(x)(\omega) = \xi(\omega)f(x)$ where $\xi \sim \mathcal{N}(0, 1)$ has its sample paths in $H^m(\mathcal{D})$ (it was obvious in the first place).

Example 3.4.6 (One dimensional case). We build a covariance function which is not pointwise differentiable at any $(q, q') \in \mathbb{Q} \times \mathbb{Q}$, and such that the corresponding Gaussian process has its sample paths in $H^1(\mathbb{R})$. Let $h_a(x) :=$

$\max(0, 1 - |x - a|)$ be the hat function centered around $a \in \mathbb{R}$. It lies in $H^1(\mathbb{R})$ but it is not differentiable at $x = a, a - 1$ and $a + 1$. Let (q_n) be an enumeration of $\mathbb{Q}$. Then the following positive definite function over $\mathbb{R}$

$$k(x, x') \coloneqq \sum_{n=0}^{+\infty} \frac{1}{2^n} h_{q_n}(x) h_{q_n}(x') \tag{3.4.12}$$

is not differentiable in the classical sense at each point (x, x') of the form (q_n, q_m), but the map ii^*, with $i : H_k \to H^1(\mathbb{R})$ the canonical imbedding, is trace-class (use equations (3.4.9) and (3.4.11)):

$$\begin{aligned} \mathrm{Tr}(ii^*) &= \mathrm{Tr}(\mathcal{E}_k) + \mathrm{Tr}(\mathcal{E}_k^1) && (3.4.13)\\ &\leq \sum_{n=0}^{+\infty} \frac{1}{2^n} \|h_{q_n}\|_2^2 + \sum_{n=0}^{+\infty} \frac{1}{2^n} \|h'_{q_n}\|_2^2 && (3.4.14)\\ &\leq \sum_{n=0}^{+\infty} \frac{1}{2^n} + \sum_{n=0}^{+\infty} \frac{1}{2^n} \times 2^2 = 10. && (3.4.15) \end{aligned}$$

Before proving Proposition 3.4.4, we will require a number of lemmas concerning the Mercer decomposition of Hilbert-Schmidt operators over $L^2(\mathcal{D})$. They are proved in Section 3.7.

Lemma 3.4.7. *Let k be a measurable positive definite function defined on an open set $\mathcal{D}$. Suppose that $\sigma \in L^1_{loc}(\mathcal{D})$. Then $k \in L^1_{loc}(\mathcal{D} \times \mathcal{D})$. Given a multi-index α, its distributional derivative $D^{\alpha,\alpha}k$ exists and we can introduce the associated continuous bilinear form over $C_c^\infty(\mathcal{D})$*

$$b_\alpha(\varphi, \psi) \coloneqq D^{\alpha,\alpha}k(\varphi \otimes \psi) = \int_{\mathcal{D}\times\mathcal{D}} k(x, y) \partial^\alpha \varphi(x) \partial^\alpha \psi(y) dx dy. \tag{3.4.16}$$

Suppose that it verifies the estimate

$$\forall \varphi, \psi \in E_2, \quad |b_\alpha(\varphi, \psi)| \leq C_\alpha \|\varphi\|_2 \|\psi\|_2, \tag{3.4.17}$$

where E_2 is the set given in Lemma 3.2.2. Then b_α can be extended to a continuous bilinear form over $L^2(\mathcal{D})$ and there exists a unique bounded, self-adjoint and nonnegative operator $\mathcal{E}_k^\alpha : L^2(\mathcal{D}) \longrightarrow L^2(\mathcal{D})$ such that

$$\forall \varphi, \psi \in C_c^\infty(\mathcal{D}), \quad b_\alpha(\varphi, \psi) = \langle \mathcal{E}_k^\alpha \varphi, \psi \rangle_{L^2(\mathcal{D})}. \tag{3.4.18}$$

Lemma 3.4.8. *Let $k \in L^2(\mathcal{D} \times \mathcal{D})$ be a be a positive definite function and α a multi-index. Suppose that the weak derivative $\partial^{\alpha,\alpha}k$ exists and lies in $L^2(\mathcal{D} \times \mathcal{D})$. Then the associated Hilbert-Schmidt integral operator defined on $L^2(\mathcal{D})$*

$$(\mathcal{E}_k^\alpha f)(x) = \int_{\mathcal{D}} \partial^{\alpha,\alpha} k(x, y) f(y) dy \tag{3.4.19}$$

is self-adjoint and nonnegative.

Lemma 3.4.9. *Let $k \in L^2(\mathcal{D} \times \mathcal{D})$ be a positive definite function and $\mathcal{E}_k$ be its associated nonnegative definite Hilbert-Schmidt operator. Let*

$$k(x, y) = \sum_{i=1}^{+\infty} \lambda_i \phi_i(x) \phi_i(y) \tag{3.4.20}$$

be a symmetric, nonnegative expansion of k in $L^2(\mathcal{D} \times \mathcal{D})$ where (λ_i) is a nonnegative sequence decreasing to 0; it may or may not be its Mercer expansion (i.e. (ϕ_i) may or may not be an orthonormal basis of $L^2(\mathcal{D})$; they are still assumed to be elements of $L^2(\mathcal{D})$ though). Then

(i) if the partial mixed weak derivative $\partial^{\alpha,\alpha} k$ exists and lies in $L^2(\mathcal{D} \times \mathcal{D})$, then for all $i \in \mathbb{N}$ such that $\lambda_i \neq 0, \partial^\alpha \phi_i \in L^2(\mathcal{D})$.

(ii) if for all $i \in \mathbb{N}$ such that $\lambda_i \neq 0, \partial^\alpha \phi_i \in L^2(\mathcal{D})$, then we define

$$Tr_0(\mathcal{E}_k^\alpha) \coloneqq \sum_{i=1}^{+\infty} \lambda_i \|\partial^\alpha \phi_i\|^2_{L^2(\mathcal{D})}. \tag{3.4.21}$$

If $\mathcal{E}_k^\alpha$ is bounded, then $Tr_0(\mathcal{E}_k^\alpha) = Tr(\mathcal{E}_k^\alpha)$, whether these quantities are finite or not. If $Tr_0(\mathcal{E}_k^\alpha) < +\infty$, then the series of functions $\sum_{i\in\mathbb{N}} \lambda_i \partial^\alpha \phi_i(x) \partial^\alpha \phi_i(y)$ is norm convergent in $L^2(\mathcal{D} \times \mathcal{D})$ (i.e. $\sum_{i\in\mathbb{N}} \lambda_i \|\partial^\alpha \phi_i \otimes \partial^\alpha \phi_i\|_{L^2} < +\infty$), $\partial^{\alpha,\alpha} k$ lies in $L^2(\mathcal{D} \times \mathcal{D})$, $\mathcal{E}_k^\alpha$ is bounded and we have the following equality:

$$\partial^{\alpha,\alpha} k(x, y) = \sum_{i=1}^{+\infty} \lambda_i \partial^\alpha \phi_i(x) \partial^\alpha \phi_i(y) \quad \text{in} \quad L^2(\mathcal{D} \times \mathcal{D}). \tag{3.4.22}$$

Equation (3.4.22) then holds for asymmetric derivatives, as for all $|\alpha|, |\beta| \leq m$, we also have $\sum_{i\in\mathbb{N}} \lambda_i \|\partial^\beta \phi_i \otimes \partial^\alpha \phi_i\|_{L^2} < +\infty$.

We can now prove Proposition 3.4.4.

Proof. (Proposition 3.4.4) We successively prove $(ii) \implies (i)$, $(i) \implies (ii)$, $(ii) \iff (iii)$, $(iii) \implies (iv)$ and $(iv) \implies (iii)$.
Before all things, the assumptions and Lemma 3.2.5 show that the sample paths of U lie in $L^1_{loc}(\mathcal{D})$, that the random variable given by the formula

$$U_\varphi^\alpha : \Omega \ni \omega \longmapsto (-1)^{|\alpha|} \int_{\mathcal{D}} U(x)(\omega) \partial^\alpha \varphi(x) dx \tag{3.4.23}$$

is well defined and that $(U_\varphi^\alpha)_{\varphi \in F_2}$ is a Gaussian sequence (see equation (3.2.17) for the definition of F_2).
$(ii) \implies (i)$: From Lemma 3.4.8, $\mathcal{E}_k^\alpha$ is a self-adjoint, nonnegative Hilbert-Schmidt operator; it is actually trace-class by assumption. We can thus define $A_\alpha \coloneqq \sqrt{\mathcal{E}_k^\alpha}$, which is a Hilbert-Schmidt, self-adjoint, nonnegative operator.

From Proposition 3.4.3, $A_\alpha(B)$ is a GB-set (B is the closed unit ball of $L^2(\mathcal{D})$). Therefore, using the canonical Gaussian process of $L^2(\mathcal{D})$,

$$\mathbb{P}(\sup_{\psi\in A_\alpha(B)} |V_\psi| < +\infty) = 1, \tag{3.4.24}$$

which, since $F_2 \subset B$, yields in particular that

$$\mathbb{P}(\sup_{\varphi\in F_2} |V_{A_\alpha(\varphi)}| < +\infty) = 1. \tag{3.4.25}$$

We now observe that the two Gaussian sequences $(V_{A_\alpha(\varphi)})_{\varphi\in F_2}$ and $(U^\alpha_\varphi)_{\varphi\in F_2}$ have the same finite dimensional marginals. Indeed, they are both centered Gaussian sequences with the same covariance:

$$\mathbb{E}[V_{A_\alpha(\varphi)}V_{A_\alpha(\psi)}] = \langle A_\alpha(\varphi), A_\alpha(\psi)\rangle_{L^2} = \langle A^2_\alpha(\varphi), \psi\rangle_{L^2} = \langle \mathcal{E}^\alpha_k\varphi, \psi\rangle_{L^2}. \tag{3.4.26}$$

$$\begin{aligned}\mathbb{E}[U^\alpha_\varphi U^\alpha_\psi] &= \mathbb{E}\left[\int_{\mathcal{D}} U(x)\partial^\alpha\varphi(x)dx \int_{\mathcal{D}} U(y)\partial^\alpha\psi(y)dy\right] \\ &= \int_{\mathcal{D}\times\mathcal{D}} k(x,y)\partial^\alpha\varphi(x)\partial^\alpha\psi(y)dxdy \\ &= \int_{\mathcal{D}\times\mathcal{D}} \partial^{\alpha,\alpha}k(x,y)\varphi(x)\psi(y)dxdy = \langle \mathcal{E}^\alpha_k\varphi, \psi\rangle_{L^2}. \end{aligned} \tag{3.4.27}$$

As in the proof of Proposition 3.3.1 (e.g. equation (3.3.26)), we deduce that the two random variables $\sup_{\varphi\in F_2} |U^\alpha_\varphi|$ and $\sup_{\varphi\in F_2} |V_{A_\alpha(\varphi)}|$ have the same law, and from equation (3.4.25), we obtain that

$$\mathbb{P}(\sup_{\varphi\in F_2} |U^\alpha_\varphi| < +\infty) = \mathbb{P}(\sup_{\varphi\in F_2} |V_{A_\alpha(\varphi)}| < +\infty) = 1. \tag{3.4.28}$$

Since equation (3.4.28) holds for all $|\alpha| \le m$, this provides a set of probability 1 on which all the sample paths of U lie in $H^m(\mathcal{D})$, which proves (i).
$\underline{(i) \implies (ii)}$: From Lemma 3.2.4 and the assumption from (i),

$$\mathbb{P}(\sup_{\varphi\in F_2} |U^\alpha_\varphi| < +\infty) = 1. \tag{3.4.29}$$

From Proposition 3.2.6, we have that

$$C_\alpha := \mathbb{E}\big[\sup_{\varphi\in F_2} |U^\alpha_\varphi|^2\big] < +\infty. \tag{3.4.30}$$

Introduce b_α, the continuous bilinear form over $C^\infty_c(\mathcal{D})$ given by

$$b_\alpha(\varphi,\psi) = \int_{\mathcal{D}\times\mathcal{D}} k(x,y)\partial^\alpha\varphi(x)\partial^\alpha\psi(y)dxdy. \tag{3.4.31}$$

Consider now φ and ψ in F_2. Then,

$$|b_\alpha(\varphi,\psi)| = \left|\int_{\mathcal{D}\times\mathcal{D}} k(x,y)\partial^\alpha\varphi(x)\partial^\alpha\psi(y)dxdy\right| = |\mathbb{E}[U_\varphi^\alpha U_\psi^\alpha]|$$
$$\leq \mathbb{E}[|U_\varphi^\alpha U_\psi^\alpha|] \leq \frac{1}{2}\mathbb{E}\big[(U_\varphi^\alpha)^2 + (U_\psi^\alpha)^2\big] \leq \mathbb{E}\big[\sup_{\varphi\in F_2}(U_\varphi^\alpha)^2\big] = C_\alpha. \tag{3.4.32}$$

From Lemma 3.4.7, b_α can be extended to a continuous bilinear form over $L^2(\mathcal{D})$ and there exists a unique bounded, self-adjoint and nonnegative operator $\mathcal{E}_k^\alpha$ which verifies, given any $\varphi,\psi \in C_c^\infty(\mathcal{D})$,

$$\int_{\mathcal{D}\times\mathcal{D}} k(x,y)\partial^\alpha\varphi(x)\partial^\alpha\psi(y)dxdy = b_\alpha(\varphi,\psi) = \langle\mathcal{E}_k^\alpha\varphi,\psi\rangle_{L^2}. \tag{3.4.33}$$

Since $\mathcal{E}_k^\alpha$ is self-adjoint and nonnegative, we can introduce its square root $A_\alpha := \sqrt{\mathcal{E}_k^\alpha}$, which is also a bounded, self-adjoint and nonnegative operator. As in equation (3.4.28), we can introduce $(V_{A_\alpha(\varphi)})_{\varphi\in F_2}$ and observe that $(V_{A_\alpha(\varphi)})_{\varphi\in F_2}$ and $(U_\varphi^\alpha)_{\varphi\in F_2}$ have the same law. Thus,

$$\mathbb{P}(\sup_{\varphi\in F_2}|V_{A_\alpha(\varphi)}| < +\infty) = \mathbb{P}(\sup_{\varphi\in F_2}|U_\varphi^\alpha| < +\infty) = 1. \tag{3.4.34}$$

Therefore, $A_\alpha(F_2)$ is a GB-set. From Proposition 3.4.2(ii), $\overline{\mathrm{Conv}(A_\alpha(F_2))}$ is compact. One then checks by elementary considerations that $\overline{\mathrm{Conv}(A_\alpha(F_2))} = \overline{A_\alpha(B)}$, where B is the unit ball of $L^2(\mathcal{D})$. This shows that A_α is a compact operator. But from Proposition 3.4.2(i), $\overline{A_\alpha(B)} = \overline{\mathrm{Conv}(A_\alpha(F_2))}$ is also a GB-set. From Proposition 3.4.3, A_α is Hilbert-Schmidt and $\mathcal{E}_k^\alpha$ is trace-class. In particular, $\mathcal{E}_k^\alpha$ is a Hilbert-Schmidt operator with a kernel k_α that lies in $L^2(\mathcal{D}\times\mathcal{D})$:

$$\forall\varphi,\psi\in C_c^\infty(\mathcal{D}),\ D^{\alpha,\alpha}k(\varphi\otimes\psi) = \int_{\mathcal{D}\times\mathcal{D}} k(x,y)\partial^\alpha\varphi(x)\partial^\alpha\psi(y)dxdy \tag{3.4.35}$$
$$= \int_{\mathcal{D}\times\mathcal{D}} k_\alpha(x,y)\varphi(x)\psi(y)dxdy$$
$$= T_{k_\alpha}(\varphi\otimes\psi). \tag{3.4.36}$$

Equation (3.4.36) shows that the distributional derivative $D^{\alpha,\alpha}k$ and the regular distribution T_{k_α} coincide on the set $\mathscr{D}(\mathcal{D})\otimes\mathscr{D}(\mathcal{D})$. From the Schwartz kernel theorem ([202], Theorem 51.7), $D^{\alpha,\alpha}k = T_{k_\alpha}$ in $\mathscr{D}'(\mathcal{D}\times\mathcal{D})$, which shows that $\partial^{\alpha,\alpha}k$ exists in $L^2(\mathcal{D}\times\mathcal{D})$ and that $\partial^{\alpha,\alpha}k = k_\alpha$. For the existence of a representative k_α with the desired properties, we refer to the previous Proposition 3.3.1(ii). This finishes to prove (ii).

$(ii) \iff (iii)$: this equivalence is fully given by Lemma 3.4.9.

$(iii) \implies (iv)$: we first study how finite difference operators behave on elements of H_k in order to use Lemma 3.2.1(iii). First, using the reproducing formula (3.4.2), observe that for suitable x and $h \in \mathcal{D}$,

$$\begin{aligned}\Delta_h f(x) &= f(x+h) - f(x) = \langle f, k(x+h,\cdot) - k(x,\cdot)\rangle_{H_k} \\ &= \langle f, \Delta_h k(x,\cdot)\rangle_{H_k}. \end{aligned} \tag{3.4.37}$$

More generally, for any finite difference operator Δ_h of order $l \leq m$, $h = (h_1, ..., h_l)$ and any open set $\mathcal{D}_0 \Subset \mathcal{D}$ such that $\sum_i |h_i| < \mathrm{dist}(\mathcal{D}_0, \partial\mathcal{D})$,

$$\Delta_h f(x) = \langle f, \Delta_h k(x,\cdot)\rangle_{H_k}. \tag{3.4.38}$$

The Cauchy-Schwarz inequality in H_k yields

$$\Delta_h f(x)^2 \leq \|f\|^2_{H_k} \|\Delta_h k(x,\cdot)\|^2_{H_k}. \tag{3.4.39}$$

Furthermore, using the bilinearity of $\langle\cdot,\cdot\rangle_{H_k}$, we have that

$$\|\Delta_h k(x,\cdot)\|^2_{H_k} = [(\Delta_h \otimes \Delta_h)k](x,x). \tag{3.4.40}$$

We then deduce that (explanation below)

$$\forall f \in H_k,\ \|\Delta_h f\|^2_{L^2(\mathcal{D}_0)} = \int_{\mathcal{D}_0} \big(\Delta_h f\big)(x)^2 dx \tag{3.4.41}$$

$$\leq \|f\|^2_{H_k} \int_{\mathcal{D}_0} [(\Delta_h \otimes \Delta_h)k](x,x)dx \tag{3.4.42}$$

$$\leq \|f\|^2_{H_k} \sum_{i=1}^{+\infty} \lambda_i \int_{\mathcal{D}_0} (\Delta_h \phi_i)(x)^2 dx \tag{3.4.43}$$

$$\leq \|f\|^2_{H_k} \sum_{i=1}^{+\infty} \lambda_i \Big(\|\phi_i\|^2_{H^m} |h_1|^2 \cdots |h_l|^2 \Big) \tag{3.4.44}$$

$$\leq \|f\|^2_{H_k} \Big(\sum_{|\alpha|\leq m} \mathrm{Tr}(\mathcal{E}_k^\alpha) \Big) \big(|h_1|^2 \cdots |h_l|^2 \big). \tag{3.4.45}$$

We used equations (3.4.39) and (3.4.40) to obtain equation (3.4.42). In equation (3.4.43), we distributed $\Delta_h \otimes \Delta_h$ on the Mercer decomposition of k (which exists by the assumption (iii)). In equation (3.4.44), we used the fact that $\phi_i \in H^m(\mathcal{D})$ (see Lemma 3.4.9(i)) conjointly with the finite difference control of Lemma 3.2.1(iii). In equation (3.4.45), the we used the trace equality from Lemma 3.4.9(ii). From equation (3.4.45) and Lemma 3.2.1(iii) again, we obtain that f lies in $H^m(\mathcal{D})$. Consider now any open set $\mathcal{D}_0 \Subset \mathcal{D}$. Equation

(3.4.45) applied to δ_h^α, the finite difference approximation of ∂^α from equation (3.2.6) with suitably chosen $h = (h_1, ..., h_l) \in (\mathbb{R}_+^*)^d$, yields that

$$\forall f \in H_k,\ \|\delta_h^\alpha f\|^2_{L^2(\mathcal{D}_0)} \leq \|f\|^2_{H_k} \Big(\sum_{|\alpha| \leq m} \mathrm{Tr}(\mathcal{E}_k^\alpha) \Big). \tag{3.4.46}$$

From Lemma 3.2.1(*iii*), we then obtain that

$$\forall f \in H_k,\ \|\partial^\alpha f\|^2_{L^2(\mathcal{D})} \leq \|f\|^2_{H_k} \Big(\sum_{|\alpha| \leq m} \mathrm{Tr}(\mathcal{E}_k^\alpha) \Big). \tag{3.4.47}$$

Summing the inequality (3.4.47) for all $|\alpha| \leq m$, we obtain that

$$\|f\|_{H^m} \leq C \|f\|_{H_k}, \tag{3.4.48}$$

with $C = \big(N \sum_{|\alpha| \leq m} \mathrm{Tr}(\mathcal{E}_k^\alpha) \big)^{1/2}$ and N is the number of multi-indexes α such that $|\alpha| \leq m$. Therefore $H_k \subset H^m(\mathcal{D})$ and the corresponding imbedding $i : H_k \to H^m(\mathcal{D})$ is continuous. Using the reproducing formula (3.4.2), its transpose $i^* : H^m(\mathcal{D}) \to H_k$ is given by

$$i^*(f)(x) = \langle i^*(f), k_x \rangle_{H_k} = \langle f, i(k_x) \rangle_{H^m} = \sum_{|\alpha| \leq m} \int_{\mathcal{D}} \partial_y^\alpha k(x, y) \partial^\alpha f(y) dy. \tag{3.4.49}$$

Above, ∂_y^α denotes differentation w.r.t. the y coordinate (note that $i^*(f)$ is indeed defined pointwise, since $i^*(f) \in H_k$). Let (ψ_j) be an orthonormal basis of $H^m(\mathcal{D})$ and $k = \sum_i \lambda_i \psi_i \otimes \psi_i$ be the Mercer decomposition of k provided by the assumption (*iii*). The trace of the nonnegative self-adjoint operator ii^* is given by (explanation below)

$$\begin{aligned}
\mathrm{Tr}(ii^*) &= \sum_j \langle \psi_j, ii^*(\psi_j) \rangle_{H^m} = \sum_j \sum_{|\beta| \leq m} \langle \partial^\beta \psi_j, \partial^\beta ii^*(\psi_j) \rangle_{L^2} \\
&= \sum_j \sum_{|\beta| \leq m} \int_{\mathcal{D}} \partial^\beta \psi_j(x) \partial^\beta ii^*(\psi_j)(x) dx \\
&= \sum_j \sum_{|\beta| \leq m} \int_{\mathcal{D}} \partial^\beta \psi_j(x) \partial_x^\beta \sum_{|\alpha| \leq m} \int_{\mathcal{D}} \partial_y^\alpha k(x, y) \partial^\alpha \psi_j(y) dy dx \qquad (3.4.50) \\
&= \sum_j \sum_i \lambda_i \sum_{|\alpha| \leq m} \sum_{|\beta| \leq m} \int_{\mathcal{D} \times \mathcal{D}} \partial^\beta \phi_i(x) \partial^\alpha \phi_i(y) \partial^\beta \psi_j(x) \partial^\alpha \psi_j(y) dy dx \qquad (3.4.51) \\
&= \sum_j \sum_i \lambda_i \Big(\sum_{|\alpha| \leq m} \int_{\mathcal{D}} \partial^\alpha \phi_i(x) \partial^\alpha \psi_j(x) dx \Big)^2
\end{aligned}$$

$$= \sum_j \sum_i \lambda_i \Big(\sum_{|\alpha| \leq m} \langle \partial^\alpha \phi_i, \partial^\alpha \psi_j \rangle_{L^2} \Big)^2 = \sum_i \lambda_i \sum_j \langle \phi_i, \psi_j \rangle_{H^m}^2$$
$$= \sum_i \lambda_i \|\phi_i\|_{H^m}^2 = \sum_{|\alpha| \leq m} \sum_i \lambda_i \|\partial^\alpha \phi_i\|_{L^2}^2 = \sum_{|\alpha| \leq m} \mathrm{Tr}(\mathcal{E}_k^\alpha). \tag{3.4.52}$$

In equation (3.4.50), we used the fact that $i^*(\psi_j)$ given by equation (3.4.49) is a representative of $ii^*(\psi_j)$ in $H^m(\mathcal{D})$. In equation (3.4.51), we used the fact that the series of functions $\sum_i \lambda_i \partial^\beta \phi_i \otimes \partial^\alpha \phi_i$ is norm convergent (Lemma 3.4.9(*ii*)) to distribute the partial derivatives over to the Mercer decomposition of k. We also used Fubini's and Tonelli's theorems ad libitum, as all the series $\sum_i \lambda_i \partial^\beta \phi_i \otimes \partial^\alpha \phi_i$ are norm convergent. Since $\sum_{|\alpha| \leq m} \mathrm{Tr}(\mathcal{E}_k^\alpha)$ is finite by assumption, equation (3.4.52) finishes to prove (*iv*) when H_k is separable.

When H_k is not separable, observe that $\ker(i)$ is closed in H_k since i is continuous. Therefore $H_k = \ker(i) \oplus \ker(i)^\perp$ and $\ker(i)^\perp$ endowed with the topology of H_k is a Hilbert space. Moreover, $i^* : H^m(\mathcal{D}) \to H_k$ is compact since ii^* is trace class. Thus its closed range $\overline{\mathrm{im}(i^*)}$ is separable ([44], Exercise 3 p. 176). Finally, observe that $\overline{\mathrm{im}(i^*)} = \ker(i)^\perp$ ([44], Theorem 4.12) so that $\ker(i)^\perp$ is a separable Hilbert space. Consider now $j \coloneqq i_{|\ker(i)^\perp}$, the restriction of i to $\ker(i)^\perp$. Then $ii^* = jj^*$, so that equation (3.4.52) indeed yields that j is Hilbert-Schmidt.

(*iv*) $\implies$ (*iii*): by assumption, ii^* is a compact self-adjoint nonnegative operator acting on the Hilbert space $H^m(\mathcal{D})$. There exists a decreasing nonnegative sequence $(\mu_j)_{j \in \mathbb{N}}$ and aN orthonormal basis of eigenvectors of ii^*, $(\psi_j)_{j \in \mathbb{N}}$ such that for all $f \in H^m(\mathcal{D})$,

$$ii^*(f) = \sum_{j=1}^{+\infty} \mu_j \langle \psi_j, f \rangle_{H^m} \psi_j \quad \text{in } H^m(\mathcal{D}). \tag{3.4.53}$$

Since ii^* is assumed trace class,

$$\sum_{|\alpha| \leq m} \sum_{j=1}^{+\infty} \mu_j \|\partial^\alpha \psi_j\|_{L^2}^2 = \sum_{j=1}^{+\infty} \mu_j \|\psi_j\|_{H^m}^2 = \sum_{j=1}^{+\infty} \mu_j < +\infty. \tag{3.4.54}$$

We now show that the following equality holds in $L^2(\mathcal{D} \times \mathcal{D})$:

$$k(x, y) = \sum_{j=1}^{+\infty} \mu_j \psi_j(x) \psi_j(y). \tag{3.4.55}$$

In conjunction with equation (3.4.54), this equation will allow us to use Lemma 3.4.9(*ii*), which will imply the point (*iii*). First, one easily shows that $\sum_{j=1}^{+\infty} \mu_j \psi_j \otimes \psi_j$, the right-hand side of equation (3.4.55), is indeed in

$L^2(\mathcal{D}\times\mathcal{D})$ (e.g. use that $\sum_j \mu_j < +\infty$). The upcoming equation (3.4.65) will then show that k is indeed in $L^2(\mathcal{D}\times\mathcal{D})$. Now, decompose $i(k_x) \in H^m(\mathcal{D})$ on the basis $(\psi_j)_{j\in\mathbb{N}}$ given any $x \in \mathcal{D}$:

$$i(k_x) = \sum_{j=1}^{+\infty} \langle \psi_j, i(k_x)\rangle_{H^m} \psi_j \quad \text{in } H^m(\mathcal{D}). \tag{3.4.56}$$

In equation (3.4.56), the scalar $\langle \psi_j, i(k_x)\rangle_{H^m}$ is obtained through the reproducing formula (3.4.2):

$$\langle \psi_j, i(k_x)\rangle_{H^m} = \langle i^*(\psi_j), k_x\rangle_{H_k} = i^*(\psi_j)(x). \tag{3.4.57}$$

Moreover, ψ_j is an eigenvector of ii^*: $\mu_j\psi_j = ii^*(\psi_j)$ in $H^m(\mathcal{D})$. In particular,

$$\|\mu_j\psi_j - ii^*(\psi_j)\|_{L^2(\mathcal{D})} = 0. \tag{3.4.58}$$

But the pointwise defined function $i^*(\psi_j)$ is a representative of $ii^*(\psi_j)$ in $H^m(\mathcal{D})$, since i is the imbedding of H_k in $H^m(\mathcal{D})$. Setting $S = \sum_j \mu_j = \mathrm{Tr}(ii^*)$, one then has (explanation below)

$$\left\| k - \sum_{j=1}^{+\infty} \mu_j \psi_j \otimes \psi_j \right\|^2_{L^2(\mathcal{D}\times\mathcal{D})} = \int_{\mathcal{D}\times\mathcal{D}} \Big(k(x,y) - \sum_{j=1}^{+\infty} \mu_j \psi_j(x)\psi_j(y) \Big)^2 dxdy \tag{3.4.59}$$

$$= \int_{\mathcal{D}}\int_{\mathcal{D}} \Big(k_x(y) - \sum_{j=1}^{+\infty} \mu_j \psi_j(x)\psi_j(y) \Big)^2 dydx \tag{3.4.60}$$

$$= \int_{\mathcal{D}}\int_{\mathcal{D}} \Big(i(k_x)(y) - \sum_{j=1}^{+\infty} \mu_j \psi_j(x)\psi_j(y) \Big)^2 dydx \tag{3.4.61}$$

$$= \int_{\mathcal{D}}\int_{\mathcal{D}} \Big(\sum_{j=1}^{+\infty} \mu_j \psi_j(y) \big({\mu_j}^{-1} i^*(\psi_j) - \psi_j(x) \big) \Big)^2 dydx \tag{3.4.62}$$

$$\leq \int_{\mathcal{D}}\int_{\mathcal{D}} S \sum_{j=1}^{+\infty} \mu_j \psi_j(y)^2 \big({\mu_j}^{-1} i^*(\psi_j) - \psi_j(x) \big)^2 dydx \tag{3.4.63}$$

$$\leq S \sum_{j=1}^{+\infty} \mu_j \int_{\mathcal{D}} \psi_j(y)^2 dy \int_{\mathcal{D}} \big({\mu_j}^{-1} ii^*(\psi_j) - \psi_j(x) \big)^2 dx \tag{3.4.64}$$

$$\leq S \sum_{j=1}^{+\infty} \mu_j \|\psi_j\|^2_{L^2(\mathcal{D})} \|{\mu_j}^{-1} ii^*(\psi_j) - \psi_j\|^2_{L^2(\mathcal{D})} = 0 \tag{3.4.65}$$

Above, we used Tonelli's theorem in equation (3.4.60). We imbedded k_x in $H^m(\mathcal{D})$ in equation (3.4.61). We used equations (3.4.56) and (3.4.57) in equation (3.4.62). We used Jensen's discrete inequality on the squaring function

$(\cdot)^2$ with the weights μ_j/S ($\mu_j/S \geq 0, \sum_j \mu_j/S = 1$) in equation (3.4.63). We imbedded $i^*(\psi_j)$ in $H^m(\mathcal{D})$ and used Tonelli's theorem in equation (3.4.64). We used equation (3.4.58) in equation (3.4.65).

Therefore we have proved that equation (3.4.55) holds. By the assumption that ii^* is trace class and using Lemma 3.4.9(ii),

$$\sum_{|\alpha|\leq m} \mathrm{Tr}(\mathcal{E}_k^\alpha) = \sum_{|\alpha|\leq m} \sum_{j=1}^{+\infty} \mu_j \|\partial^\alpha \psi_j\|_{L^2}^2 = \sum_{j=1}^{+\infty} \mu_j \|\psi_j\|_{H^m}^2 \tag{3.4.66}$$

$$= \sum_j \mu_j = \mathrm{Tr}(ii^*) < +\infty. \tag{3.4.67}$$

Therefore, Lemma 3.4.9(ii) implies that every $\mathcal{E}_k^\alpha$ is indeed trace-class, which shows (iii). □

3.5 Application to the selection of covariance kernels

This short section proposes an application of the quantitative criterion of Proposition 3.4.4, in the selection process of covariance functions. The results we present here constitute a current topic of research.

In equation (1.2.27) of Section 1.2.4, we saw that the Kriging mean, given a set of n observations $\{\ell_i(u) = y_i, 1 \leq i \leq n\}$ of a target function u, where ℓ_i is a continuous linear form over H_k, was obtained as the minimizer of the problem

$$\min_{m \in H_k} \|m\|_{H_k} \quad \text{s.t.} \quad \ell_i(m) = y_i. \tag{3.5.1}$$

The obtained solution (which we denote m_k in this section) is optimal in the RKHS norm but it may behave badly in terms of Sobolev regularity. As argued before, this can be undesireable is certain physical settings. Consider the case of Sobolev regularity of Hilbert type $H^m(\mathcal{D})$. Among all the Kriging means provided by kernels, one may then consider the one that has minimal Sobolev norm:

$$\min_{\text{kernels } k} \|m_k\|_{H^m}. \tag{3.5.2}$$

The set of all such positive definite kernels, while not without structure (it is a pointed, salient and convex cone [184]), is very large and the associated minimization problem is difficult to solve, both theoretically and numerically. As an alternative, fix now a family of functions $(\phi_i) \subset H^m(\mathcal{D})$ and consider

instead kernels of the form $k_\Lambda(x,y) \coloneqq \sum_{i=1}^d \lambda_i \phi_i(x)\phi_i(y)$, where $d \in \mathbb{N}^*$ is fixed and $\Lambda \coloneqq (\lambda_1, \dots, \lambda_d) \in \mathbb{R}_+^d$. The functions (ϕ_i) can be an orthogonal family of some Hilbert space, say Fourier modes or wavelets, but this is not a requirement. The optimization problem (3.5.2) then becomes finite dimensional:

$$\min_{\Lambda \in \mathbb{R}_+^d} \|m_{k_\Lambda}\|_{H^m}. \tag{3.5.3}$$

The Sobolev norm H^m of m_{k_Λ} may still be difficult to compute. However, from Proposition 3.4.4, we have the following convenient bound for any $f \in H_k$:

$$\begin{aligned} \|f\|_{H^m} = \|i(f)\|_{H^m} &\leq \|i\|_{\mathcal{L}(H_k, H^m)} \|f\|_{H_k} \leq \|i\|_{HS} \|f\|_{H_k} \\ &\leq \frac{1}{2}\Big(\varepsilon \|i\|_{HS}^2 + \varepsilon^{-1} \|f\|_{H_k}^2\Big). \end{aligned} \tag{3.5.4}$$

Above, $\|i\|_{\mathcal{L}(H_k, H^m)}$ is the usual operator sup norm for bounded operators. We then used the fact that $\|T\|_{\mathcal{L}} \leq \|T\|_{HS}$ for any bounded operator T conjointly with Young's inequality, $2ab \leq \varepsilon a^2 + \varepsilon^{-1} b^2$, given any $\varepsilon > 0$. For $k = k_\Lambda$ and $f = m_{k_\Lambda}$, both quantities are explicit. Indeed, $\|i\|_{HS}^2$ is given by equations (3.4.11) and (3.4.9) of Proposition 3.4.4; additionally (see e.g. [36], p. 3),

$$\|m_k\|_{H_k}^2 = \ell(u)^T k(\ell, \ell)^{-1} \ell(u). \tag{3.5.5}$$

Above, $\ell(u) = (\ell_1(u), ..., \ell_n(u))^T$ and $k(\ell,\ell)_{ij} = (\ell_i \otimes \ell_j)(k)$. We recover the usual Kriging formulas by taking $\ell_i = \delta_{x_i}$ for some x_i in the domain of definition of u. Putting both results together, we thus obtain a relaxed version of the optimization problem (3.5.3) in the form of

$$\min_{\Lambda \in \mathbb{R}_+^d} \varepsilon \sum_{i=1}^d \lambda_i \|\phi_i\|_{H^m}^2 + \frac{1}{\varepsilon} \ell(u)^T K_\Lambda^{-1} \ell(u), \tag{3.5.6}$$

where $K_\Lambda \coloneqq \sum_{i=1}^d \lambda_i V_i V_i^T, (V_i)_j \coloneqq \ell_j(\phi_i)$. Note that quantities similar to $\|i\|_{HS}^2$ have recently been used to select covariance functions in [4]. The ε parameters offers a tradeoff between the size of the RKHS inside the Sobolev space H^m, and the RKHS norm of the interpolant. In equation (3.5.6), we have the restrictive constraint that $n \leq d$ for K_Λ to be invertible. To alleviate this constraint, we make use of Tikhonov regularization with regularization parameter $\lambda_0 > 0$, which amounts to replacing K_Λ with $K_\Lambda + \lambda_0 I$.

For optimization purposes, it is interesting to observe that the minimization problem (3.5.6) is convex.

Proposition 3.5.1. *Let $\varepsilon > 0$ and $F \in \mathbb{R}^n$. Then the map given by*

$$\mathcal{L} : \Lambda \mapsto \varepsilon \sum_{i=1}^d \lambda_i \|\phi_i\|_{H^m}^2 + \frac{1}{\varepsilon} F^T (K_\Lambda + \lambda_0 I)^{-1} F, \tag{3.5.7}$$

is convex in the variable $\Lambda \in \mathbb{R}^d_+$. *As a result, any local solution of Problem* (3.5.6) *is global.*

Proof. The result is readily checked by verifying that the Hessian of the minimized function is nonnegative definite. The computations are rather "straightforward" but they are also tedious. We first set

$$K_{\text{reg}} \coloneqq K_\Lambda + \lambda_0 I. \tag{3.5.8}$$

We compute the partial derivatives of $\mathcal{L}$ with reference to λ_j. For this, we make use of the following matrix differentiation identities,

$$\partial_{\lambda_j} K_{\text{reg}}^{-1} = -K_{\text{reg}}^{-1}(\partial_{\lambda_j} K_{\text{reg}})K_{\text{reg}}^{-1}, \tag{3.5.9}$$
$$\partial_{\lambda_j} K_{\text{reg}} = V_j V_j^T. \tag{3.5.10}$$

They imply that

$$\partial_{\lambda_j}\mathcal{L} = \varepsilon\|\phi_j\|^2_{H^m} - \frac{1}{\varepsilon}F^T K_{\text{reg}}^{-1}V_j V_j^T K_{\text{reg}}^{-1}F \tag{3.5.11}$$
$$= \varepsilon\|\phi_j\|^2_{H^m} - \frac{1}{\varepsilon}\big(F^T K_{\text{reg}}^{-1}V_j\big)^2. \tag{3.5.12}$$

This next yields that

$$\begin{aligned}\partial^2_{\lambda_i\lambda_j}\mathcal{L} &= -\frac{2}{\varepsilon}\big(F^T K_{\text{reg}}^{-1}V_j\big)\partial_{\lambda_i}\big(F^T K_{\text{reg}}^{-1}V_j\big) = -\frac{2}{\varepsilon}\big(F^T K_{\text{reg}}^{-1}V_j\big)\big(F^T \partial_{\lambda_i} K_{\text{reg}}^{-1}V_j\big)\\ &= \frac{2}{\varepsilon}\big(F^T K_{\text{reg}}^{-1}V_j\big)\big(F^T K_{\text{reg}}^{-1}V_i V_i^T K_{\text{reg}}^{-1}V_j\big)\\ &= \frac{2}{\varepsilon}\big(F^T K_{\text{reg}}^{-1}V_j\big)\big(F^T K_{\text{reg}}^{-1}V_i\big)\big(V_i^T K_{\text{reg}}^{-1}V_j\big).\end{aligned} \tag{3.5.13}$$

At this point it is convenient to introduce the vectors $W_i \coloneqq K_{\text{reg}}^{-1/2}V_i$ and $G \coloneqq K^{-1/2}F$. This yields that

$$\partial^2_{\lambda_i\lambda_j}\mathcal{L} = \frac{2}{\varepsilon}(G^T W_i)(G^T W_j)(W_i^T W_j). \tag{3.5.14}$$

Taking $\mu = (\mu_1, ...\mu_d) \in \mathbb{R}^d_+$, we then have that

$$\frac{\varepsilon}{2}\mu^T\nabla^2\mathcal{L}\mu = \sum_{i,j=1}^d \mu_i\mu_j(G^T W_i)(G^T W_j)(W_i^T W_j) \tag{3.5.15}$$
$$= \left(\sum_{i=1}^d \mu_i(G^T W_i)W_i\right)^T\left(\sum_{j=1}^d \mu_j(G^T W_j)W_j\right) \geq 0, \tag{3.5.16}$$

which finishes the proof. □

Remark 3.5.2. It is in fact possible to show that much stronger property that the map $\mathcal{L}$ of Proposition 3.5.1 is convex in the *joint variable* $(\Lambda, F) \in \mathbb{R}_+^d \times \mathbb{R}^n$ (but not in the variable $(\varepsilon, \Lambda, F) \in \mathbb{R}_+^* \times \mathbb{R}_+^d \times \mathbb{R}^n$). This property is interesting, in particular when reformulating (potentially non linear) PDE constrained Kriging problems as a constrained minimization of the quadratic form $F \mapsto F^T K_{\text{reg}}^{-1} F$ ([36], Proposition 2.3). The study of the applications of this convexity property is a current subject of research.

Following Proposition 3.5.1, we can study the solution of Problem 3.5.6. The next Proposition deals with this question, in the limit where λ_0 goes to zero.

Proposition 3.5.3. *Let $F \in \mathbb{R}^n$, and let V be the $(n \times d)$ matrix defined by $V := (V_1|...|V_d)$. Assume that the V has full column rank (ie $\dim(Ran(V)) = d$), then the $(d \times d)$ Gram matrix $V^T V$ is invertible. Set $a = V^+ F$ where V^+ is the Moore-Penrose pseudo inverse of V. Then in the limit $\lambda_0 \to 0$, the minimum of the functional (3.5.7) is obtained at Λ such that $\lambda_i = |a_i|/(\varepsilon \|\phi_i\|_{H^m})$. Moreover, set $F_0 := (I - VV^+)F = F - Va$. Then for all $\lambda_0 > 0$, we have the non asymptotic bound on $\|m_k\|_{H^m}$ with $k = k_\Lambda$,*

$$\|m_k\|_{H^m}^2 \leq \sum_{i=1}^d |a_i| \|\phi_i\|_{H^m} \left(\frac{\|F_0\|^2}{\varepsilon \lambda_0} + \sum_{i=1}^d |a_i| \|\phi_i\|_{H^m} \right), \tag{3.5.17}$$

which corresponds to the product $\|i\|_{HS}^2 \|m_k\|_{H_k}^2$ evaluated at the near optimal $\lambda_i = |a_i|/(\varepsilon \|\phi_i\|_{H^m})$.

Proof. Assume that the solution to Problem (3.5.6) is located in the interior of $\mathbb{R}_+^d$ and furthermore that $\varepsilon = 1$ (without loss of generality). Following equation (3.5.12), fhe first order optimality conditions over λ_i are thus that $\|\phi_i\|_{H^m} = \left| V_i^T (K_\Lambda + \lambda_0 I)^{-1} F \right|$. Therefore there exists $\varepsilon_i \in \{-1, 1\}$ such that

$$\|\phi_i\|_{H^m} = \varepsilon_i V_i^T (K_\Lambda + \lambda_0 I)^{-1} F. \tag{3.5.18}$$

Since $\varepsilon_i^{-1} = \varepsilon_i$, this yields

$$\sum_{i=1}^d \lambda_i \varepsilon_i \|\phi_i\|_{H^m} V_i = \sum_{i=1}^d \lambda_i \varepsilon_i^2 V_i V_i^T (K_\Lambda + \lambda_0 I)^{-1} F \tag{3.5.19}$$

$$= K_\Lambda (K_\Lambda + \lambda_0)^{-1} F. \tag{3.5.20}$$

Setting $R := K_\Lambda^{1/2}$ and recalling that $R(RR^T + \lambda_0 I)^{-1}$ converges to R^+ when λ_0 converges to zero, we obtain that

$$K_\Lambda (K_\Lambda + \lambda_0)^{-1} = R \times R(RR^T + \lambda_0 I)^{-1} \xrightarrow[\lambda_0 \to 0]{} RR^+. \tag{3.5.21}$$

Moreover, RR^+ is the orthogonal projector onto the range or R. As such, $RR^+ = \Pi_{\mathrm{Ran}(K_\Lambda^{1/2})} = \Pi_{\mathrm{Span}(V_1,\dots,V_d)}$, where Π_E is the orthogonal projector onto $E \coloneqq \mathrm{Span}(V_1, \dots, V_d)$. Recall that $V = (V_1|\dots|V_d)$. Thus, we also have that $\Pi_E = VV^+$.

Define the vector χ defined by $\chi_i \coloneqq \|\phi_i\|_{H^m}\varepsilon_i\lambda_i$. The limit system corresponding to equation (3.5.20) when λ_0 goes to zero then writes

$$V\chi = \Pi_E F = VV^+F. \tag{3.5.22}$$

Since V^TV is assumed invertible, multiplying the equation above with V^T yields that $\chi = V^+F = a$. From the definition of χ, this gives (since $\lambda_i > 0$)

$$\lambda_i = |a_i|/\|\phi_i\|_{H^m}. \tag{3.5.23}$$

We now turn to the bound on the minimal value of the functional $\mathcal{L}$, which in turn bounds $\|m_k\|_{H^m}$ thanks to equation (3.5.4). For this, we use the limit solution $\lambda_i = |a_i|/\|\phi_i\|_{H^m}$ as a proxy for the solution in the non asymptotic case. First, the associated Hilbert-Schmidt norm term is given by

$$\|i\|_{HS}^2 = \sum_{i=1}^d \lambda_i \|\phi_i\|_{H^m}^2 = \sum_{i=1}^d |a_i|\|\phi_i\|_{H^m}. \tag{3.5.24}$$

For the RKHS norm term, decompose the data vector F as $F = \Pi_E F + \Pi_{E^\perp} F$. Informally, $\Pi_E F$ corresponds to the data which can be explained by the kernel k_Λ, while $\Pi_{E^\perp}F$ corresponds to measurement noise or data which cannot be explained by the kernel k_Λ. We can then write

$$F^T(K_\Lambda + \lambda_0 I)^{-1}F = \frac{\|\Pi_{E^\perp}F\|^2}{\lambda_0} + (\Pi_E F)^T(K_\Lambda + \lambda_0 I)^{-1}\Pi_E F. \tag{3.5.25}$$

This equality can be proved by writing the matrix $K_\Lambda + \lambda_0 I$ in a blockwise diagonal form, in an orthogonal basis of $\mathbb{R}^n$ corresponding to the orthogonal decomposition $\mathbb{R}^n = E \oplus E^\perp$, and by inverting it blockwise. Similar computations are described in the upcoming Section 4.3.4.1. Recall that we have $Va = \Pi_E F$. Set $F_0 \coloneqq \Pi_{E^\perp}F$. Then equation (3.5.25) is rewritten as

$$F^T(K_\Lambda + \lambda_0 I)^{-1}F = \frac{\|F_0\|^2}{\lambda_0} + (Va)^T(K_\Lambda + \lambda_0 I)^{-1}Va. \tag{3.5.26}$$

Next, write $K_\Lambda = \sum_{i=1}^d \lambda_i V_i V_i^T = VD_\Lambda V^T$, where D_λ is a $(d \times d)$ diagonal matrix with i^{th} diagonal coefficient d_i. From the fact that $K_\Lambda + \lambda_0 I \geq K_\Lambda$ in the sense of nonnegative definite matrices (Loewner order), it is readily checked that for all $b \in \mathrm{Ker}(K_\Lambda)^\perp = \mathrm{Ran}(K_\Lambda)$, $b^T(K_\Lambda + \lambda_0 I)^{-1}b \leq b^T K_\Lambda^+ b$. Thus, since $Va \in \mathrm{Span}(V_1, ..., V_d) = \mathrm{Ran}(K_\Lambda)$,

$$(Va)^T(K_\Lambda + \lambda_0)^{-1}Va \leq (Va)^T K_\Lambda^+ Va. \tag{3.5.27}$$

Moreover, V is assumed to have full column rank, D_Λ is invertible and thus $D_\lambda V^T$ has full row rank. Thus, from [92], p. 518, the following pseudo-inverse product formula holds:

$$K_\Lambda^+ = (VD_\Lambda V^T)^+ = (D_\Lambda V^T)^+ V^+ = (V^T)^+ D_\Lambda^{-1} V^+. \tag{3.5.28}$$

From this and the fact that transposition and pseudo-inversion commute, we obtain that

$$\begin{aligned}(Va)^T(K_\Lambda + \lambda_0)^{-1}Va &\leq (Va)^T(V^T)^+ D_\Lambda^{-1}V^+Va \\ &\leq (V^+Va)^T D_\Lambda^{-1}(V^+Va).\end{aligned} \tag{3.5.29}$$

Finally, since V^+V is an orthogonal projector, since $a = V^+Va + (I - V^+V)a$ and since D_Λ is diagonal, we have that $(V^+Va)^T D_\Lambda^{-1}(I - V^+V)a = 0$ which yields that $(V^+Va)^T D_\Lambda^{-1}(V^+Va) \leq a^T D_\Lambda^{-1} a$. This leads to the conclusion that

$$\begin{aligned}(Va)^T(K_\Lambda + \lambda_0)^{-1}Va &\leq (V^+Va)^T D_\Lambda^{-1}(V^+Va) \\ &\leq a^T D_\Lambda^{-1} a = \sum_{i=1}^d |a_i| \|\phi_i\|_{H^m}.\end{aligned} \tag{3.5.30}$$

More generally, if we consider the general problem with any $\varepsilon > 0$, we obtain the rescaling $\lambda_i = |a_i|/(\varepsilon\|\phi_i\|_{H^m})$, which is e.g. visible in the first order optimality conditions corresponding to arbitrary $\varepsilon > 0$. This yields the following bound,

$$\|m\|_{H^m}^2 \leq \|i\|_{HS}^2 \|m_k\|_{H_k}^2 \tag{3.5.31}$$

$$\leq \frac{1}{\varepsilon}\sum_{i=1}^d |a_i|\|\phi_i\|_{H^m}\left(\frac{\|F_0\|^2}{\lambda_0} + \varepsilon\sum_{i=1}^d |a_i|\|\phi_i\|_{H^m}\right) \tag{3.5.32}$$

$$\leq \sum_{i=1}^d |a_i|\|\phi_i\|_{H^m}\left(\frac{\|F_0\|^2}{\varepsilon\lambda_0} + \sum_{i=1}^d |a_i|\|\phi_i\|_{H^m}\right), \tag{3.5.33}$$

which finishes the proof. □

We see that the term $\|F_0\|^2\varepsilon^{-1}\lambda_0^{-1}$ blows up as λ_0 goes to zero, unless $\|F_0\| = 0$, that is, the kernel can fully explain the data. Otherwise, the regularization parameter λ_0 has to be non-zero. One can also use large values of ε to recover stability (it is really the product $\varepsilon\lambda_0$ that matters). This limit corresponds to discarding the RKHS norm in the optimization problem.

3.6 Concluding remarks and perspectives

Given $p \in (1, +\infty)$ and $m \in \mathbb{N}$, we showed that the $W^{m,p}$-Sobolev regularity of integer order of a measurable Gaussian process $((U(x))_{x\in\mathcal{D}} \sim GP(0, k)$ is fully equivalent to the fact that $\partial^{\alpha,\alpha}k$ lies in $L^p(\mathcal{D} \times \mathcal{D})$ combined with the integrability in $L^p(\mathcal{D})$ of the associated standard deviation. Using general results on Gaussian measures over Banach spaces of type 2 and cotype 2, we translated this criteria as the existence of suitable nuclear decompositions of the covariance. These can be understood as generalizations to Banach spaces of the eigenfunction expansion of symmetric, nonnegative and trace class operators. In the Hilbert space case $p = 2$, we linked this property with the Hilbert-Schmidt nature of the imbedding of the RKHS in $H^m(\mathcal{D})$, and gave explicit formulas for the traces of the involved integral operators in terms of the Mercer decomposition of the kernel.

The results presented in this article provide a theoretical background w.r.t. the use of Gaussian processes for solving physics-related machine learning problems, in particular when modelling solutions of PDEs as sample paths of some Gaussian process. These results also come along with suitable quantities for controlling the Sobolev norm of the corresponding sample paths (see Remark 3.3.6). The application of the Gaussian process principles identified here to PDE-related machine learning problems, e.g. following the approach of [36], is certainly an interesting continuation of the results of this article. Controlling the small ball probability (see e.g. [140] for further details) of the Sobolev norm of a Gaussian process, perhaps in terms of some nuclear norm, is also a relevant question for further applications of Gaussian process techniques in such machine learning problems. Finally, the following question (which was implicit in this article) is interesting for probability theory: are all Gaussian measures over $W^{m,p}(\mathcal{D})$ induced by some Gaussian process? Proposition 3.2.9 states that this is true for $m = 0$, i.e. $L^p(\mathcal{D})$.

The following directions are interesting for generalizing the results presented here. First, similar spectral/integral criteria should be obtained for fractional Sobolev and Besov spaces. Second, similar results should be sought to tackle the limit cases $p = 1$ and $p = +\infty$. Linked to the case $p = 1$, results should be sought for the space of functions of bounded variations ([33], p. 269), which are important in many problems related to physics.

Finally, the last section introduced an optimization problem which is useful for selecting covariance functions, when the Sobolev regularity of the interpolant has to be controlled. We partially solved this problem and provided bounds over the Sobolev norm of the Kriging mean. Further applications of this optimization problem have to be studied, notably in numerical settings. Finally, studying this problem in the general case $1 < p < +\infty$ (for which

Propositions 3.3.1 and 3.3.5 also provide quantitative bounds) is an interesting direction of research.

3.7 Proofs of intermediary results and lemmas

Proof. (Lemma 3.2.1) This proof follows exactly the lines of the proof of Proposition 9.3 from [33].
$(i) \iff (ii)$: suppose that $u \in W^{m,p}(\mathcal{D})$, use the fact that the distributional derivative $D^\alpha u$ is a regular distribution represented by a function that lies in $L^p(\mathcal{D})$, denoted by $\partial^\alpha u$:

$$\forall \varphi \in C_c^\infty(\mathcal{D}), \quad \int_{\mathcal{D}} u(x)\partial^\alpha \varphi(x)dx = (-1)^{|\alpha|}\int_{\mathcal{D}} \partial^\alpha u(x)\varphi(x)dx. \tag{3.7.1}$$

Hölder's inequality yields (3.2.7) with $C_\alpha = \|\partial^\alpha u\|_{L^p}$. Conversely, suppose that (3.2.7) holds and consider any $|\alpha| \leq m$. Since $C_c^\infty(\mathcal{D})$ is dense in $L^q(\mathcal{D})$ (whatever the open set $\mathcal{D}$, [169], section 2.30), equation (3.2.7) shows that the linear form $L_\alpha : \varphi \longmapsto (-1)^{|\alpha|}\int_{\mathcal{D}} u(x)\partial^\alpha\varphi(x)dx, \varphi \in C_c^\infty(\mathcal{D})$, can be extended to a continuous linear form over $L^q(\mathcal{D})$. From Riesz' representation lemma, there exists $v_\alpha \in L^p(\mathcal{D})$ such that $L_\alpha(\varphi) = \langle v_\alpha, \varphi\rangle_{L^p,L^q}$ for all $\varphi \in L^q(\mathcal{D})$. In particular, this is valid for all $\varphi \in C_c^\infty(\mathcal{D})$, which shows that for all $|\alpha| \leq m, \partial^\alpha u$ exists and is equal to v_α. Thus $u \in W^{m,p}(\mathcal{D})$. Finally, Hölder's inequality and the density of $C_c^\infty(\mathcal{D})$ in $L^q(\mathcal{D})$ yield

$$\|\partial^\alpha u\|_{L^p(\mathcal{D})} = \sup_{\varphi \in C_c^\infty(\mathcal{D})\setminus\{0\}} \left| \int_{\mathcal{D}} u(x)\frac{\partial^\alpha\varphi(x)}{\|\varphi\|_{L^q(\mathcal{D})}}dx \right|.$$

$(iii) \implies (ii)$: suppose (iii), let us show (ii). Let $|\alpha| \leq m$ and let $\varphi \in C_c^\infty(\mathcal{D})$. Note $K := \mathrm{Supp}(\varphi)$ its compact support and consider an open set $\mathcal{D}_0$ such that $K \subset \mathcal{D}_0 \Subset \mathcal{D}$. Let $\alpha \$ in \mathbb{N}^d$ and $h = (h_1, ..., h_d) \in (\mathbb{R}_+^*)^d$ be such that $\sum_i \alpha_i h_i < \mathrm{dist}(\mathcal{D}_0, \partial\mathcal{D})$. Recall that δ_h^α from equation (3.2.6) is a finite difference approximation of ∂^α and from (iii),

$$\left| \int_{\mathcal{D}} \delta_h^\alpha u(x)\varphi(x)dx \right| \leq \|\varphi\|_{L^q(\mathcal{D}_0)}\|\delta_h^\alpha u\|_{L^p(\mathcal{D}_0)} \leq C\|\varphi\|_{L^q(\mathcal{D})}. \tag{3.7.2}$$

Note also that we have the discrete integration by parts formula since h is suitably chosen:

$$\int_{\mathcal{D}} \delta_h^\alpha u(x)\varphi(x)dx = \int_{\mathcal{D}} u(x)(\delta_h^\alpha)^*\varphi(x)dx. \tag{3.7.3}$$

Therefore,

$$\left| \int_{\mathcal{D}} u(x)(\delta_h^\alpha)^*\varphi(x)dx \right| \leq C\|\varphi\|_{L^q(\mathcal{D})}. \tag{3.7.4}$$

The Lebesgue dominated convergence theorem yields that the left hand side converges to $\left| \int_{\mathcal{D}} u(x)\partial^{\alpha}\varphi(x)dx \right|$. We therefore have (ii).
$(i) \implies (iii)$: We will use recursively the fact that if $f \in W^{1,p}(\mathcal{D})$, then for all $\mathcal{D}_0 \Subset \mathcal{D}$ and $h \in \mathbb{R}^d$ such that $|h| < \mathrm{dist}(\mathcal{D}_0, \partial\mathcal{D})$, there exists an open set $\mathcal{D}_1 \Subset \mathcal{D}$ which verifies $\mathcal{D}_0 + th \subset \mathcal{D}_1$ for all $t \in [0,1]$ and

$$\|\Delta_h f\|^p_{L^p(\mathcal{D}_0)} = \|\tau_h f - f\|^p_{L^p(\mathcal{D}_0)} \leq |h|^p \|\nabla f\|^p_{L^p(\mathcal{D}_1)} = |h|^p \sum_{j=1}^{d} \|\partial_{x_j} f\|^p_{L^p(\mathcal{D}_1)}. \tag{3.7.5}$$

(this is equation 4 p. 268 in [33], found in the proof of Proposition 9.3 in [33]). First, one easily checks that weak partial derivatives and finite difference operators all commute together. Let $l \leq m$, $\mathcal{D}_0 \Subset \mathcal{D}$ and $h = (h_1, ..., h_l) \in (\mathbb{R}^d)^l$ such that $\sum_i |h_i| < \mathrm{dist}(\mathcal{D}_0, \partial\mathcal{D})$. Recall that

$$\Delta_h = \prod_{i=1}^{l} \Delta_{h_i}. \tag{3.7.6}$$

Note now that $\prod_{i=2}^{l} \Delta_{h_i} u$ lies in $W^{1,p}(\mathcal{D})$. Since $|h_1| \leq \sum_i |h_i| < \mathrm{dist}(\mathcal{D}_0, \partial\mathcal{D})$, from equation (3.7.5) there exists an open set $\mathcal{D}_1 \Subset \mathcal{D}$ such that $\mathcal{D}_0 + th_1 \subset \mathcal{D}_1$ for all $t \in [0,1]$. Moreover, one can choose $\mathcal{D}_1$ small enough so that $\mathrm{dist}(\mathcal{D}_1, \partial\mathcal{D}) < \sum_{i=2}^{l} |h_i|$.

$$\|\Delta_h u\|^p_{L^p(\mathcal{D}_0)} = \left|\left|\Delta_{h_1} \prod_{i=2}^{l} \Delta_{h_i} u\right|\right|^p_{L^p(\mathcal{D}_0)} \leq |h_1|^p \left|\left|\nabla \prod_{i=2}^{l} \Delta_{h_i} u\right|\right|^p_{L^p(\mathcal{D}_1)} \tag{3.7.7}$$

$$\leq |h_1|^p \sum_{j=1}^{d} \left|\left|\partial_{x_j} \prod_{i=2}^{l} \Delta_{h_i} u\right|\right|^p_{L^p(\mathcal{D}_1)} \leq |h_1|^p \sum_{j=1}^{d} \left|\left| \prod_{i=2}^{l} \Delta_{h_i} \left(\partial_{x_j} u\right)\right|\right|^p_{L^p(\mathcal{D}_1)}. \tag{3.7.8}$$

We used equation (3.7.5) in equation (3.7.7) which then yields equation (3.7.8). But note that for all j, $\partial_{x_j} u \in W^{1,p}(\mathcal{D})$. One can then proceed by induction and perform the above step sequentially over $i \in \{2, ..., l\}$, which yields a sequence of open sets $\mathcal{D}_0 \subset \mathcal{D}_1 \subset ... \subset \mathcal{D}_l \Subset \mathcal{D}$ such that

$$\|\Delta_h u\|^p_{L^p(\mathcal{D}_0)} \leq |h_1|^p \times ... \times |h_l|^p \sum_{|\beta| \leq l} \|\partial^{\beta} u\|^p_{L^p(\mathcal{D}_l)} \tag{3.7.9}$$

$$\leq |h_1|^p \times ... \times |h_l|^p \|u\|^p_{W^{l,p}(\mathcal{D})} \leq |h_1|^p \times ... \times |h_l|^p \|u\|^p_{W^{m,p}(\mathcal{D})}, \tag{3.7.10}$$

which shows equation (3.2.9) with $C = \|u\|_{W^{m,p}(\mathcal{D})}$. We finally show that $\|\partial^{\alpha} u\|_{L^p(\mathcal{D})} \leq C$ given any C which verifies equation (3.2.9). For this, copy

the previous steps of $(iii) \implies (ii)$, which prove that for all $\varphi \in C_c^\infty(\mathcal{D})$, the control from equation (3.2.7) holds for this C. Using the extremal equality case of Hölder's inequality in equation (3.2.7) indeed yields

$$\|\partial^\alpha u\|_{L^p(\mathcal{D})} = \sup_{\varphi \in C_c^\infty(\mathcal{D})\setminus\{0\}} \left| \int_{\mathcal{D}} u(x) \frac{\partial^\alpha \varphi(x)}{\|\varphi\|_{L^p(\mathcal{D})}} dx \right| \leq C. \tag{3.7.11}$$

□

Proof. (Lemma 3.2.4) We begin by explicitly constructing the family (Φ_n^q). First, use the fact that $L^q(\mathcal{D})$ is a separable Banach space ([169], Theorem 2.21) : let $(f_n)_{n\in\mathbb{N}^*} \subset L^q(\mathcal{D})$ be a dense countable subset of $L^q(\mathcal{D})$. For all $n \in \mathbb{N}^*$, let $(\phi_{nm})_{m\in\mathbb{N}^*} \subset C_c^\infty(\mathcal{D})$ be such that $\phi_{nm} \longrightarrow f_n$ for the $L^q(\mathcal{D})$ topology (recall that $C_c^\infty(\mathcal{D})$ is dense in $L^q(\mathcal{D})$, [169], Corollary 2.30). We relabel the countable family $(\phi_{nm})_{n,m\in\mathbb{N}^*}$ as $(\varphi_n)_{n\in\mathbb{N}^*}$, which is thus dense in $L^q(\mathcal{D})$. Second, let $(h_n)_{n\in\mathbb{N}^*} \subset C_c^\infty(\mathcal{D})$ be a dense subset of $C_c^\infty(\mathcal{D})$ for its LF-space topology (see Lemma 3.2.3). We then define E_q to be the set of all finite linear combinations of elements of (φ_n) and (h_n) with rational coefficients :

$$E_q = \mathrm{Span}_{\mathbb{Q}}\{\varphi_n, n \in \mathbb{N}^*\} + \mathrm{Span}_{\mathbb{Q}}\{h_m, m \in \mathbb{N}^*\} \tag{3.7.12}$$

$$= \bigcup_{n,m\in\mathbb{N}^*} \Big\{ \sum_{i=1}^{n} q_i\varphi_i + \sum_{j=1}^{m} r_j h_j, (q_1, ..., q_n, r_1, ..., r_m) \in \mathbb{Q}^{n+m} \Big\}. \tag{3.7.13}$$

Note that E_q is countable, as a countable union of countable sets. We then define the family (Φ_n^q) to be an enumeration of E_q : $E_q = \{\Phi_n^q, n \in \mathbb{N}^*\}$.
Proof of (i): Suppose that $T = T_v$ for some $v \in L^p(\mathcal{D})$. Then the control (3.2.13) is obviously true. Now, suppose that this countable control holds : let us show that $T = T_v$ for some $v \in L^p(\mathcal{D})$.

We begin by showing that the map $T_{|E_q}$,the restriction of T to the set E_q, can be uniquely extended to a continuous linear form $\tilde{T}$ over $L^q(\mathcal{D})$. Begin with the fact that for all $f, g \in E_q$, then $f - g \in E_q$ and from equation (3.2.18),

$$|T(f) - T(g)| = |T(f - g)| \leq C\|f - g\|_q. \tag{3.7.14}$$

Equation (3.7.14) shows that $T_{|E_q}$ is Lipschitz over E_q and therefore uniformly continuous on E_q. Since $\mathbb{R}$ is complete and E_q is dense in $L^q(\mathcal{D})$, $T_{|E_q}$ can be uniquely extended by a map $\tilde{T}$ defined over $L^q(\mathcal{D})$, which is itself uniformly continuous ([171], Problem 44, p. 196). We briefly recall the construction procedure of $\tilde{T}$ over $L^q(\mathcal{D})$. Given $f \in L^q(\mathcal{D})$ and $(f_n) \subset E_q$ *any* sequence such that $\|f_n - f\|_{L^q} \to 0$, one shows that the sequence $(T(f_n))_{n\in\mathbb{N}^*}$ is Cauchy, thus convergent and one sets $\tilde{T}(f) := \lim_n T(f_n)$. One proves that the value $\tilde{T}(f)$ does not depend on the sequence (f_n), which implies that $\tilde{T}$ is well defined and coincides with T on E_q.

We now check that $\tilde{T}$ remains linear. Let $f, g \in L^q(\mathcal{D})$ and $\lambda \in \mathbb{R}$. Let $(f_n), (g_n) \subset E_q$ and $(\lambda_n) \subset \mathbb{Q}$ be sequences such that $f_n \to f, g_n \to g$ both in $L^q(\mathcal{D})$ and $\lambda_n \to \lambda$. Then $\lambda_n f_n + g_n \to \lambda f + g$ in $L^q(\mathcal{D})$, and the sequence $(\lambda_n f_n + g_n)$ is contained in E_q. Since $\tilde{T}$ is well defined, we have that

$$\tilde{T}(\lambda f + g) = \lim_{n\to\infty} T(\lambda_n f_n + g_n) = \lim_{n\to\infty} \lambda_n T(f_n) + T(g_n) = \lambda \tilde{T}(f) + \tilde{T}(g). \tag{3.7.15}$$

Thus, $\tilde{T}$ is a (uniformly) continuous linear form over $L^q(\mathcal{D})$. Riesz' representation lemma yields a function $v \in L^p(\mathcal{D})$ such that

$$\forall f \in L^q(\mathcal{D}), \quad \tilde{T}(f) = \int_{\mathcal{D}} f(x)v(x)dx. \tag{3.7.16}$$

We now need to check that in fact $\tilde{T}(\varphi) = T(\varphi)$ if $\varphi \in C_c^\infty(\mathcal{D})$, to show that $\tilde{T}$ is indeed an extension of T. For this, notice that T and $\tilde{T}$ both define continuous linear forms over $C_c^\infty(\mathcal{D})$, w.r.t. its LF-topology (v lies in $L^1_{loc}(\mathcal{D})$). Note also that T and $\tilde{T}$ coincide on E_q, by construction of $\tilde{T}$:

$$\forall n \in \mathbb{N}^*, \quad T(\Phi_n) - \tilde{T}(\Phi_n) = 0. \tag{3.7.17}$$

But E_q is chosen so that it contains (h_n), which is a dense subset of $C_c^\infty(\mathcal{D})$. Given $\varphi \in C_c^\infty(\mathcal{D})$, consider (j_n) a subsequence of (h_n) such that $j_n \longrightarrow \varphi$ for the topology of $C_c^\infty(\mathcal{D})$. Then,

$$(T - \tilde{T})(\varphi) = \lim_{n\to\infty} (T - \tilde{T})(j_n) = \lim_{n\to\infty} 0 = 0, \tag{3.7.18}$$

which shows that in fact, $\tilde{T}(\varphi) = T(\varphi)$.
Proof of (ii): if b can be extended to a continuous linear form over $L^q(\mathcal{D})$, then the estimate (3.2.15) is obviously true, by continuity over $L^q(\mathcal{D})$ of the said extension. Suppose now that (3.2.15) holds. Let $\varphi \in E_q$. Then L_φ, the continuous linear form over $C_c^\infty(\mathcal{D})$ defined by

$$\forall \psi \in C_c^\infty(\mathcal{D}), \quad L_\varphi(\psi) = b(\varphi, \psi) \tag{3.7.19}$$

verifies

$$\forall \psi \in E_q, \quad |L_\varphi(\psi)| \leq C\|\varphi\|_q \|\psi\|_q. \tag{3.7.20}$$

From the point (i), L_φ is a regular distribution with a representer $v_\varphi \in L^p(\mathcal{D})$ which is unique in $L^p(\mathcal{D})$. Define the map $B : E_q \to L^p(\mathcal{D})$ by $B\varphi = v_\varphi$. Then B verifies

$$\forall \varphi \in E_q, \forall \psi \in L^q(\mathcal{D}), \quad |\langle B\varphi, \psi \rangle_{L^p, L^q}| = |L_\varphi(\psi)| \leq C\|\varphi\|_q \|\psi\|_q. \tag{3.7.21}$$

Taking the supremum w.r.t. $\psi \in L^q(\mathcal{D})$ yields

$$\forall \varphi \in E_q, \quad \|B\varphi\|_p \leq C\|\varphi\|_q. \tag{3.7.22}$$

Observe now that the bilinearity of b yields $B(\varphi+\lambda\psi) = B\varphi+\lambda B\psi$ if $\varphi, \psi \in E_q$ and $\lambda \in \mathbb{Q}$. Taking the exact same steps as for the proof of point (i) and using equation (3.7.22), $B : E_q \to L^p(\mathcal{D})$ is Lipschitz continuous over E_q, and can thus be uniquely extended as a uniformly continuous map $\tilde{B} : L^q(\mathcal{D}) \to L^p(\mathcal{D})$. This relies on the fact that E_q is dense in $L^q(\mathcal{D})$ and that $L^q(\mathcal{D})$ is complete. As above, one checks that $\tilde{B}$ is linear. Being uniformly continuous, it is then a bounded operator from $L^q(\mathcal{D})$ to $L^p(\mathcal{D})$ (its adjoint $\tilde{B}^*$ is then automatically bounded). Denote by $\tilde{b}$ the continuous bilinear form over $L^q(\mathcal{D})$ defined by

$$\tilde{b}(f, g) = \langle \tilde{B}f, g\rangle_{L^p,L^q} \quad \forall f, g \in L^q(\mathcal{D}). \tag{3.7.23}$$

We now need to check that $\tilde{b}$ indeed coincides with b over $C_c^\infty(\mathcal{D})$, so that it is indeed an extension of b. For this, let $\varphi, \psi \in C_c^\infty(\mathcal{D})$ and $(\varphi_n), (\psi_n)$ two sequences of elements of E_q that converge to φ and ψ respectively. Then b and $\tilde{b}$ coincide on E_q:

$$b(\varphi_n, \psi_m) = \tilde{b}(\varphi_n, \psi_m). \tag{3.7.24}$$

Observe the following chain of equalities, which rely on the sequential continuity (for the LF topology of $C_c^\infty(\mathcal{D})$) of the linear forms $\varphi \mapsto b(\varphi, \psi), \psi \mapsto b(\varphi, \psi)$ and $T_v : \varphi \mapsto T_v(\varphi) = \langle v, \varphi\rangle_{L^q,L^p}$ for any $v \in L^q(\mathcal{D})$, as well equation (3.7.24).

$$\begin{aligned} b(\varphi, \psi) &= \lim_{n\to\infty} b(\varphi_n, \psi) = \lim_{n\to\infty}\lim_{m\to\infty} b(\varphi_n, \psi_m) = \lim_{n\to\infty}\lim_{m\to\infty} \tilde{b}(\varphi_n, \psi_m) \\ &= \lim_{n\to\infty}\lim_{m\to\infty} \langle \tilde{B}\varphi_n, \psi_m\rangle_{L^p,L^q} = \lim_{n\to\infty}\lim_{m\to\infty} T_{\tilde{B}\varphi_n}(\psi_m) = \lim_{n\to\infty} T_{\tilde{B}\varphi_n}(\psi) \\ &= \lim_{n\to\infty} \langle \tilde{B}\varphi_n, \psi\rangle_{L^p,L^q} = \lim_{n\to\infty} \langle \varphi_n, \tilde{B}^*\psi\rangle_{L^q,L^p} = \lim_{n\to\infty} T_{\tilde{B}^*\psi}(\varphi_n) = T_{\tilde{B}^*\psi}(\varphi) \\ &= \langle \varphi, \tilde{B}^*\psi\rangle_{L^q,L^p} = \langle \tilde{B}\varphi, \psi\rangle_{L^p,L^q} = \tilde{b}(\varphi, \psi). \end{aligned} \tag{3.7.25}$$

The uniqueness of b follows from the uniqueness of $\tilde{B}$ as an extension of B. □

Proof. (Lemma 3.2.5) Let (K_n) be an increasing sequence of compact subsets of $\mathcal{D}$ such that $\bigcup_n K_n = \mathcal{D}$. From the measurability of U and Tonelli's theorem, $\omega \mapsto \int_{K_n} |U_\omega(x)|dx$ is measurable and we have that

$$\mathbb{E}\left[\int_{K_n} |U(x)|dx\right] = \int_{K_n} \mathbb{E}[|U(x)|]dx = \sqrt{\frac{2}{\pi}}\int_{K_n} \sigma(x)dx < +\infty. \tag{3.7.26}$$

From equation (3.7.26), $\omega \mapsto \int_{K_n} |U_\omega(x)|dx$ is finite almost surely. Since the family (K_n) is countable, one obtains a set $\Omega_0 \subset \Omega$ of probability one such

that for all $\omega \in \Omega_0$ and for all $n \in \mathbb{N}^*$, $\int_{K_n} |U_\omega(x)|dx < +\infty$. Given now any compact subset K of $\mathcal{D}$, there exists $N \in \mathbb{N}^*$ such that $K \subset K_N$ and thus for all $\omega \in \Omega_0$, $\int_K |U_\omega(x)|dx < +\infty$. Therefore, the sample paths of U lie in $L^1_{loc}(\mathcal{D})$ almost surely. From this fact and Fubini's theorem, we next obtain that given any $\varphi \in C_c^\infty$ and $|\alpha| \leq m$, the following map

$$U_\varphi^\alpha : \Omega \ni \omega \longmapsto \int_{\mathcal{D}} U_\omega(x)\partial^\alpha\varphi(x)dx \tag{3.7.27}$$

is a well defined random variable (i.e. it is measurable; see e.g. [63], Theorem 2.7, p. 62). Moreover, one can show that it is a limit in probability of suitably chosen Riemann sums of the integrand ([63], Theorem 2.8, p. 65). But here, those Riemann sums are all Gaussian random variables because U is a Gaussian process. Thus U_φ^α is a Gaussian random variable. a a limit in probability of Gaussian random variables. This also shows that $\{U_\varphi^\alpha, \varphi \in C_c^\infty(\mathcal{D})\}$ is in fact a Gaussian process, since the linearity of ∂^α yields

$$\sum_{i=1}^n a_i U_{\varphi_i}^\alpha = U^\alpha_{(\sum_{i=1}^n a_i\varphi_i)}, \tag{3.7.28}$$

and thus $\sum_{i=1}^n a_i U_{\varphi_i}^\alpha$ is a Gaussian random variable. An alternative proof is found in [29], Example 2.3.16. p. 58-59. □

Proof. (Lemma 3.4.7) First, the map k is measurable over $\mathcal{D} \times \mathcal{D}$. Then, given a compact set $K \subset \mathcal{D} \times \mathcal{D}$, there exists a compact set $K_0 \subset \mathcal{D}$ such that $K \subset K_0 \times K_0$ (see e.g. the text before equation (3.3.11)). Then, using the Cauchy-Schwarz inequality for k,

$$\int_K |k(x,y)|dxdy \leq \int_{K_0\times K_0} \sigma(x)\sigma(y)dxdy = \left(\int_{K_0} \sigma(x)dx\right)^2 < +\infty. \tag{3.7.29}$$

Therefore, $k \in L^1_{loc}(\mathcal{D} \times \mathcal{D})$ and for all mutli-index α, b_α is a bilinear continuous form over $C_c^\infty(\mathcal{D})$. From Lemma 3.2.2, b_α can be uniquely extended to a continuous bilinear form over $L^2(\mathcal{D})$. Denote by $\mathcal{E}_k^\alpha$ the associated bounded operator over $L^2(\mathcal{D})$. We now need to show that $\mathcal{E}_k^\alpha$ is self-adjoint and non-negative. First note that for all $\varphi, \psi \in C_c^\infty(\mathcal{D})$,

$$\langle \mathcal{E}_k^\alpha\varphi, \psi\rangle_{L^2} = \int_{\mathcal{D}\times\mathcal{D}} k(x,y)\partial^\alpha\varphi(x)\partial^\alpha\psi(y)dydx = \langle \varphi, \mathcal{E}_k^\alpha\psi\rangle_{L^2}. \tag{3.7.30}$$

Equation (3.7.30), conjoined with the density of $C_c^\infty(\mathcal{D})$ in $L^2(\mathcal{D})$ and the continuity of the bilinear form $(f,g) \mapsto \langle \mathcal{E}_k^\alpha f, g\rangle_{L^2}$ yields that $\langle \mathcal{E}_k^\alpha f, g\rangle_{L^2} = \langle f, \mathcal{E}_k^\alpha g\rangle_{L^2}$ for all $f, g \in L^2(\mathcal{D})$. Therefore $\mathcal{E}_k^\alpha$ is self-adjoint. For the positivity, consider again $\varphi \in C_c^\infty(\mathcal{D})$. Then from Fubini's theorem (justified below),

$$\langle \mathcal{E}_k^\alpha\varphi, \varphi\rangle = \int_{\mathcal{D}\times\mathcal{D}} k(x,y)\partial^\alpha\varphi(x)\partial^\alpha\varphi(y)dydx$$

$$= \int_{\mathcal{D}\times\mathcal{D}} \mathbb{E}[U(x)U(y)]\partial^\alpha\varphi(x)\partial^\alpha\varphi(y)dydx$$
$$= \mathbb{E}\left[\left(\int_{\mathcal{D}} U(x)\partial^\alpha\varphi(x)dx\right)^2\right] \geq 0. \tag{3.7.31}$$

Indeed the following integrability condition holds, setting $K = \mathrm{Supp}(\varphi)$:

$$\mathbb{E}\left[\int_{\mathcal{D}\times\mathcal{D}} |\partial^\alpha\varphi(x)\partial^\alpha\varphi(y)U(x)U(y)|dxdy\right]$$
$$= \int_{K\times K} |\partial^\alpha\varphi(x)\partial^\alpha\varphi(y)|\mathbb{E}[|U(x)U(y)|]dxdy$$
$$\leq \int_{K\times K} |\partial^\alpha\varphi(x)\partial^\alpha\varphi(y)|\sigma(x)\sigma(y)dxdy = \left(\int_K |\partial^\alpha\varphi(x)|\sigma(x)dx\right)^2$$
$$\leq \sup_{x\in K} |\partial^\alpha\varphi(x)|^2\left(\int_K \sigma(x)dx\right)^2 < +\infty. \tag{3.7.32}$$

Equation (3.7.32), conjoined with the density of $C_c^\infty(\mathcal{D})$ in $L^2(\mathcal{D})$ and the continuity of the quadratic form $f \mapsto \langle \mathcal{E}_k^\alpha f, f\rangle_{L^2}$ yields that $\langle \mathcal{E}_k^\alpha f, f\rangle_{L^2} \geq 0$ for all $f \in L^2(\mathcal{D})$. Therefore $\mathcal{E}_k^\alpha$ is nonnegative. □

Proof. (Lemma 3.4.8) Introduce b_α the continuous bilinear map over $C_c^\infty(\mathcal{D})$ defined by

$$b_\alpha(\varphi,\psi) = \int_{\mathcal{D}\times\mathcal{D}} k(x,y)\partial^\alpha\varphi(x)\partial^\alpha\psi(y)dxdy = \int_{\mathcal{D}\times\mathcal{D}} \partial^{\alpha,\alpha}k(x,y)\varphi(x)\psi(y)dxdy$$
$$= \langle \mathcal{E}_k^\alpha\varphi,\psi\rangle_{L^2}. \tag{3.7.33}$$

From Cauchy-Schwarz's inequality, it verifies

$$\forall\varphi,\psi \in C_c^\infty(\mathcal{D}),\ |b_\alpha(\varphi,\psi)| \leq \|\partial^{\alpha,\alpha}k\|_2\|\varphi\|_2\|\psi\|_2 \tag{3.7.34}$$

From Lemma 3.4.7, there exists a unique bounded, self-adjoint and nonnegative operator B_α over $L^2(\mathcal{D})$ such that $b_\alpha(\varphi,\psi) = \langle B_\alpha\varphi,\psi\rangle_{L^2}$ for all $\varphi,\psi \in C_c^\infty(\mathcal{D})$. The uniqueness of B_α and equation (3.7.33) yield $B_\alpha = \mathcal{E}_k^\alpha$, and thus $\mathcal{E}_k^\alpha$ is self-adjoint and nonnegative. □

Proof. (Lemma 3.4.9) $\underline{(i)}$: Let $n \in \mathbb{N}$ be such that $\lambda_n \neq 0$. Let $\varphi \in C_c^\infty(\mathcal{D})$. Then

$$\lambda_n\left(\int_{\mathcal{D}} \phi_n(x)\partial^\alpha\varphi(x)dx\right)^2 \leq \sum_{i=1}^{+\infty} \lambda_i\left(\int_{\mathcal{D}} \phi_i(x)\partial^\alpha\varphi(x)dx\right)^2$$
$$\leq \sum_{i=1}^{+\infty} \lambda_i \int_{\mathcal{D}\times\mathcal{D}} \phi_i(x)\phi_i(y)\partial^\alpha\varphi(x)\partial^\alpha\varphi(y)dxdy$$

$$\begin{aligned}
&\leq \int_{\mathcal{D}\times\mathcal{D}} k(x,y)\partial^\alpha\varphi(x)\partial^\alpha\varphi(y)dxdy \\
&\leq \int_{\mathcal{D}\times\mathcal{D}} \partial^{\alpha,\alpha}k(x,y)\varphi(x)\varphi(y)dxdy \\
&\leq \|\partial^{\alpha,\alpha}k\|_{L^2(\mathcal{D}\times\mathcal{D})}\|\varphi\|^2_{L^2(\mathcal{D})}. \qquad (3.7.35)
\end{aligned}$$

Therefore, from Lemma 3.2.1, $\partial^\alpha\phi_n \in L^2(\mathcal{D})$.
$\underline{(ii)}$: introduce the finite rank kernel k_n defined by

$$k_n(x,y) = \sum_{i=1}^n \lambda_i\phi_i(x)\phi_i(y). \qquad (3.7.36)$$

Then its mixed derivative $\partial^{\alpha,\alpha}k_n(x,y)$ is equal to $\sum_{i=1}^n \lambda_i\partial^\alpha\phi_i(x)\partial^\alpha\phi_i(y)$ in $L^2(\mathcal{D}\times\mathcal{D})$ and the associated operator $\mathcal{E}^\alpha_{k_n}$ is trace class, with

$$\begin{aligned}
\mathrm{Tr}(\mathcal{E}^\alpha_{k_n}) &= \sum_{j=1}^{+\infty}\langle\mathcal{E}^\alpha_{k_n}\phi_j,\phi_j\rangle_{L^2} = \sum_{j=1}^{+\infty}\sum_{i=1}^n \lambda_i\langle\partial^\alpha\phi_i,\phi_j\rangle^2_{L^2} \qquad (3.7.37)\\
&= \sum_{i=1}^n \lambda_i\sum_{j=1}^{+\infty}\langle\partial^\alpha\phi_i,\phi_j\rangle^2_{L^2} = \sum_{i=1}^n \lambda_i\|\partial^\alpha\phi_i\|^2_{L^2}. \qquad (3.7.38)
\end{aligned}$$

Now, observe that $\mathcal{E}^\alpha_{k_n} \leq \mathcal{E}^\alpha_k$ in the sense of the Loewner order. Indeed, let first $\varphi \in C^\infty_c(\mathcal{D})$:

$$\begin{aligned}
\langle(\mathcal{E}^\alpha_k - \mathcal{E}^\alpha_{k_n})\varphi,\varphi\rangle_{L^2} &= \langle(\mathcal{E}_k - \mathcal{E}_{k_n})\partial^\alpha\varphi,\partial^\alpha\varphi\rangle_{L^2} \\
&= \sum_{i=n+1}^{+\infty}\lambda_i\langle\phi_i,\partial^\alpha\varphi\rangle^2_{L^2} \geq 0. \qquad (3.7.39)
\end{aligned}$$

The density of $C^\infty_c(\mathcal{D})$ in $L^2(\mathcal{D})$ and the continuity of the quadratic form $f \mapsto \langle(\mathcal{E}^\alpha_k - \mathcal{E}^\alpha_{k_n})f,f\rangle_{L^2}$ over $L^2(\mathcal{D})$ yields indeed that $\mathcal{E}^\alpha_{k_n} \leq \mathcal{E}^\alpha_k$. Taking the trace :

$$\sum_{i=1}^n \lambda_i\|\partial^\alpha\phi_i\|^2_{L^2} = \mathrm{Tr}(\mathcal{E}^\alpha_{k_n}) = \sum_{j=1}^{+\infty}\langle\mathcal{E}^\alpha_{k_n}\phi_j,\phi_j\rangle_{L^2} \leq \sum_{j=1}^{+\infty}\langle\mathcal{E}^\alpha_k\phi_j,\phi_j\rangle_{L^2} = \mathrm{Tr}(\mathcal{E}^\alpha_k). \qquad (3.7.40)$$

Taking the limit when n goes to infinity yields $\sum_{i=1}^{+\infty}\lambda_i\|\partial^\alpha\phi_i\|^2_{L^2} \leq \mathrm{Tr}(\mathcal{E}^\alpha_k)$. Suppose now that $\mathrm{Tr}(\mathcal{E}^\alpha_k) < +\infty$. Equation (3.7.40) shows that the series of functions $\sum_i \lambda_i\partial^\alpha\phi_i \otimes \partial^\alpha\phi_i$ converges in norm in $L^2(\mathcal{D}\times\mathcal{D})$. Moreover, we check that it is equal to $\partial^{\alpha,\alpha}k$: taking $\varphi \in C^\infty_c(\mathcal{D}\times\mathcal{D})$, then

$$\int_{\mathcal{D}\times\mathcal{D}} k(x,y)\partial^{\alpha,\alpha}\varphi(x,y)dxdy$$

$$= \sum_i \lambda_i \int_{\mathcal{D}\times\mathcal{D}} \phi_i(x)\phi_i(y)\partial^{\alpha,\alpha}\varphi(x,y)dxdy \tag{3.7.41}$$

$$= \sum_i \lambda_i \int_{\mathcal{D}\times\mathcal{D}} \partial^\alpha\phi_i(x)\partial^\alpha\phi_i(y)\varphi(x,y)dxdy \tag{3.7.42}$$

$$= \int_{\mathcal{D}\times\mathcal{D}} \left(\sum_i \lambda_i \partial^\alpha\phi_i(x)\partial^\alpha\phi_i(y)\right)\varphi(x,y)dxdy. \tag{3.7.43}$$

We can then write, following the steps of equation (3.7.37)

$$\mathrm{Tr}(\mathcal{E}_k^\alpha) = \sum_{j=1}^{+\infty}\langle \mathcal{E}_k^\alpha\phi_j,\phi_j\rangle_{L^2} = \sum_{j=1}^{+\infty}\sum_i \lambda_i\langle\partial^\alpha\phi_i,\phi_j\rangle_{L^2}^2 = \sum_{i=1}^{+\infty}\lambda_i\|\partial^\alpha\phi_i\|_{L^2}^2. \tag{3.7.44}$$

Suppose now that $\sum_{i=1}^{+\infty}\lambda_i\|\partial^\alpha\phi_i\|_{L^2}^2 < +\infty$. Then as observed before, the series of functions $\sum_i \lambda_i\partial^\alpha\phi_i\otimes\partial^\alpha\phi_i$ converges in norm in $L^2(\mathcal{D}\times\mathcal{D})$, one verifies that $\partial^{\alpha,\alpha}k$ exists in $L^2(\mathcal{D})$ and is in fact given by

$$\partial^{\alpha,\alpha}k = \sum_i \lambda_i\partial^\alpha\phi_i\otimes\partial^\alpha\phi_i \quad \text{in} \quad L^2(\mathcal{D}\times\mathcal{D}). \tag{3.7.45}$$

Finally,

$$\sum_{i=1}^{+\infty}\lambda_i\|\partial^\alpha\phi_i\|_{L^2}^2 = \sum_{i=1}^{+\infty}\lambda_i\sum_j\langle\partial^\alpha\phi_i,\phi_j\rangle_{L^2}^2 \tag{3.7.46}$$

$$= \sum_j\sum_{i=1}^{+\infty}\lambda_i\left(\int_{\mathcal{D}}\partial^\alpha\phi_i(x)\phi_j(x)dx\right)^2 \tag{3.7.47}$$

$$= \sum_j\int_{\mathcal{D}\times\mathcal{D}}\sum_i\lambda_i\partial^\alpha\phi_i(x)\partial^\alpha\phi_i(y)\phi_j(x)\phi_j(y)dxdy \tag{3.7.48}$$

$$= \sum_j\langle\mathcal{E}_k^\alpha\phi_j,\phi_j\rangle_{L^2} = \mathrm{Tr}(\mathcal{E}_k^\alpha). \tag{3.7.49}$$

Therefore $\mathcal{E}_k^\alpha$ is trace class and $\mathrm{Tr}(\mathcal{E}_k^\alpha) = \sum_{i=1}^{+\infty}\lambda_i\|\partial^\alpha\phi_i\|_{L^2}^2$. For asymmetric derivatives, simply observe that for all $|\alpha|,|\beta|\leq m$,

$$\|\partial^\alpha\phi_i\otimes\partial^\beta\phi_i\|_2 = \|\partial^\alpha\phi_i\|_2\|\partial^\beta\phi_i\|_2 \leq \frac{\|\partial^\alpha\phi_i\|_2^2+\|\partial^\beta\phi_i\|_2^2}{2}. \tag{3.7.50}$$

Therefore the norm convergence of the series $\sum_{i\in\mathbb{N}^*}\lambda_i\|\partial^\alpha\phi_i\otimes\partial^\alpha\phi_i\|_{L^2}$ for all $|\alpha|\leq m$ implies that of all the series of the form $\sum_{i\in\mathbb{N}^*}\lambda_i\|\partial^\alpha\phi_i\otimes\partial^\beta\phi_i\|_{L^2}$ converge, provided that $|\alpha|\leq m$ and $|\beta|\leq m$. As previously, one then deduces that $\partial^{\alpha,\beta}k = \sum_{i=0}^{\infty}\lambda_i\partial^\alpha\phi_i\otimes\partial^\beta\phi_i$. □

Chapter 4

Covariance models and Gaussian process regression for the wave equation. Application to related inverse problems

---

This chapter corresponds to the paper [98] (currently under review), where the subsection 4.3.4 was added.

Abstract

In this article, we consider the general task of performing Gaussian process regression (GPR) on pointwise observations of solutions of the 3 dimensional homogeneous free space wave equation. In a recent article, we obtained promising covariance expressions tailored to this equation: we now explore the potential applications of these formulas. We first study the particular cases of stationarity and radial symmetry, for which significant simplifications arise. We next show that the true-angle multilateration method for point source localization, as used in GPS systems, is naturally recovered by our GPR formulas in the limit of the small source radius. Additionally, we show that this GPR framework provides a new answer to the ill-posed inverse problem of reconstructing initial conditions for the wave equation from a limited number of sensors, and simultaneously enables the inference of physical parameters from these data. We finish by illustrating this "physics informed" GPR on a number of practical examples.

Contents

4.1 Introduction 169
4.2 Background on Gaussian process regression 172
4.2.1 Random fields, Gaussian processes, positive definite functions 172
4.2.2 Gaussian process regression [166] 173
4.3 Gaussian process priors for the 3D wave equation . . 175
4.3.1 General solution to the wave equation 175
4.3.2 Gaussian process priors for the wave equation 175
4.3.3 The point source limit 186
4.3.4 Computational speedups 196
4.3.5 Initial condition reconstruction and error bounds . . . 200
4.4 Numerical experiments 203
4.4.1 Test case for $k_{\mathrm{u}}^{\mathrm{wave}}$ 207
4.4.2 Test case for $k_{\mathrm{v}}^{\mathrm{wave}} + k_{\mathrm{u}}^{\mathrm{wave}}$ 208
4.5 Conclusion and perspectives 213

4.1 Introduction

Machine learning techniques have proved time and again that they can provide efficient solutions to difficult problems in the presence of field data. A key element to this success is the incorporation of "expert knowledge" in the corresponding statistical models. In many practical applications, this knowledge takes the form of mathematical models which are sometimes already well understood. This is e.g. common when dealing with problems arising from physics, in which case the mathematical models often take the form of Partial Differential Equations (PDEs), such as the wave equation at hand in this article. Because of the broadness of the applications PDEs offer, large efforts have been devoted to studying and solving them, both theoretically [73] and numerically [93]. These equations impose very specific (yet often simple) structures on the observed data which can be very difficult to capture or mimic with general machine learning models.

In this article, we will focus on the linear 3 dimensional homogeneous free space wave equation. This equation is the prototype for describing simple 3D phenomena which propagate at finite speed; although particularly simple in the landscape of PDEs, it is in fact central for many applications emerging from different fields such as acoustics or electromagnetics. The homogeneity assumption is also commonly encountered in physics, when modelling conservation laws. Given that the main structures of the solutions of this PDE are well known, one may thus attempt to incorporate them in the machine learning models that work with such solutions.

The class of models we will deal with is that of Gaussian Process Regression (GPR), which is a Bayesian framework for function regression and interpolation [166]. It is especially adapted to performing inference in the presence of limited/scattered data, say measurements from a small number of scattered sensors. It is also a "kernel method", meaning that it is built upon a positive definite function, the kernel in question. In the language of Bayesian inference, GPR puts a *prior* probability distribution on a suitable function space in which the unknown function u is assumed to lie. This prior is then conditioned on available field data involving u thanks to Bayes' law, which in turn provides a *posterior* probability distribution from which statistical estimators related to u can be computed. The posterior expectation in particular plays the role of an approximant of u while the posterior covariance provides posterior error bounds. In the case of GPR, these prior and posterior distributions are in many ways generalizations to infinite dimensions of the multivariate normal distribution, and are fully specified by a mean and covariance functions. These priors are naturally obtained by modelling u as a sample path of a Gaussian process and we will thus say that we put a Gaussian

process (GP) prior over u. Imposing strict linear constraints on a GP prior as well as on the posterior expectation it provides is straightforward in principle; we will apply this observation to the case where the linear constraint is the homogeneous wave equation itself, as in [97].

Thus, we will first be concerned with building GP priors which incorporate *beforehand* the knowledge that the sought function is in fact a solution to the wave equation, thus drastically lowering the dimension of the function space upon which the prior is set. In practice, the main consequence will be that all the possible estimators of u provided by GPR will also be solutions to the same wave equation. Nevertheless, from a random field perspective, it is remarkable that this property will in fact also hold at the level of the sample paths of the GP, when the PDE is understood in the distributional sense ([97], Proposition 4.1). Those covariance formulas are particular cases of general ones first described in [97] (i.e. Chapter 2), which take the form of multidimensional convolutions against the PDE's Green's function. They were derived by putting generic Gaussian process priors over the initial conditions of the wave equation and propagating them through the solution map of the said equation, leading to "wave equation-tailored" covariance functions. Though interesting for theoretical purposes, these convolutions are very expensive to evaluate numerically, which constitutes a limitation for their use in GPR. In this article, we explore the particular cases where the initial condition priors are either stationary (Proposition 4.3.3) or radially symmetric (Proposition 4.3.5), as then notable simplifications can be obtained. We then study the case of point sources, for which we show that the task of recovering the position of the point source using multilateration (as e.g. in GPS systems, see [76]) is unexpectedly recovered by maximizing the likelihood attached to the GPR models we previously obtained for the wave equation, in the limit of the small source radius (Figure 4.1). We will also discuss applications in physical parameter estimation and initial condition reconstruction. Recovering the initial position in particular is the purpose of photoacoustic tomography (PAT, [10], Chapter 3), an exercise for which we will provide a simple proof of concept application, in the presence of radial symmetry.

Related literature The idea of solving and "learning" linear ODEs and PDEs thanks to GPR probably goes back to [90] and has been re-explored ever since. A large part of the subsequent works inspired by [90] deal with PDEs of the form $L(u) = f$ where f is a partially known *interior* source term: that is, f and u have the same input space. We will not be interested in this case as we will impose the strict condition that $f \equiv 0$, as is e.g. the case in PAT. In our case, the initial conditions will instead play the role of the source terms. For dealing with interior source terms, see [176, 9, 8, 175, 137, 163, 164] and [6, 7]

for subsequent applications to inhomogeneous wave equations. See also [36] for an alternative method applicable to nonlinear PDEs. Compared to these approaches, ensuring (deterministically) the homogeneity constraint $f = 0$ in the wave equation will allow us to drastically reduce the dimensionality of the problem of approximating u given scattered measurements of u.

Ensuring homogeneous PDE constraints on centered GPs is done by appropriately constraining its covariance kernel (Proposition 2.3.5 from Chapter 2). Such PDE constrained kernels have been explicitly built for a number of classical PDEs, namely: divergence-free vector fields [146, 182], curl-free vector fields [81, 182, 209, 109], the Laplace equation [179, 142, 5], Maxwell's equations [123], the heat equation in 1D [5] and 2D [86], Helmholtz' 2D equations [5], and linear solid mechanics [108]. See also [207] where generic PDE-constrained kernels are built under stationarity assumptions. For further discussions and references on PDE constrained random fields, we refer to Section 2.1 from Chapter 2. This article is the continuation of a previous work [97] (Chapter 2), where we described a covariance kernel tailored to the wave equation at hand in this article. In parallel with homoegeneous PDEs, [124, 94, 189] enforce homogeneous *boundary conditions* on the covariance kernel. We finish by mentioning that fine properties of a stochastic three dimensional wave equation are studied in [53]. The wave equation in [53] is not homogeneous, and because of the nonlinearity they consider, a precise investigation of the covariance function of the solution process is not considered.

The approach presented in this article falls in the field of Bayesian methods for solving PDE related inverse problems, the literature of which is extensive; see [195, 54, 45, 55] and the many references therein. However, the method we adopt here differs from the standard Bayesian inversion methods aforementioned in that we incorporate the PDE constraint *beforehand*, i.e. directly in the prior; the PDE does not only appear in the likelihood. See [151] for a point of view similar with that of the present article, which uses PDE-tailored GP priors for building optimal finite dimensional approximations of solution spaces of elliptic PDEs.

The inverse problems we will study deal with approximating the initial conditions of (4.3.1) as well as the related physical parameters (wave speed, source location and source size), given scattered measurements of the solution u. A general methodology for estimating the parameters of a linear PDE using GPR is described in [163], using the forward differential operator. Here we will rather use its inverse, i.e. the Green's function. The task of approximating the initial position in particular is the purpose of photoacoustic tomography (PAT), which is a technique commonly used e.g. in biomedical imaging [10]. See e.g. [119, 11] for details on the standard mathematical techniques and models used in PAT. Note that the solution is often assumed available on a

surface enclosing the source [216], in order to use Radon transforms or similar inversion formulas. Our method instead allows the sensors to be arbitrarily scattered. As the corresponding PAT problem becomes ill-posed, we do not aim for a full reconstruction of the initial conditions. Instead, we show that our method amounts to computing an orthogonal projection of the solution over a well-chosen finite dimensional space. Of course, the geometry of the sensor locations plays a crucial role in the accuracy of our model, but the reconstruction formula we introduce remains nonetheless independent of any underlying geometry assumptions. In the two dimensional setting, it is worth noting that [158] already showed that a GPR methodology based on Radon transforms could be set up for solving x-ray tomography problems in the presence of limited (scattered) data.

Organization of the paper For self-containment, section 4.2 is dedicated to reminders on (Gaussian) random fields and GPR. Section 4.3 is dedicated to the study of GP priors tailored to the wave equation. In section 4.4, we showcase some numerical applications of the previous section on wave equation data. We conclude in Section 4.5.

Notations Let $\mathcal{D}$ be a set, $m : \mathcal{D} \to \mathbb{R}$ and $k : \mathcal{D} \times \mathcal{D} \to \mathbb{R}$. Given $x \in \mathcal{D}$, k_x denotes the function $y \mapsto k(x, y)$. If $X = (x_1, ..., x_n)^T$ is a column vector in $\mathcal{D}^n$, we denote $m(X)$ the column vector such that $m(X)_i = m(x_i)$, $k(X, X)$ the square matrix such that $k(X, X)_{ij} = k(x_i, x_j)$ and given $x \in \mathcal{D}$, $k(X, x)$ the column vector such that $k(X, x)_i = k(x_i, x)$. The variables $(r, \theta, \phi), r \geq 0, \theta \in [0, \pi], \phi \in [0, 2\pi]$, denote spherical coordinates and S denotes the unit sphere of $\mathbb{R}^3$. We write $d\Omega = \sin\theta d\theta d\phi$ its surface differential element; $\gamma = (\sin\theta\cos\phi, \sin\theta\sin\phi, \cos\theta)^T \in S$ denotes the unit length vector parametrized by (θ, ϕ).

4.2 Background on Gaussian process regression

4.2.1 Random fields, Gaussian processes, positive definite functions

Let $\mathcal{D}$ be a set. A random field $(U(x))_{x\in\mathcal{D}}$ is a collection of random variables defined on the same probability space $(\Omega, \mathcal{F}, \mathbb{P})$. It is second order if for all $x \in \mathcal{D}$, $\mathbb{E}[U(x)^2] < +\infty$. Its sample paths are the deterministic functions $x \mapsto U(x)(\omega)$, given $\omega \in \Omega$. $(U(x))_{x\in\mathcal{D}}$ is a GP if for all $(x_1, ..., x_n) \in \mathcal{D}^n$, the law of $(U(x_1), ..., U(x_n))^T$ is a multivariate normal distribution. The law of a

GP is characterized by its mean and covariance functions ([107], Section 8), defined by $m(x) \coloneqq \mathbb{E}[U(x)]$ and $k(x,x') = \mathrm{Cov}(U(x),U(x')) = \mathbb{E}[U(x)U(x')] - m(x)m(x')$, and we write $(U(x))_{x\in\mathcal{D}} \sim GP(m,k)$. Given $\omega \in \Omega$, the associated sample path is the deterministic function $U_\omega : x \mapsto U(x)(\omega)$. The mean function can be chosen arbitrarily, but the covariance function has to be positive definite, which means that for all $(x_1,...,x_n) \in \mathcal{D}^n$, the matrix $(k(x_i,x_j))_{1\leq i,j\leq n}$ is non negative definite. The mathematical properties of the GP are encoded in the function k. Furthermore, there is a bijection between positive definite functions and covariance functions of centered GPs ([107], Theorem 8.2). We will thus focus on the design of positive definite kernels. A covariance kernels is *stationary* if $k(x,x')$ only depends on the increment $x - x'$: $k(x,x') = k_S(x-x')$ for some function k_S. Common examples of stationary kernels are the squared exponential and Matérn kernels [166]; see equation (4.4.1). Informally, if the covariance function of a GP is stationary, then its sample paths "look similar at all locations" ([166], p.4).

4.2.2 Gaussian process regression [166]

4.2.2.1 Kriging equations

GPs can be used for function interpolation. Let u be a function defined on $\mathcal{D}$ for which we know a dataset of values $B = \{u(x_1),...,u(x_n)\}$. Conditioning the law of a GP $(U(x))_{x\in\mathcal{D}} \sim GP(m,k)$ on the data B yields a second GP defined by $V(x) \coloneqq (U(x)|U(x_i) = u(x_i), i = 1,...,n)$. Its mean and covariance functions $\tilde{m}$ and $\tilde{k}$ are given by the so-called *Kriging* equations (4.2.1) and (4.2.2). Note $X = (x_1,...,x_n)^T$ and assume that $K(X,X)$ is invertible, then [166]

$$\begin{cases} \tilde{m}(x) &= m(x) + k(X,x)^T k(X,X)^{-1}(u(X) - m(X)), & (4.2.1) \\ \tilde{k}(x,x') &= k(x,x') - k(X,x)^T k(X,X)^{-1} k(X,x'). & (4.2.2) \end{cases}$$

The function $\tilde{m}$ is an estimator of u and for all x in $\mathcal{D}$, $\tilde{m}(x)$ can be used for predicting the value $u(x)$. By construction, for all observation points x_i, we have $\tilde{m}(x_i) = u(x_i)$ and $\tilde{k}(x_i,x_i) = 0$. If observing noisy data $U_i = U(x_i) + \varepsilon_i$ with $(\varepsilon_1,...,\varepsilon_n)^T \sim \mathcal{N}(0,\sigma^2 I_n)$ independent from U, one replaces $K(X,X)$ with $K(X,X) + \sigma^2 I$ in the Kriging equations and leaves the other terms $k(X,x)$ unchanged. This amounts to applying Tikhonov regularization on $k(X,X)$, which is also relevant for approximating equations (4.2.1) and (4.2.2) when $k(X,X)$ is ill-conditioned.

4.2.2.2 Tuning covariance kernels [166]

Covariance functions are usually chosen among a parametrized family of kernels $\{k_\theta, \theta \in \Theta \subset \mathbb{R}^q\}$. θ contains the *hyperparameters* of k_θ. One then attempts to find the value θ which fits best the observations $u_{obs} = (u_1, ..., u_n)^T$, the set of observations of u at locations $X = (x_1, ..., x_n)$. This is performed by maximizing the *marginal likelihood*, which is the probability density of the random vector $(U(x_1), ..., U(x_n))^T$ at point u_{obs}, given θ. Denote $p(u_{obs}|\theta)$ the associated marginal likelihood at θ, one searches for $\hat{\theta}$ such that $\hat{\theta} = \text{argmax}_{\theta\in\Theta} p(u_{obs}|\theta)$. Explicitly, assuming that $m \equiv 0$, then we have $(U(x_1), ..., U(x_n))^T \sim \mathcal{N}(0, k_\theta(X, X))$ and

$$p(u_{obs}|\theta) = \frac{1}{(2\pi)^{n/2} \det k_\theta(X, X)^{1/2}} e^{-\frac{1}{2} u_{obs}^T k_\theta(X,X)^{-1} u_{obs}}. \tag{4.2.3}$$

Equivalently, for noisy observations with identical noise standard deviation σ, set

$$\begin{aligned} \mathcal{L}(\theta, \sigma^2) :&= -2 \log p(u_{obs}|\theta) - n \log 2\pi \\ &= u_{\text{obs}}^T (k_\theta(X, X) + \sigma^2 I_n)^{-1} u_{\text{obs}} + \log \det(k_\theta(X, X) + \sigma^2 I_n). \end{aligned} \tag{4.2.4}$$

We call $\mathcal{L}(\theta, \sigma^2)$ the negative log marginal likelihood, and one may rather attempt to find $\hat{\theta}$ such that $\hat{\theta} = \arg\min_{\theta\in\Theta} \mathcal{L}(\theta, \sigma^2)$. Note that σ can also be interpreted as a hyperparameter and estimated through negative log marginal likelihood minimization.

4.2.2.3 The RKHS point of view

The Kriging equations (4.2.1) and (4.2.2) can alternatively be viewed as orthogonal projections of u in a suitable Hilbert space. Given a positive definite kernel k defined on a set $\mathcal{D}$, one may build a Reproducing Kernel Hilbert Space (RKHS) of functions defined on $\mathcal{D}$, which we denote by $\mathcal{H}_k$. The inner product of $\mathcal{H}_k$ verifies the reproducing property [212]: $\langle k(x, \cdot), k(x', \cdot)\rangle_{\mathcal{H}_k} = k(x, x')$. One may then formulate the following regularized interpolation problem [77, 212]

$$\inf_{v\in\mathcal{H}_k} ||v||_{\mathcal{H}_k} \quad \text{s.t.} \quad v(x_i) = u(x_i) \quad \forall i \in \{1, ..., n\}. \tag{4.2.5}$$

Then $\tilde{m}$ in equation (4.2.1) is the unique solution of (4.2.5). One can also show [212] that equation (4.2.1) amounts to $\tilde{m} = m + p_F(u - m)$, where p_F stands for the orthogonal projection operator on $F := \text{Span}(k(x_1, \cdot), ..., k(x_n, \cdot))$ with reference to the inner product of $\mathcal{H}_k$. If in particular $m \equiv 0$, then $\tilde{m} = p_F(u)$. Likewise, equation (4.2.2) amounts to $\tilde{k}(x, \cdot) = P_{F^\perp}(k(x, \cdot))$. Viewing the

Kriging mean as an orthogonal projection over a finite dimensional deterministic space is reminiscent of Fourier series or Galerkin reconstruction approaches.

4.3 Gaussian process priors for the 3D wave equation

4.3.1 General solution to the wave equation

Denote the 3D Laplace operator $\Delta = \partial^2_{xx} + \partial^2_{yy} + \partial^2_{zz}$ and the d'Alembert operator with the box symbol, $\Box = c^{-2}\partial^2_{tt} - \Delta$ with constant wave speed $c > 0$. Consider then the following initial value problem in the free space $\mathbb{R}^3$

$$\begin{cases} \Box w & = 0 & \forall (x,t) \in \mathbb{R}^3 \times \mathbb{R}^*_+, \\ w(x,0) & = u_0(x), \;\; \partial_t w(x,0) = v_0(x) & \forall x \in \mathbb{R}^3. \end{cases} \tag{4.3.1}$$

The solution of this problem is unique in the distributional sense ([69], p. 164). It can be extended to all $t \in \mathbb{R}$ and is represented as follow ([69], p. 295)

$$w(x,t) = (F_t * v_0)(x) + (\dot{F}_t * u_0)(x) \qquad \forall (x,t) \in \mathbb{R}^3 \times \mathbb{R}. \tag{4.3.2}$$

$(F_t)_{t\in\mathbb{R}}$ is the Green's function of the wave equation ([68], p. 202), and is a family of singular measures. $\dot{F}_t$ is its "time derivative" ([69], equation (18.16) p. 297), understood as a continuous linear form over $C^1(\mathbb{R}^3)$. Explicitly, F_t and $\dot{F}_t$ are given by

$$F_t = \frac{\sigma_{c|t|}}{4\pi c^2 t}, \qquad \text{and} \qquad \langle \dot{F}_t, \varphi \rangle_{C^1(\mathbb{R}^3)', C^1(\mathbb{R}^3)} = \partial_t \int_{\mathbb{R}^3} \varphi(x) F_t(dx). \tag{4.3.3}$$

where σ_R is the surface measure of the sphere of center 0 and radius R. If $u_0 \in \mathcal{C}^1(\mathbb{R}^3)$ and $v_0 \in \mathcal{C}^0(\mathbb{R}^3)$, then w as defined in (4.3.2) is a pointwise defined function given by the Kirschoff formula ([73], p. 72), which writes in spherical coordinates:

$$w(x,t) = \int_S t v_0(x - c|t|\gamma) + u_0(x - c|t|\gamma) - c|t|\gamma \cdot \nabla u_0(x - c|t|\gamma) \frac{d\Omega}{4\pi}. \tag{4.3.4}$$

4.3.2 Gaussian process priors for the wave equation

4.3.2.1 General covariance structure

Suppose that the initial conditions u_0 and v_0 are realizations of two independent centered Gaussian processes, $U^0 \sim GP(0, k_{\mathrm{u}})$ and $V^0 \sim GP(0, k_{\mathrm{v}})$.

That is, $u_0 = U^0_\omega$ and $v_0 = V^0_\omega$ for some $\omega \in \Omega$. This assumption is relevant e.g. when u_0 and v_0 are unknown, in which case U^0 and V^0 are interpreted as GP priors over u_0 and v_0. We will assume that the sample paths of V^0 are continuous and that of U^0 are continuously differentiable, in order to use the formula (4.3.4) (see Section 2.4.2 from Chapter 2 for more details and discussions on these assumptions). By solving (4.3.1), one obtains a time-space random field $W(x,t)$ defined by

$$W(x,t) : \Omega \ni \omega \longmapsto (F_t * V^0_\omega)(x) + (\dot{F}_t * U^0_\omega)(x). \tag{4.3.5}$$

The next result, which describes the covariance function of W, is the starting point of this paper.

Proposition 4.3.1 ([97], Proposition 4.1, i.e. Proposition 2.4.1)**.** *Denote $z = (x,t)$ and $z' = (x',t')$ the space-time variables. Let k_{u} (resp. k_{v}) be a positive definite function such that the sample paths of the associated GP are continuously differentiable (resp. continuous). In particular, $k_{\mathrm{v}} \in C^0(\mathbb{R}^3 \times \mathbb{R}^3)$ and $k_{\mathrm{u}}(x,\,.), k_{\mathrm{u}}(.\,,x') \in C^1(\mathbb{R}^3)$ for all $x, x' \in \mathbb{R}^3$. Define then the two functions*

$$k^{\mathrm{wave}}_{\mathrm{v}}(z,z') = [(F_t \otimes F_{t'}) * k_{\mathrm{v}}](x,x'), \tag{4.3.6}$$
$$k^{\mathrm{wave}}_{\mathrm{u}}(z,z') = [(\dot{F}_t \otimes \dot{F}_{t'}) * k_{\mathrm{u}}](x,x'). \tag{4.3.7}$$

(i) Then $(W(z))_{z\in\mathbb{R}^3\times\mathbb{R}}$ is a centered GP whose covariance kernel is given by

$$k_{\mathrm{w}}(z,z') = k^{\mathrm{wave}}_{\mathrm{v}}(z,z') + k^{\mathrm{wave}}_{\mathrm{u}}(z,z'). \tag{4.3.8}$$

(ii) Conversely, any centered second order random field with a.s. continuous sample paths and with covariance function k_W has its sample paths solution of the wave equation (4.3.1) for some u_0 and v_0, in the sense of distributions, almost surely.

The proof of equation (4.3.8) relies on Fubini's theorem, to permute $\mathbb{E}[\cdot]$ and integrals over the sphere S (see equation (4.3.4)). To apply Fubini's theorem, one needs the maps $(x,\omega) \mapsto V(x)(\omega)$ and $(x,\omega) \mapsto \partial_{x_i} U(x)(\omega), i \in \{1,2,3\}$ to be measurable. In our case this property holds, up to a modification, because the random fields V and $\partial_{x_i} U(x)$ are assumed a.s. continuous (see Section 2.2.1.2 for further discussions). Complete expressions of equations (4.3.6) and (4.3.7) in terms of integrals of k_{u}, its first derivatives and k_{v} over the unit sphere can be found in equations (2.4.16) and (2.4.17), Chapter 2. They are derived from the Kirschoff formula (4.3.4).

Remark 4.3.2. A more general result holds if one drops the GP assumption over $(V^0(x))_{x\in\mathbb{R}^3}$ and $(U^0(x))_{x\in\mathbb{R}^3}$. If we only assume that V^0 (resp. U^0) is a

centered second order random field with a.s. continuous (resp. a.s. continuously differentiable) sample paths and covariance function k_{v} (resp. k_{u}), then W in equation (4.3.5) is well-defined, centered, and its covariance function is k_{w} in equation (4.3.8). Only the Gaussianity of W is lost. Indeed, the proof of Proposition 4.3.1 from Chapter 2 only uses the aforementioned relaxed assumptions over U^0 and V^0 to obtain the formula (4.3.8). The Gaussianity of U^0 and V^0 is only used to show that W is also a GP. Non Gaussian (say log normal or exponential) priors are relevant e.g. for modelling nonnegative initial conditions. They are especially interesting for the wave equation because the nonnegativity of the measure F_t yields the following remarkable positivity preserving property: if $u_0 = 0$ and $v_0 \geq 0$, then w in equation (4.3.2) verifies $w(x,t) \geq 0$ for all $t \geq 0$.

Observe now that for all $z = (x,t) \in \mathbb{R}^3 \times \mathbb{R}$, we have $\Box k_{\mathrm{w}}(z,\cdot) = 0$. Using equation (4.2.1), one then deduces that all the Kriging mean obtained using the kernel k_{w} always verifies $\Box \tilde{m} = 0$. For this reason, we call WIGPR ("Wave equation informed GPR") the act of performing GPR with a covariance kernel of the form (4.3.8). Note that the inheritance of the distributional PDE constraint over the sample paths of the conditioned GP is proved in [97], Proposition 3.8 (i.e., Proposition 2.3.9 from Chapter 2).

In applications, a first obstacle of WIGPR is the cost of the evaluation of expressions (4.3.6) and (4.3.7), both in computational resources and in memory. Indeed, their computation requires 4-dimensional convolutions. This motivates the study of special cases of expressions (4.3.6) and (4.3.7). In the next paragraphs, we focus on stationarity and radial symmetry assumptions.

4.3.2.2 Stationary initial conditions

Many standard covariance kernels used for GPR are stationary [166]. More generally, for general centered second order random fields, this covariance structure corresponds to *wide sense stationarity*. Because of the popularity of both these GPR and random field models, we study equation (4.3.6) when k_{v} is stationary. For conciseness, we restrict ourselves to the case where $u_0 = 0$, i.e. $k_{\mathrm{u}} = 0$.

Proposition 4.3.3. *Assume that k_{v} is continuous and stationary: $k_{\mathrm{v}}(x,x') = k_S(x-x')$.*
(i) Then $k_{\mathrm{v}}^{\mathrm{wave}}$ is stationary in space and

$$[(F_t \otimes F_{t'}) * k_{\mathrm{v}}](x,x') = (F_t * F_{t'} * k_S)(x-x'). \tag{4.3.9}$$

(ii) Moreover, the measure $F_t * F_{t'}$ is absolutely continuous over $\mathbb{R}^3$. Denoting $|h|$ the Euclidean norm of $h \in \mathbb{R}^3$ and identifying $F_t * F_{t'}$ with its density, we

have

$$(F_t * F_{t'})(h) = \frac{sgn(t)sgn(t')}{8\pi c^2|h|}\mathbb{1}_{\left[c\left||t|-|t'|\right|,c(|t|+|t'|)\right]}(|h|). \tag{4.3.10}$$

Proof of Proposition 4.3.3. (i) : Assume for simplicity that $c = 1$. Using the definition of the convolution against the measure $F_t \otimes F_{t'}$ (see e.g. [202], Exercise 26.1 p. 282),

$$\begin{aligned}[(F_t \otimes F_{t'}) * k_{\mathrm{v}}](x, x') &= \int_{\mathbb{R}^3\times\mathbb{R}^3} k(x - s_1, x' - s_2)dF_t(s_1)dF_{t'}(s_2) \\ &= \int_{\mathbb{R}^3\times\mathbb{R}^3} k_S(x - x' - s_1 + s_2)dF_t(s_1)dF_{t'}(s_2).\end{aligned}$$

But S is invariant under the change of variable $S \ni \gamma \longmapsto -\gamma$ and thus for any continuous function f, $\int_{\mathbb{R}^3} f(s_2)dF_{t'}(s_2) = \int_{\mathbb{R}^3} f(-s_2)dF_{t'}(s_2)$. This yields

$$[(F_t \otimes F_{t'}) * k_{\mathrm{v}}](x, x') = \int_{\mathbb{R}^3\times\mathbb{R}^3} k_S(x - x' - s_1 - s_2)dF_t(s_1)dF_{t'}(s_2).$$

Applying the definition of the convolution of measures (see e.g. [29], p. 101) to $F_t * F_{t'}$,

$$\begin{aligned}(F_t * F_{t'} * k_S)(h) &= \int_{\mathbb{R}^3} k_S(h - s)d(F_t * F_{t'})(s) \\ &= \int_{\mathbb{R}^3}\int_{\mathbb{R}^3} k_S(h - s_1 - s_2)dF_t(s_1)dF_{t'}(s_2).\end{aligned}$$

Setting $h = x - x'$ finishes the proof of Point (i).
(ii) : Without loss of generality we assume that $c = 1$. The computation is carried out in the Fourier domain. Recall that F_t and $\dot{F}_t$ are tempered distributions whose Fourier transforms are given by ([69], equation (18.12) p. 294)

$$\mathcal{F}(F_t)(\xi) = \frac{\sin(ct|\xi|)}{c|\xi|} \quad \text{and} \quad \mathcal{F}(\dot{F}_t)(\xi) = \cos(ct|\xi|). \tag{4.3.11}$$

We then obtain that ([69], Theorem 14.33)

$$\begin{aligned}\mathcal{F}(F_t * F_{t'})(\xi) &= \mathcal{F}(F_t)(\xi)\mathcal{F}(F_{t'})(\xi) \\ &= \frac{\sin(t|\xi|)\sin(t'|\xi|)}{|\xi|^2} = \frac{\cos(a|\xi|) - \cos(b|\xi|)}{2|\xi|^2}.\end{aligned} \tag{4.3.12}$$

with $a = t - t', b = t + t$. We then compute the inverse Fourier transform of the quantity above. Let $h \in \mathbb{R}^3$. In spherical coordinates, noting the unit

vectors $\gamma_h = h/|h|$ and $\gamma = \xi/|\xi| = \xi/r$, we define f_a by

$$f_a(h) = \int_{\mathbb{R}^3} e^{i\langle h,\xi\rangle} \frac{\cos(a|\xi|)}{|\xi|^2} d\xi = \int_0^{+\infty} \int_0^{2\pi} \int_0^{\pi} e^{ir\langle h,\gamma\rangle} \frac{\cos(ar)}{r^2} r^2 \sin\theta d\theta d\phi dr \tag{4.3.13}$$

$$= \int_0^{+\infty} \cos(ar) \int_S e^{ir|h|\langle \gamma,\gamma_h\rangle} d\Omega dr.$$

Above, we used the spherical coordinate change $\xi = r\gamma, d\xi = r^2 \sin\theta d\theta d\phi dr$. We now make use of radial symmetry in the interior integral, as follow. Note e_3 the third vector of the canonical basis of $\mathbb{R}^3$ and M an orthogonal matrix such that $M\gamma_h = e_3$. We perform the change of variable $\gamma' = M\gamma$, using that $MS := \{M\gamma, \gamma \in S\} = S$ and that the corresponding Jacobian is equal to 1:

$$\int_S e^{ir|h|\langle \gamma,\gamma_h\rangle} d\Omega = \int_{MS} e^{ir|h|\langle M^T\gamma',\gamma_h\rangle} d\Omega' = \int_S e^{ir|h|\langle \gamma',M\gamma_h\rangle} d\Omega' \tag{4.3.14}$$

$$= \int_S e^{ir|h|\langle \gamma,e_3\rangle} d\Omega = 2\pi \int_0^{\pi} e^{ir|h|\cos(\theta)} \sin(\theta) d\theta$$

$$= 2\pi \left[-\frac{e^{ir|h|\cos(\theta)}}{ir|h|} \right]_0^{\pi} = 2\pi \frac{e^{ir|h|} - e^{-ir|h|}}{ir|h|} = 4\pi \frac{\sin(r|h|)}{r|h|}, \tag{4.3.15}$$

and thus

$$f_a(h) = 4\pi \int_0^{\infty} \frac{\cos(ar)\sin(|h|r)}{r|h|} dr = 4\pi \int_0^{\infty} \frac{\sin((|h|+a)r) + \sin((|h|-a)r)}{2r|h|} dr$$

$$= \frac{2\pi}{|h|} \int_0^{\infty} \frac{\sin(\alpha r)}{r} + \frac{\sin(\beta r)}{r} dr, \tag{4.3.16}$$

with $\alpha = |h| + a, \beta = |h| - a$. Finally, we have the Dirichlet integral

$$\int_0^{\infty} \frac{\sin(\alpha r)}{r} dr = \mathrm{sgn}(\alpha) \frac{\pi}{2}. \tag{4.3.17}$$

We define the function f_b exactly as f_a, and compute it by replacing a by b in every step above. Putting (4.3.12), (4.3.16) and (4.3.17) together, the inverse Fourier transform of $\mathcal{F}(F_t * F_{t'})$ is an absolutely continuous measure whose density f is given by

$$f(h) = \frac{1}{(2\pi)^3} \frac{1}{2} \big(f_a(h) - f_b(h)\big) = \frac{1}{16\pi|h|} \Big(\mathrm{sgn}(|h| + t - t') + \mathrm{sgn}(|h| - t + t') \tag{4.3.18}$$

$$- \mathrm{sgn}(|h| + t + t') - \mathrm{sgn}(|h| - t - t') \Big)$$

$$=: \frac{1}{16\pi|h|} K(|h|, t, t'). \tag{4.3.19}$$

$K(|h|, t, t')$ is defined in equation (4.3.19). Note that $K(|h|, -t, t') = -K(|h|, t, t')$ and likewise with t', thus $K(|h|, t, t') = \mathrm{sgn}(t)\mathrm{sgn}(t')K(|h|, T, T')$ with $T = |t|, T' = |t'|$. Using the symmetries in t and t' in equation (4.3.18) and the fact that $\mathrm{sgn}(s) = 1$ if $s > 0$, we obtain

$$\begin{aligned} K(|h|, T, T') = &\ \mathrm{sgn}(|h| + |T - T'|) + \mathrm{sgn}(|h| - |T - T'|) \\ &- \mathrm{sgn}(|h| + T + T') - \mathrm{sgn}(|h| - T - T') \\ = &\ 1 + \mathrm{sgn}(|h| - |T - T'|) - 1 - \mathrm{sgn}(|h| - T - T') \\ = &\ \mathrm{sgn}(|h| - |T - T'|) - \mathrm{sgn}(|h| - T - T'). \end{aligned} \tag{4.3.20}$$

From equation (4.3.20), one checks that $K(|h|, T, T') = 0$ if $|h| < |T - T'|$ or $|h| > T + T'$ and $K(|h|, T, T') = 2$ if $|T - T'| < |h| < T + T'$. Thus, $K(|h|, T, T') = 2 \times \mathbb{1}_{[|T-T'|, T+T']}(|h|)$. Identifying the measure $F_t * F_{t'}$ with its density, we obtain

$$(F_t * F_{t'})(h) = \frac{\mathrm{sgn}(t)\mathrm{sgn}(t')}{8\pi|h|} \mathbb{1}_{\left[\left||t|-|t'|\right|, |t|+|t'|\right]}(|h|). \tag{4.3.21}$$

which concludes the proof. □

If k_{u} is assumed zero, and if V^0 only satisfies the minimal assumptions of Remark 4.3.2 as well as wide sense stationarity, then the covariance expression (4.3.9) still holds for the solution process W in equation (4.3.5). Formally, one can obtain similar formulas for $k_{\mathrm{u}}^{\mathrm{wave}}$ by differentiating the formulas above with respect to t and t', as $\dot{F}_t = \partial_t F_t$ ($\dot{F}_t * \dot{F}_{t'}$ will only be a generalized function though).

We underline that the proof of Point (ii) in Proposition 4.3.3 makes use of the specificities of the dimension 3. First in equation (4.3.13), where the scalars r^2 cancel each other out; second in (4.3.15) where an exact antiderivative of the integrated function can be computed. None of these two simplifications hold in higher dimension or in dimension 2, and formulas as simple as equation (4.3.10) are not expected to hold.

Remark 4.3.4. Expression (4.3.10) with $h = x - x'$ is the covariance kernel of the solution process U with initial condition the "formal" white noise process V^0 with the stationary Dirac delta covariance kernel $k_{\mathrm{v}}(x, x') = \delta_0(x - x')$:

$$[(F_t \otimes F_{t'}) * k_{\mathrm{v}}](x, x') = (F_t * F_{t'} * \delta_0)(x - x') = (F_t * F_{t'})(x - x'). \tag{4.3.22}$$

Somewhat surprisingly, although formula (4.3.10) yields a summable function over $\mathbb{R}^3$ when t and t' are fixed, it can not be used for practical computations

as the diagonal terms of the related covariance matrices are all singularities: $(F_t * F_t)(0) = +\infty$... Yet, formula (4.3.10) may be used together with explicit kernels k_S to yield usable expressions. For instance, if $k_{\mathrm{v}}(x, x') = k_S(x - x') = C\exp(-|x - x'|^2/2L^2)$, we state without proof that

$$(F_t * F_{t'} * k_S)(h) = \\ \operatorname{sgn}(tt')\frac{\sqrt{2\pi}}{2}\frac{CL^3}{c^2}\left(\frac{\Phi\left(\frac{R_1+|h|}{L}\right) - \Phi\left(\frac{R_1-|h|}{L}\right)}{2|h|} - \frac{\Phi\left(\frac{R_2+|h|}{L}\right) - \Phi\left(\frac{R_2-|h|}{L}\right)}{2|h|}\right). \tag{4.3.23}$$

where $h = x - x'$, $\Phi(s) = (2\pi)^{-1/2}\int_{-\infty}^{s}\exp(-t^2/2)dt$, $R_1 = c\big||t| - |t'|\big|$, $R_2 = c(|t| + |t'|)$. Such a kernel always takes finite values: when h goes to 0, the above formula reduces to well defined derivatives.

Although these formulas are interesting in their own right, the study of propagation phenomena is usually done thanks to compactly supported initial conditions, which can never be modelled with wide sense stationary random fields. We partially deal with compactly supported initial conditions in Section 4.3.2.3, within the context of radial symmetry.

4.3.2.3 Radially symmetric initial conditions

Assume that the sample paths of the process V^0 enjoy radial symmetry around some $x_0 \in \mathbb{R}^3$. This can be expressed in terms of differential operators in (r, θ, ϕ), the spherical coordinate system around x_0:

$$\mathbb{P}(\{\omega \in \Omega : \partial_\theta V^0_\omega = 0\}) = 1, \quad \text{and} \quad \mathbb{P}(\{\omega \in \Omega : \partial_\phi V^0_\omega = 0\}) = 1. \tag{4.3.24}$$

Then by Proposition 2.3.5 of from Chapter 2, k_{v} verifies, in the sense of distributions,

$$\forall x \in \mathcal{D}, \quad \partial_\theta(k_{\mathrm{v}}(x, \cdot)) = 0 \quad \text{and} \quad \partial_\phi(k_{\mathrm{v}}(x, \cdot)) = 0. \tag{4.3.25}$$

Thus, there exists a function k^0_{v} defined on $\mathbb{R}_+ \times \mathbb{R}_+$ such that $k_{\mathrm{v}}(x, x') = k^0_{\mathrm{v}}(r^2, r'^2)$, with $r = |x|$, $r' = |x'|$ (directly using the squares r^2 and r'^2 will simplify computations later on). Similarly, assume that the sample paths of U^0 exhibit radial symmetry and write $k_{\mathrm{u}}(x, x') = k^0_{\mathrm{u}}(r^2, r'^2)$. Because of the generality of Proposition 4.3.1 from Chapter 2, the Gaussianity of V^0 and U^0 are not required. Furthermore, the same theorem states that equations (4.3.24) and (4.3.25) are in fact equivalent. From the radial representations of k_{v} and k_{u}, we can deduce the following convolution-free formulas for $k^{\mathrm{wave}}_{\mathrm{v}}$ and $k^{\mathrm{wave}}_{\mathrm{u}}$:

Proposition 4.3.5. *Set* $K_{\mathrm{v}}(r,r') = \int_0^r \int_0^{r'} k_{\mathrm{v}}^0(s,s')dsds'$. *Then for all* $z = (x,t) \in \mathbb{R}^3 \times \mathbb{R}$ *and* $z' = (x',t') \in \mathbb{R}^3 \times \mathbb{R}$,

$$k_{\mathrm{v}}^{\mathrm{wave}}(z,z') = \frac{sgn(tt')}{16c^2rr'} \sum_{\varepsilon,\varepsilon' \in \{-1,1\}} \varepsilon\varepsilon' K_{\mathrm{v}}\big((r+\varepsilon c|t|)^2, (r'+\varepsilon' c|t'|)^2\big), \tag{4.3.26}$$

$$k_{\mathrm{u}}^{\mathrm{wave}}(z,z') = \frac{1}{4rr'} \sum_{\varepsilon,\varepsilon' \in \{-1,1\}} (r+\varepsilon c|t|)(r'+\varepsilon' c|t'|) \times k_{\mathrm{u}}^0\big((r+\varepsilon c|t|)^2, (r'+\varepsilon' c|t'|)^2\big). \tag{4.3.27}$$

Proof. Without loss of generality, we assume that $c = 1$ and $x_0 = 0$. We first derive expression (4.3.26). Let f be a function defined on $\mathbb{R}_+$ and g the function defined on $\mathbb{R}^3$ by $g(x) = f(|x|^2)$. Let F be an antiderivative of f and let $x \in \mathbb{R}^3$. As in (4.3.14), let M be an orthogonal matrix such that $M(x/|x|) = e_3$ and use the change of variable $\gamma' = M\gamma$. As $MS = S$, we have

$$\begin{aligned}
(F_t * g)(x) &= \frac{1}{4\pi t} \int_S g(x - t\gamma) t^2 d\Omega = \frac{t}{4\pi} \int_S f(|x - t\gamma|^2) d\Omega \\
&= \frac{t}{4\pi} \int_S f(|x|^2 + t^2 - 2|t|\langle x, \gamma\rangle) d\Omega \\
&= \frac{t}{4\pi} \int_{MS} f\left(|x|^2 + t^2 - 2|t||x|\left\langle \frac{x}{|x|}, M^T\gamma' \right\rangle\right) d\Omega' \\
&= \frac{t}{4\pi} \int_S f(|x|^2 + t^2 - 2|t||x|\langle e_3, \gamma\rangle) d\Omega \\
&= \frac{t}{4\pi} \int_{\phi=0}^{2\pi} \int_{\theta=0}^{\pi} f(|x|^2 + t^2 - 2|t||x|\cos(\theta)) \sin(\theta) d\theta d\phi \\
&= \frac{t}{2} \int_{\theta=0}^{\pi} f(|x|^2 + t^2 - 2|t||x|\cos(\theta)) \sin(\theta) d\theta \\
&= \frac{t}{4|x||t|} \Big[F(|x|^2 + t^2 - 2|t||x|\cos(\theta)) \Big]_{\theta=0}^{\theta=\pi} \\
&= \frac{\mathrm{sgn}(t)}{4|x|} \Big(F((|x| + |t|)^2) - F((|x| - |t|)^2) \Big) \\
&= \frac{\mathrm{sgn}(t)}{4|x|} \sum_{\varepsilon \in \{-1,1\}} \varepsilon F((|x| + \varepsilon|t|)^2).
\end{aligned} \tag{4.3.28}$$

Introduce now the functions

$$k_0^1(r,r') \coloneqq \int_0^{r'} k_0(r,s)ds \quad \text{and} \quad K_{\mathrm{v}}(r,r') \coloneqq \int_0^r \int_0^{r'} k(s,s')ds'ds. \tag{4.3.29}$$

We apply twice result (4.3.28) on k_{v}: first by setting $g(x') = k_0(|x-t\gamma|^2, |x'|^2)$ where $x - t\gamma$ is fixed, which integrates to $F(s) = k_0^1(|x - t\gamma|^2, s)$. Second, by setting $g(x) = k_0^1(|x|^2, (|x'|+\varepsilon|t'|)^2)$ where $|x'|+\varepsilon'|t'|$ is fixed, which integrates to $F(s) = K_{\mathrm{v}}(s, (|x'| + \varepsilon'|t'|)^2)$. In detail, we obtain

$$\begin{aligned}
[(F_t \otimes F_{t'}) * k_{\mathrm{v}}](x, x') &= \frac{1}{4\pi t}\frac{1}{4\pi t'}\int_S\int_S k_0(|x - t\gamma|^2, |x' - t'\gamma'|^2)t'^2 d\Omega' t^2 d\Omega \\
&= \frac{1}{4\pi t}\frac{\mathrm{sgn}(t')}{4|x'|}\int_S \sum_{\varepsilon' \in \{-1,1\}} \varepsilon' k_0^1(|x - t\gamma|^2, (|x'| + \varepsilon'|t'|)^2)t^2 d\Omega \\
&= \frac{\mathrm{sgn}(tt')}{16rr'} \sum_{\varepsilon,\varepsilon' \in \{-1,1\}} \varepsilon\varepsilon' K_{\mathrm{v}}\big((r + \varepsilon|t|)^2, (r' + \varepsilon'|t'|)^2\big).
\end{aligned} \tag{4.3.30}$$

We can then use this result to compute

$$[(\dot{F}_t \otimes \dot{F}_{t'}) * k_{\mathrm{u}}](x, x') = \partial_t \partial_{t'} [(F_t \otimes F_{t'}) * k_{\mathrm{u}}](x, x'). \tag{4.3.31}$$

First, we compute it for $t \neq 0$ and $t' \neq 0$ by differentiating (4.3.30) with reference to t and t', using that for $t \neq 0$, $d|t|/dt = \mathrm{sgn}(t)$ and $d\mathrm{sgn}(t)/dt = 0$. This yields

$$\begin{aligned}
&[(\dot{F}_t \otimes \dot{F}_{t'}) * k_{\mathrm{u}}](x, x') \\
&\quad = \frac{1}{4rr'} \sum_{\varepsilon,\varepsilon' \in \{-1,1\}} (r + \varepsilon|t|)(r' + \varepsilon'|t'|) k_{\mathrm{u}}^0\big((r + \varepsilon|t|)^2, (r' + \varepsilon'|t'|)^2\big).
\end{aligned} \tag{4.3.32}$$

For the case where either $t = 0$ or $t' = 0$, note first from equation (4.3.11) that $\mathcal{F}(\dot{F}_0)(\xi) = 1$ and thus $\dot{F}_0 = \delta_0$, the Dirac mass at 0, which is the neutral element for the convolution. Therefore, when we have both $t = 0$ and $t' = 0$:

$$[(\dot{F}_0 \otimes \dot{F}_0) * k_{\mathrm{u}}](x, x') = [(\delta_0 \otimes \delta_0) * k_{\mathrm{u}}](x, x') = [\delta_{(0,0)} * k_{\mathrm{u}}](x, x') = k_{\mathrm{u}}(x, x').$$

which is also the result provided by (4.3.32) evaluated at $t = t' = 0$. When $t' = 0$ and $t \neq 0$, we still have $d|t|/dt = \mathrm{sgn}(t)$ and $d\mathrm{sgn}(t)/dt = 0$, yielding

$$\begin{aligned}
[(\dot{F}_t \otimes \dot{F}_0) * k_{\mathrm{u}}](x, x') &= [(\dot{F}_t \otimes \delta_0) * k_{\mathrm{u}}](x, x') = \partial_t [(F_t \otimes \delta_0) * k_{\mathrm{u}}](x, x') \\
&= \partial_t \int_{\mathbb{R}^3}\int_{\mathbb{R}^3} k_{\mathrm{u}}^0(|x - y|^2, |x' - y'|^2) F_t(dy)\delta_0(dy') \\
&= \partial_t \frac{1}{4\pi t}\int_S k_{\mathrm{u}}^0(|x - t\gamma|^2, |x'|^2)t^2 d\Omega \\
&= \partial_t \frac{\mathrm{sgn}(t)}{4r} \sum_{\varepsilon \in \{-1,1\}} \varepsilon k_0^1((r + \varepsilon|t|)^2, |x'|^2)
\end{aligned}$$

$$= \frac{1}{2r} \sum_{\varepsilon \in \{-1,1\}} (r + \varepsilon|t|) k_{\mathrm{u}}^0((r + \varepsilon|t|)^2, |x'|^2).$$

which is also the result provided by (4.3.32) evaluated at $t' = 0$. The same arguments apply to show that expression (4.3.32) is valid when $t = 0$ and $t' \neq 0$. Therefore the expression (4.3.32) is valid whatever the value of $t, t' \in \mathbb{R}$. □

The expressions (4.3.26) and (4.3.27) are interesting in that they are much easier and faster to compute than (4.3.6) and (4.3.7), which require to compute convolutions.

4.3.2.4 Compactly supported initial conditions

Suppose that v_0 is compactly supported on a ball $B(x_0, R)$. The Strong Huygens Principle for the 3 dimensional wave equation ([73], p. 80) states that $F_t * v_0$ is supported on the spherical shell $B(x_0, R + c|t|) \setminus B(x_0, (R - c|t|)_+)$, where $x_+ := \max(0, x)$. From a GP modelling perspective, assuming that $\mathrm{Supp}(V^0) \subset B(x_0, R)$ amounts to imposing that $V^0(x) = 0$ *a.s.* if $x \notin B(x_0, R)$. This is equivalent to $\mathrm{Var}(V^0(x)) = k_{\mathrm{v}}(x, x) = 0$ since V^0 is assumed centered. The same reasoning in terms of support can be applied to u_0 and U^0. In the next proposition, we explore the consequences of such compactness assumptions on the radial formulas (4.3.26) and (4.3.27). The new formulas are readily deduced from Proposition 4.3.5, but we state them on their own as they are the ones used in Section 4.4.

Proposition 4.3.6. *Let $R_{\mathrm{v}} > 0$ and $R_{\mathrm{u}} > 0$. Let $\alpha \in (0, 1)$ and $\varphi_\alpha : \mathbb{R}_+ \to [0, 1]$ be a C^1 decreasing function such that $\varphi_\alpha(s) = 1$ if $s < \alpha$ and $\varphi_\alpha(s) = 0$ if $s \geq 1$. Set the truncated kernels*

$$k_{\mathrm{v}}^{R_{\mathrm{v}}}(x, x') = k_{\mathrm{v}}^{0,R_{\mathrm{v}}}(r^2, r'^2) = k_{\mathrm{v}}^0(r^2, r'^2) \mathbb{1}_{[0,R_{\mathrm{v}}]}(r) \mathbb{1}_{[0,R_{\mathrm{v}}]}(r'), \tag{4.3.33}$$

$$k_{\mathrm{u}}^{R_{\mathrm{u}}}(x, x') = k_{\mathrm{u}}^{0,R_{\mathrm{u}}}(r^2, r'^2) = k_{\mathrm{u}}^0(r^2, r'^2) \varphi\big(r/R_{\mathrm{u}}\big) \varphi\big(r'/R_{\mathrm{u}}\big). \tag{4.3.34}$$

Assume now that $V^0 \sim GP(0, k_{\mathrm{v}}^{R_{\mathrm{v}}})$ and $U^0 \sim GP(0, k_{\mathrm{u}}^{R_{\mathrm{u}}})$. Then, defining the function $K_{\mathrm{v}}(r, r') = \int_0^r \int_0^{r'} k_{\mathrm{v}}^0(s, s') ds ds'$, the two following formulas hold

$$k_{\mathrm{v}}^{\mathrm{wave}}(z, z') = \frac{sgn(tt')}{16c^2 r r'} \times \sum_{\varepsilon, \varepsilon' \in \{-1,1\}} \varepsilon \varepsilon' K_{\mathrm{v}}\Big(\min\big((r + \varepsilon c|t|)^2, R_{\mathrm{v}}^2\big), \min\big((r' + \varepsilon' c|t'|)^2, R_{\mathrm{v}}^2\big)\Big), \tag{4.3.35}$$

$$k_{\mathrm{u}}^{\mathrm{wave}}(z, z') = \frac{1}{4 r r'} \times$$

$$\sum_{\varepsilon,\varepsilon'\in\{-1,1\}} (r+\varepsilon c|t|)(r'+\varepsilon' c|t'|)k_{\mathrm{u}}^{0,R_{\mathrm{u}}}\big((r+\varepsilon c|t|)^2,(r'+\varepsilon' c|t'|)^2\big). \tag{4.3.36}$$

Proof. When using the kernel $k_{\mathrm{v}}^{0,R_{\mathrm{v}}}$, we can directly use equation (4.3.26) by substituting K_{v} with $K_{\mathrm{v}}^{R_{\mathrm{v}}}(r,r') \coloneqq \int_0^r \int_0^{r'} k_{\mathrm{v}}^{0,R_{\mathrm{v}}}(s,s')dsds'$ and observing that for all $r, r' \geq 0$,

$$K_{\mathrm{v}}^{R_{\mathrm{v}}}(r^2,r'^2) \coloneqq \int_0^{r^2}\int_0^{r'^2} k_{\mathrm{v}}^{0,R_{\mathrm{v}}}(s,s')dsds' = K_{\mathrm{v}}\Big(\min\left(r^2,R_{\mathrm{v}}^2\right),\min\left(r'^2,R_{\mathrm{v}}^2\right)\Big)$$

which directly proves (4.3.35). Additionally, (4.3.36) is only a substitution of k_{u}^0 with $k_{\mathrm{u}}^{0,R_{\mathrm{u}}}$ in (4.3.27): all the mathematical steps are justified as $\varphi \in C^1(\mathbb{R}_+)$. □

Notice that the truncated kernels $k_{\mathrm{v}}^{R_{\mathrm{v}}}$ and $k_{\mathrm{u}}^{R_{\mathrm{u}}}$ are the covariance kernels of the truncated processes $V_{\mathrm{trunc}}^0(x) = \mathbb{1}_{[0,R_{\mathrm{v}}]}(|x-x_0|)V^0(x)$ and $U_{\mathrm{trunc}}^0(x) = \varphi\big(|x-x_0|/R_{\mathrm{u}}\big)U^0(x)$ respectively. For $k_{\mathrm{u}}^{R_{\mathrm{u}}}$, the truncation procedure has to be sufficiently smooth to compute $(\dot{F}_t * \dot{F}_{t'}) * k_{\mathrm{u}}^{R_{\mathrm{u}}}$, which requires to differentiate $k_{\mathrm{u}}^{R_{\mathrm{u}}}$. In contrast, we used a blunt truncation for $k_{\mathrm{v}}^{R_{\mathrm{v}}}$. Strictly speaking, the sample paths of $V_{\mathrm{trunc}}^0(x)$ are not continuous and Proposition 4.3.1 cannot be used on this GP. However, as discussed in Section 2.4.2.1 of Chapter 2, it is easily checked that for $V_{\mathrm{trunc}}^0(x)$, all the computations leading to equation (4.3.6) still hold, and thus equation (4.3.35) also holds.

We also observe that such compactly supported kernels can never be stationary as their sample paths are compactly supported. Using equation (4.3.35), one can indeed check that $k_{\mathrm{v}}^{\mathrm{wave}}(z,z) = \mathrm{Var}(V(z)) = 0$ as soon as $(r-c|t|)^2 > R_{\mathrm{v}}^2$, ie $V(z) = 0$ *a.s.* and likewise for $k_{\mathrm{u}}^{\mathrm{wave}}$: this is the expression of the strong Huygens principle on the kernels $k_{\mathrm{v}}^{\mathrm{wave}}$ and $k_{\mathrm{u}}^{\mathrm{wave}}$. Such compactly supported kernels may lead to sparse covariance matrices which may then be used for computational speedups (a topic we leave aside in this article).

4.3.2.5 Estimation of physical parameters

The wave kernel (4.3.8), using for k_{u} and k_{v} radially symmetric kernels supported in $B(x_0^{\mathrm{u}},R_{\mathrm{u}})$ and $B(x_0^{\mathrm{v}},R_{\mathrm{v}})$ respectively, has for hyperparameters $\theta = (c, x_0^{\mathrm{u}}, R_{\mathrm{u}}, \theta_{k_{\mathrm{u}}^0}, x_0^{\mathrm{v}}, R_{\mathrm{v}}, \theta_{k_{\mathrm{v}}^0})$ Among those, $(c, x_0^{\mathrm{u}}, R_{\mathrm{u}}, x_0^{\mathrm{v}}, R_{\mathrm{v}})$ all correspond to physical parameters. Their estimation via likelihood maximisation is numerically investigated in Section 4.4. Note that finding the correct radii R_{u} and R_{v} is not a well posed problem: if $\mathrm{Supp}(U^0) \subset B(x_0^{\mathrm{u}},R_{\mathrm{u}})$ then $\mathrm{Supp}(U^0) \subset B(x_0^{\mathrm{u}},\alpha R_{\mathrm{u}})$ for any $\alpha \geq 1$ and αR_{u} is also a suitable candidate for R_{u}. This is discussed in Section 4.4.

Remark 4.3.7 (GPR, radial symmetry and the 1D wave equation). It is known that the radially symmetric 3D wave equation is equivalent to the 1D wave equation, by introducing $\tilde{w}(r,t) = rw(x,t)$, $r = |x|$. However, the joint problem of approximating a radially symmetric solution w of Problem (4.3.1) with GPR *and* searching for the correct source location parameters $(x_0^{\mathrm{u}}, R_{\mathrm{u}}, x_0^{\mathrm{v}}, R_{\mathrm{v}})$ cannot be reduced to the one dimensional case, as the source centers x_0^{u} and x_0^{v} both lie in $\mathbb{R}^3$.

4.3.3 The point source limit

The case of the point source deserves a study on its own as it plays a central role for linear PDEs, both in theory [68] and in applications. For the wave equation, modelling the source term as a point source (i.e. a Dirac mass) is relevant in a number of real life cases: a localized detonation in acoustics, an electric point source in electromagnetics, a mass point in mechanics and so forth. In this section, we will not make use of the Kriging equations (4.2.1) and (4.2.2) as reconstructing an initial condition that is a point source is actually of little interest. Also, reconstructing the wave equation's Green's function thanks to a pointwise approximation such as GPR is expected to yield poor results because this Green's function in particular is not even defined pointwise: it is a family of singular measures, see equation (4.3.3). However, estimating the physical parameters attached to it, essentially the position parameter x_0, is a relevant question and an attainable goal. This is the topic of this section, where we study the behaviour of the log marginal likelihood that comes with WIGPR when the initial condition reduces to a point source. On a more general level, this section also serves as an illustration of the very explicit links one may draw between classical PDE based models and Bayesian kernel methods using physics informed kernels. We will restrict ourselves to the case $u_0 = 0$ in equation (4.3.1) and thus focus on the kernel $k_{\mathrm{v}}^{\mathrm{wave}}(z,z')$. We begin by clarifying the setting in which we will work.

4.3.3.1 Setting, assumptions and objectives

(i) Note $x_1, ..., x_q$ the q sensor locations and assume that we have N time measurements in $[0,T]$ corresponding to times $0 = t_1 < ... < t_N = T$ for each sensor; we have overall $n = Nq$ pointwise observations of a function w that is a solution of the problem (4.3.1). The space-time observation locations (x_i, t_j) are stored in a vector $Z = (Z_1|\cdots|Z_q)^T$ where $Z_i := ((x_i,t_1), ..., (x_i,t_N))$ corresponds to the i^{th} sensor. The observations are then stored in the column vector $w_{\mathrm{obs}} = (w(Z_1)|...|w(Z_q))^T$.

(ii) We assume that the initial condition v_0 corresponding to w is almost a point source: in particular it is supported on a small ball $B(x_0^*, R^*)$ where $R^* \ll 1$.

(iii) We are interested in finding x_0^*, the correct source location. To do so, we study the log marginal likelihood associated to the observations w_{obs}, using a covariance kernel associated to initial conditions truncated around a ball $B(x_0, R)$ to be estimated. Set first

$$k^{\mathrm{R}}_{x_0}(x, x') := (4\pi R^3/3)^{-2} k_{\mathrm{v}}(x, x') \mathbb{1}_{B(x_0,R)}(x) \mathbb{1}_{B(x_0,R)}(x'), \tag{4.3.37}$$

where k_{v} is a given a covariance function. The pre-factor $(4\pi R^3/3)^{-2}$ is an anticipation of the upcoming Proposition 4.3.8. We will then use the wave kernel

$$k^{\mathrm{wave,R}}_{\mathrm{x_0}}((x,t),(x',t')) = [(F_t \otimes F_{t'}) * k^{\mathrm{R}}_{x_0}](x, x'). \tag{4.3.38}$$

We then view (x_0, R) as hyperparameters of $k^{\mathrm{wave,R}}_{\mathrm{x_0}}$, and we denote (x_0^*, R^*) the real source position and size.

(iv) We assume that except for x_0, all the other hyperparameters θ of $k^{\mathrm{wave,R}}_{\mathrm{x_0}}$ are fixed. In particular, we assume that $c = c^*$ and $R = R^*$, where c^* is the true value of the celerity parameter.

In that framework, the log-marginal likelihood $p(w_{\text{obs}}|\theta)$ only depends on x_0. We thus write $K_{x_0} := k^{\mathrm{wave,R}}_{x_0}(Z, Z)$ and $\mathcal{L}(\theta, \lambda) = \mathcal{L}(x_0, \lambda)$, λ being a Tikhonov regularization parameter (see equation (4.3.39) below). The log-marginal likelihood then writes

$$\mathcal{L}(\theta, \lambda) = \mathcal{L}(x_0, \lambda) = w_{\text{obs}}^T (K_{x_0} + \lambda I_n)^{-1} w_{\text{obs}} + \log\det(K_{x_0} + \lambda I_n). \tag{4.3.39}$$

4.3.3.2 Level sets of $\mathcal{L}(x_0, \lambda)$ and GPS localization

In Figure 4.1, we provide a 3 dimensional image which displays the numerical values of the map $x_0 \mapsto \mathcal{L}(x_0, \lambda)$ that are below a suitable threshold, on a test case. This figure constitutes visual evidence that in the limit $R \to 0$, recovering a point source location from minimizing the log marginal likelihood provided by the kernel (4.3.38) reduces to the classic true-angle multilateration method used for example in GPS systems (see e.g. [76]). In this localization method, the user who is located on a sphere (Earth) sends signals to satellites gravitating around the Earth. From the corresponding time measurements, the distance between the satellite and the user is deduced, which in turn defines a sphere (one for each satellite) on which the user is located. The location of the user lies at the intersection of those spheres, and the Earth. At least three satellites are needed for this intersection to be reduced to a point.

On Figure 4.1, three facts in particular are noteworthy; our task will be to explain them mathematically. First, as a function of x_0, $\mathcal{L}(x_0, \lambda)$ reaches local minima over the whole surface of spheres centered on each sensor. Second, at the intersection of two of those spheres, the local minima are smaller. Third, the spheres all intersect at a single point x_0^*, which is the global minima of $\mathcal{L}(x_0, \lambda)$ and the real source location.

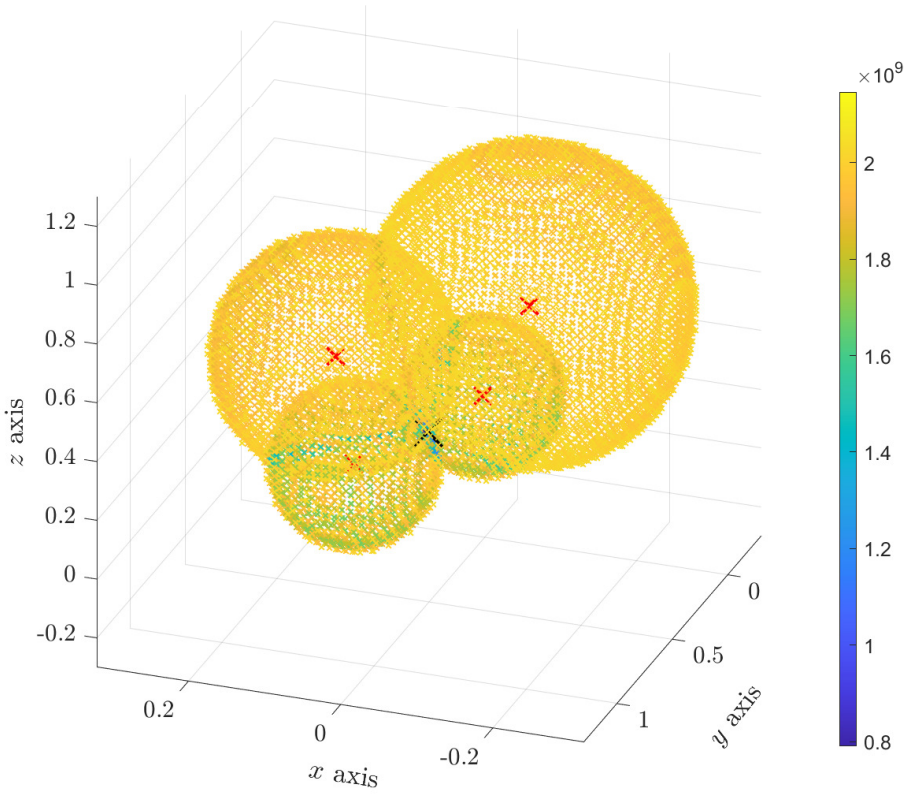

Figure 4.1 – Negative log marginal likelihood as a function of $x_0 \in \mathbb{R}^3$. Are only represented values of the negative log marginal likelihood that are below 2.035×10^9. There only remains thin spherical shells. Red crosses: sensor locations. Black cross: source position. The source is located at the intersection of spheres centered at the sensor locations.

On our way to explaining these three facts, we begin with a convergence statement describing the point source limit, from a covariance point of view.

Proposition 4.3.8. *Let k be a continuous positive definite function defined on $\mathbb{R}^3 \times \mathbb{R}^3$ and let $x_0 \in \mathbb{R}^3$. For $R > 0$, define $k_{x_0}^{\mathrm{R}}$ its truncation around x_0*

by

$$k^{\mathrm{R}}_{x_0}(x,x') = k(x,x')\mathbb{1}_{B(x_0,R)}(x)\mathbb{1}_{B(x_0,R)}(x')/(4\pi R^3/3)^2.$$

Let $t,t' \in \mathbb{R}$. Then $(F_t \otimes F_{t'}) * k^{\mathrm{R}}_{x_0}$ defines an absolutely continuous Radon measure over $\mathbb{R}^3\times\mathbb{R}^3$. Furthermore we have the following weak-$\star$ convergence in the space of Radon measures (i.e. the dual of $C_c(\mathbb{R}^3\times\mathbb{R}^3)$, the latter space being the space of continuous functions over $\mathbb{R}^3\times\mathbb{R}^3$ with compact support):

$$[(F_t \otimes F_{t'}) * k^{\mathrm{R}}_{x_0}] \xrightarrow[R\to 0]{C_c(\mathbb{R}^3\times\mathbb{R}^3)'} k(x_0,x_0)\times(\tau_{x_0}F_t)\otimes(\tau_{x_0}F_{t'}), \tag{4.3.40}$$

where $\tau_x\mu$, the translation of μ by x, is defined by $\int f(y)\tau_x\mu(dy) := \int f(x+y)\mu(dy)$.

Proof. The proof is carried out by direct computations. First, equation (4.3.4) yields

$$[(F_t \otimes F_{t'}) * k^{\mathrm{R}}_{x_0}](x,x') = tt'\int_{S\times S} k^{\mathrm{R}}_{x_0}(x-c|t|\gamma, x'-c|t'|\gamma')\frac{d\Omega d\Omega'}{(4\pi)^2}. \tag{4.3.41}$$

The integrated function in equation (4.3.41) is piecewise continuous over $\mathbb{R}^3\times\mathbb{R}^3$ and the integral in (4.3.41) is well defined, whatever the values of x and x'. Let f be a continuous compactly supported function on $\mathbb{R}^3\times\mathbb{R}^3$. We define

$$I_R := \langle (F_t \otimes F_{t'}) * k^{\mathrm{R}}_{x_0}, f\rangle/(4\pi R^3/3)^2,$$

and wish to show that $I_R \to k(x_0,x_0)\langle \tau_{x_0}F_t\otimes\tau_{x_0}F_{t'}, f\rangle$ when $R\to 0$. Using equation (2.4.16) from Chapter 2 and Fubini's theorem, we have

$$\begin{aligned}
I_R &= \frac{1}{(\frac{4}{3}\pi R^3)^2}\int_{\mathbb{R}^3\times\mathbb{R}^3} f(x,x')[(F_t\otimes F_{t'})*k^{\mathrm{R}}_{x_0}](x,x')dxdx' \\
&= \frac{1}{(\frac{4}{3}\pi R^3)^2}\int_{\mathbb{R}^3\times\mathbb{R}^3} f(x,x')tt'\int_{S\times S} k^{\mathrm{R}}_{x_0}(x-c|t|\gamma, x'-c|t'|\gamma')\frac{d\Omega d\Omega'}{(4\pi)^2}dxdx' \\
&= \frac{1}{(\frac{4}{3}\pi R^3)^2}\,tt'\int_{S\times S}\int_{\mathbb{R}^3\times\mathbb{R}^3}\Bigg(f(x,x')k_{x_0}(x-c|t|\gamma, x'-c|t'|\gamma') \\
&\qquad\qquad \times \mathbb{1}_{[0,R]}(|x-c|t|\gamma-x_0|)\mathbb{1}_{[0,R]}(|x'-c|t'|\gamma'-x_0|)\Bigg)dxdx'\frac{d\Omega d\Omega'}{(4\pi)^2}.
\end{aligned}$$

The first indicator function restricts the integration domain of x to $B(x_0 + c|t|\gamma, R)$, and symmetrically for the second indicator function and x'. For x in $B(x_0+c|t|\gamma,R)$, in spherical coordinates around $x_0+c|t|\gamma$, write $x =$

$x_0 + c|t|\gamma + R\rho\gamma_x$ with $\rho \in [0,1]$, $\gamma_x \in S$ and associated surface differential element $d\Omega_x$. We do symmetrically for $x' \in B(x_0 + c|t'|\gamma', R)$, which yields

$$I_R = tt' \int_{S\times S}\int_{S\times S}\int_0^1\int_0^1 \Big(f(x_0 + c|t|\gamma + R\rho\gamma_x, x_0 + c|t'|\gamma' + R\rho'\gamma_{x'}) \\ \times k(x_0 + R\rho\gamma_x, x_0 + R\rho'\gamma_{x'}) \Big) \times 9\rho^2 d\rho\rho'^2 d\rho' \frac{d\Omega_x d\Omega_{x'}}{(4\pi)^2}\frac{d\Omega d\Omega'}{(4\pi)^2}.$$

The integration domain above is a compact subset of $\mathbb{R}^{10}$. Since f is continuous and k is assumed continuous in the vicinity of (x_0, x_0), Lebesgue's dominated convergence theorem can be applied when $R \to 0$, which yields

$$I_R \xrightarrow[R\to 0]{} tt' k(x_0,x_0) \int_{S\times S} f(x_0 + c|t|\gamma, x_0 + c|t'|\gamma')\frac{d\Omega d\Omega'}{(4\pi)^2} \times \left(3\int_0^1 \rho^2 d\rho\right)^2 \\ = k(x_0,x_0)\langle \tau_{x_0}F_t \otimes \tau_{x_0}F_{t'}, f\rangle.$$

which concludes the proof. □

As before, the kernel $k^{\mathrm{R}}_{x_0}$ of Proposition 4.3.8 is the covariance kernel of the truncated process $V^0_{\mathrm{trunc}}(x) = \mathbb{1}_{B(x_0,R)}(x)V^0(x)/(4\pi R^3/3)$. The limit object we obtain in equation (4.3.40) is not a function but a singular measure, and thus it cannot be a covariance function. This means that we do not obtain a Gaussian process in the point source limit. More precisely, the Gaussian process associated to the covariance function $k^{\mathrm{wave,R}}_{\mathrm{x_0}}$ degenerates into a Gaussian measure [29] over the locally convex space $C_c(\mathbb{R}^3 \times \mathbb{R}^3)$ when R goes to zero, though we leave aside this observation for now. On a formal level though, Proposition 4.3.8 provides an entry point for studying the log marginal likelihood (4.3.39) associated with the kernel (4.3.38) when R is small. Indeed, Proposition 4.3.8 states that for small values of R, the kernel (4.3.38) behaves like a rank one kernel, i.e. a kernel of the form $k(z,z') = f(z)f(z')$ for some particular function f. This observation will prove to be enough for explaining the patterns observed in Figure 4.1.

Properly dealing with the limit $R \to 0$ implies that we use a mathematical framework compatible with general Radon measures, as indicated by Proposition 4.3.8. This also implies an additional layer of technicality. Instead, we introduce regularized (mollified) versions of both the limit object in Proposition 4.3.8 and $\mathcal{L}(x_0,\lambda)$, and study these regularized terms. This is the content of Propositions 4.3.9 and 4.3.11, which are statements on the regularized log marginal likelihood $\mathcal{L}_{\mathrm{reg}}(x_0,\lambda)$ introduced in equation (4.3.42). Note however that proving a rigorous mathematical statement linking the behaviours of $\mathcal{L}(x_0,\lambda)$ and $\mathcal{L}_{\mathrm{reg}}(x_0,\lambda)$ is an open question.

4.3.3.3 Point source mollification

We start with regularizing F_t thanks to a mollifier $\varphi(x)$ on $\mathbb{R}^3$ which we choose to be radially symmetric as in [74], section 4.2.1. Define $\varphi_R(y) = \varphi(y/R)/R^3$, then a $\mathcal{C}_c^\infty$ regularization of F_t is obtained by setting $f_t^{\mathrm{R}}(x) := (F_t * \varphi_R)(x)$ for all x in $\mathbb{R}^3$. As F_t, f_t^{R} exhibits radial symmetry. We will next use the following regularizations:

- Note $k_{x_0}^{\mathrm{reg}}((x,t),(x',t')) := f_t^{\mathrm{R}}(x - x_0) f_{t'}^{\mathrm{R}}(x' - x_0)$, which plays the role of a regularized version of the limit measure in Proposition 4.3.8. The same proposition states that in some sense, when R approaches 0, $k_{\mathrm{x_0}}^{\mathrm{wave,R}}$ is close to $k_{x_0}^{\mathrm{reg}}$. Denote also $F_{x_0} := (F_{x_0}^1 | \cdots | F_{x_0}^q)^T$, with $F_{x_0}^i := (f_{t_1}^{\mathrm{R}}(x_i - x_0), ..., f_{t_N}^{\mathrm{R}}(x_i - x_0))$. The covariance matrix corresponding to the hyperparameter x_0 is then given by $K_{x_0}^{\mathrm{reg}} = k_{x_0}^{\mathrm{reg}}(Z,Z) = F_{x_0} F_{x_0}^T$. In particular it is rank one.
- We also assume that $w(x_i,t_j)$ can be approximated by $\tilde{w}(x_i,t_j) = f_{t_j}^{\mathrm{R}}(x_i - x_0^*)$ as in the point source limit, $v_0 = \delta_{x_0^*}$ and in that case we would have $w(x_i,t_j) = (F_{t_j} * v_0)(x_i) = F_{t_j}(x_i - x_0^*)$ (forgetting for a second that F_t is not defined pointwise). We thus introduce the column vector of "approximated observations" $W = \big(\tilde{w}(x_i,t_j)\big)_{i,j}$ and we assume that W is ordered as $W = (W_1 | \cdots | W_q)^T$ where W_i corresponds to the i^{th} sensor: $W_i = (\tilde{w}(x_i,t_1), ..., \tilde{w}(x_i,t_N)) \in \mathbb{R}^N$.

We may then introduce the "regularized" log marginal likelihood built by replacing k with $k_{x_0}^{\mathrm{reg}}$ and w_{obs} by W:

$$\mathcal{L}_{\mathrm{reg}}(x_0,\lambda) := W^T (K_{x_0}^{\mathrm{reg}} + \lambda I_n)^{-1} W + \log\det(K_{x_0}^{\mathrm{reg}} + \lambda I_n), \tag{4.3.42}$$

where we recall that $K_{x_0}^{\mathrm{reg}} = k_{x_0}^{\mathrm{reg}}(Z,Z) = F_{x_0} F_{x_0}^T$. We will then study $\mathcal{L}_{\mathrm{reg}}(x_0,\lambda)$ in the place of $\mathcal{L}(x_0,\lambda)$; as stated before, we expect that $\mathcal{L}(x_0,\lambda)$ behaves similarly to $\mathcal{L}_{\mathrm{reg}}(x_0,\lambda)$, although proofs of such statements are lacking for the moment. We begin with a proposition which describes the asymptotic behaviour of $\mathcal{L}_{\mathrm{reg}}(x_0,\lambda)$ in the limit of $\lambda \to 0$. This limit corresponds to noiseless observations, and the limit object in Proposition 4.3.9 provides an explanation of the patterns of Figure 4.1.

Proposition 4.3.9 (Asymptotic behaviour of $\mathcal{L}_{\mathrm{reg}}(x_0,\lambda)$ when $\lambda \to 0$)**.** *Let $\varepsilon > 0$ and $E_\varepsilon := \{x_0 \in \mathbb{R}^3 : ||F_{x_0}||_{\mathbb{R}^n}^2 > \varepsilon\}$. Define the correlation coefficient between F_{x_0} and W by $r(x_0) = Corr(F_{x_0}, W) = \langle F_{x_0}, W\rangle_{\mathbb{R}^n} / (||W||_{\mathbb{R}^n} ||F_{x_0}||_{\mathbb{R}^n})$. We set $r(x_0) = 0$ if $F_{x_0} = 0$. Then we have the following pointwise convergence:*

$$\forall x_0 \in \mathbb{R}^3, \quad \big|\lambda \mathcal{L}_{\mathrm{reg}}(x_0,\lambda) - ||W||_{\mathbb{R}^n}^2 \big(1 - r(x_0)^2\big)\big| = O_{\lambda\to 0}(\lambda \log \lambda),$$

and the uniform convergence on E_ε

$$\sup_{x_0 \in E_\varepsilon} \big|\lambda \mathcal{L}_{\mathrm{reg}}(x_0,\lambda) - ||W||_{\mathbb{R}^n}^2 \big(1 - r(x_0)^2\big)\big| = O_{\lambda\to 0}(\lambda \log \lambda).$$

The set E_ε is the set of values of x_0 for which the vectors F_{x_0} are uniformly large enough for the Euclidean norm. This is interpreted by saying that the elements x_0 of E_ε are potential source positions for which the chosen sensor locations should capture a signal with sufficient L^2 energy (at least ε across all sensors) over the window $[0, T]$, should the source be located at x_0. Loosely speaking, such locations x_0 are "visible" candidate source positions. From a covariance perspective, we have that $\rho(K_{x_0}^{reg}) = ||F_{x_0}||^2_{\mathbb{R}^n}$, where ρ denotes the spectral radius.

Proof of Proposition 4.3.9. Suppose first that $||F_{x_0}||^2_{\mathbb{R}^n} = 0$. Then by definition, $r(x_0) = 0$ and $\mathcal{L}_{\text{reg}}(x_0, \lambda) = ||W||^2_{\mathbb{R}^n}/\lambda + n \log \lambda$ which indeed shows that

$$\left|\lambda \mathcal{L}_{\text{reg}}(x_0, \lambda) - ||W||^2_{\mathbb{R}^n}\right| = O_{\lambda \to 0}(\lambda \log \lambda). \tag{4.3.43}$$

Now, let $\varepsilon > 0$ and assume that $||F_{x_0}||^2_{\mathbb{R}^n} \geq \varepsilon$. We first deal with the first term in equation (4.3.42). Using the Sherman–Morrison formula ([157], Section 2.7.1), we may invert $(K_{x_0}^{\text{reg}} + \lambda I_n)$ explicitly:

$$(K_{x_0}^{\text{reg}} + \lambda I_n)^{-1} = \frac{1}{\lambda} I_n - \frac{1}{\lambda^2} \frac{F_{x_0} F_{x_0}^T}{1 + \frac{1}{\lambda} F_{x_0}^T F_{x_0}} = \frac{1}{\lambda}\Big(I_n - \frac{F_{x_0} F_{x_0}^T}{\lambda + ||F_{x_0}||^2_{\mathbb{R}^n}}\Big).$$

The determinant term in equation (4.3.42) is also easily derived. Indeed, $F_{x_0} F_{x_0}^T$ has only one non zero eigenvalue equal to $||F_{x_0}||^2_{\mathbb{R}^n}$, since $(F_{x_0} F_{x_0}^T) F_{x_0} = F_{x_0}(F_{x_0}^T F_{x_0}) = ||F_{x_0}||^2_{\mathbb{R}^n} F_{x_0}$:

$$\log \det(K_{x_0}^{\text{reg}} + \lambda I_n) = (n-1) \log \lambda + \log(\lambda + ||F_{x_0}||^2_{\mathbb{R}^n}). \tag{4.3.44}$$

(The same argument shows that $\rho(K_{x_0}^{\text{reg}}) = ||F_{x_0}||^2_{\mathbb{R}^n}$.) Thus,

$$\begin{aligned}
\mathcal{L}_{\text{reg}}(x_0, \lambda) &= W^T (K_{x_0}^{\text{reg}} + \lambda I_n)^{-1} W + \log \det(K_{x_0}^{\text{reg}} + \lambda I_n) \\
&= \frac{1}{\lambda}\left(||W||^2_{\mathbb{R}^n} - \frac{\langle F_{x_0}, W\rangle^2_{\mathbb{R}^n}}{\lambda + ||F_{x_0}||^2_{\mathbb{R}^n}}\right) + (n-1)\log\lambda + \log(\lambda + ||F_{x_0}||^2_{\mathbb{R}^n}) \\
&= \frac{||W||^2_{\mathbb{R}^n}}{\lambda}\left(1 - \frac{\langle F_{x_0}, W\rangle^2_{\mathbb{R}^n}}{||W||^2_{\mathbb{R}^n}(\lambda + ||F_{x_0}||^2_{\mathbb{R}^n})}\right) + (n-1)\log\lambda + \log(\lambda + ||F_{x_0}||^2_{\mathbb{R}^n}).
\end{aligned}$$

Therefore,

$$\begin{aligned}
&\lambda \mathcal{L}_{\text{reg}}(x_0, \lambda) - ||W||^2_{\mathbb{R}^n}(1 - r(x_0)^2) \\
&\qquad = ||W||^2_{\mathbb{R}^n}\left(\frac{\langle F_{x_0}, W\rangle^2_{\mathbb{R}^n}}{||W||^2_{\mathbb{R}^n}||F_{x_0}||^2_{\mathbb{R}^n}} - \frac{\langle F_{x_0}, W\rangle^2_{\mathbb{R}^n}}{||W||^2_{\mathbb{R}^n}(\lambda + ||F_{x_0}||^2_{\mathbb{R}^n})}\right) \\
&\qquad\quad + (n-1)\lambda\log\lambda + \lambda\log(\lambda + ||F_{x_0}||^2_{\mathbb{R}^n}).
\end{aligned} \tag{4.3.45}$$

Moreover, for the term in equation (4.3.45) which is multiplied by $||W||^2_{\mathbb{R}^n}$,

$$\begin{aligned}\frac{\langle F_{x_0}, W\rangle^2_{\mathbb{R}^n}}{||W||^2_{\mathbb{R}^n}||F_{x_0}||^2_{\mathbb{R}^n}} - \frac{\langle F_{x_0}, W\rangle^2_{\mathbb{R}^n}}{||W||^2_{\mathbb{R}^n}(\lambda + ||F_{x_0}||^2_{\mathbb{R}^n})} &= \frac{\langle F_{x_0}, W\rangle^2_{\mathbb{R}^n}}{||W||^2_{\mathbb{R}^n}}\left(\frac{1}{||F_{x_0}||^2_{\mathbb{R}^n}} - \frac{1}{\lambda + ||F_{x_0}||^2_{\mathbb{R}^n}}\right)\\ &= \frac{\langle F_{x_0}, W\rangle^2_{\mathbb{R}^n}}{||W||^2_{\mathbb{R}^n}} \frac{\lambda}{||F_{x_0}||^2_{\mathbb{R}^n}(\lambda + ||F_{x_0}||^2_{\mathbb{R}^n})}\\ &\leq r(x_0)^2 \frac{\lambda}{\lambda + ||F_{x_0}||^2_{\mathbb{R}^n}} \leq \frac{\lambda}{||F_{x_0}||^2_{\mathbb{R}^n}} \leq \frac{\lambda}{\varepsilon}, \end{aligned} \tag{4.3.46}$$

and obviously, since $\lambda \geq 0$,

$$\frac{\langle F_{x_0}, W\rangle^2_{\mathbb{R}^n}}{||W||^2_{\mathbb{R}^n}||F_{x_0}||^2_{\mathbb{R}^n}} - \frac{\langle F_{x_0}, W\rangle^2_{\mathbb{R}^n}}{||W||^2_{\mathbb{R}^n}(\lambda + ||F_{x_0}||^2_{\mathbb{R}^n})} \geq 0. \tag{4.3.47}$$

Also, one sees that $F_{x_0} = 0$ as soon as $\sup_i |x_0 - x_i| > cT + R$, ie x_0 is too far from the receivers for them to capture non zero signal during the time interval $[0, T]$. Thus the function $x_0 \longmapsto ||F_{x_0}||^2_{\mathbb{R}^n}$ is zero outside of a compact set. It is obviously continuous on $\mathbb{R}^3$ and is thus bounded on $\mathbb{R}^3$ by some constant $M > 0$. Using this together with equations (4.3.46) and (4.3.47) inside equation (4.3.45), and assuming that $\lambda \leq 1$ yields

$$\left|\lambda \mathcal{L}_{\text{reg}}(x_0, \lambda) - ||W||^2_{\mathbb{R}^n}(1 - r(x_0)^2)\right| \leq \frac{\lambda}{\varepsilon}||W||^2_{\mathbb{R}^n} + (n-1)|\lambda \log \lambda| + \lambda \log(M+1),$$

which shows the uniform convergence statement as well as the pointwise one (together with (4.3.43)). □

Remark 4.3.10. In the proof of Proposition 4.3.9, the determinant term in (4.3.42) has no influence in the limit object and only pollutes the rate of convergence. Discarding it leads to a $O_{\lambda \to 0}(\lambda)$ rate of convergence.

It also makes sense to inspect the case $N \to \infty$, which is the content of the next proposition; the obtained limit object is similar to that of Proposition 4.3.9. The limit $N \to \infty$ corresponds to having the sampling frequency of the sensors go to infinity. In this case, the discrete objects in Proposition 4.3.9 behave as Riemann sums if the time steps t_k are equally spaced and we obtain integrals in the limit $N \to \infty$. Notation wise, we highlight the dependence in N in $\mathcal{L}_{\text{reg}}(x_0, \lambda)$ by noting it instead $\mathcal{L}^N_{\text{reg}}(x_0, \lambda)$.

Proposition 4.3.11 (Asymptotic behaviour of $\mathcal{L}^N_{\text{reg}}(x_0, \lambda)$ when $N \to \infty$)**.** *Define the following vector valued functions in* $L^2([0, T], \mathbb{R}^q)$*:*

$$\begin{aligned}\forall t \in [0, T], \quad I_{\text{w}}(t) &:= \left(\tilde{w}(x_1, t), ..., \tilde{w}(x_q, t)\right)^T,\\ \forall t \in [0, T], \quad I_{x_0}(t) &:= \left(f^{\text{R}}_t(x_1 - x_0), ..., f^{\text{R}}_t(x_q - x_0)\right)^T.\end{aligned}$$

Denote $||\cdot||_{L^2}$ *and* $\langle,\rangle_{L^2}$ *the norm and the dot product of the usual Euclidean structure of* $L^2([0,T],\mathbb{R}^q)$*. Assume that the observations are such that* $||I_{\mathrm{w}}||_{L^2} > 0$*. Introduce then the correlation function, defined whenever* $||I_{x_0}||_{L^2} > 0$*:*

$$r_\infty(x_0) \coloneqq \frac{\langle I_{\mathrm{w}}, I_{x_0}\rangle_{L^2}}{||I_{\mathrm{w}}||_{L^2}||I_{x_0}||_{L^2}}. \tag{4.3.48}$$

Assume that for all $k \in \{1,...,N\}$*,* $t_k = T(k-1)/(N-1)$*, i.e. the* t_k *are equally spaced in* $[0,T]$*. Then for all* x_0 *such that* $||I_{x_0}||_{L^2} \neq 0$*, we have the following pointwise convergence at* x_0

$$\frac{\lambda}{N}\mathcal{L}^N_{\mathrm{reg}}(x_0,\lambda) \xrightarrow[N\to\infty]{} ||I_{\mathrm{w}}||^2_{L^2}\big(1 - r_\infty(x_0)^2\big) + q\lambda\log\lambda. \tag{4.3.49}$$

Proof of Proposition 4.3.11. In all concerned mathematical objects, we highlight the N dependency with an exponent, i.e. W^N, $F^N_{x_0}$, etc. We use the exact same tools as in the previous proof, namely that we the following equality holds:

$$\begin{aligned}\mathcal{L}^N_{\mathrm{reg}}(x_0,\lambda) = \frac{||W^N||^2_{\mathbb{R}^n}}{\lambda}\left(1 - \frac{\langle F^N_{x_0}, W^N\rangle^2_{\mathbb{R}^n}}{||W^N||^2_{\mathbb{R}^n}\big(\lambda + ||F^N_{x_0}||^2_{\mathbb{R}^n}\big)}\right)\\ + (n-1)\log\lambda + \log(\lambda + ||F^N_{x_0}||^2_{\mathbb{R}^n}).\end{aligned}$$

But we also have $||W^N||^2_{\mathbb{R}^n} = \sum_{i=1}^q\sum_{k=1}^N \tilde{w}(x_i,t_k)^2$, $||F^N_{x_0}||^2_{\mathbb{R}^n} = \sum_{i=1}^q\sum_{k=1}^N f^{\mathrm{R}}_{t_k}(x_i - x_0)^2$ and $\langle F^N_{x_0}, W^N\rangle_{\mathbb{R}^n} = \sum_{i=1}^q\sum_{k=1}^N f^{\mathrm{R}}_{t_k}(x_i-x_0)\tilde{w}(x_i,t_k)$. Since the time steps are equally spaced, we can study the limit $N\to\infty$ of the above objects thanks to Riemann sums. When $N\to\infty$,

$$\frac{1}{N}||W^N||^2_{\mathbb{R}^n} \longrightarrow \sum_{i=1}^q\int_0^T \tilde{w}(x_i,t)^2dt = ||I_{\mathrm{w}}||^2_{L^2}, \tag{4.3.50}$$

$$\frac{1}{N}||F^N_{x_0}||^2_{\mathbb{R}^n} \longrightarrow \sum_{i=1}^q\int_0^T f_t(x_i-x_0)^2dt = ||I_{x_0}||^2_{L^2}, \tag{4.3.51}$$

$$\frac{1}{N}\langle W^N, F^N_{x_0}\rangle_{\mathbb{R}^n} \longrightarrow \sum_{i=1}^q\int_0^T \tilde{w}(x_i,t)f_t(x_i-x_0)dt = \langle I_{\mathrm{w}}, I_{x_0}\rangle_{L^2}. \tag{4.3.52}$$

Assume that x_0 is such that $||I_{x_0}||_{L^2} \neq 0$, then because of equation (4.3.51), the quantity $||F^N_{x_0}||_{\mathbb{R}^n}$ is bounded from below by a constant $C > 0$ for sufficiently large N (say $C = ||I_{x_0}||_{L^2}/2$). From the three equations above, we then have the following convergence:

$$\frac{\langle F^N_{x_0}, W^N\rangle^2_{\mathbb{R}^n}}{||W^N||^2_{\mathbb{R}^n}(\lambda + ||F^N_{x_0}||^2_{\mathbb{R}^n})} = \frac{(\frac{1}{N}\langle F^N_{x_0}, W^N\rangle_{\mathbb{R}^n})^2}{\frac{1}{N}||W^N||^2_{\mathbb{R}^n}(\frac{\lambda}{N} + \frac{1}{N}||F^N_{x_0}||^2_{\mathbb{R}^n})} \xrightarrow[N\to\infty]{} r_\infty(x_0). \tag{4.3.53}$$

Likewise, since $n = qN$, when $N \to \infty$ we have that

$$\begin{aligned}\frac{(n-1)\log\lambda}{N} + \frac{1}{N}\log(\lambda + ||F_{x_0}||^2_{\mathbb{R}^n}) \\ &= \frac{(Nq-1)\log\lambda}{N} + \frac{\log N}{N} + \frac{1}{N}\log\left(\frac{\lambda}{N} + \frac{1}{N}||F_{x_0}||^2_{\mathbb{R}^n}\right) \\ &\xrightarrow[N\to\infty]{} q\log\lambda.\end{aligned}$$

which, together with equation (4.3.53), shows the announced result. □

4.3.3.4 Discussion: location of the point source

Propositions 4.3.9 and 4.3.11 enable us to explain the patterns observed in Figure 4.1 where the correct source position is located at the intersection of spheres centered on receivers. For that purpose, we analyze the limit term in Proposition 4.3.9 (the same can be done with the one in Proposition 4.3.11). We denote $L(x_0)$ the said limit object from Proposition 4.3.9:

$$L(x_0) = ||W||^2_{\mathbb{R}^n}\left(1 - r(x_0)^2\right) = ||W||^2_{\mathbb{R}^n}\left(1 - \frac{\left(\sum_{i=1}^q \langle F^i_{x_0}, W_i\rangle_{\mathbb{R}^n}\right)^2}{||W||^2_{\mathbb{R}^n}||F_{x_0}||^2_{\mathbb{R}^n}}\right).$$

Note T_i the time of arrival of the point source wave at sensor i: $|x_i - x_0^*| = c^*T_i$. Define also $S_i := S(x_i, cT_i)$, the sphere centered on x_i, and A_i the thin spherical shell of thickness $2R$ that surrounds S_i, given by $A_i := \overline{B(x_0, cT_i + R) \setminus B(x_0, cT_i - R)}$. Then:

(i) $L(x_0)$ reaches a local minima over the whole sphere S_i. When x_0 is located inside A_i, the subvectors W_i and $F^i_{x_0}$ of W and F_{x_0} respectively become almost colinear because f^{R}_t is radially symmetric. They become exactly colinear when $x_0 \in S_i$. This maximizes the term $\langle F^i_{x_0}, W_i\rangle$ in virtue of the Cauchy-Schwarz inequality. When x_0 lies in one and only one of those spherical shells A_i, the other terms $\langle F^j_{x_0}, W_j\rangle$ are all zero.

(ii) The local minima of $L(x_0)$ located at the intersection of two or more spheres S_i are smaller. More generally, when I is a subset of $\{1, ..., q\}$ and when $x_0 \in \bigcap_{i\in I} A_i \setminus \bigcap_{j\notin I} A_j$, the term $\sum_{i\in I}\langle F^i_{x_0}, W_i\rangle$ is (almost) maximized while $\sum_{j\notin I}\langle F^j_{x_0}, W_j\rangle = 0$, which explains why the intersection of spheres are darker coloured than the other parts of the spheres in Figure 4.1.

(iii) The spheres S_i intersect at a single point, which is exactly x_0^* as well as the global minima of $L(x_0)$. The quantity $r(x_0)$ reaches a global maximum when all subvectors W_i and $F^i_{x_0}$ are colinear, which is the case only when $x_0 \in \bigcap_i S_i$. When there are at least 4 sensors, the intersection of all the spheres $\bigcap_i S_i$ is reduced to at most one point. Recall that we have assumed that $c = c^*$: this implies that $x_0^* \in \bigcap_i S_i$, and thus the minimum of $L(x_0)$ is located at $x_0 = x_0^*$.

Note that if the speed c in $k^{\mathrm{R}}_{x_0}$ does not correspond to the real speed c^*, the intersection $\bigcap_i S_i$ will be empty. Additionally, from an optimization point of view, numerically solving $\inf_{x_0} \mathcal{L}(x_0, \lambda)$ is obviously highly non convex and none of our numerical experiments lead to the correct solution.

4.3.4 Computational speedups

In the Kriging formulas (4.2.1) and (4.2.2) as well as in the log marginal likelihood equation (4.2.4), we are interested in inverting matrices of the form $K + \lambda I$ where K in positive semidefinite. Using basic algebra, we show an exact computational shortcut to computing $(K+\lambda I)^{-1}$ when K has null lines, which is typically the case when using kernels of the form (4.3.35) because of finite speed propagation. It may provide huge computational speedups in the limit of small source size, as is the case in the previous subsection.

4.3.4.1 Inversion shortcut for Tichonov-regularized positive semi definite matrices with null columns

Let K be a symmetric nonnegative definite matrix of size n. Assume that it has p non zero columns $i_1, ..., i_p$ and $q = n - p$ zero columns $i_{p+1}, ..., i_n$. Since K is symmetric, its lines $i_1, ..., i_p$ are also zero. Finally, a simple necessary and sufficient condition for its column j to be zero is $K_{jj} = 0$, because of the Cauchy-Schwarz inequality for nonnegative definite matrices: $|a_{ij}| \leq \sqrt{a_{ii}}\sqrt{a_{jj}}$. Define the matrix $\tilde{K}$ of the extracted non-zero columns of K, of size $p \times p$ by $\tilde{K}_{k,l} = K_{i_k,i_l},\ \forall k, l \in \{1, ..., p\}$. Note $\mathcal{E} = (e_1, ..., e_n)$ the canonical basis of $\mathbb{R}^n$ and $\mathcal{F} = (e_{i_1}, ..., e_{i_n})$ a permutation according to the indexes $i_1, ..., i_p$ and $i_{p+1}, ..., i_n$ defined above (this permutation is unique up to additional permutations of the null columns of K). Then, for the orthogonal permutation matrix P such that

$$\forall k \in \{1, ..., n\}, \quad Pe_k = e_{i_k}, \tag{4.3.54}$$

we have

$$K = P^T \times \left(\begin{array}{c|c} \tilde{K} & 0_{p,q} \\ \hline 0_{q,p} & 0_{q,q} \end{array}\right) \times P. \tag{4.3.55}$$

Consequently, we have the following blockwise inversion formula,

$$(K + \lambda I_n)^{-1} = P^T \times \left(\begin{array}{c|c} (\tilde{K} + \lambda I_p)^{-1} & 0_{p,q} \\ \hline 0_{q,p} & \frac{1}{\lambda} I_q \end{array}\right) \times P. \tag{4.3.56}$$

Note that the matrix P is easy to find, as one only has to compute the diagonal elements of K in order to find the null lines/columns of K (since K is

nonnegative definite). In particular, we only need to invert a matrix of size $(p \times p)$. For a in $\mathbb{R}^n$, we define $a_{\text{in}} \in \mathbb{R}^p$ the first p components of Pa and $a_{\text{out}} \in \mathbb{R}^{n-p}$ the last $n-p$ components of Pa, ie

$$Pa = \begin{pmatrix} (Pa)_1 \\ \vdots \\ (Pa)_p \\ \hline (Pa)_{p+1} \\ \vdots \\ (Pa)_n \end{pmatrix} = \begin{pmatrix} a_{\text{in}} \\ \hline a_{\text{out}}. \end{pmatrix} \tag{4.3.57}$$

Using equations (4.3.56) and (4.3.57), we immediately have that

$$a^T(K + \lambda I_n)^{-1}a = a_{\text{in}}^T(\tilde{K} + \lambda I_p)^{-1}a_{\text{in}} + \frac{1}{\lambda}||a_{\text{out}}||^2. \tag{4.3.58}$$

In the term $a^T(K + \lambda I_n)^{-1}a$, a_{in} corresponds to the coordinates of a that are "kept" by the non zero elements of K and a_{out} corresponds to those that are left out by the non zero elements of K.

4.3.4.2 Computational shortcuts for Kriging

We may now use the previous section to speed up GPR computations when using a covariance kernel k_θ. This is summarized in Proposition 4.3.12, in which we use the following notations.

• Note $X = (x_1, ..., x_n)^T \in \mathbb{R}^n$ the observation locations, $Y \in \mathbb{R}^n$ the vector of observations ($Y_i = u(x_i)$ for noiseless observations).

• Note $K_\theta := k_\theta(X, X)$ the associated covariance matrix, P_θ and $\tilde{K}_\theta$ the matrices P and $\tilde{K}$ defined by equation (4.3.54) for $K = K_\theta$, p_θ the number of non zero columns of K_θ and $q_\theta = n - p_\theta$.

• As in equation (4.3.57), note X_{in}^θ the first p_θ coordinates of $P_\theta X$ and X_{out}^θ the q_θ last, and likewise for Y_{in}^θ and Y_{out}^θ.

Plugging equation (4.3.56) into the log-marginal likelihood and Kriging formulas, we obtain the following Proposition.

Proposition 4.3.12. *If using a covariance kernel k_θ with hyperparameter θ for GPR, we have the following exact computational shortcuts.*
(i) For the log-marginal likelihood,

$$\begin{aligned}\mathcal{L}(\theta, \lambda) = (Y_{\text{in}}^\theta)^T(\tilde{K}_\theta + \lambda I_{p_\theta})^{-1}Y_{\text{in}}^\theta \\ + \frac{1}{\lambda}||Y_{\text{out}}^\theta||^2 + \log\det(\tilde{K}_\theta + \lambda I_{p_\theta}) + q_\theta \log\lambda.\end{aligned} \tag{4.3.59}$$

(ii) For the Kriging formulas,

$$\begin{cases} \tilde{m}(x) &= m(x) + k_\theta(X^\theta_{\text{in}}, x)^T(\tilde{K}_\theta + \lambda I_{p_\theta})^{-1}(Y^\theta_{\text{in}} - m(X^\theta_{\text{in}})), & (4.3.60) \\ \tilde{k}(x, x') &= k_\theta(x, x') - k_\theta(X^\theta_{\text{in}}, x)^T(\tilde{K}_\theta + \lambda I_{p_\theta})^{-1}k_\theta(X^\theta_{\text{in}}, x'). & (4.3.61) \end{cases}$$

(iii) if $k_\theta(x, x) = 0$ *then* $\tilde{m}(x) = m(x)$ *and* $\tilde{k}(x, x') = 0$.

Proof. As in equation (4.3.58), we immediately have that

$$Y^T(K_\theta + \lambda I_n)^{-1}Y = (Y^\theta_{\text{in}})^T(\tilde{K}_\theta + \lambda I_{p_\theta})^{-1}Y^\theta_{\text{in}} + \frac{1}{\lambda}||Y^\theta_{\text{out}}||^2. \tag{4.3.62}$$

It is also clear from equation (4.3.55) that $\log\det(K_\theta + \lambda I_n) = \log\det(\tilde{K}_\theta + \lambda I_{p_\theta}) + q_\theta \log\lambda$, which proves equation (4.3.59). For the Kriging equations, assume without loss of generality that $m \equiv 0$. The Kriging mean is, as in equation (4.3.58), given by

$$\begin{aligned} \tilde{m}(x) &= k(X, x)^T(K + \lambda I_n)^{-1}Y \\ &= k(X^\theta_{\text{in}}, x)^T(\tilde{K}_\theta + \lambda I_{p_\theta})^{-1}Y^\theta_{\text{in}} + \frac{1}{\lambda}k(X^\theta_{\text{out}}, x)^T Y^\theta_{\text{out}}. \end{aligned} \tag{4.3.63}$$

Now, assume that the observation location x_i is such that $k_\theta(x_i, x_i) = (K_\theta)_{ii} = 0$, which is exactly the case of all the coordinates of X^θ_{out} (by definition). Then from the Cauchy-Schwarz inequality (2.2.2), the function $x \longmapsto k(x, x_i)$ is identically zero. Thus, for all x, we have that $k(X^\theta_{\text{out}}, x)^T Y^\theta_{\text{out}} = 0$ which, when plugged in equation (4.3.63), proves equation (4.3.60). The same reasoning leads to equation (4.3.61). Finally, for the same reason, if $k_\theta(x, x) = 0$ then the vector $k_\theta(X_{\text{in}}, x)$ is null, which implies that $\tilde{m}(x) = 0$. □

We remind that the formulas (4.3.59), (4.3.60) and (4.3.61) are exact. There are actually three shortcuts for the Kriging equations (4.3.60) and (4.3.61). First, the smaller matrix inversion, which is especially useful during the log marginal likelihood optimization step (hyperparameter calibration). Second, the selection of the pertinent data points in $k_\theta(X_{\text{in}}, x)$ by using X_{in} instead of X. Third, the selection of the pertinent evaluation points thanks to the point *(iii)* of Proposition 4.3.12. These last two are useful when $\tilde{m}$ and/or $\tilde{k}$ have to be evaluated many times. Note also that all the mathematical objects on the right-hand side of equations (4.3.59), (4.3.60) and (4.3.61) depend on θ and have to be recomputed for each new value of θ. However this is rather fast, since checking which columns of K_θ are zero only requires to compute the diagonal of K_θ, which only requires n calls to k_θ.

Remark 4.3.13. In equation (4.3.59), the term $\frac{1}{\lambda}||Y^\theta_{\text{out}}||^2$ can be understood as a very heavy penalization term that sanctions non zero observations that do not lie in the support of k_θ. When applying this to kernel (4.3.8), the term $\frac{1}{\lambda}||Y^\theta_{\text{out}}||^2$ penalizes the non zero observations that do not lie in the space time domain (or "light cone") allowed by Huygens' principle.

4.3.4.3 Expected numerical gain when using the truncated wave kernel (4.3.8)

In the case of this kernel, to examine if a point (x,t) is such that the variance $k_\theta((x,t),(x,t))$ is zero, one only needs to check that (x,t) lies in the light cone that corresponds to θ (among others, θ contains (x_0,R,c)). Explicitly, the condition to check is whether or not $x \in B(x_0,c|t|+R)\setminus B(x_0,(c|t|-R)_+)$ or equivalently, $c|t|-R \leq |x-x_0| \leq c|t|+R$. This is actually much cheaper than evaluating $k_\theta((x,t),(x,t))$.

• *Computational gain for the log-marginal likelihood*: using Cholesky decomposition to invert $\tilde{K}_\theta+\lambda I_{p_\theta}$, only $p_\theta^3/3$ flops are required versus $n^3/3$ previously (in both cases, the computation of the determinant term in (4.3.59) is immediate from the Cholesky decomposition).

• *Computational gain for the Kriging formulas*: we assume here that we are performing GPR using the truncated wave kernel (4.3.8). Suppose that the hyperparameter vector θ has been previously estimated: in particular, it provides estimated wave speed c, radius R and source position x_0. Now, equation (4.3.60) states that

$$\tilde{m}(x,t) = \sum_{i=1}^{p_\theta} a_i k_\theta\big((x,t),(X_{\text{in}}^\theta)_i\big) \tag{4.3.64}$$

for some fixed real numbers $a_1,...,a_{p_\theta}$. Suppose that we want to compute $\tilde{m}(x,t)$ over a cubic spatial grid $[0,L]^3$ of side length L at a fixed time t. Suppose that the space step Δx of this grid verifies $\Delta x \ll L$: then the number of grid points inside a volume V is approximately $V/\Delta x^3$ (each grid point occupies a cubic volume of Δx^3). In compliance with the strong Huygens principle, computing $\tilde{m}(x,t)$ over the whole grid using Proposition 4.3.12 results in N_θ calls to k, with

$$N_\theta \simeq p_\theta \times \frac{\text{Vol}\Big([B(x_0,ct+R)\setminus B(x_0,(ct-R)_+)]\cap[0,L]^3\Big)}{\Delta x^3} \tag{4.3.65}$$

The set $B(x_0,ct+R)\setminus B(x_0,(ct-R)_+)$ corresponds to the admissible domain allowed by the strong Huygens principle at time t. This is to be compared to $N_{\text{full}} = n\times L^3/\Delta x^3$, the number of calls to k needed without using Proposition 4.3.12; obviously, $N_\theta < N_{\text{full}}$ and actually, $N_\theta \ll N_{\text{full}}$ when R is small. More precise estimations of the number of grid points inside the volume in equation (4.3.65) can be derived, though this is actually a difficult research topic in itself (see for instance [13] or the Gauss circle problem for its 2D counterpart). Also, the volume appearing in (4.3.65) can be explicitly derived but we consider the additional insights this provides to be negligible.

4.3.5 Initial condition reconstruction and error bounds

4.3.5.1 Initial condition reconstruction procedure

Consider a set of space locations $(x_i)_{1\leq i\leq q}$ and moments $(t_j)_{1\leq j\leq N}$ (imagine q sensors each collecting measurements at time t_j for all j). Consider now the following inverse problem:

$$\begin{gathered}\text{Build an approximation of } u_0 \text{ and } v_0 \text{ from a finite set of} \\ \text{measurements} \{w(x_i,t_j)\}_{i,j} \text{ where } (w,u_0,v_0) \text{ are subject to (4.3.1).}\end{gathered} \tag{4.3.66}$$

We now show that WIGPR provides an answer to the problem (4.3.66). This is not surprising, because the covariance models described in the previous section were derived by putting GP priors over u_0 and v_0.

As already observed in Section 4.3.2.1, performing GPR on any data with kernel (4.3.8) automatically produces a prediction $\tilde{m}$ that verifies $\Box\tilde{m}=0$ in the sense of distributions. Therefore, this function $\tilde{m}$ is the solution of the Cauchy problem (4.3.1) for some initial conditions $\tilde{u}_0$ and $\tilde{v}_0$:

$$\tilde{m}(x,t)=(F_t*\tilde{v}_0)(x)+(\dot{F}_t*\tilde{u}_0)(x). \tag{4.3.67}$$

These initial conditions are simply given by $\tilde{u}_0(x)=\tilde{m}(x,0)$ and $\tilde{v}_0(x)=\partial_t\tilde{m}(x,0)$. If the data $\{w(x_i,t_j)\}_{i,j}$ on which GPR is performed is comprised of observations of a function w that is another solution of problem (4.3.1), the initial conditions $(\tilde{u}_0,\tilde{v}_0)$ can be understood as approximations of the initial conditions (u_0,v_0) corresponding to w. More precisely, following Section 4.2.2.3, we have $\tilde{m}=p_F(w)$ and thus

$$\tilde{u}_0(x)=\tilde{m}(x,0)=p_F(w)(x,0) \qquad \forall x\in\mathbb{R}^3, \tag{4.3.68}$$

$$\tilde{v}_0(x)=\partial_t\tilde{m}(x,0)=\partial_t p_F(w)(x,0)=p_F(\partial_t w)(x,0) \qquad \forall x\in\mathbb{R}^3, \tag{4.3.69}$$

where F denotes the finite dimensional space $\mathrm{Span}(k_{\mathrm{w}}(z_1,\cdot),...,k_{\mathrm{w}}(z_n,\cdot))$ and p_F is the orthogonal projector on F with reference to the Hilbert space structure of $H_{k_{\mathrm{w}}}$. Here, z_m is of the form $z_m=(x_i,t_k)\in\mathbb{R}^4$. This use of WIGPR provides a flexible framework for tackling the problem (4.3.66), as the sensors are not constrained in number or location by any integration formula such as Radon transforms. Taking a look at equations (4.3.68) and (4.3.69), we can qualitatively discuss the matter of optimal sensor locations for WIGPR. Indeed, we expect that $\tilde{m}$ will provide a better approximation of w when the functions $k_{\mathrm{w}}(z_i,\cdot)_{i=1,...,n}$ are as orthogonal as possible in $\mathcal{H}_{k_{\mathrm{w}}}$, since $\tilde{m}$ is an orthogonal projection on F with reference to the $\mathcal{H}_{k_{\mathrm{w}}}$ inner product. The optimal situation is when given two different sensors x_i and x_j, the following should hold for most times t_k,t_l:

$$\langle k_{\mathrm{w}}((x_i,t_k),\cdot),k_{\mathrm{w}}((x_j,t_l),\cdot)\rangle_{\mathcal{H}_{k_{\mathrm{w}}}}=k_{\mathrm{w}}((x_i,t_k),(x_j,t_l))\ll 1. \tag{4.3.70}$$

A close inspection of the explicit covariance expressions (equations (2.4.16) and (2.4.17)) shows that the property (4.3.70) can be obtained for most times t_k and t_l when the sensors are far apart from each other, as soon as the kernels k_{u} and k_{v} are such that $k(x,x') \longrightarrow 0$ when $|x-x'| \longrightarrow +\infty$ (which is common, see e.g. the kernel (4.4.1)). Computing optimal sensor locations and obtaining quantitative guaranties of the accuracy of the reconstruction provided by WIGPR is a hard question left for future research.

4.3.5.2 Time-dependent error bounds in terms of the initial condition reconstructions

Now that we have showed that WIGPR provides approximations of the initial conditions of (4.3.1), we underline the fact that these initial condition reconstructions induce a control of the spatial error between the target function u and the Kriging mean $\tilde{m}$, at all times. Indeed, we have the following L^p control in terms of the initial condition reconstruction error. Given $p \in [1,+\infty]$, denote $W^{1,p}(\mathbb{R}^3)$ the Sobolev space of functions $f \in L^p(\mathbb{R}^3)$ whose weak derivatives $\partial_{x_i} f, 1 \leq i \leq d$, exist and lie in $L^p(\mathbb{R}^3)$.

Proposition 4.3.14. *For any $p \in [1,+\infty]$ and any pair $v_0 \in L^p(\mathbb{R}^3)$, $u_0 \in W^{1,p}(\mathbb{R}^3)$ we have the following L^p estimates for all $t \in \mathbb{R}$:*

$$||F_t * v_0||_p \leq |t| \; ||v_0||_p, \tag{4.3.71}$$

$$||\dot{F}_t * u_0||_p \leq ||u_0||_p + C_p c|t| \; ||\nabla u_0||_p, \tag{4.3.72}$$

where $C_p = \left(\int_S |\gamma|_q^p \, d\Omega/4\pi \right)^{1/p} \leq 3^{1/q} \leq 3, 1/p + 1/q = 1$ ($C_\infty = 1, C_1 \leq 1$). Assume that the correct speed c is known and plugged in k_{w}, equations (4.3.71) and (4.3.72) then lead to the following L^p error estimate between the target w and its approximant $\tilde{m}$:

$$||w(\cdot,t) - \tilde{m}(\cdot,t)||_p \leq |t| \; ||v_0 - \tilde{v}_0||_p + ||u_0 - \tilde{u}_0||_p + C_p c|t| \; ||\nabla(u_0 - \tilde{u}_0)||_p, \tag{4.3.73}$$

where $\tilde{u}_0$ and $\tilde{v}_0$ are defined in (4.3.68) and (4.3.69), and $\tilde{m}$ is given in equation (4.3.67).

Equations (4.3.71) and (4.3.72) are simple stability estimates for the 3D wave equation, although we have not found them in that form in the literature (notably the explicit control constants $|t|$ and $C_p c|t|$). They fall in the category of Strichartz estimates with L^p control for the space variable and L^∞ control for the time variable. We thus provide a proof of Proposition 4.3.14.

Proof of Proposition 4.3.14. We have $(F_t * v_0)(x) = t\int_S v_0(x - c|t|\gamma)d\Omega/4\pi$, where $d\Omega/4\pi$ is the normalized Lebesgue measure on the unit sphere S. Assume first that $p \in [1, +\infty[$. Jensen's inequality on the function $t \longmapsto |t|^p$ yields

$$\begin{aligned}||F_t * v_0||_p^p &= t^p \int_{\mathbb{R}^3} |(F_t * v_0)(x)|^p dx = |t|^p \int_{\mathbb{R}^3} \left| \int_S v_0(x - c|t|\gamma)\frac{d\Omega}{4\pi}\right|^p dx \\ &\leq |t|^p \int_{\mathbb{R}^3}\int_S |v_0(x - c|t|\gamma)|^p \frac{d\Omega}{4\pi}dx = |t|^p \int_S \int_{\mathbb{R}^3} |v_0(x - c|t|\gamma)|^p dx\frac{d\Omega}{4\pi} \\ &\leq \int_S ||v_0||_p^p \frac{d\Omega}{4\pi} = |t|^p||v_0||_p^p, \end{aligned} \tag{4.3.74}$$

which yields equation (4.3.71). Next,

$$\begin{aligned}(\dot{F}_t * u_0)(x) &= \partial_t(F_t * u_0)(x) = \partial_t\left(t\int_S u_0(x - c|t|\gamma)\frac{d\Omega}{4\pi}\right) \\ &= \int_S u_0(x - c|t|\gamma)\frac{d\Omega}{4\pi} + t\int_S -c\gamma \cdot \nabla u_0(x - c|t|\gamma)\frac{d\Omega}{4\pi} \\ &=: I_1(x) + I_2(x).\end{aligned}$$

The functions I_1 and I_2 are defined in the equation above. We have $||\dot{F}_t * u_0||_p = ||I_1 + I_2||_p \leq ||I_1||_p + ||I_2||_p$. As in (4.3.74), $||I_1||_p \leq ||u_0||_p$. From Jensen's inequality,

$$\begin{aligned}||I_2||_p^p &= |ct|^p \int_{\mathbb{R}^3} \left| \int_S \gamma \cdot \nabla u_0(x - c|t|\gamma)\frac{d\Omega}{4\pi}\right|^p dx \\ &\leq |ct|^p \int_{\mathbb{R}^3}\int_S |\gamma \cdot \nabla u_0(x - c|t|\gamma)|^p \frac{d\Omega}{4\pi}dx.\end{aligned}$$

Next, we use Hölder's inequality in $\mathbb{R}^3$: $|\gamma \cdot \nabla u_0| \leq |\nabla u_0|_p \times |\gamma|_q$ with $1/p + 1/q = 1$, where $|v|_p = (|v_1|^p + |v_2|^p + |v_3|^p)^{1/p}$ and likewise for $|v|_q$. Thus,

$$\begin{aligned}||I_2||_p^p &\leq c^p|t|^p \int_{\mathbb{R}^3}\int_S |\nabla u_0(x - c|t|\gamma)|_p^p \times |\gamma|_q^p \frac{d\Omega}{4\pi}dx \\ &\leq c^p|t|^p \int_S |\gamma|_q^p \int_{\mathbb{R}^3} |\nabla u_0(x - c|t|\gamma)|_p^p dx\frac{d\Omega}{4\pi} = c^p|t|^p\left(\int_S |\gamma|_q^p \frac{d\Omega}{4\pi}\right)||\nabla u_0||_p^p.\end{aligned}$$

which yields equation (4.3.71). Finally, the case $p = +\infty$ is trivial. Equation (4.3.73) is then the result of equations (4.3.71) and (4.3.72) applied to the function

$$w(x,t) - \tilde{m}(x,t) = [F_t * (v_0 - \tilde{v}_0)](x) + [\dot{F}_t * (u_0 - \tilde{u}_0)](x).$$

This finishes the proof. □

Equation (4.3.73) shows that L^p approximations of the initial conditions provide an L^p control between the solution w and the approximation $\tilde{m}$, for any time t. This is one reason why in our numerical applications (Section 4.4), we focus on initial condition reconstruction.

When c is unknown and estimated by $\hat{c}$ through maximizing the log marginal likelihood, we have instead (highlighting the dependence in c by writing $F_t^c = \sigma_{c|t|}/4\pi c^2 t$)

$$||w(\cdot,t)-\tilde{m}(\cdot,t)||_p = ||F_t^c * u_0 - F_t^{\hat{c}} * \tilde{u}_0 + \dot{F}_t^c * v_0 - \dot{F}_t^{\hat{c}} * \tilde{v}_0||_p$$
$$= ||F_t^c * (u_0 - \tilde{u}_0) + (F_t^c - F_t^{\hat{c}}) * \tilde{u}_0 + \dot{F}_t^c * (v_0 - \tilde{v}_0) + (\dot{F}_t^c - \dot{F}_t^{\hat{c}}) * \tilde{v}_0||_p,$$

and thus

$$||w(\cdot,t) - \tilde{m}(\cdot,t)||_p \leq |t|\ ||v_0 - \tilde{v}_0||_p + ||u_0 - \tilde{u}_0||_p + C_p c|t|\ ||\nabla(u_0 - \tilde{u}_0)||_p$$
$$+ ||(F_t^c - F_t^{\hat{c}}) * \tilde{u}_0||_p + ||(\dot{F}_t^c - \dot{F}_t^{\hat{c}}) * \tilde{v}_0||_p. \qquad (4.3.75)$$

The terms containing $F_t^c - F_t^{\hat{c}}$ and $\dot{F}_t^c - \dot{F}_t^{\hat{c}}$ may be further controlled in terms of $|c - \hat{c}|$ with additional assumptions such as Lipschitz continuity of u_0 and v_0. Likewise, the quantity $||w(\cdot,t) - \tilde{m}(\cdot,t)||_p$ may be further controlled if additional assumptions are made on u_0 and/or v_0. We leave such results to the interested reader.

4.4 Numerical experiments

In this section, we showcase WIGPR on functions w that are solutions of Problem (4.3.1), using the kernels (4.3.35) and (4.3.36) separately as well as together, as in equation (4.3.8). The goal is twofold: reconstructing the target function w, which more or less amounts to reconstructing its initial conditions (Proposition 4.3.14), and estimating the physical parameters attached. Note that with badly estimated physical parameters, the reconstruction step is more or less bound to fail, especially with inaccurate wave speed c and/or source centers x_0^{u} and x_0^{v}.

Running an extensive numerical study of the capabilities and limitations of WIGPR is a large task in itself. For the time being we will settle for simple test cases; in particular we only consider compactly supported and radially symmetric initial conditions, for which we can use the formulas (4.3.35) and (4.3.36) which can be evaluated numerically with a low computational cost. We will denote with a star the corresponding true source position x_0^* and celerity c^*. whereas their starless counterpart will denote the hyperparameters of the WIGPR kernels. The estimated hyperparameters will be denoted with a hat, e.g. $\hat{c}$. Two test cases for WIGPR are considered here. A first test

case for $k_{\mathrm{u}}^{\mathrm{wave}}$ described in Subsection 4.4.1, for which $u_0 \neq 0$ and $v_0 = 0$. This would correspond to PAT, though real life PAT test cases would be very unlikely to enjoy radial symmetry properties. A second test case for $k_{\mathrm{u}}^{\mathrm{wave}} + k_{\mathrm{v}}^{\mathrm{wave}}$ described in Subsection 4.4.2, for which $u_0 \neq 0$ and $v_0 \neq 0$. For each test case, the full procedure described below is performed.

Numerical simulation and database generation Given initial conditions u_0 and v_0, we numerically simulate the solution w over a given time period. We use a basic two step explicit finite difference time domain (FDTD) numerical scheme for the wave equation as described in [27], equation A.24, over the cube $[0,1]^3$. We also use first order Engquist-Majda transparent boundary conditions [70], in order to mimic a full space simulation. We use a sample rate $SR = 200\ Hz$ (time step $\Delta t = 1/200$ s), a space step $\Delta x = 43\ mm$, and a wave speed $c^* = 0.5\ m/s$. The simulation duration is $T = 1.5\ s$.

30 sensors are scattered in the cube $[0.2, 0.8]^3$ using a Latin hypercube repartition and a minimax space filling algorithm. Signal outputs correspond to time series for each sensor, with a sample rate of 50 Hz, so 75 data points altogether spanned over the time interval $[0, T]$ for each sensor. This leads to $30 \times 75 = 2250$ observations. Each signal is then polluted by a centered Gaussian white noise with standard deviation $\sigma_{\mathrm{noise}} = 0.45$ (resp. 0.09) for the test case #1 (resp. test case #2). These values correspond to around 10% of the maximal amplitude of the signals, see Figures 4.2a and 4.4.

Perform WIGPR on simulated data We perform WIGPR on portions of the dataset obtained above, using the `kergp` package [58] from R [160]. For that we use kernels (4.3.35) and/or (4.3.36) which are "fast" to evaluate, with K_{v} and k_{u}^0 both 1D 5/2−Matérn kernels. This Matérn kernel is stationary and writes, in term of the increment $h = x - x'$,

$$k_{5/2}(h) = \sigma^2\big(1 + |h|/\rho + |h|^2/3\rho^2\big)\exp\big(-|h|/\rho\big). \tag{4.4.1}$$

It has two hyperparameters on its own, ρ and σ^2. ρ is the length scale of the kernel (4.4.1) and should correspond to the typical variation length scale of the function approximated with GPR; σ^2 is the variance of the kernel. We tackle two different questions related to WIGPR which are respectively the estimation of physical parameters and the sensitivity to sensor locations.

(P_1) We first study how well the physical parameters (c^*, x_0^*, R^*) can be estimated with WIGPR. For this, we first select N_s time series corresponding to the first N_s sensors with $N_s \in \{3, 5, 10, 15, 20, 25, 30\}$. The corresponding Kriging database contains $75 \times N_s$ data points. For this database, we perform

negative log marginal likelihood minimization to estimate the corresponding hyperparameters, which are

$$\theta = \begin{cases} (x_0^{\mathrm{u}}, R_{\mathrm{u}}, \theta_{k_{\mathrm{u}}^0}, c, \lambda) \in \mathbb{R}^8 & \text{if } v_0 = 0 \text{ and } u_0 \neq 0, \\ (x_0^{\mathrm{u}}, R_{\mathrm{u}}, \theta_{k_{\mathrm{u}}^0}, x_0^{\mathrm{v}}, R_v, \theta_{k_{\mathrm{v}}^0}, c, \lambda) \in \mathbb{R}^{14} & \text{if } v_0 \neq 0 \text{ and } u_0 \neq 0. \end{cases}$$

λ corresponds to σ^2 in Section 4.2.2.2, and is viewed as an additional hyperparameter in the log marginal likelihood. We use a COBYLA optimization algorithm to optimize $\mathcal{L}(\theta, \lambda)$ and a multistart procedure with $n_{\mathrm{mult}} = 100$ different starting points. That is, 100 different values of θ_0 are scattered over an hypercube $H \subset \mathbb{R}^8$ or $H \subset \mathbb{R}^{14}$, and the COBYLA log marginal likelihood optimization procedure is run using each value of θ_0 as a starting point. The resulting hyperparameter value providing the minimal negative log marginal likelihood is selected. The multistart procedure mitigates the risk of getting stuck in local maxima. COBYLA is a gradient-free optimization method used in `kergp` and is available in the `nloptr` package from R. We then reconstruct the initial conditions using WIGPR, which we evaluate in terms of the indicators in equation (4.4.2).

(P_2) Next, we study the sensibility of the reconstruction step with respect to the sensor locations. Consider 40 different Latin hypercube layouts of the 30 sensors, each obtained with a minimax space filling algorithm. For each layout, we provide the correct set of hyperparameter values to the model; these values are described in each test case. We then reconstruct the initial conditions using GPR and N_s sensors, with $N_s \in \{3, 5, 10, 15, 20, 25, 30\}$. L^p relative errors (see equation (4.4.2)) are computed between the reconstructed initial condition and the real initial condition. For each number of sensors N_s, statistics over the 40 different datasets for these L^p errors are summarized in boxplots (see e.g. Figure 4.3a). Each box plot shows the median, the first and the third quartiles of a dataset corresponding to results obtained on the 40 different receiver dispositions. The dots inside a circle correspond to the median of each boxplot. The black crosses are the mean of each box plot, which are linked together with the dashed line. The circles are outliers.

In both cases, the approximated initial position $\tilde{u}_0$ is recovered by evaluating the WIGPR Kriging mean at $t = 0$ over a 3D grid and the initial speed $\tilde{v}_0$ is recovered by evaluating the Kriging mean at $t = 0$ and $t = \Delta t = 10^{-7}$ over the same 3D grid: $\tilde{v}_0 \simeq (\tilde{m}(\cdot, \Delta t) - \tilde{m}(\cdot, 0))/\Delta t$. Figures are displayed using MATLAB [141].

Numerical indicators For (P_1), we indicate in Tables 4.1 and 4.2 the distances between the true physical parameters and the estimated ones, depending on the number of sensors used. Additionally, for every $p \in \{1, 2, \infty\}$, we

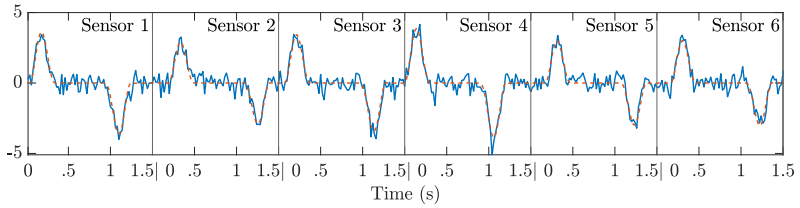

(a) Test case #1, excerpt of captured signals. Dashed line: noiseless data. Solid line: noisy data.

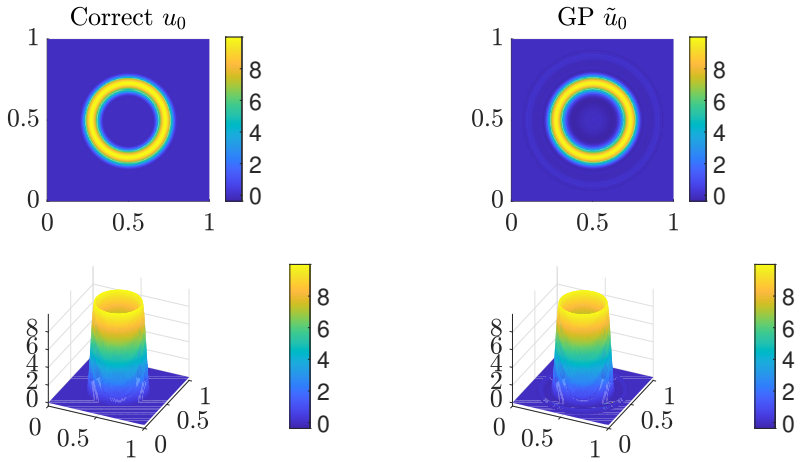

(b) Test case #1: True u_0 (left column) vs WIGPR u_0 (right column). 15 sensors were used. The images correspond to the 3D functions evaluated at $z = 0.5$.

Figure 4.2 – Visualization of signal and WIGPR results for the test case #1

indicate relative L^p reconstruction errors $e_{p,\text{rel}}$ defined below depending on the number of sensors used:

$$e^{\text{u}}_{p,\text{rel}} = ||u_0 - \tilde{u}_0||_p / ||u_0||_p \quad \text{and} \quad e^{\text{v}}_{p,\text{rel}} = ||v_0 - \tilde{v}_0||_p / ||v_0||_p. \tag{4.4.2}$$

A relative error of over 100% means that $||u_0 - \tilde{u}_0||_p \geq ||u_0||_p$, in which case the trivial estimator $\hat{u}_0 = 0$ performs better than the estimator $\tilde{u}_0$, in the L^p sense. Note that we deal with three dimensional functions, for which approximation errors are typically larger than for their one dimensional counterpart. Thus, relatively large errors may still correspond to pertinent approximations. For (P_2) are plotted boxplots of the relative L^p errors over the 40 different sensor layouts, depending on the number of sensors used. Integrals for the L^p error plots are approximated using Riemann sums over 3D grids containing the support of the integrated functions, with space step $dx = 0.01$.

The datasets, the code for generating the datasets and the code for performing WIGPR are available online at

https://github.com/iain-pl-henderson/wave-gpr

4.4.1 Test case for $k_{\mathrm{u}}^{\mathrm{wave}}$

In this test case, v_0 is assumed null and thus we set $k_{\mathrm{v}} = 0$, which yields $k_{\mathrm{v}}^{\mathrm{wave}} = 0$. We thus use $k_{\mathrm{u}}^{\mathrm{wave}}$ defined in (4.3.36) for GPR. We use the 1D Matérn kernel (4.4.1) for k_{u}^0 in equation (4.3.36). The initial condition u_0 is a radial ring cosine described as follows. We set $x_0^* = (0.5, 0.5, 0.5)^T$, $R_1 = 0.15, R_2 = 0.3$ and $A = 5$, the corresponding initial conditions (IC) are given by $v_0(x) = 0$ and

$$u_0(x) = A\mathbb{1}_{[R_1,R_2]}(|x - x_0^*|)\left(1 + \cos\left(\frac{2\pi(|x - x_0^*| - \frac{R_1+R_2}{2})}{R_2 - R_1}\right)\right). \tag{4.4.3}$$

See Figure 4.2b, left column, for a graphical representation of u_0. See Figure 4.2a for an excerpt of the corresponding Kriging database. For problem (P_1), the optimization domain is chosen to be the following hypercube of $\mathbb{R}^8$

$$\begin{aligned}\theta &= (x_0, R, \rho, \sigma^2, c, \lambda)\\ &\in [0,1]^3 \times [0.03, 0.5] \times [0.02, 2] \times [0.1, 5] \times [0.2, 0.8] \times [10^{-8}, 1].\end{aligned} \tag{4.4.4}$$

For problem (P_2), the hyperparameter θ_0 provided to the model is

$$\theta_0 = (x_0, R, (\rho, \sigma^2), c, \lambda) = ((0.65, 0.3, 0.5), 0.3, (0.2, 3), 0.5, \sigma^2_{\mathrm{noise}}), \tag{4.4.5}$$

with $\sigma^2_{\mathrm{noise}} = 0.45^2 = 0.2025$. The value of 0.2 provided for ρ is a visual estimation of the length scale of u_0 based on Figure 4.2b.

4.4.1.1 Discussion on the numerical results

For problem (P_1), Table 4.1 shows that the physical parameters x_0 and c are well estimated. The source size parameter R is overestimated, as could be expected from Section 4.3.2.5. The relative errors show that the overall function reconstruction is overall satisfying, with relative errors below 15% for $N_s = 20, 25$. The noise level σ^2_{noise} is often overestimated. For problem (P_2) (figures 4.3a, 4.3b and 4.3c), the relative errors stagnate below 10%. The IQR (interquartile range, i.e. the difference between the 3^{rd} and the 1^{st} quartiles) remains below 2%. This means that for this test case, the reconstruction step is not very sensitive to the sensors layout when they are scattered as a Latin hypercube.

N_{sensors}	3	5	10	15	20	25	30	Target
$\lvert\hat{x_0} - x_0^*\rvert$	0.204	0.003	0.004	0.008	0.003	0.004	0.015	0
$\hat{R}_{\text{u}}$	0.386	0.432	0.462	0.431	0.414	0.471	0.452	0.25
$\lvert\hat{c} - c^*\rvert$	0.084	0.004	0.005	0.005	0.006	0.001	0.004	0
$\hat{\sigma}^2_{\text{noise}}$	0.917	0.879	0.93	0.99	0.361	0.988	0.377	0.2025
$\hat{\rho}$	0.02	0.02	0.025	0.02	0.035	0.024	0.032	~ 0.05
$\hat{\sigma}^2$	2.367	3.513	4.903	3.168	4.446	4.619	4.79	Unknown
$e^{\text{u}}_{1,\text{rel}}$	1.275	0.157	0.128	0.168	0.11	0.103	0.248	0
$e^{\text{u}}_{2,\text{rel}}$	1.056	0.095	0.082	0.124	0.088	0.064	0.213	0
$e^{\text{u}}_{\infty,\text{rel}}$	1.037	0.132	0.128	0.198	0.136	0.101	0.321	0

Table 4.1 – Hyperparameter estimation and relative errors, test case #1

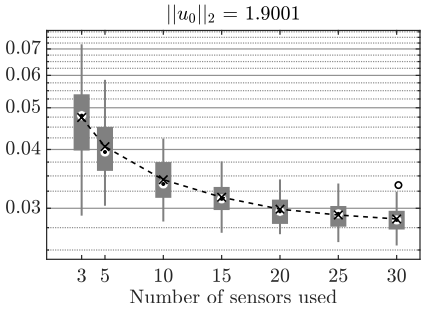

(a) L^2 rel. error for u_0 (test case #1)

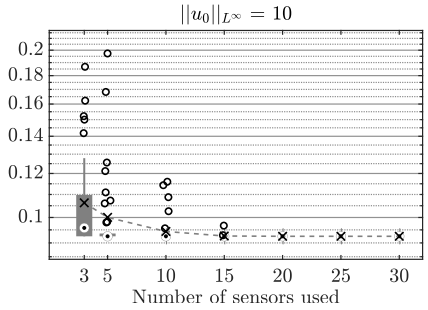

(b) L^∞ rel. error for u_0 (test case #1)

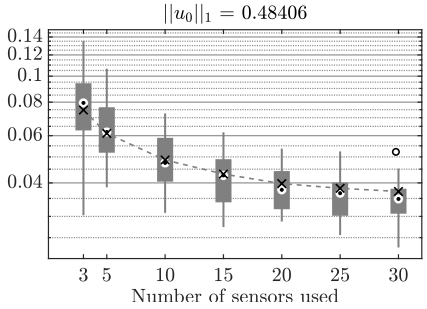

(c) L^1 rel. error for u_0 (test case #1)

Figure 4.3 – Box plots for the sensibility analysis, test case #1

4.4.2 Test case for $k_{\text{v}}^{\text{wave}} + k_{\text{u}}^{\text{wave}}$

For this test case, the initial position is a raised cosine, while the initial speed is a ring cosine. We set $x_0^{\text{u}*} = (0.65, 0.3, 0.5)^T$, $R_u = 0.25$, $A_{\text{u}} = 2.5$, $x_0^{\text{v}*} = (0.3, 0.6, 0.7)^T$, $R_1^{\text{v}} = 0.05$, $R_2^{\text{v}} = 0.15$ and $A_{\text{v}} = 30$. The co<rresponding

IC are given by

$$\begin{cases} u_0(x) &= A_{\mathrm{u}} \mathbb{1}_{[0,R_u]}(|x - x_0^{\mathrm{u}*}|)\left(1 + \cos\left(\frac{\pi|x-x_0^{\mathrm{u}*}|}{R_u}\right)\right), & (4.4.6) \\ v_0(x) &= A_{\mathrm{v}} \mathbb{1}_{[R_1^{\mathrm{v}},R_2^{\mathrm{v}}]}(|x - x_0^{\mathrm{v}*}|)\left(1 + \cos\left(\frac{2\pi\left(|x-x_0^{\mathrm{v}*}| - \frac{R_1^{\mathrm{v}}+R_2^{\mathrm{v}}}{2}\right)}{R_2^{\mathrm{v}}-R_1^{\mathrm{v}}}\right)\right). & (4.4.7) \end{cases}$$

See Figures 4.5a and 4.5b, left columns, for graphical representations of u_0 and v_0. See Figure 4.4 for a visualization of the database. For problem (P_1), the optimization domain is chosen to be the following hypercube

$$\begin{aligned} \theta =& (x_0^{\mathrm{u}}, R_u, (\rho_{\mathrm{u}}, \sigma_{\mathrm{u}}^2), x_0^{\mathrm{v}}, R_{\mathrm{v}}, (\rho_{\mathrm{v}}, \sigma_{\mathrm{v}}^2), c, \lambda) \\ \in& [0,1]^3 \times [0.05, 0.4] \times [0.02, 2] \times [0.1, 5] \\ \times& [0,1]^3 \times [0.05, 0.4] \times [0.02, 2] \times [0.1, 5] \times [0.2, 0.8] \times [10^{-8}, 2 \times 10^{-2}]. \end{aligned} \tag{4.4.8}$$

For problem (P_2), the hyperparameter value θ_0 provided to the model is

$$\theta_0 = ((0.65, 0.3, 0.5), 0.3, (0.06, 3), (0.3, 0.6, 0.7), 0.15, (0.025, 3.5), 0.5, \sigma^2_{\mathrm{noise}}), \tag{4.4.9}$$

with $\sigma^2_{\mathrm{noise}} = 0.0081$. The provided values for $(\rho_{\mathrm{u}}, \sigma_{\mathrm{u}}^2)$ and $(\rho_{\mathrm{v}}, \sigma_{\mathrm{v}}^2)$ are the estimated values from (P_1).

4.4.2.1 Discussion of the numerical results

Table 4.2 shows that the physical parameters x_0^{u}, x_0^{v} and c are well estimated. The source radii R_{u} and R_{v} are overestimated, as expected from Section 4.3.2.5. The noise level σ^2_{noise} is generally overestimated. The reconstruction of the initial position u_0 yielded satisfactory results with L^2 and L^∞ relative errors below 25%, and an L^1 relative error below 35% ($N_s = 10, 15, 20, 25, 30$). The higher L^1 relative error means that the reconstructed function $\tilde{u}_0$ is supported on a larger set than the true function u_0, as the L^1 norm favours sparsity. For the initial speed v_0, the numerical indicators are not as good, reaching minimal values for $N_s = 25$. The corresponding errors for the L^1, L^2 and L^∞ errors are 64%, 28% and 64% respectively. Note though that Figure 4.5b (corresponding to $N_s = 20$) shows that WIGPR still managed to capture the ring structure of v_0; the corresponding L^1 error for $N_s = 20$ is 150% (Table 4.2), confirming that the misestimated support radius R_{v} is heavily penalized by the L^1 norm. The reconstruction of v_0 for $N_s = 30$ failed (Table 4.2). For problem (P_2), the numerical indicators are better. For

u_0, Figures 4.6a, 4.6c and 4.6e show that relative error medians stagnate below 5% for $N_s \geq 15$. The corresponding IQR are around 2%. For v_0 (Figures 4.6b, 4.6d and 4.6f), the L^1, L^2 and L^∞ relative error medians stagnate at $30\%, 25\%$ and 40% respectively. The corresponding IQR stagnate at $10\%, 5\%$ and 10% respectively.

N_{sensors}	3	5	10	15	20	25	30	Target
$\lvert\hat{x}_0^{\text{u}} - x_0^{\text{u}*}\rvert$	0.163	0.144	0.013	0.024	0.023	0.033	0.015	0
$\hat{R}_{\text{u}}$	0.4	0.274	0.384	0.309	0.352	0.286	0.313	0.25
$\lvert\hat{x}_0^{\text{v}} - x_0^{\text{v}*}\rvert$	0.163	0.18	0.035	0.028	0.037	0.006	0.05	0
$\hat{R}_{\text{v}}$	0.252	0.166	0.313	0.356	0.348	0.266	0.339	0.15
$\lvert\hat{c} - c^*\rvert$	0.165	0.156	0.028	0.036	0.042	0.011	0.04	0
$\hat{\sigma}^2_{\text{noise}}$	0.0178	0.0184	0.0188	0.0161	0.0187	0.0145	0.0116	0.0081
$\hat{\rho}_{\text{u}}$	0.034	0.069	0.102	0.027	0.031	0.061	0.034	~ 0.05
$\hat{\sigma}^2_{\text{u}}$	4.649	4.472	4.575	2.493	0.678	3.272	2.541	Unknown
$\hat{\rho}_{\text{v}}$	0.057	0.027	0.044	0.053	0.085	0.022	0.012	~ 0.02
$\hat{\sigma}^2_{\text{v}}$	3.91	2.538	3.05	1.545	4.886	3.575	4.346	Unknown
$e^{\text{u}}_{1,\text{rel}}$	2.414	1.676	0.243	0.311	0.358	0.315	0.317	0
$e^{\text{u}}_{2,\text{rel}}$	1.276	1.053	0.174	0.223	0.228	0.261	0.205	0
$e^{\text{u}}_{\infty,\text{rel}}$	0.732	0.608	0.136	0.174	0.231	0.212	0.228	0
$e^{\text{v}}_{1,\text{rel}}$	2.865	2.796	1.315	1.42	1.51	0.645	9.784	0
$e^{\text{v}}_{2,\text{rel}}$	1.492	1.812	0.694	0.616	0.736	0.284	35.75	0
$e^{\text{v}}_{\infty,\text{rel}}$	1.083	1.608	0.817	0.763	0.845	0.635	2416.682	0

Table 4.2 – Hyperparameter estimation and relative errors, test case #2

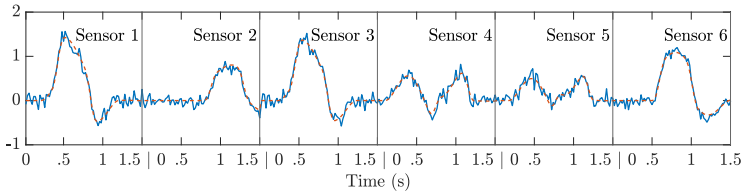

Figure 4.4 – Test case #2, excerpt of captured signals. Dashed line: noiseless data. Solid line: noisy data.

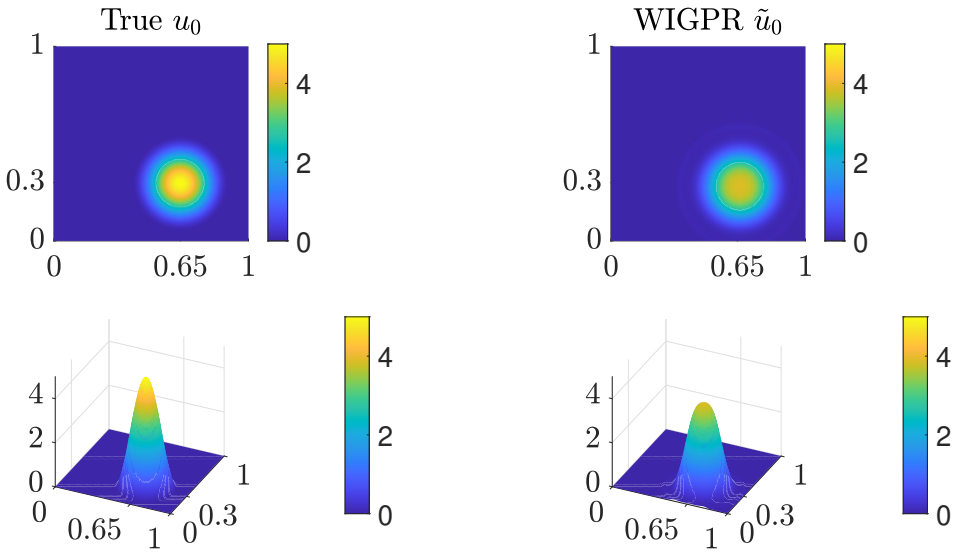

(a) True u_0 vs WIGPR u_0. The images correspond to the 3D solutions evaluated at $z = 0.5$.

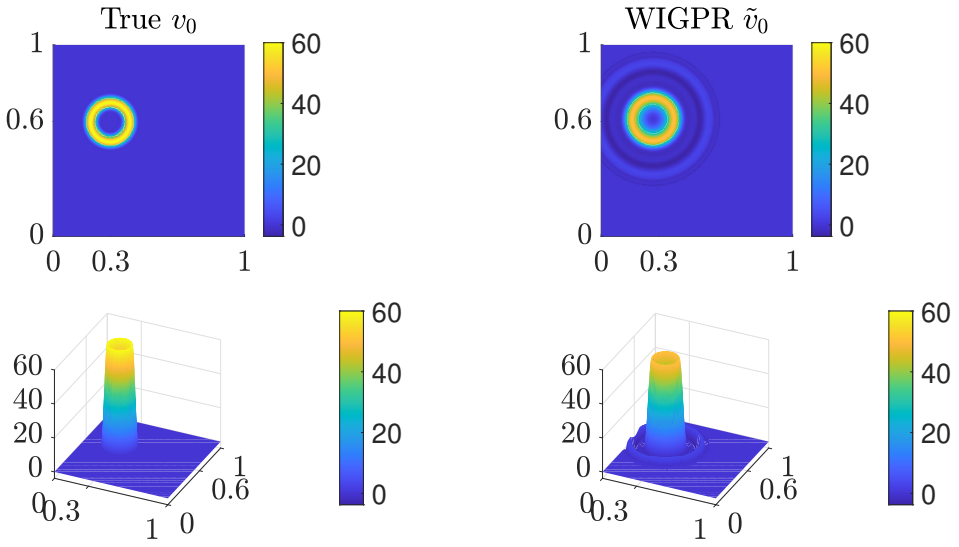

(b) True v_0 vs WIGPR v_0. The images correspond to the 3D solutions evaluated at $z = 0.7$.

Figure 4.5 – Test case #2: top and lateral view of the reconstructions of u_0 (Figure 4.5a) and v_0 (Figure 4.5b) provided by WIGPR, in comparison with u_0 and v_0. Left columns: true IC. Right columns: WIGPR IC reconstructions. 20 sensors were used.

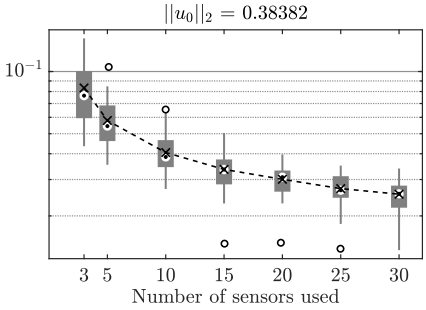

(a) L^2 rel. error for u_0 (test case #2)

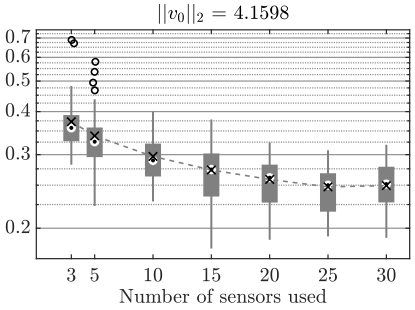

(b) L^2 rel. error for v_0 (test case #2)

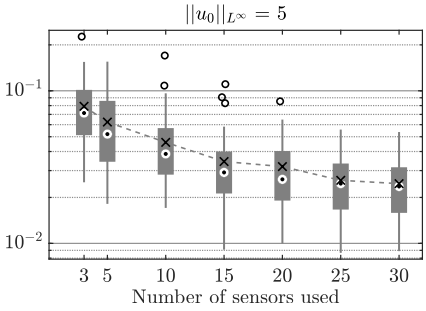

(c) L^∞ rel. error for u_0 (test case #2)

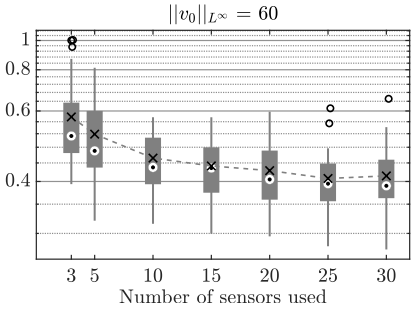

(d) L^∞ rel. error for v_0 (test case #2)

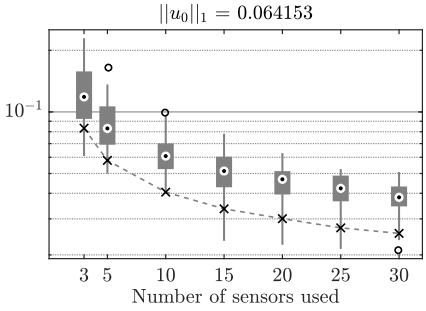

(e) L^1 rel. error for u_0 (test case #2)

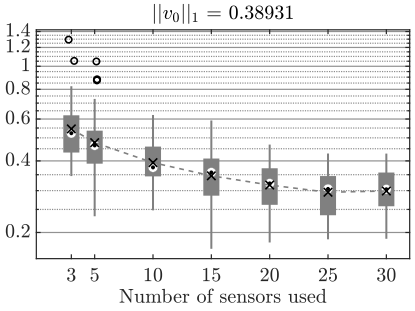

(f) L^1 rel. error for v_0 (test case #2)

Figure 4.6 – Box plots for the sensibility analysis, test case#2

4.5 Conclusion and perspectives

In Section 4.3, we described several covariance models tailored to the wave equation; they are particular cases of general ones first derived in a previous work. They correspond to the cases where either wide sense stationarity or radial symmetry assumptions over the initial conditions hold. In addition, the sample paths of the associated random fields (not necessarily Gaussian) are a.s. solution to the homogeneous wave equation. These covariances fully specify centered Gaussian process priors, which can then be used in the context of Gaussian process regression (WIGPR). In that framework, the physical parameter of the PDE system (e.g. source location or wave celerity) can be interpreted as hyperparameters of the WIGPR prior, as in [163]. We then showed that in the limit of the small source radius, the multilateration method for point source localization was naturally recovered by the hyperparameter estimation step of WIGPR. We furthermore showed that WIGPR naturally provides a reconstruction of the initial conditions of the wave equation, as should be expected when putting probability priors over them.

The radial symmetry WIGPR formulas from Section 4.3 were then showcased in Section 4.4, where two practical questions were tackled. First, WIGPR can correctly estimate certain physical parameters attached to the corresponding wave equation, namely the wave speed and source position. When these parameters are well estimated, WIGPR is capable of providing non trivial reconstructions of the initial condition, which we studied in terms of L^1, L^2 and L^∞ relative errors. We furthermore observed that the reconstruction step was not very not very sensitive to the layout of the sensors, assuming that the correct set of hyperparameters is provided to the model.

Future possible investigations concern the practical use of the more general formula (4.3.8) without any radial symmetry assumptions, e.g. for PAT applications. To compute the convolutions efficiently, one may then resort to multidimensional fast Fourier transforms. Moreover, in this first study, we have only used simple methods for GP numerical evaluation. More advanced GP techniques such as inducing points [159] should now be used to handle large datasets such as the ones we have used in Section 4.4. The case of the two dimensional wave equation is also of practical interest, e.g. in oceanography [125], and presents many different properties when compared to its 3D counterpart ([73], p. 80). It would thus deserve a theoretical and practical study in its own right when coupled with GPR.

Finally, the surprising link drawn between our GPR method and the multilateration localization method suggests that other very explicit links should exist between well-chosen kernel methods and traditional mathematical or numerical methods tailored to given physical models. This is certainly an im-

portant direction of research, where GPR stands out as a favourable environment through which the communities of machine learning and mathematical physics may be brought together.

Chapter 5

Gaussian process regression and finite difference schemes

Contrarily to the previous chapters, this chapter does not correspond to a an article or a preprint. Its subject is a current topic of research; the propositions described here constitute a first series of results which motivate the topic of this chapter as a short term perspective of research.

Abstract

This chapter presents perspectives in the application of kernel or GP methods to the design of finite difference schemes for solving PDEs. The first section is dedicated to the description of certain concepts which are central in the theory of finite difference schemes such as consistency and stability. We next describe how GPR can be used to obtain "finite difference-like schemes". The case of an asymptotic regime (the so-called "flat limit") is investigated, explicit links with well-known finite difference schemes are established and some other new schemes are proposed. A non asymptotic regime is then considered, which is obtained by solving an optimization problem constrained on the consistency equations. This regime avoids the vanishing posterior property of the flat limit, thus enabling a Bayesian interpretation of the associated scheme. A final section is dedicated to the topic of transparent boundary conditions for the wave equation.

Contents

5.1 Introduction 217
5.2 Finite difference schemes for the advection equation 221
5.2.1 First order hyperbolic PDEs 221
5.2.2 Finite difference schemes 222
5.2.3 Gaussian process regression and finite difference schemes in the flat limit regime 227
5.2.4 Finite difference schemes via GPR in the non flat regime 240
5.3 Transparent boundary conditions 247
5.3.1 Context 247
5.3.2 The two dimensional wave equation 249
5.3.3 A matched Dirichlet boundary condition strategy . . . 250
5.4 Conclusion and perspectives 251
5.5 Appendix : proofs 254

5.1 Introduction

In the previous three chapters, we have studied physics-informed kernels in continuous settings. We only encountered discretization in Sections 4.3.3 and 4.4 of Chapter 4. Section 4.3.3 in particular showed that some very explicit links may be drawn between physics-informed kernel methods and standard numerical methods used to solve problems arising from meaningful physical considerations. This chapter goes a step further by directly considering numerical methods for solving PDEs, and trying to interpret them as kernel methods; or rather, we consider kernel methods and attempt to interpret them as standard numerical methods.

This content of this chapter is the subject of current research; the presented examples are simple (but instructive), and many directions of research are yet to be explored.

As the kernel setting is firstly designed to deal with regression problems involving pointwise evaluations of the target function (see Section 1.2.4 in the introduction), we will focus on the finite difference method. Given a PDE, say the advection equation

$$\partial_t u + c\partial_x u = 0, \tag{5.1.1}$$

the finite difference method consists in approximating each derivative with a finite difference counterpart, given a space step $\Delta x > 0$ and a time step $\Delta t > 0$. For example, if one uses forward difference approximations for ∂_t and ∂_x, we obtain

$$\frac{u_k^{n+1} - u_k^n}{\Delta t} + c\frac{u_{k+1}^n - u_k^n}{\Delta x} = 0. \tag{5.1.2}$$

Here, the values u_k^n play the role of approximations of the values $u(k\Delta x, n\Delta t)$ of the target function at the grid points. Equation (5.1.2) can in turn be written as a recurrence relation: setting $\lambda = c\Delta t/\Delta x$, we have

$$u_k^{n+1} = (1+\lambda)u_k^n - \lambda u_{k+1}^n. \tag{5.1.3}$$

This relation is (in this case) easily implemented on computer machines. Such a recurrence equation is called a finite difference scheme.

The main questions concerning finite difference schemes (and in fact, other numerical methods) are the following : (i) is the scheme actually approximating the PDE We are trying to solve? (consistency) (ii) Is the solution of the recurrence equation even bounded in some sense? (stability) (iii) What is the precision of the numerical approximation $u(k\Delta x, n\Delta t) \simeq u_k^n$? (accuracy) Another notion, which has to be studied on its own for nonlinear PDEs, is that

of the convergence of the scheme: does the numerical solution converge to the true solution as the mesh size goes to zero? In the linear case, this question is settled by the Lax equivalence theorem, which states that any finite difference scheme which is stable and consistent is convergent ([132], Section 8.3.2).

The history of finite difference schemes may be traced back as far as Euler and his method for approximating derivatives, to solve ordinary differential equations ([95], p. 35). In the context of partial differential equations, this method received a lot of attention throughout the twentieth century, perhaps starting from the 1928 article from Courant, Friedrichs and Lewy (we refer to its English translation [47]; see also [132], p. 69). For time dependent linear PDEs in particular, finite difference methods remain widely used. Important applications include electromagnetics [120] and acoustics [28].

The topic of this chapter stems from the following observation. Consider a space time function $u(x,t)$, and consider the matter of estimating the value $u(0,\Delta t)$ from the sampled values $u^0_{-1} \coloneqq u(-\Delta x, 0)$, $u^0_0 \coloneqq u(0,0)$ and $u^0_1 \coloneqq u(\Delta x, 0)$. This regression problem can be tackled with Gaussian process regression. In this case, given a space-time covariance function k, the Kriging formula writes

$$\tilde{m}(0,\Delta t) = A^T U(X,0) = a_{-1}u^0_{-1} + a_0 u^0_0 + a^0_1 u^0_1, \tag{5.1.4}$$

where $X = (-\Delta x, 0, \Delta x)^T$, $u(X,0) = (u^0_{-1}, u^0_0, u^0_1)^T$ and $A = K^{-1}V$, where $K_{ij} = k((i\Delta x, 0), (j\Delta x, 0)$ and $V_j = k((0,\Delta t), (j\Delta x, 0))$. Here, we conveniently index the matrix K and vector V over $\{-1,0,1\}$ instead of $\{1,2,3\}$. At this point, equation (5.1.4) looks awfully close to a finite difference scheme, and the natural question is whether the coefficients obtained this way yield relevant numerical schemes, especially when the kernel k is well-chosen. In particular, if k is "physics-informed" with reference to a given PDE (say the advection equation), it is somewhat reasonable to hope that equation (5.1.4) reduces to some finite difference scheme, either well-known or yet unknown. Section 5.2.3, which contains the important results of this chapter, is dedicated to the study of this question.

Overview of the chapter This chapter begins with a review of the relevant literature. After a motivation for the study of finite difference methods for the advection equation through the prism of general first order hyperbolic PDEs, we provide the basics of the finite difference method. We then describe how explicit links can be made between Gaussian process regression and finite difference schemes, with a focus on centered three point finite difference schemes in particular. This process is primarily based on the study of physics-informed GPR in the *flat limit* regime. This regime consists in considering a

kernel with lengthscale $\ell > 0$, $k_\ell(x, x') = k(x/\ell, x'/\ell)$ where k is given, and in studying the behaviour of the associated Kriging mean $\tilde{m}_\ell$ when $\ell \to +\infty$. This regime is called "flat" as then, if k_0 is continuous at the vicinity of $(0, 0)$, $k_\ell(x, x') \to k(0, 0)$ when $\ell \to +\infty$, for all x, x'.

In the case of three-point schemes, the thorough investigation of flat limits of physics-informed kernels tailored to the advection equation yields a continuous family of finite difference schemes, which notably contains the well-known upwind scheme and the Lax-Wendroff scheme. Their consistency, stability and accuracy is studied; theorems and conjectures are provided. This example will serve as a motivation for further investigation of potential applications of flat limits in the contexts of numerical methods for PDEs.

We then study a non asymptotic regime in which the Kriging coefficients are constrained to verify the consistency equations corresponding to the advection equation. Theoretical results pertaining to the stability of the resulting numerical scheme are provided, as well as related conjectures.

A final section is dedicated to the design of transparent boundary conditions thanks to physics-informed Gaussian process regression.

Relevant literature The study of numerical tasks (integration, linear algebra, optimization, numerical schemes) with a general Bayesian perspective has received some attention in the past ten years. A notable work which brought attention upon the subject of adding uncertainty measurements in such numerical tasks is [100], which dates from 2015. The resulting field of research is now called "Probabilistic numerics", or "Probabilistic numerical methods". We refer to [156] for an extended description of the literature attached to this discipline, as well as the recent book [99]. The topic of this field is actually heavily inspired from the seminal 1988 paper [60], whose origins can apparently even be traced back to Poincaré's course in probability [151].

The approach described in this chapter is rather different than that of probabilistic numerics. Indeed we will be using physics-informed kernels in the sense of Section 1.3.5, while the physics-informed probabilistic numerical methods as e.g. described in [156] more or less amount to the collocation method described in [212], section 16.3, where the PDE is only enforced on some finite number of collocation points, or against some finite dimensional trial space. The main difference between [156] and [212] is the Bayesian interpretation of the collocation method. By adopting our different approach, we will recover some well-known schemes as well as some new ones.

It turns out that several results of this chapter have already been described in much earlier works from Miranker and Micchelli, namely the two articles [144] and [143] published in 1973 and 1974 respectively (we could also add the 1971 paper [145]). It is however also true that the papers [144] and [143]

have gone completely unnoticed by the community [1]; I stumbled upon them after completing a good part of my research on flat limits. Perhaps they were published too soon, at a time when kernel methods were not nearly as widespread as now. It seems though that the recent attention that physics-informed machine learning has received, as well as other works aiming at "optimizing" numerical methods using machine learning (see e.g. [57]), brings back the topic of those papers back to the agenda.

We will see that most of the results presented here are closely related to (multivariate) interpolation. In this context, convergence to Lagrange polynomial interpolation using flat limits of smooth kernels has first been observed in [66] (but this fact was already contained in [144] for cartesian grids), and has been systematically studied ever since [2]: [79, 126, 178, 131, 177, 19]. The non smooth case (typically, Matérn kernels) is investigated in [191, 130, 129], where it is shown that the limit interpolant corresponds to a polyharmonic spline interpolant. Again, versions of this fact were already contained in the earlier work [143]. Note that the article [191] is concerned with standard polyharmonic splines (of integer order) while [130] (as [143]) considers "generalized polyharmonic splines" in which the regularity exponent is an arbitrary positive real number. A one dimensional theory for such generalized fractional splines is given in [204].

It has to be noted that strictly speaking, the two works [144, 143] were not concerned with flat limits but rather with the convergence regime of numerical schemes, that is, $\Delta x \to 0$ and $\Delta t \to 0$ where Δx and Δt are the space step and the time step of the numerical scheme, respectively. We will see though that this convergence regime and the flat limit regime more or less amount to the same (Section 5.2.3.2). Finally, note that the framework used in all the works mentioned above is that of reproducing kernel Hilbert spaces, not a GP or Bayesian one. Such a framework has only been considered recently in [18]. We will see that this framework is a bit awkward as then the posterior distribution completely vanishes in the flat limit (it becomes deterministic); we will propose an alternative solution in Section 5.2.4.

Finally, it is worth mentioning that radial basis collocation methods, as described in [212], section 16.3, have been used in conjunction with finite difference methods. We refer to [80], Chapter 5, for an introduction to the subject. Flat limits are also evoked in this reference book (Sections 3.2.2 to 3.2.4).

1. At least, as suggests their Google Scholar page.

2. I would like to thank Toni Karvonen for pointing me towards those numerous references, the exploration of which eventually lead to the discovery of the papers [144] and [143].

5.2 Finite difference schemes for the advection equation

5.2.1 First order hyperbolic PDEs

One dimensional first order hyperbolic PDEs are of the form

$$\partial_t u + \partial_x f(u) = 0, \quad u(x,0) = u_0(x). \tag{5.2.1}$$

In multiple dimensions as well as for systems, an additional *hyperbolicity* condition is required on the Jacobian ∇f ([73], Section 7.3), which amounts to a specific diagonalisability condition; in our one dimensional setting, this condition is always fulfilled.

Equation (5.2.1) is a first order Cauchy problem. Hyperbolic PDEs appear in many physical problems including fluid mechanics and aerodynamics, and typically model conservation laws, such as conservation of mass, momentum or energy. The form of equation (5.2.1) is *conservative*, meaning that the final operation over each term is a partial derivative. The function f is called the flux function. Equation (5.2.1) can be written in *non conservative* form using the chain rule:

$$\partial_t u + f'(u)\partial_x u = 0, \quad u(x,0) = u_0(x). \tag{5.2.2}$$

The advection equation corresponds to the linear flux function $f(u) = cu$, where $c \in \mathbb{R}$:

$$\partial_t u + c\partial_x u = 0, \quad u(x,0) = u_0(x). \tag{5.2.3}$$

Its solution is given by translations of the initial condition:

$$u(x,t) = u_0(x - ct). \tag{5.2.4}$$

This solution verifies equation (5.2.1) in the sense of distributions. The parameter c corresponds to the propagation speed of the solution. In this setting, $f'(u)$ in equation (5.2.2) is thus interpreted as a local advection speed, and solutions of hyperbolic PDEs are expected to locally behave as solutions of the advection equation with speed $f'(u)$.

Properties of hyperbolic PDEs It is readily seen from equation (5.2.4) that hyperbolic PDEs typically do not smooth their initial conditions, contrarily to parabolic equations such the heat equation. This property is even more prevalent for nonlinear hyperbolic PDEs, as solutions corresponding to arbitrarily smooth initial conditions may become discontinuous in finite time.

A typical example is the Burger's equation, corresponding to $f(u) = u^2/2$ ([73], p. 139). This PDE is the simplest model for fluid propagation: its non conservative form $\partial_t u + u\partial_x u = 0$ is a one dimensional analogue of the first terms of the momentum equation in the Navier-Stokes system. It is also of interest to consider the *viscous* relaxation of the hyperbolic PDE (5.2.1) ([73], Section 7.3.2.b),

$$\partial_t u + \partial_x f(u) = \varepsilon \partial^2_{xx} u, \quad u(x,0) = u_0(x). \tag{5.2.5}$$

where $\varepsilon > 0$. The Laplacian term is viewed as a parabolic regularization term, and the associated solution u_ε is a smoothened approximation of the solution of equation (5.2.1) ([73], Sections 4.4.1.b, 4.5.2 and 10.1). In the case of Burger's equation, $u_\varepsilon \in C^\infty(\mathbb{R})$ for all $t > 0$ [43]. General nonlinear hyperbolic PDEs are not solvable analytically and their solutions have to be approximated numerically. This is the purpose of numerical schemes, the most commonly used being finite difference methods, finite element methods and finite volume methods. However, we will focus on the linear advection equation for three reasons:

- Given a finite difference scheme for the linear advection equation, one obtains a scheme for general hyperbolic PDEs by replacing the parameter c appearing in the scheme by the local advection speed $f'(u_k^n)$, where u_k^n denotes the approximation of the solution at the grid point $(k\Delta x, n\Delta t)$ (for finite volume and finite element methods though, the procedure is different).
- The advection equation constitutes a good benchmark for numerical schemes, as its solution is explicit, and is discontinuous if its initial data is discontinuous.
- Some important properties of numerical schemes for nonlinear PDEs, such as stability, can be expected to carry out from their behaviour on linearized PDEs (here, an advection equation). Among others, a similar remark is made in [208], Section 4.2.

5.2.2 Finite difference schemes

Finite difference schemes amount to replace the derivatives appearing in equations (5.2.1) or (5.2.2) by Euler type discretizations. They are closely related to finite volume schemes, which instead aim at approximating local averages over grid cells, in time and space, of the true solution.

Cartesian grids Given a space step Δx and a time step Δt, the associated space-time cartesian grid is the set $\{(k\Delta x, n\Delta t),\ k \in \mathbb{Z},\ n \in \mathbb{N}\}$. In relation

to the advection equation, we will introduce the so-called Courant number

$$\lambda := c\Delta t/\Delta x, \tag{5.2.6}$$

where c is the advection speed of the advection equation. Finite difference methods aim at approximating the values of the true solution at the grid points $u(k\Delta x, n\Delta t)$, by a sequence $(u_k^n)_{k\in\mathbb{Z},\ n\in\mathbb{N}}$. An approximation of the continuous solution is then recovered e.g. by means of linear interpolation. FD methods are very well-suited to cartesian grids and their analysis usually relies on Taylor expansions.

Explicit schemes, implicit schemes Replacing partial derivatives in equation (5.2.3) with Euler type discretizations lead to a recurrence relation of the form

$$\sum_{i=-p_1}^{q_1} b_i u_{i+k}^{n+1} = \sum_{i=-p_0}^{q_0} a_i u_{i+k}^n \quad \forall k \in \mathbb{Z} \tag{5.2.7}$$

(assuming that only two time steps are used to approximate the time derivative). Note that here we do not care about boundary conditions. A finite difference scheme is *explicit* if $p_1 = q_1 = 0$, and *implicit* otherwise. In this chapter we will only focus on explicit schemes and we set $b_0 = 1$, leading to schemes of the form

$$u_k^{n+1} = \sum_{i=-p}^{q} a_i u_{i+k}^n \quad \forall k \in \mathbb{Z} \tag{5.2.8}$$

Typically, the coefficients of finite difference schemes only depend on the Courant number λ.

Consistency and order of accuracy A numerical scheme is *consistent* if, in the limit of $\Delta x,\ \Delta t \to 0$, the finite difference equation reduces to the initial PDE. Consistency is a minimal requirement for any finite difference scheme. A scheme is of order $s > 0$ if the convergence rate of the numerical solution towards the true solution is of order $O(\Delta x^s)$ or $O(\Delta y^s)$ ([132], Section 8.1.1). It is known that explicit finite difference schemes for the advection equation are consistent if the two following linear equations are satisfied ([194])

$$\sum_{i=-p}^{q} a_i = 1, \quad \sum_{i=-p}^{q} i a_i = -\lambda. \tag{5.2.9}$$

If the coefficients of the scheme depend on Δx and not only on λ (which is not at all standard in usual numerical methods), it can be checked that the constraints can be relaxed to

$$\sum_{i=-p}^{q} a_i = 1 + o(1), \quad \sum_{i=-p}^{q} i a_i = -\lambda + o(\Delta x). \tag{5.2.10}$$

Stability Given a normed subspace $(E, ||\cdot||_E)$ of the space of sequences indexed by $\mathbb{Z}$ (say $\ell^p(\mathbb{Z})$ endowed with the p norm), the scheme (5.2.8) is said to be *stable* in the norm $||\cdot||_E$ (and in the Lax-Richtmyer sense) if there exists a constant α such that its solution verifies ([132], Section 8.3)

$$\left|\left|u^{n+1}\right|\right|_E \leq (1 + \alpha\Delta t)\left|\left|u^n\right|\right|_E \quad \forall n \in \mathbb{N}. \tag{5.2.11}$$

If $\alpha = 0$ then the method is stable for arbitrary large time. It can be shown that an explicit finite difference scheme is stable for arbitrary large time in the discrete ℓ^2 norm if and only if its amplification factor ($\equiv$ the modulus of the discrete Fourier transform of the scheme coefficients) is less than one:

$$\forall \omega \in [0, 2\pi], \quad \left| \sum_{j=-p}^{q} a_j e^{ij\omega} \right| \leq 1. \tag{5.2.12}$$

This is the so-called Von Neumann stability condition ([132], Section 8.3.3). For many finite difference schemes, this condition is shown to be equivalent to a so-called Courant-Friedrichs-Lewy (CFL) condition, typically of the form $|\lambda| \leq 1$, where λ is given in equation (5.2.6). Note that given a space step Δx and a finish time T, then the larger the Courant number is, the fewer the number of iterations in time are required to solve a numerical problem. This explains why one often attempts to maximize the Courant number. As in equation (5.2.10) and following equation (5.2.11), the Von Neumann condition may be relaxed to ([132], Section 8.3.3)

$$\forall \omega \in [0, 2\pi], \quad \left| \sum_{j=-p}^{q} a_j e^{ij\omega} \right| \leq 1 + \alpha\Delta t. \tag{5.2.13}$$

It may further happen that a scheme is consistent or stable only for a fixed value $\lambda = \lambda_0$; we will not be interested in such cases as for general PDEs of the form (5.2.1), the Courant number will be local ($\lambda_k^n = f'(u_k^n)\Delta t/\Delta x$, as e.g. in [132], p. 234), and thus we will rather be interested in schemes which are consistent and stable for a whole range of values of the Courant number, $\lambda_{\min} \leq \lambda \leq \lambda_{\max}$.

Explicit centered three point schemes Consider the case where $p = q = 1$. Such schemes that are consistent are parametrized by three scalars a_{-1}, a_0, a_1 and constrained by the two equations (5.2.9). It can be then shown that such schemes have the form

$$\begin{cases} a_{-1} = \lambda/2 + D/2, \\ a_0 = 1 - D, \\ a_1 = -\lambda/2 + D/2. \end{cases} \tag{5.2.14}$$

where D is a free parameter which can depend on λ. As a result, the associated finite difference scheme can be written as

$$u_k^{n+1} - u_k^n + \frac{\lambda}{2}(u_{k+1}^n - u_{k-1}^n) = \frac{D}{2}(u_{k+1}^n - 2u_k^n + u_{k+1}^n), \tag{5.2.15}$$

or, in terms of discrete derivatives,

$$\frac{u_k^{n+1} - u_k^n}{\Delta t} + c\frac{u_{k+1}^n - u_{k-1}^n}{2\Delta x} = \frac{D\Delta x^2}{2\Delta t}\frac{u_{k+1}^n - 2u_k^n + u_{k+1}^n}{\Delta x^2}. \tag{5.2.16}$$

The term on the right hand side is a discrete Laplacian. Following equation (5.2.5), the coefficient $D\Delta x^2/2\Delta t$ is then understood as a discrete viscosity coefficient whose presence regularizes the numerical solution. The upwind scheme corresponds to $D = |\lambda|$, the Lax-Friedrichs scheme corresponds to $D = 1$, the Lax-Wendroff scheme corresponds to $D = \lambda^2$ and the centered scheme corresponds to $D = 0$. As an illustration of stability analysis, we state the following theorem, which will also be of interest to us later on. Note that this result is stated without proof in [144].

Proposition 5.2.1. *The scheme* (5.2.14) *is stable in the* ℓ^2 *norm if and only if* $\lambda^2 \leq D \leq 1$.

The proof of this proposition is deferred to the appendix, for readability. This proof relies on the Von Neumann stability criterion, as well as interesting algebraic simplifications. From Proposition 5.2.1, we obtain that the upwind scheme ($D = |\lambda|$), the Lax-Friedrichs scheme ($D = 1$) and the Lax-Wendroff scheme ($D = \lambda^2$) are conditionally stable under the CFL condition $|\lambda| \leq 1$, while the centered scheme ($D = 0$) is unconditionally unstable. This shows that the discrete Laplacian stabilizes the numerical scheme, much like the Laplacian smoothens the solution in the continuous setting (equation (5.2.5)).

Modified equation analysis ([210]; [132], Section 8.6) By considering a function u whose values on the grid $u(x_k, t_n)$ verify exactly the finite difference equation (5.2.16), one can show that the function u is actually a

solution to PDE which is *different* than the target PDE (it reduces to the target PDE in the convergence regime $\Delta x,\ \Delta t \to 0$). This fact is of course approximate, but nevertheless the numerical solution is indeed closer to this new PDE than the target PDE. This PDE is the scheme's *modified (partial differential) equation*. Such equations are obtained by performing Taylor expansions on functions whose grid values exactly verify the numerical scheme. Modified equations are not unique; the preferred one is typically the one in which only spatial derivatives appear, at the exception of the time derivative appearing in the target PDE $\partial_t u + c\partial_x u = 0$. Indeed, the other spatial derivative terms are often more easily interpreted. For the scheme (5.2.14), a modified equation of this type is given in Proposition 5.2.2 below.

Proposition 5.2.2. *The following PDE*

$$\partial_t u + c\partial_x u = \frac{c\lambda\Delta x}{2}\left(\frac{D}{\lambda^2} - 1\right)\partial^2_{xx} u + \frac{c\Delta x^2}{6}(3D - 2\lambda^2 - 1)\partial^3_{xxx} u + O(\Delta x^3), \quad (5.2.17)$$

is a modified equation corresponding to the three-point scheme (5.2.14).

The proof of Proposition 5.2.2 is deferred to the appendix of the chapter. We call the coefficient in front of the $\partial^2_{xx} u$ term the *numerical* viscosity or diffusion coefficient, which is to be distinguished with the *discrete* viscosity coefficient D (the term discrete is a reference to the discrete Laplacian in equation (5.2.16)). Properties of the numerical scheme can be deduced from its modified equation. For example, for the Lax-Wendroff scheme ($D = \lambda^2$), it turns out that the diffusion coefficient in front of the term $\partial^2_{xx} u$ is null, the next term being the *dispersive* differential operator ∂^3_{xxx}. "Dispersive" means that waves (say Fourier modes $e^{i(k\cdot x - \omega t)}$ which are solutions to the given PDE) associated to different wavelengths travel at different speeds, thus "dispersing" the solution. This explains why the Lax-Wendroff scheme typically produces oscillations : the different sines and cosines propagate at different speeds. Moreover, the absence of numerical viscosity justifies that this scheme does not attenuate or dampen its numerical solution (at least, at the order of accuracy of equation (5.2.17); the next fourth order diffusive term $\partial^4_{xxxx} u$ is non zero), contrarily to other schemes with nonzero numerical viscosity. We can also see that the numerical viscosity becomes smaller and smaller as Δx approaches zero.

Note that the modified equation and the discrete equation do not agree: indeed, the modified equation associated to the Lax-Wendroff scheme is purely dispersive while its discrete viscosity $D = \lambda^2$ is non zero. Note finally that

the (incomplete) stability criterion $D \geq \lambda^2$ can be obtained by requiring that the numerical viscosity is nonnegative (as $c\lambda \geq 0$).

5.2.3 Gaussian process regression and finite difference schemes in the flat limit regime

5.2.3.1 Physics informed kernels for the advection equation and finite difference schemes

Introduce a space and a time step, Δx and Δt. Consider a stationary kernel k over $\mathbb{R}$, and consider a function u_0, say in $C^0(\mathbb{R}) \cap L^2(\mathbb{R})$, which we sample at points $x_j = j\Delta x$. Denote $u_j^0 \coloneqq u_0(j\Delta x)$, and consider the task of approximating $u_j^1 \coloneqq u_0(x_j - c\Delta t)$, which is the value of the true solution of equation (5.2.3) at $x = x_j$ and $t = \Delta t$, from the samples u_{j-1}^0, u_j^0 and u_{j+1}^0. As noted in the introduction, tackling this problem using GPR yields a relation of the form

$$u_j^1 = a_{-1}u_{j-1}^0 + a_0 u_j^0 + a_1 u_{j+1}^0, \tag{5.2.18}$$

where the vector $A = (a_{-1}, a_0, a_1)^T$ is given by

$$A = K^{-1}V, \quad K_{ij} = k((i-j)\Delta x), \quad V_j = k(j\Delta x - c\Delta t). \tag{5.2.19}$$

Above, we used the abusive but convenient indexation $i, j \in \{-1, 0, 1\}$ (instead of indexing over $\{1, 2, 3\}$) for the three dimensional matrix K and vector V. Because k is stationary, the coefficients a do not depend on x_j, or rather, j. As noted in the introduction, equation (5.2.18) looks like a finite difference scheme, and the question now will be whether the coefficients obtained this way yield relevant numerical schemes, or if they can be related to standard numerical schemes such as the ones mentioned in Section 5.2.2. The answer is yes. We will investigate two different regimes: the flat limit regime, in which we let the lengthscale of the kernel go to infinity, and a non asymptotic regime constrained on the consistency equations (5.2.9).

As a preliminary remark, note that we targeted the interpolation to take place at location $j\Delta x - c\Delta t$. In other words, we used the prior knowledge that value of the solution of the PDE, at $x = x_j$ and $t = \Delta t$, is exactly $u_0(x_j - c\Delta t)$. This can alternatively be understood in terms of physics-informed kernels. As in Example 2.3.8, we can directly incorporate the shape of the solution of the advection equation in the regression kernel, leading to a space time covariance function

$$k((x,t),(x',t')) = k_0(x - ct, x' - ct') = k_S(x - x' - c(t - t')). \tag{5.2.20}$$

where we assumed that the kernel k_0 modelling the initial conditions was stationary. Note that as in Proposition 2.4.1, we have the nice representation

$$k_0(x - ct, x' - ct') = [(\delta_{ct} \otimes \delta_{ct}) * k_0](x, x'), \tag{5.2.21}$$

where δ_{ct} is the Dirac mass at $x = ct$. δ_{ct} is also the (initial value) Green's function of the advection equation: that is, it is the distributional solution to the PDE (5.2.3), with $u_0 = \delta_0$. Using the kernel above to approximate $u(x_k, \Delta t)$ using the samples $u(x_{k-1}, 0), u(x_k, 0)$ and $u(x_{k+1}, 0)$ yields exactly equation (5.2.19).

Throughout this chapter, we will restrain our study at the origin $x_j = 0$, because the scheme is translation-invariant. It will also be of interest to us to observe that the vector A which contains the Kriging coefficients (equation (5.2.19)) is a minimizer of the following quadratic form over $\mathbb{R}^3$ (it is readily generalized to $\mathbb{R}^n$):

$$Q(b) := \int_{\mathbb{R}} \left| e^{ic\Delta t\xi} - b^T e^{i\xi X} \right|^2 \mu(d\xi). \tag{5.2.22}$$

In equation (5.2.22), we have $b \in \mathbb{R}^3, X = (-\Delta x,\ 0,\ \Delta x)^T, (e^{i\xi X})_j = e^{i\xi X_j}$ and μ is the spectral measure of k. Moreover, the minimum of this quadratic form (attained at $b = A$) is equal to the posterior variance :

$$Q(A) = 1 - k(x, X)^T k(X, X)^{-1} k(x, X) = \tilde{k}(x, x). \tag{5.2.23}$$

This quadratic form is also introduced in [212], pp. 174-176, in an expanded fashion for general non stationary kernels; the fact that the Kriging coefficients minimize this quadratic form is given in [212], Theorem 11.5. In the case of stationary kernels, the representation (5.2.22) thanks to the spectral measure was already described and used in the Micchelli et al. papers [144, 143, 130, 129], in a deterministic setting. In a probabilistic setting, this quadratic form can also be written as

$$Q(b) = \mathbb{E}\big[\big(U(c\Delta t) - b^T U(X)\big)^2\big]. \tag{5.2.24}$$

5.2.3.2 Flat limits in the context of interpolation

The previous section shows that finite difference schemes for the advection equation reduce to interpolation procedures. Indeed, Strang's "most accurate schemes" ([194, 56]) are based on Lagrange interpolation polynomials evaluated at $c\Delta t$ (forward space in time is equivalent to a translation in space), or rather, λ, after a normalization by Δx.

In the context of interpolation, the flat limit regime consists in considering the Kriging mean obtained with a kernel of the form $k_\ell(x, x') = k(x/\ell, x'/\ell)$,

and investigating the behaviour of this interpolant in the limit where $\ell \to +\infty$. It is known that flat limits with smooth kernels yield Lagrange polynomial interpolation (see e.g. [177]), which then correspond to Strang's most accurate schemes in the context of finite different schemes (cartesian grids).

Flat limits in the non smooth case (typically, Matérn kernels) are investigated in [191], [130], [129], where it is shown that the limit interpolant corresponds to a (generalized fractional) polyharmonic spline interpolant. The associated finite difference schemes are described in an implicit fashion in [143], where the coefficients of the scheme are the solution to a generalized polyharmonic spline interpolation problem.

The following illustrative example describes an explicit investigation of the 1/2-Matérn kernel in the flat limit regime, which yields the upwind scheme seen as a three point scheme.

Example 5.2.3 (The 1/2-Matérn kernel). In the case of the 1/2-Matérn kernel, many computations can be performed explicitly, in a non asymptotic fashion. This will serve as a motivating example for the rest of the chapter. Note that this example is detailled in [144] but there is a sign error in this reference (in equation (2.22) in [144]), leading to the wrong limits. It is also somewhat described in [145], but there is also an error leading to inconsistent formulas (equation (3.6) in [145], while the consistency constraints in (3.5) should be enforced). Let $p, q \in \mathbb{N}$ and consider the following set of collocation points $X \coloneqq (-p\Delta x,\ -(p-1)\Delta x,\ \ldots,\ (q-1)\Delta x,\ q\Delta x)$. We thus have $n = p+q+1$ collocation points. The coefficient (i, j) of the associated covariance matrix is $e^{-|i-j|\Delta x/\ell}$, where ℓ is the length scale of the 1/2-Matérn kernel. To work with dimensionless quantities, we write the lengthscale as a multiple of the space step, setting

$$\alpha \coloneqq \ell/\Delta x. \tag{5.2.25}$$

Finally, we set $\rho \coloneqq \exp(-1/\alpha) < 1$. The covariance matrix is then given by $K_{ij} = \rho^{|i-j|}$. This is a so-called Kac-Murdock-Szegö (KMS) matrix, whose inverse ($\rho \neq 1$) is the following explicit tridiagonal matrix ([65], Section 1.3):

$$K^{-1} = \frac{1}{1-\rho^2}\begin{pmatrix} 1 & -\rho & 0 & \ldots & 0 \\ -\rho & 1+\rho^2 & -\rho & & 0 \\ \vdots & \ddots & \ddots & \ddots & \vdots \\ 0 & \ldots & -\rho & 1+\rho^2 & -\rho \\ 0 & \ldots & 0 & -\rho & 1 \end{pmatrix} \tag{5.2.26}$$

Note that this explicit inverse is also given in [48], p. 133. Moreover, the vector v is given by $v_i = \rho^{|i-\lambda|}$, using again an abusive indexing $i \in \{-p, \ldots, 0, \ldots, q\}$.

For all $i \in \{-p+1, \ldots, 0, \ldots, q-1\}$, we thus obtain that

$$a_i(\rho) = \frac{1}{1-\rho^2}\Big(-\rho\rho^{|i-1-\lambda|} + (1+\rho^2)\rho^{|i-\lambda|} - \rho\rho^{|i+1-\lambda|}\Big). \tag{5.2.27}$$

Assume that $|\lambda| \leq 1$, as in the CFL conditions encountered previously. Then $1-\lambda \geq 0$ and $1+\lambda \geq 0$, and for $2 \leq i \leq q-1$ we get

$$a_i(\rho) = \frac{1}{1-\rho^2}\Big(-\rho^{i-\lambda} + (1+\rho^2)\rho^{i-\lambda} - \rho^{2+i-\lambda}\Big) = 0. \tag{5.2.28}$$

Similarly, $a_i = 0$ for $-p+1 \leq i \leq -2$, and one also checks that $a_{-p} = a_q = 0$. For the other coefficients, we now study the limit $\alpha \to +\infty$, that is, $\rho \to 1$. For $i = 0$, we get

$$a_0(\rho) = \frac{1}{1-\rho^2}\Big(-\rho^2\rho^{\lambda} + (1+\rho^2)\rho^{|\lambda|} - \rho^2\rho^{\lambda}\Big) \tag{5.2.29}$$

$$= \frac{1}{1-\rho^2}\Big(\rho^2(\rho^{|\lambda|} - \rho^{\lambda} - \rho^{-\lambda}) + \rho^{|\lambda|}\Big)$$

$$= \frac{1}{1-\rho^2}\Big(-\rho^2\rho^{-|\lambda|} + \rho^{|\lambda|}\Big) \tag{5.2.30}$$

$$= \rho^{-|\lambda|} + \rho^{|\lambda|}\frac{1-\rho^{-2|\lambda|}}{1-\rho^2} \xrightarrow[\rho\to 1]{} 1 - |\lambda|. \tag{5.2.31}$$

For $i = 1$, we also obtain

$$a_1(\rho) = \frac{1}{1-\rho^2}\Big(-\rho^{1+|\lambda|} + (1+\rho^2)\rho^{1-\lambda} - \rho^{3-\lambda}\Big) = \frac{1}{1-\rho^2}\Big(\rho^{1-\lambda} - \rho^{1+|\lambda|}\Big)$$

$$= \rho^{1-\lambda}\frac{1-\rho^{|\lambda|+\lambda}}{1-\rho^2} \xrightarrow[\rho\to 1]{} \frac{\lambda+|\lambda|}{2}. \tag{5.2.32}$$

The formula for a_{-1} is obtained by replacing λ with $-\lambda$ in equation (5.2.32), giving $a_{-1}(\rho) \to (-\lambda+|\lambda|)/2$ when $\rho \to 1$. We observe that the coefficients obtained in the limit $\alpha \to +\infty$ correspond to the upwind scheme (seen as a three point scheme). Interestingly, the obtained limit does not depend on the number of collocation points used, provided that $p \geq 1$ and $q \geq 1$. A possible explanation is that the inverse of the KMS matrix is tridiagonal. Among symmetric Toeplitz matrices, this fact is unique to the KMS matrix ([65]). This property is also known in the Gaussian Markov process framework ([166], Appendix B), for which the inverse of the covariance matrix is sparse ([136]). Indeed, the Gaussian process with covariance function the 1/2-Matérn kernel is a first order autoregressive process ($AR(1)$ process), which is known to be the only first order Gaussian Markov process ([166], Appendix B.2.1). p^{th} order autoregressive Gaussian processes are those with covariance function the $p+1/2$-Matérn kernels ([166], Appendix B.2.1), for which one may thus expect that the Kriging coefficients $(a_{-p}, ..., a_q)$ remain "sparse". At this stage, this property is only a conjecture.

A natural question arises, namely whether the schemes we have computed above are also relevant schemes in the non asymptotic regime ($\rho < 1$.) Two answers are possible. The schemes are not consistent in the sense of the equations (5.2.9): they do not verify the first consistency equation (coefficients sum up to one), let alone the second one. They are consistent though, in the sense of the relaxed consistency equations (5.2.10). This is due to the limits (5.2.31) and (5.2.32), and the fact that the upwind scheme is consistent.

We will describe a way of constructing strictly consistent schemes in non asymptotic regimes in Section 5.2.4, obtained by solving a constrained optimization problem. Note also that when $1 \leq \lambda \leq 2$, the indexes of the non zero coefficients are shifted by one unit (change of variable in equation (5.2.27)), but then the second consistency equation is not verified.

Finally, this example showed that the asymptotic regime to consider was $\alpha \to +\infty$. This regime can mainly be understood in two different ways. It can first be obtained by letting $\ell \to +\infty$ and keeping Δx fixed. This is the flat limit regime. The second way consists in letting $\Delta x \to 0$ and keeping ℓ fixed. This corresponds to the *convergence* regime for the numerical scheme, which was the one considered in the papers [144, 143]. Of course, a combination ob both regimes can be considered, or even divergent regimes, e.g. $\ell \sim n^2$ and $\Delta x \sim n$.

5.2.3.3 Centered three point schemes

For centered three point schemes, many derivations can be done explicitely. Of course, this is not a good approach when $n \geq 4$, but the computations are interesting nevertheless. In the general case, variational approaches can be used, following [130, 129, 144, 143]. In the case of a cartesian grid, the covariance matrix has the following Toeplitz form :

$$K = \begin{pmatrix} a & b & c \\ b & a & b \\ c & b & a \end{pmatrix} \tag{5.2.33}$$

where $a = k_S(0) + \sigma^2, b = k_S(\Delta x)$ and $c = k_S(2\Delta x)$. The term σ^2 in a is a nugget term, which we will assume to be null. In this case, we can assume without loss of generality that $a = k_S(0) = 1$. The inverse of K can be explicitly derived using the comatrix formula :

$$K^{-1} = \frac{1}{\det K} \begin{pmatrix} a^2 - b^2 & -b(a-c) & b^2 - ac \\ -b(a-c) & a^2 - c^2 & -b(a-c) \\ b^2 - ac & -b(a-c) & a^2 - b^2 \end{pmatrix}, \tag{5.2.34}$$

where $\det K = (a-c)(a(a+c)-2b^2)$. When $a=1$, we obtain that $\det K = (1-c)(1+c-2b^2)$. This assumption also yields

$$A = K^{-1}V = \frac{1}{\det K}\begin{pmatrix} (1-b^2)v_{-1} - b(1-c)v_0 + (b^2-c)v_1 \\ -b(1-c)v_{-1} + (1-c^2)v_0 - b(1-c)v_1 \\ (b^2-c)v_{-1} - b(1-c)v_0 + (1-b^2)v_1 \end{pmatrix}. \tag{5.2.35}$$

It is convenient to observe that simplifications can be obtained between the coordinates of A and the $\det K$ term. In fact,

$$a_{-1} + a_1 = \frac{v_{-1} + v_1 - 2bv_0}{1+c-2b^2}, \tag{5.2.36}$$

$$a_{-1} - a_1 = \frac{v_{-1} - v_1}{1-c}, \tag{5.2.37}$$

$$a_0 = \frac{(1+c)v_0 - b(v_{-1}+v_1)}{1+c-2b^2}. \tag{5.2.38}$$

Those explicit expressions can now be studied in the flat limit regime. In the case of the Matérn kernel of order $\nu > 0$, we have the following asymptotic expansion around 0 :

$$k_\nu(r) = 1 + Ar^2 + C_\nu r^{2\nu} + O(r^{\min(4,2\nu+2)}). \tag{5.2.39}$$

This expansion can be deduced from equation (1.2.16) as well as [1], equations 9.6.2 and 9.6.10. For all $\nu > 0$ with $\nu \neq 1$, we set

$$D(\nu,\lambda) \coloneqq \frac{|\lambda+1|^{2\nu} + |\lambda-1|^{2\nu} - 2|\lambda|^{2\nu} - 2}{4^\nu - 4}. \tag{5.2.40}$$

This quantity will play the role of a discrete diffusion coefficient, as in equation (5.2.14). In particular, we can already observe that $D(\nu,\lambda) = D(\nu,-\lambda)$, $D(\nu,0) = 0$, $D(\nu,1) = 1$, $D(1/2,\lambda) = |\lambda|$ (upwind scheme) and $D(2,\lambda) = \lambda^2$ (Lax-Wendroff scheme). The four next propositions describe the scheme obtained in the flat limit using Matérn priors. We delay the proof of the two first propositions (the most important ones) to the appendix of the chapter, while we state the two other ones without proof. These schemes are implicitly described in [143], Section 4, as solutions of a linear system corresponding to a spline interpolation problem.

Proposition 5.2.4. *Assume that $0 < \nu < 1$. Then as $\alpha \to +\infty$,*

$$a_{-1} = \frac{D(\nu,\lambda)}{2} + \frac{1}{2}\frac{|\lambda+1|^{2\nu} - |\lambda-1|^{2\nu}}{4^\nu}, \tag{5.2.41}$$

$$a_0 = 1 - D(\nu,\lambda), \tag{5.2.42}$$

$$a_1 = \frac{D(\nu,\lambda)}{2} - \frac{1}{2}\frac{|\lambda+1|^{2\nu} - |\lambda-1|^{2\nu}}{4^\nu}, \tag{5.2.43}$$

with speed of convergence $O(\alpha^{-2\min(\nu,1-\nu)})$. *In particular, the limit scheme verifies the first consistency equation but not the second one unless* $\nu = 1/2$, *in which case we recover the upwind scheme.*

Proposition 5.2.5. *Assume that* $1 < \nu < 2$. *Then we recover the scheme* (5.2.14) *with* $D = D(\nu, \lambda)$, *with order of convergence* $O(\alpha^{-2\min(\nu-1,2-\nu)})$ *when* α *goes to infinity. In particular, it is consistent.*

Note that the diffusivity coefficient $D(\nu, \lambda)$ is highly reminiscent of the covariance function of the fractional Brownian motion, or of the energy distance ([198], Theorem 1 p. 1266). A rigorous and explicit link is yet to be established. We now state without proof the two following propositions.

Proposition 5.2.6. *Assume that* $\nu > 2$. *Then we recover the Lax-Wendroff scheme.*

The proof of this result stems from the fact that, as in the proof of Proposition 5.2.5, the terms with even order α^{-2k} cancel each other out. The next result gaps the hole between Propositions 5.2.4 and 5.2.5.

Proposition 5.2.7. *When* $\nu = 1$, *we obtain the "ln" scheme with*

$$D(1, \lambda) = \frac{|\lambda + 1|^2 \ln|\lambda + 1| + |\lambda - 1|^2 \ln|\lambda - 1| - 2|\lambda|^2 \ln|\lambda|}{4 \ln 2}. \tag{5.2.44}$$

In particular it is consistent. When $\nu = 2$, *we obtain the Lax-Wendroff scheme.*

The ln-scheme can be formally obtained by computing the limits in either of Propositions 5.2.4 or 5.2.5, when $\nu \to 1^+$ or $\nu \to 1^-$. It can be rigorously obtained using the definition of modified Bessel functions of integer order, but this proof is tedious as Bessel functions of integer order have complicated asymptotic expansions at the origin ([1], equation 9.6.11). Observe that the map $x \mapsto |x|^2 \ln|x|$ (which is evaluated at $x = \lambda$, $x = \lambda - 1$ and $x = \lambda + 1$ in equation (5.2.44)) is exactly the thin plate spline, which is a particular polyharmonic spline. Given $\nu \in [1, 2] \cup \{1/2\}$, we call the ν-scheme the numerical scheme associated to the discrete diffusion coefficient $D = D(\nu, \lambda)$. In particular the 1/2-scheme is the upwind scheme, the 1-scheme is the ln-scheme and the 2-scheme is the Lax-Wendroff scheme. A comparison of the ν-scheme coefficients is given in Figure 5.1.

Observe that the speed of convergence described in Propositions 5.2.4 and 5.2.5 is increasingly bad as ν gets close to an integer, suggesting that obtaining the scheme coefficients by numerical limits is in those cases not a well conditioned procedure. This fact is perhaps related to the "uncertainty principle" of flat limits (see e.g. [191], p. 486 and the references therein).

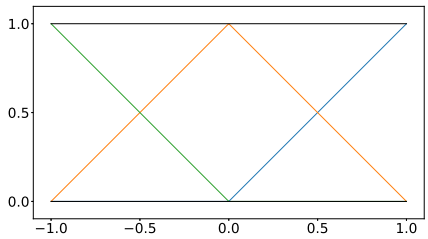

(a) Upwind scheme ($\nu = 1/2$).

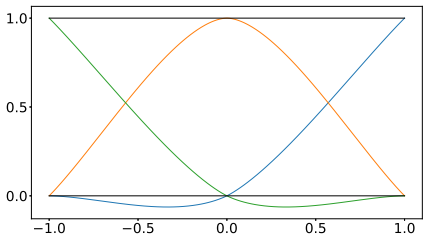

(b) ln-scheme ($\nu = 1$).

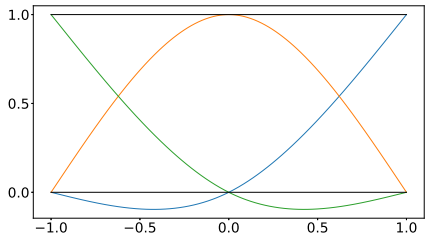

(c) ν-scheme, $\nu = 3/2$.

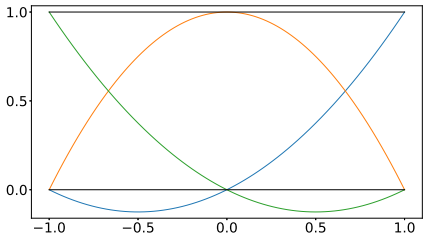

(d) Lax-Wendroff scheme ($\nu = 2$).

Figure 5.1 – Coefficients a_{-1} (blue), a_0 (orange) and a_1 (green) of the ν-scheme for $\nu = 1/2,\ 1,\ 3/2,\ 2$, as functions of $\lambda \in [-1, 1]$.

We have the following conjecture, which has consequences on the stability of the ν-schemes.

Conjecture 5.2.8 (Stability of the ν-scheme)**.** *The following facts hold :*

(i) (Weak conjecture) For all $\nu \in [1/2, 2]$ and $\lambda \in [-1, 1]$,

$$\lambda^2 \leq D(\nu, \lambda) \leq |\lambda|. \tag{5.2.45}$$

Thus the ν-scheme is stable for all $\nu \in [1, 2]$ under the CFL condition $|\lambda| \leq 1$.

(ii) (Strong conjecture) For a fixed $\lambda \in [-1, 1]$, the map $\nu \mapsto D(\nu, \lambda)$ is strictly decreasing over $[1/2, 2]$.

This conjecture does not seem too difficult to prove at first sight, however I was not able to do so. Perhaps some standard convexity considerations are sufficient. The strong conjecture implies the weak one, as $D(1/2, \lambda) = |\lambda|$ and $D(2, \lambda) = \lambda^2$ and both are stable under the CFL $|\lambda| \leq 1$. This conjecture can be checked to be true numerically, as visible from Figure 5.2.

Assuming that the strong conjecture is true, we can deduce the qualitative behaviour of the numerical scheme associated to $D = D(\nu, \lambda)$ using the modified equation (5.2.17), and the facts that $D(1/2, \lambda) = |\lambda|$ and $D(2, \lambda) = \lambda^2$. Indeed, this yields that the ν-schemes are a continuous family of schemes that

offer a trade-off between diffusivity and dispersivity, the most consistent diffusive scheme (apart from the upwind scheme) being the ln-scheme while the most dispersive is the 2-scheme, i.e. the Lax-Wendroff scheme. This behaviour is numerically confirmed in Figures 5.4c and 5.4d.

5.2.3.4 Numerical study of the ν-schemes, $\nu \in [1, 2]$

There is hope that the ν-schemes have some form of fractional order of accuracy, following the theoretical study of fractional splines in [204], Section 4. Such a property could be interesting for taking advantage of Hölder-like or fractional Sobolev regularity, e.g. in the case where the initial data is a little smoother than continuous but not quite differentiable. For the numerical study of the ν-schemes, we consider two different problems. Both consist in numerically solving the advection equation over the time domain $(x, t) \in [0, L] \times [0, T]$, with periodic boundary conditions, $u(0, t) = u(1, t)$. The simulation parameters are $L = 1$, $T = 0.5$, $c = 1$ and $\lambda = 0.75$. The two problems correspond to the two different initial conditions

$$u_{0,1}(x) = \exp(-(x - m)^2/2\sigma^2) \quad \text{(Gaussian)}, \tag{5.2.46}$$

$$u_{0,2}(x) = \mathbb{1}_{[a,b]}(x) \quad \text{(door)}, \tag{5.2.47}$$

with $m = 1/3$, $\sigma = 1/30$, $a = 1/4$ and $b = 1/3$. The smooth initial condition $u_{0,1}$ enables the study of the order of accuracy of the scheme, while the discontinuous initial condition $u_{0,2}$ enables the study of other qualitative properties of the scheme, such as diffusivity and dispersivity.

Given $N \in \mathbb{N}^*$ the number of grid points, we set $\Delta x = L/N = 1/N$. We denote $u_{\text{num}} \in \mathbb{R}^N$ the numerical solution at time $t = T$ and $u_T \in \mathbb{R}^N$ the

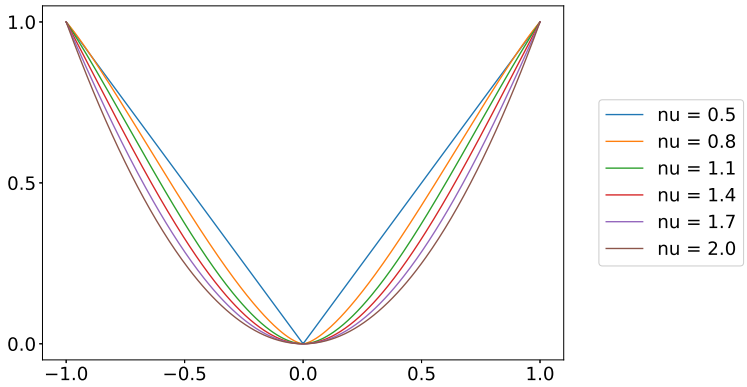

Figure 5.2 – Plot of the map $\lambda \mapsto D(\nu, \lambda)$, $\lambda \in [-1, 1]$, for several values of $\nu \in [1/2, 2]$. These plots confirm Conjecture 5.2.8.

discretization of the true solution on the grid at time T. We introduce the ℓ^p numerical error defined as

$$E_{\nu,p}(\Delta x) \coloneqq \left(\Delta x \sum_{j=1}^{N} |(u_{\text{num}})_j - (u_T)_j|^p\right)^{1/p} = \|u_{\text{num}} - u_T\|_p. \tag{5.2.48}$$

We will consider the case $p \in \{1, 2, \infty\}$, the case $p = \infty$ being defined as $E_{\nu,p}(\Delta x) \coloneqq \sup_{1\leq j\leq N} |(u_{\text{num}})_j - (u_T)_j|$.

Smooth Gaussian initial condition A visualization of the associated numerical solution is given in Figures 5.4a and 5.4b, for $N = 1000$ and $\lambda = 0.75$. Already for this value of N, the true solution and the Lax-Wendroff solution are hardly distinguishable, the lax-Wendroff being of order 2 (i.e. its error behaves as $O(\Delta x^2)$). For the ν-schemes, the convergence study in the smooth case is summarized in Figures 5.3d, 5.3e and 5.3f. For readability, the two black and red lines indicate the slope of $O(\Delta x)$ and $O(\Delta x^2)$ convergence rates. These figures show the following. For smooth solutions, as Δx tends to zero and the Courant number λ is kept constant, the approximation error of the ν-scheme with $\nu \in [1, 2)$ essentially behaves as

$$E_{\nu,p}(\Delta x) \underset{\Delta x\to 0}{\sim} A_{\nu,p}\Delta x, \tag{5.2.49}$$

where $A_{\nu,p} > 0$ is a constant and the map $\nu \mapsto A_{\nu,p}$ is strictly decreasing. In particular, those ν-schemes are of order one, but the constant $A_{\nu,p}$ is improved as ν is closer to 2. When $\nu = 2$, we recover the Lax-Wendroff scheme which is of order two. More precisely, for the ν-scheme with $\nu \in (1, 2)$, there seem to be two regimes. In the first one, when Δx is greater than some $\delta_0(\nu)$, the error $E_{\nu,p}(\Delta x)$ behaves as $O(\Delta x^\beta)$ for some $\beta \in (0, 2)$ (possibly $\beta = \nu$, although the behaviour of the curves in Figures 5.3d, 5.3e and 5.3f for $\nu \in (1, 3/2)$ seems to indicate that $\beta < 1$ for such ν). Then, when $\Delta x < \delta_0(\nu)$, the error starts behaving as $O(\Delta x)$. This two-regime behaviour is especially visible for the values $\nu = 1.95$ and $\nu = 1.98$, in Figures 5.3d, 5.3e and 5.3f.

Door type initial condition A visualization of the numerical solution associated to the ν-scheme, for several values of ν, is given in Figures 5.4c and 5.4d. In this case, $N = 2000$ and $\lambda = 0.75$. These figures show that even for very very small values of Δx, the numerical overshoot associated to the different schemes is non negligible. This fact is also visible in the ℓ^∞ plot in Figure 5.3c. This is also especially true as ν gets closer to 2, the limiting case being the Lax-Wendroff scheme whose oscillations do not seem to be dampened as time evolves. Time-dependent plots given in Figures 5.5a

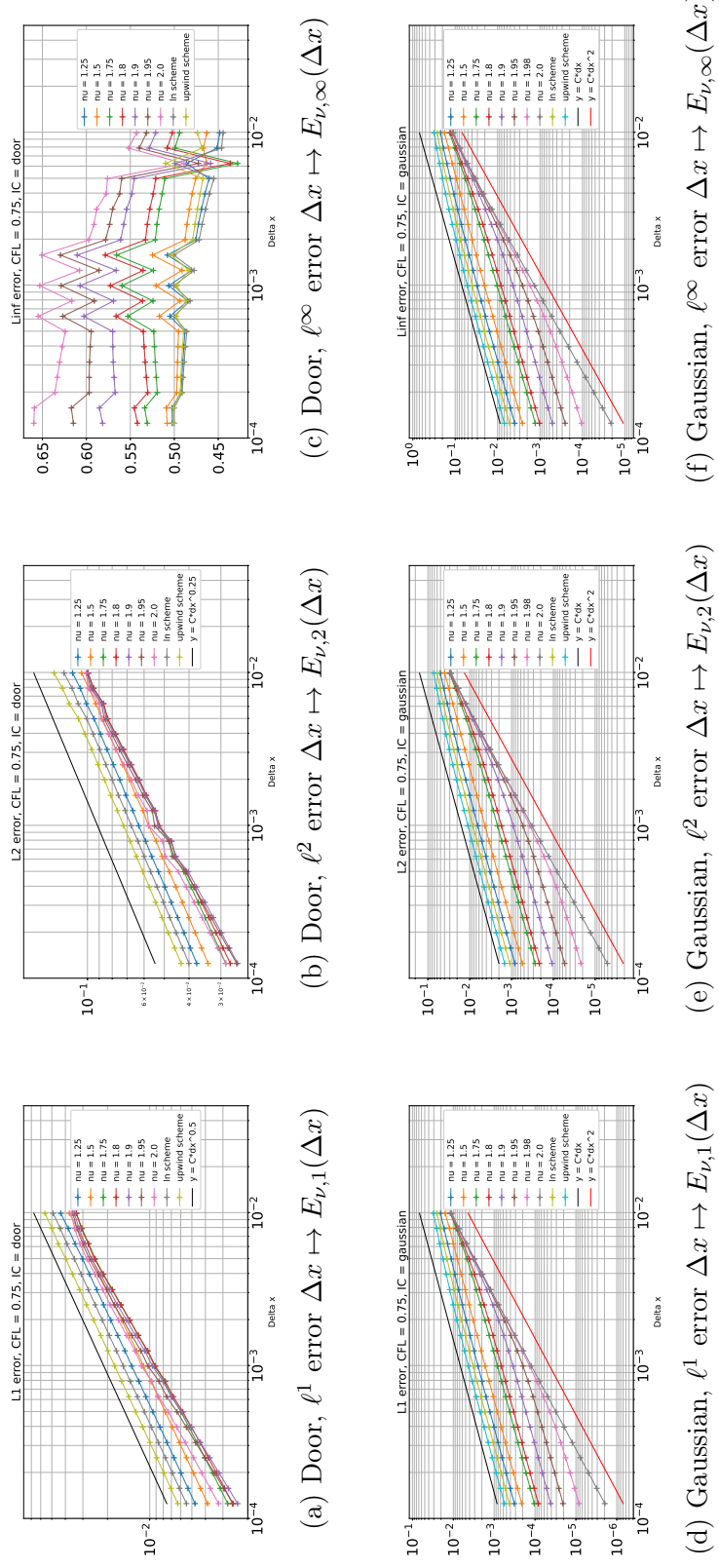

(a) Door, ℓ^1 error $\Delta x \mapsto E_{\nu,1}(\Delta x)$ (b) Door, ℓ^2 error $\Delta x \mapsto E_{\nu,2}(\Delta x)$ (c) Door, ℓ^∞ error $\Delta x \mapsto E_{\nu,\infty}(\Delta x)$

(d) Gaussian, ℓ^1 error $\Delta x \mapsto E_{\nu,1}(\Delta x)$ (e) Gaussian, ℓ^2 error $\Delta x \mapsto E_{\nu,2}(\Delta x)$ (f) Gaussian, ℓ^∞ error $\Delta x \mapsto E_{\nu,\infty}(\Delta x)$

Figure 5.3 – Convergence plots for several ν-schemes, with $\lambda = 0.75$

and 5.5b show the value of the numerical overshoot observed in Figure 5.4c, for several values of ν. This general behaviour can in fact be explained by the modified equation (5.2.17) and Conjecture 5.2.8: the numerical diffusion vanishes as ν approaches to 2, the next non zero term being a dispersive term. Indeed, the oscillations visible in Figures 5.4c and 5.4d are typical of dispersive PDEs.

The convergence analysis summarized in Figures 5.3a, 5.3b and 5.3c shows that the ν-schemes are convergent in the L^1 and L^2 norm. The convergence rate is of order $O(\Delta x^{1/2})$ and $O(\Delta x^{1/4})$ respectively, as indicated by the black line in Figures 5.3a and 5.3b. For the ℓ^∞ norm however, the convergence fails (at least at the time scale of the numerical simulation). This is not surprising, from both Figures 5.4d or 5.5b.

The upwind scheme has the interesting property of being positivity preserving, meaning that the associated numerical solution remains nonnegative if its initial data is nonnegative. This property is desirable as it holds in the continuous setting for the advection equation, as well as other general first order hyperbolic PDEs. This property also prevents the appearance of overshoots as the ones induces by the other ν-schemes. A drawback of such methods is that they are first order accurate at best, from Godunov's order barrier theorem ([213], Theorems 9.2.1 and 9.2.2).

It can be conjectured from numerical observations that the ln-scheme is also positivity preserving. This is not true as shown by Figure 5.1b, since positivity preserving schemes must have nonnegative coefficients ([213], Theorem 9.2.1). However, the negative overshoot of the ln-scheme is numerically very small, as visible in Figure 5.5, and in fact quickly vanishes at time advances. Here, we define the negative overshoot of a vector $u \in \mathbb{R}^N$ as

$$\mathcal{O}(u) := (\min u)_- = \min(0, \min_{1 \le j \le N} u_j). \tag{5.2.50}$$

In particular, if $u_j > 0$ for all j, then $\mathcal{O}(u) = 0$ ($-\infty$ in log scale). In our context, this quantity aims at measuring the size of the first negative oscillation (if it exists) of the numerical solution, located right after the first discontinuity of the true solution (starting from the left). Figure 5.5 shows that the ln-scheme is "approximately" positivity preserving. The ln-scheme is also of order one, but as is visible from Figure 5.3, the constant associated to its $O(\Delta x)$ convergence rate is better than that of the upwind scheme, ensuring a slightly faster convergence.

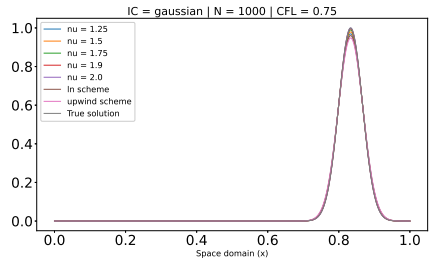

(a) Gaussian, numerical solution.

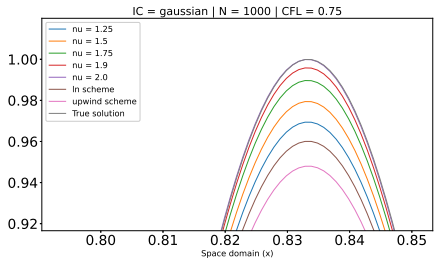

(b) Gaussian, numer. solution, zoomed.

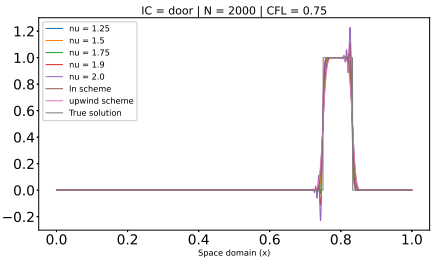

(c) Door, numerical solution.

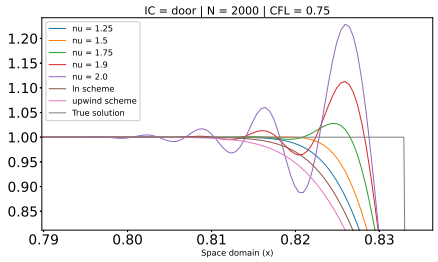

(d) Door, numerical solution, zoomed.

Figure 5.4 – Visualization of the numerical solutions associated to ν-schemes, with smooth (Gaussian) and non smooth (door type) initial conditions.

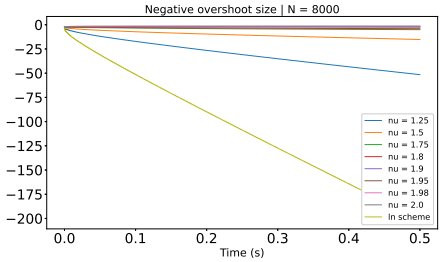

(a) Values of overshoot

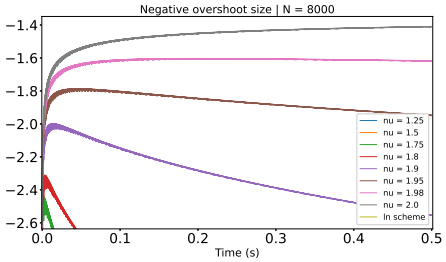

(b) Zoom on top four curves.

Figure 5.5 – Absolute value of the negative overshoot (equation (5.2.50)) of the solution associated to the ln-scheme with a door type initial condition, as a function of time, in log scale. The overshoots are less and less dampened as ν approaches 2, while those of the Lax-Wendroff scheme actually seem to grow.

5.2.4 Finite difference schemes via GPR in the non flat regime

Vanishing posterior in the flat limit An issue associated to the flat limit regime is that the corresponding posterior completely vanishes (while the prior "converges" to the rank one kernel given by $k(x, x') = 1$ for all x, x'). This is the content of the next proposition.

Proposition 5.2.9. *Consider a stationary covariance kernel k over $\mathbb{R}^d$ such that its spectral measure μ verifies $\int_{\mathbb{R}^d} |\xi|^2 \mu(d\xi) < +\infty$. Consider the Kriging mean and covariance functions $\tilde{m}_\ell$ and $\tilde{k}_\ell$, obtained by solving an interpolation problem using the scaled kernel $k_\ell(h) = k(h/\ell)$, given a set of observations $\{(x_j, y_j) \in \mathbb{R}^d \times \mathbb{R},\ 1 \leq j \leq n\}$. Then in the flat limit regime, the posterior variance converges to zero:*

$$\tilde{k}_\ell(x, x) \xrightarrow[\ell \to +\infty]{} 0. \tag{5.2.51}$$

Proof. Set $X = (x_1, ..., x_n)^T$. Let $x \in \mathbb{R}^d$. Consider the quadratic form given in (5.2.22), using this time the kernel k_ℓ and extending the definition of this quadratic form to $\mathbb{R}^d$ and n observations:

$$Q_\ell(b) = \int_{\mathbb{R}} \left| e^{i\xi \cdot \frac{x}{\ell}} - b^T e^{i\xi \cdot \frac{X}{\ell}} \right|^2 \mu(d\xi), \tag{5.2.52}$$

where $b \in \mathbb{R}^n$, $x \cdot \xi$ stands for the dot product of $\mathbb{R}^d$ and the vector $e^{i\xi \cdot X/\ell} \in \mathbb{R}^n$ has entries $(e^{i\xi \cdot X/\ell})_j = e^{i\xi \cdot x_j/\ell}$. Again, the posterior variance $\tilde{k}_\ell(x, x)$ minimizes the quadratic form (5.2.52) (see e.g. [212], Theorem 11.5). We perform a zeroth order Taylor expansion of the integrated term in the quadratic form, for a fixed $\xi \in \mathbb{R}^d$, when $\ell \to +\infty$. First,

$$e^{i\xi \cdot \frac{x}{\ell}} - b^T e^{i\xi \cdot \frac{X}{\ell}} = 1 - b^T \mathbb{1} + O\left(\frac{1}{\ell}\right). \tag{5.2.53}$$

where $\mathbb{1}$ is the vector made of ones. In particular, for $b = n^{-1}\mathbb{1}$, we have that

$$e^{i\xi \cdot \frac{x}{\ell}} - \frac{1}{n} \mathbb{1}^T e^{i\xi \cdot \frac{X}{\ell}} = O\left(\frac{1}{\ell}\right). \tag{5.2.54}$$

Moreover, we have the standard estimate for complex exponentials, $|1 - e^{is}| = 2|\sin(s/2)| \leq |s|$ for all $s \in \mathbb{R}$. Denote $e^{i\xi \cdot (X-x)/\ell}$ the vector such that $(e^{i\xi \cdot (X-x)/\ell})_j = e^{i\xi \cdot (x_j - x)/\ell}$. The estimate yields a constant $C > 0$, depending on x, X and n such that for all $\xi \in \mathbb{R}^d$,

$$\left| e^{i\xi \cdot \frac{x}{\ell}} - \frac{1}{n} \mathbb{1}^T e^{i\xi \cdot \frac{X}{\ell}} \right| = \left| 1 - \frac{1}{n} \mathbb{1}^T e^{i\xi \cdot \frac{X-x}{\ell}} \right| = \left| \frac{1}{n} \sum_{j=1}^{n} \left(1 - e^{i\xi \cdot \frac{x_j - x}{\ell}} \right) \right| \tag{5.2.55}$$

$$\leq \frac{1}{n}\sum_{j=1}^{n}\left|1-e^{i\xi\cdot\frac{x_j-x}{\ell}}\right| \leq C|\xi|. \tag{5.2.56}$$

In equation (5.2.55), we first factored by the unit norm complex number $e^{i\xi\cdot x/\ell}$ and expanded the dot product between $\mathbb{1}$ and $e^{i\xi\cdot(X-x)/\ell}$. The convergence (5.2.54) for fixed ξ when $\ell \to +\infty$, the domination (5.2.56), the assumption that $\int |\xi|^2\mu(d\xi) < +\infty$ and the Lebesgue dominated convergence theorem yield that

$$Q_\ell(n^{-1}\mathbb{1}) \xrightarrow[\ell\to+\infty]{} 0. \tag{5.2.57}$$

But the posterior variance is the minimum of Q_ℓ, and thus

$$\tilde{k}_\ell(x,x) = \arg\min_{b\in\mathbb{R}^d} Q_\ell(b) \leq Q_\ell(n^{-1}\mathbb{1}) \xrightarrow[\ell\to+\infty]{} 0, \tag{5.2.58}$$

which shows the desired result. □

Proposition 5.2.9 states that the posterior Gaussian measure associated to the mean $\tilde{m}_\ell$ and covariance $\tilde{k}_\ell$ converges to a Dirac mass (in a suitable function space, and in a suitable sense) which is localized at the Kriging mean m_ℓ. Considering higher order Taylor expansions in equation (5.2.53) yields a system of equations (the first of them being $b^T\mathbb{1} = 1$) which exactly correspond to a Lagrange interpolation matrix system (at least in one dimension), which then yields Strang's "most accurate" schemes as defined in [194] and [56]. As such, the proof above can be adapted to show that the limit interpolant (if it exists) corresponds to either a Lagrange polynomial interpolant (if a sufficient number of moments of μ exist) or a generalized polyharmonic spline interpolant (if μ admits less moments than n, the number of observations).

Proposition 5.2.9 shows that the flat limit regime is not well-suited to the Bayesian analysis of numerical schemes. The next paragraph proposes an alternative way of constructing finite difference schemes, outside of the flat limit regime.

Non asymptotic regime We have seen that the consistency relations were only enforced in the flat limit regime; but this regime prevents the Bayesian interpretation of GPR as the posterior degenerates to zero. To circumvent this apparent incompatibility, a possibility is to consider the quadratic form (5.2.22) and minimize it under the constraint that the consistency relations be fulfilled. We now illustrate this approach in the three point scheme setting. For this, consider the quadratic form given in equation (5.2.24). We then solve the problem

$$\min_{b\in\mathbb{R}^3} Q(b) \quad s.c. \quad \mathbb{1}^T b = 1,\ E^T b = -\lambda, \tag{5.2.59}$$

where $\mathbb{1} = (1,1,1)^T$ and $E = (-1,0,1)^T$. The constraints exactly express the consistency relations (5.2.9). Note that the exact same constrained problem has already been considered in [145], Section 2.2, but outside of the probabilistic context. Such a constrained system (in a Bayesian framework) has also been considered in [113], in the context of numerical integration.

To solve this optimization problem, two possible solutions exist. The most general one consists in introducing Lagrange multipliers, leading to the global minimization of the following functional, where $\mu = (\mu_1, \mu_2)^T \in \mathbb{R}^2$:

$$\mathcal{L}(b, \mu) = Q(b) + \mu_1(\mathbb{1}^T b - 1) + \mu_2(E^T b + \lambda). \tag{5.2.60}$$

Equating its gradient to zero yields the following system, which takes the following block matrix form, where $\Lambda = (1, -\lambda)^T$ and V is the 3×2 matrix defined column-wise by $V = (\mathbb{1} \mid E)$:

$$\begin{pmatrix} K & V \\ V^T & 0 \end{pmatrix} \begin{pmatrix} b \\ \mu \end{pmatrix} = \begin{pmatrix} k(0, X) \\ \Lambda \end{pmatrix} \tag{5.2.61}$$

This system of equations exactly takes the form of that associated to interpolation with conditionally positive functions ([212], Section 8.5), at the exception that the vector Λ is non zero. Such a system with $\Lambda = 0$ is e.g. encountered in in the context of spline interpolation. This system (still with $\Lambda = 0$) is also encountered in a Bayesian context (e.g. [48], equation (5.4.15)), when using *intrinsic random functions* ([48], Section 5.4), which generalizes Kriging. The case where $\Lambda \neq 0$ is briefly treated in [212] (Theorem 11.1) but it is not discussed much more. As a result, the interpretation of this matrix system is not really obvious in our setting.

A second approach to this problem, which is not really well-suited to more general frameworks, consists in observing that consistent schemes necessarily take the form of equation (5.2.14). As a result, the three dimensional problem of minimizing $Q(b)$ (or rather, the five dimensional problem of (5.2.61)) is reduced to the optimization of one single variable, which is the diffusivity coefficient D. Rearranging the random variables inside the expectation where $b \in \mathbb{R}^3$ is of the form of equation (5.2.14), we have

$$\begin{aligned} U(c\Delta t) - b^T U(X) = U(c\Delta t) &- \left(\frac{\lambda}{2} + \frac{D}{2}\right) U(-\Delta x) \\ &- (1 - D)U(0) - \left(-\frac{\lambda}{2} + \frac{D}{2}\right) U(\Delta x) \qquad (5.2.62) \\ = U(c\Delta t) - U(0) &+ \lambda \frac{U(\Delta x) - U(-\Delta x)}{2} \\ &- \frac{D}{2}\Big(U(-\Delta x) - 2U(0) + U(\Delta x)\Big). \qquad (5.2.63) \end{aligned}$$

Denote the linear operators S and Δ_d acting on functions by

$$S(u)(h) \coloneqq u(c\Delta t + h) - u(h) + \lambda \frac{u(\Delta x + h) - u(-\Delta x + h)}{2}, \tag{5.2.64}$$

$$\Delta_d(u)(h) \coloneqq \frac{1}{2}\Big(u(-\Delta x + h) - 2u(h) + u(\Delta x + h)\Big). \tag{5.2.65}$$

Δ_d is a discrete Laplace operator (note the $1/2$ prefactor) while S applies the centered scheme. The optimization problem becomes

$$\min_{D\in\mathbb{R}} \mathbb{E}\Big[\big(S(U)(0) - D\Delta_d(U)(0)\big)^2\Big]. \tag{5.2.66}$$

The meaning of the solution to this problem is now clear : it corresponds to the discrete diffusion coefficient minimizing the mean square error of the consistent numerical scheme, under the probability measure induced by the GP prior over the set of "all" (up to the regularity assumptions induced by the GP) solutions of the advection equation. Indeed, viewing the numerical scheme as an interpolation problem means that we only consider exact solutions of this PDE.

To compute the associated solution, note that $\big(S(U)(0), \Delta_d(U)(0)\big)^T$ is a Gaussian random vector. Therefore this problem is solved by a one-point Kriging formula (a direct minimization of a polynomial of degree two is also possible...). This yields the following result.

Proposition 5.2.10. *Let $k : \mathbb{R}\times\mathbb{R} \to \mathbb{R}$ be a stationary covariance kernel. Then the numerical scheme associated to the constrained minimization problem (5.2.59) is the scheme (5.2.14) with*

$$D = \frac{Cov(S(U)(0), \Delta_d(U)(0))}{Var(\Delta_d(U)(0))} = \frac{[(S\otimes\Delta_d)k](0,0)}{[(\Delta_d\otimes\Delta_d)k](0,0)}. \tag{5.2.67}$$

Proof. One obtains $D = \mathrm{Cov}(S(U)(0), \Delta_d(U)(0))/\mathrm{Var}(\Delta_d(U)(0))$ by a direct minimization of equation (5.2.66). The second part of equation (5.2.67) is a consequence of the bilinearity of the covariance. □

Note that the result above still holds if k is not assumed stationary, in which case the scheme coefficient D will depend on the location $x_j = j\Delta x$ (replace $(0,0)$ by $(j\Delta x, j\Delta x)$ in equation (5.2.67)). The exploration of such non stationary schemes is an interesting perspective of research. For the time being though, we restrict the next paragraphs to the stationary case.

The question now is whether the scheme of Proposition 5.2.10 is stable or not. A way to assess this is Proposition 5.2.1. As a simple test case, consider the one dimensional cosine kernel of angular frequency ξ (considering $-\xi$ is equivalent)

$$k_\xi(x, x') = \cos(\xi(x - x')) = \cos(\xi x)\cos(\xi x') + \sin(\xi x)\sin(\xi x'). \tag{5.2.68}$$

Thanks to Bochner's theorem, every stationary kernel can be obtained thanks to this kernel by means of integrals of such kernels over the ξ-domain ([166], Theorem 4.1). Explicitly, given a stationary kernel over $\mathbb{R}^d$, this theorem states that there exists a nonnegative Radon measure μ over $\mathbb{R}^d$ such that

$$k_S(h) = \int_{\mathbb{R}^d} e^{ih\cdot\xi}\mu(d\xi), \tag{5.2.69}$$

where $h \cdot \xi$ is the inner product of $\mathbb{R}^d$. The measure μ is called the spectral measure of k_S. If $\mu(d\xi) = f(\xi)d\xi$ for some nonnegative function f, then the latter is called the spectral density of the kernel. If k_S is assumed real valued, then the imaginary part of equation (5.2.69) is null and we obtain

$$k_S(h) = \int_{\mathbb{R}^d} \cos(h \cdot \xi)\mu(d\xi). \tag{5.2.70}$$

For conciseness we denote $\cos_\xi := \cos(\xi\cdot)$ and likewise for $\sin_\xi$. Using the parity of the sin and cos functions, it is then readily checked that

$$\Delta_d(\sin_\xi)(0) = 0, \tag{5.2.71}$$
$$\Delta_d(\cos_\xi)(0) = \cos(\xi\Delta x) - 1, \tag{5.2.72}$$
$$S(\cos_\xi)(0) = \cos(c\Delta t\xi) - 1 = \cos(\lambda\Delta x\xi) - 1. \tag{5.2.73}$$

Distributing the tensorised operators over the expanded expression of the cosine kernel (equation (5.2.68)), we obtain from the equations above that

$$\begin{aligned}[(\Delta_d \otimes \Delta_d)k](0,0) &= \Delta_d(\cos_\xi)(0)\Delta_d(\cos_\xi)(0) + \Delta_d(\sin_\xi)(0)\Delta_d(\sin_\xi)(0)\\ &= (\cos(\xi\Delta x) - 1)^2 = \Big(2\sin^2\big(\xi\Delta x/2\big)\Big)^2\\ &= 4\sin^4\big(\xi\Delta x/2\big).\end{aligned} \tag{5.2.74}$$

Likewise for the $[(S \otimes \Delta_d)k](0,0)$ term,

$$\begin{aligned}[(S \otimes \Delta_d)k](0,0) &= (\cos(\xi\Delta x) - 1)(\cos(\lambda\Delta x\xi) - 1)\\ &= 4\sin^2\big(\xi\Delta x/2\big)\sin^2\big(\lambda\xi\Delta x/2\big).\end{aligned} \tag{5.2.75}$$

Therefore, setting $\delta = \xi\Delta x/2$, we obtain

$$D = \sin^2(\lambda\delta)/\sin^2(\delta). \tag{5.2.76}$$

The stability criteria of Proposition 5.2.1 therefore reads

$$\lambda^2\sin^2(\delta) \le \sin^2(\lambda\delta) \le \sin^2(\delta). \tag{5.2.77}$$

The right hand side inequality is ensured as soon as $\delta \leq \pi/2$ and $|\lambda| \leq 1$, the $\sin^2(\cdot)$ function being increasing over $[0, \pi/2]$. The left hand side inequality can be reformulated as

$$\operatorname{sinc}^2(\delta) = \frac{\sin^2(\delta)}{\delta^2} \leq \frac{\sin^2(\lambda\delta)}{\lambda^2\delta^2} = \operatorname{sinc}^2(\lambda\delta), \tag{5.2.78}$$

which is obviously true when $\delta \in [0, \pi]$ and $|\lambda| \leq 1$, the cardinal sine being an even function which is decreasing over $[0, \pi]$. We have thus proved the following theorem (recall that above, $\delta = \xi\Delta x/2$).

Proposition 5.2.11. *The scheme associated to the cosine kernel with angular frequency ξ is stable if $\Delta x|\xi|/2 \leq \pi/2$ under the CFL condition $|\lambda| \leq 1$, which ensures both inequalities in equation (5.2.77). This constraint amounts to $|\xi| \leq \pi/\Delta x$.*

Bochner's theorem then yields the following criteria.

Proposition 5.2.12. *Let k be a stationary kernel over $\mathbb{R}$ and let μ be its spectral measure. If Supp$(\mu) \subset [-\pi/\Delta x, \pi/\Delta x]$, then the associated scheme is stable under the CFL condition $|\lambda| \leq 1$.*

Proof. From Bochner's theorem (equation (5.2.70)), write

$$\begin{aligned} k(x, x') &= \int_{\mathbb{R}} \cos(\xi(x - x'))\mu(d\xi) \\ &= \int_{\mathbb{R}} \Big(\cos(\xi x)\cos(\xi x') + \sin(\xi x)\sin(\xi x') \Big)\mu(d\xi). \end{aligned} \tag{5.2.79}$$

Use then the definition of D in equation (5.2.67) and the stability criteria from Proposition 5.2.1. The first stability equation writes

$$\lambda^2[(\Delta_d \otimes \Delta_d)k](0, 0) \leq [(S \otimes \Delta_d)k](0, 0), \tag{5.2.80}$$

which also writes, by commuting the integral and the translation-like operators Δ_d and S, and by using equations (5.2.74) and (5.2.75),

$$\int_{\mathbb{R}} \lambda^2 4\sin^4\big(\xi\Delta x/2\big)\mu(d\xi) \leq \int_{\mathbb{R}} 4\sin^2\big(\xi\Delta x/2\big)\sin^2\big(\lambda\xi\Delta x/2\big)\mu(d\xi). \tag{5.2.81}$$

Similarly, the second stability equation writes

$$\int_{\mathbb{R}} 4\sin^2\big(\xi\Delta x/2\big)\sin^2\big(\lambda\xi\Delta x/2\big)\mu(d\xi) \leq \int_{\mathbb{R}} 4\sin^4\big(\xi\Delta x/2\big)\mu(d\xi). \tag{5.2.82}$$

Proposition 5.2.11, the support assumption with reference to μ and the non-negativity of μ yield that both equations (5.2.81) and (5.2.82) hold, thus proving the stability of the associated finite difference scheme. □

Interestingly, Proposition 5.2.12 provides the same criteria as the Nyquist-Shannon condition $\omega_{\max} \leq \omega_S/2$ which ensures the perfect reconstruction of a signal from its equally spaced samples thanks to cardinal sine series, if its Fourier transform has compact support within $[-\omega_{\max}, \omega_{\max}]$ ([187], Theorem 1). Indeed, the (spatial) sampling period is in our case $T_S = \Delta x$, and the sampling radial frequency is $\omega_S = 2\pi/T_S = 2\pi/\Delta x$. Defining $\omega_{\max}$ as the largest radial frequency contained in the support of the spectral measure of the kernel, the criterion from Proposition 5.2.12 then reads $\omega_{\max} \leq \pi/\Delta x = \omega_S/2$. The appearance of this Nyquist-Shannon criterion (which concerns the kernel, not the function that is approximated by the numerical scheme) in the context of the stability of a numerical scheme is yet to be fully understood.

When working with kernels with a lengthscale hyperparameter, Proposition 5.2.11 can be understood in terms of the normalized quantity $\alpha = \ell/\Delta x$.

Proposition 5.2.13. *Let k be a stationary kernel whose spectral measure μ is supported in a compact interval $[-\omega_{\max}, \omega_{\max}]$. Let $k_\ell(h) \coloneqq k(h/\ell)$. Then the scheme (5.2.14) where D is given in equation (5.2.67), using the kernel k_ℓ, is stable if $\alpha \geq \omega_{\max}/\pi$ under the CFL condition $|\lambda| \leq 1$.*

Proof. From the definition of k_ℓ and Bochner's theorem, we can write that

$$k_\ell(h) = k(h/\ell) = \int_{\mathbb{R}} \cos\left(\frac{h}{\ell} \cdot \xi\right) \mu(d\xi) = \int_{\mathbb{R}} \cos\left(h \cdot \frac{\xi}{\ell}\right) \mu(d\xi). \tag{5.2.83}$$

From Proposition 5.2.12, the scheme using the kernel k_ℓ is stable if and only if $\omega_{\max}/\ell \leq \pi/\Delta x$, which is equivalent to

$$\alpha \geq \frac{\omega_{\max}}{\pi}, \tag{5.2.84}$$

which finishes the proof. □

Note that the criteria from Propositions 5.2.12 and 5.2.13 are very restrictive as kernels with compactly supported spectral measure are automatically analytic (by writing the complex exponential as its series expansion and using the compact support assumption over the spectral measure). More generally, we expect that the criteria from Propositions 5.2.12 and 5.2.13 are only sufficient and not necessary. Indeed, one may expect that unstable frequencies can be compensated by stable ones if the spectral measure or density puts enough weight on stable frequencies, so that the criteria $\lambda^2 \leq D \leq 1$ holds. For covariance functions with decreasing spectral density converging to zero at infinity, the counterpart of the size of the support of the spectral measure is simply the lengthscale in the frequency domain, which is the inverse of the spatial lengthscale (up to some multiple of π, depending of one's definition of the Fourier transform). This leads to the next conjecture :

Conjecture 5.2.14. *Let k be a stationary kernel with decreasing spectral density converging to zero at infinity (e.g. the Gaussian kernel), with spatial lengthscale parameter $\ell > 0$. Then there exists $\delta > 0$, depending only on k, such that if $\ell^{-1} \leq \delta/\Delta x$ (or equivalently, $\alpha = \ell/\Delta x \geq \delta^{-1}$), then the scheme is stable under the CFL condition $|\lambda| \leq 1$.*

Proposition 5.2.13 states that this result holds for $\delta = \pi/\omega_{\max}$, if $\omega_{\max} := \sup\big(\mathrm{Supp}(\mu)\big) < +\infty$. A fully open question is the order of accuracy of those schemes. We conclude this section with this final conjecture concerning the constrained ν-schemes, with $\nu \in (0, 1)$.

Conjecture 5.2.15. *Consider the scheme associated the to constrained problem (5.2.59), when using a Matérn kernel of order $\nu \in (0, 1)$. Then in the flat limit regime, this constrained scheme converges to the scheme (5.2.14) with $D = D(\nu, \lambda)$, similarly to Proposition 5.2.5 dealing with $\nu \in (1, 2)$. This would yield a family of consistent ν-schemes for $\nu \in (0, 1)$.*

Similarly to a previous discussion concerning the ln-scheme, those schemes may perhaps be (approximately) positivity preserving. The final section of this chapter is concerned with another important topic in numerical analysis, which is that of transparent boundary conditions (TBC).

5.3 Transparent boundary conditions

This section is much shorter than the rest of the chapter, as the results presented here are much more prospective.

5.3.1 Context

The search for perfect or approximated transparent boundary conditions for numerical schemes is an active research topic. They became a popular research topic in 1970' [70] and several different strategies have since been set up to deal with them : see e.g. [22],[70], [102], or [114] for an overview of these different methods. A "friendly review" of TBC and other techniques aiming to deal with the same problem can also be found in [12]. The need for them rises from the fact that numerical simulation domains are necessarily finite and thus bounded; or at the very least, discretized thanks to a finite grid. To numerically solve a free space PDE such as (2.4.1), one first uses an adapted numerical scheme (finite differences, finite elements, etc) for the desired PDE applied in the interior domain, i.e. at the interior points of the discretization grid. At the boundaries of the numerical domain, one is then forced to

encode boundary conditions : common examples are the Dirichlet and Neumann boundary conditions, which cause reflections on the boundaries of the domain. For the free space problem, the question is then the following : can we numerically implement boundary conditions that produce no reflections?

In standard TBC methods, numerical domains containing angles are the most difficult to deal with. Since kernel methods are inherently meshless, they are in theory well equipped to deal with arbitrary geometry, angular in particular. We recall that WIGPR designates the general procedure of using the kernels (2.4.7) and (2.4.8), already encountered in Chapters 2 and 4, for Kriging (or in fact, any other purpose whatsoever).

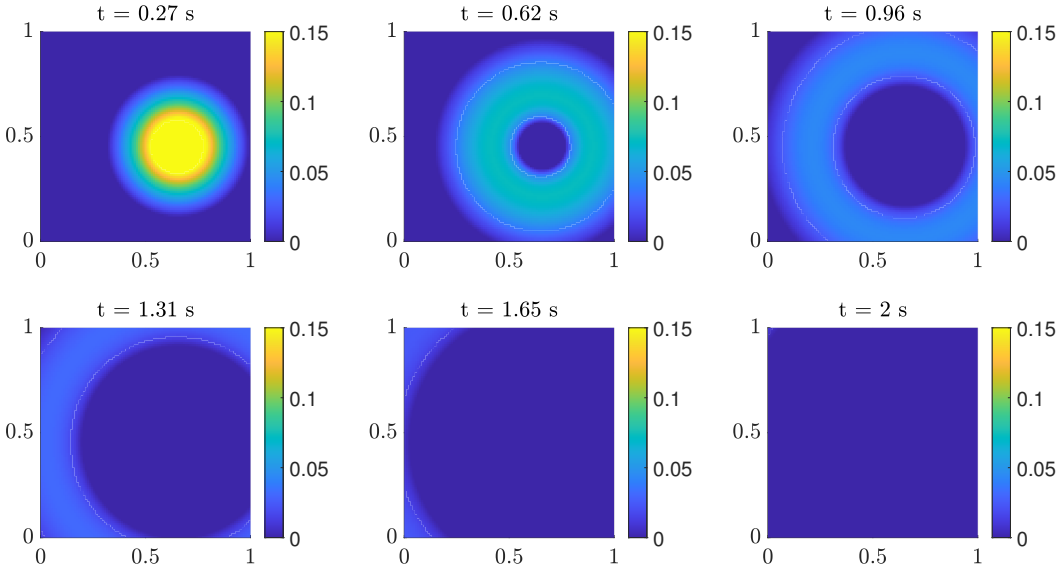

Figure 5.6 – Numerical example showing that the outgoing waves produced by WIGPR do not suffer from numerical reflection issues.

Figure 5.6 shows that WIGPR provides numerical solutions to problem (2.4.1) that do not suffer from numerical reflection issues. The reason is simple: these numerical reconstructions are evaluations on a grid of functions that are exact solutions of the free space problem (2.4.1). While being a promising start for new types of transparent boundary conditions, the discussion above is not enough to provide viable transparent boundary conditions in the sense of numerical schemes. Given the covariance kernels from (2.4.8) and (2.4.7), two questions should be investigated. (*i*) How can WIGPR be associated to classical numerical schemes such as finite difference schemes for the wave equation? (*ii*) Is the corresponding numerical transparent boundary condition numerically stable? The study of the stability of numerical schemes with given boundary conditions is a research topic in itself, see e.g. [46] or the reference (but yet unfinished) book [201], Section 6.4.

For the time being, we describe a simple strategy designed to deal with the following initial value problem for the two dimensional wave equation,

$$\begin{cases} \Box w & = 0 & \forall (x,t) \in \mathbb{R}^2 \times \mathbb{R}_+^*, \\ w(x,0) & = u_0(x) & \forall x \in \mathbb{R}^2, \\ (\partial_t w)(x,0) & = v_0(x) & \forall x \in \mathbb{R}^2. \end{cases} \tag{5.3.1}$$

We next illustrate it on a numerical example.

5.3.2 The two dimensional wave equation

We focus on the two dimensional wave equation (5.3.1), which has applications e.g. in oceanography [125]. As in equation (2.4.2), the solution of this PDE can also be written as

$$w(x,t) = (F_t * v_0)(x) + (\dot{F}_t * u_0)(x). \tag{5.3.2}$$

In dimension two, F_t is a locally integrable function given by

$$F_t(x) = \frac{\operatorname{sgn}(t) \mathbb{1}_{[0,c|t|]}(|x|)}{2\pi\sqrt{c^2t^2 - |x|}}, \tag{5.3.3}$$

where $|\cdot|$ is the Euclidean norm in $\mathbb{R}^2$ (see e.g. [68], Section 3.4 and its equation (3.4.13)). $\dot{F}_t$ remains the distributional time derivative of F_t.

We admit that the formulas (2.4.7) and (2.4.8) still hold in dimension two, where the distributions F_t and $\dot{F}_t$ are given above. As already observed in Chapter 4 (after the proof of Proposition 4.3.3), there are many simplifications which hold in dimension three but not in dimension two. It remains true however that the Fourier transforms of the distributions F_t and $\dot{F}_t$ are equal to

$$\mathcal{F}(F_t)(\xi) = \frac{\sin(ct|\xi|)}{c|\xi|} \quad \text{and} \quad \mathcal{F}(\dot{F}_t)(\xi) = \cos(ct|\xi|), \tag{5.3.4}$$

where this time $|\cdot|$ is the Euclidean norm in $\mathbb{R}^2$ ([69], equation (18.12) p. 294). We will thus use those formulas conjointly with a four-multidimensional fast Fourier transforms (FFT), to compute the kernels (2.4.7) and (2.4.8).

Note also that contrarily to dimension three, F_t is supported on the whole two-dimension ball $B(0, c|t|)$ and not only the sphere $S(0, c|t|)$. This is Huygens' principle for the wave equation in even dimensions ([73], p. 80).

5.3.3 A matched Dirichlet boundary condition strategy

In this section, we illustrate a particular strategy for building TBC, which consists in building matched Dirichlet boundary conditions using the WIGPR Kriging mean. Since this topic is only a recent topic of research, we will not delve into the details of the method, both from the point of view of theory and implementation. Moreover, we will not compare the results with other TBC methods. This necessary study is left for future research.

Given an arbitrary domain $\mathcal{D} \subset \mathbb{R}^2$, a possible strategy consists in using a standard finite difference numerical scheme inside the domain $\mathcal{D}$ and in matching the numerical value at the boundary of the domain using the WIGPR Kriging mean. We choose to constrain it on a finite number samples of the initial conditions: this implies that the matched boundary conditions can be computed offline.

Since we have not found any mathematical simplifications which would justify using particular kernels in this two dimensional setting, we directly consider kernels of the following form, for the kernels k_{u} and k_{v}

$$k(x, x') = \chi(x)\chi(x')k_S(x - x'). \tag{5.3.5}$$

Above, k_S is a stationary kernel over $\mathbb{R}^2$ and the function χ is compactly supported. Recall that kernels k_{u} and k_{v} are those associated to GP priors over the initial conditions, u_0 and v_0. In this setting, we choose k_S to be a 3/2-Matérn kernel and the function χ to be a smoothed indicator function for the support of the initial condition (either u_0 for k_{u} and v_0 for k_{v}).

Figure 5.7 shows an example of numerical result obtained from this method. This test case considers cosine type initial conditions for both u_0 and v_0, as the one given in equation (4.4.6). Note that we do not use the radial symmetry of such initial conditions; wWe only use the knowledge of their support.

In the left and middle columns of Figure 5.7, the circles indicate the support of the initial conditions: green for u_0 and yellow for v_0. The colored dots contained in those circles (left column) indicate the location of the points against which the WIGPR Kriging mean is constrained at $t = 0$. There are 78 green and yellow points each, yielding a covariance matrix of size 156×156. In the interior domain, we used the two step explicit finite difference scheme given in [28], Section 11.3.1 (with $\alpha = 2/3$ in its equation (11.16), yielding a fourth order accurate scheme) with Courant number $\lambda = \sqrt{3}/2 - 10^{-6}$. This respects the CFL condition given in [28], equation (11.17).

The energy functional computed in the right column is the one given in [28], Section 11.2.2, equation (11.14). It is a discretized version of the energy function given in the introduction chapter, equation (1.3.11). Our objective is that this numerical energy vanishes as the numerical simulation progresses.

Note though that Huygens' principle in even dimensions implies that this energy will never completely vanish in finite time in the continuous setting (and thus probably also in the numerical setting).

Figure 5.7 shows that most of the initial data effectively escapes the numerical domain. These are qualitatively good results. Those should now be compared with the performance of the Engquist-Majda transparent boundary conditions described in [70].

Observe that spurious reflections are visible, particularly in the last three images of Figure 5.7. This is to be expected. Indeed, the numerical solution produced by the numerical scheme is only approximately a solution to the wave equation, while the Kriging mean is an exact solution to the wave equation. Such spurious reflections are in fact common in TBC or similar boundary conditions, and one expects that they vanish in the limit $\Delta x \to 0$. In our case, the number of initial interpolation points should also increase as $\Delta x \to 0$.

An important problem associated to the FFT approach is that it implicitely periodizes the signal. In our two dimensional setting, this corresponds to paving $\mathbb{R}^2$ with squares whose length are proportional to the number of points used in the frequency domain used for computing the FFT. As a result, if using FFTs to approximate the convolution with F_t for large t, then the matched Dirichlet boundary conditions will actually produce a wave *penetrating* the numerical domain. This ingoing wave is the outgoing wave corresponding to the periodized domain located right above the true numerical domain. This means that a sufficient amount of zero padding is needed for the FFT, and that the numerical simulation has to be stopped at a given time T. Alternatively, the matched Dirichlet boundary conditions can be switched to homogeneous Dirichlet or Neumann boundary conditions after most of the energy of the solution has escaped the numerical domain. This is obviously not an optimal fix and research is ongoing on how to fix this issue.

5.4 Conclusion and perspectives

The first part of this chapter was dedicated to the study of several links between finite difference schemes and physics-informed GPR. We described two different ways of building finite difference schemes from GPR models. From the results we described, many research directions are possible. For instance, we can consider the case of an arbitrary number of points in the scheme (we focused on three point schemes), as well as different smoothness regimes. For PDEs with non constant coefficients, the symbol ([101], p. 237) of the PDE may be found to be helpful. In the non asymptotic regime of Section 5.2.4, non stationary kernels may also be relevant for incorporating

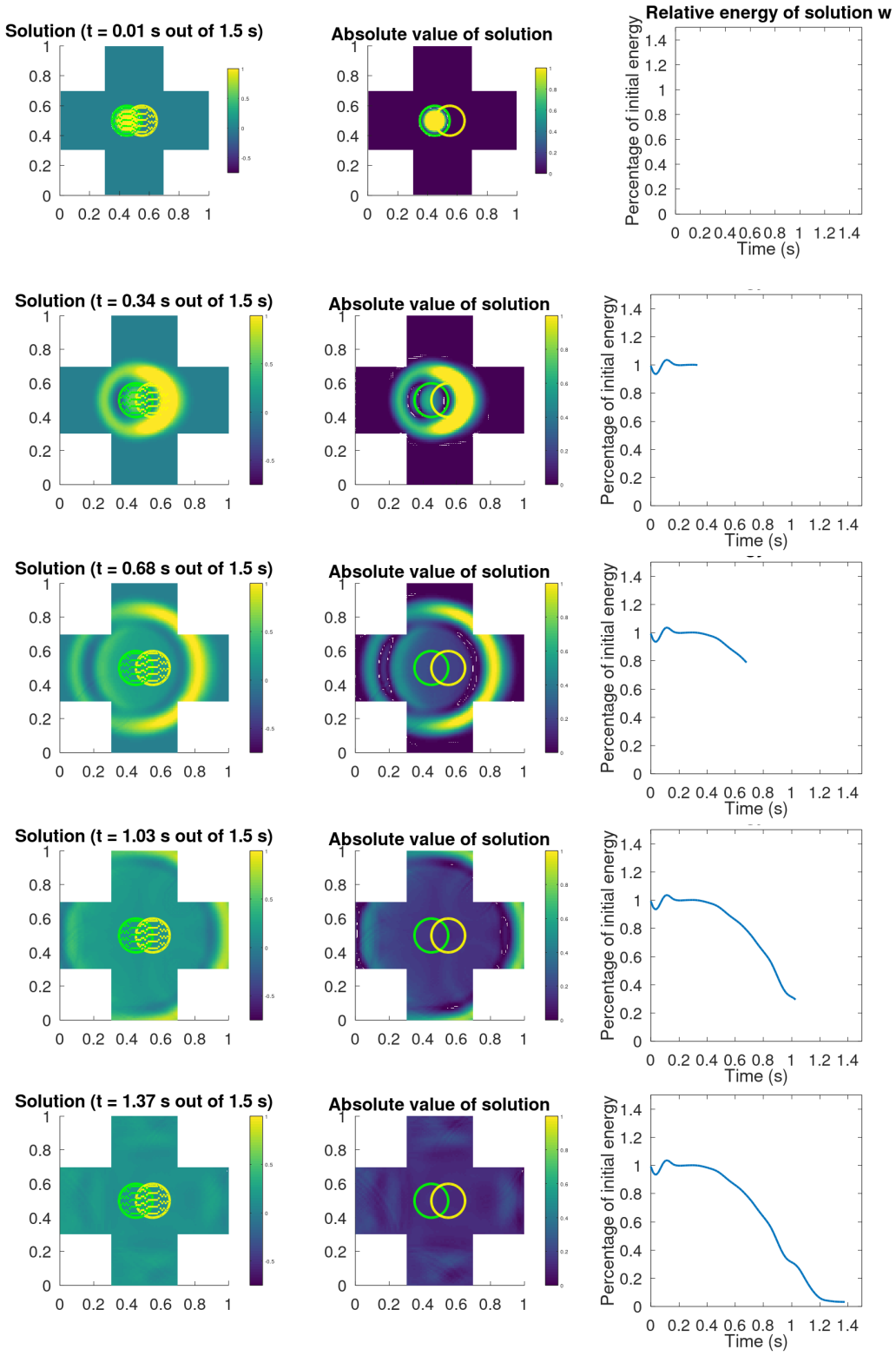

Figure 5.7 – Numerical example of matched Dirichlet transparent boundary conditions using WIGPR.

prior information such as a constrained support, which e.g. could result in removing certain non physical spurious oscillations (it can be checked that flat limits of stationary kernels yield the same results as that of Section 5.2.3). The stability and accuracy analysis of such non stationary schemes should be fully carried out. The case of multidimensional time dependent PDEs is also an obvious direction of research. Likewise, the study of *systems* of linear PDEs is another major direction of research. Systems are particularly important within the framework of hyperbolic systems of conservation laws [186]. Even more generally, we may also consider other general linear PDEs.

Note also that the finite difference scheme setting naturally appeared as we directly considered interpolation problems which, in the RKHS setting, correspond to linear forms of the form $\ell_x : u \mapsto u(x) = \langle u, k_x \rangle_k$. Different linear forms can be considered, such as integrals of the target function. This may lead to links with the finite element method (integrals against test functions) or the finite volume (local averages of the function). It is in fact known that finite element methods in one dimension are easily seen as kernel methods, as $H^1(\mathbb{R})$ is an RKHS, from the Sobolev embedding theorem. This could lead to a unifying framework for numerical methods, encompassing finite difference methods on the one side, finite element methods on the other side and finite volume methods on yet another side. Perhaps that hybrid methods, which could mix finite difference, finite element and finite volume approaches, can be obtained in such a framework.

Concerning TBC, there are many directions which are left to be explored. The method we have described should obviously be compared to other TBC methods. Alternatives to this method should also be considered. For example, a possibility consists in conditioning the Kriging mean of WIGPR on neighbouring points instead that on initial condition values, similarly to the finite difference method. It is possible that such a method would only require the knowledge of the Green's function over a single time step, that is, $F_{\Delta t}$ and $\dot{F}_{\Delta t}$. This would avoid the periodization problem of FFT described earlier. Such an approach could also be relevant for nonlinear PDEs as they can be locally linearized, whereas the method we have introduced is in fact non local (as TBC usually are!). In this context, the relevance of the stationary formulas from Proposition 4.3.3 (only valid in the three dimensional setting) is to be investigated.

5.5 Appendix : proofs

Proof of Proposition 5.2.1: Consider the discrete Fourier transform of the coefficients of the scheme

$$G(\omega) = a_{-1}e^{-i\omega} + a_0 + a_1 e^{i\omega} = 1 - D + D\cos(\omega) - i\lambda\sin(\omega). \tag{5.5.1}$$

The Von Neumann stability condition is ensured by the negativity of the following quantity, given $\omega \in [-\pi, \pi]$:

$$\begin{aligned}|G(\omega)|^2 - 1 &= \big(1 - D + D\cos(\omega)\big)^2 + \lambda^2\sin^2(\omega) - 1\\ &= (1-D)^2 + 2D(1-D)\cos(\omega) + D^2\cos^2(\omega) + \lambda^2\big(1 - \cos^2(\omega)\big) - 1\\ &= (1-D)^2 + \lambda^2 - 1 + 2D(1-D)\cos(\omega) + (D^2 - \lambda^2)\cos^2(\omega).\end{aligned}$$

We will thus study the sign of the following polynomial function over $[-1, 1]$:

$$P(x) := (1-D)^2 + \lambda^2 - 1 + 2D(1-D)x + (D^2 - \lambda^2)x^2. \tag{5.5.2}$$

Quite surprisingly, its discriminant is a perfect square.

$$\begin{aligned}\Delta &= 4D^2(1-D)^2 - 4((1-D)^2 + \lambda^2 - 1)(D^2 - \lambda^2)\\ &= 4D^2(1-D)^2 - 4\Big(D^2(1-D)^2 - (1-D)^2\lambda^2 + D^2\lambda^2 - \lambda^4 - D^2 + \lambda^2\Big)\\ &= 4\Big((1-D)^2\lambda^2 - D^2\lambda^2 + \lambda^4 + D^2 - \lambda^2\Big)\\ &= 4\Big(\lambda^2 - 2D\lambda^2 + D^2\lambda^2 - D^2\lambda^2 + \lambda^4 + D^2 - \lambda^2\Big)\\ &= 4(D^2 - 2D\lambda^2 + \lambda^4) = 4(D - \lambda^2)^2 \geq 0.\end{aligned} \tag{5.5.3}$$

The two roots of $P(x)$ are then given by

$$r_\pm = \frac{-D(1-D) \pm (D - \lambda^2)}{D^2 - \lambda^2}. \tag{5.5.4}$$

This yields $r = 1$ or $r = (D^2 - 2D + \lambda^2)/(D^2 - \lambda^2)$. The polynomial $x - 1$ being negative over $[-1, 1]$, the condition for $P(x)$ to be negative over $[-1, 1]$ is

$$\frac{P(x)}{x-1} = (D^2 - \lambda^2)\left(x - \frac{D^2 - 2D + \lambda^2}{D^2 - \lambda^2}\right) \geq 0, \quad \forall x \in [-1, 1]. \tag{5.5.5}$$

Since this is a polynomial of degree one, equation (5.5.5) amounts to having the condition enforced at both ends of the interval $[-1, 1]$:

$$(D^2 - \lambda^2)\left(1 - \frac{D^2 - 2D + \lambda^2}{D^2 - \lambda^2}\right) \geq 0, (D^2 - \lambda^2)\left(-1 - \frac{D^2 - 2D + \lambda^2}{D^2 - \lambda^2}\right) \geq 0.$$

After expanding the products, one finds that the first equation amounts to $D \geq \lambda^2$ while the second amounts to $D(1-D) \geq 0$, that is, $D \in [0,1]$, which finishes the proof. □

Proof of Proposition 5.2.2 : For short we denote $u_t = \partial_t u$, $u_{tt} = \partial^2_{tt} u$ and likewise for $\partial_x u = u_x$, $\partial^2_{xx} u = u_{xx}$ and so forth for other derivatives such as u_{xxt}. The computations are "straighforward" but they are also tedious. Note that a general algorithmic procedure for obtaining modified equations is given in [210]. We start by expanding the function u with its Taylor series around $(k\Delta x, n\Delta t)$. This yields

$$\left(u_t + \frac{\Delta t}{2} u_{tt} + \frac{\Delta t^2}{6} u_{ttt}\right) + c\left(u_x + \frac{\Delta x^2}{6} u_{xxx}\right) = (D_0 \Delta x) u_{xx} + O(\Delta x^3), \quad (5.5.6)$$

where we used that $O(\Delta x) = O(\Delta t)$ when the Courant number is kept constant, and where we denoted $D_0 \coloneqq cD/2\lambda$, which is of order $O(1)$ and verifies $D\Delta x^2/2\Delta t = D_0 \Delta x$. The time partial derivatives of order 2 and 3 can be expressed as space derivatives thanks to the following procedure. We first assume that all the derivatives of u, up to order 4, are bounded, and we begin with the u_{xxx} term. Now, note that equation (5.5.6) states that

$$u_t + c u_x = O(\Delta x), \quad (5.5.7)$$

where the term $O(\Delta x)$ is carried by a derivative of order 2. Because we assumed that derivatives of order 3 are bounded, by differentiating equation (5.5.7) with respect to x and t we obtain that

$$u_{tt} + c u_{tx} = O(\Delta x), \quad (5.5.8)$$
$$u_{xt} + c u_{xx} = O(\Delta x), \quad (5.5.9)$$

where now the $O(\Delta x)$ term is carried by a third order derivative. Differentiating the equations above with respect to x and t together with the assumption that fourth order derivatives are bounded, we next obtain that

$$u_{ttt} + c u_{ttx} = O(\Delta x), \quad (5.5.10)$$
$$u_{xtt} + c u_{xtx} = O(\Delta x), \quad (5.5.11)$$
$$u_{xxt} + c u_{xxx} = O(\Delta x), \quad (5.5.12)$$

which yields in particular that

$$u_{ttt} = -c^3 u_{xxx} + O(\Delta x). \quad (5.5.13)$$

Since the coefficient associated to the derivative u_{ttt} in equation (5.5.6) is already of order $O(\Delta x^2)$, equation (5.5.13) can be plugged in equation (5.5.6) to yield

$$u_t + cu_x = (D_0\Delta x)u_{xx} - \frac{\Delta t}{2}u_{tt} + \left(\frac{c^3\Delta t^2}{6} - c\frac{\Delta x^2}{6}\right)u_{xxx} + O(\Delta x^3). \quad (5.5.14)$$

We now deal with the u_{tt} term. For this, notice now that equation (5.5.6) states that

$$u_t + cu_x = (D_0\Delta x)u_{xx} - \frac{\Delta t}{2}u_{tt} + O(\Delta x^2). \quad (5.5.15)$$

As previously, by differentiating the equation above with respect to x and t and using equations (5.5.10), (5.5.11) and (5.5.12), we deduce that

$$\begin{aligned} u_{tt} + cu_{tx} &= (D_0\Delta x)u_{txx} - \frac{\Delta t}{2}u_{ttt} + O(\Delta x^2) && (5.5.16)\\ &= -c(D_0\Delta x)u_{xxx} + c^3\frac{\Delta t}{2}u_{xxx} + O(\Delta x^2), && (5.5.17)\\ u_{xt} + cu_{xx} &= (D_0\Delta x)u_{xxx} - \frac{\Delta t}{2}u_{xtt} + O(\Delta x^2) && (5.5.18)\\ &= (D_0\Delta x)u_{xxx} - c^2\frac{\Delta t}{2}u_{xxx} + O(\Delta x^2), && (5.5.19)\end{aligned}$$

Thus,

$$\begin{aligned} u_{tt} &= -cu_{tx} - c(D_0\Delta x)u_{xxx} + c^3\frac{\Delta t}{2}u_{xxx} + O(\Delta x^2) && (5.5.20)\\ &= -c\Big(- cu_{xx} + (D_0\Delta x)u_{xxx} - c^2\frac{\Delta t}{2}u_{xxx}\Big) && (5.5.21)\\ &\qquad - c(D_0\Delta x)u_{xxx} + c^3\frac{\Delta t}{2}u_{xxx} + O(\Delta x^2) && (5.5.22)\\ &= c^2u_{xx} + \left(c^3\Delta t - 2cD_0\Delta x\right)u_{xxx} + O(\Delta x^2). && (5.5.23)\end{aligned}$$

Plugging this equation in equation (5.5.14) yields

$$u_t + cu_x = \left(D_0\Delta x - c^2\frac{\Delta t}{2}\right)u_{xx} + \left(\frac{c^3\Delta t^2}{6} - c\frac{\Delta x^2}{6} - c^3\frac{\Delta t^2}{2} + cD_0\Delta x\Delta t\right)u_{xxx} + O(\Delta x^3). \quad (5.5.24)$$

This equation is simplified by further computing that

$$D_0\Delta x - c^2\frac{\Delta t}{2} = \frac{c\lambda\Delta x}{2}\left(\frac{D}{\lambda^2} - 1\right), \tag{5.5.25}$$

and that

$$\begin{aligned}\frac{c^3\Delta t^2}{6} - c\frac{\Delta x^2}{6} - c^3\frac{\Delta t^2}{2} + cD_0\Delta x\Delta t &= \frac{c\Delta x^2}{6}(\lambda^2-1) - \frac{c\lambda^2\Delta x^2}{2} + \frac{cD\Delta x^2}{2}\\ &= \frac{c\Delta x^2}{6}(3D - 2\lambda^2 - 1). \end{aligned}\tag{5.5.26}$$

This finally yields equation (5.2.17). □

Proof of Proposition 5.2.4 : We use equation (5.2.39), and in fact we will only need the following expansion (recall that $0 < \nu < 1$, thus $2\nu < 2$) :

$$k_\nu(r) = 1 + C_\nu r^{2\nu} + O(r^2). \tag{5.5.27}$$

We set $\gamma := \alpha^{-2}$, with $\alpha = \ell/\Delta x$. Then, in the limit when α goes to infinity, γ goes to zero and

$$b = 1 + C_\nu(1/\alpha)^{2\nu} + O(\alpha^{-2}) = 1 + C_\nu\gamma^\nu + O(\gamma), \tag{5.5.28}$$

$$c = 1 + C_\nu(2/\alpha)^{2\nu} + o(\alpha^{-2}) = 1 + C_\nu 4^\nu\gamma^\nu + O(\gamma). \tag{5.5.29}$$

This implies that

$$\begin{aligned}1 + c - 2b^2 &= 2 + C_\nu 4^\nu\gamma^\nu + O(\gamma) - 2(1 + C_\nu\gamma^\nu + O(\gamma))^2\\ &= C_\nu(4^\nu - 4)\gamma^\nu + O(\gamma^{\min(2\nu,1)}), \end{aligned}\tag{5.5.30}$$

$$1 - c = -C_\nu 4^\nu\gamma^\nu + O(\gamma). \tag{5.5.31}$$

Observe that in equation (5.5.30), the product term $\gamma^{2\nu}$ obtained by squaring $C_\nu\gamma^{2\nu}$ is of lower order that γ when $0 < \nu < 1/2$. This will have no influence on the obtained limits; only the order approximation is impacted.

We first focus on a_{-1} and a_1. Observe that for v_{-1}, v_0 and v_1, the asymptotic expansion (5.5.27) yields

$$v_{-1} = 1 + C_\nu\left|\frac{c\Delta t - \Delta x}{\alpha\Delta x}\right|^{2\nu} + O(\gamma) = 1 + C_\nu|\lambda - 1|^{2\nu}\gamma^\nu + O(\gamma), \tag{5.5.32}$$

$$v_1 = 1 + C_\nu\left|\frac{c\Delta t + \Delta x}{\alpha\Delta x}\right|^{2\nu} + O(\gamma) = 1 + C_\nu|\lambda + 1|^{2\nu}\gamma^\nu + O(\gamma), \tag{5.5.33}$$

$$v_0 = 1 + C_\nu\left|\frac{c\Delta t}{\alpha\Delta x}\right|^{2\nu} + O(\gamma) = 1 + C_\nu|\lambda|^{2\nu}\gamma^\nu + O(\gamma). \tag{5.5.34}$$

Storing all the $O(\gamma^{\min(2\nu,1)})$ (lowest order) terms in the same one at the end, we have that

$$\begin{aligned} v_{-1} + v_1 - 2bv_0 &= 2 + C_\nu(|\lambda-1|^{2\nu} + |\lambda+1|^{2\nu})\gamma^\nu \\ &\quad - 2(1 + C_\nu\gamma^\nu)(1 + C_\nu|\lambda|^{2\nu}\gamma^\nu) + O(\gamma^{\min(2\nu,1)}) \\ &= C_\nu(|\lambda-1|^{2\nu} + |\lambda+1|^{2\nu} - 2|\lambda|^{2\nu} - 2)\gamma^\nu + O(\gamma^{\min(2\nu,1)}). \quad (5.5.35) \end{aligned}$$

Similarly,

$$\begin{aligned} v_{-1} - v_1 &= 1 + C_\nu|\lambda-1|^{2\nu}\gamma^\nu - 1 - C_\nu|\lambda+1|^{2\nu}\gamma^\nu + O(\gamma) \quad (5.5.36) \\ &= C_\nu(|\lambda-1|^{2\nu} - |\lambda+1|^{2\nu})\gamma^\nu + O(\gamma). \quad (5.5.37) \end{aligned}$$

This yields that

$$\begin{aligned} a_{-1} - a_1 &= \frac{C_\nu(|\lambda-1|^{2\nu} - |\lambda+1|^{2\nu})\gamma^\nu + O(\gamma)}{-C_\nu 4^\nu\gamma^\nu + O(\gamma)} \\ &= \frac{|\lambda+1|^{2\nu} - |\lambda-1|^{2\nu}}{4^\nu} + O(\gamma), \quad (5.5.38) \\ a_{-1} + a_1 &= \frac{C_\nu(|\lambda-1|^{2\nu} + |\lambda+1|^{2\nu} - 2|\lambda|^{2\nu} - 2)\gamma^\nu + O(\gamma^{\min(2\nu,1)})}{C_\nu(4^\nu - 4)\gamma^\nu + O(\gamma^{\min(2\nu,1)})} \quad (5.5.39) \\ &= D(\nu,\lambda) + O(\gamma^{\min(\nu,1-\nu)}). \quad (5.5.40) \end{aligned}$$

From this we conclude that

$$a_{-1} = \frac{D(\nu,\lambda)}{2} + \frac{1}{2}\frac{|\lambda+1|^{2\nu} - |\lambda-1|^{2\nu}}{4^\nu} + O(\gamma^{\min(\nu,1-\nu)}). \quad (5.5.41)$$

Similarly for a_1,

$$a_1 = \frac{D(\nu,\lambda)}{2} - \frac{1}{2}\frac{|\lambda+1|^{2\nu} - |\lambda-1|^{2\nu}}{4^\nu} + O(\gamma^{\min(\nu,1-\nu)}). \quad (5.5.42)$$

Finally, for a_0 and dropping the approximation term $O(\gamma^{\min(2\nu,1)})$ (it is now implicit in each equality, for readability),

$$\begin{aligned} (1+c)v_0 - b(v_{-1} + v_1) &= (2 + C_\nu 4^\nu\gamma^\nu)(1 + C_\nu|\lambda|^{2\nu}\gamma^\nu) \\ &\quad - (1 + C_\nu\gamma^\nu)(2 + C_\nu(|\lambda-1|^{2\nu} + |\lambda+1|^{2\nu})\gamma^\nu) \quad (5.5.43) \\ &= 2 + C_\nu(4^\nu + 2|\lambda|^{2\nu})\gamma^\nu \\ &\quad - (2 + C_\nu(|\lambda-1|^{2\nu} + |\lambda+1|^{2\nu} + 2)\gamma^\nu) \quad (5.5.44) \\ &= C_\nu(4^\nu - 2 + 2|\lambda|^{2\nu} - |\lambda-1|^{2\nu} - |\lambda+1|^{2\nu})\gamma^\nu. \quad (5.5.45) \end{aligned}$$

and thus, up to a term of order $O(\gamma^{\min(\nu,1-\nu)})$,

$$a_0 = \frac{C_\nu(4^\nu - 2 + 2|\lambda|^{2\nu} - |\lambda-1|^{2\nu} - |\lambda+1|^{2\nu})\gamma^\nu}{C_\nu(4^\nu - 4)\gamma^\nu} \quad (5.5.46)$$

$$= \frac{4^\nu - 4 + 2 + 2|\lambda|^{2\nu} - |\lambda - 1|^{2\nu} - |\lambda + 1|^{2\nu}}{4^\nu - 4} \tag{5.5.47}$$

$$= 1 - \frac{|\lambda + 1|^{2\nu} + |\lambda - 1|^{2\nu} - 2|\lambda|^{2\nu} - 2}{4^\nu - 4} = 1 - D(\nu, \lambda), \tag{5.5.48}$$

which finishes the proof. □

Proof of Proposition 5.2.5 : The idea is the same as previously, but we need to go higher in the asymptotic expansion :

$$k_\nu(r) = 1 + Ar^2 + C_\nu r^{2\nu} + O(r^4). \tag{5.5.49}$$

With the convention $\gamma = \alpha^{-2}$, we then obtain, up to a $O(\gamma^2)$ term (recall that $1 < \nu < 2$, thus $2 < 2\nu$ and $O(\gamma^{2\nu}) \in O(\gamma^2)$ when $\gamma \to 0$),

$$\begin{aligned} 1 + c - 2b^2 &= 2 + 4A\gamma + C_\nu 4^\nu \gamma^\nu - 2(1 + A\gamma + C_\nu \gamma^\nu)^2 \\ &= 2 + 4A\gamma + C_\nu 4^\nu \gamma^\nu - 2(1 + 2A\gamma + 2C_\nu \gamma^\nu) \\ &= C_\nu(4^\nu - 4)\gamma^\nu + O(\gamma^2). \end{aligned} \tag{5.5.50}$$

Likewise,

$$1 - c = -4A\gamma + O(\gamma^\nu). \tag{5.5.51}$$

We begin with a_{-1} and a_1. First, up to a $O(\gamma^2)$ term,

$$\begin{aligned} v_{-1} + v_1 - 2bv_0 &= 2 + A(|\lambda - 1|^2 + |\lambda + 1|^2)\gamma + C_\nu(|\lambda - 1|^{2\nu} + |\lambda + 1|^{2\nu})\gamma^\nu \\ &\quad - 2(1 + A\gamma + C_\nu\gamma)(1 + A\lambda^2\gamma + C_\nu|\lambda|^{2\nu}\gamma^\nu) \qquad (5.5.52) \\ &= 2 + 2A(\lambda^2 + 1)\gamma + C_\nu(|\lambda - 1|^{2\nu} + |\lambda + 1|^{2\nu})\gamma^\nu \\ &\quad - 2(1 + A(\lambda^2 + 1)\gamma + C_\nu(1 + |\lambda|^{2\nu})\gamma^\nu) \qquad (5.5.53) \\ &= C_\nu(|\lambda - 1|^{2\nu} + |\lambda + 1|^{2\nu} - 2|\lambda|^{2\nu} - 2)\gamma^\nu + O(\gamma^2). \qquad (5.5.54) \end{aligned}$$

Next, up to a $O(\gamma^\nu)$ term,

$$v_{-1} - v_1 = 1 + A|\lambda - 1|^2\gamma - 1 - A|\lambda + 1|^2\gamma = -4A\lambda\gamma + O(\gamma^\nu). \tag{5.5.55}$$

Therefore,

$$a_{-1} - a_1 = \frac{-4A\lambda\gamma + O(\gamma^\nu)}{-4A\gamma + O(\gamma^\nu)} = \lambda + O(\gamma^{\nu-1}), \tag{5.5.56}$$

$$\begin{aligned} a_{-1} + a_1 &= \frac{C_\nu(|\lambda - 1|^{2\nu} + |\lambda + 1|^{2\nu} - 2|\lambda|^{2\nu} - 2)\gamma^\nu + O(\gamma^2)}{C_\nu(4^\nu - 4)\gamma^\nu + O(\gamma^2)} \\ &= D(\nu, \lambda) + O(\gamma^{2-\nu}), \end{aligned} \tag{5.5.57}$$

which finally yields that

$$a_{-1} = \frac{\lambda}{2} + \frac{D(\nu, \lambda)}{2} + O(\gamma^{\min(\nu-1, 2-\nu)}), \tag{5.5.58}$$

$$a_1 = -\frac{\lambda}{2} + \frac{D(\nu,\lambda)}{2} + O(\gamma^{\min(\nu-1,2-\nu)}). \tag{5.5.59}$$

For a_0, we study each term in $(1+c)v_0 - b(v_{-1}+v_1)$ independently. First, up to a $O(\gamma^2)$ term,

$$\begin{aligned}(1+c)v_0 &= (2+4A\gamma + C_\nu 4^\nu \gamma^\nu)(1 + A\lambda^2\gamma + C_\nu|\lambda|^{2\nu}) \\ &= 2 + (2A\lambda^2 + 4A)\gamma + C_\nu(4^\nu + 2|\lambda|^{2\nu})\gamma^\nu + O(\gamma^2). \end{aligned} \tag{5.5.60}$$

For the second term, up to a $O(\gamma^2)$ term and using that $(\lambda+1)^2 + (\lambda-1)^2 = 2(\lambda^2+1)$,

$$\begin{aligned}&b(v_{-1}+v_1) \\ &\quad = (1 + A\gamma + C_\nu\gamma^\nu)(2 + 2A(\lambda^2+1)\gamma + C_\nu(|\lambda-1|^{2\nu} + |\lambda+1|^{2\nu})\gamma^{2\nu}) \\ &\quad = 2 + 2A(\lambda^2+2)\gamma + C_\nu(|\lambda+1|^{2\nu} + |\lambda-1|^{2\nu} + 2)\gamma^\nu + O(\gamma^2). \end{aligned} \tag{5.5.61}$$

Therefore the terms of order γ cancel out, yielding

$$\begin{aligned}&(1+c)v_0 - b(v_{-1}+v_1) \\ &\qquad = C_\nu(4^\nu + 2|\lambda|^{2\nu} - |\lambda+1|^{2\nu} - |\lambda-1|^{2\nu} - 2)\gamma^\nu + O(\gamma^2). \end{aligned} \tag{5.5.62}$$

Thus,

$$\begin{aligned}a_0 &= \frac{C_\nu(4^\nu - 2 + 2|\lambda|^{2\nu} - |\lambda+1|^{2\nu} - |\lambda-1|^{2\nu})\gamma^\nu + O(\gamma^2)}{C_\nu(4^\nu - 4)\gamma^\nu + O(\gamma^2)} \\ &= 1 - D(\nu,\lambda) + O(\gamma^{2-\nu}), \end{aligned} \tag{5.5.63}$$

which finishes the proof (observe that the speed of convergence for the central coefficient is the slightly better $O(\gamma^{2-\nu})$). □

Chapter 6

General conclusion and perspectives

A retrospective overview of the manuscript

Some general comments are now called for, in hindsight of the results described in Chapters 2, 3, 4 and 5. Discarding the introductive chapter, the first two chapters of the manuscript were dedicated to the identification of mathematical frameworks in which the use of GPR methods was compliant with certain key principles stemming from PDE theory. Those principles, functional analytic in essence, bear in them important physical meaning (Chapter 1, Section 1.3). Explicitly, Chapter 2 shows how to strictly encode homogeneous distributional linear PDE constraints on a GP, while Chapter 3 shows how to control the Sobolev regularity of a GP. Both chapters adopt very general frameworks; in particular, the assumption that the process is continuous in probability (which is otherwise standard in random field theory) is dropped whenever possible. Indeed, for distributional formulations as well as for Sobolev regularity, relevant or interesting solutions may very well be discontinuous and thus continuity assumptions should be avoided. The criteria identified in those chapters, which are both necessary and sufficient, are phrased solely in terms of the first two moments of the process. Finally, efforts were made so that the results hold at the level of the sample paths of the process. As a result, the conditions identified in Propositions 2.3.5, 3.3.1 and 3.4.4 each provide a framework within which the statistical modeling associated to GPR (which consists in viewing the unknown function as a realization of some Gaussian process) is *justified*: this means here that the statistical modeling takes into account the properties of the target PDE, using the language of PDE theory (here, distributional derivatives and Sobolev spaces).

The next two chapters were more applied in nature. Chapter 4 dealt with the practical application of general covariance formulas identified in Chapter 2, which are tailored to the three dimensional wave equation. Applications concerned the resolution of ill-posed inverse problems constrained by the wave equation. Chapter 5 was concerned with the study of the finite difference method for hyperbolic PDEs in particular, from the point of view of kernel

methods. In their approach, these two chapters are complementary to the two first ones. Indeed, while Chapters 2 and 3 were concerned with enforcing notions from PDE theory on GPR methods, Chapters 4 and 5 were concerned with applying GPR methods to certain typical PDE problems. The underlying hope was that GPR methods based on "physics-informed" kernels could shed a new light on well-known (numerical) methods of resolution, as well as provide some new answers, methods and perspectives for solving such PDE related problems. In our case, the soundness of this idea was confirmed by the results from Section 4.3.3 (unexpected at first sight), which link the hyperparameter estimation step of "wave equation-informed GPR" with the more intuitive multilateration method for point source localization. This correspondence suggested the existence of other links between physics-informed kernel methods and standard numerical methods for PDEs, thus paving the way for Chapter 5.

A review of the results of Chapters 2 to 5, with perspectives

Chapter 2 deals with the distributional formulation of homogeneous linear PDEs. "Homogeneous" means here that the source term is null, as e.g. encountered in conservation laws. This distributional formulation of linear PDEs consists in multiplying the PDE with a test function (smooth and compactly supported), and transferring all the derivatives to the test function by means of integration by parts. In effect, this reduces to the minimum the regularity assumption required over the target solution, which need only be locally integrable. Such a formulation is sometimes required in practice, for example when dealing with hyperbolic PDEs. The core result of Chapter 2 is Proposition 2.3.5, which states that the sample paths of a general measurable second order random field verify a given homogenous PDE if and only if the functions $k(x, \cdot)$ verify the same PDE. Here, k is the covariance function of the process and all the PDEs are understood in the distributional sense. From a modeling perspective, this result is practical because it enables to conveniently constrain the sample paths of a second order random field by constraining the kernel. A general covariance formula tailored to the homogeneous three dimensional full space wave equation was then described, in a very general framework.

A complimentary result to Proposition 2.3.5 would consist in describing the kernels which verify the constraint $\mathcal{L}(k_x) = 0$, e.g. in terms of the PDE's Green's function. This seems like a sound approach when the coefficients of the PDE are constant, as then the Malgrange-Ehrenpeis theorem ensures the existence of such a function (rather, distribution); see e.g. [33], p. 117. Moreover, the covariance formulas for the wave equation were derived by in-

corporating a representation formula for the solution of the full space problem in the GP prior; a fact which is then inherited to the associated numerical approximation formula (here, the Kriging mean). Incorporating the shape of the full space solution in the numerical approximation is a typical strategy for the design of transparent boundary conditions (TBC), which aim at emulating transparent boundaries (as if one was solving a full space problem) of the finite numerical simulation domain, thus allowing outgoing waves to escape out of the simulation domain. The design of TBC is a difficult problem, especially if the numerical domain contains corners. In principle at least, it seems that physics-informed kernels such as the ones described in Proposition 2.4.1 can help tackle arbitrary geometry, as kernel interpolation methods are inherently meshless. The design and the analysis of TBC obtained by such physics-informed kernel methods is thus an interesting direction of research.

Chapter 3 provided several necessary and sufficient conditions ensuring that the sample paths of a measurable Gaussian process lie in a given Sobolev space $W^{m,p}(\mathcal{D})$, where $m \in \mathbb{N}$, $p \in (1, +\infty)$ and $\mathcal{D}$ is an arbitrary open set of $\mathbb{R}^d$. As a consequence of the lack of regularity assumptions over the open set $\mathcal{D}$, those results were proved by reverting to using elementary characterizations of Sobolev regularity. Likewise, because the (kernel of the) Gaussian process is not assumed continuous, various technical difficulties had to be dealt with, in particular when it came to defining, in an unambiguous fashion, the integral of discontinuous kernels over the diagonal $\{(x, x),\ x \in \mathcal{D}\}$ which has null Lebesgue measure in $\mathcal{D} \times \mathcal{D}$.

From a theoretical perspective, obvious possible extensions concern generalizations of the results of Chapter 3 to fractional Sobolev spaces, which naturally appear in PDEs involving boundary problems, as well as Besov spaces. Moreover, now that the Sobolev regularity of GPs is well understood (within the assumptions of Chapter 3), extensions of Proposition 2.3.5 to variational or weak formulations would constitute a nice complement. Indeed, certain important PDEs, such as $\operatorname{div}(a\nabla u) = f$ with $a_{ij} \in L^\infty(\mathcal{D})$, do not admit strong or distributional formulations in the sense of Definitions 2.3.1 and 2.3.3, due to the lack of regularity of its inner coefficients a. The PDE $\operatorname{div}(a\nabla u) = f$ only makes sense through its weak formulation.

From an applied perspective, the use of the numerical quantities identified in Propositions 3.3.1 and 3.4.4 in the study of kernel methods applied to PDEs is certainly a good direction of research. In particular, they fit (or even extend) the theoretical framework of the article [36] which describes a relaxed "physics-informed" kernel method adapted to nonlinear PDEs, where the PDE is only enforced locally. Finally, the Sobolev kernel selection criterion described in Section 3.5 also deserves a more thorough study.

Chapter 4 dealt with practical applications of covariance formulas obtained in Chapter 2. We derived several "explicit" covariance formulas, in the context of stationarity (Proposition 4.3.3) and radial symmetry (Propositions 4.3.5 and 4.3.6). A toy numerical example within the framework of radial symmetry was then described, showing that such a method was, in principle, capable of tackling several inverse problems linked to the wave equation. These comprised the approximation of the initial conditions of the PDE as well as the estimation of its physical parameters, given scattered sensor measurements of the space-time solution. The approximation of the initial condition in particular is the purpose of photoacoustic tomography (PAT), which has practical applications in many different fields.

In this context, a first step in extending the applicability of the GPR method described in Chapter 4 (say to PAT problems) is to work outside of the context of radial symmetry. Specific algorithms and formulas should then be sought in order to compute the convolutions which, even when using FFTs, are very costly in memory as well as in computation time. At the very least, the fact that the measures F_t and $\dot{F}_t$ are supported on two dimensional manifolds (spheres) should be taken into account to lower the dimensionality of the FFT. Alternatively, it is possible that the stationary formulas from Proposition 4.3.3 may provide relevant GPR models for PAT. Another issue is the large number of data points associated to numerous sensor measurements, as then the covariance matrix becomes prohibitively difficult to invert. The use of low rank approximation methods such as *inducing points* [159] or other methods [190] appears to be an interesting numerical alternative, which is yet to be tested in our context.

More general applications concern wave equations with variable wave speed, as in layered media. In this context, obtaining usable formulas such as the ones from Proposition 2.4.1 appears much more involved, as then the Green's function becomes a function of two space-time variables, $G((x,t),(x',t'))$, because the differential operator is not translation invariant (note though that Proposition 2.3.5 holds in that framework). It is possible that a locally constant approximation procedure may be used, in order to reduce to the case described in Chapter 4. A slightly less demanding generalization concerns the inclusion of boundary conditions with simple geometry (say rectangular or radially symmetric), as then relatively explicit Green's functions (still of the form $G((x,t),(x',t'))$, because now the *domain* is not translation invariant) exist ([68], Chapter 3).

Note that we did not apply the formulas from Proposition 4.3.3, which correspond to stationary initial conditions. The argument was that stationary initial conditions was an unnatural assumption in the context of initial value (hyperbolic) PDEs. Be that as it may, those formulas still correspond to

important random field models. Moreover, the compact explicit expression of $F_t * F_{t'}$ is a "fortunate" consequence of several mathematical simplifications specific to dimension three. Their application should thus be investigated, in PAT or in the design of TBC.

Chapter 5 was dedicated to the study of certain links between kernel regression methods and finite difference schemes for solving PDEs. In the so-called flat limit regime, we described a family of three point centered finite difference schemes indexed by a continuous parameter $\nu > 0$. Interestingly, this family contains the upwind scheme ($\nu = 1/2$) as well as the Lax-Wendroff scheme ($\nu \geq 2$). We next studied their properties, both quantitatively (consistency, stability, accuracy) and qualitatively (diffusivity, dispersivity). In the following section, we studied an alternative regime in which the quadratic form minimized by the Kriging weights is constrained on the consistency equations, yielding other families of schemes. We provided partial results concerning their stability.

At this point, many research perspectives are available. The study of the schemes obtained in the flat limit, for an arbitrary number of points and using kernels with arbitrary smoothness, is a clear direction of research. Considering different (multidimensional) PDEs, or systems of PDEs, is also an interesting perspective. In the non asymptotic constrained regime, the stability and accuracy analysis should be pursued. Moreover, applications of such non degenerate (and potentially non stationary) priors should be sought. The use of linear forms over the RKHS that are different from pointwise evaluations, such as local averages (as in the finite volume method) or integrals against test functions (as in the finite element method), should be investigated. In this setting, hybrid methods combining pointwise evaluations and (weighted) integrals of the numerical solution constitutes an interesting research opportunity.

Concerning transparent boundary conditions (TBC), the kernel-based "matched Dirichlet boundary condition" method described in Chapter 5 should be compared to other standard TBC methods. Alternatives to this method should also be sought, e.g. by constraining the "physics-informed" kriging mean only on points neighbouring the boundary points. For example, it is possible that such a method could only require the knowledge and the computation of $F_{\Delta t}$ and $\dot{F}_{\Delta t}$.

Other research directions. In all the GPR models considered in this manuscript, linear forms that are not pointwise evaluations can in fact be considered. For instance, they may be integrals against some test function. The study of such linear forms is e.g. described in [24], Section 4.9.1.1. The choice of different linear forms may have interesting impacts on the quality of the Kriging mean, a fact which is yet to be studied in our case.

We noted in Chapter 1 that both the Kriging mean and covariance have their counterpart in the scattered data interpolation framework. One is the data interpolant, while the other is the so-called *power function* (see Section 1.2.4). In the Bayesian setting though, there exists quantities that do not have a clear equivalent in the RKHS setting. A first example is the marginal likelihood, which is useful for tuning the hyperparameters of the kernel. A second example concerns the quantities of the form

$$\mathbb{P}(\sup_{t\in T} |U(t)| > \alpha), \quad \mathbb{P}(\|V\| \leq \alpha), \tag{6.0.1}$$

where $(U(t))_{t\in T}$ is a centered Gaussian process and $\|V\|$ is some norm of the sample paths of another centered Gaussian process $(V(x))_{x\in\mathcal{D}}$. We have seen in Chapter 3 that many interesting sample path norms $\|V\|$ are in fact equal to a supremum of the form $\sup_{t\in T} |U(t)|$, in which case both quantities in equation (6.0.1) are equal up to a complement event [1]. When $\alpha \to 0$, the quantity $\mathbb{P}(\|V\| \leq \alpha)$ is known as a *small ball probability*, while the quantity $\mathbb{P}(\sup_{t\in T} |U(t)| \geq \alpha)$ is called an *excursion probability* [2, 16]. We refer to [140] as well as references within for an introduction to the study of small ball probabilities when the norm $\|\cdot\|$ is that of a Hilbert space. For excursion probabilities, asymptotic expansions when $\alpha \to +\infty$ are known ([2], Chapter 14; [16], Chapter 8), as well as non asymptotic bounds with the Borell-TIS inequality in particular ([2], Chapter 2). The use of theoretical results concerning small ball probabilities as well as excursion probabilities constitutes an interesting direction of research within the framework of physics-informed GPR, especially in uncertainty quantification contexts where probabilities of extreme events are target quantities.

1. The indexation set T may become very large though: for example, if $\|\cdot\|$ is an L^p norm, $1 < p < +\infty$, then T becomes the unit ball of L^q which is not compact. In such a setting, many common bounds and techniques for controlling $\sup_{t\in T} |U(t)|$ fall apart, such as Dudley's bound ([199], equation (A.23)). As a result, in Chapter 3, we resorted to alternative methods based on Gaussian measure theory to avoid such problems.

Bibliography

[1] M. Abramowitz, I. A. Stegun, and R. H. Romer. *Handbook of mathematical functions with formulas, graphs, and mathematical tables*. American Association of Physics Teachers, 1965 (cited on pages 232, 233).

[2] R. J. Adler and J. E. Taylor. *Random Fields and Geometry*. Springer Monographs in Mathematics. New York, NY: Springer, 2007 (cited on pages 47, 50, 78, 85, 96, 117, 118, 122, 266).

[3] R. J. Adler. *The Geometry of Random Fields*. Classics in Applied Mathematics. Philadelphia, PA: SIAM, 2010 (cited on page 85).

[4] J.-L. Akian, L. Bonnet, H. Owhadi, and É. Savin. Learning "best" kernels from data in Gaussian process regression. With application to aerodynamics. *J. Comput. Phys.*, 470:Paper No. 111595, 29, 2022 (cited on page 151).

[5] C. G. Albert and K. Rath. Gaussian process regression for data fulfilling linear differential equations with localized sources. *Entropy*, 22(2):Paper No. 152, 16, 2020 (cited on pages 75, 171).

[6] P. A. Alvarado, M. A. Alvarez, G. Daza-Santacoloma, A. Orozco, and G. Castellanos-Dominguez. A latent force model for describing electric propagation in deep brain stimulation: a simulation study. In *2014 36th Annual International Conference of the IEEE Engineering in Medicine and Biology Society*, pages 2617–2620, 2014 (cited on page 170).

[7] P. A. Alvarado, M. A. Álvarez, and Á. A. Orozco. A three spatial dimension wave latent force model for describing excitation sources and electric potentials produced by deep brain stimulation, 2016. arXiv: 1608.04972 (cited on page 170).

[8] M. Álvarez, D. Luengo, and N. Lawrence. Linear latent force models using Gaussian processes. *IEEE Trans. Pattern Anal. Mach. Learn. Intell.*, 35:2693–2705, 2013 (cited on pages 75, 170).

[9] M. Álvarez, D. Luengo, and N. D. Lawrence. Latent force models. In D. van Dyk and M. Welling, editors, *Proceedings of the Twelth International Conference on Artificial Intelligence and Statistics*, volume 5 of *Proc. Mach. Learn. Res.* Pages 9–16, Hilton Clearwater Beach Resort, Clearwater Beach, Florida USA. PMLR, 2009 (cited on page 170).

[10] H. Ammari, editor. *Mathematical modeling in biomedical imaging. II*, volume 2035 of *Lecture Notes in Mathematics*. Springer, Heidelberg, 2012. Optical, ultrasound, and opto-acoustic tomographies, Mathematical Biosciences Subseries (cited on pages 170, 171).

[11] M. A. Anastasio, J. Zhang, D. Modgil, and P. J. La Rivière. Application of inverse source concepts to photoacoustic tomography. *Inverse Problems*, 23(6):S21–S35, 2007 (cited on page 171).

[12] X. Antoine, E. Lorin, and Q. Tang. A friendly review of absorbing boundary conditions and perfectly matched layers for classical and relativistic quantum waves equations. *Molecular Physics*, 115(15-16):1861–1879, 2017 (cited on page 247).

[13] L. Arkhipova. Number of lattice points in a sphere. *Moscow University Mathematics Bulletin*, 63:214–215, 2008 (cited on page 199).

[14] N. Aronszajn. Theory of reproducing kernels. *Trans. Amer. Math. Soc.*, 68(3):337–404, 1950 (cited on pages 21, 22).

[15] S. Arora, S. S. Du, Z. Li, R. Salakhutdinov, R. Wang, and D. Yu. Harnessing the power of infinitely wide deep nets on small-data tasks. *ICLR 2020*, 2020 (cited on page 24).

[16] J.-M. Azaïs and M. Wschebor. *Level sets and extrema of random processes and fields*. Hoboken, NJ: Wiley & Sons, Inc., 2009 (cited on pages 99, 109, 123, 266).

[17] F. Bach. On the relationship between multivariate splines and infinitely-wide neural networks, 2023. arXiv: 2302.03459 (cited on page 25).

[18] S. Barthelmé, P.-O. Amblard, N. Tremblay, and K. Usevich. Gaussian process regression in the flat limit, 2022. arXiv: 2201.01074 (cited on page 220).

[19] S. Barthelmé and K. Usevich. Spectral properties of kernel matrices in the flat limit. *SIAM J. Matrix Anal. Appl.*, 42(1):17–57, 2021 (cited on page 220).

[20] M. Belkin, D. Hsu, S. Ma, and S. Mandal. Reconciling modern machine-learning practice and the classical bias–variance trade-off. *Proc. Natl. Acad. Sci. USA PNAS*, 116(32):15849–15854, 2019 (cited on page 6).

[21] M. Belkin, S. Ma, and S. Mandal. To understand deep learning we need to understand kernel learning. In J. Dy and A. Krause, editors, *Proceedings of the 35th International Conference on Machine Learning*, volume 80 of *Proceedings of Machine Learning Research*, pages 541–549. PMLR, 2018 (cited on page 25).

[22] J.-P. Bérenger. *Perfectly Matched Layer (PML) for Computational Electromagnetics*, volume 2 of number 1 in *Synthesis Lectures on Computational Electromagnetics*. Springer Cham, 2007, pages 1–117 (cited on page 247).

[23] C. Berg, J. P. R. Christensen, and P. Ressel. *Harmonic analysis on semigroups: theory of positive definite and related functions*, volume 100. Springer, 1984 (cited on page 8).

[24] A. Berlinet and C. Thomas-Agnan. *Reproducing Kernel Hilbert Spaces in Probability and Statistics*. New York, NY: Springer, 2004 (cited on pages 21, 76, 84, 85, 108, 138, 265).

[25] K. Bhattacharya, B. Hosseini, N. B. Kovachki, and A. M. Stuart. Model reduction and neural networks for parametric PDEs. *SMAI J. Comput. Math.*, 7:121–157, 2021 (cited on page 40).

[26] A. Bietti and F. Bach. Deep Equals Shallow for ReLU Networks in Kernel Regimes. In *ICLR 2021 - International Conference on Learning Representations*, pages 1–22, Virtual, Austria, 2021 (cited on page 25).

[27] S. Bilbao. *Wave and Scattering Methods for Numerical Simulations*. John Wiley & Sons, Ltd, 2004 (cited on page 204).

[28] S. Bilbao. *Numerical sound synthesis: finite difference schemes and simulation in musical acoustics*. John Wiley & Sons, 2009 (cited on pages 218, 250).

[29] V. I. Bogachev. *Gaussian measures*, number 62 in Mathematical Surveys and Monographs. American Mathematical Soc., 1998 (cited on pages 16, 19, 50, 115, 116, 118, 119, 126, 131, 138, 162, 178, 190).

[30] V. I. Bogachev and M. A. S. Ruas. *Measure theory*, volume 1. Springer, 2007 (cited on pages 117, 124, 126).

[31] L. Breiman. Reflections after refereeing papers for NIPS. In *The Mathematics of Generalization*, pages 11–15. CRC Press, 1995 (cited on page 6).

[32] S. C. Brenner and L. R. Scott. *The mathematical theory of finite element methods*, volume 15 of *Texts in Applied Mathematics*. Springer, New York, third edition, 2008 (cited on page 107).

[33] H. Brézis. *Functional Analysis, Sobolev Spaces and Partial Differential Equations*. Universitext. New York, NY: Springer, 2010 (cited on pages 26, 34, 50, 51, 81, 88, 112, 156, 157, 158, 262).

[34] C. Brislawn. Kernels of trace class operators. *Proc. Amer. Math. Soc.*, 104(4):1181–1190, 1988 (cited on pages 116, 120, 133, 135).

[35] Q. Chen and P. Monk. Discretization of the time domain CFIE for acoustic scattering problems using convolution quadrature. *SIAM J. Math. Anal.*, 46(5):3107–3130, 2014 (cited on page 36).

[36] Y. Chen, B. Hosseini, H. Owhadi, and A. M. Stuart. Solving and learning nonlinear PDEs with Gaussian processes. *J. Comput. Phys.*, 447:Paper No. 110668, 29, 2021 (cited on pages 39, 75, 107, 151, 153, 156, 171, 263).

[37] S. A. Chobanjan and V. I. Tarieladze. Gaussian characterizations of certain Banach spaces. *J. Multivariate Anal.*, 7(1):183–203, 1977. ISSN: 0047-259X (cited on page 119).

[38] Z. Ciesielski. Modulus of smoothness of the Brownian paths in the L^p norm. *Constructive theory of functions (Varna, Bulgaria, 1991)*:71–75, 1991 (cited on page 108).

[39] Z. Ciesielski. Quelques espaces fonctionnels associés à des processus gaussiens. *Studia Mathematica*, 107:171–204, 1993 (cited on pages 108, 109).

[40] B. S. Cirel'son, I. A. Ibragimov, and V. N. Sudakov. Norms of Gaussian sample functions. In *Proceedings of the Third Japan—USSR Symposium on Probability Theory*, pages 20–41. Springer, 1976 (cited on page 108).

[41] A. Cohen. From linear to nonlinear n-width : optimality in reduced modelling. In *Journées "Réduction de modèles et traitement géométrique des données", IHP*, 2021 (cited on page 6).

[42] A. Cohen and R. DeVore. Approximation of high-dimensional parametric PDEs. *Acta Numer.*, 24:1–159, 2015 (cited on page 9).

[43] J. D. Cole. On a quasi-linear parabolic equation occurring in aerodynamics. *Quart. Appl. Math.*, 9:225–236, 1951 (cited on page 222).

[44] J. B. Conway. *A course in functional analysis*, volume 96. Springer, 2019 (cited on page 148).

[45] S. L. Cotter, M. Dashti, and A. M. Stuart. Approximation of Bayesian inverse problems for PDEs. *SIAM J. Numer. Anal.*, 48(1):322–345, 2010 (cited on page 171).

[46] J.-F. Coulombel. Stability of finite difference schemes for hyperbolic initial boundary value problems. *SIAM J. Numer. Anal.*, 47(4):2844–2871, 2009 (cited on page 248).

[47] R. Courant, K. Friedrichs, and H. Lewy. On the partial difference equations of mathematical physics. *IBM J. Res. Develop.*, 11:215–234, 1967 (cited on page 218).

[48] N. Cressie. *Statistics for spatial data*. John Wiley & Sons, 1993 (cited on pages 229, 242).

[49] N. Cressie. The origins of Kriging. *Math. Geol.*, 22(3):239–252, 1990 (cited on page 21).

[50] F. Cucker and S. Smale. On the mathematical foundations of learning. *Bull. Amer. Math. Soc. (N.S.)*, 39(1):1–49, 2002 (cited on page 9).

[51] F. Cucker and D. X. Zhou. *Learning theory: an approximation theory viewpoint*, volume 24. Cambridge University Press, 2007 (cited on page 9).

[52] G. Da Prato and J. Zabczyk. *Stochastic equations in infinite dimensions*, volume 44 of *Encyclopedia of Mathematics and its Applications*. Cambridge: Cambridge University Press, 1992 (cited on page 78).

[53] R. C. Dalang and M. Sanz-Solé. Hölder-Sobolev regularity of the solution to the stochastic wave equation in dimension three. *Mem. Amer. Math. Soc.*, 199(931), 2009 (cited on page 171).

[54] M. Dashti, K. J. Law, A. M. Stuart, and J. Voss. MAP estimators and their consistency in Bayesian nonparametric inverse problems. *Inverse Problems*, 29(9):095017, 2013 (cited on page 171).

[55] M. Dashti and A. M. Stuart. The Bayesian approach to inverse problems. In R. Ghanem, D. Higdon, and H. Owhadi, editors, *Handbook of Uncertainty Quantification*, pages 311–428, Cham. Springer International Publishing, 2017 (cited on pages 12, 171).

[56] B. Després. Uniform asymptotic stability of Strang's explicit compact schemes for linear advection. *SIAM J. Numer. Anal.*, 47(5):3956–3976, 2009 (cited on pages 228, 241).

[57] B. Després and H. Jourdren. Machine learning design of volume of fluid schemes for compressible flows. *J. Comput. Phys.*, 408:109275, 27, 2020 (cited on page 220).

[58] Y. Deville, D. Ginsbourger, O. Roustant, and N. Durrande. *kergp: Gaussian Process Laboratory*. R package version 0.5.5. 2021 (cited on page 204).

[59] E. Di Nezza, G. Palatucci, and E. Valdinoci. Hitchhiker's guide to the fractional Sobolev spaces. *Bulletin des sciences mathématiques*, 136(5):521–573, 2012 (cited on page 109).

[60] P. Diaconis. Bayesian numerical analysis. *Statistical decision theory and related topics IV*, 1:163–175, 1988 (cited on page 219).

[61] J. Dieudonné. Sur les espaces de Montel métrisables. French. *C. R. Acad. Sci., Paris*, 238:194–195, 1954 (cited on page 88).

[62] Y. Dodge. *The concise encyclopedia of statistics*. Springer Science & Business Media, 2008 (cited on page 5).

[63] J. L. Doob. *Stochastic processes*. Wiley Classics Library. New York, NY: John Wiley & Sons, Inc., 1990 (cited on pages 49, 77, 78, 79, 120, 162).

[64] J. L. Doob. Stochastic processes depending on a continuous parameter. *Trans. Amer. Math. Soc.*, 42(1):107–140, 1937 (cited on pages 78, 121).

[65] M. Dow. Explicit inverses of Toeplitz and associated matrices. *ANZIAM Journal*, 44(E):E185–E215, 2003 (cited on pages 229, 230).

[66] T. A. Driscoll and B. Fornberg. Interpolation in the limit of increasingly flat radial basis functions. *Comput. Math. Appl.*, 43(3-5):413–422, 2002 (cited on page 220).

[67] R. M. Dudley. The sizes of compact subsets of Hilbert space and continuity of Gaussian processes. *J. Funct. Anal.*, 1(3):290–330, 1967 (cited on pages 47, 138, 139).

[68] D. G. Duffy. *Green's functions with applications*. Chapman and Hall/CRC, second edition edition, 2015 (cited on pages 175, 186, 249, 264).

[69] J. J. Duistermaat and J. A. C. Kolk. *Distributions*. Boston, MA: Birkhäuser Boston, Inc., 2010 (cited on pages 86, 95, 96, 175, 178, 249).

[70] B. Engquist and A. Majda. Absorbing boundary conditions for the numerical simulation of waves. *Math. Comp.*, 31(139):629–651, 1977 (cited on pages 204, 247, 251).

[71] I. Erdélyi. A generalized inverse for arbitrary operators between Hilbert spaces. *Proc. Cambridge Philos. Soc.*, 71:43–50, 1972 (cited on page 23).

[72] A. Estrade and J. Fournier. Anisotropic Gaussian wave models. *ALEA Lat. Am. J. Probab. Math. Stat.*, 17, 2020 (cited on page 74).

[73] L. C. Evans. *Partial differential equations*, volume 19 of *Graduate Studies in Mathematics*. Providence, RI: American Mathematical Society, second edition, 2010 (cited on pages 26, 28, 72, 75, 86, 94, 96, 103, 107, 108, 169, 175, 184, 213, 221, 222, 249).

[74] L. C. Evans and R. F. Gariepy. *Measure theory and fine properties of functions*. Textbooks in Mathematics. Boca Raton, FL: CRC Press, revised edition, 2015 (cited on pages 81, 191).

[75] M. Fan, D. Paul, T. C. M. Lee, and T. Matsuo. Modeling tangential vector fields on a sphere. *J. Amer. Statist. Assoc.*, 113(524):1625–1636, 2018 (cited on page 74).

[76] B. T. Fang. Trilateration and extension to global positioning system navigation. *J. Guid. Control Dyn.*, 9(6):715–717, 1986 (cited on pages 60, 170, 187).

[77] G. E. Fasshauer. *Meshfree approximation methods with MATLAB*, volume 6 of *Interdisciplinary Mathematical Sciences*. Hackensack, NJ: World Scientific Publishing Co. Pte. Ltd., 2007 (cited on pages 21, 94, 174).

[78] J. Fiedler. *Distances, Gegenbauer expansions, curls, and dimples: On dependence measures for random fields*. PhD thesis, 2016 (cited on page 74).

[79] B. Fornberg, G. Wright, and E. Larsson. Some observations regarding interpolants in the limit of flat radial basis functions. *Comput. Math. Appl.*, 47(1):37–55, 2004 (cited on page 220).

[80] B. Fornberg and N. Flyer. *A primer on radial basis functions with applications to the geosciences*. SIAM, 2015 (cited on page 220).

[81] E. J. Fuselier Jr. *Refined error estimates for matrix-valued radial basis functions*. Ann Arbor, MI: ProQuest LLC, 2006, page 87. Thesis (Ph.D.)–Texas A&M University (cited on pages 75, 171).

[82] J. Gapaillard and J. Michaux. Sur les processus linéaires définis sur un espace nucléaire. *Ann. Fac. Sci. Toulouse Math. (5)*, 8(1):75–92, 1986/87 (cited on page 88).

[83] A. Geist and S. Trimpe. Learning constrained dynamics with Gauss' principle adhering Gaussian processes. In *Proceedings of the 2nd Conference on Learning for Dynamics and Control*, volume 120 of *Proc. Mach. Learn. Res.* Pages 225–234. PMLR, 2020 (cited on page 74).

[84] I. M. Gel'fand and N. Y. Vilenkin. *Generalized functions. Vol. 4: Applications of harmonic analysis*. New York-London: Academic Press, 1964 (cited on page 88).

[85] B. Ghorbani, S. Mei, T. Misiakiewicz, and A. Montanari. When do neural networks outperform kernel methods ? *Adv. Neural Inf. Process Syst. (NEURIPS)*, 33:14820–14830, 2020 (cited on pages 24, 25).

[86] D. Ginsbourger, O. Roustant, and N. Durrande. On degeneracy and invariances of random fields paths with applications in Gaussian process modelling. *J. Statist. Plann. Inference*, 170:117–128, 2016 (cited on pages 40, 42, 71, 74, 76, 83, 84, 85, 171).

[87] R. Godement. Les fonctions de type positif et la théorie des groupes. *Trans. Amer. Math. Soc.*, 63:1–84, 1948 (cited on page 8).

[88] G. H. Golub and C. F. Van Loan. *Matrix computations*. JHU press, 2013 (cited on page 10).

[89] A. Gossard. *Méthodes d'apprentissage pour l'IRM computationnelle*. PhD thesis (cited on page 7).

[90] T. Graepel. Solving Noisy Linear Operator Equations by Gaussian Processes: Application to Ordinary and Partial Differential Equations. In *Proc. 20th Int. Conf. Mach. Learn.* Pages 234–241. AAAI Press, 2003 (cited on pages 74, 170).

[91] R. B. Gramacy. *Surrogates: Gaussian process modeling, design, and optimization for the applied sciences*. CRC press, 2020 (cited on pages 8, 24).

[92] T. N. E. Greville. Note on the generalized inverse of a matrix product. *SIAM Rev.*, 8:518–521, erratum, ibid. 9 (1966), 249, 1966 (cited on page 155).

[93] C. Grossmann, H.-G. Roos, and M. Stynes. *Numerical treatment of partial differential equations*. Springer, 2007 (cited on page 169).

[94] M. Gulian, A. Frankel, and L. Swiler. Gaussian process regression constrained by boundary value problems. *Comput. Methods Appl. Mech. Engrg.*, 388:Paper No. 114117, 18, 2022 (cited on pages 75, 171).

[95] E. Hairer, S. P. Nørsett, and G. Wanner. *Solving ordinary differential equations. 1, Nonstiff problems*. Springer-Verlag, 1993 (cited on page 218).

[96] I. Henderson. Sobolev regularity of Gaussian random fields, 2022. arXiv: 2209.02703 (cited on pages 41, 105).

[97] I. Henderson, P. Noble, and O. Roustant. Characterization of the second order random fields subject to linear distributional pde constraints. *Bernoulli*, 29(4):3396–3422, 2023. ISSN: 1350-7265. DOI: 10.3150/23-BEJ1588 (cited on pages 41, 69, 170, 171, 176, 177).

[98] I. Henderson, P. Noble, and O. Roustant. Wave equation-tailored Gaussian process regression with applications to related inverse problems. Working paper or preprint, 2023 (cited on pages 41, 167).

[99] P. Hennig, M. A. Osborne, and H. P. Kersting. *Probabilistic Numerics: Computation as Machine Learning*. Cambridge University Press, 2022 (cited on page 219).

[100] P. Hennig, M. A. Osborne, and M. Girolami. Probabilistic numerics and uncertainty in computations. *Proc. R. Soc. A*, 471(2179):20150142, 17, 2015 (cited on page 219).

[101] L. Hörmander. *The analysis of linear partial differential operators I: Distribution theory and Fourier analysis*. Springer, 2015 (cited on page 251).

[102] F. Q. Hu. Absorbing boundary conditions. *International Journal of Computational Fluid Dynamics*, 18(6):513–522, 2004 (cited on page 247).

[103] B. R. Hunt, T. Sauer, and J. A. Yorke. Prevalence: a translation-invariant "almost every" on infinite-dimensional spaces. *Bull. Amer. Math. Soc. (N.S.)*, 27(2):217–238, 1992 (cited on page 15).

[104] I. Ibragimov. Conditions for Gaussian homogeneous fields to belong to classes H_p^r. *Journal of Mathematical Sciences*, 68(4):484–497, 1994 (cited on page 108).

[105] V. Isakov. *Inverse problems for partial differential equations*, volume 127. Springer, 2006 (cited on page 29).

[106] A. Jacot, F. Gabriel, and C. Hongler. Neural tangent kernel: convergence and generalization in neural networks. In S. Bengio, H. Wallach, H. Larochelle, K. Grauman, N. Cesa-Bianchi, and R. Garnett, editors, *Adv. Neural Inf. Process Syst. (NEURIPS)*, volume 31. Curran Associates, Inc., 2018 (cited on page 25).

[107] S. Janson. *Gaussian Hilbert spaces*, volume 129 of *Cambridge Tracts in Mathematics*. Cambridge: Cambridge University Press, 1997 (cited on pages 78, 173).

[108] C. Jidling, J. Hendriks, N. Wahlstrom, A. Gregg, T. Schon, C. Wensrich, and A. Wills. Probabilistic modelling and reconstruction of strain. *Nucl. Instrum. Methods Phys. Res. B: Beam Interact. Mater. At.*, 436:141–155, 2018 (cited on pages 75, 171).

[109] C. Jidling, N. Wahlström, A. Wills, and T. B. Schön. Linearly constrained Gaussian processes. In *Adv. Neural Inf. Process Syst.* Volume 30. Curran Associates, Inc., 2017 (cited on pages 74, 75, 171).

[110] J. Jørgensen. *Probability With a View Towards Statistics, Volume II*. Chapman and Hall/CRC, 1994 (cited on pages 16, 17, 117).

[111] M. Kanagawa, P. Hennig, D. Sejdinovic, and B. K. Sriperumbudur. Gaussian processes and kernel methods: a review on connections and equivalences, 2018. arXiv: 1807.02582 (cited on pages 48, 140).

[112] G. E. Karniadakis, I. G. Kevrekidis, L. Lu, P. Perdikaris, S. Wang, and L. Yang. Physics-informed machine learning. *Nat. Rev. Phys.*, 3(6):422–440, 2021 (cited on pages 7, 39).

[113] T. Karvonen, C. J. Oates, and S. Sarkka. A Bayes-Sard cubature method. *Adv. Neural Inf. Process Syst. (NEURIPS)*, 31, 2018 (cited on page 242).

[114] M. Kazakova and P. Noble. Discrete transparent boundary conditions for the linearized Green-Naghdi system of equations. *SIAM J. Numer. Anal.*, 58(1):657–683, 2020 (cited on page 247).

[115] G. Kerkyacharian, S. Ogawa, P. Petrushev, and D. Picard. Regularity of Gaussian processes on Dirichlet spaces. *Constr. Approx.*, 47(2):277–320, 2018 (cited on pages 108, 109).

[116] N. Kovachki, Z. Li, B. Liu, K. Azizzadenesheli, K. Bhattacharya, A. Stuart, and A. Anandkumar. Neural operator: learning maps between function spaces with applications to PDEs. *J. Mach. Learn. Res.*, 24(89):1–97, 2023 (cited on page 40).

[117] A. Krizhevsky, I. Sutskever, and G. E. Hinton. Imagenet classification with deep convolutional neural networks. In F. Pereira, C. Burges, L. Bottou, and K. Weinberger, editors, *Adv. Neural Inf. Process Syst. (NEURIPS)*, volume 25. Curran Associates, Inc., 2012 (cited on page 7).

[118] P. Kuchment and L. Kunyansky. Mathematics of photoacoustic and thermoacoustic tomography. In *Handbook of mathematical methods in imaging. Vol. 1, 2, 3*, pages 1117–1167. New York: Springer, 2015 (cited on page 76).

[119] P. Kuchment and L. Kunyansky. Mathematics of photoacoustic and thermoacoustic tomography. In *Handbook of mathematical methods in imaging. Vol. 1, 2, 3*, pages 1117–1167. Springer, New York, 2015 (cited on page 171).

[120] K. S. Kunz and R. J. Luebbers. *The finite difference time domain method for electromagnetics*. CRC press, 1993 (cited on page 218).

[121] P. T. Lai. Noyaux d'Agmon. fre. *Séminaire Jean Leray*, 277(4):1–37, 1973-1974 (cited on page 141).

[122] S. Lang. *Real and functional analysis*, volume 142 of *Graduate Texts in Mathematics*. New York, NY: Springer-Verlag, third edition, 1993 (cited on page 82).

[123] M. Lange-Hegermann. Algorithmic linearly constrained Gaussian processes. In *Adv. Neural Inf. Process Syst. (NEURIPS)*, volume 31. Curran Associates, Inc., 2018 (cited on pages 74, 75, 107, 171).

[124] M. Lange-Hegermann. Linearly constrained Gaussian processes with boundary conditions. In A. Banerjee and K. Fukumizu, editors, *Proceedings of The 24th International Conference on Artificial Intelligence and Statistics*, volume 130 of *Proceedings of Machine Learning Research*, pages 1090–1098. PMLR, 2021 (cited on pages 74, 75, 171).

[125] D. Lannes and P. Bonneton. Derivation of asymptotic two-dimensional time-dependent equations for surface water wave propagation. *Physics of Fluids*, 21(1):016601, 2009 (cited on pages 213, 249).

[126] E. Larsson and B. Fornberg. Theoretical and computational aspects of multivariate interpolation with increasingly flat radial basis functions. *Comput. Math. Appl.*, 49(1):103–130, 2005 (cited on page 220).

[127] J.-F. Le Gall. *Mouvement brownien, martingales et calcul stochastique*, volume 71 of *Mathématiques & Applications (Berlin)*. Heidelberg: Springer, 2013 (cited on pages 49, 77, 98).

[128] J. Lee, Y. Bahri, R. Novak, S. S. Schoenholz, J. Pennington, and J. Sohl-Dickstein. Deep neural networks as Gaussian processes. In *ICLR 2018 - International Conference on Learning Representations* (cited on page 25).

[129] Y. J. Lee, C. A. Micchelli, and J. Yoon. A study on multivariate interpolation by increasingly flat kernel functions. *J. Math. Anal. Appl.*, 427(1):74–87, 2015 (cited on pages 25, 220, 228, 229, 231).

[130] Y. J. Lee, C. A. Micchelli, and J. Yoon. On convergence of flat multivariate interpolation by translation kernels with finite smoothness. *Constr. Approx.*, 40(1):37–60, 2014 (cited on pages 64, 220, 228, 229, 231).

[131] Y. J. Lee, G. J. Yoon, and J. Yoon. Convergence of increasingly flat radial basis interpolants to polynomial interpolants. *SIAM J. Math. Anal.*, 39(2):537–553, 2007 (cited on page 220).

[132] R. J. LeVeque. *Finite volume methods for hyperbolic problems*, volume 31. Cambridge university press, 2002 (cited on pages 28, 37, 218, 223, 224, 225).

[133] Z. Li, N. B. Kovachki, K. Azizzadenesheli, K. Bhattacharya, A. Stuart, A. Anandkumar, et al. Fourier neural operator for parametric partial differential equations. In *International Conference on Learning Representations*, 2021 (cited on page 40).

[134] V. Linde, V. I. Tarieladze, and S. A. Chobanyan. Characterization of certain classes of Banach spaces by properties of Gaussian measures. *Theory of Probability & Its Applications*, 25(1):159–164, 1980 (cited on pages 117, 119, 132).

[135] F. Lindgren, D. Bolin, and H. Rue. The SPDE approach for Gaussian and non-Gaussian fields: 10 years and still running. *Spat. Stat.*:100599, 2022 (cited on pages 26, 73).

[136] F. Lindgren, H. Rue, and J. Lindström. An explicit link between Gaussian fields and Gaussian Markov random fields: the stochastic partial differential equation approach. *J. R. Stat. Soc. Ser. B Stat. Methodol.*, 73(4):423–498, 2011. With discussion and a reply by the authors (cited on page 230).

[137] A. F. López-Lopera, N. Durrande, and M. Álvarez. Physically-inspired Gaussian process models for post-transcriptional regulation in drosophila. *IEEE/ACM Transactions on Computational Biology and Bioinformatics*, 18:656–666, 2021 (cited on page 170).

[138] L. Lu, P. Jin, G. Pang, Z. Zhang, and G. Karniadakis. Learning nonlinear operators via deeponet based on the universal approximation theorem of operators. *Nat. Mach. Intell.*, 3:218–229, 2021 (cited on page 40).

[139] B. Malgrange. L. Schwartz et la théorie des distributions. In number 131, pages 25–33. 1985. Colloquium in honor of Laurent Schwartz, Vol. 1 (Palaiseau, 1983) (cited on page 34).

[140] A. Mas. Representation of small ball probabilities in Hilbert space and lower bound in regression for functional data. *Electron. J. Stat.*, 6:1745–1778, 2012 (cited on pages 156, 266).

[141] *MATLAB version 9.8.0.1721703 (R2020a) Update 7*. The Mathworks, Inc. Natick, Massachusetts, 2020 (cited on page 205).

[142] F. M. Mendes and E. A. da Costa Júnior. Bayesian inference in the numerical solution of Laplace's equation. *AIP Conference Proceedings*, 1443(1):72–79, 2012 (cited on pages 75, 171).

[143] C. A. Micchelli and W. L. Miranker. Asymptotically optimal approximation in fractional Sobolev spaces and the numerical solution of differential equations. *Numer. Math.*, 22:75–87, 1974 (cited on pages 26, 219, 220, 228, 229, 231, 232).

[144] C. A. Micchelli and W. L. Miranker. Optimal difference schemes for linear initial value problems. *SIAM J. Numer. Anal.*, 10:983–1009, 1973 (cited on pages 219, 220, 225, 228, 229, 231).

[145] W. L. Miranker. Difference schemes with best possible truncation error. *Numer. Math.*, 17:124–142, 1971 (cited on pages 219, 229, 242).

[146] F. J. Narcowich and J. D. Ward. Generalized Hermite interpolation via matrix-valued conditionally positive definite functions. *Math. Comp.*, 63(208):661–687, 1994 (cited on pages 75, 171).

[147] R. M. Neal. *Bayesian learning for neural networks*, volume 118. Springer Science & Business Media, 1996 (cited on page 24).

[148] N. C. Nguyen and J. Peraire. Gaussian functional regression for linear partial differential equations. *Comput. Methods Appl. Mech. Engrg.*, 287:69–89, 2015 (cited on pages 75, 76).

[149] S. M. Nikol'skii. *Approximation of functions of several variables and imbedding theorems*, volume 205. Springer Science & Business Media, 2012 (cited on page 108).

[150] J. P. Nolan. *Univariate Stable Distributions*. Springer Series in Operations Research and Financial Engineering. Springer Cham, 2012 (cited on page 16).

[151] H. Owhadi. Bayesian numerical homogenization. *Multiscale Model. Simul.*, 13(3):812–828, 2015 (cited on pages 75, 107, 171, 219).

[152] H. Owhadi. Do ideas have shape? Idea registration as the continuous limit of artificial neural networks. *Phys. D*, 444:Paper No. 133592, 41, 2023 (cited on page 25).

[153] H. Owhadi. Gaussian process hydrodynamics, 2023. arXiv: 2209.10707 [physics.flu-dyn] (cited on page 39).

[154] H. Owhadi and C. Scovel. Separability of reproducing kernel spaces. *Proc. Amer. Math. Soc.*, 145(5):2131–2138, 2017 (cited on page 138).

[155] A. Pazy. *Semigroups of linear operators and applications to partial differential equations*, volume 44 of *Applied Mathematical Sciences*. New York: Springer-Verlag, 1983 (cited on page 95).

[156] M. Pförtner, I. Steinwart, P. Hennig, and J. Wenger. Physics-informed Gaussian process regression generalizes linear PDE solvers, 2023. arXiv: 2212.12474 [cs.LG] (cited on page 219).

[157] W. H. Press, S. A. Teukolsky, W. T. Vetterling, and B. P. Flannery. *Numerical recipes 3rd edition: The art of scientific computing*. Cambridge university press, 2007 (cited on page 192).

[158] Z. Purisha, C. Jidling, N. Wahlström, T. B. Schön, and S. Särkkä. Probabilistic approach to limited-data computed tomography reconstruction. *Inverse Problems*, 35(10):105004, 20, 2019 (cited on page 172).

[159] J. Quiñonero-Candela and C. E. Rasmussen. A unifying view of sparse approximate Gaussian process regression. *J. Mach. Learn. Res.*, 6:1939–1959, 2005 (cited on pages 26, 213, 264).

[160] R Core Team. *R: A Language and Environment for Statistical Computing*. R Foundation for Statistical Computing. Vienna, Austria, 2020 (cited on page 204).

[161] A. Radford, L. Metz, and S. Chintala. Unsupervised representation learning with deep convolutional generative adversarial networks, 2016. arXiv: `1511.06434 [cs.LG]` (cited on page 7).

[162] M. Raissi, P. Perdikaris, and G. Karniadakis. Physics-informed neural networks: a deep learning framework for solving forward and inverse problems involving nonlinear partial differential equations. *J. Comput. Phys.*, 378:686–707, 2019 (cited on pages 7, 39, 107).

[163] M. Raissi, P. Perdikaris, and G. E. Karniadakis. Machine learning of linear differential equations using Gaussian processes. *J. Comput. Phys.*, 348:683–693, 2017 (cited on pages 75, 76, 107, 170, 171, 213).

[164] M. Raissi, P. Perdikaris, and G. E. Karniadakis. Numerical Gaussian processes for time-dependent and nonlinear partial differential equations. *SIAM J. Sci. Comput.*, 40(1):A172–A198, 2018 (cited on page 170).

[165] M. Raissi, A. Yazdani, and G. E. Karniadakis. Hidden fluid mechanics: learning velocity and pressure fields from flow visualizations. *Science*, 367(6481):1026–1030, 2020 (cited on page 39).

[166] C. E. Rasmussen and C. K. I. Williams. *Gaussian processes for machine learning*. Adaptive Computation and Machine Learning. Cambridge, MA: MIT Press, 2006 (cited on pages 8, 10, 13, 14, 18, 19, 22, 25, 77, 79, 93, 169, 173, 174, 177, 230, 244).

[167] M. Refinetti, S. Goldt, F. Krzakala, and L. Zdeborová. Classifying high-dimensional Gaussian mixtures: where kernel methods fail and neural networks succeed. In *International Conference on Machine Learning*, pages 8936–8947. PMLR, 2021 (cited on page 24).

[168] K. Ritter. *Average-case analysis of numerical problems*, volume 1733 of *Lecture Notes in Mathematics*. Berlin: Springer-Verlag, 2000 (cited on page 100).

[169] J. J. F. F. Robert A. Adams. *Sobolev spaces*. Pure and Applied Mathematics. Academic Press, 2nd edition, 2003 (cited on pages 32, 49, 107, 108, 109, 111, 125, 129, 141, 157, 159).

[170] L. Roques, D. Allard, and S. Soubeyrand. Spatial statistics and stochastic partial differential equations: a mechanistic viewpoint. *Spat. Stat.*:100591, 2022 (cited on page 73).

[171] H. L. Royden and P. Fitzpatrick. *Real analysis*, volume 32. Macmillan New York, 1988 (cited on page 159).

[172] B. Roynette. Mouvement Brownien et espaces de Besov. *Stochastics*, 43(3-4):221–260, 1993 (cited on page 108).

[173] W. Rudin. *Functional analysis*. International Series in Pure and Applied Mathematics. New York, NY: McGraw-Hill, Inc., second edition, 1991 (cited on pages 26, 72, 79, 80, 81, 91).

[174] T. J. Santner, B. J. Williams, and W. I. Notz. *The design and analysis of computer experiments*. Springer Series in Statistics. Springer, New York, 2018. Second edition (cited on pages 8, 24).

[175] S. Särkkä, M. Álvarez, and N. Lawrence. Gaussian process latent force models for learning and stochastic control of physical systems. *IEEE Trans. on Automat. Control*, 64:2953–2960, 2019 (cited on page 170).

[176] S. Särkkä. Linear operators and stochastic partial differential equations in Gaussian process regression. In T. Honkela, W. Duch, M. Girolami, and S. Kaski, editors, *Artificial Neural Networks and Machine Learning – ICANN 2011*, pages 151–158, Berlin, Heidelberg. Springer Berlin Heidelberg, 2011. ISBN: 978-3-642-21738-8 (cited on page 170).

[177] R. Schaback. Limit problems for interpolation by analytic radial basis functions. *J. Comput. Appl. Math.*, 212(2):127–149, 2008 (cited on pages 220, 229).

[178] R. Schaback. Multivariate interpolation by polynomials and radial basis functions. *Constr. Approx.*, 21(3):293–317, 2005 (cited on pages 64, 220).

[179] R. Schaback. Solving the Laplace equation by meshless collocation using harmonic kernels. *Adv. Comput. Math.*, 31(4):457–470, 2009 (cited on pages 75, 171).

[180] H. H. Schaefer and M. P. Wolff. *Topological vector spaces*, volume 3 of *Graduate Texts in Mathematics*. New York, NY: Springer-Verlag, second edition, 1999 (cited on page 88).

[181] M. Scheuerer. Regularity of the sample paths of a general second order random field. *Stochastic Process. Appl.*, 120(10):1879–1897, 2010 (cited on pages 92, 103, 108, 109, 110, 122, 141).

[182] M. Scheuerer and M. Schlather. Covariance models for divergence-free and curl-free random vector fields. *Stoch. Models*, 28(3):433–451, 2012 (cited on pages 74, 75, 171).

[183] L. Schwartz. Généralisation de la notion de fonction, de dérivation, de transformation de Fourier et applications mathématiques et physiques. *Ann. Univ. Grenoble. Sect. Sci. Math. Phys. (N.S.)*, 21:57–74 (1946), 1945 (cited on page 33).

[184] L. Schwartz. Sous-espaces Hilbertiens d'espaces vectoriels topologiques et noyaux associés (noyaux reproduisants). *J. Anal. Math.*, 13(1):115–256, 1964 (cited on pages 17, 22, 84, 150).

[185] T. J. Sejnowski. The unreasonable effectiveness of deep learning in artificial intelligence. *Proc. Natl. Acad. Sci. USA PNAS*, 117(48):30033–30038, 2020 (cited on page 6).

[186] D. Serre. *Systems of conservation laws. Vol 1.* Cambridge: Cambridge University Press, 1999 (cited on pages 28, 71, 91, 253).

[187] C. E. Shannon. Communication in the presence of noise. *Proceedings of the IRE*, 37(1):10–21, 1949 (cited on page 246).

[188] H. A. Simon. The architecture of complexity. *Proc. Am. Philos. Soc.*, 106(6):467–482, 1962 (cited on page 4).

[189] A. Solin and M. Kok. Know your boundaries: constraining Gaussian processes by variational harmonic features. In *Proc. 22nd Int. Conf. Artif. Intell. Stat.* Volume 89 of *Proc. of Mach. Learn. Res.* Pages 2193–2202. PMLR, 2019 (cited on page 171).

[190] A. Solin and S. Särkkä. Hilbert space methods for reduced-rank Gaussian process regression. *Stat. Comput.*, 30(2):419–446, 2020 (cited on pages 26, 264).

[191] G. Song, J. Riddle, G. E. Fasshauer, and F. J. Hickernell. Multivariate interpolation with increasingly flat radial basis functions of finite smoothness. *Adv. Comput. Math.*, 36(3):485–501, 2012 (cited on pages 26, 220, 229, 233).

[192] E. M. Stein. *Singular integrals and differentiability properties of functions.* Princeton Mathematical Series, No. 30. Princeton University Press, Princeton, N.J., 1970 (cited on pages 108, 134, 135).

[193] I. Steinwart. Convergence types and rates in generic Karhunen-Loeve expansions with applications to sample path properties. *Potential Anal.*, 51(3):361–395, 2019 (cited on pages 78, 108, 109, 110, 141).

[194] G. Strang. Trigonometric polynomials and difference methods of maximum accuracy. *Journal of Mathematics and Physics*, 41(1-4):147–154, 1962 (cited on pages 223, 228, 241).

[195] A. M. Stuart. Inverse problems: a Bayesian perspective. *Acta Numer.*, 19:451–559, 2010 (cited on pages 16, 171).

[196] J. Suuronen, T. Soto, N. K. Chada, and L. Roininen. Bayesian inversion with α-stable priors, 2022. arXiv: 2212.05555 [stat.CO] (cited on page 16).

[197] C. Szegedy, W. Zaremba, I. Sutskever, J. Bruna, D. Erhan, I. Goodfellow, and R. Fergus. Intriguing properties of neural networks, 2014. arXiv: 1312.6199 [cs.CV] (cited on page 6).

[198] G. J. Székely and M. L. Rizzo. Energy statistics: a class of statistics based on distances. *J. Statist. Plann. Inference*, 143(8):1249–1272, 2013 (cited on page 233).

[199] M. Talagrand. *Upper and lower bounds for stochastic processes*, volume 60. Springer, 2014 (cited on pages 47, 50, 138, 266).

[200] T. Tao. *Nonlinear dispersive equations: local and global analysis*, number 106. American Mathematical Soc., 2006 (cited on page 31).

[201] L. N. Trefethen. Finite difference and spectral methods for ordinary and partial differential equations, 1996 (cited on page 248).

[202] F. Trèves. *Topological vector spaces, distributions and kernels*. New York-London: Academic Press, 1967 (cited on pages 17, 26, 48, 79, 80, 81, 82, 83, 86, 88, 96, 97, 113, 131, 145, 178).

[203] H. Triebel. Über die approximationszahlen der einbettungsoperatoren $J(B^r_{p,q}(\Omega) \to B^{r'}_{p',q'}(S))$. *Archiv der Mathematik*, 19(3):305–312, 1968 (cited on page 141).

[204] M. Unser and T. Blu. Fractional splines and wavelets. *SIAM review*, 42(1):43–67, 2000 (cited on pages 25, 220, 235).

[205] A. Van Der Vaart and H. Van Zanten. Information rates of nonparametric Gaussian process methods. *J. Mach. Learn. Res.*, 12(6), 2011 (cited on page 107).

[206] R. van der Meer, C. W. Oosterlee, and A. Borovykh. Optimally weighted loss functions for solving PDEs with neural networks. *J. Comput. Appl. Math.*, 405:Paper No. 113887, 18, 2022 (cited on page 39).

[207] R. C. Vergara, D. Allard, and N. Desassis. A general framework for SPDE-based stationary random fields. *Bernoulli*, 28(1):1–32, 2022 (cited on pages 73, 74, 76, 77, 171).

[208] A. C. Vliegenthart. On finite-difference methods for the Korteweg-de Vries equation. *J. Engrg. Math.*, 5:137–155, 1971 (cited on page 222).

[209] N. Wahlstrom, M. Kok, T. B. Schön, and F. Gustafsson. Modeling magnetic fields using Gaussian processes. *Proc. IEEE Int. Conf. Acoust. Speech Signal Process.*:3522–3526, 2013 (cited on pages 75, 107, 171).

[210] R. F. Warming and B. J. Hyett. The modified equation approach to the stability and accuracy analysis of finite-difference methods. *J. Comput. Phys.*, 14:159–179, 1974 (cited on pages 225, 255).

[211] L. Wasserman. *All of statistics: a concise course in statistical inference*, volume 26. Springer, 2004 (cited on pages 14, 22).

[212] H. Wendland. *Scattered data approximation*, volume 17. Cambridge university press, 2004 (cited on pages 21, 22, 23, 25, 39, 174, 219, 220, 228, 240, 242).

[213] P. Wesseling. *Principles of computational fluid dynamics*, volume 29. Springer Science & Business Media, 2009 (cited on page 238).

[214] P. Whittle. On stationary processes in the plane. *Biometrika*:434–449, 1954 (cited on page 73).

[215] E. P. Wigner. The unreasonable effectiveness of mathematics in the natural sciences. richard courant lecture in mathematical sciences delivered at new york university, may 11, 1959. *Comm. Pure Appl. Math.*, 13(1):1–14, 1960 (cited on page 6).

[216] M. Xu and L. V. Wang. Universal back-projection algorithm for photoacoustic computed tomography. *Phys. Rev. E*, 71(1):016706, 2005 (cited on page 172).

[217] O. C. Zienkiewicz, R. L. Taylor, and J. Z. Zhu. *The finite element method: its basis and fundamentals*. Elsevier, 2005 (cited on page 30).

Méthodes de régression à noyau sous contraintes d'équations aux dérivées partielles

Résumé: Ce manuscrit traite de l'étude de méthodes de régression à noyau construites spécifiquement pour résoudre des problèmes contrôlés par des équations aux dérivées partielles (EDPs). En particulier, la question du choix d'un noyau respectant les propriétés d'une EDP donnée est étudiée, notamment du point de vue du processus aléatoire sous-jacent au noyau utilisé. Un chapitre introductif est dédié à une description pédagogique de notions importantes issues de l'inférence bayésienne, de la théorie des processus aléatoires et de la théorie des EDPs. Le chapitre 2 donne une caractérisation nécessaire et suffisante pour que les trajectoires d'un processus aléatoire général d'ordre deux vérifient une EDP linéaire homogène donnée, au sens des distributions. Etant donnés $m \in \mathbb{N}$ et $1 < p < +\infty$, le chapitre 3 décrit plusieurs caractérisations nécessaires et suffisantes pour que les trajectoires d'un processus gaussien centré possèdent une régularité Sobolev $W^{m,p}$, presque sûrement. Les caractérisations de ces deux chapitres sont formulées uniquement en terme des deux premiers moments du processus; certaines d'entre elles sont relativement faciles à appliquer en pratique. Les cadres théoriques de ces deux chapitres sont choisis de façon à être les plus généraux possible, en évitant toute hypothèse de continuité non nécessaire.

Le chapitre 4 décrit quelques fonctions de covariance adaptés à l'équation des ondes (au sens du chapitre 2) en trois dimensions. Ces dernières sont ensuite utilisées pour estimer les paramètres physiques de l'équation ainsi que ses conditions initiales, étant donné une base de données d'observations de la solution issues de quelques capteur ponctuelles. Le chapitre 5 décrit comment des schémas numériques de type différences finies pour l'équation d'advection peuvent être obtenus à l'aide d'une régression à noyau basée sur une fonction de covariance adaptée à cette EDP. Certains schémas classiques sont retrouvés et de nouveaux sont proposés. Une étude théorique et numérique (accompagnée de conjectures) de ces schémas est proposée.

Mots-clés : régression par processus gaussiens, machine learning informé par la physique, équations aux dérivées partielles, équation des ondes

PDE constrained kernel regression methods

Abstract: This thesis manuscript deals with the study of certain kernel regression methods, which are specifically built to approximate functions which are related to partial differential equations (PDEs). In particular, the matter of the construction of covariance kernels which respect the properties of the PDE is studied. This question is mostly studied from the point of view of the random field underlying the kernel. Chapter 1 contains a user friendly description of important notions stemming from Bayesian inference, random field theory and PDE theory. Chapter 2 describes a necessary and sufficient condition ensuring that the sample paths of a general second order random field are solutions to a given linear homogeneous PDE, in the sense of distributions, almost surely. Chapter 3 provides several necessary and sufficient conditions ensuring that the realizations of a centered Gaussian process lie in a given Sobolev space $W^{m,p}$, where $m \in \mathbb{N}$ and $1 < p < +\infty$, almost surely. The results contained in Chapters 2 and 3 only involve the two first moments of the process; some of these results are relatively easy to use in practice. The theoretical frameworks of both chapters are chosen to be as general as possible, avoiding unnecessary continuity assumptions.

Chapter 4 describes several covariance kernels tailored to the three dimensional wave equation (in the sense of Chapter 2). These kernels are then used to estimate the physical parameters of the wave equation as well as its initial conditions, given a database of observations of a solution to the PDE thanks to scattered sensors. Chapter 5 describes how numerical methods akin to finite difference schemes can be obtained for the advection equation, thanks to a kernel tailored to this PDE. Certain well-known finite difference schemes are recovered and new ones are proposed. A theoretical and numerical study of those schemes is then described, along with related conjectures.

Keywords: Gaussian process regression, physics-informed machine learning, partial differential equations, wave equation